Proteomic analysis of Vascular Endothelial Growth Factor (VEGF) signalling: Studies of the mechanism of VEGF-induced Heat Shock Protein 27 phosphorylation and its role in endothelial cell signalling and function

Gary Britton

University College London

2010

A thesis submitted for the degree of Doctor of Philosophy

Declaration

I, Gary Britton, confirm that the work presented in this thesis is my own. Where information has been derived from other sources, I confirm that this has been indicated in the thesis.

Abstract

Vascular Endothelial Growth Factor (VEGF) is essential for angiogenesis and endothelial function. Proteomic analysis of Human Umbilical Vein Endothelial Cells (HUVEC) identified Heat Shock Protein 27 (Hsp27) as a major VEGF-regulated protein. Hsp27 is implicated in actin organization, cell survival and migration, and is a potential mediator of these VEGF functions in the endothelium. Studies of pharmacological inhibitors indicated that VEGF-stimulated Hsp27 serine 82 (S82) phosphorylation was resistant to p38 mitogen-activated protein kinase inhibition and mediated by Protein Kinase C (PKC). VEGF activated Protein Kinase D (PKD), and this effect was inhibited by small interfering (si)RNAs targeting selected PKC isoforms. PKD2 siRNA inhibited VEGF-induced Hsp27 S82 phosphorylation, and PKD2 immunoprecipitated from VEGF-treated cells selectively phosphorylated Hsp27 at S82. Hsp27 siRNAs markedly inhibited VEGF-induced cell migration, increased apoptosis and reduced tubulogenesis. Furthermore, inhibition of PKC but not p38 kinase inhibited VEGF-stimulated cell migration. Overexpression of S82A and S82D Hsp27 mutants using adenoviral vectors (Ad) had no significant effect on migration. However, VEGF reduced Hsp27 oligomeric size, and Ad-overexpressed S82D Hsp27 also formed smaller oligomers than wild-type Hsp27. These findings identify a VEGF/PKC/PKD/Hsp27 S82 pathway, indicate a role for PKD and HSP27 in VEGF-induced endothelial migration, and also suggest a specific role for Hsp27 S82 phosphorylation in regulation of Hsp27 oligomerisation.

Further proteomic analysis of HUVECs identified Stomatin-Like Protein 2 (SLP2) as a major component of anti-phosphotyrosine immunoprecipitates. The function of SLP2 is little understood. VEGF did not alter the amount of anti-phosphotyrosine-associated SLP2, and further investiga-

tions suggested that SLP2 may not be directly tyrosine phosphorylated. SLP2 was localized to mitochondria and co-immunoprecipitated with Prohibitin, a protein implicated in mitochondrial function. However, siRNA-mediated SLP2 knockdown did not affect mitochondrial membrane potential, apoptosis or migration of endothelial cells, and the function of this protein remains unknown.

Contents

List of Figures

List of Tables

Publications

Evans IM*, Britton G*, Zachary IC (2008). Vascular endothelial growth factor induces heat shock protein (HSP) 27 serine 82 phosphorylation and endothelial tubulogenesis via protein kinase D and independent of p38 kinase. *Cell Signal* 20(7):1375–1384

* Joint first authors

Acknowledgements

First and foremost I would like to thank my supervisors, Professor Ian Zachary and Dr. Ian Evans. Their guidance, patience, support and willingness to help whenever required has gone beyond what might be expected, and this is genuinely appreciated.

Thanks to the European Commission and the British Heart Foundation for funding the work in this thesis.

Thanks also to those who have repeatedly helped me with once unfamiliar methods, in particular Drs. Derek Gilroy and Pauliina Lehtolainen (FACS analysis), Mr. Mark Crawford (mass spectrometry), and Dr. Paul Frankel and especially Dr. Izabela Piotrowska (molecular biology). Thanks to Drs. Sean Davidson (Hatter Institute, UCL) and Glenn Baggott (School of Biological and Chemical Sciences, Birkbeck College) for invaluable discussions on mitochondrial methods and statistical analysis respectively.

Thanks to members of the Centre for Cardiovascular Biology and Medicine at UCL for doing the things that lab colleagues do – helping with methods, donating reagents, giving advice, and generally making the lab a pleasant place to be.

Finally, thank you to my family and friends for their support and belief – Grandma, you can now have your coffee morning, although you may need to reheat the coffee. In particular, thank you to Diana, who has lived through this with me, tolerating my absence and unavailability without complaining (much), continually supporting and encouraging. This is what it was for.

Selected abbreviations

Standard one and three letter amino acid codes, and one letter DNA and RNA base codes used throughout. Standard scientific units and prefixes and basic chemical formulae are also used. Abbreviations not listed are defined on first use. Amino acid residue numbering corresponds to human protein variants unless stated.

aa	amino acid(s)
Ad	adenovirus
APS	ammonium persulphate
ATP	adenosine 5'-triphosphate
BAEC	bovine aortic endothelial cells
BAPTA-AM	1,2-bis(2-aminophenoxy)ethane-N,N,N',N'-tetraacetic acid
bp	base pair(s)
BSA	bovine serum albumin
CaM	Ca^{2+}/calmodulin complex
cAMP	adenosine 3',5'-cyclic monophosphate
cDNA	complementary DNA
CHAPS	3-((cholamidopropyl)-dimethylammonio)-1-propanesulfonate
cytC	cytochrome C
Da	daltons
DMEM	Dulbecco's modified Eagle's medium
DMSO	dimethyl sulphoxide
DNA	2'-deoxyribonucleic acid
DNase	2'-deoxyribonuclease
ds	double-stranded
dT	2'-deoxythymidine phosphate
DTT	dithiothreitol
E	embryonic day (time after fertilisation) *or* early gene cassette (from adenovirus genome)
EBM	endothelial basal medium
EC	endothelial cell
EDTA	ethylenediaminetetraacetic acid
EGTA	ethylene glycol-bis(β-aminoethyl ether)-N,N,N',N'-tetraacetic acid
ESI	electrospray ionisation

F-actin	filamentous (polymerised) actin
FBS	foetal bovine serum
FCCP	carbonyl cyanide p-trifluoromethoxyphenylhydrazone
FITC	fluorescin isothiocyanate
GF109203X	bisindolylmaleimide I, Gö6850; 2-[1-(3-dimethylaminopropyl)-1H-indol-3-yl] -3-(1H-indol-3-yl)-maleimide
Gö6976	12-(2-Cyanoethyl)-6,7,12,13-tetrahydro-13-methyl-5-oxo-5H-indolo(2,3-a) pyrrolo(3,4-c)-carbazole
Gö6983	2-[1-(3-dimethylaminopropyl)-5-methoxyindol-3-yl]-3-(1H-indol-3-yl)-maleimide
GFP	green fluorescent protein
GST	glutathione-S-transferase
H_2O_2	hydrogen peroxide
HBSS	HEPES-buffered saline solution
HCAEC	human coronary artery endothelial cells
HEPES	4-(2-hydroxyethyl)-1-piperazineethanesulfonic acid
HRP	horseradish peroxidase
Hsp	heat shock protein
HSPG	heparan sulphate proteoglycan
HUVECs	human umbilical vein endothelial cells
IC_{50}	concentration of inhibitor required to prevent 50
Ig	immunoglobulin
IL-1	interleukin-1
IP	immunoprecipitation/immunoprecipitate
IP_3	inositol-1,4,5-triphosphate
IPG	immobilised pH gradient
kb	kilobases (of nucleic acid)
LB	Luria-Bertani
LDS	lithium dodecyl sulphate
M_r	relative molecular mass
MALDI-TOF	matrix-assisted laser desorption and ionisation-time of flight
MAPK	mitogen-activated protein kinase
MAPKAPK or MK	MAPK-activated protein kinase
MOPS	3-(N-morpholino)propanesulfonic acid
MS	mass spectrometry
NF-κB	nuclear factor-κB
NO	nitric oxide
NRP	neuropilin
nt	nucleotide(s)
p38 /p38 MAPK	p38 mitogen-activated protein kinase, more specifically p38α variant CSBP2
P-	phosphorylated/phospho-
PAGE	polyacrylamide gel electrophoresis
PBS	phosphate-buffered saline
PCR	polymerase chain reaction
PGI_2	prostacyclin
PKC	protein kinase C
PKD	protein kinase D
PLC	phospholipase C

PlGF	placental growth factor
PMA	phorbol 12-myristate 13-acetate. Also named 12-O-Tetradecanoylphorbol 13-acetate (TPA)
PP2	pyrazolopyrimidine 2; 4-amino-5-(4-chlorophenyl)-7-(t-butyl)pyrazolo [3,4-d]pyrimidine
RIPA	radioimmunoprecipitation assay
RNA	ribonucleic acid
RNase	ribonuclease
RT	reverse transcriptase/reverse transcription
SB202190	4-(4-fluorophenyl)-2-(4-hydroxyphenyl)-5-(4-pyridyl)1H-imidazole
SB203580	4-(4-fluorophenyl)-2-(4-methylsulphinylphenyl)-5-(4-pyridyl)1H-imidazole
SDS	sodium dodecyl sulphate
SEM	standard error of the mean
SH2/3	src homology 2/3
sHsp	small heat shock protein
shRNA	short hairpin RNA
siRNA	small interfering RNA
SLP2	stomatin-like protein 2
SMC	smooth muscle cell
SU5614	5-Chloro-3-[(3,5-dimethylpyrrol-2-yl)methylene]-2-indolinone
TEMED	N,N,N,N'-tetramethylethylenediamine
TMRM	tetramethylrhodamine
TNF	tumour necrosis factor
Tris	tris(hydroxymethyl)aminomethane
UV	ultraviolet
VEGF	vascular endothelial growth factor, more specifically VEGF-A_{165}
VEGFR	vascular endothelial growth factor receptor
vSMC	vascular smooth muscle cell

Chapter 1

Introduction

The vascular circulation is an internal transport system that has evolved in large multicellular organisms to supply tissues with nutrients, remove waste products, and to carry substances generated by one tissue to other parts of the body. It consists of the transport fluid, blood, which is pumped around the blood vessels or vasculature by the heart.

The vasculature consists of five main types of vessel: the arteries, arterioles, capillaries, venules and veins (Pocock and Richards 2006). Blood leaving the heart initially enters the elastic great arteries, which help to smooth the pulsed blood flow generated by the heart, before passing through muscular arteries and arterioles, key resistance vessels containing smooth muscle which constrict and dilate to target blood to areas of need and to regulate blood pressure. Blood then enters capillaries – thin-walled vessels that are the site of most substance exchange between the blood and underlying tissues, before returning to the heart via the venules and veins.

Most vessels apart from capillaries are composed of three distinct layers (tunicae) separated by elastic laminae: the intima, media and adventitia, although the width and exact composition of these layers varies between vessels. The innermost, blood-contacting layer is the tunica intima, composed of a layer of endothelial cells on their basement membrane and a thin layer of connective tissue. The tunica media, separated from the intima by the internal elastic lamina, is composed of smooth muscle cells arranged in a circular layer, and extracellular matrix components such

as elastin and collagen, and may be innervated for the regulation of vascular tone. The tunica adventitia, separated from the media by the external elastic lamina, consists of loose connective tissue and longitudinally-arranged smooth muscle cells, and may also contain other components such as capillaries to supply nutrients to the vessel itself.

Capillaries are composed of a single layer of endothelial cells on their basement membrane with some supporting cells (pericytes) attached on the tissue-facing side. As the blood passes through the capillary lumen, a small quantity of fluid crosses the capillary wall by filtration to contribute to the interstitial fluid that bathes cells. This fluid can be returned to the capillary by absorption when the blood pressure in the capillary (controlled by upstream arterioles) is sufficiently low, the rest enters the lymphatic system, where it is known as lymph.

This thesis is primarily concerned with the effects of Vascular Endothelial Growth Factor (VEGF) on endothelial cells, particularly those related to VEGF-stimulated intracellular signalling, with a focus on the role of Heat Shock Protein 27 (Hsp27) and its functions. After a discussion of the biology of the endothelium, including its role in blood vessel formation and pathology, the effects of VEGF on endothelial cells will be considered along with the signalling mechanisms involved, before considering Hsp27 function and signalling with particular reference to endothelial cells. An overview of the biology of some enzymes and cytokines relevant to the results of this thesis is also given.

1.1 Structure of the endothelium

Endothelial cells are asymmetric, polarised cells with a blood-contacting apical/luminal surface facing the vessel lumen, and a basolateral/abluminal surface facing the basement membrane and tissues. Some cellular components are unevenly distributed, and the apical and basolateral surfaces express distinct proteins (Muller and Gimbrone 1986).

1.1.1 Cell junctions and basement membrane

ECs are connected to one another by three types of junction commonly found in other epithelia: tight, adherens and gap (reviewed by Dejana 2004). All junction types present consist of a transmembrane protein on one cell interacting homotypically with another molecule of the same protein on an adjacent cell. Other proteins bind the cytoplasmic tail of the transmembrane molecule, linking it directly or indirectly to the actin cytoskeleton.

Tight junctions (TJs) form a belt around the endothelial cell, the zonula occludens, and act as a barrier to the transport of substances across the endothelium via the paracelluar route (between cells). TJs also have fence-like properties, restricting the diffusion of membrane components and allowing the maintenance of differing compositions of the apical and basolateral plasma membrane. The key transmembrane proteins of TJs are the claudins, although occludin, junctional adhesion molecules (JAMs) and nectins may also be present. Endothelial cells express claudins 1, 5 and 12.

Adherens junctions (AJs) also form a belt around endothelial cells, the zonula adherens, and provide mechanical strength to cell-cell contacts but are also involved in signalling EC–EC contact. Cadherins, the key transmembrane proteins involved, are indirectly linked to the actin cytoskeleton by binding to intracellular catenins. All ECs express vascular endothelial (VE)-cadherin, which is only present on a few cell types and is the main cadherin present in EC AJs (reviewed by Vestweber 2008). VE-cadherin associates with vascular endothelial growth factor receptor 2 (VEGFR2) in confluent cells, regulating endothelial cell survival (Carmeliet *et al.* 1999a, discussed later). Neuronal (N)-cadherin is also known to be expressed in ECs, but does not localise to adherens junctions in endothelial cells and is unlikely to be involved in EC–EC adhesion but may be involved in adhesion to other cell types such as pericytes. E-cadherin is also expressed in brain ECs. Ca^{2+} binds to the extracellular domain of cadherins, and is required for their structural integrity and ability to bind homotypically to an adjacent cell.

Catenins, including β-catenin, plakoglobin/γ-catenin and p120, are able to bind to the cytoplasmic tail of VE-cadherin, and link it to the actin cytoskeleton. Catenins can translocate to the nucleus and regulate transcription, allowing EC–EC contact to influence gene expression. Sequestering of β-catenin by VE-cadherin in juxtaposed endothelial cells is thought to be involved in contact inhibition of cell growth.

Gap junctions do not form a belt, but exist as fluid-filled channels (connexons) which form direct links between the cytoplasm of adjacent ECs, allowing the passage of ions and small molecules, so aiding cell–cell communication. Connexons are composed of individual protein subunits called connexins (Cx) – ECs express Cx43, Cx40 and Cx37, forming channels around 20 nm in diameter. ECs also form gap junctions with underlying smooth muscle cells.

Platelet endothelial cell adhesion molecule (PECAM, also known as CD31), a transmembrane immunoglobulin-like molecule which can participate in homophilic or heterophilic interactions, is concentrated at EC–EC junctions. Although not part of a defined junctional complex, PECAM is important in EC–EC adhesion. PECAM staining is often used as a marker for endothelium.

The endothelium, as for other epithelia, rests on a basement membrane produced by the endothelial cells themselves (Kramer *et al.* 1984). The basement membrane is usually continuous but may be discontinuous, and encloses ECs in a sheath in intact vessels. Pericytes are enclosed within the basement membrane, smooth muscle cells are not. All basement membranes consist primarily of type IV collagens, laminins, nidogens (entactins) and heparan sulphate proteoglycans (HSPGs) such as perlecan, with lower amounts of other components such as thrombospondin, fibronectin and vitronectin (reviewed by Hallmann *et al.* 2005). The basement membrane may influence cell behaviour by binding growth factors such as VEGF (via HSPGs), and through the binding of integrins to components such as laminins.

ECs are tethered to their basement membrane by discrete structures called focal adhesions, which are linked to the actin cytoskeleton. The key transmembrane proteins present in focal adhesions and responsible for cell–matrix adhesion are integrins, heterodimeric proteins of one α and one

β subunit. Key integrins expressed by endothelial cells include the collagen receptors $\alpha_1\beta_1$ and $\alpha_2\beta_1$, fibronectin receptors $\alpha_4\beta_1$ and $\alpha_5\beta_1$, laminin receptors $\alpha_3\beta_1$, $\alpha_6\beta_1$ and $\alpha_6\beta_4$, and vitronectin receptors $\alpha_v\beta_3$ and $\alpha_v\beta_5$ (Silva *et al.* 2008).

Focal adhesion formation is initiated by binding of integrins to an extracellular substrate, leading to clustering of integrins at a particular location in the cell membrane and subsequent activation of the cytoplasmic tyrosine kinase focal adhesion kinase (FAK, reviewed by Romer *et al.* 2006; Mitra *et al.* 2005). Integrin-dependent signalling is an important stimulator of endothelial cell survival (Brooks *et al.* 1994), and loss of integrin attachment to the extracellular matrix leads to anoikis of ECs – detachment-induced apoptosis of normally adherent cells (Brooks *et al.* 1994, reviewed by Michel 2003).

1.1.2 Endothelial heterogeneity

The properties of the endothelium vary with location in the vascular network (e.g. arterial versus venous or capillary endothelium) and the requirements of the organ being supplied, resulting from tissue-specific endothelial differentiation (reviewed by Aird 2007). Endothelium can be broadly classified based on morphology and permeability as continuous, fenestrated or discontinuous. Most capillary endothelia are continuous, and do not permit unregulated passage of plasma proteins or other macromolecules across the endothelium. The porosity of the endothelial barrier can be increased by the presence of small holes in the endothelial cell body (fenestrae) or, in discontinuous endothelium, large gaps between endothelial cells. These features are not present on all endothelium, however. For example, fenestrae in the kidney glomerulus allow the increased fluid transport rate required for blood filtration, whereas the discontinuous endothelium of liver sinusoids or lymph node high endothelial venules allow passage of large volumes of plasma constituents across the endothelium, improving nutrient absorption by hepatocytes and blood screening by lymphocytes respectively. In contrast to these permeability-increasing adaptations, ECs of the cerebral circulation show reduced permeability to ions and hormones due to the

nature of the tight junctions between cells and lack of fenestrations, so forming the blood-brain barrier (Brightman and Reese 1969).

Endothelial heterogeneity may be due to either environmental/extrinsic factors, or developmental programming/intrinsic factors. Local variations in factors such as associating cells, blood flow, cytokine concentrations, or extracellular matrix components can also alter the properties of the endothelium. Some differences in gene expression observed in freshly isolated ECs were lost during cell culture (Lacorre *et al.* 2004), indicating the importance of local factors, whereas other differences were maintained (Chi *et al.* 2003), indicative of programming, possibly due to epigenetic factors.

1.2 Physiological roles of the endothelium

1.2.1 Blood/tissue gatekeeper and transport role

The endothelium is the barrier between the blood and the tissues, and actively regulates the passage of materials across it. Many blood-borne substances (e.g. nutrients) must physically cross the endothelium to reach their destination cell from their site of synthesis, although signalling molecules may instead cause the endothelium to produce a second molecule released basolaterally which can then contact the target.

Substances can cross the endothelium from the blood to the tissue or vice versa by either the paracellular route, travelling through the junctions between endothelial cells, or the transcellular route, travelling through the endothelial cell body itself. Permeability can be either selective as in receptor-mediated transcytosis, non-selective e.g. by creating holes in endothelial junctions or the EC body, or semi-selective. The relative contribution of the different trans-endothelial pathways to the transport of specific substances in vivo depends on the region of the vascular tree in question and the nature and concentration of the substance.

The endothelium contains a number of structures which increase the permeability of the endothe-

lial cell body, the presence or function of which can be regulated by various cytokines (reviewed by Mehta and Malik 2006). These structures include caveolae, fenestrations and vesicular-vacuolar organelles (VVOs).

Caveolae (literally, 'little caves') can often be observed as flask-shaped invaginations of the plasma membrane, but may also be present wholly within the cytosol, appearing as spherical vesicles 60–70 nm in diameter (reviewed by Gratton *et al.* 2004). Caveolae form from lipid rafts, specialised sections of the plasma membrane rich in cholesterol and sphingolipids, and contain an abundance of receptors for trans/endocytosis (e.g. LDL, albumin) and signalling (e.g. eNOS, Ca^{2+} channels, VEGFR2) (Sonveaux *et al.* 2004). The defining constituent of caveolae is caveolin-1, a transmembrane protein with cholesterol-binding and scaffolding abilities responsible for the sequestration of cholesterol and receptors into caveolae. ECs derived from caveolin-1-null mice do not contain caveolae (Razani *et al.* 2001). The abundance of caveolae in ECs is thought to reflect the need for high levels of transcytotic transport.

Fenestrae are small pores, around 70 nm in diameter and sealed with a diaphragm, which form a continuous channel through an endothelial cell and increase the transport rate of water, ions and small molecules. The diaphragm is a bike wheel-like structure containing plasmalemma protein-1, composed of a central knob with radiating spokes, and may function in pore selectivity e.g. by acting as a size filter (Stan *et al.* 1999; Stan 2007).

VVOs are large organelles forming a continuous channel through the body of an endothelial cell (a trans-endothelial channel). VVOs contain caveolin-1 and appear to be formed from interconnected vesicles (Feng *et al.* 1996, 2002), suggesting formation by caveolae fusion, although other vesicular systems (e.g. clathrin-coated vesicles) may contribute.

1.2.2 Control of vascular tone

Vascular tone is the degree of contraction of vascular smooth muscle present in the vessel wall, and influences both blood distribution and overall blood pressure, with relaxation of vSMC re-

sulting in vasodilation. Regulation of vascular tone is important in arterioles, which control blood distribution, but not in capillaries which do not contain smooth muscle.

Vascular tone can by adjusted by direct actions on vascular smooth muscle cells (vSMCs), e.g. by cytokines or autonomic nervous stimulation. However the effects of many blood-borne cytokines, and haemodynamic factors such as shear stress, are mediated by the endothelium. ECs produce a number of important substances acting directly on vSMCs, the production of which can be modulated by various vasoactive cytokines acting on the endothelium. Some of the vasoactive cytokines which function by adjusting endothelial production of these second messengers include VEGF, acetylcholine, histamine, serotonin, thrombin, angiotensin and adrenaline. Blood flow (shear stress) also modulates EC production of vasoactive substances. Thus ECs integrate a variety of signals, adjusting the output to vSMCs as appropriate.

Endothelial-synthesised vasodilators include nitric oxide (NO), prostacyclin (PGI_2) (both reviewed by Moncada 2006) and endothelial-derived hyperpolarising factor (EDHF). Endothelial-synthesised vasoconstrictors include endothelin-1 and thromboxane A2. NO and PGI_2, which are also synthesised by non-endothelial cells, additionally inhibit proliferation of vSMCs, instead maintaining them in a quiescent, contractile phenotype. NO and other factors also affect other cell types, including the endothelium itself and platelets. Platelet-related effects of NO and PGI_2 are discussed later.

1.2.3 Haemostasis

Interactions between platelets, the endothelium, and plasma proteins are the basis of haemostasis, the prevention of blood loss from damaged vessels by formation of a localised clot or thrombus.

The haemostatic response involves two interlinked processes – platelet aggregation, leading to the formation of a platelet plug, and blood coagulation, stabilising the plug as a clot – which serve to seal the injured site. The response is initiated by the binding of blood-borne coagulation factors and platelets to tissue-resident proteins including fibrous collagens, von Willebrand factor (vWF)

and tissue factor. These event initiate platelet activation (including thromboxane A2 synthesis) and aggregation, and also activate a proteolytic cascade leading to generation of thrombin, the key effector protease. Thrombin cleaves the plasma peptide fibrinogen to fibrin monomers, which then polymerise and bind aggregated platelets together, stabilising the clot.

Unwanted thrombosis is an important event in a number of diseases, and blockage of key blood vessels by a clot can lead to stroke or myocardial infarction. Undamaged endothelium forms an anti-thrombotic surface, expressing a number of anti-coagulant species. The anti-coagulant properties of endothelium are important in prevention of thrombus formation in the absence of injury, and in localising the clotting process to the site of injury (reviewed by Arnout *et al.* 2006).

1.2.4 Inflammation and immunity

Inflammation is the acute response of an area of the body to tissue damage or infection, characterised by increased blood flow to the affected area (manifested as redness and heat), and increased tissue oedema as fluid enters the tissues (pain and swelling). Inflammation brings plasma proteins (e.g. complement) and immune cells to the affected region, where they leave the blood and enter the tissues to engage antigen.

On pathogen recognition, tissue-resident immune cells produce a variety of cytokines to initiate the inflammatory response, some of which bind to and activate the endothelium, such as histamine and in particular tumour necrosis factor-α (TNFα) and interleukin-1 (IL-1). On activation, the endothelium switches from a non-adhesive to an leukocyte-adhesive surface by displaying new leukocyte adhesion molecules on its surface, secretes various cytokines and chemokines, and increases its permeability to aid extravasation of both cells and plasma proteins (Kuldo *et al.* 2005, reviewed by Pober and Sessa 2007).

Activated endothelium is a major source of the chemokine interleukin-8 (IL8/CXCL8), responsible for recruiting neutrophils to the site of injury, and later produces the monocyte chemoattractant CCL2 (MCP-1).

The main adhesion molecules known to be newly expressed on activated endothelium and participating in leukocyte binding are the selectins and the cell adhesion molecules (CAMs) (reviewed by Ley and Reutershan 2006). Selectins are lectins which bind to a modified trisaccharide (sialyl-Lewis^x) present in leukocyte glycoproteins such as P-selectin glycoprotein ligand-1. CAMs are immunoglobulin family members, containing a number of Ig-like domains, and bind to integrins present on leukocytes. The best studied CAMs involved in leukocyte adhesion are Intercellular CAM-1 and Vascular CAM-1, both of which are upregulated on activated endothelium. A number of other CAMs are also able to bind leukocytes, including PECAM-1, ICAM-2, and mucosal addressin cell adhesion molecule-1 (MAdCAM-1).

1.3 Formation and remodelling of the vasculature

1.3.1 Overview

Blood vessel formation is a central physiological process during development and growth, but occurs only in specific situations in adult life. During development, a complex vascular network is produced from a single fertilised cell. Post-natal growth requires an expansion of the vascular network to supply growing organs. In adulthood, vessel growth is required during wound healing, the menstrual cycle and exercise-induced muscle enlargement.

Angiogenesis is also a key process in the pathogenesis of several chronic diseases, particularly ocular disorders and cancer. Vascularisation of tumours is required for tumour growth and progression to life-threatening metastatic cancer, and therapies targeted against the pro-angiogenic effects of VEGF to decrease blood vessel growth are now in routine clinical use for some cancers.

The major processes involved in blood vessel growth are termed vasculogenesis and angiogenesis (reviewed by Fischer *et al.* 2006). Vasculogenesis refers to the *de novo* formation of a primitive vascular network by aggregation and differentiation of endothelial precursor cells to ECs, whereas angiogenesis refers to the remodelling of an existing vascular network and involves growth of new

vessels, pruning and remodelling of existing vessels, and recruitment of pericytes. A major distinction between these processes is that during vasculogenesis ECs are produced by differentiation of distinct non-EC precursor cells, whereas during angiogenesis ECs are produced by proliferation of other pre-existing ECs. Vasculogenesis was thought to be restricted to early embryonic development, but recent evidence suggests that endothelial differentiation from bone marrow-derived stem cells occurs in the adult (discussed in section 1.3.2.2).

Arteriogenesis, the conversion of capillaries into larger arteries by recruitment of vSMCs and enlargement of the vessel lumen is also involved in remodelling vessel networks to meet tissue demands. Arteriogenesis can also occur in pathological situations, such ischaemic heart disease, to produce a 'biological bypass', or collateral artery, around an occluded coronary artery. Endothelial cells play a key role in vascularisation, forming the initial tubular structures and directing the subsequent recruitment of perivascular cells – pericytes or smooth muscle cells – which stabilise newly-formed vessels.

1.3.2 Vasculogenesis

Vasculogenesis consists of the differentiation of mesodermal cells to endothelial precursor cells (angioblasts), followed by subsequent angioblast differentiation to endothelial cells, in combination with the development of an initial vessel network, the primary vascular plexus. This initial network is subsequently expanded and remodelled by angiogenesis.

Vasculogenesis occurs in two separate locations in the embryo during development – the extraembryonic tissues (i.e. those not forming part of the foetus at birth, such as the yolk sac), and inside the embryo itself. The first clear evidence of blood vessel development in the embryo is observed in the yolk sac after the onset of gastrulation (around E7.5 in mice), where mesodermal cells migrate to the yolk sac and form aggregates which subsequently differentiate to blood islands, with the outermost cells giving rise to angioblasts and then endothelial cells, and the inner cells forming haematopoetic precursors and then primitive erythrocytes and other blood cells. Blood islands

then fuse to form an initial vessel network, the primary vascular plexus, and so vessels are formed with blood already inside of them. The major steps of vasculogenesis are shown in figure 1.1.

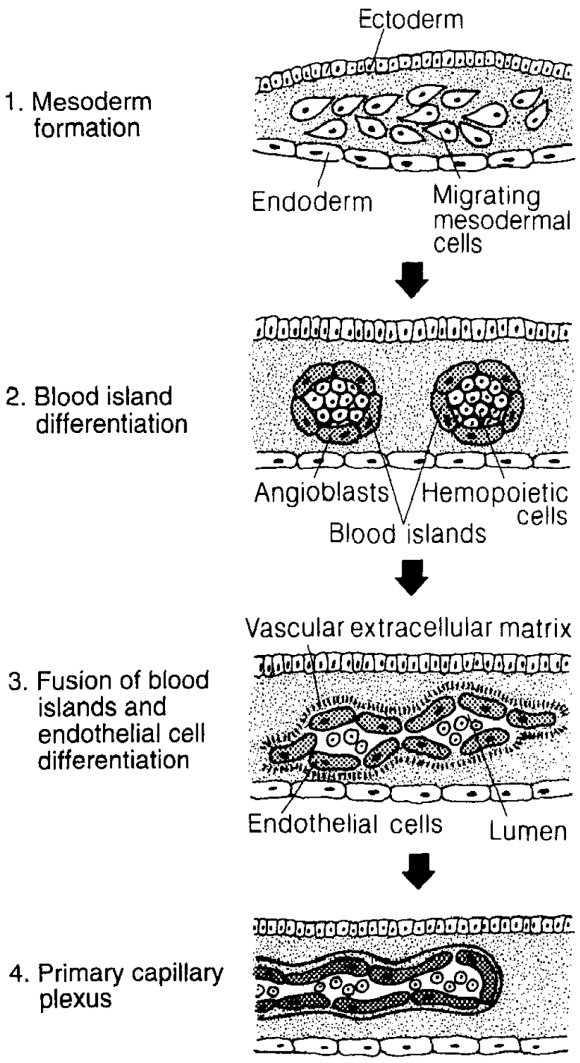

Figure 1.1: Processes involved in vasculogenesis (from Risau and Flamme 1995)

The haemangioblast is defined as the immediate precursor of haematopoetic stem cells and angioblasts, and so is able to give rise to both blood and endothelial cells. Migration of mesoderm-derived haemangioblasts into the yolk sac or dorsal aorta followed by their aggregation and bi-directional differentiation are thought to result in the formation of blood islands and intra-aortic haematopoetic precursors, where cells expressing blood and endothelial markers are tightly associated.

For a long time, the haemangioblast was assumed to exist but had not been identified in living

animals. Supporting evidence for the existence of a haemangioblast includes the close proximity of blood and endothelial cell differentiation in blood islands, and the presence of common cell surface markers in ECs and haematopoetic stem cells, some of which are later downregulated in one or other cell type (e.g. VEGFR2 is lost from haematopoetic stem cells). More recent fate-mapping studies suggest that some but not all embryonic ECs derive from haemangioblasts (Vogeli *et al.* 2006).

1.3.2.1 Endothelial arterial/venous fate

ECs belonging to arteries and veins differ in their protein expression, indicating that the expression of some proteins is restricted during development to ECs destined to become either arteries or veins. Proteins exhibiting lineage restriction include the Ephs and ephrins, and neuropilins.

Ephrins are cell surface-expressed ligands which bind to Eph receptor tyrosine kinases, forming a bi-directional signalling complex, with signals transduced in both the ephrin- and Eph-expressing cells (Kuijper *et al.* 2007). Ephrin B2 is predominantly expressed in arterial ECs whereas its receptor, EphB4, is expressed mainly in venous ECs (Wang *et al.* 1998), although this distinction is lost during tissue culture (Korff *et al.* 2006). Upregulation of ephrinB2 and downregulation of EphB4 in arterial endothelium is under the control of the Notch pathway.

EphrinB2-null and EphB4-null mice show impaired vasculogenesis and angiogenesis (Adams *et al.* 1999; Gerety *et al.* 1999). Vascular morphogenesis requires bi-directional ephrinB2 signalling, as mice expressing a truncated form of ephrinB2 lacking the cytoplasmic domain, but not the full-length form, showed similar vascular defects to ephrinB2-null mice (Adams *et al.* 2001). Endothelial cell-specific ephrinB2 knockout mice show identical defects to ephrinB2-null mice (Gerety and Anderson 2002), indicating that endothelial ephrinB2 is required for normal vascular development.

Neuropilins (NRPs), co-receptors for several heparin-binding growth factors including VEGF (discussed below), also display arterio-venous restriction. In the adult vasculature, NRP1 is found only

on arterial ECs, whereas NRP2 is only found on venous ECs (Yuan *et al.* 2002). NRP expression is an earlier marker of arterial and venous ECs than the ephrin/Eph distinction, and segregation of NRP1 and NRP2 expression occurs in chick embryo blood islands before the onset of flow (Herzog *et al.* 2005). So whereas blood flow and associated pressure may alter protein expression in ECs, the artery/vein decision also has a strong genetic component.

Certain members of the Notch pathway such as Notch3 and Dll4 are expressed in arterial but not venous ECs (Eichmann *et al.* 2005). The Notch pathway (reviewed by Roca and Adams 2007) is a conserved signalling mechanism for communicating between adjacent cells, and is an important regulator of arterial versus venous endothelial differentiation. Notch receptors are heterodimers with a transmembrane and extracellular subunits, and mammalian Notches bind to the ligands Delta-like ligand (Dll) and Jagged, transmembrane proteins expressed by an adjacent cell. On ligand binding, the extracellular domain of Notch is proteolytically cleaved and, bound to its ligand, is endocytosed by the ligand-expressing cell. Notch is then cleaved again at the membrane by γ-secretase, releasing the intracellular domain which enters the nucleus to modify gene expression. Thus both the Notch-expressing and the ligand-expressing cell receive signals from the interaction.

1.3.2.2 Post-natal vasculogenesis

Vasculogenesis involves the formation of vessels from non-EC precursor cells, and was until recently thought to be confined to the embryo, with all post-natal vessel growth believed to occur via angiogenesis. Peripheral blood-isolated cells expressing CD34 (commonly used as a marker for haematopoetic stem cells) and the VEGF receptor VEGFR2 were able to integrate into sites of neovascularisation in a hindlimb ischaemia model, producing spindle-shaped cells which lost haematopoetic markers (CD45) but gained typical endothelial properties, such as production of NO in response to acetylcholine and VEGF (Asahara *et al.* 1997). These cells, termed endothelial progenitor cells (EPCs), were incorporated directly into nascent capillaries, but did not integrate

into quiescent vessels, suggesting that a population of blood-borne cells expressing haematopoetic markers homed specifically to the injured site, differentiated to endothelial or endothelial-like cells and incorporated into a new vessel.

In addition to its role in promoting differentiation of EPCs to ECs, VEGF also increases the concentration of $CD34^+$ cells in the blood, termed EPC mobilisation from the bone marrow (Asahara *et al.* 1999). These mobilised cells integrated into newly growing vessels in a corneal injury model, and the greater mobilisation of EPCs was suggested to have led to greater incorporation of EPCs into the newly forming vessels and the subsequent higher levels of neovascularisation occurring in the VEGF-treated animals. Ischaemia and Granulocyte-Macrophage CSF were also observed to mobilise EPC-like cells from the bone marrow (Takahashi *et al.* 1999a), and these effects may occur in conjunction with those of VEGF (e.g. via ischaemia-enhanced production of VEGF). However it should be noted that VEGF and other cytokines are pro-survival and mitogenic factors for ECs, and may affect non-EPC targets such as other ECs, which may contribute to increased vessel growth without the involvement of EPCs.

While impressive improvements in blood flow have been observed with stem cells in animal models, clinical trials in humans have shown much more modest effects (Abdel-Latif *et al.* 2007). These difficulties may be related to underpowered trials, but may also be ascribed to a lack of understanding of which cells to use. At the time of writing there is no agreement about the definition of an EPC, and researchers have been using different protocols to purify their cells, probably resulting in studying different cell populations which may have distinct properties. A number of EPC markers have been proposed, including presence of CD31, CD34, CD133, and VEGFR2, and absence of CD45.

Another fundamental question about EPCs concerns their mode of action. Large therapeutic benefits have been observed in animal models with only a small degree of incorporation of cells into growing vessels. Even more surprisingly, benefits have in some cases been observed within hours of cell administration, too rapidly for differentiation and incorporation into new tissue, suggesting

a paracrine effect – that is, the EPCs release factors which act on the target tissue (e.g. endothelial cells) and have a beneficial effect.

The very existence of EPCs continues to be questioned. It does appear that circulating endothelial progenitors are not normal ECs sloughed off from the endothelium – they proliferate far more rapidly than sloughed ECs (Lin *et al.* 2000). However, a number of 'EPC' markers are expressed on immature circulating cells with multiple possible fates, rather than on endothelial-restricted cells.

1.3.3 Angiogenesis

Angiogenesis involves a number of distinct steps (reviewed by Fischer *et al.* 2006; Adams and Alitalo 2007, summarised in figure 1.2), beginning with dilation of the parent vessel and increased trans-endothelial permeability due to increased fenestration and a loosening of EC–EC junctions. Extravasation of plasma proteins such as fibronectin provides a scaffold for endothelial cells to migrate on. Increased expression and secretion of proteases such as matrix metalloproteases (MMPs) degrades the endothelial basement membrane and stromal extracellular matrix, removing a tether that holds the ECs in place and freeing a path for subsequent migration. Protease-mediated liberation of matrix-sequestered growth factors may also be important. Natural inhibitors of MMPs, termed tissue inhibitors of metalloproteases (TIMPs), are present throughout the tissues localising MMP action. Other non-MMP proteases, such as urokinase- or tissue-type plasminogen activator may also be important at this stage.

Released from the basement membrane and with a cleared path, endothelial cells proliferate and migrate under the influence of a chemoattractant gradient. During migration, ECs fuse to form solid cords and later acquire a lumen, behaving in a tentacle-like fashion as they reach out to contact other sprouts. If all cells in a sprout behaved in a similar manner without co-ordination, this sort of behaviour would not be possible, and capillary integrity would not be maintained. Instead, a sprouting capillary is organised as a blind-ended tube consisting of a tip cell, which lacks a lumen,

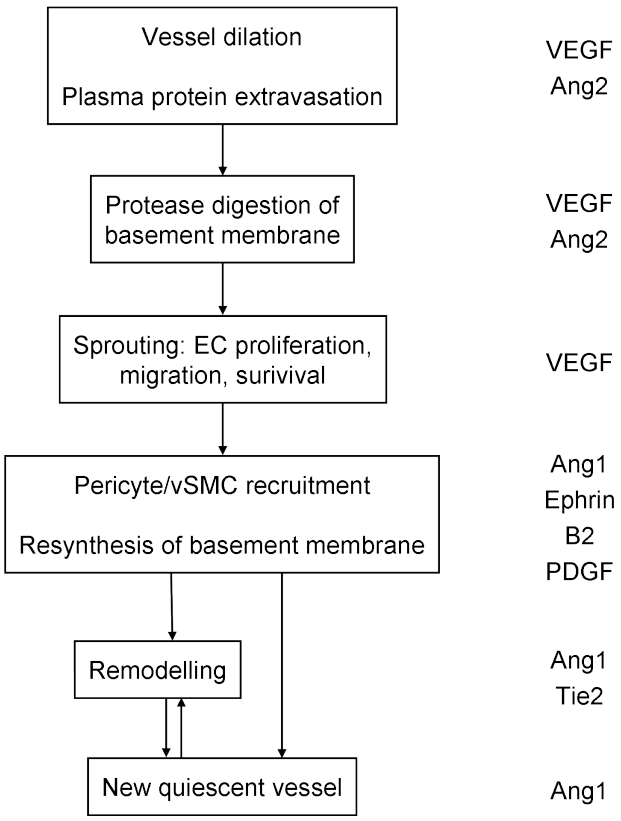

Figure 1.2: Sprouting angiogenesis
The main cytokines influencing the different processes are shown to the right of each step. Further details are given in the text.

and a number of stalk cells, which contain a lumen. Proliferation of endothelial cells in either the stalk or tip (stalk in mouse retina: Gerhardt *et al.* 2003, tip in zebrafish: Siekmann and Lawson 2007) extends the length of the capillary as it grows, whereas the direction of growth is determined by a tip cell which projects many filopodia and responds to gradients of chemoattractant such as VEGF (Lawson and Weinstein 2002; Gerhardt *et al.* 2003). This manner of growth is similar to that used by nerves, with a nerve growth cone performing the role of the tip cell.

Newly-formed endothelial tubes are susceptible to regression via apoptosis of the constituent endothelial cells on withdrawal of soluble pro-survival factors. Coverage of these nascent vessels with peri-endothelial cells stabilises the new vessels, adding structural support and stimulating ECM deposition, inhibiting further endothelial proliferation and migration, and preventing vessel regression on reduction of angiogenic growth factor concentrations (Jo *et al.* 2006). VSMCs and pericytes both act as peri-endothelial cells, depending on the vascular bed. VSMCs are present

in arteries and veins, on the outer side of the endothelial basement membrane, whereas pericytes cover capillaries, venules and arterioles, and are in direct contact with the ECs themselves. The origins of peri-endothelial cells are complex and appear to depend on the identity of the newly vascularised tissue.

The lymphatic system is formed by sprouting from the wall of the embryonic cardinal vein, in a process termed lymphangiogenesis. Cells in the wall of the cardinal vein begin to express the transcription factor Prox1, leading expression of VEGF receptor 3 and subsequent VEGF-C-driven lymphangiogensis (Makinen *et al.* 2007).

In addition to the formation of additional blood-carrying vessels by sprouting and intussusception, angiogenesis involves the remodelling of the vasculature into large and small vessels via appropriate circumferential growth, branching, and vessel regression. Remodelling converts a uniform vasculature into one adapted to the needs of the tissue, and is in part regulated by local haemodynamic factors such as shear and wall stretch.

1.3.3.1 Angiogenic factors and signalling

In addition to Vascular Endothelial Growth Factors (VEGFs, discussed in detail later), important angiogenic roles have been defined for other growth factors including angiopoietins (Ang)-1 and 2, fibroblast growth factor (FGF), and platelet-derived growth factor (PDGF), Ephs/ephrins, and Notch and its ligands. Indeed, any cytokine or other molecule which affects any of the multiple processes involved in angiogenesis is potentially pro- or anti-angiogenic. The complex, highly choreographed interplay between a number of different factors is responsible for formation of the mature vasculature.

Angiopoietin-1 (Ang1) is a ligand for the endothelial receptor Tie2 (also called tek). Mice lacking either Tie2 (Dumont *et al.* 1994; Sato *et al.* 1995) or Ang1 (Suri *et al.* 1996) died during gestation with vascular defects including reduced vessel branching, indicating a requirement for Ang1 in remodelling. The endothelial cells in Ang1-null mice did not associate with pericytes and showed

very high levels of vascular leakage. In contrast, mice overexpressing Ang1 formed vessels that were resistant to leakage induced by inflammatory agents and VEGF (Thurston *et al.* 1999). The anti-leakage role of Ang1 may persist in quiescent adult vessels, as overexpression of Ang1 in adult mice prevented large scale vascular leakage due to VEGF overexpression (Thurston *et al.* 2000). Ang1 is expressed by cultured pericytes (Sundberg *et al.* 2002), strengthening the association between ECs and pericytes. Disruption of this interaction, leading to a loss of pericyte coverage, would then cause a loss of pericyte-produced vessel stabilisation signals, leading to vascular leakage and vessel regression. Ang1 binding to Tie2 may also directly promote vessel-stabilising pathways – Ang1 alters EC junctional proteins in cultured ECs (Gamble *et al.* 2000).

Ang2 is a Tie2 antagonist, so acting as a competitive inhibitor of Ang1, stimulating matrix degradation and increased permeability (Maisonpierre *et al.* 1997). In the early stages of angiogenesis, when the mother vessel must be disrupted to allow endothelial proliferation and migration, Ang2 is required to overcome Ang1-induced vessel stabilisation, and allow VEGF-induced permeability increases. In the later stages of angiogenesis, when endothelial tubes have formed a circuit and recruited pericytes, Ang1 stabilises EC-pericyte interactions.

PDGF-B binds to a receptor tyrosine kinase, PDGFR-β. Expression of PDGF-B by endothelial cells is involved in recruitment of vSMCs and pericytes to endothelial tubes (Hellstrom *et al.* 1999). Mice lacking PDGF-B or PDGFRβ develop blood vessels with reduced perivascular cell coverage, which is completely lacking in some regions. Microaneurysms and haemorrhage are observed, presumably due to the inability of the uncoated vessel to withstand blood pressure, leading to structural failure.

Fibroblast growth factor (FGF) was the earliest pro-angiogenic factor to be identified (Shing *et al.* 1984). The fibroblast growth factor (FGF) family contains three angiogenic members: FGF1 (acidic FGF), FGF2 (basic FGF), and FGF4, of which FGF2 is the best studied. FGF2-null mice are viable whereas knockout of FGFR1, a receptor tyrosine kinase which is the major receptor for FGF2, is lethal during gastrulation, before the onset of vasculogenesis (Yamaguchi *et al.* 1994;

Deng *et al.* 1994). Expression of a truncated FGFR1 by adenovirus infection of embryos at E9 (after vasculogenesis begins) resulted in abnormal vascular development (Lee *et al.* 2000), indicating that FGF signalling also plays a post-gastrulation role in vascular development. FGF2 lacks export sequences, indicating that FGF2 may not be a secreted factor, and how it promotes angiogenesis is not clear, although FGF2-stimulated VEGF production may be involved.

Ephrins and Ephs, mentioned above as markers of arterio-venous identity, are also involved in angiogenesis. EphrinB2-null, EphB4-null and EphB2/B3 double-null mice showed defective vascular formation (Adams *et al.* 1999; Gerety *et al.* 1999). Although expressed on other sites, ephrinB2 is required in the endothelium for normal angiogenesis (Gerety and Anderson 2002). Pericytes and vSMCs lacking ephrinB2 do not properly cover newly-formed vessels leading to lethality due to vascular leakage (Foo *et al.* 2006), and indicating a role for ephrinB2 in perivascular cell coverage.

Notch signalling is involved in regulating tip cell formation, with Notch pathway mutants resulting in inappropriate and excessive tip cell formation and angiogenic sprouting, suggesting that Notch signalling is required to maintain non-tip endothelial cells as stalk cells. Disruption of Dll4/Notch signalling by deletion of Notch1 or one allele of Dll4 in endothelial cells led to increased tip cell formation, and vessel sprouting and branching in the mouse retina, whereas activation of Notch signalling with soluble jagged1 resulted in reduced tip cell formation and vessel branching (Hellstrom *et al.* 2007). Similar findings have been reported in zebrafish (Siekmann and Lawson 2007; Leslie *et al.* 2007), and the regulation of tip cell formation and angiogenic sprouting by Notch may be important in turning off VEGF-induced EC migration once a sprout has connected with another sprout to make a vessel circuit. A simple mechanism for tip-cell mediated inhibition of further tip cell formation via Notch would involve enhanced expression of Dll4 in a tip cell, leading to Notch activation in adjacent cells, preventing these adjacent cells from becoming tip cells. However, Hellstrom *et al.* (2007) reported that Dll4 did not appear concentrated in tip cells, but was distributed evenly within the angiogenic sprout.

1.4 VEGF

Vascular endothelial growth factor (VEGF) was initially characterised as a vascular endothelial cell-specific mitogen, purified from medium conditioned by bovine pituitary follicular cells (Ferrara and Henzel 1989). When purified and sequenced, it was realised that VEGF was the same substance as the previously identified vascular permeability factor, which had been shown to increase fluid leakage through capillaries (Senger *et al.* 1983; Keck *et al.* 1989; Leung *et al.* 1989). Since these initial findings it has been shown that VEGF-A_{165}, the substance characterised in these early studies, is a member of a wider family encompassing a number of related genes, which have multiple effects on endothelial and other cells, and play a central role in blood vessel development. The pro-angiogenic role of VEGF has attracted clinical interest for its possible uses in gene therapy to improve the blood supply to ischaemic tissues (therapeutic angiogenesis) and as a target for anti-angiogenic drugs that prevent tumour vascularisation. In addition to its roles in blood vessel development during embryogenesis and post-natal growth, VEGF also has roles in adult angiogenesis during wound healing, the menstrual cycle and exercise-induced muscle enlargement, and in vascular maintenance (Maharaj and D'Amore 2007). A historical discussion of the discovery of VEGF and its functions is given by Ribatti (2005).

1.4.1 The VEGF gene family

VEGFs are secreted disulphide-linked glycoproteins, with an approximate molecular weight of 40 kDa. There are currently five members of the mammalian VEGF gene family: VEGFs A, B, C, D and placental growth factor (PlGF), with additional VEGF-like proteins in parapoxvirus and snake venom, termed VEGFs E and F respectively (Wise *et al.* 1999; Ogawa *et al.* 1998; Takahashi *et al.* 2004; Holmes and Zachary 2005). The first discovered and most intensively studied is the prototypical isoform, VEGF-A. VEGF-A binds to two different cell surface receptors, VEGFR1 and VEGFR2, and some VEGF-A isoforms also bind to other cell-surface molecules, neuropilins (NRPs) 1 and 2. Binding to VEGFRs and NRPs is thought to be responsible for the biological

activities of VEGF-A. An additional VEGF receptor, VEGFR3, is also expressed, and the various VEGFs vary in which receptor combination they bind to. Some VEGFs also bind to heparin sulphate proteoglycans, and this may be required for their activity. The receptor binding specificity of the VEGFs is shown in table 1.1.

Table 1.1: Summary of transmembrane receptor binding by VEGF family members

	VEGFR1	VEGFR2	VEGFR3	NRP1	NRP2
VEGF-A	+	+	-	+	+
VEGF-B	+	-	-	+	nd
VEGF-C	-	+	+	+	+
VEGF-D	-	+	+	+	+
PlGF	+	-	-	+	nd
VEGF-E	-	+	+	+	+
VEGF-F	+	+	-	-	nd

Key: + binds, - does not bind, nd no data found. Not all splice variants of each VEGF bind to the same receptors. VEGF-C and VEGF-D bind VEGFR2 with high affinity after proteolytic processing. References and further details are given in the text discussing each family member.

1.4.1.1 VEGF genes and their role in vascular development

The roles of the VEGFs in mouse development have been examined using gene disruption. Table 1.2 details the phenotypes corresponding to deletion of specific VEGF-related genes. In a number of studies, the coding region of the studied VEGF gene was replaced by a detectable reporter gene such as β-galactosidase but the gene promoter was retained, so that in heterozygous (+/-) mice which express both the studied VEGF and the reporter gene, the time at which the gene is activated during development could be monitored.

VEGF-A is composed of a number of splice variants, all of which bind to VEGFR1 and VEGFR2 and some (including VEGF-A_{165}) bind to neuropilins (further discussed below). The major VEGF-A isoforms VEGF-A_{165}, VEGF-A_{121} (Larcher *et al.* 1998) and VEGF-A_{189} are pro-angiogenic when expressed in vivo.

Table 1.2: Mouse knockout phenotypes of VEGF and related proteins

Protein	+/-	-/-	Phenotype	References
VEGF-A	Lethal E11–12	Lethal	Large-scale defects in vascularisation	Carmeliet *et al.* (1996); Ferrara *et al.* (1996)
VEGF-B	Viable	Viable	Slight cardiac alterations	Bellomo *et al.* (2000); Aase *et al.* (2001)
VEGF-C	Viable	Lethal	Failure of lymphatic vascular development	Karkkainen *et al.* (2004)
VEGF-D	Viable	Viable	No observed phenotype	Baldwin *et al.* (2005)
PlGF	Viable	Viable	Impaired pathological angiogenesis	Carmeliet *et al.* (2001)
VEGFR-1	Viable	Lethal E8.5–9.5	Excessive endothelial cells leading to disorganised vessels	Fong *et al.* (1995, 1999a)
VEGFR-2	Viable	Lethal E8.5–9.5	Absence of vasculature and blood islands. No mature ECs	Shalaby *et al.* (1995)
VEGFR-3	Viable	Lethal E12.5	Defect in remodelling of blood vessels	Dumont *et al.* (1998)
NRP1	Viable	Lethal E12.5–13.5	Various defects in blood vessel formation and peripheral nervous system	Kawasaki *et al.* (1999)
NRP2	Viable	Viable	Reduced lymphatics and abnormal nerve guidance	Yuan *et al.* (2002)
NRP1+2	Viable	Lethal E8.5	Severe cardiovascular defects, avascular areas in yolk sac and embryo	Takashima *et al.* (2002)

Heterozygous VEGF-A deletion was lethal at E11–12, resulting in impaired vasculogenesis and angiogenesis in both the embryo and yolk sac (Carmeliet *et al.* 1996; Ferrara *et al.* 1996). Lethal haploid insufficiency is extremely rare and indicates the importance of VEGF-A concentration, not just its presence, in embryonic vascular development. Endothelial cells were still formed, even in VEGF-A-null embryos, although their development appeared delayed with reduced numbers observed in the dorsal aorta (Carmeliet *et al.* 1996). Mild overexpression of VEGF-A (2–3-fold by removal of DNA coding for the 3' untranslated region of VEGF-A mRNA) causes vascular defects and is also embryonic lethal (Miquerol *et al.* 2000), further indicating the importance of the correct VEGF concentration during vascular development. Of therapeutic importance, VEGF-A-null embryonic stem cells did not form the usual tumours when injected into mice, indicating a role for VEGF-A in cancer (Ferrara *et al.* 1996). The importance of VEGF-A production by endothelial cells themselves was shown in an EC-specific VEGF-A knockout (Lee *et al.* 2007). A third of these mice died in utero, and around 10% died shortly after birth.

This thesis concentrates on work with VEGF-A, the biology of which is discussed in more detail below. Isoform-specific VEGF-A knockout mice are discussed in section 1.4.2.2.

VEGF-B binds to VEGFR1 and NRP1 (Olofsson *et al.* 1998), can heterodimerise with VEGF-A, and is angiogenic in vivo, promoting capillary growth into a subcutaneous matrigel plug (Silvestre *et al.* 2003). VEGF-B knockout mice are healthy and fertile (Bellomo *et al.* 2000; Aase *et al.* 2001). Both knockout studies noted that VEGF-B appears to have a role in cardiac development, but the reported phenotypes differed. Bellomo *et al.* (2000) reported that one month-old VEGF-B-null mice have smaller hearts than wild-type mice, while Aase *et al.* (2001) reported that the electrocardiogram PQ interval was slightly extended, which they attributed to an atrial conduction defect. They further reported that VEGF-A-induced angiogenesis was normal in an ocular model.

VEGFs-C and D bind to both VEGFR2 and VEGFR3 (Joukov *et al.* 1996; Achen *et al.* 1998). Proteolytic cleavage of VEGFs C and D is required to allow receptor binding and biological activity – partly processed forms bind to VEGFR3, whereas in humans fully processed forms also

bind to VEGFR2 (Joukov *et al.* 1997; Stacker *et al.* 1999). However, mouse VEGF-D binds to VEGFR3 only (Baldwin *et al.* 2005). VEGF-C and D are pro-angiogenic in in vivo assays (Cao *et al.* 1998; Marconcini *et al.* 1999).

VEGF-C knockout is embryonic lethal, with most embryos dying at E15.5–17.5 (Karkkainen *et al.* 2004). In heterozygous animals, expression was first observed at E8.5 in the jugular region of the cardinal vein, from which endothelial cells sprout to form lymphatic sacs – these sacs later give rise to the lymphatic vasculature. Although heterozygous mice were viable and did belatedly form lymphatic vessels, these vessels contained fewer cells than normal and were functionally abnormal. In VEGF-C-null mice, oedema was observed from E12.5 onwards, and was severe at E15.5, further indicating the lack of a functional lymphatic vasculature leading to inability to drain tissue fluid and return it to the circulation. Application of VEGF-C to explants from VEGF-C-null mice caused migration of endothelial cells expressing prox1 (a lymphatic endothelial marker) towards the VEGF-C. Arteries and veins were morphologically normal in both heterozygous and knockout mice, indicating a lymphatic-specific role for VEGF-C. In agreement with this knockout data, Jeltsch *et al.* (1997) reported that overexpression of VEGF-C in mice resulted in proliferation and enlargement of the lymphatic vasculature but not circulatory vasculature, further confirming the role of VEGF-C as a lymphatic endothelial growth factor.

VEGF-D-null mice are viable and appear healthy (Baldwin *et al.* 2005). Given the similarities in receptor binding between VEGFs C and D, lymphangiogenesis in VEGF-D-null mice was examined. No vascular or lymphatic defects were observed, and no noticeable oedema was present, indicating that any key developmental roles of VEGF-D are compensated by another molecule, possibly VEGF-C. However, VEGF-D does appear to play a role in lymphangiogenesis, and ectopic expression of VEGF-D in the skin of transgenic mice under the control of the keratin 14 gene promoter induced the growth of lymphatic vessels in the dermis, whereas blood vessels were unaffected (Veikkola *et al.* 2001). VEGF-D may be less important in mice than humans, given that mouse VEGF-D lacks VEGFR2 binding capacity.

Originally isolated from a placental cDNA library (Maglione *et al.* 1991), the human **PlGF** gene is alternatively spliced to produce three isoforms, PlGFs 1, 2 and 3, whereas mice only express a single PlGF form analogous to human PlGF2. PlGF1 binds to VEGFR1 but not NRP1 whereas PlGF2 binds to both VEGFR1 and NRP1 (Park *et al.* 1994; Migdal *et al.* 1998).

PlGF expression can be observed from E10.5 in developing mice, and PlGF-null mice are viable, fertile and appear healthy, with little noticeable effect on normal vascular development – however, VEGF-A was upregulated in PlGF-null mice, and may compensate (Carmeliet *et al.* 2001). PlGF appears to have a particular role in pathological angiogenesis. Vascularisation of ES cell-derived tumours was substantially reduced when the host mouse or the implanted cells lacked PlGF, and PlGF-deficient mice showed reduced angiogenesis into ischaemic regions of the retina and myocardium (Carmeliet *et al.* 2001). Tumour cells overexpressing PlGF promote angiogenesis when injected into mice (Hiratsuka *et al.* 2001), and these findings coupled with the data from PlGF-null mice indicate that mouse PlGF can promote angiogenesis in certain situations.

PlGF has little apparent effect when administered directly to cultured endothelial cells (although it does stimulate tissue factor production, Clauss *et al.* 1996), but enhances VEGF-stimulated responses in some ECs (Park *et al.* 1994) but not others (Carmeliet *et al.* 2001) – this difference was suggested to be due to saturating PlGF production by the ECs in the second study. VEGF-stimulated proliferation, survival and migration was impaired in capillary ECs derived from PlGF-null mice, as was VEGF-stimulated increases in capillary permeability, whereas endothelial responses to FGF2 and permeability responses to histamine were unaffected (Carmeliet *et al.* 2001). Normal VEGF responses could be restored in the PlGF-null cells/mice by addition of exogenous PlGF. Together, it appears that PlGF is important for full EC responses to VEGF, but EC-produced PlGF may be adequate in most circumstances.

Given its minimal direct effect on endothelial cells, PlGF had been proposed to increase VEGF-stimulated angiogenesis by occupying soluble VEGFR1 thus preventing VEGF sequestration. This mechanism is unlikely, as no difference in embryonic VEGF concentrations was observed

in PlGF2-null mice (Carmeliet *et al.* 2001). PlGF potentiation of VEGF responses may be involve formation of VEGF/PlGF heterodimers or VEGFR1/VEGFR2 heterodimers (Autiero *et al.* 2003).

Although disruption of other members of the VEGF family also have negative effects on blood vessel development, none are as dramatic as those for VEGF-A, and VEGF-A appears to be the most important member of this family in vasculogenesis and angiogenesis in vertebrates. The remainder of this section will concentrate on the biology of VEGF-A.

1.4.2 VEGF-A

Mature VEGF-A is a dimer (M_r approx 46 kDa for the VEGF-A_{165} homodimer), consisting of two polypeptides linked by two disulphide bonds in a cysteine knot motif. This motif was revealed by the crystal structure of a protein corresponding to residues 8–109 of VEGF, present in all VEGF-A splice variants, which shows monomers associating in a head-to-tail conformation (Muller *et al.* 1997). The cysteine knot is an eight cysteine residue ring composed of one interchain and three intrachain disulphide bonds per monomer, and is also found in other growth factors including PDGF. The cysteine knot disulphide bonds stabilise the structure of VEGF and are necessary for dimerisation and biological activity. Point mutation of these cysteine residues results in monomeric VEGF-A, which biologically inactive (Claffey *et al.* 1995). As discussed later, dimerisation is important for the ability of VEGF to cross-link its receptors and so induce a downstream signal.

VEGF-A is secreted from the cell, and a 26-residue N-terminal signal sequence present in the mature VEGF-A protein is cleaved on secretion. Comparison of VEGF purified from cell-conditioned media (glycosylated at Asn75) or synthesised by *E. coli* (non-glycosylated) showed similar in vivo angiogenic activity of the two VEGFs, indicating that glycosylation is not required for VEGF biological activity (Walter *et al.* 1996), but promotes efficient secretion (Claffey *et al.* 1995).

1.4.2.1 Ischaemia-stimulated VEGF-A production

Hypoxic cells increase the expression of VEGF-A_{165} (Shweiki *et al.* 1992), so promoting blood vessel growth towards themselves. VEGF-A expression is regulated by intracellular oxygen concentrations due to the presence of a hypoxia response element (HRE) upstream of the VEGF-A promoter, which binds hypoxia inducible factor-1 (HIF-1). Under normal intracellular oxygen concentrations, the α subunit of HIF-1 is hydroxylated on key proline residues by prolyl hydroxylases, which use molecular oxygen as the rate-limiting substrate (Epstein *et al.* 2001, reviewed by Kaelin and Ratcliffe 2008). Hydroxyproline-HIF-1α is recognised by a the von Hippel-Lindau protein component of a ubiquitin ligase, and is degraded by the ubiquitin/proteasome pathway. Under low oxygen concentrations (i.e. during hypoxia), HIF-1α is not hydroxylated on proline, accumulates and forms heterodimers with HIF-1β which translocate to the nucleus. This complex binds to the HRE in the VEGF promoter, increasing VEGF transcription in response to hypoxia.

HIF-1α-null mice die at E10.5, with substantial vascular malformations and vascular regression observed, indicating substantial EC death (Kotch *et al.* 1999). Hypoxia-induced increases in VEGF mRNA expression are strongly reduced in HIF-1α-null embryonic stem cells (Carmeliet *et al.* 1998), indicating the importance of HIF-1 signalling in hypoxia-stimulated VEGF synthesis. Hypoxia can also increase the production of VEGF protein by stabilisation of its mRNA (Ikeda *et al.* 1995). Increased VEGF-A transcription and mRNA stabilisation provide a system by which hypoxic tissues increase VEGF-A production and secretion, so attracting new blood vessel growth (Shweiki *et al.* 1992).

VEGF-A mRNA expression is increased in HIF-1α-null *embryos* (Kotch *et al.* 1999), suggesting that HIF-1α has essential VEGF-independent roles in embryonic development (as HIF-1α-null mice express VEGF but still die), and further suggesting that a non-hypoxia-driven pathway also operates to increase VEGF expression in tissues requiring improved local vascularisation. In cultured cells, reduced glucose concentrations in culture medium led to increased VEGF mRNA expression (Kotch *et al.* 1999), suggesting that glucose deficiency as well as oxygen deficiency

may contribute to increased VEGF expression by ischaemic tissues.

A review of the various transcription factors involved in regulation of VEGF-A expression is given by Pages and Pouyssegur (2005).

1.4.2.2 VEGF-A splice variants and their role in vascular development

1.4.2.2.1 VEGF-A structural elements and their roles

The human VEGF-A gene is organised as eight exons separated by seven introns, and undergoes alternative splicing (Tischer *et al.* 1991). A number of variants have currently been identified: VEGF-A_{121} (equivalent to mouse VEGF-A_{120}), VEGF-A_{145}, VEGF-A_{148}, VEGF-A_{165} (equivalent to mouse VEGF-A_{164}), VEGF-A_{183}, VEGF-A_{189} (equivalent to mouse VEGF-A_{188}), and VEGF-A_{206} are generated by alternative splicing of exons 6 and 7, where the subscript refers to the number of amino acids present in each *secreted* polypeptide, excluding the signal peptide which is cleaved on secretion (Robinson and Stringer 2001). The first isoform to be identified, and the most intensively studied and apparently biologically most important isoform is VEGF-A_{165}.

Recently a number of 'b' isoforms of VEGF-A have been identified, containing a region encoded by an alternate exon 8 and producing isoforms with an identical number of amino acids as the variants listed above but causing an alteration in the six carboxy-terminal amino acids (Harper and Bates 2008). For example, VEGF-A_{165}b results from alternative exon 8 splicing of VEGF-A_{165} (Bates *et al.* 2002). VEGF-A_{165}b has been proposed to act as an anti-angiogenic isoform. Cell culture studies indicate that VEGF-A_{165}b is a weak agonist of VEGFR2, probably because it is unable to bind NRP1 (Kawamura *et al.* 2008). Overexpression of VEGF-A_{165}b in vivo has been shown to inhibit angiogenesis, but the biological or pathological role of endogenous VEGF-A_{165}b or other 'b' isoforms is currently unclear.

Figure 1.3 indicates the derivation of the splice variants from the VEGF-A gene.

VEGF-A_{165} can be cleaved by the extracellular protease plasmin, generating an N-terminal 110 aa

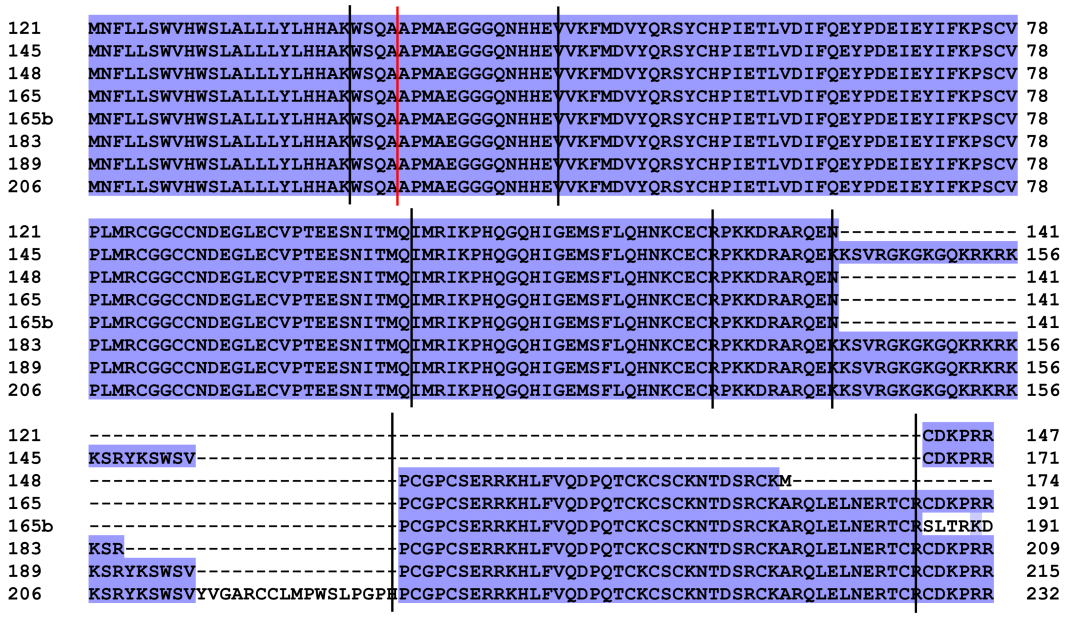

Figure 1.3: VEGF-A splice variants
Protein sequences for human VEGF-A isoforms containing the indicated number of amino acids (on left of sequence) were retrieved from the SwissProt database and aligned with ClustalX2. Residues are coloured according to Blossum62 score, with darker colours indicating better conservation. Black vertical lines indicate exon boundaries, the red vertical line indicates the boundary between the N-terminal signal sequence and mature secreted protein. Exon boundaries were determined via Ensembl. The SwissProt database accession numbers for the protein sequences used for alignment were: 121 aa isoform, P15692-7; 145, P15692-6; 148, P15692-5; 165, P15692-4; 165b, P15692-8; 183, P15692-3; 189, P15692-2; 206, P15692.

fragment containing the receptor binding domain, and a C-terminal 55 aa fragment containing a heparin-binding domain (Owens and Keyse 2007).

The VEGF receptor binding domain, or VEGF homology domain (VHD), binds to VEGFRs 1 and 2 (Keyt *et al.* 1996). It is apparent that dimerisation and receptor-binding activities of VEGF-A are encoded by this domain, since a protein formed from VEGF-A residues 8–109 (VEGF-A_{8-109}, encoded by these domains) has been crystallised as a dimer, and in complex with VEGFR1 (Muller *et al.* 1997; Wiesmann *et al.* 1997). Exons 1–5 (encoding residues 1–114, including the entire receptor-binding domain) are common to all VEGF-A variants, and include the cleavable signal sequence, glycosylation site, residues essential for VEGF dimerisation, and residues required for binding to the receptors VEGFR1 and VEGFR2.

The heparin-binding domain is a region rich in basic amino acids, and is responsible for binding

to heparin and neuropilins (Pellet-Many *et al.* 2008). This region is encoded by VEGF-A exons 6, 7 and 8, regions which are not common to all VEGF-A variants, and as a result NRP and heparin binding varies between splice variants. Of the common splice variants, VEGF-A_{165} lacks exon 6, VEGF-A_{121} lacks exons 6 and 7, and VEGF-A_{189} contains all exons including all of VEGF-A_{165} and VEGF-A_{121}, although lacking part of exon 6 present in VEGF-A_{206} (see figure 1.3).

VEGF-A_{165} binds to NRP1 and NRP2 whereas VEGF-A_{121} has been reported to bind to neither (Soker *et al.* 1998; Gluzman-Poltorak *et al.* 2000), implicating VEGF-A exon 7 in NRP binding. Regions of exon 8 are also important in NRP1 binding as VEGF-A_{165}b, differing from VEGF-A_{165} only in the six amino acids at the extreme C-terminus and encoded by exon 8, does not bind NRP1 (Kawamura *et al.* 2008). A recent study also reported that VEGF-A_{121} may, in fact, bind NRP1 via its exon 8 domain, but does not appear to promote VEGFR2/NRP1 complexation (Pan *et al.* 2007). VEGF-A_{145}, lacking exon 7 but containing part of exon 6 not present in VEGF-A_{121}, also weakly binds NRP1 implicating exon 6 in NRP1 binding (Kawamura *et al.* 2008). Thus regions of all exons of the heparin-binding domain contribute to NRP binding. The general roles of VEGF-A exons/domains are indicated in figure 1.4.

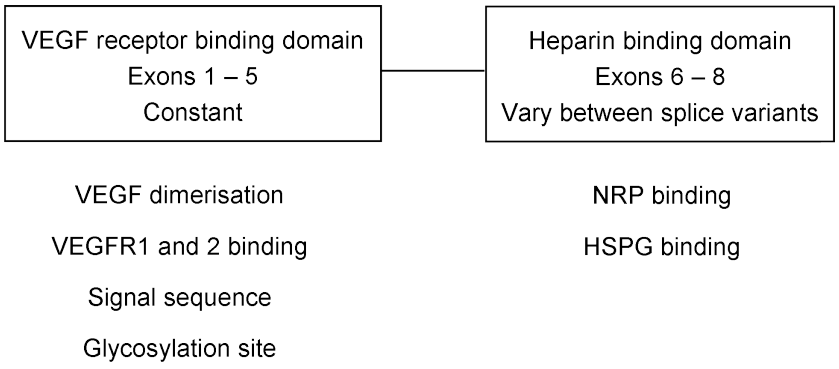

Figure 1.4: Roles of VEGF-A domains

The isolated heparin-binding domain binds to heparin, whereas the isolated receptor-binding domain (VHD) shows little heparin-binding activity (Owens and Keyse 2007). Residues from exons 6, 7 and 8 are all likely to contribute to heparin binding. Neither VEGF-A_{121} nor VEGF-A_{165}b

bind heparin, indicating a requirement for exons 6 or 7, and exon 8 respectively (Kawamura *et al.* 2008). The same paper showed that both VEGF-A_{145} (lacking exon 7) and VEGF-A_{165} (lacking exon 6) bind to heparin, indicating that residues from either region in combination with exon 8 can suffice for heparin binding, although stronger binding requires both exons.

In addition to differences in heparin and NRP1 binding, the biological activity of the splice variants also varies and it is likely that modulation of the VEGF splice variant produced (and possible heterodimerisation between VEGF isoforms) allows cells to fine-tune VEGF-A-dependent responses. For example, VEGF-A_{165} is reported to be 100-fold more potent as an EC mitogen than VEGF-A_{121} (Keyt *et al.* 1996) but these isoforms are similarly potent EC chemoattractants (Pan *et al.* 2007). VEGF-A_{165}b is reported to anti-angiogenic, inhibiting VEGF-A_{165}-activated endothelial cell processes such as proliferation, migration and arterial vasodilation (Bates *et al.* 2002). Given that the receptor-binding domain is identical in all VEGF-A splice variants, it is likely that differences in heparin and NRP binding contribute to the differences in biological activity between variants. Possible reasons for this include modulation of VEGFR activity or VEGF binding by heparin-containing species or NRPs as a result of NRP complexation with VEGFR2, or effects on VEGF protein distribution. Variation in the conformational change induced in VEGFRs (and hence VEGFR activation) on binding different VEGF-A variants may also contribute.

Differences in heparin binding are thought to contribute to differences in the diffusability of the VEGF-A splice variants. VEGF-A was recovered from the conditioned medium of cells transfected with cDNAs encoding the 121 and 165 isoforms, indicating that these forms were secreted and soluble, but not from medium conditioned by cells expressing the 189 and 206 aa VEGF-A variants (Houck *et al.* 1991). This appears to be because the longer isoforms bind strongly to heparin, and are sequestered by cell-surface HSPGs, whereas the 165 aa isoform binds more weakly and the 121 aa isoform doesn't bind to heparin at all (Houck *et al.* 1992). Extracellular matrix-sequestered VEGF can be cleaved by extracellular proteases such as plasmin, releasing a soluble bioactive fragment (Park *et al.* 1993).

Differences in heparin binding by VEGF-A splice variants, leading to differences in diffusability (lower binding isoforms diffusing further) may be important in producing a VEGF gradient to attract angiogenic sprouts, explaining the need for multiple splice variants. Ruhrberg *et al.* (2002) reported that VEGF-A binding to heparin produced the appropriate VEGF-A concentration gradient for proliferating endothelial cells to correctly form blood vessels – lack of heparin binding VEGF-A forms caused proliferating ECs to be incorporated into an existing vessel increasing its diameter, rather than forming correctly branched vessels.

1.4.2.2.2 Functional role of VEGF-A splice variants: knockout studies

A number of studies have used gene disruption in mice to determine the specific functional roles of the various VEGF-A splice variants. Mice are known to express at least three VEGF-A splice variants: VEGF-A_{120}, VEGF-A_{164} and VEGF-A_{188} (Breier *et al.* 1992), murine versions of the main three isoforms produced by most VEGF-A-expressing cells (Robinson and Stringer 2001).

Stalmans *et al.* (2002) generated mice expressing single VEGF-A splice variants, by replacing the VEGF-A genomic sequence with a fused cDNA containing the relevant exons. All heterozygous mice were apparently normal. VEGF-A_{120} mice (i.e. expressing only VEGF-A_{120}) died within two weeks of birth due to heart failure resulting from impaired myocardial angiogenesis (this defect was also observed by Carmeliet *et al.* 1999b). VEGF-A_{164} mice were apparently normal and fertile. Some VEGF-A_{188} mice died in utero, but the majority survived but with impaired growth and fertility. Retinal vessel development was normal in VEGF-A_{164} mice, but was impaired in both VEGF-A_{188} mice and most severely in VEGF-A_{120} mice, with the major defects occurring in arterial vessels. Thus VEGF-A_{164} appears to be sufficient for mouse development, and is likely to mediate the major biological functions of VEGF-A during embryogenesis and post-natal growth. That the most severe defects were observed in VEGF-A_{120} mice, a non-heparin binding and freely diffusable form, suggests that sequestration of VEGF-A in the extracellular matrix may be important to its functions, possibly required for the correct establishment of VEGF-A concentration

gradients as mentioned above.

Apparently the only VEGF-A isoform required for normal retinal angiogenesis, VEGF-A_{164} may also be the only VEGF-A isoform required for normal bone vascularisation and angiogenesis. Bone vascularisation was apparently normal in mice expressing only VEGF-A_{164} but not VEGF-A_{120} or VEGF-A_{188}, with the most severe defect observed in VEGF-A_{120}-expressing mice (Zelzer *et al.* 2002; Maes *et al.* 2002, 2004).

VEGF-A_{165} (often simply referred to as VEGF) is highly expressed and diffusible. It is believed to be the most biologically potent form of VEGF-A, is the only VEGF-A splice variant required for apparently normal mouse development, and is responsible for mediating most of the key biological functions of VEGF-A in endothelial cells. As a result, it is the most intensively studied member of the entire VEGF family and its effects on vascular endothelial cells are the topic of this thesis.

1.4.3 Receptors for VEGFs

Three signal-transducing cell surface receptors for VEGFs have been identified, termed VEGFR1, VEGFR2 and VEGFR3. In addition, HSPGs (containing heparin, abundant on the endothelial surface) and NRPs are also able to bind to various VEGF isoforms.

1.4.3.1 Overview of VEGF receptor structure

VEGFR1, 2 and 3 have a similar structure, composed of an N-terminal extracellular region of seven immunoglobulin (Ig)-like domains (six in VEGFR3, with domain 5 replaced by a disulphide bridge), a single pass transmembrane domain, a tyrosine kinase catalytic domain which is interrupted by a short region termed the kinase insert region, and a C-terminal tail (reviewed by Roskoski 2008). VEGF receptors are believed to act as classical receptor tyrosine kinases (RTKs), with a VEGF dimer bound to a dimerised receptor leading to transautophosphorylation of the receptor tyrosine residues, producing binding sites for SH2 domain-containing proteins and leading to initiation of signalling cascades.

The role of individual VEGF receptors has been analysed by overexpressing individual VEGF receptors in cells which otherwise did not detectably bind or respond to VEGF-A_{165} (for example the porcine aortic endothelial cell line (PAE), Waltenberger *et al.* 1994). The downstream signalling components of VEGF signalling pathways appear to be present in these cells, and overexpression of the appropriate VEGF receptors in these cells causes the transfected cells to respond to VEGF in a similar way to primary endothelial cells (i.e. by proliferation, migration etc). Data from these kind of experiments indicates that VEGFRs 1–3 have distinct roles in biological signalling. Heterodimers of the VEGF receptors have been reported, for example VEGFR1 with VEGFR2 (Autiero *et al.* 2003) and VEGFR2 with VEGFR3 (Dixelius *et al.* 2003), which might also have distinct roles and this may provide a method for fine-tuning VEGF-stimulated signalling.

Co-crystallisation of the extracellular domains of VEGFR1 with VEGF-A_{8-109} shows that VEGF-A binding occurs via the second and third Ig-like domains (numbered from the outermost, N-terminal regions) (Wiesmann *et al.* 1997). Analysis of deletion mutants of the VEGFR2 extracellular domain, in which a protein lacking Ig-like domains 1,4 and 5 bound VEGF with similar affinity to a protein containing domains 1–5, indicates that VEGFR2 IgG-like domains 2 and 3 are primarily responsible for VEGFR2 binding to VEGF-A (Fuh *et al.* 1998). VEGFR1 and 2 bind in the groove between the monomers of dimeric VEGF, with contacts on both monomers (Muller *et al.* 1997; Wiesmann *et al.* 1997).

Ig-like domains 2 and 3 may also be the only extracellular domains essential for VEGFR2 downstream signalling. Chimeric receptors composed of the extracellular region of VEGFR2 and intracellular and transmembrane regions from VEGFR3 transduced VEGF-stimulated mitogenic signals, even when VEGFR2 Ig-like domains 4–7 were missing (Fuh *et al.* 1998).

Evidence for the involvement of the various VEGF binding molecules in mouse development is discussed below. The role of these receptors in VEGF-stimulated signal transduction is discussed in section 1.4.4.2.

1.4.3.2 VEGFR2

VEGFR2, also known as kinase domain receptor (KDR) in humans or foetal liver kinase-1 (Flk-1) in mice, binds VEGF-A_{165} with a dissociation constant (K_d) of 0.6 nM (comparable to other growth factors and their receptors), resulting in VEGF-A_{165}-stimulated tyrosine phosphorylation of VEGFR2 (Millauer *et al.* 1993; Quinn *et al.* 1993). VEGFR2 binds to VEGF-A, fully processed VEGFs C and D, and VEGF-E.

VEGF-A_{165} stimulates autophosphorylation of VEGFR2 on tyrosine residues Y951 and Y996 in the kinase insert domain, Y1054 and Y1059 in the catalytic domain, and Y1175 and Y1214 in the C-terminal tail (Dougher-Vermazen *et al.* 1994; Takahashi *et al.* 2001; Matsumoto *et al.* 2005). VEGFR2 does not appear to become phosphorylated on Ser or Thr residues in in vitro kinase assays (Takahashi *et al.* 2001). Phosphorylation of the kinase domain residues Y1054 and Y1059 enhances VEGFR2 tyrosine kinase activity, and is required for phosphorylation of cellular substrates (Dougher and Terman 1999).

VEGFR2 is expressed in endothelial cells and their progenitors (Millauer *et al.* 1993; Quinn *et al.* 1993; Yamaguchi *et al.* 1993), and was thought to be specific for endothelial cells but has more recently been identified on other cell types including neurons and their progenitors (Yang and Cepko 1996; Nishijima *et al.* 2007).

VEGFR2-null mice die in utero at E8.5–9.5 due to a massive defect in vasculogenesis, whereas heterozygous mice were fertile and apparently normal (Shalaby *et al.* 1995). In knockout animals, no blood vessels were observed in either the embryo or yolk sac, and yolk sac blood islands were not formed. VEGFR2-null mice contained cells expressing early endothelial markers including VEGFR3 and tie2, but not the later endothelial marker tie1, and no recognisable endothelial cells were present, indicating an essential early role of VEGFR2 in endothelial differentiation. Interestingly, VEGF-A knockout mice do form some endothelial cells as discussed earlier, showing that some roles of VEGF-A in endothelial development can be compensated to some extent, possibly

by another VEGFR2 ligand such as VEGF-C. VEGFR2-null mice also developed few committed haematopoetic progenitor cells, indicating a role for VEGFR2 in blood development. VEGFR2 has been reported as a marker which defines the haemangioblast (Yamaguchi *et al.* 1993), the blood island precursor which forms endothelial and blood cells in the yolk sac, explaining the connection between loss of blood and endothelial cells in VEGFR2-deficient mice.

The importance of VEGFR2 tyrosine phosphorylation for blood vessel development was shown by studies where a Y1173F (equivalent to human Y1175F) point mutation was introduced into mice (Sakurai *et al.* 2005). These mice die at E8.5–E9.5 from a large scale vascular defect similar to that observed for VEGFR2-null mice, with no blood vessels, endothelial cells or blood vessels formed. Mutation of another VEGFR2 site, Y1212 (equivalent to human Y1214), had no effect and these mice were fertile and apparently normal. Thus VEGF-induced phosphorylation of specific sites on VEGFR2 is essential for VEGF activity, presumably because key signalling molecules bind to specific sites on VEGFR2 to activate downstream pathways.

PAE cells transfected with VEGFR2, with previously undetectable VEGF-A_{165} binding, undergo VEGF-A_{165}-stimulated increases in proliferation and migration (Waltenberger *et al.* 1994), indicating that VEGFR2 is the only receptor required for these responses. VEGFR2 is believed to be responsible for the majority of VEGF-A-stimulated signalling in endothelial cells (further discussed in section 1.4.4.2).

1.4.3.3 VEGFR1

VEGFR1, also called Fms-like tyrosine kinase-1 (Flt-1, where Fms is the macrophage colony stimulating factor receptor), binds VEGF-A_{165} with a K_d around 20 pM, substantially lower than that of VEGFR2 (De Vries *et al.* 1992; Waltenberger *et al.* 1994). VEGFR1 binds to VEGFs A and B and PlGF, and can be alternatively spliced to give a soluble, secreted 110 kDa form which also binds VEGF, so preventing VEGF binding to its cell surface receptors and acting as an antagonist (Kendall and Thomas 1993). When expressed in PAE cells, VEGFR1 undergoes VEGF-A_{165}-

dependent tyrosine phosphorylation, but to a much lesser extent than VEGFR2 (Waltenberger *et al.* 1994), suggesting that VEGFR1 is a weaker tyrosine kinase than VEGFR2. VEGF-A_{165} stimulates VEGFR1 phosphorylation at Y794, 1169, 1213, 1242, 1327 and 1333 (Ito *et al.* 1998, reviewed by Olsson *et al.* 2006) although the extent of phosphorylation of some of these residues is apparently minor, not occurring on every VEGF-stimulated receptor-expressing cell, and is disputed.

VEGFR1-null mice die in utero, apparently from a vascular defect, with lethality occurring around E8.5 (Fong *et al.* 1995). Endothelial cells are present, but these are not correctly assembled into functional vessels with endothelial cells in the interior of blood islands and the dorsal aorta, indicating that while VEGFR-1 is not required for endothelial cell differentiation it is necessary for vascular organisation. Blood cells were also formed. This is in contrast to the defect in VEGFR2 mice, where endothelial and blood cells were not formed (Shalaby *et al.* 1995).

Increased numbers of endothelial precursor cells are present in VEGFR1-null mice, due to increased commitment of mesenchymal stem cells to the (haem)angioblast lineage (Fong *et al.* 1999a). Using chimeric mice generated from mixtures of VEGFR1-null and wild-type embryonic stem cells in various proportions, the same study showed that when diluted the progeny of VEGFR1-null cells formed parts of apparently normal blood vessels, indicating that endothelial expression of VEGFR1 may not be required for an EC to participate normally in vessel formation.

VEGFR1 tyrosine kinase activity is not required for normal vascular development. Hiratsuka *et al.* (1998) deleted exons encoding the C-terminus of VEGFR1 in mice, so preserving the extracellular and transmembrane regions but removing the intracellular tyrosine kinase domain. Mice homozygous for the deletion were viable and fertile, and blood vessel development was unaffected. In contrast, the existence of VEGFR1 at the plasma membrane appears important. Around half of mice lacking both the tyrosine kinase and transmembrane domains of VEGFR1 (so only producing the soluble form) die in utero exhibiting vascular defects, whereas the other half survive to adulthood (Hiratsuka *et al.* 2005) – on another genetic background, the surviving proportion was

increased.

Overall, the primary embryonic role of VEGFR1 appears to be to regulate the production of endothelial precursors, mediated by VEGFR2 as discussed above. An explanation for the VEGFR1 mutant phenotypes is that in the embryo VEGFR1 binds to VEGF and acts as a VEGF sink (decoy receptor), so preventing excessive VEGFR2 signalling and endothelial precursor production. In agreement with this possibility, the vast majority of VEGFR1 expressed in normal mouse embryos is soluble rather than membrane associated (Carmeliet *et al.* 2001). Soluble VEGFR1 lacking either the tyrosine kinase domain or the transmembrane domain can still sequester VEGF away from VEGFR2, allowing normal vascular development. The sequestering of VEGF near the cell membrane (where VEGFR2 receptors are located) may be particularly important, explaining why mice expressing only soluble VEGFR1 forms show reduced survival, although it is not clear why this should be more important in some individuals than others. Alternatively VEGFR1/2 heterodimerisation, or phosphorylation/protein binding to non-tyrosine kinase intracellular regions of VEGFR1 may be important.

Although VEGFR1 is a weaker VEGF-A_{165}-stimulated tyrosine kinase than VEGFR2 and is not essential for many VEGF-A_{165}-induced responses of cultured endothelial cells (Waltenberger *et al.* 1994), VEGFR1 does bind other members of the VEGF family (PlGF2 and VEGF-B) and may be required for some non-embryonic effects of VEGF-A in ECs or other cell types. Deletion of the VEGFR1 tyrosine kinase domain prevented PlGF-stimulated angiogenesis in mice (Hiratsuka *et al.* 2001) and VEGF-A_{165}- and PlGF-stimulated monocyte migration (Hiratsuka *et al.* 1998), indicating that classical tyrosine kinase activity of VEGFR1 may be important in some circumstances.

1.4.3.4 VEGFR3

VEGFR3, also called Fms-like tyrosine kinase 4 (Flt4) does not bind VEGF-A, but binds VEGF-C and VEGF-D (Joukov *et al.* 1996; Achen *et al.* 1998).

VEGFR3-null mice have an abnormally underdeveloped vasculature and die in utero around E12 (Dumont *et al.* 1998). Endothelial cells and erythrocytes were formed in these mice, and angiogenesis appeared normal as intersomitic vessels were present. The primary defect seemed to be in the remodelling of blood vessels, with a number of uniformly sized vessels present in the head rather than the usual branched network. Heterozygous mice were apparently normal, and LacZ expression indicated that whereas VEGFR3 was expressed in aortic, venous and blood island endothelial cells in the embryo, expression was restricted to the lymphatic endothelium in newborn and adult mice, a restriction that had been observed previously (Kaipainen *et al.* 1995). Transgenic expression of chimeric membrane-bound VEGFR3 lacking the intracellular domains in skin cells prevented lymphatic development in the skin, whereas blood vessel development was normal (Makinen *et al.* 2001). Thus the chimeric VEGFR3 suppresses lymphangiogenesis but not angiogenesis, presumably due to competition with endogenous VEGFR3 for its ligands, and indicating a critical role for VEGFR3 signalling in the lymphatic system.

Although likely to play a role in the developing and adult lymphatic system, death of VEGFR3-null mice appeared related to blood vessel defects occurring before the development of lymphatic problems (Dumont *et al.* 1998). The fact that VEGF-C-null mice die from lymphatic defects later in development, at E15.5–17.5 (discussed above) may be because another VEGFR3 ligand such as VEGF-D compensates for VEGF-C during early blood vessel development, but is insufficient in later lymphatic development.

1.4.3.5 Neuropilins

Neuropilins (NRPs, reviewed by Pellet-Many *et al.* 2008) are transmembrane glycoproteins that bind some VEGFs, and class 3 semaphorins, secreted proteins involved in directing the growth cones of growing axons. Two neuropilin genes are known, NRP1 and NRP2, which like VEGFR1 can produce either a transmembrane receptor or, by alternative splicing, soluble forms (sNRP1 and 2) composed of the extracellular region only. The b1 and b2 domains of NRPs bind to VEGF

regions encoded by exons 7 and 8. NRP1 binds to VEGFs B–E, PlGF2 (and mouse PlGF), and some isoforms of VEGF-A (including VEGF-A_{165}, Soker *et al.* 1998), whereas NRP2 binds to some VEGF-A isoforms (including VEGF-A_{165}), and VEGFs C and D (Gluzman-Poltorak *et al.* 2000). Both NRP1 and 2 are expressed in vascular endothelial cells, but in the adult vasculature NRP1 is mainly expressed by arterial ECs whereas NRP2 is expressed by venous and lymphatic ECs (Yuan *et al.* 2002). Cultured HUVECs, however, do express NRP1.

The transmembrane receptor forms of NRP1 and 2 have a short cytoplasmic domain which has been shown to interact with an intracellular PDZ domain-containing protein, synectin. NRPs have no known signalling role acting alone, but are believed to act as co-receptors for VEGF, with the signal transduced through the plasma membrane by VEGFR2, and semaphorins, with the signal transduced by transmembrane receptors known as plexins. However, neuropilin expression is not essential and not sufficient for VEGFR2-dependent signalling, and expression of VEGFR2 without neuropilins is sufficient to confer VEGF responsiveness, at least in porcine aortic endothelial cells (Waltenberger *et al.* 1994).

Most work regarding NRPs in VEGF signalling and function has focused on NRP1. NRP1 complexes with VEGFR2 in endothelial cells, and in some reports complex formation is VEGF-dependent. Soker *et al.* (1998) reported that co-expression of NRP1 with VEGFR2 enhanced VEGF binding and VEGF-stimulated migration of porcine aortic endothelial cells over that observed in cells expressing VEGFR2 alone, while cells expressing NRP1 alone did not respond to VEGF.

The potentiation of VEGF-stimulated cell signalling by NRP1 could occur via a number of mechanisms, such as stabilisation of the VEGF/VEGFR2 signalling complex at the cell surface so increasing the duration of VEGFR2 signalling, or by transducing signals directly (e.g. via synectin) which feed in to VEGFR2 signalling. Hypothetically, synectin-mediated inhibition of a protein tyrosine phosphatase could also enhance VEGFR2-stimulated signalling.

NRP1-null mice die in utero around E12.5–13.5, showing multiple cardiovascular defects with

sparse capillaries in the yolk sac and some major vessels in the brachial region incorrectly branched, incomplete or not formed at all (Kawasaki *et al.* 1999). Nervous defects were also observed, with nerves following incorrect paths, due to a blockade of semaphorin 3-mediated signalling (Kitsukawa *et al.* 1997).

The vascular and neural effects of NRP1 were delineated by producing mice deficient in NRP1 specifically in the endothelium, or mice expressing mutant NRP1 specifically unable to bind Sema3A but able to bind VEGF-A_{165} (Gu *et al.* 2003). Endothelial-specific NRP1-null mice died in utero, displaying abnormalities in major arteries and reduced vessel branching at E12.5. In contrast, mice expressing a mutant NRP1 which binds VEGF-A but not Sema3A are born live, but exhibit nervous system defects and die soon after birth. Together these data indicate that endothelial expression of NRP1, but not Sema3A binding to NRP1, is required for normal vascular development, while Sema3A binding to NRP1 plays a restricted role in neurogenesis. However, the precise contribution of VEGF binding to NRP1 in vascular development is not yet known.

NRP2-null mice are viable, with no apparent cardiovascular defects but a reduced number of small lymphatic vessels (Chen *et al.* 2000; Yuan *et al.* 2002). The major defect appears to be neural, with abnormal guidance of cranial and spinal nerves. NRP1/NRP2 double knockout mice die in utero at E8, earlier than for single NRP1-null mice (Takashima *et al.* 2002), suggesting that NRP2 may compensate to a certain extent for NRP1 during early cardiovascular development. NRP1/NRP2 double-null mice display a severe cardiovascular abnormalities with large avascular areas in the yolk sac and embryo, and reduced connections between blood vessel sprouts. This severe phenotype, similar to that observed for VEGF-A-null and VEGFR2-null mice, may reflect insufficient VEGF-A/VEGFR2 signalling as NRP-mediated potentiation of the VEGF-A signal is lost.

1.4.3.6 Heparan sulphate proteoglycans

Several VEGF isoforms including VEGF-A_{165} contain a heparin binding domain, and so are able to bind to HSPGs. HSPGs are transmembrane proteins abundant on the surface of endothelial cells, where the covalently-linked heparan sulphate moiety (similar to the mast cell-produced polysaccharide mixture heparin) binds to the plasma protein antithrombin III and accelerates its action to inactivate thrombin, so limiting the extent of thrombus formation during the clotting cascade. HSPGs are highly negatively charged, and bind to strongly positive regions on a variety of secreted growth factors including VEGFs.

The heparin binding domain of VEGF-A is not present in some isoforms such as VEGF-A_{121} and differences in heparin binding, as well as NRP1 binding, have been suggested to account for some of the differences between VEGF-A splice variants. Additionally, HSPG binding is important in angiogenesis in establishing a VEGF concentration gradient (discussed in section 1.4.2.2.1).

A number of earlier studies reported the importance of the heparin-binding domain for VEGF biological activity, but these usually failed to distinguish between effects of heparin binding and neuropilin binding. Heparin binding itself does not appear essential for VEGF biological activity, at least in cell-based studies. VEGF-A_{164} mutants which showed a substantially reduced affinity for heparin due to mutation of specific Arg residues in the heparin binding domain showed similar abilities to bind VEGFR1 and VEGFR2 and stimulate tissue factor expression and ex-vivo angiogenesis as wild-type VEGF-A_{164} (Krilleke *et al.* 2007). A complete loss of heparin-binding ability may have more dramatic effects. Heparin has been reported to affect the interaction of VEGF-A_{165} with VEGFR2 (Tessler *et al.* 1994), and to increase VEGF-A_{165}-stimulated tubulogenesis (Ashikari-Hada *et al.* 2005), although these effects were relatively small.

1.4.4 Biological functions of VEGF-A_{165} in the endothelium and the key signalling pathways involved

1.4.4.1 Angiogenic and non-angiogenic roles of VEGF

Experimental disruption of VEGF or VEGF receptor genes in mice clearly demonstrates the importance of VEGF signalling in vascular formation as discussed previously. VEGF-A_{165} protein (hereafter referred to as VEGF) promotes angiogenesis in vivo in a number of models, including the corneal micropocket assay (Connolly *et al.* 1989; Morbidelli *et al.* 1997), chick chorioallantoic membrane assay (Wilting *et al.* 1993) and rat mesenteric assay (Norrby 1996), and implanted VEGF-expressing tumour cells attract blood vessels (Ferrara *et al.* 1993), suggesting that VEGF signalling is rate limiting for angiogenesis in a number of situations.

Tubulogenesis – the angiogenesis-like formation of endothelial tubes from cultured ECs – occurs in ECs cultured on matrigel, a mixture of growth factors and basement membrane components (Kubota *et al.* 1988). VEGF increases angiogenesis/tubulogenesis in a cell/tissue culture-based assays including EC co-culture with fibroblasts (Jia *et al.* 2001a) and capillary outgrowth from aortic rings (Nicosia *et al.* 1994).

The angiogenic effect of VEGF *alone* is difficult to assess in vivo, and in assays involving other cell types which may produce various factors (e.g. the aortic ring assay). I was unable to locate studies in defined in vitro systems (e.g. tubule formation by cultured ECs on 2-D or 3-D collagen) which demonstrated an angiogenic effect of VEGF alone, although VEGF is clearly able to promote tubulogenesis in the presence of other factors such as serum (Pepper *et al.* 1992; Ilan *et al.* 1998) and may be sufficient for angiogenesis in vivo. However, VEGF alone can directly stimulate a number of processes required for angiogenesis in cultured endothelial cells, including EC proliferation, migration and cell survival, and EC production of known vasodilators. VEGF also promotes vascular permeability and vasodilation in vivo. These pro-angiogenic roles of VEGF, and the mechanisms underlying them, are further discussed below.

In addition to its established role in the developing vascular system in the embryo, VEGF also functions in adult angiogenesis (Maharaj and D'Amore 2007). VEGF is required for angiogenesis during the menstrual cycle (Ferrara *et al.* 1998) and wound healing (Nissen *et al.* 1998). VEGF is also involved in pathological angiogenesis, such as tumour vascularisation – pathological angiogenic effects of VEGF are discussed later.

VEGF also affects a number of non-angiogenic physiological processes. Monocytes express VEGFR1, and VEGF acts as a monocyte chemoattractant (Barleon *et al.* 1996; Hiratsuka *et al.* 1998). Coupled with its role in increasing vascular permeability, these activities suggest a role for VEGF in inflammation – indeed monocyte-produced VEGF may be a key factor promoting influx of plasma proteins into injured sites.

VEGF stimulates endothelial release of NO and prostacyclin, which in vivo would subsequently act to cause vasodilation and reduce blood pressure, and also inhibit platelet aggregation (Wheeler-Jones *et al.* 1997; Laitinen *et al.* 1997). It has been proposed that low levels of VEGF protect the adult vasculature partly via NO and prostacyclin production (Zachary *et al.* 2000). Common side effects of anti-VEGF therapies (e.g. Bevacizumab, discussed in section 1.4.5) include bleeding, oedema, unwanted clotting and especially hypertension (Kamba and McDonald 2007), suggesting that VEGF does indeed play a role in protecting the adult vasculature. Furthermore, most mice with an endothelial-specific VEGF knockout survive to birth but show progressive endothelial degeneration with half dying before 25 weeks of post-natal life (Lee *et al.* 2007). Taken together, these findings indicate an important continuing role for VEGF-A in adult vascular homeostasis.

A role for VEGF in neuroprotection (and other aspects of the nervous system including axonal outgrowth, Sondell *et al.* 2000) has been noted. While this may partially occur via regulation of neural vascularisation or maintenance of the neural vasculature, VEGF acts as a direct pro-survival factor for cultured neurons (Oosthuyse *et al.* 2001), and loss of VEGF isoforms showed a defect similar to that observed in patients with amyotrophic lateral sclerosis (ALS), an adult-onset motor neuron disease. Furthermore, virus-mediated overexpression of VEGF in muscles of mice

with experimental ALS reduced disease symptoms and improved survival (Azzouz *et al.* 2004), suggesting that VEGF-dependent neuroprotection is biologically relevant.

1.4.4.2 Principles of VEGF signal transduction

The basic paradigm for VEGF receptor signal transduction is thought to be the same as for other receptor tyrosine kinases (RTKs) such as the receptors for PDGF, FGF, epidermal growth factor, insulin-like growth factor, insulin, and nerve growth factor (reviewed by Olsson *et al.* 2006, summarised in figure 1.5). VEGF dimers bind to receptor molecules at the cell surface, promoting receptor dimerisation and activation, bringing the tyrosine kinase domains of the receptor monomers into contact and leading to transautophosphorylation of the receptor at Tyr residues – that is, one receptor molecule phosphorylates the other and vice versa. Other proteins containing phosphotyrosine binding motifs (e.g. SH2 domains) are then able to bind the VEGF receptor, and either diffuse to other cellular locations or recruit other enzymes to transduce the downstream signal.

Evidence is emerging that this view of VEGF signalling may not be entirely accurate. VEGF preferentially binds to pre-dimerised VEGFR2 (Fuh *et al.* 1998), implying that it is the conformational change in the receptor dimer on VEGF binding rather than VEGF-induced receptor dimerisation per se that is responsible for initiation of the downstream signal.

In common with other RTKs, VEGFR2 is ubiquitinated and internalised into endosomes on VEGF binding – this internalisation does not terminate its signalling (Duval *et al.* 2003; Lampugnani *et al.* 2006, reviewed by Mukherjee *et al.* 2006). Endosomal VEGFR2 may be degraded by a lysosomal pathway (resulting in the observed reduction in VEGFR2 protein levels on prolonged stimulation with VEGF, Ewan *et al.* 2006; Mittar *et al.* 2009), or could be dephosphorylated and recycled to the cell membrane. Significant proportions of both VEGFR1 and VEGFR2 have been reported to be present in the Golgi apparatus and endosomes respectively in unstimulated cells (Mittar *et al.* 2009; Gampel *et al.* 2006), and translocate to the cell surface on VEGF stimulation suggesting

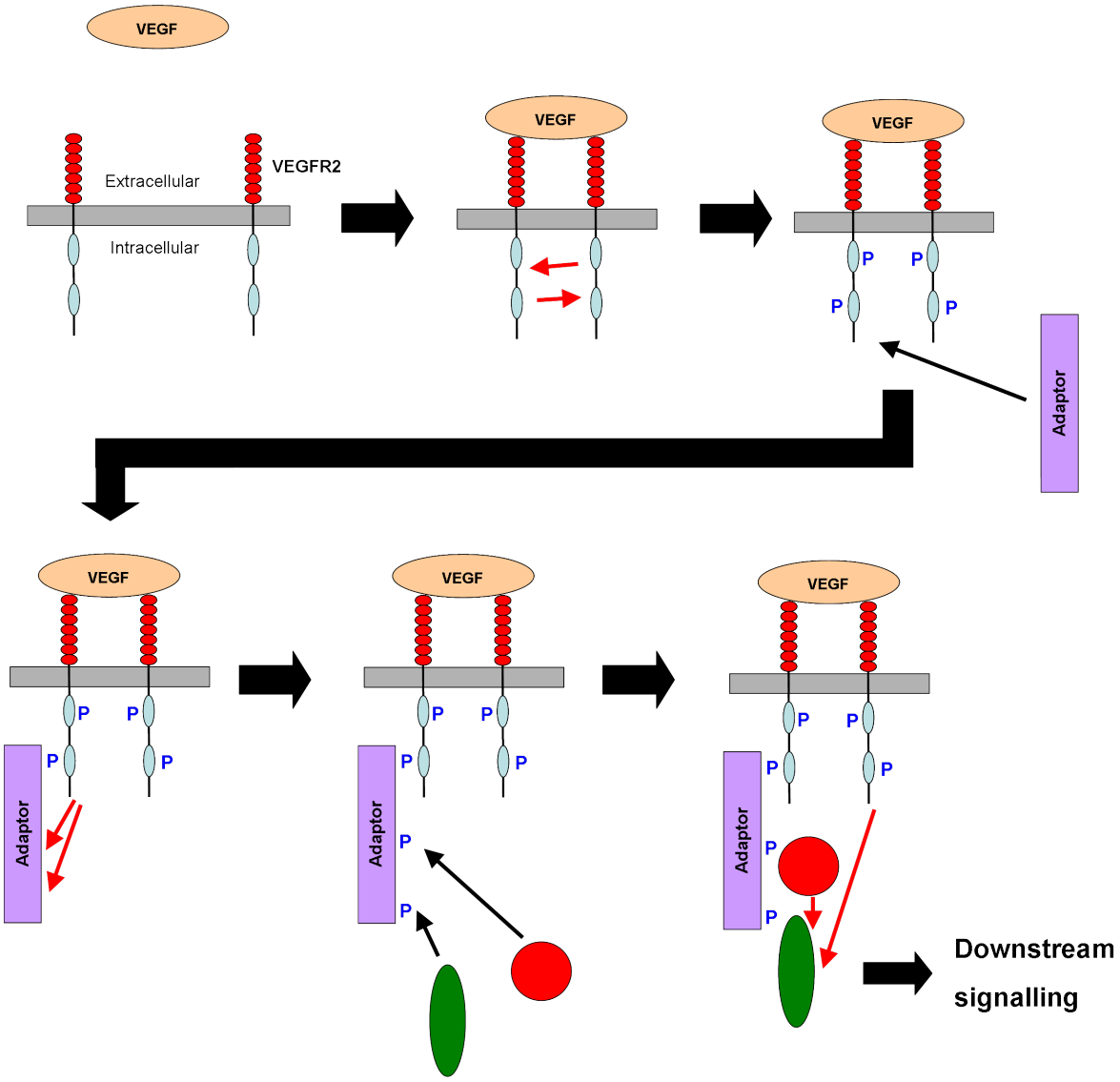

Figure 1.5: Model for the initiation of VEGF-stimulated signalling
Schematic illustration of the initiation of intracellular signalling as a consequence of VEGF binding to VEGFR2. Progression through the images is represented by thick black arrows. Thin black arrows indicate recruitment of another molecule. Thin red arrows indicate a phosphorylation event, with the added phosphate shown with a blue P. VEGF binding to VEGFR2 leads to autophosphorylation of VEGFR2 on tyrosine residues. Other proteins such as the adapator shown associate with phosphorylated VEGFR2 and may themselves become phosphorylated, providing new binding sites for other downstream signalling proteins such as those shown in red and green. These may also phosphorylate each other and diffuse to new cellular locations, initiating further signalling pathways.

that in addition to continual recycling, VEGF receptors may be stored in intracellular pools until needed.

The notion of VEGF as a molecule which acts purely by being released from cells and binding extracellularly to its receptor has also been challenged by work indicating that endothelial cells themselves produce VEGF, and that an autocrine intracellular VEGF signalling loop is required for endothelial survival and vascular maintenance (Lee *et al.* 2007).

VEGFR2, rather than VEGFR1, appears to be the key receptor transducing biologically-relevant VEGF signalling in endothelial cells. VEGF-stimulated proliferation and migration of PAE cells expressing VEGFR2 but not of cells expressing VEGFR1 (Waltenberger *et al.* 1994). siRNA-mediated knockdown of VEGFR2 was sufficient to reduce activation of major VEGF-regulated signalling pathways (Kou *et al.* 2005). Mutated forms of VEGF with reduced binding for the different VEGF receptors has also been used to probe the signalling mediated by different receptors. VEGFR2-specific ligands, but not VEGFR1-specific ligands, stimulated increases in endothelial survival (Gerber *et al.* 1998b), migration, permeability and in vivo angiogenesis (Gille *et al.* 2001), tubulogenesis in cultured ECs (Yang *et al.* 2001), and changes in gene expression (Yang *et al.* 2002).

It is possible that VEGFR1 signalling enhances VEGFR2-mediated responses as, in a number of the studies mentioned above, the response to a VEGFR2-specific ligand was substantially lower than that for wild-type VEGF. This enhancement does not appear to be critical for VEGF angiogenic signalling, at least during embryogenesis, as the tyrosine kinase domain of VEGFR1 is not required for mouse development (Hiratsuka *et al.* 1998), indicating that RTK-type signalling by VEGFR1 is redundant for developmental angiogenesis. It is possible that non-RTK signalling by VEGFR1 may be important, such as phosphorylation of VEGFR1 by VEGFR2-activated kinases or VEGFR2 itself leading to recruitment of signalling proteins to VEGFR1. RTK-type signalling by VEGFR1 does appear to be important in some circumstances – vascular permeability increases stimulated by VEGF-F (which binds to VEGFR1 and weakly to VEGFR2, but

not to NRP1 or VEGFR3) are strongly reduced in mice lacking the VEGFR1 tyrosine kinase domain (Takahashi *et al.* 2004). However, in the same study VEGF-stimulated vascular permeability was much less affected, suggesting that VEGFR1-mediated signals are less important for native VEGF. Overall, it appears that in endothelial cells VEGFR2-mediated signals are essential for most VEGF-stimulated biological processes, whereas VEGFR1-mediated signals are redundant but may increase the VEGF response in some processes.

Tyrosine phosphorylation of multiple SH2 domain-containing proteins is observed in response to VEGF treatment of ECs (Guo *et al.* 1995). Originally identified in the non-receptor tyrosine kinase src, SH2 domains bind to particular regions of proteins containing phosphorylated Tyr (pY) residues (Machida and Mayer 2005). Some of these SH2 domain-containing proteins may bind to pY on the VEGF receptor and be directly phosphorylated by the kinase domain of VEGFR2, whereas others may be phosphorylated by other enzymes as both enzyme and substrate associate at the VEGF receptor complex. Some of the pY-containing proteins are adaptor proteins, not catalytically active themselves but becoming phosphorylated on tyrosine residues and allowing other SH2 domain-containing proteins to join the VEGF receptor complex. For example, the adaptor proteins Grb2, Nck, Shc and Sck have been shown to be recruited to tyrosine-phosphorylated VEGFR2 and become tyrosine phosphorylated themselves (Kroll and Waltenberger 1997; Ratcliffe *et al.* 2002). Others are enzymes, directly activating signalling cascades. Some of these signalling cascades are activated in many cell types in response to a wide variety of stimuli, and it is likely that it is the spectrum of pathways activated, their degree of activation, and the spatio-temporal characteristics of activation of a combination of pathways that are specific to an individual cytokine and are required to elicit a particular cellular response.

1.4.4.3 Major VEGF-activated signalling cascades

The enzymes discussed below are important nodes in many signalling pathways activated by VEGF in endothelial cells. These pathways are summarised in figure 1.6.

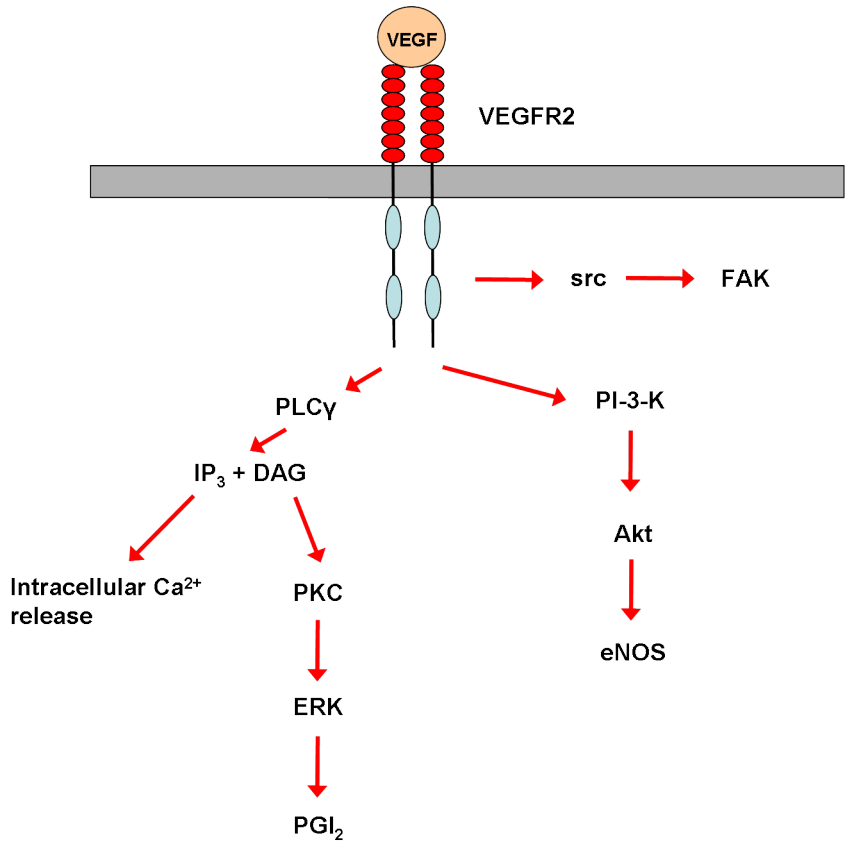

Figure 1.6: VEGF-activated signalling pathways
Schematic illustration of some of the major intracellular signalling pathways activated by VEGF in endothelial cells. See text and abbreviations for further details.

Phospholipase Cγ (PLCγ) is an SH2 domain-containing protein which binds directly to VEGFR2 pY1175, becoming tyrosine phosphorylated and activated. Adenovirus-mediated overexpression of a VEGFR2 Y1175F mutant prevented PLCγ activation (Takahashi *et al.* 2001). Activated PLCγ generates diacylglycerol (DAG) and inositol-1,4,5-triphosphate (IP_3) from the membrane lipid phosphatidylinositol-4,5-diphosphate (PIP_2). IP_3 releases Ca^{2+} from intracellular stores such as the endoplasmic reticulum, whereas DAG goes on to activate protein kinase C (PKC) isoforms and subsequently the Raf1-MEK-ERK mitogen-activated protein kinase cascade (Takahashi *et al.* 1999b, 2001; Gliki *et al.* 2001). This method of ERK activation is unusual – ERK activation by other RTKs occurs via binding of the adaptor protein Grb2 to the RTK, leading to activation of the guanine exchange factor Son of Sevenless, activation of Ras followed by activation of Raf1. PKCδ has been reported to be involved in ERK activation in vascular endothelial cells (Gliki *et al.* 2001). PKC is also involved in activation of protein kinase D (PKD). The PKC and PKD families

and their role in vascular endothelial cells is further discussed in sections 1.6.2 and 1.6.3.

Phosphoinositide 3'-kinase (PI-3-K) is another important signalling protein in vascular endothelial cells. VEGF stimulates tyrosine phosphorylation of the regulatory (p85) subunit of PI-3-K, releasing the catalytic p110 subunit (Thakker *et al.* 1999). p85 associates directly with VEGFR2, with phosphorylation of Y801 and Y1175 of VEGFR2 appearing necessary for this interaction (Dayanir *et al.* 2001). p110 phosphorylates the membrane lipid phosphatidylinositol-4,5-bisphosphosphate (PIP_2) to phosphatidylinositol-3,4,5-trisphosphosphate (PIP_3). Akt/PKB directly binds PIP_3 via its pleckstrin homology (PH) domain, so being recruited to the plasma membrane. Phosphoinositide-dependent kinase 1 (PDK1) also contains a PH domain and is similarly recruited to the membrane, where it phosphorylates and activates another kinase, Akt. Although there are multiple isoforms of PI-3-K, only p110α forms are required for angiogenesis (Graupera *et al.* 2008).

Src (also termed c-Src) is a tyrosine kinase involved in a variety of cellular processes. Src is covalently linked to a fatty acid, which targets it to the cytoplasmic face of the plasma membrane in a conformation in which the SH2 domain is bound to a C-terminal pY residue. During activation, the C-terminal pY residue is dephosphorylated, releasing the SH2 domain. Full activation occurs when the src SH3 domain binds to the proline-rich region of an activating ligand. Src has been shown to associate with VEGFR2 on VEGF stimulation of ECs (He *et al.* 1999).

VEGF increases cytosolic Ca^{2+} concentrations, causing an initial spike and then maintaining a lower but elevated plateau (Brock *et al.* 1991; Gliki *et al.* 2001), and this process can be inhibited by an antibody directed against the extracellular domain of VEGFR2 (Cunningham *et al.* 1999). The initial spike is due to IP_3-mediated release of Ca^{2+} from intracellular stores such as the endoplasmic reticulum, whereas the elevated plateau is probably dependent on extracellular Ca^{2+} entry through plasma membrane Ca^{2+} channels (Gliki *et al.* 2001; Jia *et al.* 2004). Overexpression of inactive transient receptor potential cation channel 6 inhibited VEGF-stimulated increases in intracellular Ca^{2+} concentration in microvascular ECs (Hamdollah Zadeh *et al.* 2008), indicating this may be the key plasma membrane Ca^{2+} channel family activated by VEGF.

VEGF increases endothelial production of the vasoactive molecules NO (van der Zee *et al.* 1997; Laitinen *et al.* 1997) and PGI_2 (Wheeler-Jones *et al.* 1997). NO plays an important role in VEGF-specific angiogenic pathways, as NOS inhibitors blocked VEGF- but not FGF-stimulated angiogenesis (Ziche *et al.* 1997). VEGF induces sustained eNOS activation in ECs via PI-3-K dependent Akt-catalysed phosphorylation of eNOS at S1177, the same site phosphorylated in response to shear stress (Dimmeler *et al.* 1999). Phosphorylation of this site renders eNOS active at resting Ca^{2+} concentrations. VEGF also promotes long-term NO production by inducing expression of both eNOS and the high-activity isoform iNOS (Kroll and Waltenberger 1998). Short-term (less than 10 mins after VEGF administration) NO production is independent of PI-3K, and may involve VEGF-stimulated Ca^{2+} mobilisation (Gelinas *et al.* 2002). VEGF-stimulated PGI_2 production in ECs involves PKC- and ERK-mediated activation of cytosolic phospholipase 2, and also required intracellular Ca^{2+} (Gliki *et al.* 2001; Wheeler-Jones *et al.* 1997).

It should be noted that differing reports exist in the literature regarding the involvement of particular enzymes in various signalling and functional responses, and this may be related to the importance and/or activation status of different enzymes in different assays and cell types. Many earlier studies relied on the use of a single inhibitor to demonstrate the involvement of a particular protein in a signalling pathway, and more recent large-scale target screening has shown that many inhibitors previously assumed to be specific have multiple targets, and with greater effects on 'off-target' enzymes greater than that on the 'specific' target (Davies *et al.* 2000; Bain *et al.* 2003, 2007). However even when studies have used the same inhibitors, cell type, assay and endpoint, conflicting results have been obtained, for example, in work regarding the involvement of PI-3-K in VEGF-stimulated cell migration (discussed below). It is difficult to say why this is so, but differences in cell batch or source, culture techniques, culture substrate (e.g. coating used for cultureware) and other factors frequently not reported in papers may be important.

In complex processes such as cell migration, a large number of specific actions are required to produce a coordinated biological response. The signalling in such multi-faceted processes is likely

to be complex, and inhibition or loss of any of the factors involved would retard the response if the inhibition was complete enough to make the affected factor rate-limiting for the overall response. The better-characterised signals impinging on each response are discussed below, concentrating on cell migration and survival.

1.4.4.4 Cell migration

Endothelial cell migration is a multi-faceted process, driven by actin polymerisation at the leading edge of the cell (Lee *et al.* 1996) and involving cycles of adhesion and release from the extracellular matrix, and requires activation of multiple signal transduction pathways. In culture, VEGF acts as a chemoattractant for ECs (Rousseau *et al.* 1997; Jia *et al.* 2004) and PAE cells transfected with VEGFR2 (Waltenberger *et al.* 1994). Protrusion of the leading edge of the cell via actin polymerisation, coordinated lengthening and shortening of the cell via actin filaments (stress fibres), and formation and release of focal adhesions are thought to be responsible for the migration of endothelial cells towards VEGF (Rousseau *et al.* 2000a). The effect of the enzymes discussed in this section on VEGF-stimulated migration is illustrated in figure 1.7. In vivo, endothelial cells are surrounded by extracellular matrix and must proteolytically digest a path to allow subsequent cell movement. VEGF induces expression of both matrix metalloproteases (MMPs) and plasminogen activators, both of which may contribute to this process (Lamoreaux *et al.* 1998; Pepper *et al.* 1991).

Endothelial cells interact with the extracellular matrix (ECM) via focal adhesions, which are also connected to the EC actin cytoskeleton. VEGF stimulates src-mediated phosphorylation of focal adhesion kinase (FAK) at Y861 and its subsequent recruitment to focal adhesions (Abu-Ghazaleh *et al.* 2001). Activation of focal adhesion kinase (FAK) is required for VEGF-driven chemotaxis, and requires Hsp90 (Rousseau *et al.* 2000b). Hsp90 associates directly with the intracellular domain of VEGFR2, and this association is required for FAK activation (Le Boeuf *et al.* 2004). This same study also implicated Hsp90 in RhoA-mediated FAK activation in response to VEGF. Cells

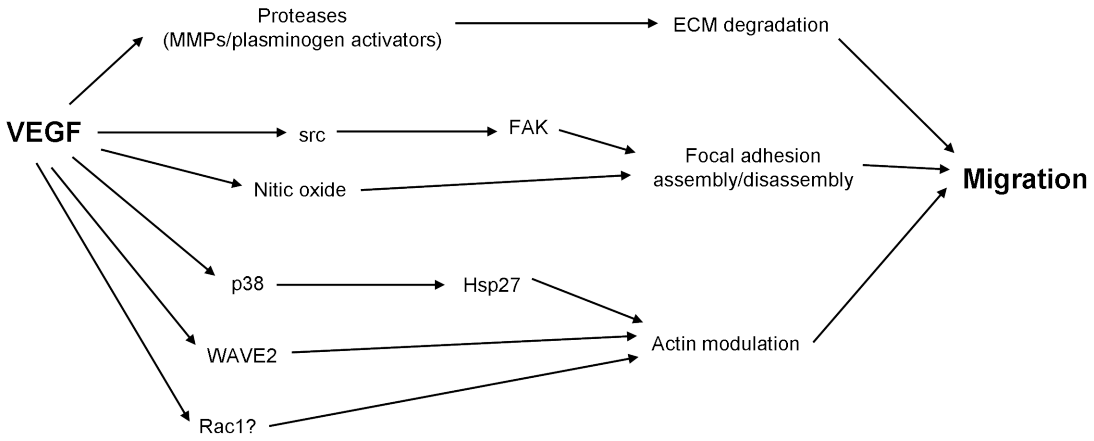

Figure 1.7: Involvement of some signalling pathways in VEGF-stimulated cell migration
Summary of some of the signalling pathways discussed in the text as contributing to VEGF-stimulated endothelial cell migration

from FAK-null mice show an increased number of focal adhesions but reduced motility (Ilic *et al.* 1995), suggesting that FAK may be particularly important in the disassembly of focal adhesions required for ECM de-adhesion during migration. NO also interferes with focal adhesion formation (Goligorsky *et al.* 1999), and VEGF-stimulated EC migration required phosphorylation of eNOS at S1177 (Dimmeler *et al.* 2000), indicating that NO may be important in the release of cell/substrate de-adhesion.

In addition to effects at focal adhesions, VEGF activates a number of modulators of the actin cytoskeleton which are involved in the actin remodelling required for cell migration. The adaptor protein IQGAP1 associates with phosphorylated VEGFR2 and activates the small GTPase Rac1 by inhibiting its intrinsic GTPase activity (Yamaoka-Tojo *et al.* 2004). Rac1 has been shown in fibroblasts to induce formation of lamellipodia. WAVE2 is also involved in VEGF-induced actin reorganisation, and endothelial cells lacking WAVE2 showed severely reduced lamellipodia formation in response to VEGF (Yamazaki *et al.* 2003).

Two other adaptor proteins, TSAd and Shb, are reported to associate with VEGFR2 and promote endothelial cell migration (Holmqvist *et al.* 2004; Matsumoto *et al.* 2005). SiRNA-mediated Shb knockdown reduced VEGF-induced phosphorylation of FAK and PI-3-K, and these effects may be responsible for the effects of Shb loss on migration

p38 MAPK has been implicated as a key enzyme in control of the actin cytoskeleton, the effects of which have been suggested to be mediated by phosphorylation of the small heat shock protein Hsp27 (discussed later). Overexpression of constitutively active MEK6, an upstream activator of p38 MAPK, in HUVECs activated p38 MAPK, induced lamellipodia and stress fibre formation and increased endothelial cell migration even in the absence of growth factor stimulation (McMullen *et al.* 2005). In the same study, co-transfection of cells with inactive p38α or unphosphorylatable Hsp27 prevented the MEK6-induced increase in migration.

p38 MAPK activity has been implicated in migration of ECs stimulated by VEGF or oestrogen. VEGF-induced HUVEC migration in transwell assays was inhibited by pre-treatment with the pharmacological p38 MAPK inhibitor SB203580 (Rousseau *et al.* 1997; McMullen *et al.* 2004) or adenovirus-mediated overexpression of inactive p38 MAPK (McMullen *et al.* 2004). Oestrogen-dependent migration of bovine aortic endothelial cells was reduced by overexpression of inactive p38 MAPK, inactive MAPKAPK2 or p38 MAPK inhibition by SB203580 (Razandi *et al.* 2000). Taken together, it seems that p38 MAPK may be a general cytoskeletal regulator and its involvement in migration may not be specific to VEGF signalling.

1.4.4.5 Cell survival

1.4.4.5.1 Overview of apoptosis

Apoptosis is a controlled, ATP-dependent process where the cell follows a particular death programme to die without rupture of the cell, thus preventing uncontrolled release of cytokines, enzymes and other cellular constituents which could adversely affect neighbouring cells. In vivo, apoptotic cells can then be phagocytosed intact by neighbouring cells (e.g. immune cells).

Characteristic hallmarks of apoptosis include cytoplasmic shrinkage, membrane blebbing, cleavage of DNA into 50–200 kb sections, appearance of phosphatidylserine in the outer leaflet of the plasma membrane, and caspase-mediated protein degradation (Saraste and Pulkki 2000). Effector caspase-mediated events are responsible for the hallmarks of apoptosis, such as activation of

endonucleases (DNA fragmentation) and cleavage of nuclear envelope proteins (nuclear condensation).

Apoptosis can proceed via two distinct modes: the extrinsic and intrinsic pathways, which both ultimately lead to activation of effector caspases, including the key apoptosis inducer, caspase 3 (reviewed by Green 2005, and Chaudhuri and Paul 2006). The intrinsic apoptotic pathway is regulated by the balance between the pro- and anti-apoptotic proteins of the Bcl2 family. Activation of the intrinsic pathway involves proteolytic cleavage of cytosolic proteins Bid or Bim, which then insert into the mitochondrial membrane and bind to Bax or Bak. Bax/Bak then dimerises and promotes release of various proteins from the mitochondria into the cytosol, including cytochrome C (CytC), which induces oligomerisation of apoptosis protease activation factor-1 (APAF1), leading to activation of procaspase-9 and caspase-3.

The extrinsic apoptotic pathway involves the binding of extracellular ligands to TNF-family transmembrane receptors such as TNFR1 and Fas (also termed APO1/CD95). These receptors contain intracellular motifs termed death domains (DD) which interact with DDs on other proteins, and ligand binding to clustered receptors leads to recruitment of intracellular DD-containing proteins, e.g. Fas-associated DD protein (FADD) and TRADD (discussed later) resulting in the formation of a death-inducing signalling complex (DISC) and activation of procaspase-8 and caspase 3.

An additional Fas-mediated pathway has also been described, in which death-domain associated protein (daxx), rather than FADD, moves from the nucleus to the cytosol and binds to clustered Fas (Salomoni and Khelifi 2006). The mechanism by which daxx binding to Fas induces apoptosis is unclear, but may involve the interaction of daxx with the kinase Ask1, which has been implicated in sustained activation of p38 MAPK and JNK associated with apoptosis.

A number of anti-apoptotic proteins normally hold apoptosis in check. Bcl2, Bcl-XL and A1 inhibit Bax/Bak dimerisation and unwanted CytC release. Various inhibitor of apoptosis (IAP) proteins also directly inhibit caspases. The kinase Akt inhibits cytC release from mitochondria (Kennedy *et al.* 1999), and phosphorylates and inhibits the apoptosis-promoting forkhead tran-

scription factor FKHRL1 (Brunet *et al.* 1999) and Bad, preventing it from binding and so inactivating pro-survival Bcl2 family members (Datta *et al.* 1997).

1.4.4.5.2 VEGF stimulation of EC survival

VEGF is a survival factor for endothelial cells in culture, inhibiting apoptosis due to serum withdrawal (Gerber *et al.* 1998b), and also acts as a survival factor for newly-formed capillaries in vivo. Exposure of premature babies to hyperoxia causes retinal capillary regression via a reduction in VEGF expression (Alon *et al.* 1995; Meeson *et al.* 1999). In some vascular beds the continued presence of circulating VEGF in the adult is required to maintain endothelial health, for example administration of an anti-VEGF antibody caused death of kidney endothelium and associated renal dysfunction (Sugimoto *et al.* 2003), and a kidney podocyte-specific VEGF knockout caused peri-natal lethality (Eremina *et al.* 2003).

The fenestrated endothelium found in kidney vessels may be a special case – a general loss of capillaries on treatment with anti-VEGF therapies has not been reported. Retinal capillaries are resistant to the anti-VEGF aptamer Pegaptanib unless an anti-PDGF receptor antibody (which reduced pericyte coverage of vessels) was also administered (Jo *et al.* 2006), suggesting that coverage of vessels with peri-endothelial cells protects against VEGF withdrawal.

As discussed earlier, endothelial-produced VEGF is required for vessel maintenance, including maintenance of vessels covered with peri-endothelial cells (Lee *et al.* 2007). Interestingly, exogenous VEGF administration is unable to compensate for loss of endothelial-produced VEGF in endothelial survival, suggesting that an intracellular VEGF signalling loop may be important.

In common with other growth factors, activation of Akt is critically involved in VEGFR2-mediated survival effects on vascular endothelial cells (Gerber *et al.* 1998b). VEGF additionally promotes expression of a number of anti-apoptotic proteins including Bcl2, A1, and the IAPs survivin and X chromosome-linked IAP (Gerber *et al.* 1998a; Tran *et al.* 1999). The pro-survival effects of VEGF on apoptotic signalling pathways are summarised in figure 1.8.

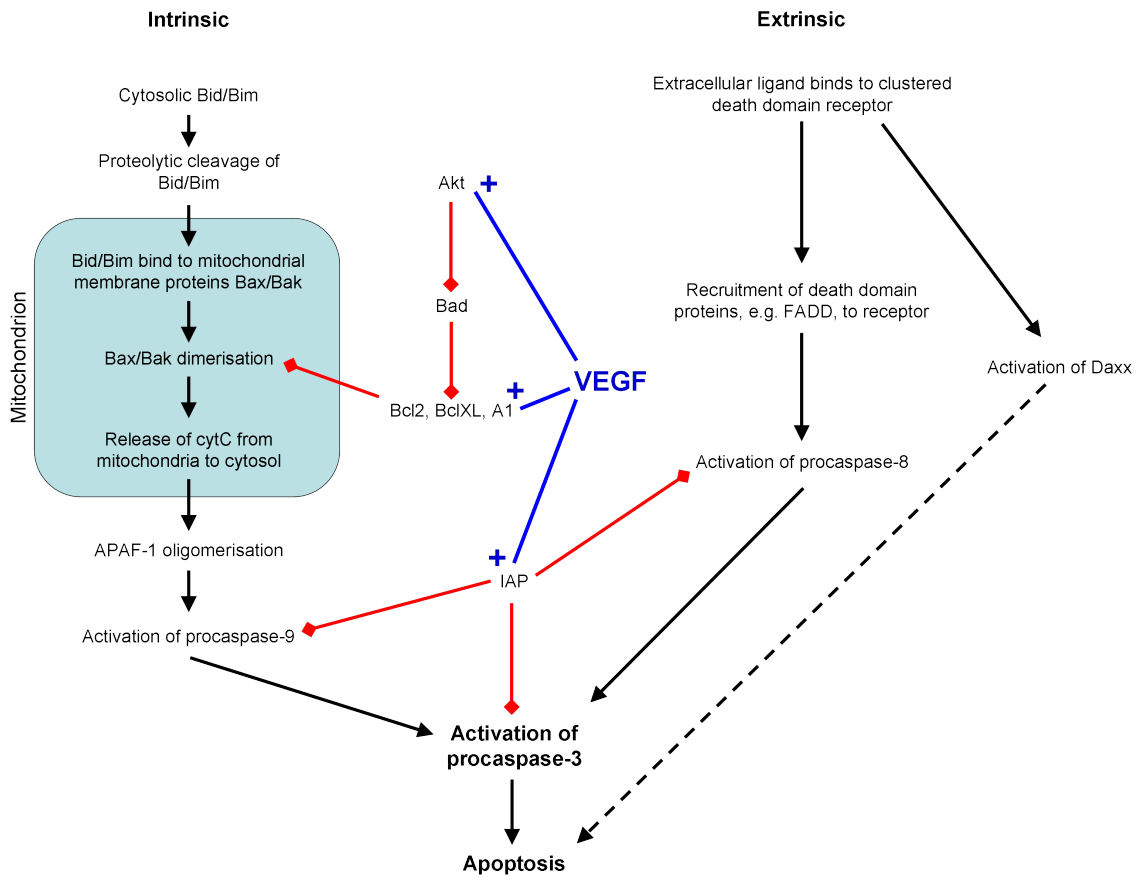

Figure 1.8: VEGF modulation of apoptosis signalling
Summary of apoptotic signalling, showing the anti-apoptotic effects of VEGF described in the text. Black arrows indicate the transition between steps in the pathways. Red diamond-tipped lines indicate inhibition of an apoptotic step by the indicated regulatory protein. VEGF either activates or increases the expression of various apoptotic modulators (indicated with plus-tipped blue lines), so inhibiting apoptosis. The dashed black arrow indicates that the mechanism by which Daxx stimulates apoptosis is not understood.

VEGF-dependent endothelial cell survival is dependent on VEGFR2, PI-3-K, and the adherens junction components VE-cadherin and β-catenin. Truncation of the cytoplasmic domain VE-cadherin prevented its interaction with β-catenin and also prevented VEGF-induced cell survival by reducing activation of PI-3-K and Akt (Carmeliet *et al.* 1999a). These data indicate that VEGF promotes survival in ECs with intact adherens junctions (i.e. cells that have made contact with another cell) but not in single isolated cells.

1.4.4.6 Proliferation

Transit through the cell cycle G1/S-phase checkpoint and subsequent DNA synthesis and mitosis requires the activity of cyclin-dependent kinase 4, which is activated by binding to cyclin D1.

Although control of the cell cycle is complex, the ERK and Akt pathways are commonly involved (reviewed by Shaw and Cantley 2006). Mitogenesis of many cells is regulated by the Raf1/MEK/ERK pathway, leading to activation of a number of transcription factors including c-myc and subsequent increased expression of cyclin D1. The PI-3-K/Akt pathway is another common regulator of the cell cycle, acting via glycogen synthase kinase 3 (GSK3). In unstimulated cells, GSK3 phosphorylates cell cycle regulators cyclinD1 and c-Myc, preventing DNA synthesis. Activated Akt phosphorylates and inhibits GSK3, allowing S-phase entry.

VEGF increases the proliferation of cultured ECs (Ferrara and Henzel 1989; Leung *et al.* 1989), though there is debate as to how effective a mitogen VEGF is.

Adenovirus-mediated overexpression of a VEGFR2 Y1175F mutant or microinjection of an anti-pY1175 antibody prevented VEGF-induced PLCγ tyrosine phosphorylation and DNA synthesis whereas overexpression of Y801F or Y1214F VEGFR2 mutants had no effect (Takahashi *et al.* 2001). Inhibitor studies showed that VEGF-stimulation of primary endothelial cell proliferation was blocked by inhibitors of MEK (Wu *et al.* 2000; Takahashi *et al.* 1999b; Yu and Sato 1999). PKC inhibition prevented HUVEC proliferation induced by VEGF but not EGF or FGF (Wu *et al.* 2000; Takahashi *et al.* 1999b). Treatment of ECs with PKC-activating phorbol esters was sufficient to stimulate DNA synthesis in the absence of VEGF (Takahashi *et al.* 1999b), suggesting that PKC activation may be of central importance in VEGF-stimulated proliferation. Together, these data suggest that PLCγ activation by VEGFR2 leads to cell proliferation via PKC-mediated activation of the Raf1/MEK/ERK cascade.

Data on the involvement of PI-3-K/Akt in proliferation is contradictory. Takahashi *et al.* (1999b) reported that two structurally distinct PI-3-K inhibitors, wortmannin and LY294002, did not effect VEGF-stimulated DNA synthesis in HUVECs. In contrast, Yu and Sato (1999) also working in HUVECs showed that VEGF-stimulated proliferation was inhibited by both wortmannin and LY294002. The reason for these differences is not clear. Similarly some studies have reported reductions in VEGF-stimulated ERK phosphorylation by PI-3-K inhibitors, suggesting that PI-3-

K may be involved in ERK regulation, whereas other studies using the same cell type and inhibitors showed no effect.

1.4.4.7 Vascular permeability

Enhancement of fluid leakage from capillaries was one of the first activities ascribed to VEGF (Senger *et al.* 1983, 1990). VEGF induces multiple permeability-enhancing changes in endothelial cells (reviewed by Bates and Harper 2002), and the most important adaptation depends on the affected vascular bed and other stimuli present. VEGF induces the formation of endothelial structures such as fenestrae (Roberts and Palade 1995; Esser *et al.* 1998b) and vesiculo-vacuolar organelles (Feng *et al.* 1996).

VEGF also increases paracellular permeability (Roberts and Palade 1995), adjusting the properties of endothelial cell–cell junction proteins. VEGF promotes phosphorylation of the tight junction proteins occludin and zonula occludens 1 (Antonetti *et al.* 1999), and other junctional components such as VE-cadherin and PECAM (Esser *et al.* 1998a). It is likely that these phosphorylations are involved in regulation of endothelial junction integrity.

Inhibitors of PI-3-K, PKC, ERK and eNOS reduced the VEGF-stimulated increase in permeability of capillaries to FITC-labelled dextran (Aramoto *et al.* 2004). Reduction of VEGF-stimulated albumin permeability by inhibitors of eNOS and PKC has also been shown by other groups (Wu *et al.* 1999; Murohara *et al.* 1998). Src is also involved, and VEGF-induced vessel permeability and angiogenesis was prevented in src-null mice (Eliceiri *et al.* 1999).

1.4.4.8 Vasodilation

VEGF increases vasodilation of arteries, mediated at least in part by NO and PGI_2 production and the subsequent effect of these two mediators on vascular smooth muscle (Ku *et al.* 1993; Li *et al.* 2002). Thus, the signalling pathways discussed above that are responsible for NO production (Akt, Ca^{2+}) are also important in VEGF-stimulated vasodilation (Aramoto *et al.* 2004). The

importance of VEGF-mediated vasodilation has been shown in clinical trials of the anti-VEGF antibody Becavizumab, which causes an increase in blood pressure (Jain *et al.* 2006).

1.4.5 VEGF, angiogenesis and disease

VEGF is a key stimulator of angiogenesis, and is a target of both pro- and anti-angiogenic therapeutic strategies.

Angiogenesis and VEGF have a key role in cancer progression. Tumour cells from a variety of sources produce VEGF (Senger *et al.* 1983), and an anti-VEGF monoclonal antibody was shown to reduce tumour vascularisation and growth when injected into mice (Kim *et al.* 1993). Without attracting blood vessel growth, tumours are unable to grow to a problematic size due to the limitations of obtaining nutrients via diffusion. The discovery of VEGF launched a huge effort to develop anti-VEGF therapies for the treatment of cancer, with a variety of agents produced including anti-VEGF antibodies, VEGF receptor tyrosine kinase inhibitors and aptamers. Bevacizumab (Avastin), a humanised anti-VEGF-A monoclonal antibody, received FDA approval in 2004 for treatment of colorectal cancer. A phase III trial showed that Bevacizumab slowed tumour growth and improved survival when used in combination with other chemotherapeutic agents (Hurwitz *et al.* 2004), and other trials have shown varying degrees of efficacy of Bevacizumab with different cancers (Jain *et al.* 2006).

There is considerable debate as to the mechanism of action of Bevacizumab. One proposed mode of action is that VEGF inhibition 'normalises' the tumour vasculature and reduces its permeability, thus having the dual effect of reducing oedema and interstitial fluid pressure, and producing a less chaotic and tortuous tumour vasculature, both of which allow more effective penetration of the tumour mass by cytotoxic drugs.

Anti-VEGF therapies do not cause a complete block on tumour angiogenesis, probably because other tumour-produced pro-angiogenic factors are also able to promote angiogenesis. Cells overexpressing VEGFs B and C (Salven *et al.* 1998), D and PlGF (Donnini *et al.* 1999) have been

isolated from tumours. Non-VEGF family factors such as FGF may also contribute. Additionally, anti-VEGF therapies can only reduce VEGF concentrations, not entirely eliminating it. As a result, anti-VEGF therapies tend to be used in combination with other drugs for cancer therapy.

VEGF-mediated angiogenesis is also involved in eye disease. Blood vessel growth in normal eyes is minimised, as the vessels interfere with vision. However growth of blood vessels into the eye with advancing age, and the leakage of fluid from these vessels, in particular in the retinal region around the optic nerve (the macula), termed wet age-related macular degeneration, is a common cause of blindness in older people. VEGF is synthesised by retinal epithelial cells (Adamis *et al.* 1993), and is overexpressed in retinopathies (Aiello *et al.* 1994).

Anti-VEGF therapies Pegaptanib (Macugen) and Ranibizumab (Lucentis) are FDA-approved for the treatment of age-related macular degeneration, working in part by preventing VEGF-stimulated blood vessel growth in the retina (Ciulla and Rosenfeld 2009). Pegaptanib (discovery and development reviewed by Ng *et al.* 2006) is an RNA aptamer – a oligonucleotide designed to bind proteins for a therapeutic purpose, whereas Ranibizumab is a fragment of the same antibody that Bevacizumab was developed from. Pegaptanib binds specifically to VEGF-A_{165}, whereas Ranibizumab and Bevacizumab bind to all VEGF-A isoforms. In clinical trials, both Pegaptanib and Ranibizumab have been shown to slow the onset of macular degeneration and in some patients improve visual performance (Gragoudas *et al.* 2004; Rosenfeld *et al.* 2006; Brown *et al.* 2006, reviewed in Ciulla and Rosenfeld 2009).

As discussed earlier, VEGF-reducing therapies suffer from a number of intrinsic problems due to loss of VEGF-dependent vascular protection, including bleeding, oedema, unwanted clotting and hypertension (Kamba and McDonald 2007).

In other pathologies, a pro-angiogenic strategy might be useful. Atherosclerosis leads to build-up of deposits on artery walls, narrowing the lumen of vessels and increasing their chance of blockage. Atherosclerosis of the coronary or cerebral arteries may lead to life-threatening events such as myocardial infarction or stroke. Stimulation of collateral vessel growth to bypass a vessel

narrowing is of major interest in treating conditions such as angina and peripheral vascular disease, and preventing heart attack.

VEGF may have a role in collateral growth under normal and ischaemic conditions (Rissanen *et al.* 2005; Clayton *et al.* 2008), and adenovirus-mediated overexpression of VEGF in skeletal muscle promotes capillary enlargement (Rissanen *et al.* 2003). However, in trials virus-mediated VEGF expression had little effect on patient outcomes in a variety of ischaemic diseases (for example Stewart *et al.* 2009, reviewed by Yla-Herttuala *et al.* 2007). This may be due to a number of factors, including insufficient VEGF delivery to the region of interest (largely countered using adenovirus vectors), inability to establish an appropriate spatially patterned concentration gradient (including effective VEGF concentrations), or other required angiogenic factors becoming limiting or out of balance when excess VEGF is present.

The possibility of conferring VEGF-expressing abilities on a benign tumour or cancerous cell, or increasing plasma VEGF concentrations resulting in undesirable angiogenesis or oedema, is a concern with strategies involving VEGF gene therapy.

1.5 Hsp27

Heat shock protein 27 (Hsp27) is a small heat shock protein implicated in a wide variety of cellular processes including cell migration and apoptosis. Phosphorylation of Hsp27 contributes to regulation of its structural organisation and functional properties, and can be stimulated by VEGF in endothelial cells. Thus Hsp27 is a potential mediator of VEGF-stimulated chemotactic and pro-survival signalling. Hsp27, its properties and role in the vasculature have been reviewed by Ferns *et al.* (2006).

After an initial description of the heat shock response, the phosphorylation of Hsp27 and its role in modulating Hsp27 is function is discussed, followed by the evidence for the involvement of Hsp27 in biological functions, particularly migration and survival, and the involvement of Hsp27

in disease.

1.5.1 Heat shock, the heat shock response and Hsps

1.5.1.1 Cellular consequences of heat shock

An increase in the ambient temperature experienced by an organism beyond the normal range experienced can disrupt protein structure and enzyme function, leading to a number of metabolic problems such as misfolding of proteins during synthesis (reviewed in Liberek *et al.* 2008). Misfolded proteins may be insoluble and precipitate within a cell, as hydrophobic sections of the protein (such as the internal residues of a globular protein) remain external in the misfolded protein and subsequently interact with other externally hydrophobic, misfolded proteins. A number of human diseases are due to abnormal protein folding including Creutzfeldt-Jakob disease, Parkinson's disease, Huntington's disease and Alzheimer's disease (Chiti and Dobson 2006). These diseases are neurodegenerative – the protein aggregates accumulate in the brain or nervous system. In these conditions, β-sheet-containing protein monomers stack up to form a fibril, termed a cross-beta filament or protofilament. A number of these filaments twist together to form amyloid fibrils, the constituent of the deposits found in these diseases.

1.5.1.2 The heat shock response

To counteract potential problems of protein misfolding during heat and other cellular stresses, cells have developed the heat shock response (HSR). The HSR is an evolutionarily conserved metabolic programme whereby an organism experiencing environmental stress such as heat shock – an increase in cellular temperature above that normal for the organism – rapidly increases the synthesis of a subset of proteins which help protect the cell from the environmental insult. Some of these proteins act as molecular chaperones – binding to external hydrophobic regions of misfolded proteins and aiding in their refolding. Others promote the degradation of proteins which cannot be correctly folded. Others directly protect the cell from apoptosis by interacting with the component

of the apoptotic pathways. Some proteins involved in the HSR perform more than one of these roles.

The HSR is the primary mechanism for dealing with misfolded proteins in the cytosol (Westerheide and Morimoto 2005) – a second mechanism, the unfolded protein response, handles misfolded proteins in the endoplasmic reticulum (Ron and Walter 2007). Despite the name, the HSR can be triggered by a variety of environmental stresses and although inducible, many of the proteins upregulated in the heat shock response are also present in unstressed cells and perform roles in normal cellular metabolism.

The HSR is primarily controlled by the transcription factor HSF1. A variety of cellular stresses (not just heat shock) causes HSF1 to trimerise, enter the nucleus and act as a transcription factor, binding to heat shock elements in the promoters of genes involved in the HSR and increasing their transcription. On heat shock, fibroblasts derived from wild-type or heterozygous mice rapidly increased the expression of the HSR proteins Hsp70 and Hsp27, but HSF1-null mice did not (McMillan *et al.* 1998). The details of how HSF1 is activated in response to cellular stress are not fully established, but may be related to the release of HSF1 from complexes with chaperone proteins when these chaperones are required by unfolded proteins, leaving HSF1 free to trimerise. Other factors in addition to HSF1 are involved in activating the HSR, as increases in expression of some genes are still observed in HSF1-null cells (Trinklein *et al.* 2004).

The protective nature of proteins upregulated in the heat shock response is believed to be responsible for thermotolerance: the phenomenon whereby an initial mild heat shock followed by a recovery period at normal temperature protects cells from a later severe heat shock which is lethal to non-preshocked cells. This is presumably because the initial heat shock induces the heat shock response, increasing the level of the protective proteins, which then protected the cell from the second heat shock. Cells which had not previously been exposed to a heat shock had lower starting levels of the protective proteins and were unable to synthesise them rapidly enough under the severe environmental conditions to protect the cell. HSF1-null fibroblasts, which do not induce

the HSR, do not exhibit thermotolerance (McMillan *et al.* 1998). As the heat shock response is able to protect against various environmental stresses, its manipulation has attracted interest in the treatment of conditions such as ischaemia-reperfusion injury. The involvement of Hsp27 in thermotolerance is discussed in section 1.5.2.2.

1.5.1.3 Heat shock proteins

Although all known organisms from bacteria to animal cells exhibit a heat shock response, exactly which proteins are upregulated varies between organisms. Some of the key proteins recognised to be transcriptionally upregulated during the heat shock response are termed the heat shock proteins (Hsps). Currently, two main classifications of mammalian Hsps have been recognised – the high molecular weight Hsps and the small Hsps (Lanneau *et al.* 2008).

The high molecular weight Hsps are ATP-dependent chaperones and include three major families: Hsp90, Hsp70 and Hsp60. Some members of these families are constitutively expressed, whereas others are inducible on heat shock. Although all display chaperone activity, the roles of these families are overlapping but distinct. Hsp90 associates with a variety of signalling-related proteins such as VEGFR2 (Le Boeuf *et al.* 2004) and eNOS, and is required for the activity of these proteins. Hsp70 has a variety of roles including aiding folding of newly translated proteins and assisting protein translocation across membranes.

Small Hsps are ATP-independent chaperones that form large oligomers (heat shock granules) in cells. Structurally, small Hsps contain an N-terminal region, a conserved 80–100 aa α-crystallin domain, and a C-terminal region. Current members of the mammalian small heat shock protein family are Hsp27/HspB1, HspB2, HspB3, α-A crystallin/HspB4, α-B crystallin/HspB5, Hsp20/HspB6, HspB7, Hsp22/HspB8, HspB9, HspB10 (Taylor and Benjamin 2005) and HspB11 (Bellyei *et al.* 2007). Hsp27, α-B-crystallin, Hsp20 and Hsp22 are widely expressed and heat-inducible, other members are restricted in their expression sites (e.g. to muscle, eye lens or testis) and so are unlikely to play general cellular roles. Hsp27 and α-B-crystallin (reviewed by Arrigo

et al. 2007) are the most-studied and best-characterised small Hsps.

Amino acid sequence alignment of human small Hsps reveals a reasonable degree of amino acid identity between most members in the α-crystallin domain (figure 1.9). Across many species, the amino acid sequence of the α-crystallin domain is variable at most positions, but always forms a β-sheet sandwich structure, composed of two layers of three and five antiparallel strands (Haslbeck *et al.* 2005).

Heat shock of vascular endothelial cells was reported to increase the synthesis of proteins with molecular weights of 99, 85, 72, 45 and 27 kDa, as determined by leucine radiolabelling (Darbon *et al.* 1990) and, although not identified in this study, the 27 kDa protein likely to be the small heat shock protein Hsp27. Later studies using proteomic analysis showed that ECs constitutively express a number of Hsps including Hsp27, Hsp90 and various members of the Hsp60 and Hsp70 families, and that expression of a number of these proteins (including Hsp27) was increased by cellular stresses including heat shock (Portig *et al.* 1996; Dreher *et al.* 1995; Wagner *et al.* 1999).

1.5.2 Hsp27 as a conserved small Hsp

Hsp27 (HspB1, mouse homologue known as Hsp25) is a highly conserved member of the mammalian small heat shock protein family, and constitutively expressed in a wide variety of human tissues including endothelial cells (Piotrowicz *et al.* 1995). Highly similar proteins are expressed in a variety of mammalian species, Xenopus and zebrafish, although the closest related proteins in lower organisms such as nematode worms and yeast, while similar to each other, are distinct from Hsp27 (figure 1.10). Human Hsp27 was originally cloned by Hickey *et al.* (1986), mouse Hsp25 was cloned by Gaestel *et al.* (1993). Hsp27 protein expression and phosphorylation is increased on heat shock (Arrigo and Welch 1987). The heat-induced increase in Hsp27 expression is HSF1-dependent, but basal expression is HSF1-independent (McMillan *et al.* 1998).

The C-terminal half of Hsp27 contains a large α-crystallin domain of approximately 100 aas. This domain is involved in protein-protein interactions, binding to another α-crystallin domain in a

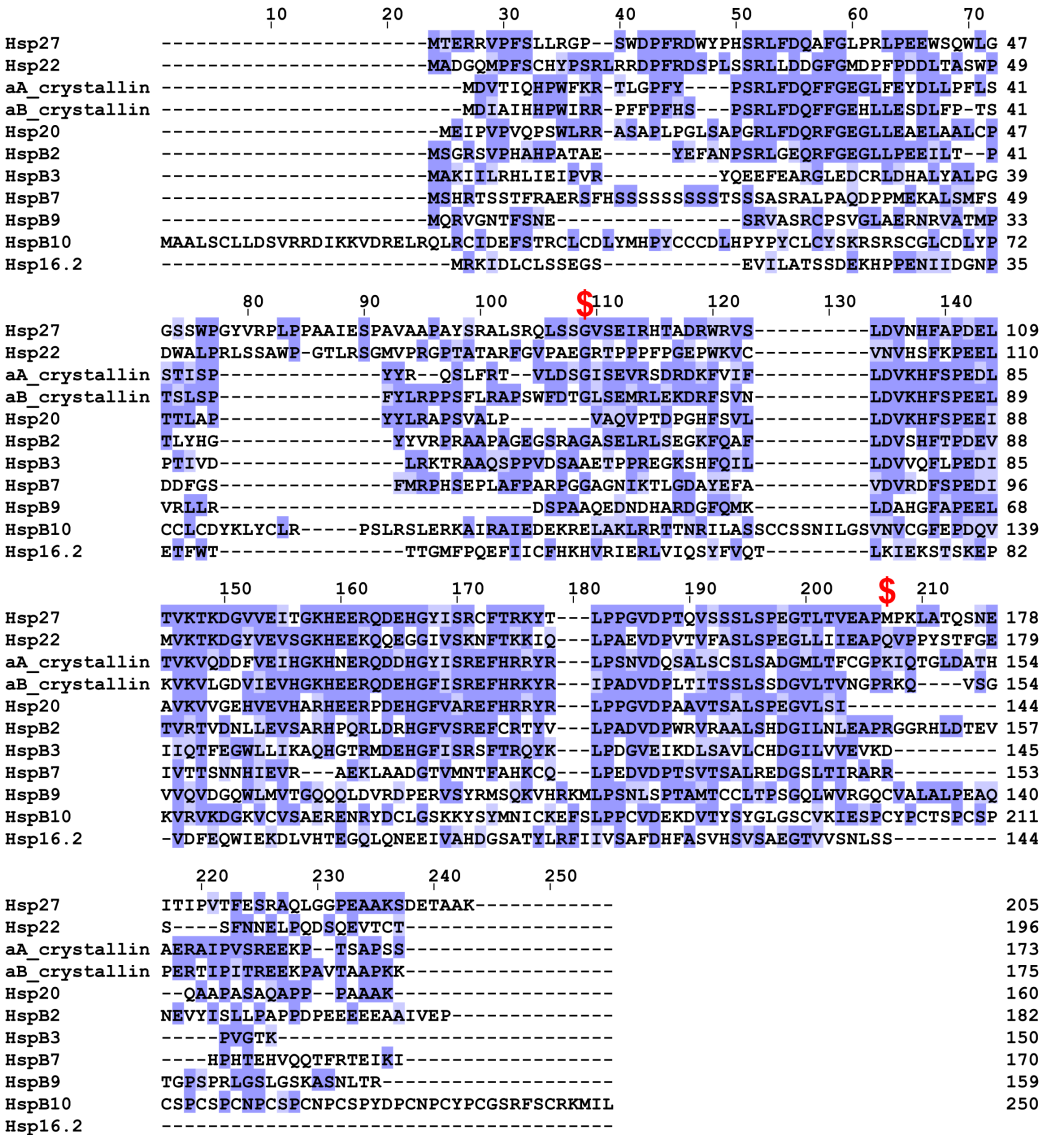

Figure 1.9: Amino acid sequence alignment of human small heat shock proteins
Reference protein sequences for human small heat shock proteins (HspB1–HspB11) were retrieved via Entrez Gene and aligned with Clustal X2. Residues are coloured according to Blossum62 score, with darker colours indicating better conservation. The first and last residues of the α-crystallin domain in Hsp27 (as reported in the RefSeq record) are indicated with a dollar sign ($). The RefSeq database accession numbers for the protein sequences used for alignment were: Hsp27 NP_001531.1; HspB2 NP_001532.1; HspB3 NP_006299.1; α-A-crystallin NP_000385.1; α-B-crystallin NP_001876.1; Hsp20 NP_653218.1; HspB7 NP_055239.1; Hsp22 NP_055180.1; HspB9 NP_149971.1; HspB10 NP_077721.2; HspB11 NP_057210.2.

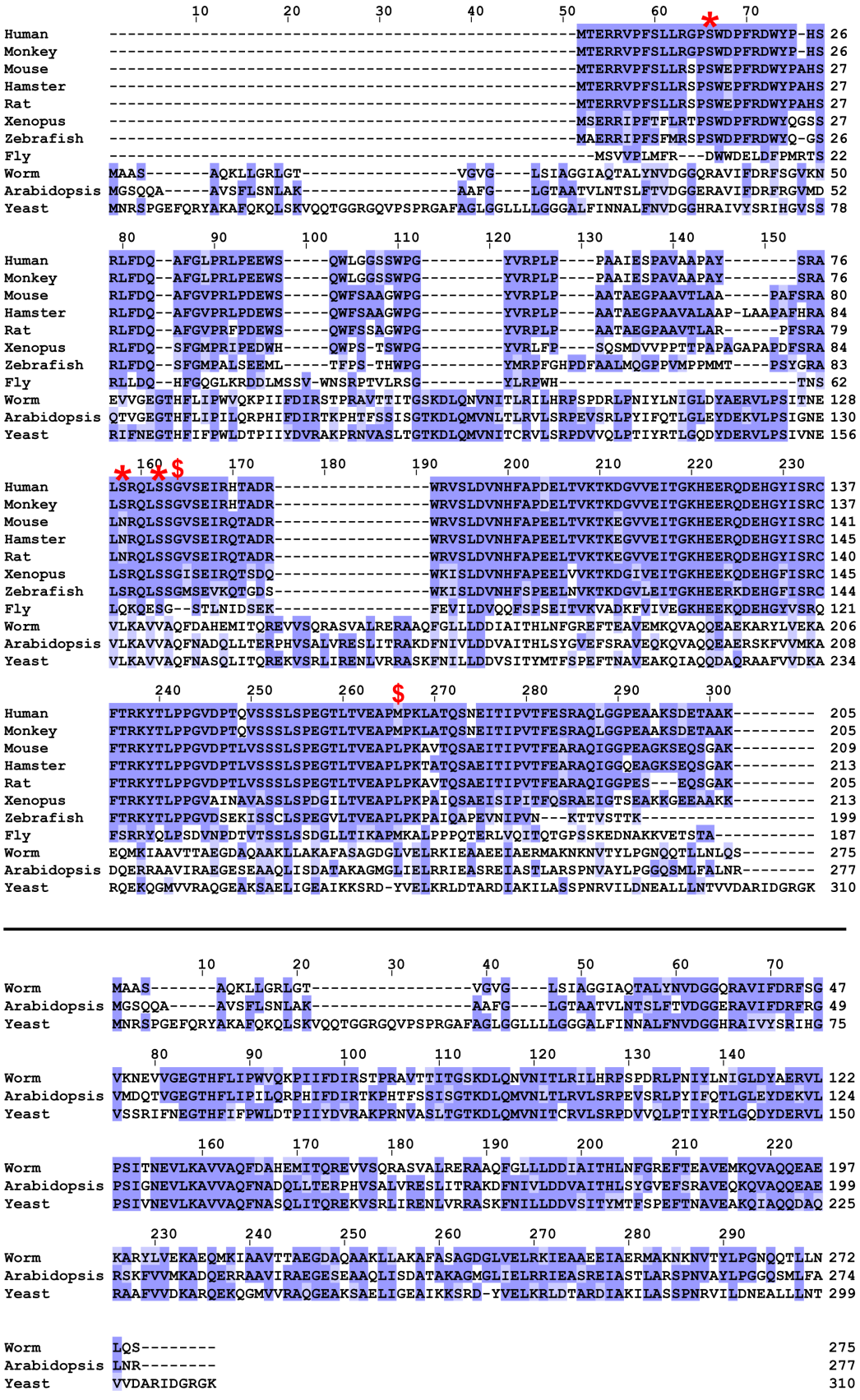

Figure 1.10: Amino acid sequence alignment of Hsp27 homologues in multiple species (legend overleaf)

Figure 1.10: Amino acid sequence alignment of Hsp27 homologues in multiple species (continued)
Upper: Amino acid sequences for proteins homologous to human Hsp27 were retrieved via Unigene, supplemented with HspB1 sequences for hamster and rat retrieved via Entrez Gene, and aligned with Clustal X2. Residues are coloured according to Blossum62 score, with darker colours indicating better conservation. The first and last residues of the α-crystallin domain in human Hsp27 (as reported in the RefSeq record) are indicated with a dollar sign ($). The location of the human Hsp27 phosphorylation sites (S15, S78, S82) are indicated with an asterisk (*). The RefSeq database accession numbers for the protein sequences used for alignment were: Human NP_001531.1; Monkey XP_001109274.1; Mouse NP_038588.2; Rat NP_114176.3; Xenopus NP_001087285.1 ; Zebrafish NP_001008615.1; Fly NP_523827.1; Worm NP_490929.1; Arabidopsis NP_198893.1; Yeast NP_011747.2. The GenBank accession number for the non-Refseq hamster sequence was P15991.1.
Lower: ClustalX2 alignment of the worm, Arabidopsis and yeast sequences from above. These three sequences, though dissimilar to human Hsp27, are similar to one another.

separate molecule and leading to the formation of Hsp27 dimers (discussed in section 1.5.4.1).

1.5.2.1 Role of Hsp27 in development

Hsp25-null mice have been generated by replacement of the coding sequence of mouse HspB1 (Hsp25) with a lacZ reporter gene (Huang *et al.* 2007). Hsp25-null mice were viable, fertile and exhibited no apparent morphological abnormalities (monitored for one year after birth), indicating that any roles of Hsp25 in development are redundant. Examining heterozygous animals, which express both normal Hsp25 and LacZ under control of the Hsp27 promoter, β-galactosidase activity was first observed at E8.5 in the cardiac region, and was evident in the developing vascular system at E10.5. Generally, Hsp25 was widely expressed in both embryonic and adult mice, increasing during development, with adult expression most prominent in the musculature. High muscular expression of Hsp25 had previously been reported (Gernold *et al.* 1993).

Similar to humans, mice contain at least ten small Hsp genes and it is possible that some functions of Hsp25 may go unnoticed due to compensation by other sHsp proteins. However, Huang *et al.* (2007) examined the expression of other sHsps at the mRNA level in a number of muscles, and other Hsps (e.g. Hsp70, Hsp60, Hsp90) at the protein level in a wider variety of tissues, and did not observe any differences in expression of other Hsp proteins between Hsp25-null and wild-type

mice.

1.5.2.2 Involvement of Hsp27 in thermotolerance

Along with other Hsps, Hsp27 expression increases after mild heat shock and is correlated with the development of a thermotolerant phenotype. The first direct evidence of a protective role for Hsp27 came from work by Landry *et al.* (1989), who showed dramatically increased survival, determined by colony forming ability after heat shock, in hamster or mouse cell lines stably overexpressing human Hsp27 after exposure a heat stress lethal to control transfectants. In this study, whereas overexpression of Hsp27 under its own promoter (giving both constitutive and heat-inducible expression) was protective against usually lethal heat shock, transfection with Hsp27 under the control of an Hsp70 promoter (giving heat-inducible but little constitutive expression) was not, indicating that elevated Hsp27 protein levels may be required at the time of heat challenge.

This question was addressed by Lavoie *et al.* (1993a), who transfected the mouse cell line NIH3T3 with a construct containing the human Hsp27 coding sequence fused to a metallothionin promoter, allowing induction of Hsp27 expression by addition of low concentrations of cadmium chloride which did not detectably increase expression of other heat shock proteins. Cadmium chloride pre-treatment of the cells increased survival of a subsequent severe heat shock. Taken together, these and a number of other studies have shown that overexpression of Hsp27, simulating upregulation of Hsp27 by sub-lethal heat shock, improves cell survival in response to a normally lethal heat shock or other cellular stress.

Further evidence of the importance of Hsp27 in thermotolerance comes from studies in a fibroblast line established from Hsp25-null mouse embryos (Huang *et al.* 2007). Hsp25-null fibroblasts developed a lower degree of thermotolerance (less cells survived a severe heat shock after an earlier mild heat shock) than control cells, indicating that this function of Hsp25 is not fully compensated for by other heat shock proteins. Fibroblasts from Hsp70-null embryos also showed impaired thermotolerance similar to those obtained from Hsp27-null embryos. Interestingly, fibroblasts

derived from Hsp27/Hsp70 double-null embryos showed a further lowering of the thermotolerance response, beyond that observed with either single knockout with survival similar to that for cells not previously exposed to mild heat shock (the survival status at birth etc of Hsp27/Hsp70-double null mice was not reported). Thus it appears that Hsp25 and Hsp70 are key proteins involved in the quantitatively most important processes in the acquisition of thermotolerance, and seem to have some distinct functions in thermotolerance acquisition due to the lack of full compensation of their functions.

In addition to protection against heat-induced cellular injury, enhanced expression of Hsp27 has been shown in to be protective (i.e. increased viability of cells after stress) against cell death due to oxidative stress (e.g. H_2O_2) and TNFα (Mehlen *et al.* 1996a), radiation, serum starvation (Garrido *et al.* 1998), Fas ligand (Mehlen *et al.* 1996b), and anti-cancer drugs (Garrido *et al.* 1997). In endothelial cells, overexpression of Hsp27 can protect from apoptosis induced by hypoxia/reoxygenation (Kabakov *et al.* 2003). However, Hsp25-null transformed mouse fibroblasts showed similar susceptibility to cell death induced by etoposide, which induces double-strand DNA breaks, X-rays, serum starvation or oxidative stress (Huang *et al.* 2007). Given the importance of Hsp25 in thermotolerance, it appears that the importance of Hsp27 in survival of cellular stresses may be dependent on the particular stress employed. Hsp25 does not have a non-redundant role in protection against all stresses or under basal conditions, although this does not preclude the notion that increased expression or post-translational modification of Hsp25 might result in enhanced protection from some of these stresses.

Hsp27 is a multi-functional protein, acting as a molecular chaperone, modulator of apoptosis signalling and regulator of the actin cytoskeleton (discussed below). While it is likely that these properties contribute to the protective effect of Hsp27, the relative contribution of each individual property is unknown and may vary depending on the nature of the cellular stress involved.

1.5.3 Phosphorylation of Hsp27

Initial studies of heat shock proteins in endothelial cells indicated that heat shock, phorbol ester and arsenite could increase the phosphorylation of an $\sim$27 kDa protein whose synthesis was increased on heat shock (Robaye *et al.* 1989; Darbon *et al.* 1990; Santell *et al.* 1992). Phosphorylation sites were initially identified by chromatographic examination of tryptic peptides containing radiolabelled phosphate as S78 and S82 (and possibly S15) in human Hsp27 (Landry *et al.* 1992), and S15 and S86 in mouse Hsp25 (Gaestel *et al.* 1991). The major site of labelled phosphate incorporation into Hsp27 in arsenite-treated MCF7 human breast cancer cells was S82, which contained 80% of Hsp27-incorportated phosphate (Landry *et al.* 1992). A large number of studies using subsequently-developed phospho-specific antibodies have shown that human Hsp27 is phosphorylated at S15, S78 and S82 in response to diverse stress stimuli. S15 and S82 are conserved sites in all other mammalian Hsp27 proteins, while S78 is not (figure 1.10).

In addition to heat shock, arsenite and phorbol esters, Hsp27 phosphorylation in endothelial cells can be stimulated by treatment of cells with VEGF (Rousseau *et al.* 1997), TNFα (Robaye *et al.* 1989; Kiemer *et al.* 2002), H_2O_2 (Barchowsky *et al.* 1994; Huot *et al.* 1997), IL-1 (Saklatvala *et al.* 1991), thrombin (Santell *et al.* 1992), oestrogen (Razandi *et al.* 2000) and fluid shear stress (Li *et al.* 1996). Phosphorylation of Hsp27 has been observed in other cell types in response to diverse stress stimuli including UV irradiation, anisomycin (a protein synthesis inhibitor), and sorbitol-induced osmotic shock. Cytokines including TGFβ and PDGF (Hedges *et al.* 1999), and serum and TGFβ (Zhou *et al.* 1993) have also been reported to induce Hsp27 phosphorylation in vascular smooth muscle cells and a hamster fibroblast line respectively. Phosphorylation of Hsp27 occurs rapidly after cell stimulation with all of these agents, with 5–30 min treatments employed in most studies.

1.5.3.1 p38 MAPK pathway

p38 MAPK is a protein kinase activated by treatment of cells with many of the stresses and cytokines listed above as stimulators of Hsp27 phosphorylation, including VEGF, TNFα, IL-1β, H_2O_2 and anisomycin. Stress-induced p38 MAPK activation occurs via the upstream kinases MEK3 and 6 which directly phosphorylate p38 MAPK on its activation loop residues (T180/Y182). MEK3 and 6 are in turn activated by upstream kinases, although the identity of these is uncertain and may vary depending on the stimulus. Downstream, p38 MAPK phosphorylates a number of target proteins, the most relevant for Hsp27 being mitogen-activated protein kinase-activated protein kinases (MAPKAPKs) 2 and 3, with MAPKAPK2 playing the dominant role. Isoforms of p38 that phosphorylate MAPKAPK2 can be inhibited by the compounds SB203580 or SB202190, and pretreatment of cells with these compounds prevents MAPKAPK2 phosphorylation and activation. The p38 MAPK/MAPKAPK2 pathway is discussed in more detail in section 1.6.1.

In vitro, MAPKAPK2 phosphorylates Hsp27 at the sites observed to be phosphorylated in response to diverse stimuli in vivo: S15, S78 and S82 for human Hsp27, S15 and S86 for mouse Hsp25, with S82/S86 being the major phosphorylation sites (Stokoe *et al.* 1992b). MAPKAPK2 partially purified from arsenite-, sorbitol- or IL-1-treated cells phosphorylated Hsp27 in vitro, and this were prevented by pre-incubation of the cells with SB203580 (Cuenda *et al.* 1995), indicating that in vivo Hsp27 phosphorylation in response to these stimuli was mediated by p38 MAPK, probably via the p38/MAPKAPK2 pathway. It is likely that MAPKAPK2 can directly phosphorylate Hsp27 in intact cells, as an overexpressed constitutively active MAPKAPK2 phosphorylated Hsp27 in the absence of other stimuli (Xu *et al.* 2006).

A large number of studies have shown that Hsp27 phosphorylation induced by a variety of stimuli in various cell types is blocked by SB203580. Inhibition of MAPKAPK2 activity and Hsp27 phosphorylation by SB203580 is highly likely to be due to p38 MAPK inhibition, rather than non-p38 effects of this inhibitor. Eyers *et al.* (1999) generated fibroblast cell lines expressing an

inducible SB203580-resistant p38 MAPK, and transiently transfected them with Hsp27. Before induction, UV- or anisomycin-stimulated Hsp27 phosphorylation at S15 or S78 was inhibited by SB203580, whereas after induction (i.e. in cells expressing drug-resistant p38 MAPK), Hsp27 phosphorylation was not inhibited by SB203580. Similar results were observed for MAPKAPK2 activity.

The importance of p38 MAPK and MAPKAPK2/3 in Hsp27 phosphorylation was shown in cells derived from knockout mice. Hsp27-phosphorylating kinases activated by UV, anisomycin or H_2O_2 present in normal cardiomyocytes were absent in p38α-null cardiomyocytes (Adams *et al.* 2000). Some endogenous phosphorylated Hsp25 was detected in cardiac tissue of MAPKAPK2-null mice, indicating that other kinases may also phosphorylate Hsp27 in vivo, although the increases in Hsp25 phosphorylation stimulated by lipopolysaccharide (LPS) (Kotlyarov *et al.* 1999) and arsenite (Shi *et al.* 2003) were prevented. MAPKAPK3 overexpression can compensate for the loss of arsenite-stimulated Hsp25 kinase activity in MAPKAPK2-null cells (Ronkina *et al.* 2007), indicating that MAPKAPK2 and 3 act as stress-stimulated Hsp27 kinases. Together, these data indicate that p38α and MAPKAPK2/3 mediate stress-induced Hsp27 phosphorylation, and that MAPKAPK2 appears to be the major stress-activated direct Hsp27 kinase.

Interestingly, the phorbol ester PMA stimulated Hsp27 phosphorylation in p38α-null cardiomyocytes (Adams *et al.* 2000) indicating that, in contrast to 'stress' stimuli, phorbol esters stimulate a p38α-independent pathway to phosphorylate Hsp27. As MAPKAPK2 was not detectably activated in PMA-stimulated p38α-null cardiomyocytes (Adams *et al.* 2000), it is likely that phorbol ester-stimulated Hsp27 phosphorylation is also independent of MAPKAPK2, suggesting that additional enzymes can directly phosphorylate Hsp27 in vivo.

1.5.3.2 PKC

Phorbol esters are known activators of classical and novel PKC isoforms, and the PMA-stimulated Hsp27 phosphorylation observed in p38α-null cardiomyocytes (Adams *et al.* 2000) may be medi-

ated by PKC.

After initial work showing phorbol ester treatment of intact cells stimulated Hsp27 phosphorylation, the importance of PKC in Hsp27 phosphorylation was called into question by the inability of long-term phorbol ester treatment (which downregulates PKC isoforms) or the broad-specificity PKC inhibitor staurosporine to prevent TNFα- and IL-1β-stimulated Hsp27 phosphorylation (Saklatvala *et al.* 1991). Coupled with the discovery of the p38/MAPKAPK2/Hsp27 pathway and its implication in Hsp27 phosphorylation induced by IL-1 (Freshney *et al.* 1994) and a variety of stress stimuli including heat shock, arsenite and osmotic stress (Rouse *et al.* 1994), interest in a PKC/Hsp27 pathway appears to have decreased.

In endothelial cells, phorbol ester treatment increased Hsp27 phosphorylation, and long-term phorbol ester treatment prevented Hsp27 phosphorylation stimulated by phorbol ester, thrombin or histamine, and reduced IL-1β-stimulated phosphorylation (Santell *et al.* 1992). Also in endothelial cells, PKC inhibitors did not prevent H_2O_2-induced Hsp27 phosphorylation (Barchowsky *et al.* 1994). These differences were further investigated by Faucher *et al.* (1993), who showed in the MCF7 breast cancer cell line that PKC inhibition with the broad-specificity PKC inhibitor GF109203X substantially reduced phosphate incorporation into Hsp27 induced by phorbol ester treatment but had no effect on heat shock-induced phosphate incorporation. The importance of PKC in Hsp27 phosphorylation is therefore stimulus-dependent, indicating the presence of additional signalling pathways for Hsp27 phosphorylation, but leaving it uncertain whether a PKC-dependent pathway is physiologically relevant.

Maizels *et al.* (1998) examined the ability of various recombinant PKC isoforms to phosphorylate recombinant Hsp25 in vitro. PKCδ and, to a lesser extent, PKCα phosphorylated Hsp25, whereas PKCs β, ϵ and ζ caused relatively little phosphorylation. Whether direct phosphorylation of Hsp27 by PKC occurs in vivo is unknown.

1.5.3.3 Other pathways

In addition to MAPKAPK2/3, MAPKAPK5 (p38 regulated/activated kinase, PRAK) has also been reported to phosphorylate Hsp27 in response to arsenite (New *et al.* 1998). However, Shi *et al.* (2003) found that while recombinant MAPKAPK5 is activated by p38 in vitro, and can then phosphorylate Hsp27, this does not occur in vivo and MAPKAPK5 immunoprecipitated from cells treated with p38 activators is unable to phosphorylate Hsp27. The same group also showed that the antibody used by New *et al.* in their original paper was able to immunoprecipitate an Hsp27 kinase from arsenite-activated mouse embryonic fibroblasts derived from MAPKAPK5-null mice but not from MAPKAPK2-null mice, suggesting this antibody cross-reacts with MAPKAPK2 and so may give erroneous results. Although MAPKAPK5 is apparently not responsible for p38 MAPK-mediated Hsp27 phosphorylation, it has recently been reported to be involved in forskolin-stimulated actin re-organisation via direct Hsp27 phosphorylation (Kostenko *et al.* 2009), suggesting that MAPKAPK5 may be a relevant Hsp27 kinase under some conditions. These studies were performed with overexpressed proteins, and no evidence on the effect of MAPKAPK5 knockdown on forskolin-stimulated Hsp27 phosphorylation was presented despite the use of a MAPKAPK5 siRNA in this study.

Akt has been reported to associate with and phosphorylate Hsp27 at S82 but not S15 or S78. Recombinant Akt phosphorylated Hsp27 in vitro, and co-transfection of HEK293 cells with constitutively active Akt and wild type Hsp27 led to phosphorylation of the transfected Hsp27 at S82 (Rane *et al.* 2003). The authors proposed a p38/MAPKAPK2- and PI-3-K-dependent model for Akt activation in their human neutrophil system but did not examine whether PI-3-K inhibition (e.g. by wortmannin or LY294002) prevented Hsp27 phosphorylation in untransfected cells. Another group reported that in a mouse fibroblast line Hsp27 exists in complex with Akt, p38 and MAPKAPK2, with Hsp27 dissociating from the complex on p38 or Akt activation, but did not report Akt-stimulated Hsp27 phosphorylation (Zheng *et al.* 2006). The existence of direct Hsp27 phosphorylation by Akt in human endothelial cells has not been shown.

Lee *et al.* (2005) overexpressed various fragments and deletion mutants of mouse Hsp25 and mouse PKCδ in L929 mouse fibroblasts, showing by co-immunoprecipitation that Hsp25 and PKCδ interact when both proteins are overexpressed, with the V5 region at the C-terminus of the PKCδ catalytic domain and the amino acids 90–103 of Hsp25 were responsible for the interaction. PKCδ mutants mimicking autophosphorylation (S643D or S662D) did not interact with Hsp25 whereas PKCδ forms with these residues mutated to Ala did, and an S15D S86D Hsp25 mutant did not interact with PKCδ whereas a non-phosphorylatable (S15A S86A) form did, suggesting an interaction between the unphosphorylated forms of Hsp25 and PKCδ. Immunoprecipitated PKCδ phosphorylated Hsp25 in vitro at S15 and S86, although whether this phosphorylation occurs in vivo in the absence of overexpression is unknown.

T143 has been suggested as an additional Hsp27 phosphorylation site. cGMP-dependent protein kinase (PKG) catalyses phosphate incorporation into a purified Hsp27 S15D S78D S82D (3D) mutant protein in vitro, but not of a Hsp27 3D + T143E mutant, whereas MAPKAPK2 is unable to incorporate phosphate into either (Butt *et al.* 2001). Treatment of human platelets with a PKG-activating cGMP analogue induced phosphorylation of Hsp27 without affecting p38 MAPK activation loop phosphorylation, and PKG was unable to phosphorylate MAPKAPK2 in vitro, indicating that cGMP-activated Hsp27 phosphorylation in platelets is unlikely to occur via the p38 MAPK/MAPKAPK2 pathway. However, there are no reports of T143 phosphorylation in non-platelets or in response to any other stimuli, and a number of early studies examining Hsp27 after stimulation by a number of cytokines and stress-inducing stimuli could detect phospho-serine, but not phospho-threonine or pY in purified Hsp27.

1.5.3.4 VEGF-stimulated Hsp27 phosphorylation

At the outset of this work, the p38 MAPK/MAPKAPK2 pathway was thought to be the major pathway responsible for Hsp27 phosphorylation in vivo. Rousseau *et al.* (1997) reported that VEGF activates p38 MAPK, and that the p38 MAPK/MAPKAPK2 pathway was responsible for

VEGF-induced Hsp27 phosphorylation, showing that 15 mins VEGF treatment of HUVECs increased the incorporation of radiolabelled phosphate from ATP into Hsp27, and this was prevented by pre-incubation of the cells for 15 mins with the p38 MAPK inhibitor SB203580 (1 μM). The sites of phosphorylation were not determined, and quantitative data was not presented. The same group reported that VEGF-stimulated p38 MAPK activation occurred via VEGFR2 (Rousseau *et al.* 2000b).

McMullen *et al.* (2004) showed that adenovirus-mediated overexpression of an non-activatable p38α form prevented VEGF-stimulated Hsp27 phosphorylation in HUVECs, suggesting involvement of the p38/MAPKAPK2 pathway. Activation of all p38 isoforms by overexpression of constitutively active MEK6 caused Hsp27 phosphorylation in HUVECs (McMullen *et al.* 2005). This activation was prevented by overexpression of kinase-dead p38α, indicating that p38α is the primary enzyme responsible for MEK6-mediated Hsp27 phosphorylation. In both studies, the phosphorylation site recognised by the phospho-Hsp27 antibody used was not indicated.

The mechanism of VEGF-stimulated p38 MAPK activation is controversial. McMullen *et al.* (2004) reported that VEGF-stimulated p38 MAPK phosphorylation in HUVECs was reduced by chelation of extracellular calcium, or adenovirus-mediated overexpression of either kinase-inactive src or a mutant form of the non-receptor tyrosine kinase Pyk2 which is unable to bind src. In this study, neither PKC inhibition nor overexpression of an inactive cdc42 mutant prevented VEGF-stimulated p38 phosphorylation (McMullen *et al.* 2004). Another study on HUVECs reported that VEGF-stimulated p38 MAPK phosphorylation was inhibited by the PKC inhibitor GF109203X (Yashima *et al.* 2001). A third study showed that overexpression of cdc42 carrying the same mutation as used by McMullen *et al.* (2004) reduced VEGF-stimulated p38 MAPK phosphorylation and Hsp27 phosphate incorporation in NIH3T3 cells additionally transfected with VEGFR2, p38, and (for the Hsp27 data) MAPKAPK2 (Lamalice *et al.* 2004). Lamalice also showed that VEGF-stimulated p38 MAPK phosphorylation occurred in cells transfected with wild-type VEGFR2 but not a VEGFR2 Y1214F mutant.

The signalling pathways believed at the outset of this thesis to contribute to VEGF-stimulated Hsp27 phosphorylation are depicted in figure 1.11. During the course of this thesis, it was reported that VEGF is able to activate protein kinase D (PKD) via PKC (Wong and Jin 2005), and that PKD is able to phosphorylate Hsp27 in vitro at S82 (Doppler *et al.* 2005), suggesting a VEGF/PKC/PKD/Hsp27 pathway. Further discussion of the mechanism, regulation and roles of PKC and PKD is given in section 1.6. The following sections discuss the relevance of Hsp27 phosphorylation to its cellular roles.

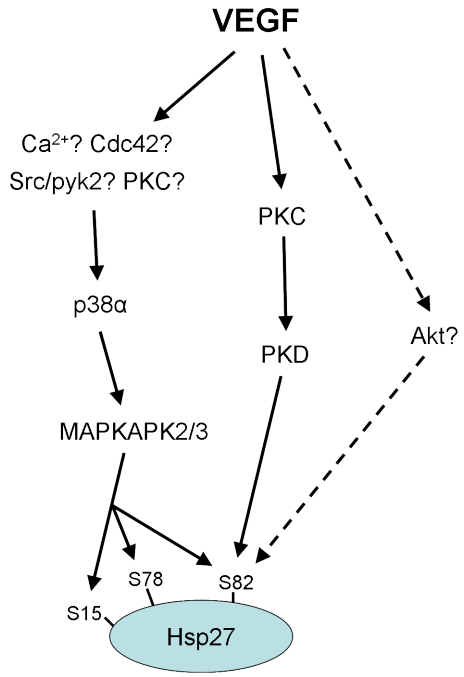

Figure 1.11: Pathways contributing to VEGF-stimulated Hsp27 phosphorylation in endothelial cells
Solid arrows indicate signal transduction events. Dashed arrows indicate that, while VEGF activates Akt and Akt has been reported to phosphorylate Hsp27 at S82, this pathway has not been shown to operate in endothelial cells. While a number of potential mediators of p38 activation have been suggested, as discussed in the text the actual pathway is uncertain.

1.5.4 Hsp27 structure and oligomerisation

In common with other members of the small heat shock protein family, Hsp27 is able to form oligomers and multimers of varying size. sHsp oligomers can either be homomers (i.e. composed of a single sHsp) or heteromers. Hsp27 can form hetero-oligomers with other sHsps including α-

B-crystallin (Zantema *et al.* 1992), Hsp20 (Bukach *et al.* 2009), and Hsp22 (Benndorf *et al.* 2001), although at least two studies have reported that Hsp27 in vivo is mainly a homomer (Zantema *et al.* 1992; Lambert *et al.* 1999).

1.5.4.1 Importance of α-crystallin domain for dimerisation

Although the crystal structure of Hsp27 has not been determined, the crystal structure of two other sHsps, Hsp16.5 from the archaeon *Methanococcus jannaschii*, and Hsp16.9 from wheat have been solved (Kim *et al.* 1998; van Montfort *et al.* 2001). These structures show that two sHsp monomers interact to form a dimer, and these dimers are then arranged in higher order structures to form the oligomer. The oligomer structure of the two sHsps is different with respect to the number of subunits incorporated and the shape produced (a 24 monomer hollow ball for Hsp16.5, 12 monomer double ring for Hsp16.9). Other sHsps, whose structures were analysed by electron microscopy, showed varying oligomeric structures, with α-crystallin forming a number of different structures (reviewed by Haslbeck *et al.* 2005).

The α-crystallin domain forms a β-sheet sandwich structure composed of two layers of β sheets with one β-strand separate from the others. The separate β-strand is able to interact with the β-sheet sandwich in another sHsp molecule, allowing sHsp monomers to dimerise. The determined sHsp crystal structures show the N-terminal region as a random coil free to move, seemingly not taking part in monomer-monomer interactions.

The conserved α-crystallin domain is likely to be responsible for dimer formation between sHsp monomers. A truncation mutant of the yeast sHsp Hsp26 which lacked the entire N-terminal domain (consisting of the α-crystallin domain and short C-terminal extension) formed dimers but not higher order structures (Stromer *et al.* 2004). Additionally, a hamster Hsp27 deletion mutant lacking a short N-terminal region (R5–Y23) was unable to form species larger than dimers (Lambert *et al.* 1999). Thus it appears that the α-crystallin domain is necessary and sufficient for dimerisation, a common property of sHsps. Conservation of the α-crystallin domain between

sHsps allows heterodimerisation, and therefore hetero-oligomerisation.

Hsp25 forms dimers in non-reducing buffers (Miron *et al.* 1988). The only cysteine residue present in Hsp27, the α-crystallin domain residue C137 (C141 in Hsp25) is conserved between Hsp27 species homologues (figure 1.10) but not between human sHsps (figure 1.9). A C141A Hsp25 mutant did not form dimers, indicating the importance of this residue for dimerisation, but retained a number of Hsp25 physiological abilities suggesting large-scale structural changes do not occur as a result of this mutation (Diaz-Latoud *et al.* 2005). It is possible that monomer–monomer interactions are stabilised by the formation of an inter-subunit disulphide bond between these residues.

1.5.4.2 Involvement of the N-terminal region in higher-order oligomerisation

Deletion of regions of the N-terminal domain of Hsp27 prevents oligomer formation. Lambert *et al.* (1999) used a chimeric protein formed by the N-terminal region of hamster Hsp27 (including S15 and S90 but not the α-crystallin domain) fused to luciferase (a normally monomeric protein) to examine the role of the N-terminal region of Hsp27 in phosphorylation-sensitive oligomerisation. The fusion protein formed oligomers, with a modal size of $\sim$400 kDa, when expressed in a fibroblast line. On arsenite treatment, the average size of the fusion protein species decreased with an increase in the amount of small (probably monomeric) species. Taken together with the inability of N-terminal deletion mutant proteins to form large oligomeric species (Stromer *et al.* 2004), these data indicate that the N-terminal region is involved in Hsp27 oligomer formation, and phosphorylation of Hsp27 disrupts this interaction causing a reduction in the size of Hsp27 oligomers.

Two different studies of hamster Hsp27 deletion mutants indicated that deletion of small N-terminal regions encoded by residues 5–23 (Rogalla *et al.* 1999) or 18–30 (Theriault *et al.* 2004) prevented oligomerisation, with the second study showing that mutants lacking residues 1–14 and 28–79 formed similar sized oligomers to wild-type Hsp27, indicating that these residues are dis-

pensable for oligomer formation. Residues 15–27 (corresponding to human Hsp27 residues 14–26) contain the conserved WDPF sequence (residues 16–19 in human Hsp27), and this sequence is thought to be important in dimer–dimer interactions within the Hsp27 oligomer.

Theriault *et al.* (2004) also proposed a model for the organisation of Hsp27 oligomers, extrapolating from the crystal structure of *M. jannaschii* Hsp16.5. In their model, Hsp27 forms two 12-mer rings, one on top of the other, which would have a predicted molecular weight of 27 kDa x 24 subunits = 648 kDa, similar to that observed for wild-type Hsp27 in a number of studies. Residues around the conserved WDPF sequence are proposed to be the important N-terminal region for oligomerisation. However two different groups have reported that the number of subunits incorporated into the Hsp27 oligomer varies with protein concentration (Ehrnsperger *et al.* 1999; Theriault *et al.* 2004). Additionally, Hsp27 appears to have a range of sizes when purified from cells (although this could be an artifact), and other sHsps appear have oligomeric structures quite different to that of Hsp16.5 (Haslbeck *et al.* 2005), so the general applicability of the Theriault structure is unknown.

1.5.4.3 Influence of phosphorylation on oligomeric structure

In unstressed growing HeLa cells, Hsp27 is predominantly unphosphorylated and exists in a high molecular weight complex, with an average size around 500 kDa as determined by gel filtration chromatography, although considerable variation in size was observed (Arrigo and Welch 1987; Arrigo *et al.* 1988). Gel filtration-purified high molecular weight non-phosphorylated Hsp27 oligomers displayed reasonably uniform circular structures approximately 15 nm in diameter when analysed by electron microscopy (Arrigo and Welch 1987; Benndorf *et al.* 1994; Rogalla *et al.* 1999).

Heat shock (Zantema *et al.* 1992) or treatment of cells with Hsp27 phosphorylation-inducing stimuli, including PMA, TNFα, IL-1β and arsenite (Kato *et al.* 1994), caused a reduction in the average size of Hsp27 oligomers as assessed by sucrose density-gradient centrifugation. The same au-

thors showed that radiolabelled phosphate-containing Hsp27 was mainly present in smaller Hsp27 species (also observed by Rogalla *et al.* 1999). Ehrnsperger *et al.* (1999) showed that Hsp25 phosphorylated in vitro by MAPKAPK2 formed smaller species than untreated Hsp25, strongly indicating that phosphorylation status rather than some other modification is responsible for the difference in Hsp27 oligomeric size. Taken together these data suggested that phosphorylation of Hsp27 may cause oligomer dissociation.

The effect of phosphorylation on the oligomeric structure of Hsp27 has been further examined by overexpressing Hsp27 phosphorylation site mutants in intact cells, and fractionating the cells to determine the molecular weight of Hsp27-containing species. In the discussion that follows, a 3X Hsp27 mutant consists of a protein identical to wild-type Hsp27 but with the three MAPKAPK2-phosphorylated serine residues mutated to X (a particular amino acid). Similarly, a 2X Hsp25 mutant has S15 and S86 mutated to X, and a 2X hamster Hsp27 mutant has S15 and S90 mutated to X.

Lavoie *et al.* (1995) analysed the effect of phosphorylation on the molecular size of human Hsp27 overexpressed in CHO cells by non-denaturing gel electrophoresis, showing that arsenite induced a decrease in the oligomeric size of wild-type Hsp27 but did not affect the size of a 3G Hsp27 mutant. In the absence of arsenite simulation, the wild-type and 3G Hsp27 forms ran at similar gel positions. Another study reported that whereas wild type Hsp27 exists as a range of sizes in intact cells, the 3A Hsp27 mutant exists as large multimers but not small species (Hollander *et al.* 2004).

Direct comparisons between Hsp27 wild type, 3A and 3D mutants using gel filtration indicated that whereas wild-type Hsp27 formed a range of species (700 kDa – monomers), 3A Hsp27 formed large species only (>200 kDa) whereas 3D Hsp27 formed only small species (<200 kDa, although the precise size varied between studies) (Mehlen *et al.* 1997a; Bruey *et al.* 2000b). A hamster 2A Hsp27 mutant displayed a similar size distribution to endogenous Hsp27 in untreated hamster CCL39 cells, whereas a 2D mutant had a similar size distribution to endogenous Hsp27 in arsenite-treated cells, as analysed by SDS-PAGE analysis of glutaraldehyde cross-linked Hsp27 and density

gradient centrifugation (Lambert *et al.* 1999). Another study also reported that a 2A hamster Hsp27 mutant transfected into NIH3T3 mouse fibroblasts formed large oligomers similar to those formed when cells were transfected with wild type Hsp27, whereas a 2E mutant formed only small species, probably dimers (Theriault *et al.* 2004).

Where studies have shown a lack of influence of phosphorylation on oligomeric structure, methodological differences may be responsible. For example, Knauf *et al.* (1994) reported that in vitro-phosphorylated Hsp25 (by MAPKAPK2) elutes at a similar position, approx 700 kDa, to unphosphorylated Hsp25 using gel filtration chromatography. However, some of these authors contributed to a later paper (Ehrnsperger *et al.* 1999) which found that phosphorylated Hsp25 formed smaller oligomers than unphosphorylated Hsp25, ascribing the differing results in the earlier work to the presence of a contaminating phosphatase in the in vitro Hsp25 preparation.

Overall, a number of studies have shown that chromatographed Hsp27 exists in two forms, large and small, with less Hsp27 at intervening sizes indicating that two major oligomeric forms exist rather than a continuum of sizes. Phosphorylation of Hsp27 results in a decrease in oligomer size. Mutants mimicking phosphorylated Hsp27 (D/E) form small species, whereas mutants containing unphosphorylatable residues (G/A) form large species whose size cannot be decreased by a number of stimuli causing deoligomerisation of wild-type Hsp27. In some studies (e.g. Rogalla *et al.* 1999) mutant Hsp27 consisting of a single phospho-mimicking form of Hsp27 was present entirely as small or large species, whereas in other studies phospho-mimicking mutants showed a increased formation of smaller species but were also present as large species, indicating that phosphorylated Hsp27 tends to occur in smaller species but is not exclusively present in them.

Much of the work on the involvement of phosphorylation on Hsp27 oligomerisation has involved overexpressing mutant forms of Hsp27 or analysing Hsp27 after in vitro phosphorylation. Vertii *et al.* (2006) used MAPKAPK2-null cells, and inhibitors of p38 and MAPKAPK2, to examine the importance of phosphorylation on Hsp25 oligomerisation without the requirement for Hsp27 overexpression. Arsenite-stimulated Hsp25 S86 phosphorylation was reduced by SB203580 pre-

treatment and completely prevented in MAPKAPK2-null mouse embryonic fibroblasts. In untreated cells, Hsp25 existed as a mixture of large species (modal size approx 250 kDa) and smaller species (<70 kDa) as assessed by gel filtration chromatography, and produced a laddered pattern after glutaraldehyde cross-linking and SDS-PAGE. Arsenite treatment of wild-type cells reduced the predominant size of Hsp25 oligomers to the smaller species, whereas arsenite treatment of MAPKAPK2-null cells did not noticeably affect either the glutaraldehyde cross-linked Hsp25 pattern or the distribution of Hsp25 obtained by gel filtration. These data indicate that MAPKAPK2 is necessary for the arsenite-induced dissociation of Hsp25 oligomers, and suggests more generally that phosphorylation is required for small heat shock oligomer dissociation.

1.5.4.4 Role of individual phosphorylation sites

The involvement of the individual phosphorylation sites of Hsp27 has also been examined by site-directed mutagenesis. Arsenite treatment reduced the oligomer size of overexpressed wild-type hamster Hsp27 and an S15A mutant, but had little effect on an S90A mutant (Lambert *et al.* 1999). The same authors showed that an S15E S90A Hsp27 mutant formed large oligomers (modal size approx 600 kDa by glycerol gradient centrifugation) whereas an S15A S90E mutant predominantly formed small species (modal size $\sim$40 kDa, probably representing dimers).

Rogalla *et al.* (1999) extended some of the findings of Lambert *et al.* (1999) to human Hsp27, by examining the role of individual phosphorylation sites in Hsp27 oligomerisation using gel filtration chromatography. Wild type Hsp27 existed almost entirely as a high molecular weight species (400–700 kDa). A 3D mutant existed entirely as small species (<200 kDa), whereas an S78D S82D double mutant existed as two distinct populations, with similar amounts of the larger species and the smaller species. An S15D mutant contained a majority of large species and a low proportion of small species. Similar results were obtained when the wild-type and mutant proteins were examined by electron microscopy. After in vitro phosphorylation, Hsp27 existed with roughly equal amounts of Hsp27 present in large and small species. Taken together, the work

of Lambert *et al.* and Rogalla *et al.* indicates that S82 phosphorylation is likely to be the critical event in Hsp27 deoligomerisation. In human Hsp27, phosphorylation of S15 also contributes significantly to oligomer dissociation.

In summary, it is clear that phosphorylation of Hsp27 reduces the size of the oligomers formed. It is believed that the phosphorylation-regulated alterations in oligomerisation state, rather than phosphorylation itself, are important in regulation of Hsp27 functional properties. Distinct oligomeric species may have distinct functions (discussed below), so allowing the function of Hsp27 to be regulated in part by phosphorylation-inducing stimuli.

1.5.5 Physiological roles of Hsp27

Hsp27 has been implicated in a variety of physiological processes, including acting as a molecular chaperone, regulating the actin cytoskeleton (with related roles in cell migration), and inhibiting apoptosis. The mechanisms behind these properties are now examined, using evidence from endothelial cells where available. Information discussed in this section is summarised in figure 1.12.

1.5.5.1 Molecular chaperone

Molecular chaperones are proteins that assist the folding of other molecules, or the assembly of other macromolecular structures, but do not participate in the final complete structure. Chaperones are known to be involved in protein folding under both normal and abnormal cellular conditions. As discussed earlier, heat shock and other cellular stresses often lead to the production of misfolded proteins, which must be either refolded into their correct shape or destroyed. For this reason, many molecular chaperones concerned with protein folding are upregulated on heat shock (i.e. are heat shock proteins).

Hsp27, Hsp25 and α-B-crystallin reduced the rate of thermally-induced aggregation of citrate synthase and α-glucosidase as determined by light scattering, indicating that these proteins are molecular chaperones, whereas addition of IgG or lysozyme had no effect (Jakob *et al.* 1993). Ad-

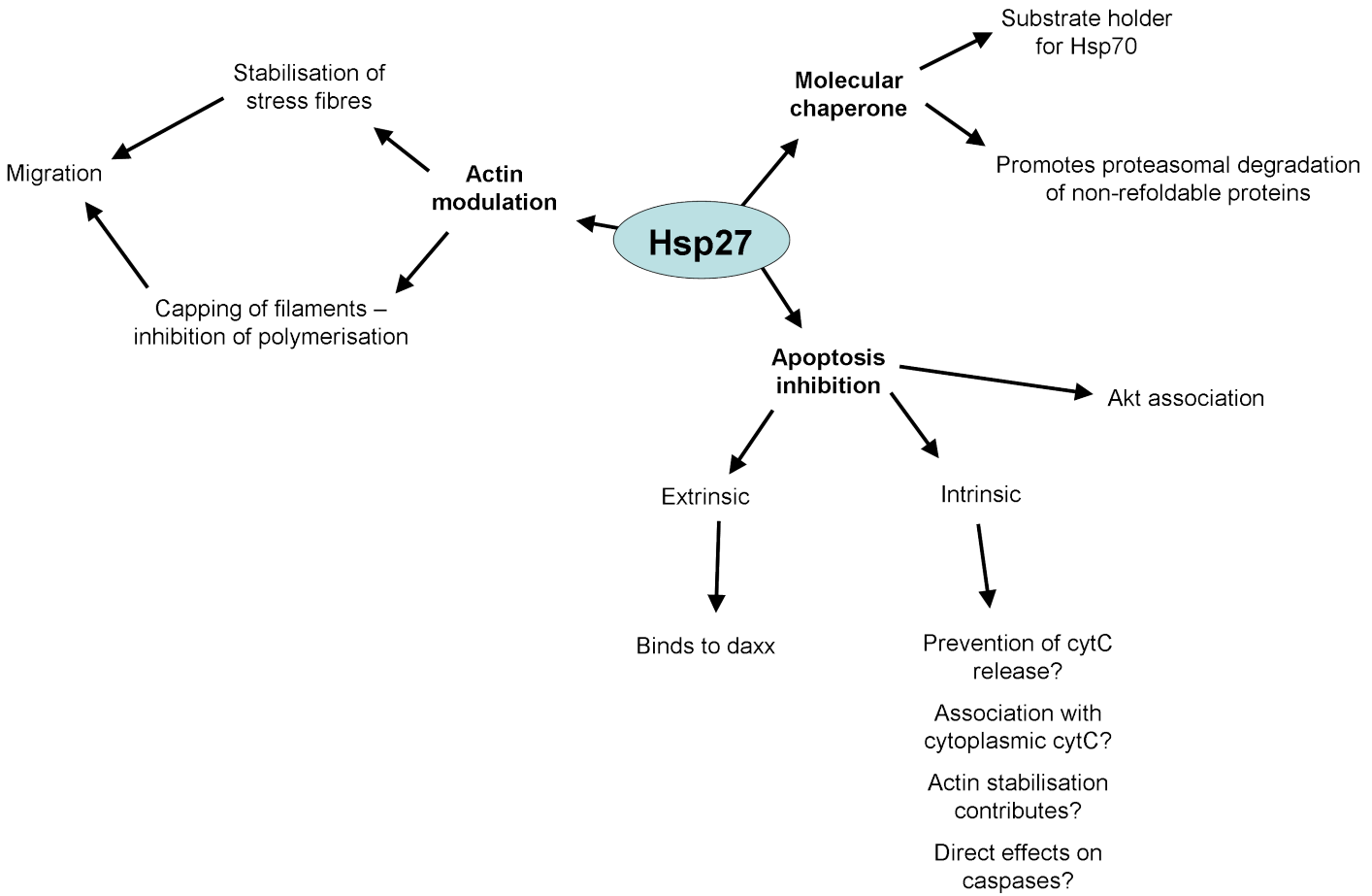

Figure 1.12: Major physiological roles of Hsp27
The major physiological roles of Hsp27 discussed in this chapter are schematically illustrated, with some suggested contributing mechanisms. Hsp27 has also been reported to influence protection against oxidative stress by regulating glutathione expression levels, and may have roles in cell growth and mRNA stability. Further details are given in the text.

ditionally, the rate of reactivation of citrate synthase and α-glucosidase was substantially higher in the presence of Hsp25 or Hsp27 than in the presence of IgG. Taken together, this study indicates that Hsp27 prevents aggregation of proteins during heat shock, and promotes refolding of denatured proteins in vitro. The presence of MgATP did not enhance the effects of Hsp27, implying that Hsp27 is an ATP-independent molecular chaperone.

1.5.5.1.1 Interaction with ATP-dependent chaperones

Ehrnsperger *et al.* (1997) examined the interplay between Hsp25 and other molecular chaperones in protein folding during heat shock. The presence of Hsp25 delayed the thermally-induced irreversible inactivation of citrate synthase but had little effect on the loss of citrate synthase activity, indicating that citrate synthase was being preserved as inactive intermediates. Addition of Hsp70 and ATP to heat shock-induced citrate synthase/Hsp25 complexes at normal cellular temperatures caused a greater reactivation of citrate synthase than addition of a control protein (IgG) or Hsp70 in the absence of ATP. These data suggest that the presence of both Hsp70 and ATP increases the reactivation of citrate synthase complexed with Hsp25 in vitro, probably by Hsp70-mediated refolding of citrate synthase, when normal cellular conditions return. Several more proteins (which were not identified) from heat shocked cells were found to bind to Hsp25-sepharose beads than from non-heat shocked cells, suggesting that after heat shock, a number of proteins adopt a (probably partially denatured) conformation that can be bound to Hsp25, and so may be trapped in the Hsp25 reservoir.

The ability of Hsp27 to act as a molecular chaperone in vivo was demonstrated by Bryantsev *et al.* (2007), who showed that refolding of a luciferase-GFP protein in heat-shocked L929 cells was enhanced in cells overexpressing Hsp27 or Hsp70, and this effect was reduced in cells co-expressing Bag1, a negative regulator of Hsp70. These data indicate that Hsp27 chaperone activity is dependent on Hsp70 activity, consistent with Ehrnsperger *et al.* (1997) and with the idea of Hsp27 as a substrate 'holder' for Hsp70.

Hsp27 is a cytosolic protein in unstressed cells, but rapidly translocates to the nucleus on heat shock and associates with large structures, before slowly returning to the cytosol (Arrigo and Welch 1987; Kato *et al.* 1993). Proteasome components co-localise with nuclear Hsp27 (Bryantsev *et al.* 2007), leading to the suggestion that nuclear Hsp27 may contain a pool of unrefoldable substrate molecules destined for degradation. The basis of the nuclear translocation is unknown, but may be passive diffusion of small Hsp27 species through nuclear pores. p38 MAPK inhibitors did not prevent Hsp27 translocation on heat shock, indicating that p38-mediated Hsp27 phosphorylation is not required, however a 3A Hsp27 mutant (forming large species) also did not translocate (Bryantsev *et al.* 2007). Cells overexpressing Hsp27 showed enhanced proteasomal degradation of ubiquitinated proteins after cellular stress (Parcellier *et al.* 2003). Hsp27 interacted with both a ubiquitinated protein (IκB) and the proteasome, suggesting that Hsp27 may directly promote proteasomal degradation of ubiquitinated proteins, although whether this mechanism is applicable to many different proteins is unknown. Speculating, it is possible that Hsp27 promotes proteasomal degradation of unrefoldable proteins, although how Hsp27 distinguishes between refoldable and non-refoldable proteins is not clear.

Chaperone activity is believed to be a common property of sHsps, which are thought to act as a reservoir for unfolded proteins similar to that observed for Hsp27, preventing their irreversible aggregation and allowing time for favourable cellular conditions to return when ATP-dependent chaperones can refold these trapped proteins (reviewed by Liberek *et al.* 2008). The heat-stimulated increase in the synthesis of chaperone proteins such as Hsp27 is believed to contribute to thermotolerance, and also explains why overexpression of small heat shock proteins simulates thermotolerance. The presence of chaperones in larger quantities than normal at the onset of severe cellular stress, due to a previous mild stress, increases the capacity to cope with misfolded proteins, reducing problems due to protein aggregation.

1.5.5.1.2 Influence of phosphorylation/oligomerisation

A number of studies have examined which molecular species is responsible for the chaperone activity of Hsp27. Hsp25 or Hsp27 phosphorylated in vitro by MAPKAPK2 slowed thermally-induced citrate synthase aggregation and reduction-induced insulin B chain precipitation less effectively than the corresponding wild-type protein (Rogalla *et al.* 1999). In contrast, Knauf *et al.* (1994) reported that purified Hsp25 either phosphorylated in vitro by MAPKAPK2 or remaining unphosphorylated showed a similar retardation of thermally-induced aggregation of α-glucosidase and a similar enhancement of reactivation of urea-denatured α-glucosidase. However, this was the same paper which stated that phosphorylation of Hsp25 had no effect on Hsp25 oligomerisation, and may have been contaminated by a phosphatase (discussed on page 112).

An Hsp27 3D mutant (composed of small species) was much less effective in retarding heat-induced citrate synthase aggregation and accelerating its refolding than wild-type Hsp27, whereas an S15D mutant and an S78D S82D double mutant (mainly larger species) had a similar effect to wild type Hsp27 as determined by light scattering (Rogalla *et al.* 1999). In contrast, Theriault *et al.* (2004) reported that wild-type hamster Hsp27, and S15A S90A and S15E S90E mutants reduced thermally-induced citrate synthase aggregation to a similar degree. The apparent differences in the results may be related to the Hsp27/denatured substrate molar ratio. When eqimolar concentrations of Hsp27 and substrate were examined by Theriault *et al.* (2004), similar to those used by Rogalla *et al.* (1999), wild-type hamster Hsp27 and a 2A mutant reduced citrate synthase aggregation to a greater degree than a 2E mutant. However, at higher molar ratios (greater molar excesses of Hsp27), differences between wild type and mutant Hsp27 forms were not observed.

The studies described above were performed using in vitro thermal denaturation/renaturation of particular proteins. Intact fibroblasts overexpressing 3D Hsp27 were much more effective at recovering luciferase activity (by correctly refolding luciferase) after heat shock than cells overexpressing wild-type, 3A or 3G Hsp27 forms (Bryantsev *et al.* 2007). Heat shock seems to cause a somewhat different Hsp27 response to phosphorylation-stimulating cellular stresses. As discussed

earlier heat shock causes transit of Hsp27 into the nucleus and its appearance in large structures, whereas phosphorylation causes a reduction in oligomeric size. 3A Hsp27 was unable to translocate into the nucleus, and this may be the key factor in this system.

On balance, it appears that larger Hsp27 species may be more effective as molecular chaperones in vitro than smaller species, but that during heat shock in cells Hsp27 must also dissociate to enter the nucleus. A model for sHsp chaperone function is described in Haslbeck *et al.* (2005). According to this model, under basal conditions sHsps exist in large oligomers (in dynamic equilibrium with individual subunits entering and leaving the oligomer) which is in a low-affinity substrate binding state. On heat shock, the oligomer remains together but subunits adopt a high-affinity state and bind denatured substrate molecules. Dimers can enter and leave the oligomer in either state, in a dynamic equilibrium. The denatured substrates are refolded by ATP-dependent chaperones such as Hsp70.

If Hsp27 is an important trap to prevent protein aggregation, it seems unlikely that the immediate phosphorylation-associated decrease in Hsp27 oligomeric size observed after heat shock and other cellular stresses acts to reduce the ability of Hsp27 to bind denatured proteins, as this would immediately impair the cell's defences against protein aggregation. It is possible that this does occur if another role of Hsp27 is initially more important (e.g. related to actin cytoskeleton stabilisation or apoptosis). Alternatively, perhaps de-oligomerisation is necessary for initial protein binding before Hsp27 monomers come together again, holding bound substrates in multimers. In support of this idea, the N-terminal region of yeast Hsp26 is required for denatured substrate binding, which may be inaccessible to larger substrates in oligomerised Hsp27 given the involvement of this region in oligomerisation (Haslbeck *et al.* 2004).

1.5.5.2 Actin modulation

Monomeric actin (also termed globular actin, G-actin) self-assembles into polymeric, double helical chains termed actin filaments (F-actin, reviewed by Mounier and Arrigo 2002). Although

joining of the initial few subunits (termed nucleation) is slow, subsequent actin polymerisation is rapid. At constant length, actin filaments lose subunits from the end closest to the nucleation site (the pointed end or minus end), and add subunits at the barbed end (also known as the plus end). Various proteins regulate the formation of the actin cytoskeleton including capping proteins which bind to and block polymerisation at one end of the filament, actin severing proteins which introduce breaks into an actin filament, and nucleating proteins, which catalyse the assembly of the initial few actin monomers to begin a filament. Actin forms multiple structures within the cell, including a filament network under the plasma membrane (the cortical web) which connects to membrane proteins giving structure to the plasma membrane, and thick bundles of actin filaments called stress fibres. Actin drives extension of parts of the cell, pushing the cell membrane forward into space via structures including filopodia, laemellipodia and pseudopodia.

Hsp27 has been reported to interact with actin in two distinct ways: as a barbed end capping protein which inhibits actin filament polymerisation, and as a stabiliser of pre-existing actin filaments (reviewed by Mounier and Arrigo 2002).

1.5.5.2.1 Inhibition of actin polymerisation

A 25 kDa protein purified from turkey smooth muscle, subsequently identified as Hsp27, was shown to act as a capping protein of the barbed end of actin filaments and an inhibitor of in vitro actin polymerisation (Miron *et al.* 1988, 1991). Benndorf *et al.* (1994) separated Hsp25 purified from tumour cells into phosphorylated monomeric, and unphosphorylated monomeric and polymeric fractions by chromatography and sucrose gradient centrifugation, and examined the effect of these species on in vitro actin polymerisation. Unphosphorylated monomeric Hsp25 reduced actin polymerisation in a dose-dependent manner, and inhibition plateaued (at around 90%) at a 1:1 ratio of unphosphorylated Hsp25 monomers to actin monomers, whereas phosphorylated monomeric and polymeric Hsp25 had little effect on actin polymerisation.

The unphosphorylated monomeric Hsp25 preparation used by Benndorf *et al.* (1994) contained

some Hsp25 dimers, but these dimers are unlikely to be able to inhibit actin polymerisation – Miron *et al.* (1988) reported that chicken Hsp27 dimerises in non-reducing buffers (probably via disulphide bond formation via the single cysteine present in Hsp27, C137 in humans), and under these conditions Hsp27 does not inhibit actin polymerisation. Unphosphorylated monomeric Hsp27 microinjected into intact cells impaired the reformation of actin stress fibres after heat shock, whereas phosphorylated monomeric Hsp27 did not (Schneider *et al.* 1998), indicating that unphosphorylated monomeric Hsp27 can act as an inhibitor of actin polymerisation in vivo. Hsp27 does not appear to be either an actin nucleating protein as it does not affect the lag time of in vitro actin polymerisation (unpublished results reported in Miron *et al.* 1991) or an actin filament severing protein as microinjected monomeric Hsp27 (phosphorylated or unphosphorylated) did not itself cause a reduction in actin stress fibres (Schneider *et al.* 1998).

Wieske *et al.* (2001) identified peptides derived from Hsp27 that inhibit actin polymerisation in vitro. One peptide included the S15 residue in human Hsp27, and a phosphorylated form of this peptide was less able to inhibit actin polymerisation, suggesting that phosphorylation at S15 may reduce the actin capping activity of Hsp27. It is unknown whether these peptides are important in the in vivo effects of intact Hsp27 on actin structures in vivo.

Hsp27 affects actin polymerisation-driven processes in endothelial cells. Untransfected BAECs formed broad laemellipodia when migrating into a cell-free area which stained strongly for Hsp27 along the leading edge (Piotrowicz *et al.* 1998). BAECs stably overexpressing human wild-type Hsp27 were more elongated, projecting further into the cell-free area than control cells, whereas 3G Hsp27-expressing cells projected less into the cell-free area with reduced laemellipodia formation. Those projections which did form did not appear to be enriched in Hsp27 at their tips. Similar results were observed with another actin polymerisation-driven process, pinocytosis, in hamster fibroblasts. Cells stably overexpressing wild-type Hsp27 showed enhanced pinocytotic activity compared to control cells, whereas cells overexpressing a non-phosphorylatable Hsp27 showed reduced pinocytotic activity (Lavoie *et al.* 1993b).

The reduction in laemellipodia formation or pinocytosis in cells overexpressing non-phosphorylatable Hsp27 may be due to inhibition of actin polymerisation by unphosphorylated Hsp27. The enrichment of Hsp27 at the leading edge of cells undergoing actin polymerisation suggests that Hsp27 inhibits actin polymerisation by capping the growing (plus/barbed) end of actin filaments, rather than by chelating all actin monomers – actin is a highly abundant protein and monomer chelation would require vast quantities of Hsp27. The need for a large amount of Hsp27 per actin monomer to effectively inhibit in vitro actin polymerisation probably reflects the ability of filament nucleation to occur anywhere, not the case in vivo.

Quite where the actin-capping unphosphorylated monomeric Hsp27 comes from is not entirely clear, as unphosphorylated Hsp27 is present in large oligomers. However as discussed previously, Hsp27 usually exists as a range of species, with phosphorylated species or mutant mimics generally smaller but also present in large oligomers, conversely indicating that naturally occurring small unphosphorylated species are likely to exist. Additionally, Hsp27 oligomers have been reported to be in dynamic equilibrium, with subunits entering and leaving the oligomer even when unphosphorylated. Thus a pool of unphosphorylated small Hsp27 species is likely to be present in the cell. It is also possible that some small phosphorylated Hsp27 species that are subsequently dephosphorylated bind to and cap actin rather than immediately re-incorporating into an oligomer. The monomeric requirement for the actin-capping species is harder to understand, given that Hsp27 dimerises via its α-crystallin domain. How this interaction is disrupted is not clear, although a dynamic equilibrium between monomers and dimers may also play a role.

1.5.5.2.2 Stabilisation of actin filaments

In addition to a plus end capping activity, Hsp27 also acts to stabilise actin filaments from disruption. Lavoie *et al.* (1993a) reported that disruption of actin stress fibres by cytochalasin D was reduced in cells stably overexpressing Hsp27, and recovery of stress fibres after removal of cytochalasin D was enhanced. Cytochalasin D-induced reduction in cellular growth was also

reduced in Hsp27 overexpressing cells. Later work showed that although overexpression of wild-type Hsp27 in cell lines protected stress fibres against dissociation in response to cytochalasin D or heat shock, overexpression of human 3G Hsp27 had no effect (Lavoie *et al.* 1995; Guay *et al.* 1997). Similarly, only wild type Hsp27 increased the rate of stress fibre reappearance. Overexpression of wild-type but not non-phosphorylatable Hsp27 also prevented H_2O_2-induced actin fragmentation in hamster fibroblasts (Huot *et al.* 1996). Mounier and Arrigo (2002) proposed a model for the protection of the actin cytoskeleton by Hsp27, in which Hsp27 coats actin microfilaments preventing the action of actin severing proteins which are also activated during the stress response.

In HUVECs, H_2O_2 induces accumulation of stress fibres, rather than the actin fragmentation observed in fibroblasts, and this can be blocked by SB203580 (Huot *et al.* 1997). This difference may be related to the high level of Hsp27 expression in ECs, as fibroblasts overexpressing Hsp27 showed a similar response to H_2O_2 as seen in HUVECs. VEGF also induced accumulation of stress fibres in HUVECs, which could be blocked by pre-incubating the cells with SB203580 (Rousseau *et al.* 1997). In both cases, the effects of SB203580 were ascribed to prevention of p38 MAPK-mediated phosphorylation of Hsp27, although no direct evidence of the involvement of Hsp27 in stress fibre formation was provided. Heat shock of endothelial cells caused association of Hsp27 with actin stress fibres (Loktionova *et al.* 1996), suggesting that Hsp27 may stabilise stress fibres under adverse cellular conditions in ECs. Direct analysis of actin filament stabilisation by Hsp27 in ECs, e.g. by cytochalasin D-mediated disruption, has not been reported.

In summary, it appears that phosphorylated Hsp27 species stabilise actin filaments, preventing filament disintegration (in cell lines) and allowing stress fibre formation (in ECs).

1.5.5.3 Migration and invasion

Cell migration is an actin polymerisation-driven process (section 1.4.4.4), and roles of Hsp27 in actin modulation are probably important in migration. Rousseau *et al.* (1997) first proposed

the involvement of Hsp27 in VEGF-stimulated endothelial cell migration, showing that the p38 MAPK inhibitor SB203580 prevented VEGF-induced HUVEC migration and Hsp27 phosphorylation, and suggested that changes in Hsp27 phosphorylation may be involved in VEGF-stimulated migration. However they did not show a relationship between Hsp27 and migration.

More direct evidence for the involvement of Hsp27 in endothelial migration was given by manipulation of the amount of Hsp27 present inside cells. Overexpression of wild type Hsp27 enhanced serum-stimulated HUVEC migration in a wound healing assay, whereas overexpression of an unphosphorylatable Hsp27 mutant inhibited migration (Piotrowicz *et al.* 1998). In a similar assay, oestrogen-stimulated BAEC migration is reduced by overexpression of a non-phosphorylatable Hsp27 mutant, which also reduced oestrogen-stimulated tubulogenesis on matrigel (Razandi *et al.* 2000). In smooth muscle cells, expression of a 3A Hsp27 mutant inhibits PDGF-stimulated migration in a transwell assay whereas overexpression of wild-type Hsp27 has no effect on migration (Hedges *et al.* 1999). Reduction of Hsp27 in cells also affects cell migration – siRNA-mediated knockdown of human Hsp27 reduced migration of HeLa cells in response to the chemokine CXCL12 in a transwell assay (Rousseau *et al.* 2006).

A large number of studies have used the inhibitor SB203580 to implicate p38 MAPK in the migration of various cell types in response to a number of stimuli. In endothelial cells, VEGF-stimulated migration of HUVECs was reduced by SB203580 or by overexpression of inactive p38 MAPK (Rousseau *et al.* 1997; McMullen *et al.* 2004), and oestrogen-stimulated migration of BAECs was reduced by overexpression of inactive p38 MAPK, inactive MAPKAPK2 or p38 MAPK inhibition with SB203580 (Razandi *et al.* 2000). Hsp27, with its role in actin dynamics, is believed to be an effector of p38 MAPK regulation of the actin cytoskeleton. Consistent with this idea, transwell endothelial cell migration induced by expression of a constitutively active form of the p38 MAPK-activating enzyme MEK6 was reversed by overexpression of unphosphorylatable p38 MAPK or unphosphorylatable Hsp27 (McMullen *et al.* 2005).

A current model for the involvement of Hsp27 in VEGF-stimulated endothelial cell migration, and

cell migration in general, is that described by Rousseau *et al.* (2000a). Under basal conditions, unphosphorylated Hsp27 caps actin filaments, preventing their elongation. VEGF or another stimulus leads to activation of p38 MAPK, which phosphorylates and activates MAPKAPK2, which directly phosphorylates Hsp27 at S15, S78 and S82. Phosphorylation of Hsp27 monomers inhibits their actin capping activity, allowing actin polymerisation to occur. At the leading edge of cells, where Hsp27 is enriched, enhanced actin polymerisation results in the formation of laemellipodia which pushes the leading edge of the cell forwards. Elsewhere in the cell, increased actin polymerisation results in formation of stress fibres, which are observed rapidly after VEGF treatment of endothelial cells and are also required for migration. Phosphorylated Hsp27 may be required to stabilise these stress fibres to allow prolonged migration, and may also assist in stabilising newly formed filaments at the leading edge. Interactions of Hsp27 with other cytoskeletal-regulating proteins may also contribute – for example, interaction with the protein hydrogen peroxide-inducible clone 5 has been suggested to regulate actin in SMCs, and hic5 is also expressed in ECs (Jia *et al.* 2001b; Srinivasan *et al.* 2008).

Although this model offers an explanation for the functions of Hsp27 in migrating endothelial cells, it does not appear to hold in all experimental situations. NIH3T3 cells stably overexpressing wild-type hamster Hsp27 showed reduced migration in a wound-healing assay and invasion on matrigel (Lee *et al.* 2008). Further analysis using phosphorylation site mutants indicated that overexpression of a 2A Hsp27 mutant enhanced migration whereas a 2E mutant inhibited migration. These results seem to contradict those observed in other studies and predicted by the model discussed above. However Lee *et al.* (2008) suggested that, in their model, overexpression of Hsp27 results in excessively strong adhesion of cells to the substrate by increased focal adhesion formation and reduced expression of the matrix metalloprotease MMP2, so retarding migration.

The effect of Hsp27 overexpression on cancer cell invasion appears to vary with cell type. TGFβ-stimulated invasion of PC3 prostate cancer cells in gelatin was reduced by Hsp27 or MAPKAPK2 siRNAs, and cells overexpressing non-phosphorylatable (3G) Hsp27 were less invasive than cells

overexpressing wild-type Hsp27 (Xu *et al.* 2006). In this study, overexpression of the non-phosphorylatable form of Hsp27 substantially reduced TGFβ-stimulated expression of MMP2, which was postulated as the cause of the reduced invasion. However, the inability to remove Hsp27 caps on actin filaments discussed above may also contribute.

The extent to which adhesion or actin polymerisation effects dominate in the response to Hsp27 overexpression may depend on the cell type and degree of overexpression. Reduction of endogenous Hsp27 in endothelial cells may be informative as to the in vivo role of Hsp27 in these cells.

1.5.5.4 Protection from apoptosis

As discussed elsewhere, increased Hsp27 expression protects cells against heat and other cellular stresses, and this protection may involve the chaperone, actin-protective, and glutathione-modulating properties of this protein (glutathione-related effects discussed in section 1.5.5.5.1). Hsp27 has also been reported to directly interact with various members of apoptosis signalling pathways, and this is believed to be an important part of the protective roles of Hsp27 (reviewed by Concannon *et al.* 2003, Lanneau *et al.* 2008). For context, an overview of apoptosis signalling is given in section 1.4.4.5. Little work on the involvement of Hsp27 in endothelial apoptosis has been reported, with most data obtained from cell lines.

1.5.5.4.1 Extrinsic/caspase 8 pathway

Initial evidence for the involvement of Hsp27 in apoptotic cell death comes from work by Mehlen *et al.* (1996b), who showed that cell death and apoptosis-related changes (DNA laddering and morphological changes such as nuclear breakup and cell shrinkage) due to antibody-mediated crosslinking of Fas were dramatically reduced in mouse L929 cells overexpressing human Hsp27. After 18 h exposure to a high concentration of antibody, almost all control cells were dead whereas less than 10% of Hsp27 overexpressing cells were dead.

Charette *et al.* (2000) examined the role of Hsp27 on Fas-mediated apoptosis. Hamster Hsp27 interacted with daxx when both proteins were overexpressed in 293 cells. In a pulldown assay using GST-Fas, less daxx was pulled down from lysates from cells overexpressing daxx and Hsp27 than lysates from cells expressing daxx alone, indicating that Hsp27 reduced the binding of daxx to Fas, probably by binding directly to daxx. A S15E S90E (2E) hamster Hsp27 form was similarly effective to wild-type Hsp27 in inhibiting the Fas/daxx interaction, whereas a S15A S90A (2A) Hsp27 mutant was less effective. In 293 cells overexpressing both daxx and Ask1, in order to enhance daxx-dependent apoptosis, overexpression of wild-type Hsp27 or the 2E mutant reduced the nuclear-to-cytoplasmic translocation of daxx and apoptosis, whereas overexpression of the 2A mutant had little effect. Overall, it appears that phospho-mimicking Hsp27 binds to daxx, preventing its translocation to the cytoplasm and its interaction with activated Fas and Ask1, so reducing apoptosis. How Hsp27 does this, given that daxx is nuclear in healthy cells and Hsp27 is cytoplasmic, is unclear. Perhaps Hsp27 interferes with a signalling pathway involved in daxx-mediated apoptosis in two separate ways, inhibiting the plasma membrane-to-nucleus signalling required for daxx translocation, and/or binding to any cytoplasmic daxx. Another possibility is that a very small amount of Hsp27 may be present in the nucleus. The authors pointed out that the effect of Hsp27 on Fas-mediated apoptosis depends on the relative contribution of the daxx and FADD-dependent pathways, which is likely to be stimulus and time dependent, as Hsp27 apparently had little effect on FADD-mediated apoptosis.

1.5.5.4.2 Intrinsic/caspase 9 pathway

Hsp27 inhibits the intrinsic apoptotic pathway at a number of points. Hsp27 overexpressed in U937 cells co-immunoprecipitates with procaspase 3 and inhibits its cleavage and activation by caspase 9 (Pandey *et al.* 2000b). Additionally, immunodepletion of Hsp27 resulted in loss of caspase 3 protein, further suggesting an association between Hsp27 and caspase 3. Less caspase 3 was present in Hsp27 IPs from cells exposed to ionising radiation and other DNA damaging stimuli, leading the authors to suggest a model whereby Hsp27 associates with and so inhibits

caspase 3 activity. Apoptosis-inducing stimuli disrupt this interaction during caspase 3 activation. Association of Hsp27 and procaspase 3, causing inhibition of caspase 3 cleavage and activation, has also been reported in monocytes (Voss *et al.* 2007).

Garrido *et al.* (1999) showed that overexpression of human Hsp27 in U937 leukaemia cells reduces cell death and apoptosis induced by the drug etoposide, which produces double-stranded breaks in genomic DNA leading to p53-mediated apoptosis. Hsp27 overexpression prevented cleavage (activation) of caspases 2, 3, 8 and 9 but did not affect the mitochondria-to-cytosol redistribution of cytC; cytC-stimulated activation of caspases 3 and 9 in cellular extracts was also blocked by immunodepletion of Hsp27. These results suggest that the anti-apoptotic effect of Hsp27 is due to inhibition of cytC-mediated activation of caspase 9.

Using the same cell type and model Bruey *et al.* (2000a) demonstrated that Hsp27 co-immunoprecipitated with cytC, suggesting a direct association of the two proteins. Neither APAF1 nor caspases 3 and 9 were present in Hsp27 IPs, nor were other heat shock proteins tested (Hsp60, Hsp70, Hsp90). The amount of cytC and procaspase 9 present in APAF1 immunoprecipitates of cytC-treated cell extracts was reduced in Hsp27 overexpressing cells. Taken together, these results indicate that Hsp27 binds to cytC released from mitochondria, preventing its association with APAF1 and subsequent activation of caspase 9 activation.

Analysis of cells transfected with Hsp27 containing various deletion mutations indicated that regions in both the N-terminal and α-crystallin domains, and the single cysteine residue of Hsp27 (C137), are essential for association of cytC with Hsp27, and for Hsp27-mediated protection against etoposide-induced apoptosis (Bruey *et al.* 2000a). In contrast amino acids 15–51 (which includes the WDPF region required for oligomerisation) and 141–205 are relatively unimportant. C137 is required for Hsp27 dimerisation (discussed above), and so it is unlikely that monomers are the cytC-interacting Hsp27 species.

Paul *et al.* (2002) reported that Hsp27 interferes with staurosporine-induced release of cytC from mitochondria of L929 fibroblasts. This contradicts work detailed above which found no effect of

Hsp27 on cytC release. After comparing cell lines expressing differing amounts of Hsp27, the authors ascribed this difference to the need for a higher level of Hsp27 expression, not achieved in the earlier studies, for inhibition of cytC release than is necessary for inhibition of procaspase 3 activation via binding to released cytosolic cytC.

The mechanism by which Hsp27 prevents cytC release is unknown, but appeared to be upstream of mitochondrial activation. The pro-apoptotic protein Bid is an activator of Bax, which forms pores in the outer mitochondrial membrane causing cytC release. Bid and Bax are normally cytosolic, and redistribute to mitochondria during activation of the intrinsic apoptotic pathway. HeLa cells expressing antisense Hsp27 showed accelerated staurosporine-induced loss of Bid from the cytosol, suggesting that Hsp27 may affect signals prior to the involvement of mitochondria. However a control antisense (scrambled)-expressing cell line was not used (Paul *et al.* 2002). Another study reported that Hsp27 overexpression in a renal epithelial cell line inhibited ATP depletion-induced Bax activation and cytC leakage from mitochondria, whereas siRNA-mediated Hsp27 knockdown increased Bax activation (Havasi *et al.* 2008).

Damage to actin microfilaments can be an activator of the intrinsic apoptotic pathway, and actin filament-stabilising properties of Hsp27 may contribute to reduction of cytC release from mitochondria. Phalloidin prevented actin damage and apoptosis induced by cisplatin, and overexpression of Bcl2 prevented cisplatin-induced apoptosis but not actin damage (Kruidering *et al.* 1998), indicating that actin damage is upstream of cytC-related events in cisplatin-stimulated apoptosis. Cytochalasin D-induced actin depolymerisation, mitochondrial cytC release and caspase activation in L929 fibroblasts, and this could all be prevented by pre-treatment of the cells with phalloidin (Paul *et al.* 2002). Furthermore, L929 fibroblasts strongly overexpressing Hsp27 showed resistance to cytochalasin D-mediated cytC release (Paul *et al.* 2002), indicating that Hsp27-mediated actin stabilisation may contribute to the anti-apoptotic properties of Hsp27.

Actin stabilisation is unlikely to be the only property of Hsp27 leading to reduced mitochondrial cytC release. In etoposide-treated L929 fibroblasts, where F-actin disruption is not noticeable,

Hsp27 still inhibited cytC release (Paul *et al.* 2002). Furthermore, phalloidin only partially protected against staurosporine-induced apoptosis.

In summary, Hsp27 inhibits the intrinsic pathway machinery by inhibiting cytC release from mitochondria, preventing the interaction of cytosolic cytC with APAF1, and inhibiting procaspase 3 activation by caspase 9. Stabilisation of the actin cytoskeleton contributes to inhibition of mitochondrial cytC release induced by some stimuli but is relatively unimportant for others. The most important mechanism for apoptosis inhibition may vary depending on the apoptotic stimulus employed.

1.5.5.4.3 Effect on Akt signalling

The protein kinase Akt is an important inhibitor of the intrinsic apoptotic pathway, and is activated via the PI-3-K pathway by a number of cytokines including VEGF. Amongst other targets, Akt phosphorylates and so inhibits the activity of the pro-apoptotic molecules procaspase 9 and Bad, so promoting cell survival (discussed in section 1.4.4.5).

Overexpression of Hsp27 decreased Bax activation and increased survival of a renal cell line exposed to ATP depleting agents (Havasi *et al.* 2008). PI-3-K inhibitors prevented the increased survival obtained due to Hsp27 overexpression, suggesting that Akt activity is required for Hsp27-dependent survival effects, at least under the circumstances examined. Whether Hsp27 anti-apoptotic effects act via Akt, or whether Akt activity is required in a permissive role, is not clear.

In some cell types (not ECs), Akt has been reported to associate with Hsp27 in a complex that also contains MAPKAPK2 and p38 (Rane *et al.* 2001; Zheng *et al.* 2006), and may directly phosphorylate Hsp27 (discussed in section 1.5.3.3). Wild-type and 3A Hsp27 associated with Akt-GST in a pulldown assay, whereas Akt-phosphorylated recombinant Hsp27 (phosphorylated at S82) and 3D Hsp27 did not (Rane *et al.* 2003). The same group suggested Hsp27 acts as a scaffolding protein, bringing together MAPKAPK2 and Akt, and is required for MAPKAPK2-dependent Akt phosphorylation. Hsp27 overexpression may promote complex formation and MAPKAPK2-mediated

Akt activation, leading to pro-survival signals. The general applicability of this mechanism has not been demonstrated.

1.5.5.5 Other cellular roles of Hsp27

1.5.5.5.1 Protection against oxidative stress

Hsp27 has been reported to improve cellular protection against oxidative stress by increasing intracellular levels of glutathione (GSH). GSH is a thiol-containing tripeptide (Glu-sCys-Glu, where sCys is the modified thiol-containing amino acid selenocysteine) which can reduce oxidants such as H_2O_2 chemically and enzymatically and has a role in protecting the cell against oxidative stress. Overexpression of small Hsps including Hsp27 raises cellular levels of GSH (Mehlen *et al.* 1996a), and siRNA-mediated Hsp27 knockdown reduces cellular GSH levels (McCollum *et al.* 2006). Chemical depletion of GSH prevents Hsp27-induced apoptosis protection against both H_2O_2 and TNFα (which causes intracellular H_2O_2 generation) (Mehlen *et al.* 1996a). The Hsp27-mediated glutathione increase may be a pro-survival mechanism important in protection against death-inducing agents which act via oxidant generation.

1.5.5.5.2 Growth

Hsp27 has been implicated in controlling the proliferation of ECs in culture. BAECs overexpressing wild-type Hsp27 proliferate more rapidly than controls and reach senescence earlier, whereas those overexpressing 3G Hsp27 proliferate at a similar rate (Piotrowicz *et al.* 1995). The earlier senescence may be a consequence of increased proliferation rate. It therefore appears that excessive small Hsp27 species may be responsible for the effect on growth rate. Why this effect occurs is not clear, but it may be related to Hsp27 regulated genes (see below) or increased nutrition via increased pinocytosis. Alternatively, it may be an artifact of improved survival of the transfection/antibiotic selection by Hsp27-expressing cells. In contrast, overexpression of Hsp27 reduces the proliferation rate of murine embryonic stem cells, whereas antisense-mediated Hsp27

reduction enhances proliferation (Mehlen *et al.* 1997b). In these cells, Hsp27 was postulated to be involved in growth arrest and differentiation of immature cells. Hsp27 expression increases during embryonic development, correlating with cell differentiation (Huang *et al.* 2007). It is possible that Hsp27 differentially affects growth rate in mature and immature cells.

1.5.5.5.3 Modulation of protein expression

Many mRNAs corresponding to pro-inflammatory genes and cytokines contain AU-rich elements (AREs) in their 3' untranslated region, and these elements are involved in rapid degradation of the mRNA with related effects on mRNA lifespan and therefore protein expression. The pathway for degradation of ARE-containing mRNAs is incompletely understood, but involves association of AUF1 with the ARE and recruitment of other proteins to the complex including Hsp70, followed by subsequent proteasomal degradation of AUF1 and mRNA degradation (Laroia *et al.* 1999, summarised in Sinsimer *et al.* 2008). MAPKAPK2, via p38 MAPK, has been reported to increase the stability of ARE mRNAs, so leading to increased inflammatory gene expression, and this required MAPKAPK2 catalytic activity (Winzen *et al.* 1999; Lasa *et al.* 2000, discussed further in section 1.6.1.2).

SiRNA-mediated Hsp27 knockdown inhibited IL-1-activated induction of the pro-inflammatory genes IL-6, IL-8 and COX2 in HeLa cells (Alford *et al.* 2007). The effect of Hsp27 knockdown appeared to be at least partly mediated by a more rapid degradation of these mRNAs, but Hsp27 did not appear to regulate the stability of large numbers of mRNAs indicating Hsp27 may be specifically involved in regulation of inflammatory pathways.

Alford *et al.* (2007) also reported that IL-1- and TNFα-stimulated activation of p38 and MAPKAPK2 (and of other enzymes including JNK and IκB kinase) was reduced by Hsp27 knockdown. Interestingly, this suggests that Hsp27 may also regulate its own phosphorylation. Given the involvement of p38/MAPKAPK2 in regulating the stability of mRNA, the authors suggested that the Hsp27 siRNA-induced reduction in inflammatory gene expression may have occurred via

effects on the activity of MAPKAPK2.

While Hsp27 may affect ARE mRNA stability via alterations in MAPKAPK2 activity, it may also have more direct effects. Hsp27 has recently been identified as a direct ARE binding protein, and has been found in an AUF1-containing complex (Sinsimer *et al.* 2008). Surprisingly, shRNA-mediated knockdown of Hsp27 increased the half-life of TNFα mRNA, or a reporter mRNA containing the TNFα ARE – this is the opposite of that expected from the studies mentioned above. Furthermore, an shRNA-mediated 63% reduction in Hsp27 protein levels extended TNFα mRNA half-life 10-fold, whereas a 90% knockdown of AUF1 increased half-life 4-fold. In another study, overexpression of 3E Hsp27 increases the half-life of a COX2-based reporter transcript (Lasa *et al.* 2000), suggesting that phosphorylation of Hsp27 may be a target of MAPKAPK2-mediated mRNA stablilisation.

Whatever the mechanism, it appears that Hsp27 can affect protein expression via affects on mRNA stability, and this effect may be important in inflammation. It may also be a reason for the rapid transit of Hsp27 to the nucleus after heat shock.

1.5.6 Role of Hsp27 in disease

1.5.6.1 Charcot-Marie-Tooth disease

Charcot-Marie-Tooth disease (CMT) is a heterogeneous neurodegenerative condition characterised by wasting and weakness of peripheral muscles, often accompanied by peripheral sensory nerve loss and skeletal deformities (Pareyson 2007). Distal hereditary motor neuropathy (dHMN) is similar to CMT affecting motor but not sensory neurons, although there may be a continuum between the two diseases.

Mutations in the Hsp27 gene associate with type 2 (axonal, rather than type 1 myelin-related) CMT, and have also been reported in dHMN sufferers (Evgrafov *et al.* 2004; Houlden *et al.* 2008). Most mutations are in the α-crystallin domain, and none occur at or immediately adjacent to

known Hsp27 phosphorylation sites. Neuronal cells overexpressing Hsp27 carrying an S135F mutation (also observed in some CMT patients) survived less well than either control cells or cells overexpressing wild type Hsp27 (Evgrafov *et al.* 2004).

Although Hsp27 mutations may occur in some CMT2 patients, genetic analysis revealed that most CMT2 sufferers did not harbour mutations in any of the genes previously reported to be associated with CMT2 – indeed, of 61 affected patients, no-one carried a mutation in the Hsp27 gene (Bienfait *et al.* 2007). In a later study, 7 out of 145 affected families had mutations in the Hsp27 gene (Houlden *et al.* 2008).

The low incidence of Hsp27 mutations in CMT sufferers may reflect the heterogeneous nature of the disease, with many pathologies giving rise to similar symptoms, and Hsp27 mutation may define a disease subset. The nature of the involvement of Hsp27 in neuropathy is unknown but may be related to its ability to modify the cytoskeleton. Overexpression of S135F Hsp27 prevented normal assembly of neurofilament light protein into filaments, whereas wild-type Hsp27 did not have this effect (Evgrafov *et al.* 2004). Other properties of Hsp27 may also be involved, such as loss of apoptosis protection. Additionally, Hsp27 dysfunction may exacerbate protein folding problems caused by another protein defect.

1.5.6.2 Cancer

Hsp27 biology is of interest in cancer. Examining cells of differing tumourigenicity, Garrido *et al.* (1998) observed that Hsp27 expression was absent in tumour cells which formed rapidly regressing tumours, but was substantial in tumour cells which formed slowly regressive tumours. Implantation of Hsp27-lacking tumour cells into rats caused small tumours which regressed rapidly, whereas implantation of tumour cells overexpressing Hsp27 caused large, prolonged, slowly regressing tumours to form (Garrido *et al.* 1998). In nude (non-immunocompetent) mice, no difference was observed in tumour formation between Hsp27-null and Hsp27-overexpressing cells, which was substantial in both cases.

Garrido *et al.* (1998) proposed that this difference between nude mice and immunocompetent rats was due to Hsp27 overexpression reducing immune cell-mediated clearance of tumours, possibly by reducing tumour cell apoptosis and so reducing the release of antigenic tumour cell debris. Indeed, anti-apoptosis effects may underlie Hsp27-mediated increases in tumourigenicity – over-expression of Hsp27 also increases the resistance of tumour cells to anti-cancer drugs (Garrido *et al.* 1997, 1998).

In addition to survival roles, Hsp27-overexpression increases the invasiveness of prostate cancer cells, and cells overexpressing a 3G Hsp27 mutant showed reduced invasion (Xu *et al.* 2006, previously discussed on page 125).

Hsp27 expression is high in a number of cancer cells (Calderwood *et al.* 2006), suggesting that Hsp27 overexpression may aid tumour progression and may therefore be an attractive target for cancer treatments. Given the relatively normal Hsp27-null mouse (Huang *et al.* 2007), reasonably few side effects might be expected for anti-Hsp27 therapies, although many subtle or pathology defence-related effects of Hsp27 may have been missed in Hsp27 knockout mice.

1.5.6.3 Ischaemia-reperfusion injury

Ischaemia-reperfusion injury (I-R) is tissue damage occurring on reperfusion of an ischaemic area, particularly the heart (Liem *et al.* 2007). Ischaemic preconditioning, where mild ischaemia and recovery subsequently protects against severe ischaemia resulting in reduced cell death and tissue damage, is reminiscent of thermotolerance. A variety of proteins are induced during ischaemic pre-conditioning, and are protective against the later, more severe insult. Induction of VEGF has been reported to be particularly important in protection of neurons (Nishijima *et al.* 2007).

Hsp27 overexpression protects against simulated I-R in endothelial cell cultures (Kabakov *et al.* 2003), myocyte cell cultures (Martin *et al.* 1997; Vander Heide 2002), and a Langendorff perfused heart model (Hollander *et al.* 2004). Overexpression of hemagglutinin-tagged human Hsp27 in mice reduced the kidney and liver damage occurring on hepatic I-R (Park *et al.* 2009; Chen *et al.*

2009).

In the Langendorff study, hearts from mice overexpressing either wild-type human Hsp27 or a non-phosphorylatable mutant were less affected by simulated ischaemia-reperfusion injury and recovered better than hearts from control animals, suggesting that phosphorylation of Hsp27 may not be required in the protection from I/R injury. Indeed, the non-phosphorylatable mutant did appear to give improved protection against the associated oxidative stress than the wild-type form. It should be noted that a significant amount of endogenous Hsp25 appeared to be present in the control hearts, and that Hsp27 is not the native form of this protein present in mice. It is likely that Hsp27 protects against I-R via its roles as a chaperone and in direct regulation of apoptosis.

1.6 p38 MAPK/MAPKAPK2 and PKC/PKD activation and signalling

1.6.1 p38 MAPK and MAPKAPK2

Mitogen-activated protein kinases (MAPKs) are protein Ser/Thr kinases activated by two phosphorylations in the activation loop in a TXY motif, and include the ERKs (motif TEY), JNKs (TPY) and p38 MAPKs (TGY) (reviewed by Raman *et al.* 2007). These phosphorylations are performed by a dual specificity MAP kinase kinase (MEK), which itself is activated by an upstream MEK kinase, forming a classical three step MAPK cascade.

p38 MAPK (p38, also originally termed cytokine suppressive anti-inflammatory drug binding protein (CSBP) or reactivating kinase) was discovered in 1994 by a number of separate groups as a MAPK (phosphorylated on Thr and Tyr, inhibited in vitro by Ser/Thr or Tyr kinases) activated by cellular stresses, distinct from ERK and JNK on the basis of activation stimuli, substrate and inhibitor specificity, and homologous to the yeast kinase HOG1 (Han *et al.* 1994; Rouse *et al.* 1994; Freshney *et al.* 1994; Lee *et al.* 1994). p38 was activated in cells by cellular stresses which did not activate ERK, and in vitro did not phosphorylate the JNK substrate c-Jun. p38 was identified as the

target of pyridinyl imidazole compounds such as SB202190 and SB203580, which block production of TNFα and IL-1β in lipopolysaccharide-stimulated monocytes (Lee *et al.* 1994), and these compounds have since been used extensively to implicate p38 in a variety of physiological processes. Importantly for this thesis, these early studies also identified p38 as able to phosphorylate and activate the Hsp27 phosphorylating kinase MAPKAPK2.

Since its initial discovery, a number of p38 isoforms have been identified, encoded by separate genes. The p38 MAPK family currently consists of the originally identified p38 (p38α/stress-activated protein kinase (SAPK) 2a/MAPK14), p38β (sometimes termed p38β2, SAPK2b/MAPK11), p38γ (SAPK3/MAPK12) and p38δ (SAPK4/MAPK13) – SAPK1 is JNK. Some isoforms have a number of splice variants – p38α is known to have four: CSBP2 (MAPK14 isoform 2, the originally identified p38), CSBP1, Mxi2 and Exip. Where p38 has been overexpressed (without denoting a subtype), CSBP2 is the form referred to. p38α, β, γ and δ (and a previously identified p38β1 isoform) have been overexpressed in a human cell line to examine their relative properties (Kumar *et al.* 1997; Goedert *et al.* 1997). All isoforms apart from β1 were activated by TNFα, IL-1, sorbitol (inducing osmotic stress) and ultraviolet irradiation. In vitro, p38α (CSBP2) and β strongly phosphorylated MAPKAPK2 and 3, and were inhibited by SB202190 and SB203580, whereas p38γ and δ were poor kinases for MAPKAPK2 and 3, and were insensitive to SB202190 and SB203580.

MAPKAPK2 was originally characterised as a protein Ser/Thr kinase which, after dephosphorylation, could be reactivated in vitro by ERK (Stokoe *et al.* 1992a), and was subsequently shown to phosphorylate Hsp27 and Hsp25 in in vitro kinase assays at the same sites (S15, S78 and S82 for Hsp27, S15 and S86 for Hsp25) as had been reported to be phosphorylated in vivo in response to cytokines and heat shock (Stokoe *et al.* 1992b). In vitro phosphorylation of S82/S86 by MAPKAPK2 was more rapid than phosphorylation at the other sites. p38 was shown to be involved in Hsp27 phosphorylation stimulated by arsenite, IL-1 and sorbitol in human cells using SB203580 (Cuenda *et al.* 1995). Given that SB203580 doesn't directly inhibit MAPKAPK2 (Kumar *et al.*

1999), it is likely that a p38–MAPKAPK2–Hsp27 pathway exists in vivo.

Other MAPKAPK2-like enzymes exist, and MAPKAPK2 is considered to form a family with MAPKAPK3 and MAPKAPK5 (reviewed by Gaestel 2006). MAPKAPK3 appears very similar to MAPKAPK2 in terms of activation and substrate specificity, and is able to phosphorylate Hsp27 at the same sites as MAPKAPK2 (McLaughlin *et al.* 1996; Clifton *et al.* 1996). In these studies, MAPKAPK3 contributed less to SB203580-sensitive phosphorylation of downstream substrates, which is likely to reflect generally lower levels of MAPKAPK3 expression. MAPKAPK5 is not activated in response to classical p38 activators such as arsenite and sorbitol, does not phosphorylate Hsp27 and appears functionally distinct to MAPKAPKs 2 and 3 (Shi *et al.* 2003).

1.6.1.1 Activation mechanism of p38 and MAPKAPK2

As for other MAPKs, activation of p38 MAPK requires phosphorylation at the activation loop residues (T180/Y182 in human p38α). Mutation of either of these residues to unphosphorylatable mimics prevents p38 activation induced by arsenite (Doza *et al.* 1995) or UV (Raingeaud *et al.* 1995) in intact cells. Pyridinyl imidazole inhibitors bind to the ATP binding site of p38, inhibiting enzymatic activity but not preventing p38 activation loop phosphorylation by its upstream kinases (Young *et al.* 1997; Kumar *et al.* 1999). MEK3 and MEK6 (also termed SKK3) have been identified as the major upstream kinases of p38 isoforms. MEK3 and 6 are activated by cellular stresses, and overexpression of constitutively active MEK3 or MEK6 in intact cells stimulated phosphorylation of overexpressed p38α (Raingeaud *et al.* 1996). p38α, β, γ and δ are phosphorylated in vitro by MEK6, p38α, γ and δ but not p38β are phosphorylated by MEK3 (Enslen *et al.* 1998; Goedert *et al.* 1997). Some phosphorylation of p38α, but not β or γ, was also observed in vitro by the JNK kinase MEK4.

The activation of p38 by MEK isoforms has been examined by the generation of MEK-null mice (Brancho *et al.* 2003), although it was not clear from the methods of this study whether all p38 isoforms were being assayed, or just p38α. Mice lacking MEK3 or MEK6 were apparently nor-

mal, whereas MEK3/6 double-null died around E11 exhibiting placental defects similar to that observed for p38α-null mice (see below). TNFα stimulated p38 activation loop phosphorylation and kinase activity in fibroblasts isolated from MEK3-null or MEK6-null embryos, but not in fibroblasts from MEK3/6 double-null embryos. UV-stimulated p38 activation was still observed at a reduced level in MEK3/6 double-null fibroblasts, but was largely abolished by siRNA-mediated MEK4 knockdown in these cells. Thus either MEK3 and 6 are required for TNFα-stimulated p38 activation, and either MEK3, 4 or 6 is required for UV-stimulated p38 activation. MEK3 and 6 appear mutually redundant.

Upstream activation of MEK3/6 is unclear - a wide variety of kinases have been reported to phosphorylate MEKs 3 and 6, including Ask1, TGFβ activated kinase 1 (TAK1), MEKK3 and others (Raman *et al.* 2007). Scaffolding proteins including OSM and JIP2 may also be involved in recruiting the a p38/MEK complex to upstream activators. In common with other MAPKs, p38 activity can be influenced by dual-specificity phosphatases which dephosphorylate MAPK activation loop residues reducing MAPK activity. Overexpression of the dual-specificity phosphatase MKP1 inhibited UV-induced p38α activity in intact cells (Raingeaud *et al.* 1995), and siRNA-mediated downregulation of MKP1 in endothelial cells prolonged TNFα-stimulated p38 activation (Wadgaonkar *et al.* 2004).

MAPKAPK2 is a phosphorylation-regulated enzyme, and dephosphorylation completely prevents its ability to phosphorylate Hsp27 in vitro. Although MAPKAPK2 is phosphorylated on a number of sites in arsenite-stimulated cells, the key regulatory sites in human MAPKAPK2 are T222 and T334, and replacement of these residues with Glu renders the enzyme constitutively active (Engel *et al.* 1995; Ben-Levy *et al.* 1995).

MAPKAPK2 contains nuclear localisation and nuclear export signals. In unstimulated cells, MAPKAPK2 is present mainly in the nucleus, and forms a complex with p38. This complex may be important for the mutual stability of the two enzymes – MAPKAPK2 protein levels are strongly reduced in p38α-null fibroblasts, whereas MAPKAPK2 mRNA expression is little affected (Sudo

et al. 2005). Conversely, p38α protein expression is reduced in MAPKAPK2-deficient tissues, the extent of which is tissue-dependent (Kotlyarov *et al.* 2002). On activation, the p38α/MAPKAPK2 complex translocates to the cytosol, and this appears to be at least partially dependent on MAPKAPK2 phosphorylation at T334 (Engel *et al.* 1998; Ben-Levy *et al.* 1998).

1.6.1.2 Knockout mice

p38α-null mice died in utero around E10.5, whereas heterozygotes were apparently normal (Allen *et al.* 2000; Adams *et al.* 2000). Lethality in p38α-null mice was due to lack of intermingling of embryonic and maternal blood vessels in the placenta. Mixing diploid embryonic stem (ES) cells from one embryo with tetraploid ES cells from another results in mice in which cells from both embryos contribute to certain extra-embryonic tissues, but the embryo proper (and so resulting mouse) is formed only from ES cells contributed by the diploid embryo (Ihle 2000). Using this method, rescue of the placental defect by mixing p38α-null diploid ES cells with wild-type tetraploid ES cells allowed birth of apparently normal p38α-null mice (Adams *et al.* 2000), indicating that p38α is required for correct development of the placenta but not for the rest of the embryo. UV, anisomycin (a protein synthesis inhibitor) and H_2O_2 failed to activate MAPKAPK2 or Hsp27-phosphorylating kinases in a p38α-null cardiomyocyte line, whereas these stimuli strongly activated MAPKAPK2 and Hsp27-phosphorylating kinases in cardiomyocytes from heterozygous mice (Adams *et al.* 2000). These data indicate that stress-stimulated MAPKAPK2 activation occurs via p38α and not other p38 isoforms or other enzymes, at least in cardiomyocytes, although the expression of other p38 isoforms was not determined.

In contrast, p38β-null mice are apparently normal, with unimpaired anisomycin-induced MAPKAPK2 activation and lipopolysaccharide-stimulated TNFα production (Beardmore *et al.* 2005). Mice lacking either p38γ or p38δ, or double-null mice lacking both isoforms, are viable, fertile and apparently healthy (Sabio *et al.* 2005). Given that stress-induced MAPKAPK2 activation can be blocked by SB203580, which does not inhibit p38γ or δ, these results indicate that p38α is

likely to be the only enzyme responsible for stress-induced activation of MAPKAPK2.

MAPKAPK2-null mice are viable, fertile and apparently healthy, but showed reduced lipopolysaccharide (LPS)-stimulated release of inflammatory cytokines with TNFα release reduced by 90% compared to wild-type mice (Kotlyarov *et al.* 1999). The role of MAPKAPK2 in TNFα production appears to be due to phosphorylation of downstream targets by MAPKAPK2, as adenovirus-mediated overexpression of wild-type but not kinase-inactive MAPKAPK2 restored LPS-stimulated TNFα production in MAPKAPK2-deficient cells (Kotlyarov *et al.* 2002). The involvement of MAPKAPK2 in TNFα production is probably due to the presence of AU-rich elements in the TNFα mRNA. p38-medited MAPKAPK2 activity has been implicated in stabilisation of ARE-containing mRNAs, and loss of MAPKAPK2 would therefore be expected to reduce TNFα mRNA lifetime and so protein expression (Winzen *et al.* 1999, discussed in section 1.5.5.5.3).

Mice deficient in either MAPKAPK3 or MAPKAPK5 are viable and fertile, and exhibit no alterations in LPS-stimulated cytokine release (Ronkina *et al.* 2007; Shi *et al.* 2003). The similarity of MAPKAPK2 and 3, and compensation between these isoforms, may mask some of the effects of MAPKAPK2 and 3 in these mice. Indeed, reductions in LPS-induced TNFα secretion, arsenite-stimulated Hsp25 phosphorylation and p38α protein expression in MAPKAPK2-null cells could be rescued by overexpression of MAPKAPK3 (Ronkina *et al.* 2007). However, MAPKAPK2/3-double null mice are also viable, fertile and overtly normal although they display greater reductions in LPS-induced TNFα secretion and p38α protein expression (Ronkina *et al.* 2007). Together, these data indicate that MAPKAPK2 and 3 are very similar enzymes, without separate known substrates, and that MAPKAPK2 is the major enzyme in most tissues due to a higher expression level.

1.6.1.3 Activation of p38 and MAPKAPK2 in ECs

TNFα, IL-1β and H_2O_2 all activated p38 MAPK in HUVECs, with strong kinase activity detected 5–20 mins after stimulus addition (Huot *et al.* 1997). Interestingly, H_2O_2-stimulated p38 MAPK and MAPKAPK2/3 activity was biphasic, with an initial increase followed by a decline at around 20 mins and then a second phase of increased activity, declining after 40 mins. TNFα, IL-1β and H_2O_2 also activated a kinase able to phosphorylate Hsp27 in vitro, assumed to be MAPKAPK2 as H_2O_2-stimulated Hsp27 phosphorylation was blocked by the p38 MAPK inhibitor SB203580. VEGF also activated p38 MAPK in HUVECs, with maximal kinase activity detected after 5–15 mins stimulation (Rousseau *et al.* 1997). The mechanism of VEGF-stimulated p38 MAPK activation in ECs is discussed in section 1.5.3.4.

1.6.2 Protein kinase C

Protein kinase C was originally identified as a Ser/Thr kinase activated by the membrane lipids phosphatidylserine (PS) and diacylglycerol (DAG), phorbol esters and Ca^{2+} (Takai *et al.* 1979). Phorbol esters (such as phorbol 12-myrisate 13-acetate, PMA) are artificial tumour-promoting compounds that are non-hydrolysable analogues of the physiological PKC activator DAG. While both phorbol esters and DAG activate PKC, prolonged treatment with phorbol esters but not DAG induces downregulation of PKC via an increased rate of PKC protein degradation (Rodriguez-Pena and Rozengurt 1984; Young *et al.* 1987; Issandou and Rozengurt 1989).

Since these early findings, a variety of PKC isoforms have been discovered and mammalian isoforms have been classified into three subcategories: classical/conventional, novel, and atypical (reviewed by Mellor and Parker 1998). The classical isoforms α, βI, βII and γ are activated by PS, DAG and Ca^{2+} (βI and βII are splice variants). The novel isoforms δ, ϵ, θ and η (eta) are activated by PS and DAG but not Ca^{2+}. The atypical isoforms ζ (zeta) and ι (iota, referred to as λ (lambda) in mice) are activated by PS but are insensitive to DAG and Ca^{2+}. These categories can be partially distinguished by inhibitor sensitivities – the compounds GF109203X (bisindolyl-

maleimide I) and Gö6983 inhibit all PKC isoforms with reduced effectiveness against atypical PKCs, whereas Gö6976 is often used as an inhibitor of the classical PKC isoforms (Toullec *et al.* 1991; Martiny-Baron *et al.* 1993).

PKCs are composed of a number of domains as shown in figure 1.13. In the absence of stimulation, PKC activity is prevented by an autoinhibitory regulatory region containing a pseudosubstrate sequence – proteolytic separation of the regulatory region from the catalytic domain renders PKC constitutively active. The regulatory region also contains a cysteine-rich C1 domain, and may contain a C2 domain. C1 domains are responsible for DAG, phorbol ester and PS binding (Colon-Gonzalez and Kazanietz 2006). Classical and novel PKC isoforms have two C1 domains, termed C1A and C1B, whereas the atypical C1 domain is unable to bind phorbol esters or DAG. Other, non-PKC proteins also contain C1 domains (for example PKD, discussed below) and so are able to bind to DAG and phorbol esters. C2 domains in classical PKC isoforms are responsible for Ca^{2+} binding, and act as Ca^{2+}-dependent phospholipid-binding domains. In novel PKCs, C2 domains bind neither Ca^{2+} nor phospholipids, and their function is unclear.

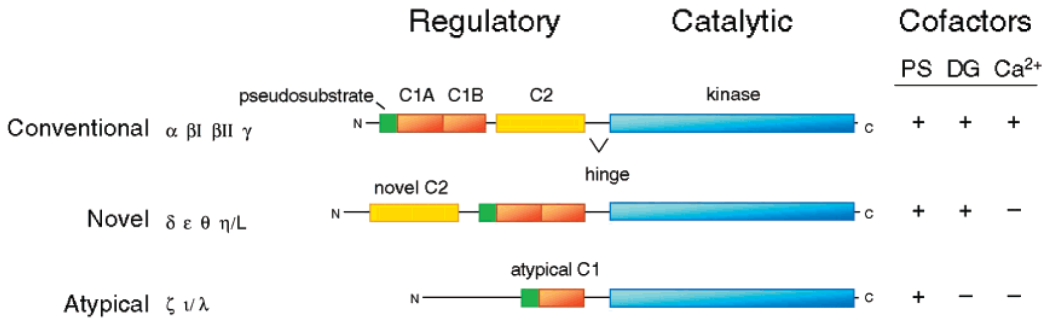

Figure 1.13: PKC domains and cofactors (adapted from Newton 2001)

Activation of PKC is a multi-step process involving phosphorylation, lipid binding and translocation, and is best understood for classical and novel PKCs. As for other AGC family kinases, PKC is phosphorylated at three sites termed the activation loop, the turn motif and the hydrophobic site (Newton 2003). Additional isoform-specific phosphorylations at other sites may also occur. Phosphorylation at the activation loop threonine residue unmasks the catalytic site and is performed

by PDK1, the same phosphoinositide-activated enzyme that is involved in Akt activation as mentioned previously. The turn motif and hydrophobic site are believed to be autophosphorylation sites.

The current model for PKC activation is as follows. PKC associates with the membrane after synthesis and is phosphorylated, perhaps constitutively, at the activation loop by PDK1. Subsequent autophosphorylations allow the pseudosubstrate sequence to bind, which maintains mature PKC in an inactive conformation, and causes translocation to the cytosol. Cytokine-mediated activation of phospholipase C leads to production of DAG and inositol-1,4,5-triphosphate (and subsequently intracellular Ca^{2+} release). PKC then translocates to the membrane, assisted by Ca^{2+}-bound C2 domains in classical PKC isoforms, and interacts with membrane-embedded DAG via the C1 domain. DAG-bound C1 domains interact with PS, and result in removal of the pseudosubstrate sequence from the active site, producing catalytically active PKC. A variety of other molecules, including phosphatases and scaffolding proteins, influence PKC localisation and activity.

PKC has been implicated in a wide variety of cellular processes in many cell types, including VEGF-stimulated processes in endothelial cells as discussed previously. Mice lacking PKCα (Braz *et al.* 2004), PKCβ (Leitges *et al.* 1996), PKCγ (Abeliovich *et al.* 1993), PKCδ (Miyamoto *et al.* 2002), PKCϵ (Castrillo *et al.* 2001), PKCθ (Sun *et al.* 2000), PKCζ (Leitges *et al.* 2001), and PKCι/λ (Soloff *et al.* 2004) have been produced. With the exception of the PKCι/λ knockout, all these mice are viable, with some defects in restricted contexts such as the immune system. The general health of these mice suggests that substantial functional redundancy exists between PKC isoforms.

PKCs α, δ, and ϵ have previously been shown in this laboratory to translocate to the membrane in VEGF-stimulated HUVECs, suggesting that they are activated in response to VEGF treatment, and expression but not translocation of PKCζ was also detected (Gliki *et al.* 2001). Other groups have also used antibodies to detect PKCs α, β, δ, ϵ and ζ in HUVECs, with Yamamura *et al.* (1996) additionally detecting PKCη and PKCθ, and Wang *et al.* (2002) detecting PKCη. PKCα

and $\beta 2$ were reported to translocate to the membrane in VEGF-treated BAECs, whereas PKCδ and ϵ did not. The isoforms activated by VEGF may be endothelial cell type-specific.

1.6.3 Protein kinase D

Protein kinase D is a more recently identified family of PKC-activated protein Ser/Thr kinases (reviewed by Rozengurt *et al.* 2005, cardiovascular aspects reviewed by Avkiran *et al.* 2008). The protein kinase D (PKD) family of enzymes comprises three members, PKD1 (also termed PKCμ, Valverde *et al.* 1994; Johannes *et al.* 1994), PKD2 (Sturany *et al.* 2001), and PKD3 (also termed PKCν (nu), Hayashi *et al.* 1999). An alignment of the human PKD isoform amino acid sequences is shown in figure 1.14. All three PKDs contain two cysteine-rich motifs similar to the PKC C1 domain, a pleckstrin homology (PH) domain and a catalytic domain. The majority of work on the activation mechanism of PKDs has been performed on PKD1.

Similar to novel PKCs, PKD is activated by phosphorylation, PS and DAG/phorbol esters, but unlike PKCs is not downregulated by long-term phorbol ester treatment (Johannes *et al.* 1995; Van Lint *et al.* 1995). Additionally, the PKD catalytic domain is more similar in sequence to Ca^{2+}/calmodulin-dependent protein kinases (CaMKs) than PKC, and PKD1 does not phosphorylate a variety of synthetic peptides phosphorylated by PKC (Valverde *et al.* 1994). PKDs are now considered a subset of the CaMK family rather than the PKA/PKG/PKC family.

A major event in PKD activation is phosphorylation of the activation loop serine residues, in the motif SFRRS (S738/742 in human PKD1, S744/748 in mouse PKD1). A PKD1 S744E/S748E double mutant was constitutively active, and the activity of this enzyme was only slightly increased by phorbol ester stimulation, whereas an S744A/S748A double mutant was incapable of phorbol ester-stimulated activation (Iglesias *et al.* 1998). Mutation of either of the activation loop Ser residues to Glu resulted in intermediate PKD activity. PKD activation loop phosphorylation occurs in intact cells as determined by a phospho-specific antibody directed against phospho-S744/748 (Waldron *et al.* 2001). The small enhancement of activity by phorbol esters of a PKD

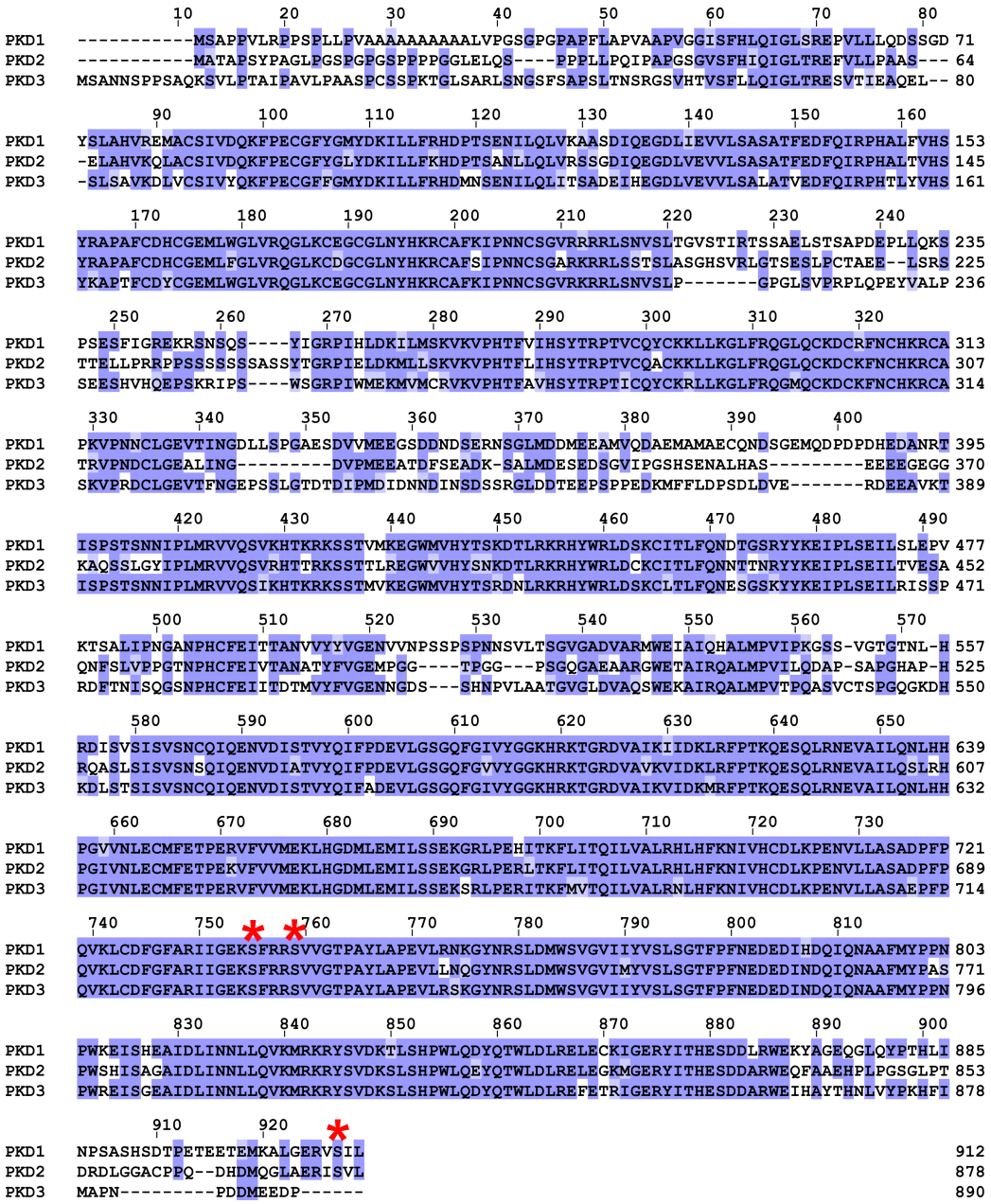

Figure 1.14: Alignment of amino acid sequences of human PKD isoforms
Reference protein sequences for human PKD1, PKD2 and PKD3 were retrieved from the RefSeq database and aligned with ClustalX2. Residues are coloured according to Blossum62 score, with darker colours indicating better conservation. The S738, S742 and S910 phosphorylation sites of human PKD1 are indicated with an asterisk (*). The RefSeq database accession numbers for the protein sequences (all human) used for alignment were: PKD1, NP_002733.2; PKD2, NP_001073349.1; PKD3, NP_005804.1.

phosphorylated activation loop mimic indicates that activation loop phosphorylation plays a much greater role in the control of PKD activity that the permissive, maturation-type role in PKC activation.

Activation loop phosphorylation is performed by an upstream kinase rather than autophosphorylation, as inactive PKD is still phosphorylated at the activation loop (Waldron *et al.* 2001). PKC inhibitors such as GF109203X blocked PKD activation loop phosphorylation in intact cells, but had no effect on purified PKD activity in vitro (Zugaza *et al.* 1997; Matthews *et al.* 1997). As these inhibitors do not directly affect PKD, their effects indicate that PKC phosphorylates PKD at the activation loop in vivo. PKC inhibitors prevent PKD activation loop phosphorylation in response to a wide range of stimuli, indicating that PKC may be a common upstream activator of PKD. Overexpression of constitutively active PKCδ or PKCϵ increased PKD activation loop phosphorylation in the absence of stimulation, whereas overexpression of PKCζ had no effect (Storz *et al.* 2004). Immunoprecipitated PKCδ directly phosphorylated the PKD activation loop residues in vitro (Storz *et al.* 2004), and immunoprecipitated PKCϵ directly phosphorylated a peptide consisting of residues surrounding the activation loop of PKD1 in vitro (Waldron and Rozengurt 2003).

In the model presented by Rozengurt *et al.* (2005), novel PKC isoforms and PKD translocate to the membrane and bind PS and phospholipase C-produced DAG. PKC is activated and phosphorylates PKD at the activation loop, resulting in PKD activation and removal of the requirement of DAG/PS binding for activity. Activated PKD can then translocate away from the membrane and phosphorylate downstream substrates. Exactly which novel PKC is responsible for PKD activation loop phosphorylation may depend on the upstream stimulus.

PKD becomes phosphorylated at a variety of other non-activation loop sites, which may be involved in PKD activation or regulation. PKD is autophosphorylated at S916 (S910 in human PKD1), and PKD catalytic activity correlates well with S910 phosphorylation (Matthews *et al.* 1999). As a result, S910 phosphorylation has been used as a surrogate for PKD activity in many studies.

PKD has been implicated in a wide variety of cellular processes in a number of cell types. At the outset of this thesis, there were no reports of VEGF-stimulated PKD activation, and little data on the role of PKD in endothelial cells. During the course of this thesis, PKD1 and 2 were reported to be expressed in endothelial cells. PKD1 and 2 have been implicated in VEGF-stimulated endothelial cell proliferation, migration and angiogenesis using siRNA-mediated PKD knockdown (Wong and Jin 2005; Qin *et al.* 2006; Hao *et al.* 2009b). PKD1 has further been implicated in phosphorylation of histone deacetylases (HDAC) 5 and 7, mediators of angiogenic gene expression (Ha *et al.* 2008a,b; Wang *et al.* 2008).

1.7 Biology of TNFα, IL-1 and H_2O_2

TNFα, IL-1 and H_2O_2 are stimulators of Hsp27 phosphorylation in endothelial cells. As these factors were used experimentally in this thesis, some details of their biological effects and activated signalling pathways are given below.

1.7.1 TNFα

Originally described as a factor which reduced tumour size in vivo and promoted death of tumour cells in culture (Carswell *et al.* 1975), tumour necrosis factor α (TNFα, reviewed by Pober and Min 2006; Bradley 2008) is an important pro-inflammatory cytokine with multiple effects on endothelial cells, promoting leukocyte recruitment to injured sites by inducing expression of E-selectin, ICAM-1 and VCAM-1 expression on nearby endothelium, and stimulating release of IL-8 and CCL2 (Pober *et al.* 1987; Mackay *et al.* 1993; Kuldo *et al.* 2005). TNFα stimulates COX2 expression, leading to prostacyclin production associated vasodilation and increased endothelial permeability.

The importance of TNFα in defence against infection was shown in mice lacking TNFα (Marino *et al.* 1997) or its receptor TNFR1 (Pfeffer *et al.* 1993; Rothe *et al.* 1993), which are viable but showed impaired clearance of bacterial infections and other immunological abnormalities.

While TNFα stimulation of immune cell activity is important for effective pathogen clearance, inappropriate/excessive TNFα production may lead to unwanted immune cell activity and tissue damage (Beutler *et al.* 1985; Pfeffer *et al.* 1993).

1.7.1.1 TNFα signalling

TNFα stimulates a wide variety of intracellular signalling in endothelial cells, including activation of NF-κB, p38 MAPK, JNK, ERK and PI-3-K/Akt (Modur *et al.* 1996, reviewed by Madge and Pober 2001). In contrast, VEGF does not appear to activate JNK or NF-κB (Mechtcheriakova *et al.* 2001). Both TNFR1 and 2 are expressed in HUVECs, but TNFα-stimulated increases in expression of E-selectin, ICAM-1 and VCAM-1 are predominantly mediated by TNFR1 (Mackay *et al.* 1993; Slowik *et al.* 1993). Indeed, inflammatory responses to TNFα were blocked in TNFR1- and TNFR1/2-null mice, but not in mice lacking only TNFR2 (Peschon *et al.* 1998).

The intracellular domain of TNFR1 (but not TNFR2) contains sequence motifs termed death domains (DD), which interact with death domains on other proteins. On ligand binding, TNFR1 displaces silencer of death domain signalling (SODD) and binds another DD-containing protein, TNFR-associated DD protein (TRADD). Recruitment of FADD directly to TRADD initiates TNFα-stimulated apoptosis via activation the extrinsic pathway (procaspase 8). Healthy ECs (and many other cell types) are usually resistant to TNFα-induced apoptosis, presumably because they are adapted to respond to macrophage-generated TNFα during inflammation.

TRADD may also bind a protein kinase (receptor interacting protein-1, RIP-1) and a ubiquitin ligase (TNFR-associated factor 2, TRAF2). Activated TRAF2 recruits and activates apoptosis signalling kinase-1 (Ask1), which phosphorylates MEKs 3, 4 and 6, which in turn phosphorylate and activate JNK and p38 MAPK (Ichijo *et al.* 1997; Nishitoh *et al.* 1998). Ask1 appears to be important for the sustained p38 MAPK activation associated with apoptosis, but not essential for p38 activation by short-term stimulation of TNFα (Saitoh *et al.* 1998).

The TRADD/RIP-1/TRAF2 complex also activates the transcription factors AP-1 and NF-κB.

AP-1 activation occurs via JNK, which phosphorylates the AP-1 subunit c-Jun. NF-κB (reviewed by Hayden and Ghosh 2008) is usually bound by the protein inhibitor of κB (IκB), which masks nuclear localisation signals in NF-κB, so maintaining it in the cytosol. TNFR1 activation leads to phosphorylation and activation of IκB kinase (IKK), which phosphorylates IκB, leading to IκB ubiquitination and degradation. Unbound NF-κB is then free to enter the nucleus and activate gene expression. TNFα-stimulated transcription of many pro-inflammatory genes, including E-selectin, ICAM-1, VCAM-1, CXCL8 and CCL2 is under the control of NF-κB and AP-1.

1.7.2 IL-1

Interleukin-1 (IL-1) classically refers to two distinct gene products, IL-1α and IL-1β, which have virtually identical effects in many cells including endothelial cells (Pober *et al.* 1987). IL-1 is an important cytokine in inflammation, with endothelial and systemic effects similar to those described above for TNFα (reviewed by Dinarello 2009). IL-1 activates endothelium, increasing leukocyte adhesion to ECs (Bevilacqua *et al.* 1985; Nawroth *et al.* 1986), via increased endothelial expression of leukocyte-binding adhesion molecules E-selectin, ICAM-1 and VCAM-1, and stimulation of endothelial production of neutrophil and monocyte chemoattractants CXCL8 and CCL2 (Kuldo *et al.* 2005).

Binding of IL-1 to its receptor IL-1R1 results in recruitment of recruitment of the adaptor molecule MyD88 and activation of IL-1R-associated kinase (IRAK), followed by recruitment of TRAF6. This signalling complex subsequently activates key signalling proteins including p38 MAPK, JNK (and so AP-1) and NF-κB. The importance of IL-1 for inflammatory responses has been demonstrated in mice lacking IL-1R1, which showed enhanced susceptibility to bacterial infection (Labow *et al.* 1997).

1.7.3 H_2O_2

Hydrogen peroxide (H_2O_2) is implicated in multiple functions in endothelial cells (reviewed by Cai 2005). H_2O_2 is a reactive molecule, oxidising the thiol (–SH) groups of susceptible cysteine residues in proteins (e.g. leading to disulphide bond formation) and reacting with other macromolecules such as DNA.

H_2O_2 was originally thought to be a purely pathological molecule, contributing to oxidant-induced cellular damage termed oxidative stress. Whereas high concentrations (mM) of H_2O_2 are toxic to many cells, and are produced along with other reactive oxygen species (ROS) to damage cells during the immune cell oxidative burst, lower concentrations (nM–μM) are now believed to be an essential component of normal intracellular signalling.

H_2O_2 is generated by reaction of superoxide (O_2^-) with water, catalysed by superoxide dismutase (SOD). O_2^- is produced by NADPH oxidase (Nox), which catalyses the reaction NADPH + $2O_2 \rightarrow$ $NADP^+ + H^+ + 2O_2^-$. However, H_2O_2 itself can form reactive radicals which damage protein – in the presence of iron (such as that in many enzymes), H_2O_2 is degraded non-enzymatically to water and oxygen radicals, including the hydroxyl radical, by the Fenton reaction. H_2O_2 is reduced to water and oxygen by peroxidases including catalase, glutathione peroxidase and peroxiredoxins, and can be sequestered by antioxidants (reducing agents) including glutathione and vitamins C and E.

H_2O_2-stimulated cellular signalling occurs by modification of some protein cysteine residues, which may lead to a loss of catalytic activity in enzymes or change of structure and so function in other proteins. In endothelial cells, H_2O_2 has been implicated as a mediator of growth, proliferation, apoptosis, barrier function, actin organisation, and production of vasoactive mediators and inflammatory cytokines (Cai 2005).

A number of cytokines increase intracellular H_2O_2 concentrations including TNFα and in ECs, VEGF (Kamata *et al.* 2005; Ushio-Fukai *et al.* 2002; Lin *et al.* 2003). Antioxidants and other

ROS-manipulating strategies have been shown to reduce signalling and impede responses to TNFα (Saitoh *et al.* 1998; Kamata *et al.* 2005) and in ECs, to VEGF (see below). Although antioxidants may also affect levels of non-H_2O_2 ROS, overexpression of catalase reduced serum-induced EC proliferation (Zanetti *et al.* 2002). This effect is presumably mediated by reductions in H_2O_2 signalling, with the extra catalase limiting H_2O_2 diffusion. Given the apparent importance of H_2O_2 in responses to various cytokines, it is likely that exogenous administration of H_2O_2 to cultured cells 'feeds in' to the various cellular signal transduction pathways at the point where it is endogenously involved.

Whether H_2O_2 feeds in to pathways activated by other cytokines such as TNFα or activates distinct pathways may depend on the dose of H_2O_2 administered. High doses (500 μM) of H_2O_2 sufficient to induce EC apoptosis stimulate PKD activation loop phosphorylation in ECs, whereas TNFα does not (Zhang *et al.* 2005b), indicating that H_2O_2 is unlikely to feed in to the TNFα pathway to activate PKD. It is possible that H_2O_2 feeds in to another pathway, or stimulates cellular damage-activated pathways. However, distinct signalling mechanisms may also operate specific to H_2O_2. H_2O_2 acts as an endothelial-derived hyperpolarising factor inducing vSMC relaxation, as EDHF-mediated relaxation of aortic rings in organ baths was completely prevented by addition of catalase to the bathing solution (Matoba *et al.* 2000). Given the importance of H_2O_2 in the vessels studied, it is likely that H_2O_2 has a specific receptor in vSMCs, which may be coupled to the cellular machinery via a distinct signalling pathway.

VEGF increases O_2^- generation by activating the NADPH oxidase catalytic subunit gp91phox, and the small GTPase Rac was required for this activation (Ushio-Fukai *et al.* 2002). The same study showed that inhibition or downregulation of gp91phox, or inhibition of Rac reduced VEGFR2 phosphorylation and VEGF-stimulated proliferation and migration of HUVECs. Furthermore, whereas VEGF-stimulated angiogenesis was reduced in vivo, sphingosine-1-phosphate-induced angiogenesis was unaffected. These findings indicate that gp91phox-mediated O_2 formation is involved in VEGF-stimulated angiogenesis, probably via cross-talk with VEGFR2-mediated sig-

nalling, and that the angiogenesis blockade observed was not due to overall inhibition of angiogenic machinery. Another group has also reported that VEGF increases intracellular H_2O_2 concentrations, and that the antioxidant N-acetyl cysteine reduced VEGF-stimulated tubulogenesis (Lin *et al.* 2003).

H_2O_2 initiates a variety of signalling pathways in ECs, including activation loop phosphorylation of PKD (Zhang *et al.* 2005b) and activation of p38 MAPK (Huot *et al.* 1997). H_2O_2-stimulated p38 MAPK activation loop phosphorylation was reduced by the inhibitor KN93, a finding which was interpreted as implicating CaMKII (Nguyen *et al.* 2004), although it is possible that another KN93 target may be responsible. Ask1, a mediator of TNFα and IL-1β-stimulated p38 MAPK activation, has also been implicated in activation of p38 by H_2O_2. The reduced forms of thioredoxin and glutaredoxin have been reported to associate with Ask1, maintaining it in an inactive state (Saitoh *et al.* 1998). Treatment of cells with TNFα or H_2O_2 results in oxidation of thioredoxin and glutaredoxin, activation of Ask1 and so p38 as previously discussed. H_2O_2-induced activation of Ask1 has also been observed in endothelial cells, although treatments shorter than 30 mins treatment were not examined (Zhang *et al.* 2005a).

1.8 Aims of the thesis

The overall goal of this thesis is to increase the understanding of VEGF signalling in endothelial cells, more specifically to:

- Analyse VEGF-stimulated endothelial signalling using proteomics, and examine the role of any up/downregulated proteins identified in VEGF-stimulated endothelial processes such as migration and apoptosis
- Examine the role of PKC and PKD in the VEGF-stimulated p38-independent phosphorylation of Hsp27
- Analyse the involvement of Hsp27 and its phosphorylation in VEGF-stimulated endothelial

cell migration and apoptosis

Chapter 2

Materials and Methods

A description of each experimental procedure used in this thesis is given below. Information regarding the principle underlying each method was obtained from Wilson and Walker (2005) and/or product literature as appropriate.

2.1 General materials

Recombinant human forms of VEGF-A_{165} (mature secreted 165 aa form lacking signal sequence, expressed in insect Sf21 cells, referred to in experimental details as VEGF) and PlGF-1 (mature 129 aa form lacking signal sequence, expressed in E. coli) were from R&D Systems. Recombinant human forms of TNFα (mature cleaved 17 kDa form, expressed in yeast, activity 100 U/ng) and IL-1β (mature 17 kDa form, expressed in E. coli) were from Sigma. H_2O_2 and phorbol 12-myristate 13-acetate (PMA) were from Sigma. Enzyme inhibitors listed in table 2.1 were obtained from Merck Biosciences, apart from dibutyryl cAMP, forskolin, IBMX, SQ22536 and sodium orthovanadate which were from Sigma. 2-D electrophoresis-specific reagents were obtained from GE Healthcare. Primers were from MWG. siRNAs were from Ambion or Dharmacon as indicated. Gateway molecular biology reagents were from Invitrogen. Protease inhibitor cocktail was Complete^{TM} from Roche. Primary antibody suppliers and dilutions are given in table 2.2. Suppliers of other key materials are given in the relevant method below. All other chemicals were

obtained from Sigma or VWR.

2.2 Human cell culture

2.2.1 Primary cells

Human umbilical vein endothelial cells (HUVECs, TCS CellWorks) or human coronary artery endothelial cells (HCAECs; TCS CellWorks) were grown in cell cultureware (Falcon, Becton Dickinson) coated with gelatin (Sigma) in a humidified 37°C, 5% CO_2 incubator. Cells were maintained in endothelial growth medium (EGM, Lonza), consisting of endothelial basal medium (EBM; Lonza) supplemented with gentamicin sulphate (30 μg/ml) and amphotericin-B (15 ng/ml), epidermal growth factor, and bovine brain extract (Singlequots; Lonza) and 10% v/v foetal bovine serum (FBS; Autogen Bioclear). Cells were passaged by trypsinisation. Unless otherwise stated, experiments were performed on confluent HUVECs or HCAECs at passage 2–5 that had been incubated overnight in EBM containing 1% v/v FBS prepared as a dilution of the EGM medium (low serum EBM, also referred to as serum deprivation) prior to the addition of factors and other treatments.

2.2.2 Cell lines

Human embryonic kidney (HEK) 293A cells (293; Invitrogen) were grown in cell cultureware in a 37°C, 5% CO_2 incubator. Cells were maintained in DMEM (Invitrogen) supplemented with 10% v/v FBS, 1% v/v penicillin-streptomycin (Sigma), and passaged by trypsinisation.

2.3 Adenovirus production

A series of adenoviruses were generated using the Gateway system (Invitrogen) to examine the effect of both wild-type and phosphorylation site-mutated Hsp27 on endothelial cell functions.

Table 2.1: Inhibitors used in this study

Compound	Effect on target	Intended target	References
dibutyryl cAMP	Activates	PKA	Hastie *et al.* (1997)
Forskolin	Activates	Adenylyl cyclase	Seamon and Daly (1981); Hastie *et al.* (1997)
Gö6976	Inhibits	PKC (classical isoforms); PKD	Martiny-Baron *et al.* (1993); Gschwendt *et al.* (1996); Zhang *et al.* (2005b)
Gö6983	Inhibits	PKC (broad, not PKD)	Gschwendt *et al.* (1996); Zhang *et al.* (2005b)
GF109203X	Inhibits	PKC (broad specificity)	Toullec *et al.* (1991); Martiny-Baron *et al.* (1993); Gliki *et al.* (2001)
Herbimycin A	Inhibits	Tyr phosphatases	Fukazawa *et al.* (1991); Uehara *et al.* (1989); Cohen *et al.* (1999)
IBMX	Inhibits	Phosphodiesterase	Hastie *et al.* (1997)
Orthovanadate	Inhibits	Tyrosine phosphatases	Swarup *et al.* (1982); Gordon (1991); Yacyshyn *et al.* (2009)
PMA	Activates	PKC	Issandou and Rozengurt (1989); Santell *et al.* (1992); Yamamura *et al.* (1996)
PP2	Inhibits	Src family Tyr kinases	Hanke *et al.* (1996); Abu-Ghazaleh *et al.* (2001)
SB202190	Inhibits	p38 MAPK (α and β)	Goedert *et al.* (1997); Kabakov *et al.* (2004)
SB203580	Inhibits	p38 MAPK (α and β)	Goedert *et al.* (1997); Rousseau *et al.* (1997)
SQ22536	Inhibits	Adenylyl cyclase	Fabbri *et al.* (1991); Hastie *et al.* (1997)
SU5614	Inhibits	VEGFR2	Sun *et al.* (1998); Fong *et al.* (1999b); Gliki *et al.* (2001)
U0126	Inhibits	MEK1/2	Davies *et al.* (2000); Jia *et al.* (2004)
Wortmannin	Inhibits	PI-3-K	Arcaro and Wymann (1993); Gliki *et al.* (2001)

The effect of a number of the inhibitors listed above has been systematically screened against a wide variety of protein kinases in vitro (Davies *et al.* 2000; Bain *et al.* 2003, 2007). IC_{50} values are not given as many of these compounds are ATP competitive and so the IC_{50} value determined by in vitro assay depends on the ATP concentration used in the assay, and also varies with the ability of the compound to penetrate the target cell type (Davies *et al.* 2000). Instead where possible references showing inhibition of the target protein and previous studies using the compound in primary endothelial cells are given. The table lists the inhibitors used to treat cells – the Ser/Thr phosphatase inhibitors sodium fluoride and β-glycerophosphate were also used in some lysis buffers as indicated in the text.

Table 2.2: Primary antibodies used in this study

Target	Manufacturer	Host	Dilution
ERK 1/2 total	CST	Rabbit	1:2000
ERK 1/2 phospho-T202/Y204	CST	Rabbit	1:1000
Hsp27 phospho-S15	AB	Rabbit	1:500
Hsp27 phospho-S78	Upstate	Mouse	1:1000
Hsp27 phospho-S82	CST	Rabbit	1:500
Hsp27 total	CST	Mouse	1:2000
Hsp27 total polyclonal	Stressgen	Rabbit	1:3000
PKCα	CST	Rabbit	1:1000
PKCδ	BD	Mouse	1:500
PKCϵ	BD	Mouse	1:1000
PKCζ	Santa Cruz	Mouse	1:3000
PKD phospho-S738/S742[1]	CST	Rabbit	1:500
PKD phospho S910[2]	CST	Rabbit	1:500
PKD total	CST	Rabbit	1:500
PKD2	Bethyl	Rabbit	1:2000
MAPKAPK2	CST	Rabbit	1:1000
p38α (total)	BD	Mouse	1:4000
p38 MAPK phospho-T180/Y182	BD	Mouse	1:1000
P-Tyr (4G10)	Upstate	Mouse	1:2000
P-Tyr (RC20)	BD	Biotinylated	1:2000
SLP2	Proteintech	Rabbit	1:2000
Prohibitin 1	Neomarkers	Mouse	1:1000
V5	Invitrogen	Mouse	1:4000

Manufacturers: CST, Cell Signalling Technology; BD, Beckton Dickinson Transduction Labs; AB, Affinity Bioreagents. Dilution is that most commonly used for western blotting.
The residue numbering quoted for the P-PKD antibodies is correct for human PKD1. The phospho-PKD S738/S742 antibody is expected to cross-react with PKDs 1, 2 and 3 whereas the phospho-PKD S910 and total PKD antibodies were expected to be PKD1 specific based on sequence analysis performed by the manufacturer proprietory (Dr. Robert Somogyi, CST, personal communication). This analysis could not be as the immunising peptide sequence was proprietory. The PKD2 antibody has been shown by the manufacturer not to cross-react with either PKD 1 or 3 in lysates from cells over-expressing these isoforms.
The phospho-p38 antibody is expected to cross-react with all p38 MAPK isoforms due to full antigen conservation. The total p38α antibody was raised against human p38α residues which are 48–65% conserved in the other three p38 isoforms, cross reactivity was not experimentally tested by the manufacturer (Dr. Martin Gueldenagel, BD, personal communication).
The anti-pY antibody antibody used was 4G10 unless stated.
Anti-PKC antibodies are quoted by the manufacturer not to cross-react with endogenous levels of other PKC isoforms.

[1]Listed by CST as S744/S748 in mouse PKD1
[2]Listed by CST as S916 in mouse PKD1

In addition to an adenovirus expressing wild-type Hsp27 protein, three viruses encoding phosphorylation site mutants of Hsp27 were produced, with S15, S78 or S82 replaced with either a phospho-mimicking residue (negatively-charged aspartate) or an unphosphorylatable residue (alanine, lacks a hydroxyl group for phosphate attachment). A LacZ control virus, synthesising V5-tagged β-galactosidase, was also produced. The side chain structures of serine, alanine, aspartate and phosphorylated serine are shown in figure 2.1 for comparison. A schematic diagram of the mutant Hsp27 forms produced by the viruses is shown in figure 2.2. The full amino acid sequence of the protein synthesised by each Hsp27 virus is given in table 2.3.

The rationale and methods used to produce the viruses is detailed below. Generation of the vectors for the wild-type Hsp27 adenovirus was performed with Dr. Izabela Piotrowska, who also helped design the primers used for mutagenesis and advised on the entire procedure.

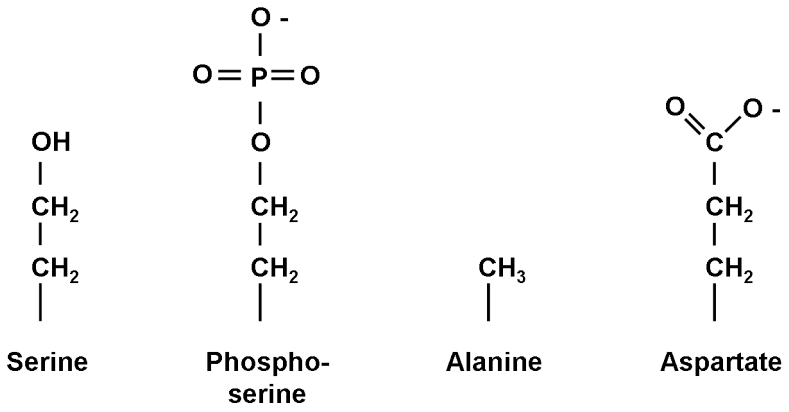

Figure 2.1: Comparison of the amino acid side chain structures of serine, phosphoserine, alanine and aspartate

2.3.1 Background

2.3.1.1 Normal adenovirus biology

Adenoviruses are non-enveloped viruses with a linear double-stranded DNA genome (reviewed by Berk 2007; Russell 2000). There are over 50 human serotypes of adenovirus, differentiated on the basis of antibody recognition of variable regions of their capsid proteins – Ad2 and Ad5

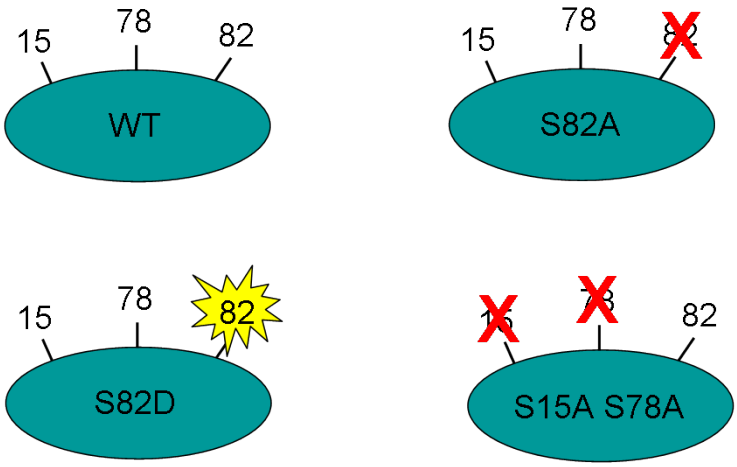

Figure 2.2: Hsp27-expressing viruses produced in this thesis
Schematic diagram of the Hsp27 forms expressed by the generated viruses. Yellow highlight indicates Ser→Asp (phospho-mimic) mutation, red cross indicates Ser→Ala (unphosphorylatable) mutation.

are the most commonly studied. Adenoviruses infect a wide variety of organisms and cell types, and in humans can cause a variety of ailments including respiratory problems, conjunctivitis and infantile gastroenteritis.

Adenovirus infection proceeds through binding of the fibre protein of the viral capsid to the extracellular domain of the coxsackie/adenovirus receptor (CAR), expressed on the surface of many cells including endothelial cells (Carson *et al.* 1999). The adenovirus is internalised into an early endosome via integrin- and clathrin-mediated endocytosis. The virus exits the early endosome and is transported to the nucleus, where viral DNA is injected through a nuclear pore. Virus DNA can be detected in the nucleus 1–2 h after infection. The adenovirus genome does not integrate into that of the host cell but the genes are episomally expressed.

The adenoviral genes are expressed in two distinct phases, early and late, separated by viral DNA replication. The first phase begins with the expression of the early 1 (E1) genes, which code for gene regulatory proteins required for expression of the remaining adenoviral genes. After synthesis of viral components assembly occurs, packaging virus DNA into its protein coat. The host cell is subsequently lysed, releasing virus particles for the next round of infection.

Table 2.3: Amino acid sequences of Hsp27 forms produced by adenoviruses

Virus	Amino acid sequence
27 WT	MTERRVPFSLLRGP***S***WDPFRDWYPHSRLFDQAFGLPRLP EEWSQWLGGSSWPGYVRPLPPAAIESPAVAAPAYSRAL***S*** RQL***S***SGVSEIRHTADRWRVSLDVNHFAPDELTVKTKDGV VEITGKHEERQDEHGYISRCFTRKYTLPPGVDPTQVSSSL SPEGTLTVEAPMPKLATQSNEITIPVTFESRAQLGGPEAA KSDETAAK
S82A	MTERRVPFSLLRGP***S***WDPFRDWYPHSRLFDQAFGLPRLP EEWSQWLGGSSWPGYVRPLPPAAIESPAVAAPAYSRAL***S*** RQL***A***SGVSEIRHTADRWRVSLDVNHFAPDELTVKTKDG VVEITGKHEERQDEHGYISRCFTRKYTLPPGVDPTQVSSS LSPEGTLTVEAPMPKLATQSNEITIPVTFESRAQLGGPEAA KSDETAAK
S82D	MTERRVPFSLLRGP***S***WDPFRDWYPHSRLFDQAFGLPRLP EEWSQWLGGSSWPGYVRPLPPAAIESPAVAAPAYSRAL***S*** RQL***D***SGVSEIRHTADRWRVSLDVNHFAPDELTVKTKDG VVEITGKHEERQDEHGYISRCFTRKYTLPPGVDPTQVSSS LSPEGTLTVEAPMPKLATQSNEITIPVTFESRAQLGGPEAA KSDETAAK
S15A S78A	MTERRVPFSLLRGP***A***WDPFRDWYPHSRLFDQAFGLPRLP EEWSQWLGGSSWPGYVRPLPPAAIESPAVAAPAYSRAL***A*** RQL***S***SGVSEIRHTADRWRVSLDVNHFAPDELTVKTKDGV VEITGKHEERQDEHGYISRCFTRKYTLPPGVDPTQVSSSL SPEGTLTVEAPMPKLATQSNEITIPVTFESRAQLGGPEAA KSDETAAK

The wild-type Hsp27 sequence was obtained from the RefSeq database, accession number NP_001531.1. S15, S78, S82 (or replacement residues) are highlighted in red bold italics. The β-galactosidase protein produced by the lacZ virus has the V5 epitope, sequence GK PIPNPLLGLDST, attached to its C-terminus, with the molecular weight of the combined β-galactosidase/V5 tag approximately 120 kDa.

2.3.1.2 Adenoviral vectors

Adenoviruses were chosen as the delivery vehicle for the Hsp27 constructs as they are able to infect a wide variety of cell types, whether dividing or not, producing strong expression of constructs inserted into their genome, and have previously been used to overexpress proteins of choice in HUVECs (de Martin *et al.* 1997; Riccioni *et al.* 1998; Rosnoblet *et al.* 1999). Additionally, Hsp27 has been overexpressed in primary vascular cells using adenoviruses (Martin *et al.* 1999; Hedges *et al.* 1999). The vector used in this study is E1 and E3 deleted, and so is unable to synthesise virus proteins, which are under control of viral transcription factors encoded by the E1 region,

and is therefore unable to produce additional virus particles to infect other cells. A sequence of interest inserted into the adenovirus genome will be expressed provided it is coupled to appropriate sequences to initiate translation by host cell enzymes. Expression levels vary with time, initially increasing and then reducing as the viral genome is diluted by cell division.

2.3.1.3 Overview of Gateway system and vectors

Gateway is a cloning technology from Invitrogen which allows a DNA fragment to be inserted into a universal entry vector (pENTR/D-TOPO), and then rapidly transferred into pre-designed, application-specific destination vectors.

The entry vector (pENTR-D/TOPO, figure 2.3) is supplied linearised with a 4 nt overhang adjacent to conjugated topoisomerase I from Vaccinia virus. Introduction of a blunt-ended PCR fragment with a 5' CACC sequence (complementary to the vector overhang sequence, and also generating a Kozak sequence required for later translation in mammalian cells) will undergo topoisomerase-catalysed recombination and insertion into the pENTR vector. The vector contains a kanamycin resistance gene for selection of positive transformants (the inserted sequence is not expressed in *E. coli* due to the presence of transcription termination sites). Once present in the entry vector, the sequence of interest can be transferred to any destination vector via enzyme catalysed recombination between the attL1/L2 sites in the entry vector and the attR1/R2 sites in the destination vector.

The pAd/CMV/V5-DEST destination vector (figure 2.3) produces replication-incompetent E1- and E3-deleted Ad5 adenovirus containing the sequence of interest when transfected into 293 cells. These cells provide the essential E1 adenoviral gene products in trans (Graham *et al.* 1977), allowing synthesis of viral proteins. When infected into mammalian cells, the inserted sequence is transcribed via the human cytomegalovirus (CMV) promoter, giving high level expression.

This destination vector adds a C-terminal tag to the inserted sequence if a stop codon is not present in the insert and the reading frame is maintained from insert into vector sequence. The tag consists

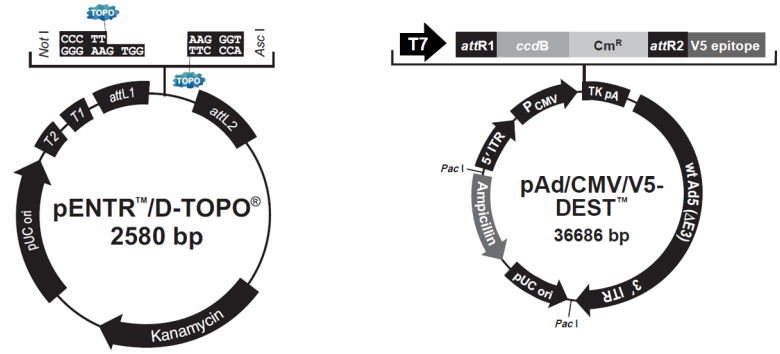

Figure 2.3: Gateway vector maps
Maps of the entry and destination vectors used in this thesis, taken from the relevant Invitrogen manuals (Entry vector, pENTR directional TOPO cloning kits; destination vector, pAd/CMV/V5-DEST and pAd/PL-DEST gateway vectors; available at `www.invitrogen.com`). Detail of all the vector components is provided in these manuals, some elements are discussed in the text.

of part of the attL2 and R2 recombination sites from the pENTR/pAd vectors and the V5 epitope. The V5 tag can then be used for immunoprecipitation, affinity purification, immunofluorescent microscopy and other techniques, but may affect the function of the protein. If the inserted sequence includes an in-frame stop codon, as do all the Hsp27 inserts used in this thesis, this sequence is not added.

The pAd/CMV/V5-DEST vector contains an ampicillin-resistance gene for selection of positive transformants. The ccdB gene, the product of which interferes with DNA gyrase and is cytotoxic to cells not expressing the ccdA gene product (Couturier *et al.* 1998) such as the TOP10 *E. coli* used for transformation, is also included but is lost from the destination vector when recombination occurs with the entry vector. Thus transformed cells containing unrecombined destination vector are not viable and colonies from such cells were not observed.

2.3.2 Preparation of Hsp27 cDNA

Total RNA was purified from HUVECs using the RNeasy kit (Qiagen) according to the manufacturer's instructions. Single-stranded complementary DNA (cDNA) was prepared from mRNA with the superscript II kit (Invitrogen) using the included oligo dT primers according to the man-

ufacturer's instructions.

2.3.3 Generation of modified Hsp27 cDNA by PCR

Hsp27 wild-type cDNA was selectively amplified by PCR using the entry primers detailed in table 2.4. The forward primer contains the CACC sequence required for integration into pENTR/D-TOPO immediately N-terminal to the start codon. The reverse primer includes a stop codon to prevent addition of the in-frame V5 tag. Only the coding sequence of Hsp27 was enclosed by the primers used – the 5' and 3' untranslated regions were not amplified and so did not form part of the final virus-produced Hsp27 mRNA. As the Hsp27 siRNA used in this study binds to the 3' untranslated region of Hsp27 mRNA (figure 2.4), this allows siRNA-mediated knockdown of endogenously-produced Hsp27 without affecting virus-produced Hsp27, a potentially useful feature.

1 μl of cDNA was amplified with 2.5 U cloned Pfu polymerase (Stratagene) and 20 pmol of each primer in MasterAmp pre-mixed PCR buffer D with ammonium sulphate (Epicentre Biotechnology). Reactions were carried out in thin-walled PCR tubes (final volume 50 μl) on a Dyad DNA Engine thermocycler (MJ Research). Amplification parameters (35 cycles) were 5 min initial melt, 94°C; melting 1 min, 94°C; annealing 1 min, 55°C; extension 2 mins (+ 5 s/cycle), 72°C; final extension 10 mins, 72°C.

Table 2.4: Nucleotide sequences of Hsp27 entry primers

Direction	Sequence (5'→3')
Forward	*CACC*ATGACCGAGCGCCGCGTCCCC
Reverse	TTACTTGGCGGCAGTCTCATCGGATTTTG

CACC sequence added before start codon to produce forward primer is highlighted in red italics, incorporated Kozak sequence is underlined.

CTCAAACACCGCCTGCTAAAAATACCCGACTGGAGGAGCATAAAAGCGCAGC
CGAGCCCAGCGCCCCGCACTTTTCTGAGCAGACGTCCAGAGCAGAGTCAGCC
AGC

ATGACCGAGCGCCGCGTCCCCTTCTCGCTCCTGCGGGGCCCCAGCTGGGACC
CCTTCCGCGACTGGTACCCGCATAGCCGCCTCTTCGACCAGGCCTTCGGGCT
GCCCCGGCTGCCGGAGGAGTGGTCGCAGTGGTTAGGCGGCAGCAGCTGGCCA
GGCTACGTGCGCCCCCTGCCCCCCGCCGCCATCGAGAGCCCCGCAGTGGCCG
CGCCCGCCTACAGCCGCGCGCTCAGCCGGCAACTCAGCAGCGGGGTCTCGGA
GATCCGGCACACTGCGGACCGCTGGCGCGTGTCCCTGGATGTCAACCACTTC
GCCCCGGACGAGCTGACGGTCAAGACCAAGGATGGCGTGGTGGAGATCACCG
GCAAGCACGAGGAGCGGCAGGACGAGCATGGCTACATCTCCCGGTGCTTCAC
GCGGAAATACACGCTGCCCCCCGGTGTGGACCCCACCCAAGTTTCCTCCTCC
CTGTCCCCTGAGGGCACACTGACCGTGGAGGCCCCCATGCCCAAGCTAGCCA
CGCAGTCCAACGAGATCACCATCCCAGTCACCTTCGAGTCGCGGGCCCAGCT
TGGGGGCCCAGAAGCTGCAAAATCCGATGAGACTGCCGCCAAGTAA

AGCCTTAGCCTGGATGCCCACCCCTGCTGCCGCCACTGGCTGTGCCTCCCCC
GCCACCTGTGTGTTCTTTTGATACATTTATCTTCTGTTTTTCTCAAATAAAG
TTCAAAGCAACCACCTGTAAAAAAAAAAAAAAAAAA

Figure 2.4: Hsp27 siRNA binding site
Wild-type Hsp27 mRNA sequence (RefSeq database accession number NM_001540.2) illustrating the binding site of the Hsp27 siRNA used in this study (black, underlined). The Hsp27 mRNA sequence is contiguous, but has been divided into three sections (top to bottom: 5' untranslated region; coding region; 3' untranslated region) for illustration purposes. The start and stop codons are coloured green and red respectively.

2.3.4 Agarose gel electrophoresis and recovery of DNA

Amplified PCR product (or other sample) was mixed with 6x loading buffer (Fermentas) and run on a 1% agarose gel containing 200 ng/ml ethidium bromide at 120 V, using TAE running buffer (40 mM tris-acetate, pH 8.3; 1 mM EDTA, Eppendorf). Separation was monitored by the migration of bromophenol blue and xylene cyanol, which have apparent sizes of 4000 bp and 300 bp respectively. After adequate separation, the gel was photographed under UV illumination using the Genetools package (Syngene) and the band of interest was excised and added to a pre-weighted tube. DNA was recovered from the gel piece using the Qiaquick Gel Extraction Kit (Qiagen) and eluted into 50 μl water. The concentration of the DNA was determined by absorbance at 260 nm on a Biophotometer (Eppendorf).

2.3.5 TOPO cloning into pENTR/D-TOPO entry vector

TOPO cloning was performed as described in the manufacturer's instructions for chemical transformation. 20 ng of gel-purified PCR product was added to 1 μl (17.5 ng) pENTR/D-TOPO vector with 1 μl of provided salt solution in a final volume of 6 μl. The reaction was mixed and incubated at room temperature for 5 mins, and 4 μl was used to transform competent TOP10 *E. coli*.

2.3.6 Transformation and growth of competent *E. coli*

One-shot chemically competent TOP10 Escherichia coli bacteria (Invitrogen) were used for all transformations. TOP10 express Dam methylase (required for site-directed mutagenesis), and do not express the ccdA gene (making them susceptible to ccdB-mediated death, relevant for the pAd/CMV/V5-DEST vector). A vial of TOP10 bacteria was thawed on ice and the plasmid for transformation was added and gently mixed. After a further 30 min incubation on ice, the bacteria were heat-shocked in a water bath at 42°C for 30 s and placed on ice. 250 μl SOC medium (Invitrogen) was added and the cells were incubated for 1 h at 37°C with shaking to allow protein production from the plasmid antibiotic resistance gene. The entire culture was plated on to pre-warmed 10 cm dishes containing LB agar (Sigma) and either 100 μg/ml kanamycin (Invitrogen, for pENTR) or 100 μg/ml ampicillin (Sigma, for pAd) as appropriate for the plasmid used for transformation. Plates were dried at 37°C for 30 mins before inversion and continued incubation overnight. The next morning, individual colonies were picked and transferred into 14 ml round-bottomed tubes containing 3–7 ml LB broth (Sigma) and the appropriate antibiotic (concentrations as for LB agar). Cells were grown overnight at 37°C with shaking, then used in the next procedure or stored at 4°C.

2.3.7 Plasmid DNA minipreps

Preparation of plasmid DNA was performed by an alkaline lysis technique modified from Sambrook *et al.* (1989). This method is based on the limited lysis of bacteria by SDS and denatura-

tion of DNA by NaOH, followed by the renaturation of plasmid (which is held together during denaturation due to supercoiling) but not genomic DNA, which is much slower to renature and precipitates.

Bacteria from a 1.5 ml overnight culture were pelleted by centrifugation (16000g, 1 min), the supernatant was discarded and the cells resuspended in 100 μl ice-cold solution A (25 mM Tris-HCl pH 8; 50 mM glucose; 10 mM EDTA) and transferred to 1.5 ml tubes. 200 μl solution B (200 mM NaOH; 1% w/v SDS, freshly diluted from separate concentrated stock solutions) was added and the tube was rapidly inverted to lyse the cells and release the plasmid DNA. 150 μl solution C (3 M potassium acetate; 2 M acetic acid) was added to neutralise the NaOH from solution B and terminate the lysis. Samples were incubated on ice for 3 mins, before precipitated material was pelleted by centrifugation (16000g, 5 mins, 4°C) and the supernatant transferred to a fresh tube. DNA was precipitated by addition of approximately 0.7 volumes (350 μl) isopropanol and pelleted by centrifugation (16000g, 20 mins, 4°C). The supernatant was discarded and the pellet was washed with 70% v/v ethanol, centrifuged (16000g, 5 mins, 4°C), and the supernatant was discarded. The pellet was air-dried at room temperature to evaporate remaining ethanol (around 5 mins), and was resuspended in TE (10 mM Tris-HCl pH 8, 1 mM sodium EDTA) containing 1 mg/ml RNase A (Sigma). These basic minipreps were used for certain procedures, e.g. diagnostic digests for screening of mutants.

For other procedures such as sequencing and cloning, protein and other contaminants were removed by proteinase K treatment and phenol-chloroform extraction using phase-lock heavy gel (Eppendorf). Phase-lock gel eases phenol-chloroform extractions by holding the lower organic phase under the gel whereas the upper aqueous phase remains above the gel, and was used according to the manufacturer's instructions. Briefly, 10 μl of 1% v/v proteinase K (Invitrogen) in TE was added to the basic miniprep and incubated at 37°C for 15 mins. The miniprep was then made up to a total volume of 100 μl with TE, and added to a pre-centrifuged phase-lock gel tube. An equal volume of phenol-chloroform-isoamyl alcohol (25:24:1, Sigma) was added and the tube was

thoroughly mixed by inversion before separation of the layers by centrifugation (16000g, 5 mins, room temperature). Remaining phenol was removed by adding 100 μl chloroform-isoamyl alcohol (24:1, Fluka), mixing and centrifugating as before. This wash was repeated once and the aqueous upper layer containing the plasmid DNA was transferred to a separate tube. DNA was then precipitated with isopropanol and washed with 70% v/v ethanol as earlier, before resuspension in water.

2.3.8 DNA sequencing

Sequencing was performed by either Cogenics or by the Advanced Biotechnology Centre, Imperial College London. The primers used for sequencing are detailed in table 2.5. The protein sequence coding for the Hsp27 variant present in the plasmid was verified by manually checking the chromatogram supplied by the sequencing service using the Sequencher software package (Gene Codes).

Table 2.5: Nucleotide sequence of primers used for sequencing

Primer	Target strand	Sequence (5'→3')
A	Forward	GCAGCAGCTGGCCAGGCTACGTG
B	Reverse	CACGTAGCCTGGCCAGCTGCTGC
C	Forward	GCTTCACGCGGAAATACACGCTGC
D	Reverse	GCAGCGTGTATTTCCGCGTGAAGC

Forward primers sequenced the sense strand, reverse primers sequenced the antisense strand

2.3.9 Site-directed mutagenesis of Hsp27-pENTR

2.3.9.1 Strategy

Wild-type Hsp27 in pENTR was mutated with the Quickchange II kit (Stratagene). This method is based on amplification of the template (unmutated) plasmid with primer pairs containing the desired nucleotide sequence alteration (one forward, one reverse, both containing the sequence

alteration). These primers anneal imperfectly to the template DNA due to sequence mismatch between the mutated template plasmid and the mutation-containing primers, but well enough to allow PCR replication of the plasmid. The unmutated template plasmid was originally derived by miniprep from cells, and so is methylated. The template plasmid is digested by Dpn I, which cleaves at GATC only when methylated on N6 of adenine (e.g. by DNA adenine methylase, Dam). The mutated plasmid produced by PCR is unmethylated, and so is preserved. The mutated plasmid can then be transformed into competent cells and replicated as normal.

A primer pair covering nucleotide residues 38–73 of the coding region of Hsp27 was used for mutation of S15, and a primer pair covering nucleotide residues 219–256 was used for S78 or S82 mutations. For mutation of both S15 and S78, two rounds of mutagenesis was performed, firstly introducing the S15 mutation, followed by transformation of competent cells, bacterial growth and miniprep. The S15-mutated plasmid was then used as template DNA for primers containing the S78 mutation. The primers used for mutagenesis are listed in table 2.6, and their binding sites in Hsp27 are shown in figure 2.5.

Table 2.6: Nucleotide sequence of primers used for mutagenesis

Mutation introduced	Sequence (5'→3')
S82A	CAGCC(G***G***GCGC)TCAGCCGGCAACTC***GC***CA GCGGGGTC
S82D	CAGCC(G***G***GCGC)TCAGCCGGCAACTC***GA***CA GCGGGGTC
S78A	CAGCC(G***G***GCGC)TC***GC***CCGGCAACTCAGCA GCGGGGTC
S15A	GGCCCC***GC***CTGGGACCCCTTCCGCGACT(G GTA***T***C)G

Forward primer only shown, reverse primer is reverse complement of forward primer. Restriction site for screening enclosed in brackets. Differences between nucleotide sequence of primer and wild-type Hsp27 sequence (mismatches) highlighted with red bold italics.

To facilitate screening of colonies produced after transformation for the presence of the desired mutation, additional silent mutations were incorporated into each primer (indicated in table 2.6).

These mutations deleted a restriction site (Kpn I for the S15 primer, Pau I for the S78/S82 primer) but did not alter the amino acid sequence of produced protein, making use of codon redundancy.

To screen colonies for the presence of a mutation, plasmid minipreps were digested with the appropriate restriction enzyme, and the size of the fragments produced determined by agarose gel electrophoresis. Loss of the restriction site (resulting in a larger DNA fragment) indicated that the colony was likely to contain Hsp27 cDNA mutated at the appropriate site. Figure 2.5 shows the location of the deleted restriction sites, and figure 2.6 shows the origin of the restriction fragments used for screening. Presence of the mutation (and absence on undesired mutations from the Hsp27 coding sequence) was verified by DNA sequencing before recombination into pAd/CMV/V5-DEST.

2.3.9.2 Mutagenesis procedure

Site-directed mutagenesis was performed using the Quickchange II kit (Stratagene) according to the manufacturer's instructions except where indicated. Nucleotide sequences of primers used for PCR are shown in table 2.6. Sites of primer binding and restriction sites for screening are shown in figure 2.5. PCR reactions, containing 30 ng wild-type pENTR-Hsp27 template plasmid and 10 pmol of each primer, were performed in a final volume of 50 μl. Cycling parameters (22 cycles) were 1.5 mins initial melt, 95°C; melting 1 min, 95°C; annealing 1.5 mins, 55°C; extension 5 mins, 68°C; final extension 10 mins, 68°C. 1 μl Dpn I was added directly to the cooled sample and digestion was allowed to proceed at 37°C for 1–2 h. 2 μl of the cooled sample was used to transform TOP10 *E. coli*, which were plated onto kanamycin-containing agar plates as before to select for the presence of the p-ENTR plasmid.

2.3.9.3 Screening procedure

Colonies from mutagenesis reactions were picked and grown as before, and plasmid DNA was recovered in a basic miniprep. Minipreps (2 μl) from an S15 mutation reaction were screened

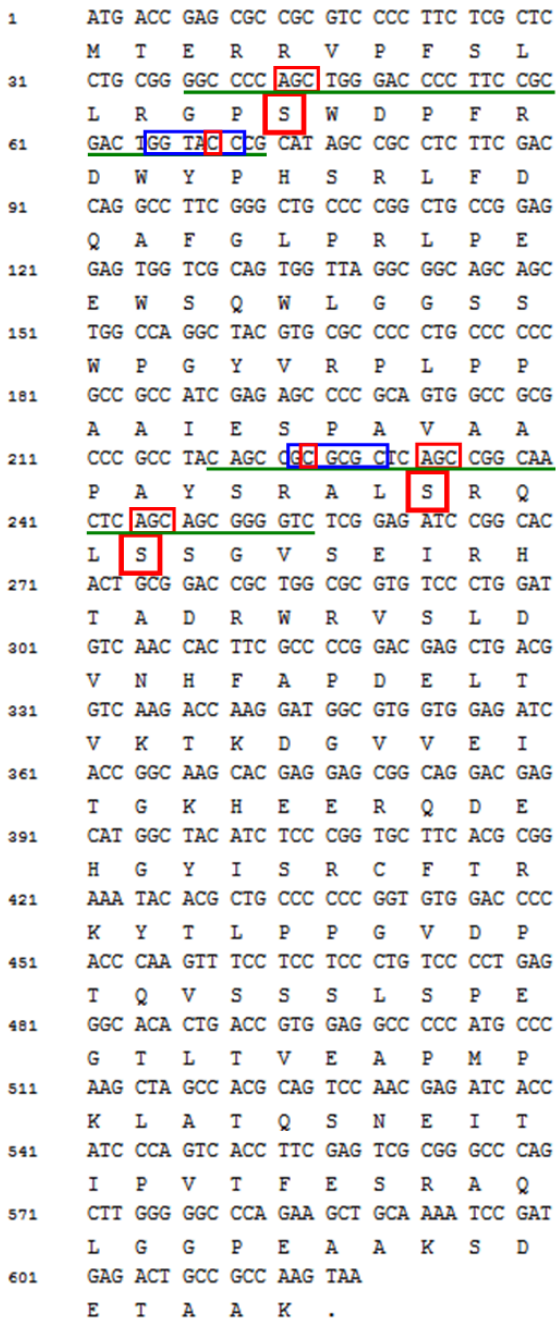

Figure 2.5: Mutagenesis primer binding sites
Wild-type Hsp27 DNA sequence (RefSeq database accession number NM_001540.2) used for illustration, with amino acid translation under each codon. Primer annealing sites are underlined in green. Restriction sites (Kpn I in S15 primer, Pau I in S78/S82 primer) used for analysis in blue box. Potential mutation site (codons for S15, S78, S82, and silent mutation in restriction sites) highlighted in red.

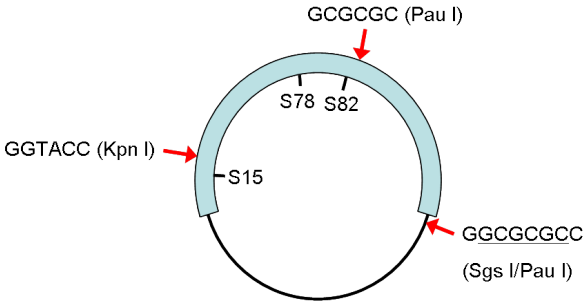

Figure 2.6: Origin of restriction fragments used for screening of mutants
Schematic illustration of the origin of the restriction fragments used for screening colonies for successful mutation of Hsp27 in pENTR. The restriction sites are shown with red arrows, with the sequence and the enzyme cutting that sequence indicated. The second Pau I (6 base cutter) site, which is within the Sgs I (8 base cutter) site, is underlined. The blue area represents Hsp27 coding sequence, the black line represents vector sequence. The relative positions of S15, S78 and S82 residues are indicated.

using a Sgs I/Kpn I double digestion in buffer tango (10 U Kpn I, 2.5 U Sgs I), S78 or S82 mutants were screened using Pau I digestion in buffer red (2.5 U Pau I). The indicated quantity of each enzyme was used per digestion in a final volume of 10 μl, and was allowed to proceed for 1–2 h before analysis by agarose gel electrophoresis. In each case, the presence of a single large fragment of the appropriate size (approximately 3000 bp) indicated successful mutagenesis, two fragments indicated unsuccessful mutagenesis. All restriction enzymes and buffers were from Fermentas.

2.3.10 Cloning into pAd/CMV/V5-DEST destination vector and DNA maxiprep

Hsp27 with the desired mutations was cloned from the pENTR/D-TOPO entry vector into the pAd/CMV/V5-DEST destination vector (Invitrogen) according to the manufacturer's instructions supplied with the destination vector. Briefly, 0.25 μl pENTR plasmid was mixed with 1 μl pAd/CMV/V5-DEST vector and made up to a final volume of 8 μl with TE, pH 8. 2 μl clonase II enzyme mix (Invitrogen) was added to initiate recombination, which was allowed to proceed at room temperature overnight. Recombination was terminated by addition of 1 μl proteinase K and incubation at 37°C for 10 mins. 3 μl of the mixture was transformed into TOP10 *E. coli* and grown overnight on ampicillin-containing selective plates. The following day, colonies were picked and grown in ampicillin-containing broth. At the end of the day, around 20 μl of this starter culture was used to inoculate 150 ml of ampicillin-containing broth, and the culture was grown overnight

at 37°C with vigorous shaking. The following day, plasmid DNA was purified from the 150 ml culture using the HiSpeed Plasmid Maxi kit (Qiagen). DNA was eluted in 750 μl DNase-free water and quantified by absorbance at 260 nm. Presence of the appropriate mutation and absence of other mutations in the coding sequence of Hsp27, and the orientation of the Hsp27 sequence in the vector, was verified by DNA sequencing and manual examination of aligned chromatograms for all pAd plasmids using Sequencher 4.7 (Gene Codes).

2.3.11 Preparation of low-titre adenoviral stock

20 μg of pAd maxiprep was digested with 8 μl Pac I (New England Biolabs) using the supplied buffer in a final volume of 200 μl at 37°C for 2 h to linearise the pAd plasmid and expose the viral inverted terminal repeat (ITR) sequences, as recommended by the Gateway manuals. Enzyme and other contaminants were removed by phenol-chloroform extraction as before, and the cut plasmid was resuspended in 50 μl water.

Fugene 6 (Roche) was used to transfect 293 cells with the cut pAd plasmid, according to the manufacturer's instructions. 6 μl Fugene 6 was mixed with 3 μg cut pAd plasmid in a total volume of 350 μl DMEM, and incubated at room temperature for 30 mins to allow the lipid-DNA complexes to form. The entire mixture was then added to a 10 cm dish of 293 cells (around 70% confluent) in complete DMEM, and cells were left for 10–14 days without changing the media until cytopathic effects were observed.

Once all cells had rounded up and half had detached from the dish, still adherent cells were removed from the dish by squirting with a pipette to produce a suspension, which was transferred to a 50 ml tube. Virus was released from the 293 cells using three freeze-thaw cycles to lyse the cells: 30 mins at -70°C, 5–10 mins at 37°C. The virus-containing supernatant was clarified by centrifugation (3000g, 15 mins), and then stored at -70°C or used immediately to produce a high-titre viral stock.

2.3.12 Preparation of high-titre adenoviral stock

Small quantities of separate lacZ-expressing and GFP-expressing adenovirus were provided for amplification by Dr. David Holmes and Dr. Birger Herzog (both Ark Therapeutics) respectively. The lacZ virus had been produced by the above method from the pAd/CMV/V5-GW/lacZ plasmid supplied by Invitrogen, whereas the backbone of the GFP virus was different. For each virus, 6 x 15 cm dishes of 293 cells (90% confluent) were used to produce the high-titre stock, with around 500 μl low-titre virus stock used to infect each dish. Cells were harvested once all cells had rounded up and half had detached from the plate, which took around 3 days. Cells were squirted off the dish as before and pelleted by centrifugation (500g, 5 mins). The supernatant was discarded and the cell pellet was resuspended in 8 ml sterile PBS. The cells were freeze-thawed 4 times as before, and the supernatant clarified and transferred to a fresh tube containing 4.4 g of caesium chloride. The virus solution was used to dissolve the CsCl, producing a final concentration of 3.3 M. The CsCl/virus mixture was transferred to an Optiseal centrifuge tube (Beckman) and centrifuged in a Ti 70.1 rotor for 18 h at 60000 rpm (240000g) at 10°C. The virus particles gave a discrete band, which was collected by piercing the Optiseal tube with a needle and withdrawing the virus. The virus was then mixed with an equal concentration of sterile 2x freezing buffer (final concentrations: 5 mM Tris-HCl pH 8; 50 mM NaCl; 0.05% w/v BSA; 25% glycerol) and stored in aliquots at -70°C. Around 3 ml of each virus was obtained after addition of storage buffer.

Viral titre was determined using the QuickTiter Adenovirus Titer Immunoassay kit (Cell Biolabs) according to the manufacturer's instructions. This method involves detection of viral coat protein production in 293 cells by immunostaining. All reagent incubations and concentrations were those recommended in the kit instructions. Briefly, 293 cells were plated in 24-well plates at 2.5x10^5 cells/ml, 1 ml/well. One hour after plating cells, 100 μl of virus at various dilutions (10^{-4}–10^{-6}) was added to each well in duplicate. The cells were allowed to grow for 2 days for virus production to occur before the cells were fixed in methanol, blocked with BSA, incubated in anti-hexon antibody and then alkaline phosphatase-conjugated secondary antibody. Virus-

containing cells were visualised by incubation in diaminobenzidine tetrahydrochloride (DAB) solution for 10 mins, and stored in PBS at 4°C. 10–100 stained cells were counted per field, with 5 random fields assessed per well. Virus titres obtained ranged from 2–8 x 10^{10} ifu/ml.

2.4 Electrophoresis and gel staining

2.4.1 Preparation of cell lysates for western blotting or 2-D analysis

For experiments without the use of inhibitors, serum-deprived cells were washed twice with warm EBM and incubated in a 37°C, 5% CO_2 incubator for the required time with either 25 ng/ml (600 pM of dimer) recombinant human VEGF-A_{165}, 100 U/ml (2 ng/ml) TNFα or other reagents as indicated.

For the examination of the effects of enzyme inhibitors, serum-deprived cells in 6-well plates were washed twice with warm EBM and pre-incubated for 30 mins in warm EBM containing the appropriate inhibitor. To begin treatment, concentrated VEGF or other reagents were then added to the inhibitor-containing medium to the final concentration desired. The contents of each well was mixed by gentle pipetting and the cells were returned to the incubator for the required time period.

To stop treatment, cells were placed on ice, washed twice with ice cold PBS and either lysed in RIPA buffer (50 mM Tris-HCl pH 7.4, 150 mM NaCl, 1 mM disodium EDTA, 1% v/v Igepal CA-630, 0.5% w/v sodium deoxycholate, 0.1% w/v SDS, protease inhibitor cocktail) or for 2-D blots, in 2-D buffer (7 M urea, 2 M thiourea, 4% w/v CHAPS, protease inhibitor cocktail) after an additional wash in tris-sucrose (10 mM Tris-HCl pH 7.4, 0.25 M sucrose). Lysis was allowed to continue on ice for 30 mins, after which time the lysates were clarified by centrifugation at 16000g for 30 mins. The supernatant was transfered to a fresh tube and the lysates were stored at -70°C for further analysis.

For downregulation of PKCs with phorbol esters, cells at 50–80% confluence were washed with

EBM and then incubated in low serum EBM containing 200 ng/ml (324 nM) PMA for 28 h. Cells were then washed twice with EBM and incubated with the appropriate factors in EBM as detailed above for other experiments.

2.4.2 Glutaraldehyde-mediated protein cross-linking

Glutaraldehyde-mediated cross-linking of proteins in cell lysates was performed as described by Lambert *et al.* (1999). After appropriate treatment, cells were lysed in ice-cold buffer H (25 mM HEPES pH 7.2; 3.3% v/v glycerol; 1 mM EDTA; 1 mM DTT) supplemented with protease inhibitors. Samples were sonicated for 5 s with a probe sonicator using medium power settings to disrupt cell membranes. Lysates were clarified by centrifugation (10 mins, 16000g, 4°C) and supernatants were transferred to a fresh tube. 7 μl buffer H containing various amounts of glutaraldehyde, was added to 28 μl clarified lysate to give the desired final glutaraldehyde concentration (spanning 0–0.3% v/v), and samples were incubated at 30°C for 30 mins to allow cross-linking to occur. Cross-linking was terminated by adding an equal volume (35 μl) of Quench (1 M Tris pH 7.2; 10% w/v SDS; 10 mM EDTA) to the lysates. Lysates were stored at -70°C until analysis.

2.4.3 SDS-PAGE and western blotting

SDS-PAGE separates proteins migrating through a gel under the influence of an electric field. Coupled with antibody detection steps, the relative abundance of a particular protein in two lysates can be determined. SDS-PAGE was performed using either tris-glycine homemade gels (BioRad mini protean II system), or precast bis-tris gels (Invitrogen NuPAGE system).

2.4.3.1 Principle of western blotting

Heating of cell lysates with SDS- and DTT-containing sample buffer denatures proteins, reducing protein disulphide bonds to thiol groups and covering the protein with SDS molecules, forming a negatively-charged complex. Under the influence of an electric field, proteins migrate through

a gel whose pore size is determined by the concentration of acrylamide and cross-linker in the gel. Larger proteins are retarded more than smaller proteins, resulting in a separation of proteins largely based on molecular size. During transfer, the protein/SDS complex is transferred out of the gel onto a protein-binding membrane under the influence of an electric field. For antibody detection, protein-binding sites on the membrane are blocked by incubating with a protein solution such as milk, and a protein of interest is then specifically bound with an antibody. This primary antibody is then detected with a secondary antibody conjugated to an enzyme, often a peroxidase. A liquid substrate is then added, which in the presence of the peroxidase enzyme emits light in a chemiluminescent reaction, and this light is detected using photographic film. Western blotting is often described as a semi-quantitative technique, with the amount of protein originally present in the lysate proportional to the amount of peroxidase enzyme bound to protein on the membrane, and so the amount of light generated and area and intensity of the band present on the film. For routine western blotting, samples were not protein assayed before loading, instead equivalent areas of cell coverage were lysed in equal amounts of buffer, and equal volumes were loaded. Blotting with a total antibody, usually total ERK, was used to visually confirm comparable protein loading.

2.4.3.2 Homemade gels

For one-dimensional blots, 4x sample buffer (250 mM Tris HCl pH 6.8, 400 mM DTT, 8% w/v SDS, 40% v/v glycerol, trace bromophenol blue) was added to the cell lysates prepared in RIPA buffer to a final concentration of 1x. The samples were then boiled for 4 mins and subjected to SDS-PAGE using homemade gels (BioRad). Standard resolving gels contained 10% w/v acrylamide-bis solution, 375 mM Tris-HCl pH 8.8, 0.2% w/v SDS, 0.05% w/v APS, 0.05% v/v TEMED, stacking gels were composed of 4% w/v acrylamide-bis solution, 125 mM Tris-HCl pH 6.8, 0.1% w/v SDS, 0.1% w/v APS, 0.1% v/v TEMED. Tris-glycine running buffer (25 mM Tris base, 192 mM glycine, 0.1% w/v SDS) was used. Samples were wet transferred on to Immobilon-P (Millipore) overnight at 30 V, 4°C, or 0.36 A, 4°C for 1h 30, using a transfer buffer of 25 mM Tris base, 192 mM glycine, 20% v/v methanol.

2.4.3.3 Precast gels

The Invitrogen Novex system, including running and transfer buffers, was used for pre-cast gels. Samples in RIPA buffer were adjusted to 1x LDS sample buffer (Invitrogen), 50 mM DTT, before heating at 80–90°C for 10 mins. Samples were cooled and subjected to SDS-PAGE on NuPAGE bis-tris gels, using MOPS running buffer before semi-dry transfer to Immobilon-P for 1 h at 35 V. Transfer buffer was made up to 20% methanol.

2.4.3.4 Blocking, antibody incubation and detection

Membranes were blocked in 5% w/v non-fat milk (5% w/v BSA for anti-pY) in PBS-T (0.1% v/v Tween 20 in PBS) for 1 h at room temperature and then incubated in primary antibody at the required concentration (listed in table 2.2) in blocking solution for either 2 h at room temperature or overnight at 4°C. Membranes were washed four times for 5 mins with PBS-T and incubated in horseradish peroxidase-conjugated secondary antibody (Swine anti-rabbit or goat anti-mouse, 1:10000–1:30000 dilution in blocking solution, Dako) for 1 h at room temperature before being washed as before. Bands were detected by a chemiluminescent procedure (ECL plus, GE Healthcare) and Hyperfilm ECL (GE Healthcare) following the manufacturer's protocols. Blots were scanned on an ImageScanner (GE Healthcare) and band intensities were quantified with the ImageJ gels module (National Institues of Health, `rsb.info.nih.gov/ij/`).

2.4.4 Protein assay

To determine the protein concentration of lysates in 2-D buffer, a modified Bradford assay was used essentially as described by Ramagli (1999), with the variation that results were determined as the absorbance ratio 595 nm/450 nm to improve assay linearity (Zor and Selinger 1996).

5 μl of clarified sample was diluted with 20 μl of 0.01 M HCl (freshly diluted from the concentrated acid), and mixed in a 96-well plate with 200 μl of a 25 % v/v solution of Bradford reagent

concentrate (BioRad). The absorbance of each well at 595 nm and 450 nm was determined. Samples containing 0–5 μg ovalbumin, assayed in the same 96-well plate, were used to construct a (linear) standard curve of protein concentration against the ratio of absorbances at 595nm/450nm. The protein concentration of unknown samples was determined by comparing to the standard curve.

2.4.5 Two-dimensional gel electrophoresis

2-D electrophoresis is a protein separation technique coupling isoelectric focusing (1st dimension) to SDS-PAGE (2nd dimension). In all 2-D gel images shown, the acidic region of the gel (low pI) is on the left, and the high molecular weight region is at the top.

2.4.5.1 Principle of isoelectric focusing

The isoelectric point (pI) of a protein is the pH at which that protein has no net charge. Proteins are composed of many amino acids with ionisable entities such as the amino and carboxyl groups. On the peptide backbone, only two of these groups are available for ionisation, at the N- and C-termini, and so the majority of ionisable groups in a protein occur on amino acid side chains (e.g. carboxyl groups on Asp and Glu, and amino groups on Lys and Arg), with the effect that the pI of a protein is determined by its amino acid sequence (the identity of the protein) and the presence of any modifications such as phosphate groups.

Each individual ionisable group acts as a weak acid or base, and whether or not the group is charged depends on the ambient pH – when pH is lower than the pK_a for that group, the majority of the group is in its protonated (more positive) form, and when ambient pH is higher than the pK_a for that group, the majority of group is in its deprotonated (more negative) form. Overall, when the pH is lower than the pI for the protein, the net charge on the protein is positive and when the pH is higher than the pI, the net charge is negative.

Isoelectric focusing occurs in an immobilised pH gradient under the influence of a high voltage,

with the low pH region at the anode and the high pH region at the cathode. If a protein is at a pH that is lower than its pI, and so the net charge on the protein is positive, the protein will migrate through the pH gradient towards the cathode. As the protein migrates, and the ambient pH becomes higher, the protein releases more protons as the acid-base equilibrium for each ionisable group shifts, with the result that the net charge on the protein becomes less positive. With continued migration, the protein reaches a pH at which the net charge on the protein has reduced to zero, and the protein has now focused at its isoelectric point. This process is schematically illustrated in figure 2.7.

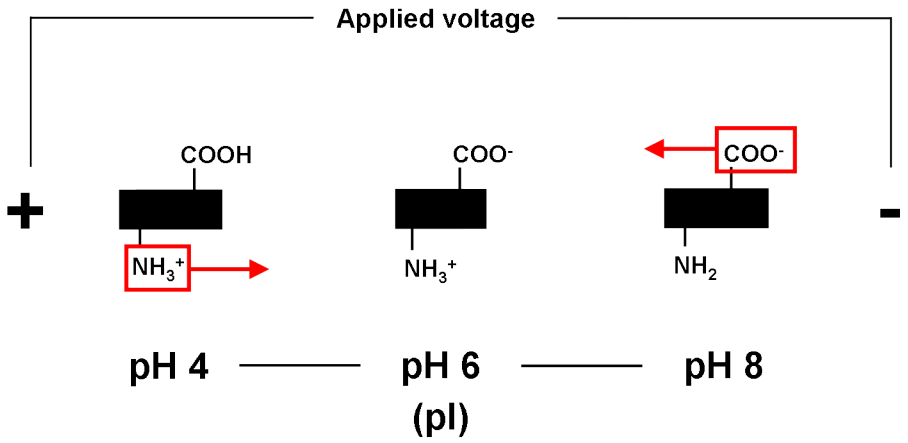

Figure 2.7: Principle of isoelectric focusing
Schematic representation of isoelectric focusing of a protein with a pI of 6. At pH 4, the net charge on the protein is positive due to the protonated amino group, causing migration towards the cathode through increasing ambient pH. At pH 8, the net charge on the protein is negative due to the deprotonated carboxyl group, causing migration towards the anode through decreasing ambient pH. At pH 6, the net charge on the protein is zero, and the protein no longer migrates. The direction of migration of each molecular species is indicated with an arrow, and the charged group responsible is highlighted with a red box.

2.4.5.2 Isoelectric focusing procedure

Lysates were prepared in 2-D buffer (7 M urea, 2 M thiourea, 4% w/v CHAPS). Immediately before running the first dimension, the samples were adjusted to 7 M urea, 2 M thiourea, 4% w/v CHAPS, 0.5% v/v IPG buffer (GE Healthcare), 1% w/v DTT, trace bromophenol blue (final concentrations). Samples were then loaded onto immobiline drystrips (GE Healthcare), overlayed with mineral oil and isoelectric focusing incorporating a 10 hr rehydration step was carried out

overnight on an IPGphor (GE Healthcare) according to the manufacturer's instructions. Focused IEF strips were then equilibrated and run in the second dimension on homemade (tris-glycine) or precast (NuPAGE bis-tris; Invitrogen) gels.

2.4.5.3 Second dimension: homemade gels

Focused IEF strips were equilibrated in SDS equilibration solution (50 mM Tris HCl pH 8.8, 6 M urea, 30% v/v glycerol, 2% w/v SDS, trace bromophenol blue) containing 1% (65 mM) w/v DTT for 15 mins, and then in SDS equilibration solution containing 2.5% (140 mM) w/v iodoacetamide for a further 15 mins. Strips were placed on top of a self-cast polyacrylamide slab gel and sealed with agarose sealing solution (1x running buffer containing 0.5% w/v agarose, trace bromophenol blue).

For 24 cm IPG strips, SDS-PAGE was conducted using the Ettan Dalt 6 system (GE Healthcare) using 1x tris-glycine running buffer in the lower chamber and 2x tris-glycine running buffer in the upper chamber, as recommended by the manufacturer. Gels contained 10% w/v acrylamide, 375 mM Tris-HCl pH 8.8, 0.2% w/v SDS, 0.1% w/v APS, 0.017% v/v TEMED. For 7 cm IPG strips, SDS-PAGE was conduced using 10% resolving gels, without a stacking gel, with buffers and recipes as described in section 2.4.3.2. In both cases, SDS-PAGE continued until the bromophenol blue tracking dye just ran off the gel.

2.4.5.4 Second dimension: precast gels

Focused IEF strips were equilibrated in 1x LDS loading buffer (Invitrogen) containing 1% w/v DTT for 15 mins, followed by 1x LDS loading buffer containing 2.5% w/v iodoacetamide for a further 15 mins. Strips were then placed on top of a pre-cast NuPAGE bis-tris gel and sealed with agarose sealing solution (1x MOPS running buffer containing 0.5% w/v agarose, trace bromophenol blue) according to the manufacturer's instructions.

For 2-D western blots, proteins were transferred to Immobilon-P and processed as described for

western blotting of one dimensional gels (section 2.4.3.2).

2.4.6 Silver staining

Silver staining of polyacrylamide gels was carried out essentially as described by Yan *et al.* (2000). On completion of electrophoresis, gels were fixed in 40% v/v ethanol, 10% v/v acetic acid overnight. Gels were then incubated for 30 mins in sensitiser (30% v/v ethanol, 1.2 M sodium acetate, 0.2% w/v sodium thiosulphate), washed 3 x 5 mins in water and impregnated with silver (0.25% w/v silver nitrate) for 20 mins. After 2 x 1 min washes with water, the gel was incubated in developer (0.25 M sodium carbonate, 0.02% v/v formaldehyde) until spots appeared. Staining was terminated by incubating the gel for 10 mins in stop solution (40 mM sodium EDTA). After washing in water (3 x 5 mins), the gel was shrunk for at least 30 mins in 50% v/v methanol and scanned.

2.4.7 Coomassie staining of PVDF membranes

Coomassie staining of proteins on PVDF membranes was performed as described by Dunn (1999). Membranes were shaken in stain (0.2% w/v Coomassie brilliant blue R250 (Sigma), 45% methanol, 10% glacial acetic acid) for 2 mins, and then destained in 45% methanol, 10% glacial acetic acid, until the background was acceptable. Membranes were air dried and scanned.

2.4.8 Difference gel electrophoresis (DIGE)

2.4.8.1 Overview of DIGE method

In this thesis a two-dye DIGE method was used, involving covalently labelling the proteins in two lysates to be compared with separate fluorescent dyes. The samples are then pooled and run on the same gel, and the gels are imaged with a fluorescent scanner to detect the two dyes (summarised in figure 2.8).

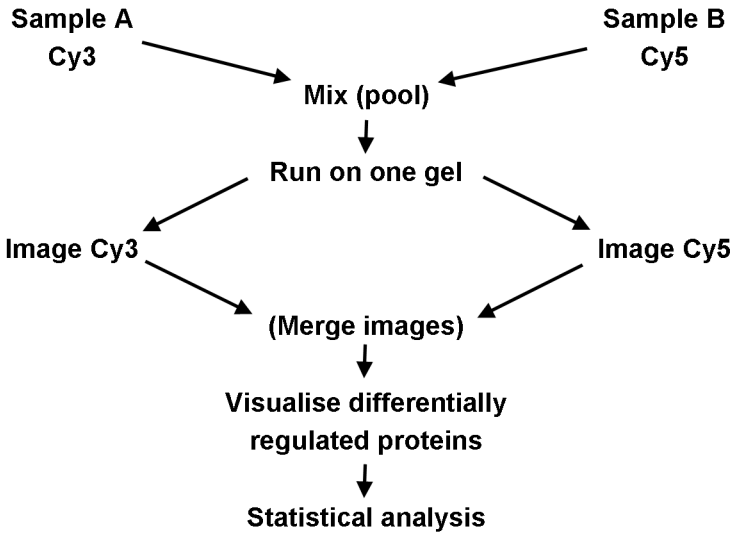

Figure 2.8: Summary of the difference gel electrophoresis method
Schematic diagram of the DIGE procedure as used in this study. Equal quantities of each of two test protein samples is mixed with a reactive dye containing either a Cy3 or Cy5 fluorophor. During a labelling reaction, the dyes covalently link to amine groups on lysine residues of proteins in the sample. The labelled samples are then mixed to produce a pooled sample and undergo 2-D electrophoresis on a single gel. The gel is then imaged for Cy3 and Cy5 separately using a fluorescent scanner. Spot matching between the two samples is simple as the any protein present in both samples will migrate to the identical positions on the gel, giving overlapping spots which are individually detectable. A computer program then compares the intensity of the two spots, determining any differences between the two samples.

Most proteins present in the pooled mixture will be composed of some protein from one sample (e.g. Control, Cy3 labelled) and some from the other sample (e.g. VEGF-treated, Cy5 labelled). Because the dyes are very similar in structure and molecular weight and have a similar effect on the molecular weight of the labelled protein, a particular protein in the Cy3-labelled (control) sample runs to an identical position in the 2-D gel as the same protein from the Cy5-labelled (VEGF-treated) sample. A comparison of the relative abundance of that protein in the two samples is then made by comparison of the ratio of Cy3 fluorescence to Cy5 fluorescence in the spot. Comparison of multiple samples from each treatment group, ideally combined with statistical testing, determines whether the protein is changed by the treatment employed.

DIGE analysis was performed as recommended by the manufacturer (GE Healthcare) using a two-dye minimal labelling protocol. Salient points are indicated below.

2.4.8.2 CyDye labelling of protein sample

CyDye labelling involves covalently attaching one fluorescent dye (a CyDye) to one protein sample, and another fluorescent dye to a second protein sample. CyDyes contain a fluorophor, either Cy3 or Cy5, and an NHS ester group that reacts with primary amines such as those on lysine groups in proteins. During the labelling reaction the dye is limiting, with the manufacturer reporting that ≈1–2% of lysine residues in a sample are labelled, and double labelling of individual protein molecules does not occur.

Labelling of protein samples with CyDyes (GE Healthcare) was performed according to the manufacturer's minimal labelling protocol. Samples were lysed in DIGE buffer (10 mM Tris-HCl, 7 M Urea, 2 M Thiourea, 4% w/v CHAPS, pH 8.5 at 4°C), clarified, re-adjusted to pH 8.5 (when ice cold) and protein assayed. 50 μg of each sample was mixed with 1 μl of working CyDye solution (400 pmol/μl in dimethylformamide) and the labelling reaction was allowed to proceed on ice in the dark for 30 mins. Labelling was quenched by the addition of 10 μl of 10 mM lysine (excess free amine groups binds remaining unreacted dye). Control and treated samples produced in a single experiment were labelled with different CyDyes, and which dye was assigned to the control sample was varied between experiments to avoid dye bias. Labelled samples were then immediately prepared for 2-D electrophoresis.

2.4.8.3 2-D separation and imaging of CyDye-labelled samples

The entire labelling reaction from two samples labelled with different CyDyes (a VEGF-treated sample labelled and a matched control sample from the same lysis) were mixed to produce a pooled sample. The pooled sample was then made up to 450 μl with 2-D buffer and adjusted to 0.5% v/v IPG buffer, 1% w/v DTT, trace bromophenol blue, and separated by 2-D electrophoresis using 24 cm pH 3–10 IEF strips and 10%acrylamide gels as described in section 2.4.5. Gels still in their glass cassettes were removed for the gel tank, rinsed in distilled water and the glass cassette was air dried. Gel-cassette assemblies were sequentially scanned by a Typhoon 8600 variable

mode imager (GE Healthcare), using excitation wavelengths of 532 nm for Cy3 and 633 nm for Cy5. Initial low-resolution scans were assessed in ImageQuant (GE Healthcare) and Typhoon photomultiplier tube voltages were adjusted so that maximum signal from each gel was 30000–70000, thus preventing image saturation (which occurs at 100000) but maximising sensitivity. Final images were acquired at 100 μm pixel size.

2.4.8.4 DIGE gel analysis

DIGE gels were analysed using DeCyder software (GE Healthcare) as recommended by the manufacturer. Matched scans (Cy3, Cy5) from each individual gel were analysed using the DeCyder differential in-gel analysis (DIA) module to automatically detect spots, normalise total Cy3 and Cy5 signals within the gel, and remove artifacts such as edge effects and dust. Spots detected in gels during DIA were then matched automatically to other gels containing independent protein samples of the same treatment duration using the DeCyder biological variation analysis (BVA) module. Automatic matching was adjusted manually where necessary to ensure accurate spot matching between gels.

Spots with a mean volume change of at least 10%, and matched between at least two of the three gels analysed at each time point, were considered to be changed. Rigorous statistical analysis was not available via DeCyder as this requires a Cy2-labelled internal standard to be run on each gel. At the time these experiments were performed, access to a Cy2-detecting imager was not available.

2.5 Mass spectrometry-based methods

Mass spectrometry (MS) is an analytical technique that separates analytes (e.g. peptides) by mass-to-charge ratio (m/z), so allowing determination of the mass of the analytes. MS analysis of peptides obtained from a protein allows identification of that protein and is commonly used to identify unknown proteins from polyacrylamide gels. The principles and techniques of the MS methods used are described below.

2.5.1 Principle of peptide mass fingerprinting

Peptide mass fingerprinting as used in this study consists of excising a spot of (hopefully) pure protein from a polyacrylamide gel, digesting the protein with trypsin, and determining the masses of the intact tryptic peptides produced, giving a peptide mass fingerprint for the unknown protein.

Masses of the peptides are determined by MS using matrix-assisted laser desorption and ionisation, and a time-of-flight detector (MALDI-TOF). The MALDI ionisation method converts the tryptic peptides (M) to singly charged ions (MH^+) by gas-phase transfer of protons from a UV-absorbing matrix without fragmentation of the peptide. As all ions formed are non-fragmented and singly-charged, separation occurs solely by peptide mass. The actual masses of the detected peptides are determined by calibrating the MS with peptides of known mass.

Trypsin cuts polypeptides immediately C-terminal to Arg or Lys residues except where the next residue is Pro (Olsen *et al.* 2004). Due to this site specificity, if the sequence of a protein is known the peptides it will produce on trypsin digestion can be deduced, and the masses of these peptides (calculated from the peptide sequences) give a theoretical peptide mass fingerprint for that protein. A computer program (Mascot was used in this thesis) can then compare the peptide mass fingerprint obtained from the gel-excised, unknown protein with the theoretical peptide mass fingerprints of known proteins in a sequence database. Mascot scores the 'goodness' of fit of the experimental data to each protein in the database based on the number of peptides matches obtained, the difference in observed and database-calculated masses of matches, and the search settings (e.g. mass tolerance) employed. A significance threshold, at $p<0.05$, is assigned to prevent spurious matches, with a match classed as significant if there is less than a 5% chance that a set of masses would produce a score (match) equally good in a database of equal size by matching to a random protein. A protein is classed as positively identified if it is the top match and has a score above the significance threshold, with other hits below the significance threshold.

2.5.2 Principle of tandem mass spectrometry

To identify post-translational modifications of protein sequences, some tryptic digests were analysed by tandem mass spectrometry (MS/MS). Peptide mass fingerprinting does not provide any direct information regarding the internal composition of each peptide, and it can be problematic to identify post-translational modification sites. For example, if a peptide is observed via MALDI-TOF MS that differs by the appropriate mass from a predicted tryptic peptide, it may be assumed that the peptide is phosphorylated. However, if the peptide contains multiple Ser, Thr and Tyr residues, it would not be possible to say which residue was phosphorylated. Due to this limitation another approach, MS/MS is more useful in identifying the sites of post-translational modifications.

In MS/MS, peptides are initially separated by the first mass spectrometry stage, and then individual peptides are fragmented by collision with an inert gas (collision-induced dissociation), and the fragments are then separated and detected by a second mass spectrometry stage, so determining the mass of the fragments produced. Computer software is able to reconstruct the peptide and determine its sequence by comparing the masses of fragments produced, and the presence of post-translational modifications such as phosphorylation.

Fragmentation of tryptic peptides can occur at a variety of sites in the peptide backbone and side chains, but is especially useful for peptide identification if it occurs at the peptide bond. Fragmentation-induced cleavages of different peptide bonds of the parent ion leads to the generation of the b- and y-ion series. In the b-ion series, the peptide charge is retained on the N-terminal fragment and in the y-ion series the charge is retained on the C-terminal fragment.

Tandem MS of peptides is usually performed coupled to an initial chromatographic step to separate the peptides, which then enter the mass spectrometer, more concentrated and more pure, as they elute off the column. Ionisation occurs via electrospray ionisation (ESI), rather than the matrix/laser method used in MALDI. ESI involves rapid drying of a droplet of peptide in the presence

of an acid (usually methanoic acid), resulting in protonation of the peptide.

2.5.3 Preparation and tryptic digestion of gel plugs

After excision from the gel, stained spots were reduced and alkylated in a Progest Investigator (Genomic Solutions) following a procedure provided by the manufacturer. Briefly, gel plugs were washed twice (hydrated with 25 mM ammonium bicarbonate (ABC), dehydrated with acetonitrile), reduced with 10 mM DTT in ABC (35 mins, 50°C) and then alkylated with 100 mM iodoacetamide in ABC (45 mins, room temperature), washed twice as before and dried in a speedvac. The dried plugs were rehydrated for 10 mins in the presence of 20 ng/μl (0.75 μM) modified pig trypsin (Trypsin Gold, Promega) in 40 mM ammonium bicarbonate, covered with 40 mM ABC/10% v/v acetonitrile to avoid dehydration, and digestion was allowed to proceed overnight at 37°C.

2.5.4 MALDI-TOF MS

1 μl droplets of each tryptic digest were spotted onto a steel target plate then covered with a 1 μl droplet of matrix solution (α-cyano-4-hydroxycinnamic acid, half-saturated, in 33% v/v acetonitrile, 0.1% v/v trifluoroacetic acid) and allowed to dry. Samples were analysed in a MALDI-TOF (Autoflex, Bruker Daltonics) mass spectrometer in positive ionisation mode. Roughly 120 shots were averaged to give each spectrum. External calibration of mass spectra was conducted using a mixture of standard peptides covering the range m/z = 1046–2465, followed where possible by internal calibration using trypsin autolysis peptides (m/z = 842.50, corresponding to peptide VATVSLPR; 1045.56, peptide LSSPATLNSR; 2211.10, peptide LGEHNIDVLEGNEQFINAAK). The monoisotopic masses of the MH^+ ions were used to search the NCBI non-redundant protein sequence database via the Mascot peptide mass fingerprint interface (Matrix Science, `www.matrixscience.com/cgi/search_form.pl?FORMVER=2&SEARCH=PMF`). For database searching, carbamidomethyl modification of cysteine was selected as a fixed modification

(due to modification of cysteine by iodoacetamide, +57.03 Da $-CH_2CONH_2$), whereas oxidation of methionine sulphur (+15.99 Da) was selected as a variable modification. Mass tolerance was 100 ppm (equivalent to a 0.1 Da error at 1000 Da) and one missed tryptic cleavage was allowed. All hits quoted were above the statistical significance threshold set by Mascot.

2.5.5 Tandem mass spectrometry (ESI-MS/MS)

Some gel spots were excised from 2-D gels and sent for external tandem MS analysis using the pick-n-post service from Alphalyse. For in-house tandem MS, tryptic digests were dried to $\approx$5 μl with a speedvac, and made up to 20 μl by addition of 0.1% HPLC-grade methanoic acid. Tandem MS, including a coupled reverse-phase chromatographic separation using a C18 column, was performed by Mark Crawford (Centre for Molecular Medicine, Department of Medicine, UCL), using an LTQ XL Orbitrap (Thermo Scientific). Protein and post-translational modification identification was performed by Mark Crawford using the Mascot database (Matrix Science, `www.matrixscience.com/cgi/search_form.pl?FORMVER=2&SEARCH=MIS`).

2.6 Small interfering RNA (siRNA) transfection

2.6.1 Principle of siRNA-mediated protein knockdown

RNA interference (RNAi) is a technique for reducing the abundance of specific mRNAs in a cell and thus reducing the amount of the encoded protein present, and is now widely used to knock down genes (Gewirtz 2007). Briefly, dsRNA is degraded to short (21–23 nt) fragments by an endonuclease, Dicer, which are then incorporated into a large multiprotein complex, RISC (RNA-induced silencing complex). Any cellular RNA complementary to the incorporated RNA fragment is recognised by RISC and degraded.

Endogenously, RNAi is used by micro RNAs (miRNAs) – short hairpin RNAs which are processed by dicer and RISC after transcription – to regulate transcript amounts (Asirvatham *et al.* 2009)

and may also help protect against certain viruses by degrading their dsRNA genome, but can be hijacked for experimental purposes by administration of dsRNAs similar to the dicer products. These sequences, termed siRNAs, can directly integrate into RISC resulting in downregulation of complementary mRNA.

SiRNAs (and other nucleic acids) are negatively charged and are not readily taken up by most cells. SiRNAs can be introduced into cells by binding with a cationic liposome-like reagents such as oligofectamine, which can then cross the cell membrane so carrying the siRNA into the cell (Akhtar and Benter 2007).

2.6.2 Experimental details

Duplex siRNAs targeting the genes of interest were obtained from Ambion (Silencer range, unmodified) or Dharmacon (On-target plus range, includes a chemical modification to reduce off-target effects) (see table 2.7 for sequences), and their effects were compared with the appropriate non-targeting, negative control siRNA (Ambion negative control siRNA #1, or Dharmacon siControl non-targeting siRNA). 1 μM siRNA in warm OptiMem (Invitrogen) was incubated with 5% v/v oligofectamine (Invitrogen) for 25 mins to allow the siRNA/oligofectamine complexes to form.

Confluent HUVECs in 6-well plates and maintained in EGM were washed with OptiMem and incubated for 4 h in OptiMem containing the complexed siRNA (final siRNA concentration 200 nM, 1 ml/well) to allow transfection to occur. The medium in each well was adjusted to 10% v/v FBS and then replaced with EGM the following day. For experiments requiring serum deprivation, the media was changed in the evening to low serum EBM and the cells were incubated in this medium overnight; otherwise the cells were left in EGM for a further night. Under both procedures, further experiments were then performed as described in the text 48 h (unless stated) after the addition of the siRNA. Knockdown was confirmed by western blotting using appropriate antibodies, and quantified with ImageJ. For functional studies, where cells are removed from the plate (e.g. for flow cytometry or migration assays), knockdown was assessed by lysing cells transfected

in parallel with the experimental cells, and analysing these lysates via western blotting.

Table 2.7: Nucleotide sequences of siRNAs used in this study

Target	Manufacturer	Sense strand sequence (5'→3')
Control	A	not provided by manufacturer
Hsp27	A	GUUCAAAGCAACCACCUGUtt
PKCα	A	GGCUUCCAGUGCCAAGUUUtt
PKCδ	A	GGCCAAAAUCCACUACAUCtt
PKCδ (B)	A	GGCUACAAAUGCAGGCAAUtt
PKCϵ	A	GGAAAUAAAAGAACUUGAGtt
PKD1	A	GGAAGAGAUGUAGCUAUUAtt
PKD2	A	GGAAAUUCCGCUGUCAGAAtt
Control	Dh	UGGUUUACAUGUCGACUAAuu
SLP2 (A)	Dh	UGUUAGACCGGAUCCGAUAuu
SLP2 (B)	Dh	AUGAGGAACUUGAUCGAGUuu
MAPKAPK2 (A)	Dh	CCACCAGCCACAACUCUUUuu
MAPKAPK2 (B)	Dh	GGCAUCAACGGCAAAGUUUuu
p38α[1]	Dh	GGAAUUCAAUGAUGUGUAUuu
		UCUCCGAGGUCUAAAGUAUuu
		GUAAUCUAGCUGUGAAUGAuu
		GUCCAUCAUUCAUGCGAAAuu

Manufacturer: A, Ambion (silencer range); Dh, Dharmacon (on-target plus range). The control siRNA used was always from the same manufacturer and range as the experimental siRNA. A letter in brackets designates one of multiple seperate siRNAs targeting this same protein.

[1]The p38 siRNA is a smart pool reagent, composed of the four different siRNAs listed, but the total concentration of siRNA used was still 200 nM.

2.7 Immunoprecipitation-based methods

Immunoprecipitation is the antibody-mediated capture of a protein from solution. Antibody directed against the a target protein of interest binds to its target in a cell lysate. This primary antibody is then bound by a secondary reagent, inert beads conjugated to Staphlococcus protein A or G, which bind to the constant region of antibodies. These beads are large, and are separated (along with their complexed antibody/target protein) from the remainder of the cell lysate by centrifuga-

tion. Other proteins bound to the target protein, such as endogenous cellular binding partners, may be co-purified with the target protein and appear in the immunoprecipitate, depending on the stability of these interactions.

2.7.1 Immunoprecipitation

Serum-deprived cells in tissue culture dishes were washed in serum free medium and treated with appropriate factors. To stop treatment, cells were washed twice in ice-cold PBS and lysed by scraping the cells in triton buffer (10 mM Tris-HCl pH 7.4, 150 mM NaCl, 4 mM EDTA, 1% v/v Triton X100, protease inhibitor cocktail, phosphatase inhibitor cocktail: 10 mM sodium fluoride; 10 mM β-glycerophosphate; 1 mM sodium orthvanadate). Lysis was allowed to continue on ice for 30 mins, after which the lysate was clarified by centrifugation (30 mins, 16000g, 4°C) and the insoluble material removed. The lysate was then pre-cleared by incubating with beads (protein A/G plus agarose, Santa Cruz) for at least 1 h followed by antibody binding overnight at 4°C. For Hsp27 IPs, a polyclonal antibody to total Hsp27 (Stressgen) was used. The following day, the lysates were further incubated with beads for 1 h at 4°C to bind the primary antibody. Immunoprecipitates were then washed three times with the immunoprecipitation lysis buffer and, if the sample was to be analysed by 2-D electrophoresis, a further two washes were performed with 10 mM Tris-HCl pH 7.4. The IP complex was then either dissociated by incubation in 2-D buffer for 30 mins, by boiling in 1x SDS-PAGE sample buffer for 4 mins, or processed for an immune complex kinase assay. Samples were stored at -70°C until used.

2.7.2 Immune complex kinase assay

Immune complexes were washed and resuspended in 90 μl kinase buffer (4 mM MOPS, 4 mM $MgCl_2$, 2.5 mM β-glycerophosphate, 1 mM EGTA, 0.4 mM EDTA, 50 μM DTT, pH 7.2) containing 3 μg recombinant Hsp27-GST fusion protein (Upstate), and the mixture was allowed to equilibrate to room temperature for 5 mins. The kinase reaction was started with the addition of

10 μl of 100 μM ATP, and an aliquot was immediately removed, mixed with an equal volume of 2x SDS-PAGE sample buffer and boiled to terminate the reaction (reaction time = 0). The reaction was allowed to proceed at room temperature, and aliquots were removed at various time points and boiled in SDS-PAGE sample buffer to produce a time course. Samples were stored at -70°C until analysis.

2.7.3 Immune complex dephosphorylation assay

Phosphate was removed from some immunoprecipitated proteins using alkaline phosphatase (AP, calf intestinal phosphatase, New England Biolabs). Immune complexes were washed in 10 mM Tris-HCl pH 7.4 and resuspended in 40 μl 1x supplied phosphatase buffer, with equal volumes then aliquoted into three separate tubes. One tube was spiked with AP to a final concentration of 10 U/μl, and an equivalent volume of 1x phosphatase buffer was added to the other two. Mock (to control for any effect of heating) and AP samples were incubated for 30 mins at 37°C to allow dephosphorylation to occur, whereas the third tube (IP) was left on ice. Reactions were terminated by addition of an equal volume of 2x SDS-PAGE sample buffer and stored at -70°C until analysis.

For analysis of alkaline phosphatase-dephosphorylated samples on 2-D gels, proteins in SDS-PAGE sample buffer were precipitated with the 2-D clean-up kit (GE Healthcare) and resuspended in 2-D buffer.

2.8 Immunofluorescent staining and microscopy

Staining of permeablised cells with fluorophor-conjugated probes such as antibodies allows the imaging of the location of the fluorophor (and so target protein) with a cell. The imaged fluorophor can be localised to a single plane using laser illumination on a confocal microscope, reducing image blurring due to excitation of fluorophor above or below the plane of focus.

Cells were grown on gelatin-coated glass cover slips (15 mm diameter) in 24-well plates. After

treatment, medium was removed and cells were fixed for 10 mins in 4% v/v formaldehyde in PBS, permeablised for 6 mins in 0.2% v/v Triton-X100 in PBS, blocked for 1 h, and incubated in primary antibody. Blocking and antibody incubations were performed in 1% w/v BSA in PBS-T. Polyclonal antibodies against Hsp27 (Stressgen) and SLP2 (Proteintech Group) were used at 1:2000 for 1–2 h at 37°C. Cells were then incubated in secondary antibody (Alexa 488-conjugated donkey anti-rabbit, Invitrogen) at 1:1000 for 1 h at room temperature. Cells were washed 3 times with PBS between each solution, but not before addition of fix. Coverslips were inverted and mounted on glass slides with fluorescence mounting medium (Dako).

For Mitotracker Red staining, cells were incubated in 400 nM Mitotracker Red CMXRos (Invitrogen) in EGM for 30 mins to allow the dye to accumulate in mitochondria. Medium was removed, cells were washed once with EGM to remove free dye and cells were then fixed in 4% formaldehyde as normal.

For antigen competition experiments with the SLP2 antibody, 1 μg SLP2 antibody was pre-mixed with 100 μg SLP2-GST fusion protein (Proteintech) in 500 μl blocking solution for 1 h at room temperature. An aliquot of this solution was then used as the primary antibody for immunostaining, maintaining an equivalent SLP2 antibody concentration.

Confocal images were taken with a a x40 oil-immersion objective on an upright Nikon Eclipse E1000 microscope running LaserSharp 2000 software (BioRad). The excitation and emission maxima of fluorophors used in this thesis are given in table 2.8.

2.9 Flow cytometry

Flow cytometry determines the properties of individual cells, including size and the absence or presence (abundance) of particular fluorescent compounds associated with the cells, and can be used to sort cells into populations defined by these parameters. Staining cells with fluorophor-conjugated probes such as antibodies allows the determination of the proportion of cells analysed

Table 2.8: Fluorophors used in this study

Probe	Fluorophor	Absorption (nm)	Emission (nm)
CyDye Cy3	Cy3	532	580
CyDye Cy5	Cy5	633	670
Donkey anti-rabbit	Alexa 488	495	519
Annexin V	Fluorescein	488	518
TMRM	TMRM	549	573
Mitotracker Red	Mitotracker Red	579	599

The mitotracker red variant used was CMXRos. Approximate absorption and emission maxima are indicated (solvent-dependent). Fluorophors were from Invitrogen, apart from the CyDyes which were from GE Healthcare and Annexin V-fluorescein which was from Roche.

that express the antigen, and the degree of expression.

After appropriate treatment (described below), cells were washed with HEPES-buffered saline solution (HBSS, Lonza) and detached by trypsinisation, which was terminated by addition of trypsin neutralising solution (Lonza). Cells were washed by dilution in PBS and pelleted by centrifugation at 250 g, 5 mins. The supernatant was removed and cells were resuspended in appropriate buffer as described and kept on ice. Flow cytometry was performed using a FACS Calibur (Beckton Dickinson) via the CellQuest Pro interface program, with at least 10,000 cells counted per sample. The excitation and emission maxima of fluorophors used are given in table 2.8. Excitation of all fluorphors was via a 488 nm argon laser.

2.9.1 TMRM mitochondrial potential assay

2.9.1.1 Assay principle

The mitochondrial matrix is negatively charged with respect to the cytosol, due to the pumping of protons from the mitochondrial matrix into the intermembrane space during oxidative phosphorylation. This difference in charge between the cytosol and mitochondrial matrix, referred to as the mitochondrial membrane potential ($\Delta\psi_m$), is important for mitochondrial functions including ATP generation and import of Ca^{2+} (Duchen *et al.* 2003).

The membrane-permeable cationic fluorescent dye tetramethylrhodamine methyl ester (TMRM) distributes across membranes and is accumulated in mitochondria. When allowed to establish an equilibrium in cells by addition of low concentrations to the culture medium, TMRM accumulation is an indicator of $\Delta\psi_m$ (Davidson *et al.* 2007). Accumulation of the similar dye tetramethylrhodamine ethyl ester (TMRE) has previously been used to assess mitochondrial membrane potential by flow cytometry (Hajek *et al.* 2007).

2.9.1.2 Procedure

TMRM was kindly donated by Dr. Sean Davidson, Hatter Institute, UCL. Confluent HUVECs in 12-well plates treated with or without siRNA for 3 days were incubated in EGM containing 25 nM TMRM for 2 h at 37°C to allow dye equilibration. Cells were washed with PBS and trypsinised. Trypsin was neutralised with trypsin neutralising solution (Lonza), mixed with PBS and pelleted by low speed centrifugation (200g, 5 mins). The cell pellet was resuspended in 500 μl of 0.5% serum in PBS. Samples were stored on ice and were analysed by flow cytometry within one hour. Geometric mean fluorescence of the sample cells was determined by flow cytometry using the FL2 channel (585$\pm$21 nm).

2.9.2 Apoptosis assay

2.9.2.1 Assay principle

During early stages of apoptosis, the phospholipid phosphatidylserine (PS) translocates from the inner to the outer leaflet of the plasma membrane (Bevers *et al.* 1999) and the cell shrinks, while the plasma membrane itself remains intact, preparing the cell for removal by phagocytic cells. At later times, the plasma membrane becomes leaky, allowing free fluid exchange, and caspase-dependent DNA fragmentation occurs.

PS present on the surface of the cell can be bound by the Ca^{2+}-dependent protein annexin V. When added as an external Ca^{2+}-containing solution, fluorescein-conjugated annexin V binds

to apoptotic cells expressing PS on their surface, tagging these cells with fluorescein. PS is not present on the surface of healthy cells and so is not accessible to the fluorescein-annexin V reagent, and so these cells are not tagged with fluorescein. Tagged and untagged cells, and so apoptotic and healthy cells, can be distinguished by flow cytometry. The DNA stain propidium iodide (PI) can enter cells and stain DNA only when the plasma membrane has become leaky, so staining cells in the later stages of apoptosis. Cells staining with PI only, but not annexin V, are classed as necrotic – plasma membrane degradation has occurred without PS translocation.

2.9.2.2 Procedure

HUVECs treated with or without siRNAs for 2 days were incubated overnight in M199 basal medium (Invitrogen), with or without 25 ng/ml VEGF, to induce apoptosis. The following day, conditioned medium was removed into a 15 ml tube. Cells were washed with HBSS, the wash was removed and added to the same 15 ml tube, and cells were trypsinised. Trypsin was neutralised with trypsin neutralising solution (Lonza), and detached cells were removed and added to the 15 ml tube. The empty well was then washed with HBSS which was added to the 15 ml tube. Washes and medium used for overnight incubation were saved to ensure maximum recovery of all detached cells. As a further wash, the 15 ml tube was topped up with PBS. Cells were pelleted by low speed centrifugation (200g, 5 mins) and the supernatant was discarded. The cell pellet was resuspended in 50 μl of binding buffer containing 1 μl of fluorescein-conjugated annexin V and 1 μl propidium iodide (PI), all sourced from the Annexin V-FLUOS staining kit (Roche). Cells were incubated in staining solution for 10 mins at room temperature, after which time binding was terminated by addition of 450 μl of ice-cold binding buffer. Samples were stored on ice and were analysed by flow cytometry within one hour. Fluorescein fluorescence was determined using the FL1 channel (530$\pm$15 nm), and PI uptake was detected with the FL2 channel. Cell debris formed a discrete population with very low forward scatter (FSC, measure of particle size) and side scatter (SSC, measure of particle granularity), and this material was removed from analysis by gating. At least 10000 gated cells were analysed per sample.

Later re-analysis of data from control samples stained with annexin V only or PI only performed in parallel with experimental samples indicated that the electronic compensation required to remove fluorescein interference from the FL2 (PI) channel was inadequate, making the PI staining data unreliable and so this was not used in analyses. PI interference in the FL1 (fluorescein) channel was not observed in control samples stained with PI only, and so the fluorescein data was deemed reliable and was used for analysis. Additionally, a subsequent experiment using correct compensation parameters produced the same results with regards to total annexin V staining as the inadequately compensated experiments.

2.10 Cell migration assay

Cell migration towards a chemoattractant was assessed with a transwell assay, in which cells in one chamber migrate through pores in a membrane towards the chemoattractant in another chamber.

HUVECs in EGM were trypsinised and resuspended in EBM at $3x10^5$ cells/ml. In some experiments, cells were incubated at this stage for 30 mins in the presence of enzyme inhibitors with mixing every 5–10 mins. Uncoated cell culture inserts (8 μm membrane pore size; Falcon, Becton Dickinson) were inserted into a 24-well plate, and 750 μl EBM with or without 25 ng/ml VEGF was added to the lower chamber. Cell suspensions were then added to the upper chamber (0.5 ml, $1.5x10^5$ cells/well) and incubated at 37°C for 4 h. Unmigrated cells were removed by scraping the upper side of the membrane with a cotton bud, and the cells were fixed and stained with the Reastain Quick Diff kit (Reagena) and mounted onto glass slides. Nuclei of migrated cells were counted in four fields, one from each quadrant of the insert, at x100 magnification using an eyepiece indexed graticule. The mean count was used as the count for that insert.

2.11 Collagen tubulogenesis assay

Collagen I solution in M199 medium was prepared by mixing PureCol (Nutracon) with 10x M199 medium (Invitrogen) and 0.1 M NaOH in the ratio 8:1:1. The solution was neutralised with a few drops of 0.5 M NaOH, assessed by medium colour change, and 750 μl was added to each well of a 12-well plate and incubated at 37°C for 1 h to solidify.

Meanwhile, HUVECs were trypsinised and resuspended in EBM containing 0.5% FBS (prepared as a dilution of EGM) at 1.5x10^5 cells/ml. For some experiments, cells were incubated for 30 mins at 37°C in the presence of inhibitors. 500 μl of cell suspension was added to a well containing set collagen, and some samples were spiked with VEGF to a final concentration of 25 ng/ml. Plates were returned to the incubator for 24 h to allow tubulogenesis to occur, after which the adhered cells were washed with PBS, fixed in 4% formaldehyde in PBS, washed three times with PBS and stored in PBS at 4°C.

For quantification of tubulogenesis, a single phase-contrast micrograph just off centre of each well was digitally acquired. Using ImageJ, lines were drawn over the tubes and the area of these lines (proportional to the total length of tubes visible in the micrograph) was determined. Tubes were defined as at least two connected cells forming an elongated structure, and the line was drawn from the tip of one end of the tube to the tip of the other end, as shown in figure 2.9.

2.12 Database sources and sequence analysis

All DNA, mRNA and protein sequences used for sequence analysis were retrieved from the RefSeq database, and were located by searching Entrez Gene, limiting results to RefSeqs. Accession numbers given are for the RefSeq database.

Protein sequence alignments were performed using Clustal 2.0.10 via the ClustalX2 program using the default settings. Alignments were imported into JalView, where sequences were coloured for

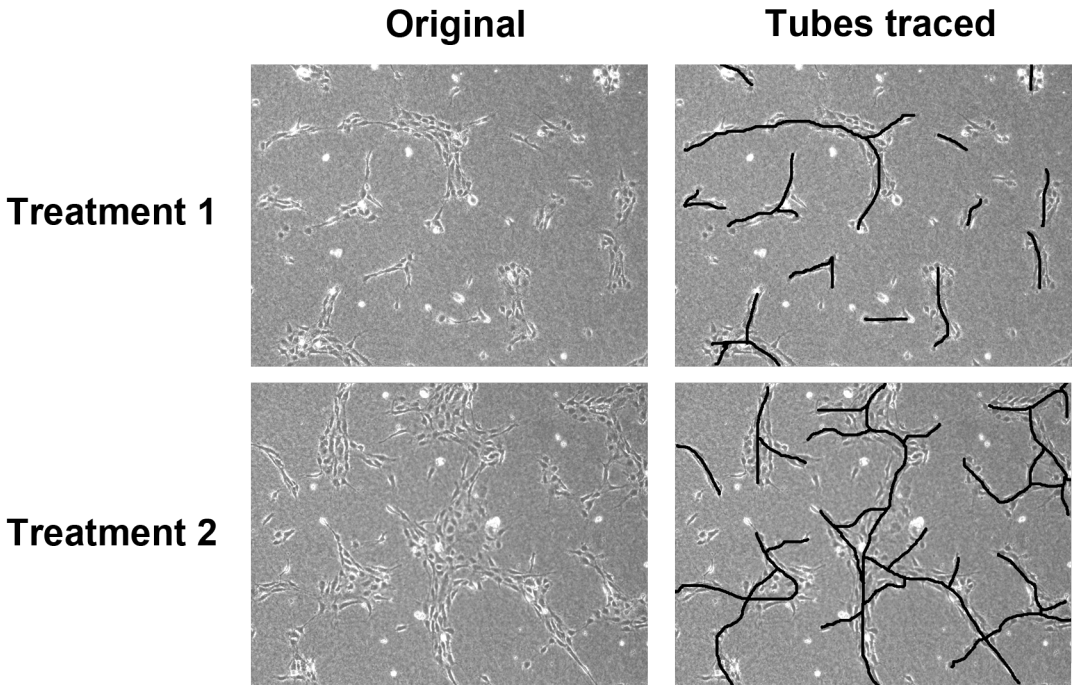

Figure 2.9: Tubulogenesis quantification method
Two original images are shown on the left, with the tubes traced on the right. The area (length) of the traced lines in the right hand images would then be used for quantification of tubule length.

similarity, using the Blossum62 symbol comparison matrix (Henikoff and Henikoff 1992).

Web addresses and references for all sequence analysis tools used in this thesis are given in table 2.9.

2.13 Statistical analysis

In order to compare between treatment groups composed of multiple individual experiments, normalisation of data was required. Without normalisation, problems arise such as comparing the same western blot exposed to film for varying times gives different raw quantification values, and large raw values from a particular experiment will dominate when results are averaged across a number of experiments.

As analysis of variance (ANOVA) methods require treatment groups for comparison to have equal variances, it was not possible to normalise replicate experiments by correcting data within an experiment to a control sample – this leads to the variability of the control group being zero.

Table 2.9: Databases and web tools used in this study

Database or website	Reference or web address
BLASTp	Altschul *et al.* (1997, 2005) www.ncbi.nlm.nih.gov/blast/Blast.cgi?PAGE=Proteins&PROGRAM=blastp
ClustalX2	Larkin *et al.* (2007)
Conserved Domain database	www.ncbi.nlm.nih.gov/Structure/cdd/wrpsb.cgi
Ensembl	www.ensembl.org/Homo_sapiens/Info/Index
Entrez Gene	Marchler-Bauer *et al.* (2007) www.ncbi.nlm.nih.gov/sites/entrez?db=gene
Jalview	Clamp *et al.* (2004)
Mascot peptide mass fingerprint	www.matrixscience.com/cgi/search_form.pl?FORMVER=2&SEARCH=PMF
Mascot tandem MS	www.matrixscience.com/cgi/search_form.pl?FORMVER=2&SEARCH=MIS
MitoProt	Claros and Vincens (1996) mips.gsf.de/cgi-bin/proj/medgen/mitofilter
Refseq database	Pruitt *et al.* (2007) www.ncbi.nlm.nih.gov/RefSeq/key.html
Scansite	Obenauer *et al.* (2003) scansite.mit.edu/motifscan_seq.phtml
Scansite pI calculator	scansite.mit.edu/cgi-bin/calcpi
SwissProt	www.uniprot.org
TargetP	Emanuelsson *et al.* (2000); Nielsen *et al.* (1997) www.cbs.dtu.dk/services/TargetP/

Instead, individual response values within an experiment were expressed as a proportion of the total response observed across all treatments within an individual experiment, giving proportion data. For example, raw results are control 10, treatment A 60, treatment B 30, then proportion data is control 0.1, A 0.6, B 0.3 (proportions of 10 + 60 + 30). The response produced by a particular treatment group was then the mean of the individual proportion data values from a number of experiments. To aid viewing, the proportion data was normalised (before determining the mean response for that treatment to preserve variation in the data) by dividing the entire dataset by the mean proportion of a selected control treatment group, so that the mean of this group would be 1. If the example data were group means, this would give control 1, A 6, B 3. Data was then said to be a proportion of that control group. Where required for some ANOVA analyses, proportion data was logarithmically transformed before analysis to equalise variances and prevent the residual error term of ANOVA increasing in line with mean data value. This normalisation method was agreed with Dr. Glenn Baggott (School of Biological and Chemical Sciences, Birkbeck College) as the most appropriate treatment for the data.

Statistical analysis was performed via Prism (GraphPad) on normalised data by either one- or two-way ANOVA as appropriate, with Bonferroni's test for multiple comparisons used to locate differences. Statistical significance was accepted at a family error rate $p<0.05$. The specifics of each statistical analysis performed are indicated in the appropriate figure legend, with the adjusted p values.

Error bars on graphs represent the standard error of the mean (SEM) unless stated. For clarity, in most figures only a single error bar is shown (e.g. bar in a bar graph represents the group mean, error bar above that bar represents the SEM). However in all cases the an identical error bar below the mean is possible, and in reality all data are mean $\pm$ SEM, although the other error bar is not shown.

Chapter 3

Results: Proteomic analysis of VEGF treatment of HUVECs

In an attempt to find new VEGF-regulated proteins, VEGF signalling in endothelial cells was analysed using proteomics. At the outset of this work, no proteomic analysis of VEGF-treated endothelial cells had been published. Here, several proteomic approaches are described which aimed to generate an overall quantitative picture of changes in endothelial protein expression and phosphorylation in response to VEGF.

3.1 Overview of proteomics

The proteome is the totality of proteins expressed in a defined biological system, such as a cell or organelle. Unlike the genome, the proteome varies with time and external influences such as stimulation by cytokines, as expression of various proteins increases and decreases. Proteomics, analysis of the proteome, involves separation of proteins from often complex mixtures, and their identification by mass spectrometry-based approaches.

A large number of proteins can be analysed and, in theory, any protein of interest can be identified, increasing the likelihood of novel and unexpected findings. Comparative proteomics, aimed at locating differences in protein expression or modification between treatments, as opposed to

cataloguing cellular proteins, can be performed in different ways, but always includes the following elements: production of protein mixtures that differ in treatment, cell type or some other influence being investigated; separation of the proteins in this mixture; detection of these proteins; location of proteins exhibiting differences between treatments; and subsequent identification of these proteins of interest.

In this chapter, protein mixtures were separated by two-dimensional electrophoresis, on the basis of isoelectric point (pI) and then molecular weight, and then detected by silver staining. Proteins of interest were then excised from 2-D gels, digested to peptides with trypsin, and the masses of these peptides were then determined by MALDI-TOF mass spectrometry, to give a peptide mass fingerprint for the protein. These fingerprints were then compared with databases of known protein sequences to identify the protein spots cut from the gel. A fuller description of peptide mass fingerprinting principles is given in section 2.5.

3.2 Analysis of whole-cell lysates by 2-D electrophoresis and silver staining

To identify changes in protein expression or modification in response to VEGF treatment of endothelial cells, whole-cell lysates were prepared from confluent, serum-deprived human umbilical vein endothelial cells (HUVEC) after treatment with 25 ng/ml VEGF for different times. Proteins in the cell lysates were separated by 2-D electrophoresis using a linear pH range of 3–10 in the first (isoelectric focusing) dimension and a 10% acrylamide gel in the second (SDS-PAGE) dimension. Gels were then silver stained. Figure 3.1 shows typical 2-D gels obtained using this approach with samples treated with or without VEGF for 10 mins.

In several independent experiments, spots A and B (figure 3.2) appeared different between gels from control cells and cells treated with VEGF for 10 mins as determined by visual inspection, spot A increasing and spot B decreasing in response to VEGF. Quantification of spots A and B by

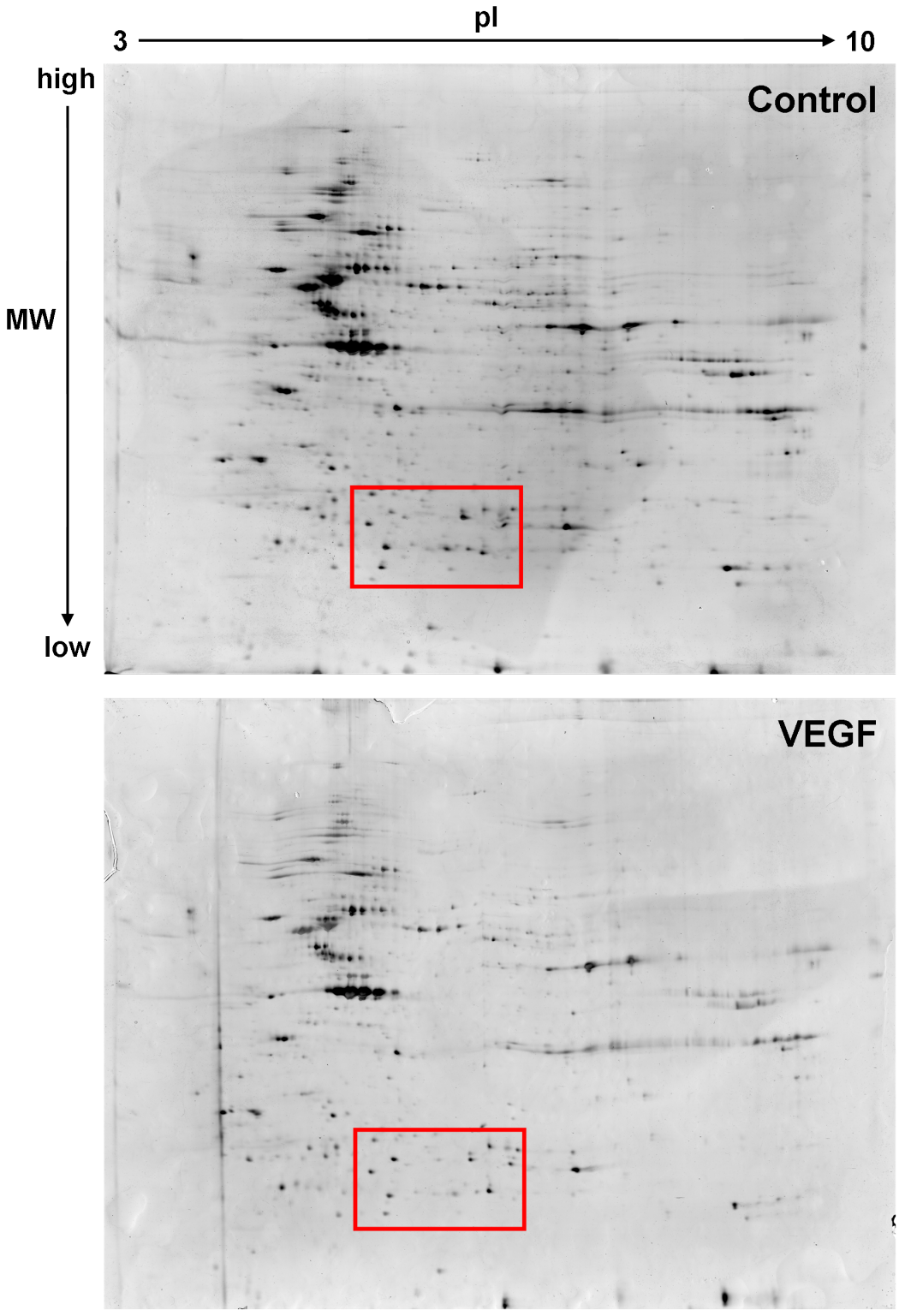

Figure 3.1: Analysis of whole-cell lysates by 2-D electrophoresis and silver staining
Confluent, serum-deprived HUVECs were treated with either 25 ng/ml VEGF or no addition (control) for 10 mins. Lysates were separated by 2-D electrophoresis and gels were silver stained. Representative 2-D gels obtained using this method are shown, with the axes of separation indicated (pI, isoelectric point; MW, molecular weight). The boxed area of the gel refers to figure 3.2A.

densitometry showed that VEGF induced an increase in the amount of spot A as a proportion of the total amount of spots A and B from 0.17 to 0.65 (figure 3.2B). Both spots were identified as forms of Heat Shock Protein 27 (Hsp27) (figure 3.2C). The increase in the more acidic form of Hsp27 (spot A) over the more basic form (spot B) without apparent change in molecular weight is consistent with VEGF causing phosphorylation of this protein, although other modifications could also be responsible for the observed spot pattern. VEGF regulation of Hsp27 is the topic of chapters 4 and 5.

No other consistent differences between control or VEGF-treated samples were found in silver-stained 2-D gels following treatment times of 5 mins, 10 mins, 30 mins, 1 h, and 24 h, in at least two independent experiments for each time point. Representative gels obtained from HUVECs treated with VEGF for 24 h are shown in figure 3.3.

3.3 Analysis of whole-cell lysates by difference gel electrophoresis

The second proteomic approach taken to quantitatively identify VEGF regulated changes in protein expression or modification used difference gel electrophoresis (DIGE). The DIGE method, described in section 2.4.8, involves covalently labelling the two samples to be compared with separate fluorescent dyes. The samples are then mixed and run on the same gel, and the gels are imaged with a fluorescent scanner.

DIGE has two major advantages over analysing samples using separate silver-stained gels described in section 3.2. Firstly, it avoids the need to locate the same protein spot on two different gels when comparing two protein samples as both samples are pooled and run on the same gel, as these spots overlap. The second major advantage over silver staining is the linear dynamic range (range over which the increase in protein abundance is proportional to the increase in detected signal) is much higher for fluorescence detection than for silver staining. Therefore, quantitation and the ability to detect small differences between protein samples is improved.

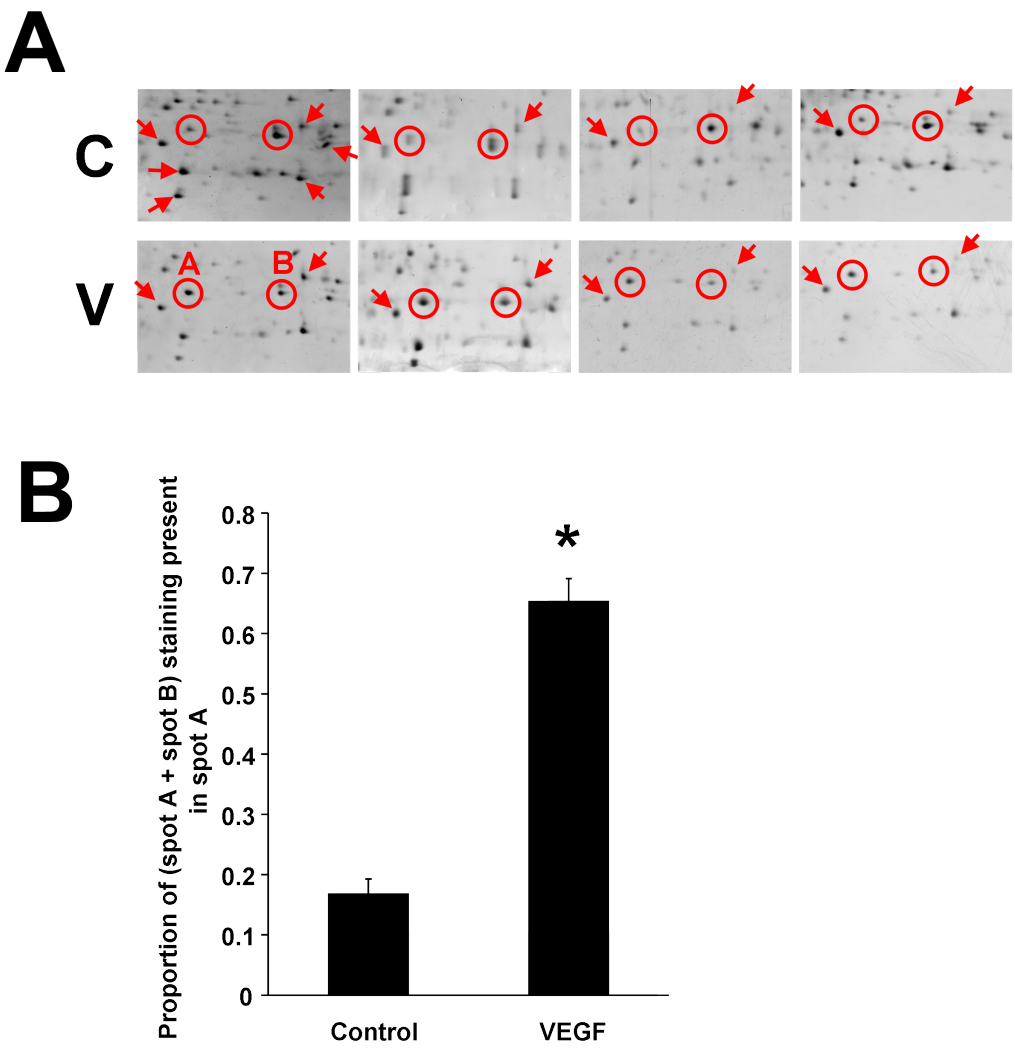

Figure 3.2: VEGF induces an acidic shift in the isoelectric point of Hsp27 consistent with phosphorylation (continued overleaf)

A. Confluent, serum-deprived HUVECs were treated with either 25 ng/ml VEGF (V) or no addition (control, C) for 10 mins. Lysates were separated by 2-D electrophoresis and gels were silver stained. The area of the gel indicated by the box in figure 3.1 is shown from four independent experiments. The two circled spots, labelled A and B, were noticed as different between gels from control- and VEGF-treated samples. Spots A and B are circled in each gel, and were identified as equivalent between separate gels by comparison with the relative positions of other nearby spots, indicated with arrows. Two of these spots are indicated on all gels to aid comparison. Spots A and B from one gel containing a VEGF-treated sample were picked and identified via peptide mass fingerprinting, both spots were Hsp27 (see part C overleaf). Cell treatments and 2-D gels were performed in conjunction with Dr. Ian Evans, Department of Medicine, UCL.

B. The intensity of staining of spots A and B from the gels shown in part A was quantified using ImageJ gels module, and data is expressed as the mean intensity ($\pm$ SEM) of spot A as a proportion of the combined intensity of spots A and B, from four independent experiments. * Proportion of staining present in spot A was significantly higher in samples treated with VEGF than in control samples ($p<0.001$ by unpaired t-test).

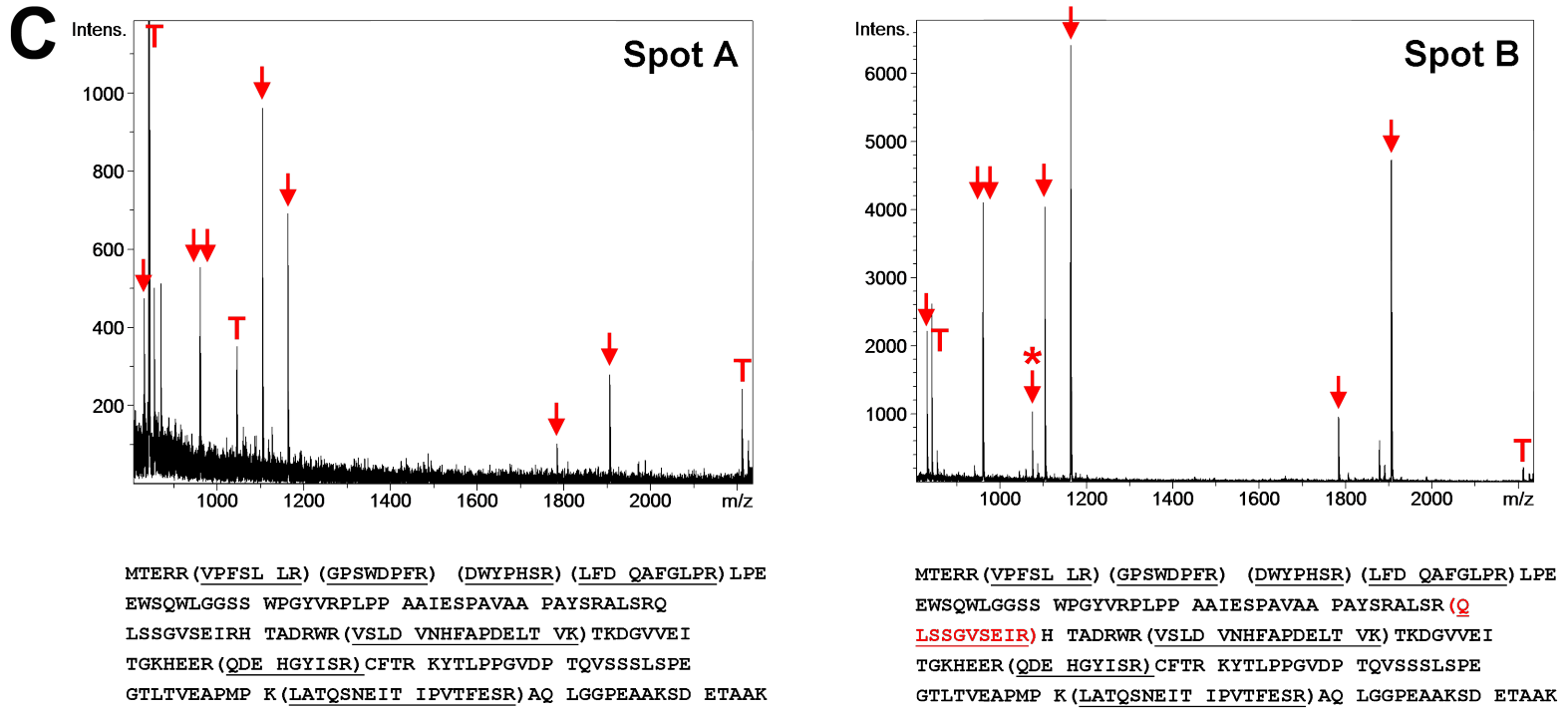

Figure 3.2: VEGF induces an acidic shift in the isoelectric point of Hsp27 consistent with phosphorylation (continued)
C. Peptide mass fingerprints obtained for spots A and B as shown in part A. The y-axis represents signal intensity, the x-axis represents mass-to-charge ratio (m/z) which, for the ions produced by MALDI-TOF, is equivalent to mass + 1. Peaks identified as derived from Hsp27 are indicated with arrows. Trypsin autolysis peptides are indicated with a 'T'. The graphs have been scaled to show the less intense Hsp27 peaks, and so some highly abundant trypsin peaks are off the scale. The Hsp27 amino acid sequence is given below each spectrum, with the identified peptides enclosed by brackets and underlined. The same peptides were identified from both samples apart from the starred peak, representing the peptide QLSSGVSEIR (amino acids 80–89, highlighted red in the spot B amino acid sequence and indicated with an asterisk on the spot B spectrum), which was observed in the spot B spectrum only.

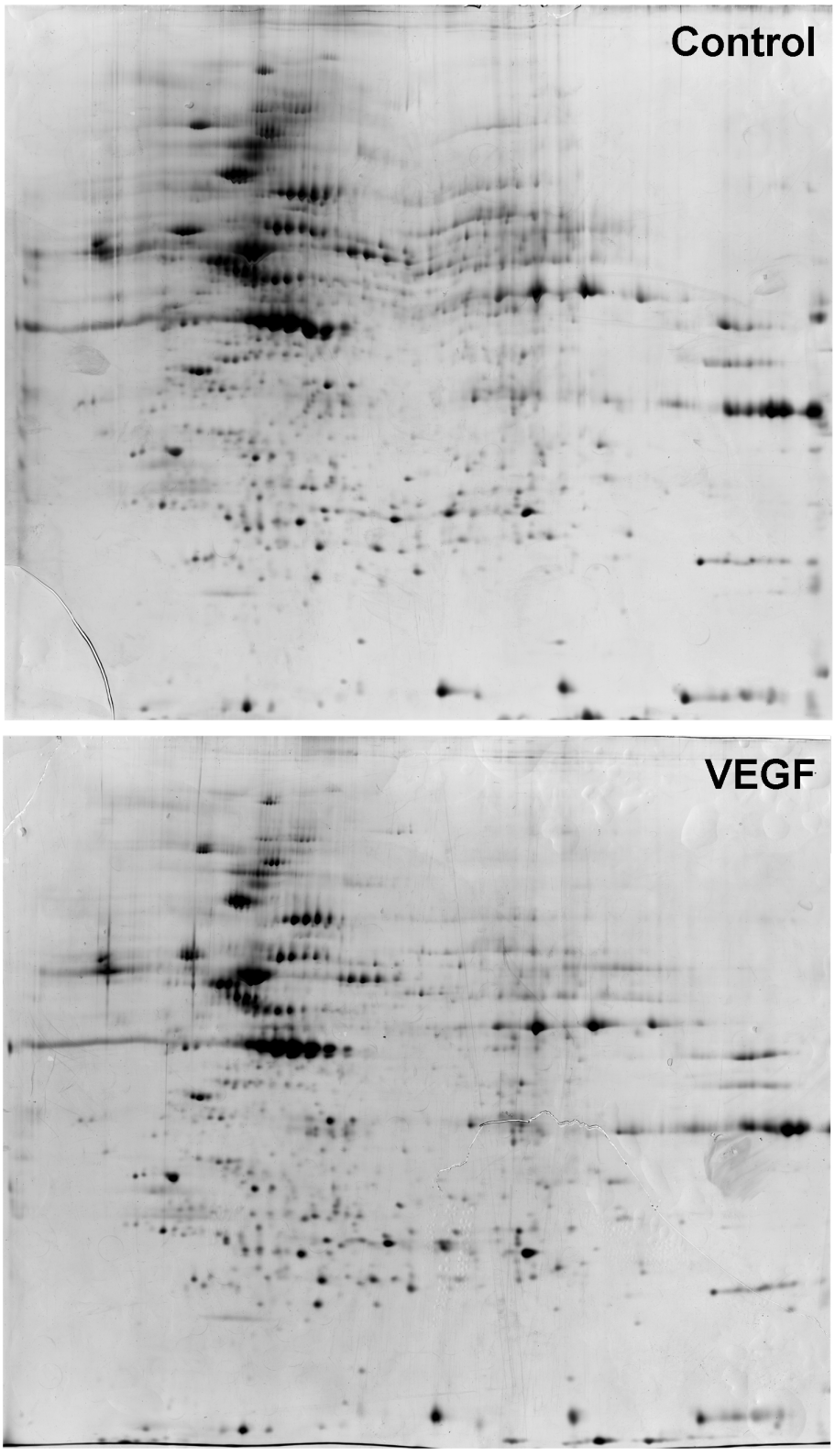

Figure 3.3: Effect of 24 h VEGF treatment on spot pattern obtained by 2-D electrophoresis and silver staining
Confluent, serum-deprived HUVECs were treated with either 25 ng/ml VEGF or no addition (control) for 24 h. Lysates were separated by 2-D electrophoresis and gels were silver stained. Gels shown are representative of six independent experiments. No consistent differences were observed between gels corresponding to VEGF-treated cells and those from control cells.

Confluent, serum-deprived HUVECs were treated with VEGF for 5 mins, 10 mins, and 24 h, and compared with time-matched controls. The number of proteins detected to change consistently on VEGF treatment by more than 10% was 2, 7, and 11 respectively, and no protein changed by more than 50% (three independent experiments per time point). Gels indicating the altered spots are shown in figure 3.4.

The gels were then silver stained, spots were picked and an attempt was made to identify the altered proteins via via MALDI-TOF mass spectrometry. None of the proteins were identified, possibly due to insufficient protein. Running preparative gels (>1 mg protein loaded per gel) to gain enough protein for mass spectrometry-based identification resulted in messy gels with poor spot resolution, and it was not possible to confidently locate the spots on the preparative gels which corresponded to those of interest from the DIGE gels. This method was not pursued further in this thesis.

3.4 Analysis of the phospho-tyrosine proteome

An alternative strategy to identify changes in proteins relevant for VEGF signalling is to analyse changes in the phospho-tyrosine (pY) proteome. This has the advantage that the potential number of proteins undergoing change is considerably smaller than in the total cellular proteome, and it was hoped that when scaling up to preparative gels adequate spot resolution would be maintained.

VEGF activates receptor protein tyrosine kinases and is known to increase tyrosine phosphorylation of a number of cellular components important in VEGF signalling such as VEGFR2, ERK, p38, src, PI-3-K, and phospholipase Cγ. The availability of good antibodies to pY also increased the likelihood of specifically isolating tyrosine phosphorylated proteins.

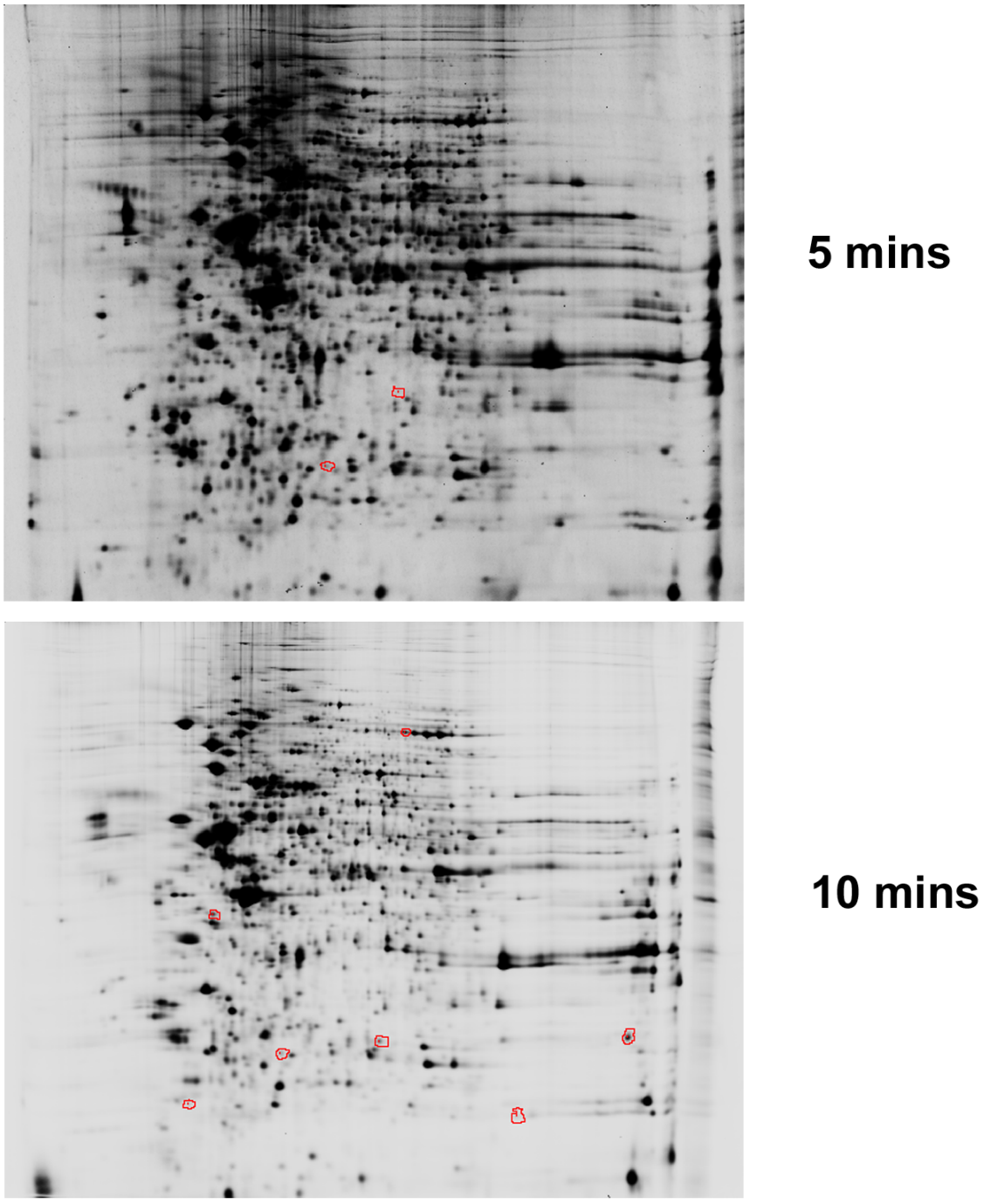

Figure 3.4: Consistent effects of VEGF treatment detected by DIGE (continued overleaf)

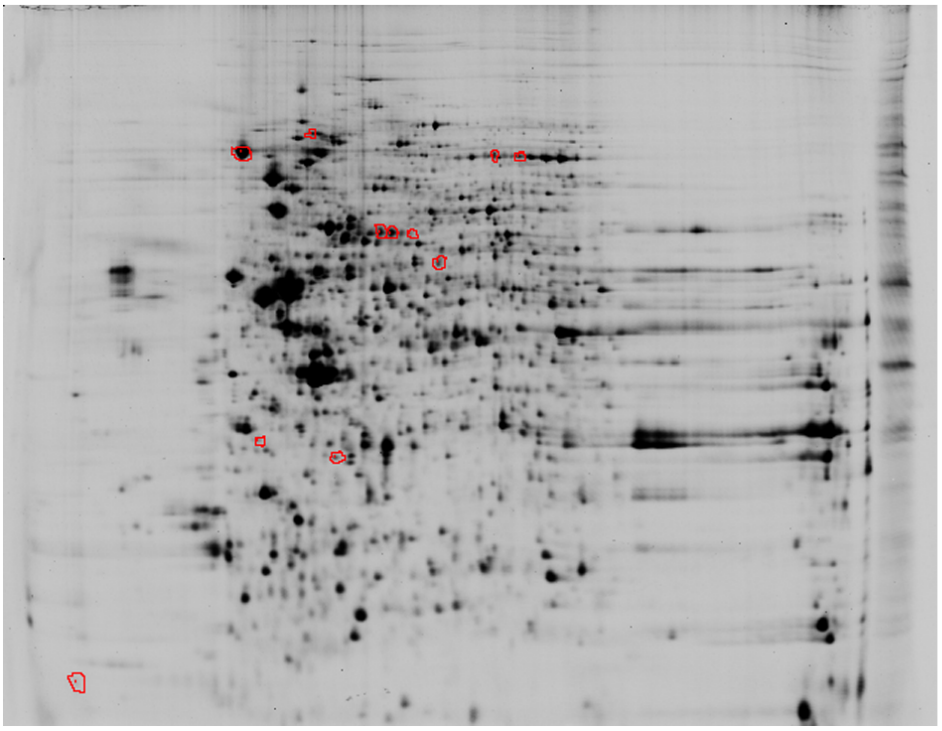

Figure 3.4: Consistent effects of VEGF treatment detected by DIGE (continued from previous page)
Serum-deprived, confluent HUVECs were treated for either 5 mins, 10 mins or 24 h, with 25 ng/ml VEGF or no addition (Control) and lysed. One sample (either control or VEGF) was labelled with Cy3 and the other with Cy5 using the dye manufacturers minimal labelling protocol – which dye was assigned to which treatment group was varied between experiments. 50 μg of protein, determined by modified Bradford assay, was separated by 2-D electrophoresis and gels were imaged using a Typhoon fluorescent imager. Three independent experiments were performed for each time point, and for each time point spots were matched between gels (1 gel per experiment) and analysed for up- or down-regulation of spot abundance on VEGF treatment using DeCyder software. Representative gels are shown for each time point, and spots determined to increase or decrease by at least 10% on VEGF treatment are circled in red. The number of spots determined to vary by greater than 10% at 5 mins, 10 mins, and 24 h, was 2, 7, and 11 respectively.

3.4.1 Whole cell lysates

Initially, samples were separated by either SDS-PAGE (figure 3.5) or 2-D electrophoresis (figure 3.6) and blotted with anti-phosphotyrosine antibodies to ensure that VEGF-induced tyrosine phosphorylation could be observed.

Treatment with VEGF for 10 mins induced phosphorylation of a number of proteins as detected by immunoblots of 1-D gels (figure 3.5A). The detection of tyrosine-phosphorylated proteins and VEGF-induced increases in tyrosine phosphorylation was improved by pre-treatment of cells with

the tyrosine phosphatase inhibitor sodium orthovanadate (figure 3.5B).

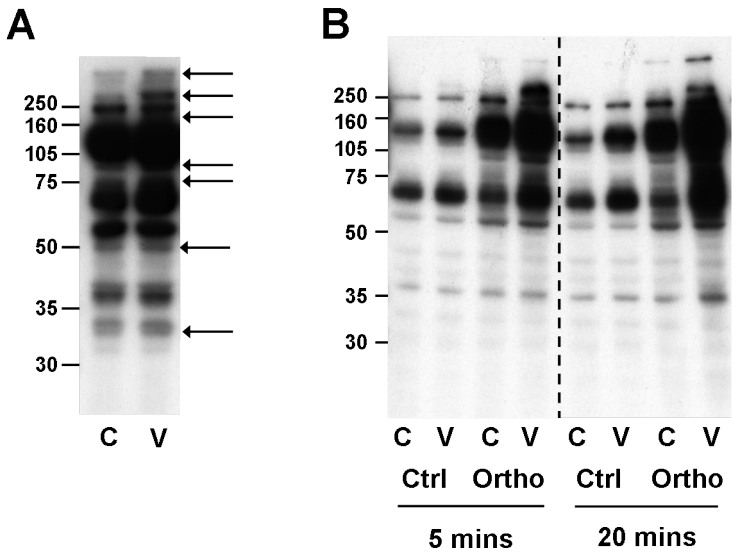

Figure 3.5: SDS-PAGE analysis of VEGF-induced tyrosine phosphorylation using whole cell extracts
A. Confluent, serum-deprived HUVECs were treated for 10 mins with 25 ng/ml VEGF (V) or no addition (C), and then lysed. Whole cell extracts were blotted and probed with 4G10 anti-phosphotyrosine antibody. Arrows indicate increases in tyrosine phosphorylation with VEGF treatment. Positions of molecular weight markers (in kDa) are given on the left of the blot.
B. Confluent, serum-deprived HUVECs were pre-incubated with either 1 mM sodium orthovanadate (O) or no inhibitor (Ctrl). After 30 mins, cells were exposed to 25 ng/ml VEGF (V) or no addition (C) for either 5 or 20 mins before lysis as indicated. Whole cell extracts were blotted and probed with 4G10 anti-phosphotyrosine antibody. Results are representative of three independent experiments.

VEGF-induced tyrosine phosphorylation was also examined by anti-pY blots of two-dimensional gels. This proved to be more problematic than the 1-D gel-based analysis, with the only consistent change observed being an increase in the phosphorylation of an ≈40 kDa protein within 5–10 min, although no difference was observed after 30 mins (figure 3.6). A number of the changes observed in the one-dimensional gels could not be seen on the 2-D gels. The lack of resolution available on the 7 cm IEF strips used may have contributed to this problem.

3.4.2 Phospho-tyrosine immunoprecipitates

To identify proteins tyrosine-phosphorylated in response to VEGF, pY-containing proteins were immunoprecipitated from VEGF-treated HUVECs. Tyrosine-phosphorylated proteins could be

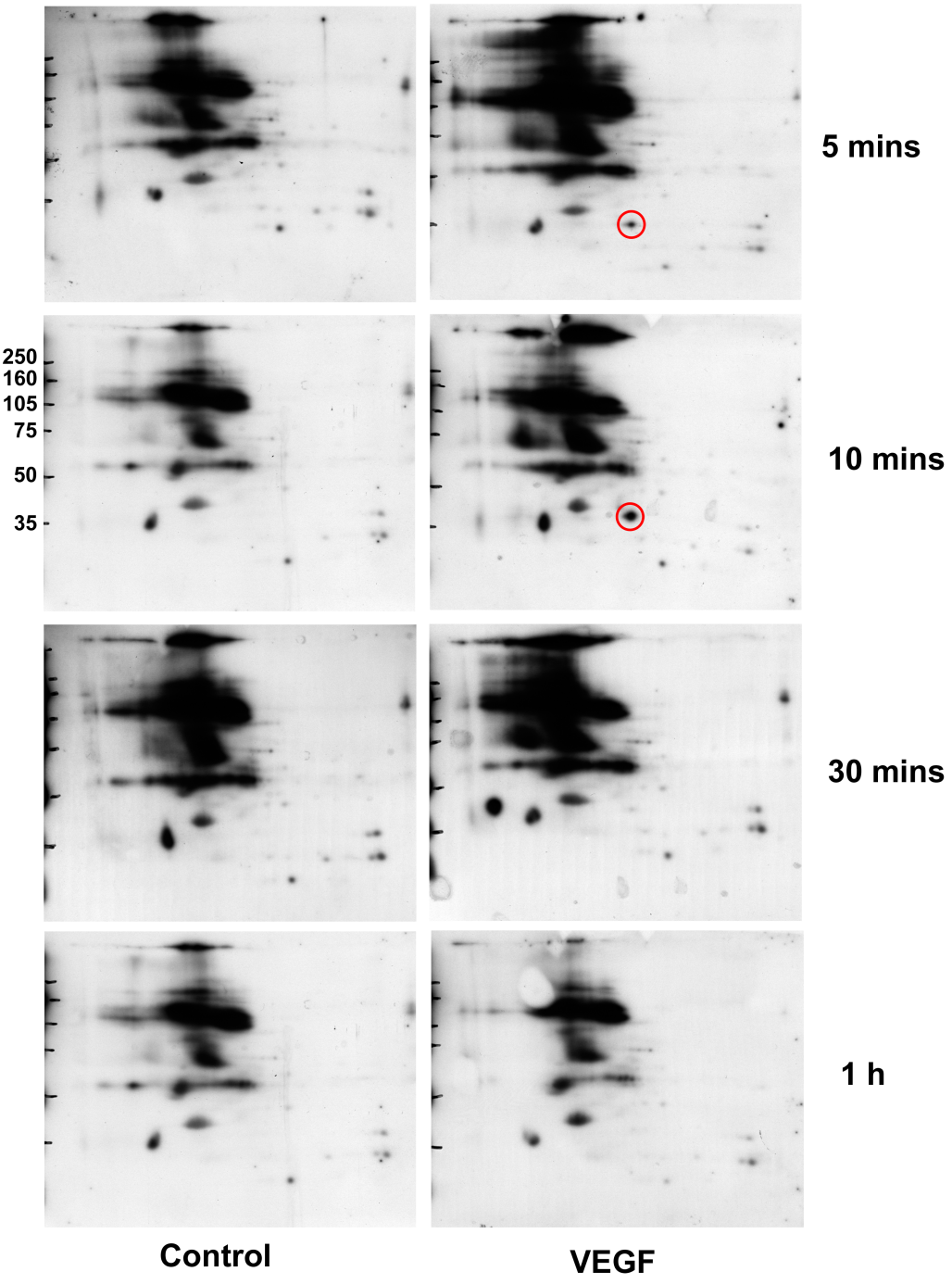

Figure 3.6: 2-D analysis of VEGF-induced tyrosine phosphorylation using whole cell extracts

Confluent, serum-deprived HUVECs were treated with no addition (Control) or 25 ng/ml VEGF for either 5, 10, 30 or 60 mins as indicated, and then lysed. Whole cell extracts were separated by 2-D electrophoresis (pH 3–10 IEF strip used), blotted and probed with 4G10 anti-phosphotyrosine antibody. Positions of molecular weight markers (in kDa) are given on the left of the blot. Results are representative of two independent experiments. The only clear and consistent change observed between control and VEGF treatment is circled.

immunoprecipitated with either the 4G10 or RC20 antibodies (figure 3.7). It is likely that the immunoprecipitated proteins are genuinely tyrosine phosphorylated as alkaline phosphatase treatment of the immunoprecipitates dramatically reduced the number of tyrosine-phosphorylated proteins detected in the protein extracts. As previously observed for analysis of whole cell lysates (figure 3.5B), orthovanadate pre-treatment of cells before lysis enhanced the degree of tyrosine phosphorylation (figure 3.7).

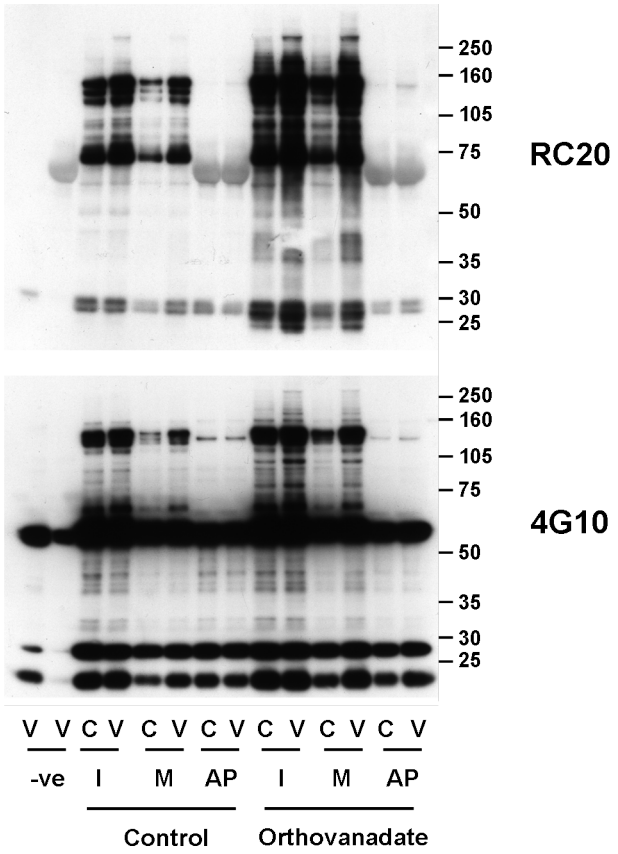

Figure 3.7: Analysis of phospho-tyrosine immunoprecipitates with 1-D gels
Serum-deprived, confluent HUVECs were incubated for 30 mins with 1 mM sodium orthovanadate or no addition (control), and then exposed to 25 ng/ml VEGF (V) or no addition (C) for 15 mins before lysis. Tyrosine-phosphorylated proteins were immunoprecipitated with either 4G10 or RC20 anti-pY antibodies, or a non-targeting control antibody of the same host species and isotype as the 4G10 antibody (-ve). Immunoprecipitates were washed and for 30 mins were either incubated with alkaline phosphatase at 37°C (AP), with no addition at 37°C (M), or on ice (I), after which proteins were then extracted by boiling with SDS-PAGE sample buffer. Extracts were immunoblotted and probed with the immunoprecipitating antibody. The mock (M) samples were included to control for any alkaline phosphatase-independent effects of a 30 min, 37°C incubation. Left and right -ve lanes are samples untreated and treated with alkaline phosphatase respectively. Results are representative of two independent experiments. Positions of molecular weight markers (in kDa) are indicated.

Often, the resolution of 1-D gels is insufficient to give a distinct band of pure protein, hindering peptide mass fingerprinting-based identification of proteins, and so, with the aim of identifying new targets, pY immunoprecipitates were analysed by 2-D gel electrophoresis followed by silver staining. In an initial experiment where HUVECs were pre-incubated with orthovanadate and then treated with VEGF for 15 mins, no consistent differences between control- and VEGF-treated samples were observed. However, the major problem was that very few strongly staining spots were detected, with other very faint spots clearly containing insufficient protein for MALDI-TOF analysis. It was decided to concentrate on methodological modifications, increasing the amount of cells used for immunoprecipitation and varying the amount of antibody used, with the intention to revisit control/VEGF comparisons once a settled method was obtained. Judging by intensity of the silver-stained spots obtained, and attempted peptide mass fingerprinting, it was not possible to obtain enough pY-containing proteins to allow MS analysis, and so control/VEGF comparisons using silver stained gels was not pursued further.

Instead, methodological alteration experiments were used to try to identify pY-containing proteins from IPs of VEGF-treated cells, so that any novel findings could be pursued by western blotting. A typical 2-D gel obtained is shown in figure 3.8. A number of proteins were identified from the gel via peptide mass fingerprinting, including stomatin-like protein 2 (SLP2). At the time this experiment was performed, SLP2 had not been reported to be present in endothelial cells, and very little was known about it. SLP2 and its role in endothelial cells is the topic of chapter 6.

3.5 Discussion

This chapter aimed to identify novel VEGF-regulated proteins using proteomic methods. Analysis of whole cell lysates by 2-D electrophoresis and silver staining, combined with peptide mass fingerprinting, identified Hsp27 as a VEGF-regulated protein, but did not reveal any other clear differences between VEGF-treated and control samples despite examination of a number of time points between 5 mins and 24 h. Difference gel electrophoresis (DIGE) revealed a number of

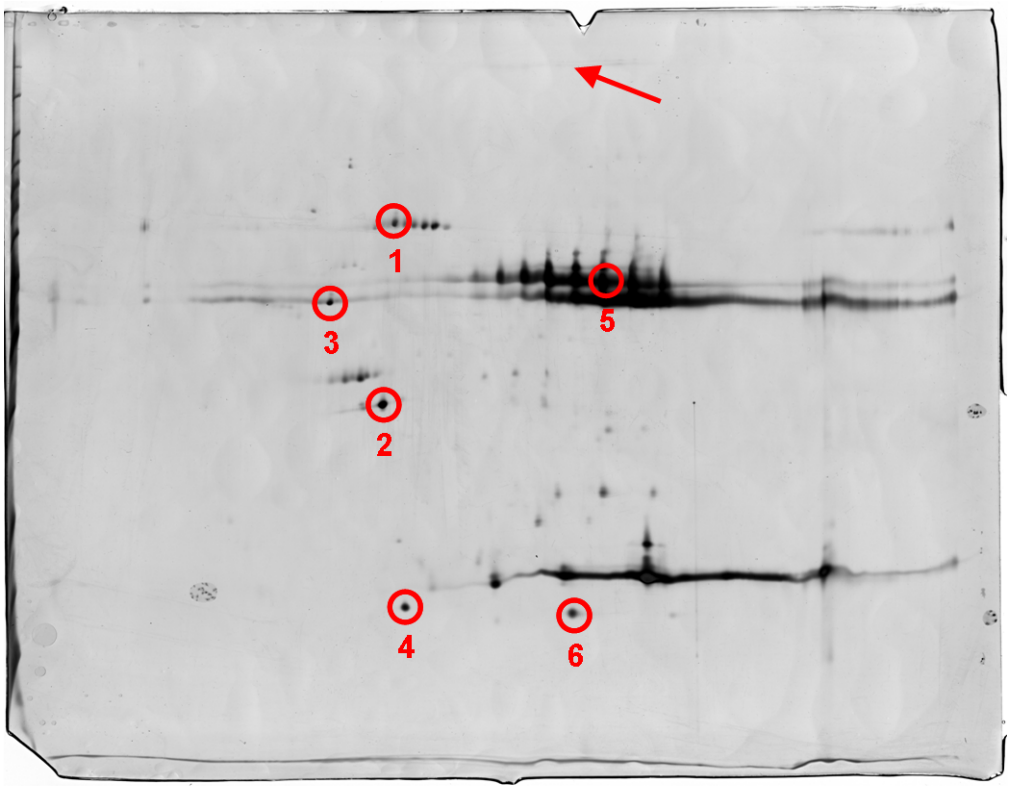

Spot	Protein ID	Mr kDa	Matched peptides	% coverage
1	Heat shock 70kDa protein 9B (Mortalin, mortalin-2)	74	12	22
2	Stomatin (EPB 72)-like 2	39	9	34
3	Vimentin	54	18	46
4	Glutathione transferase	23	8	49
5+6	IgG 2b (mouse)	53	6	13

Figure 3.8: Proteins identified in phosphotyrosine immunoprecipitates
Serum-deprived, confluent HUVECs from 6 x 15 cm dishes were treated for 15 mins with 25 ng/ml VEGF before cells were lysed and phosphotyrosine-containing proteins were immunoprecipitated with the 4G10 antibody. Extracts were separated by 2-D electrophoresis using a pH 3–10 IEF strip, and gels were silver stained. Spots were picked and identified via peptide mass fingerprinting. Matched peptides, the number of separate peptides obtained from the tryptic digest of that spot that matched the identified protein; % coverage, proportion of protein sequence covered by the matched peptides. In other gels, myosin was positively identified in the region shown by the arrow. Spot pattern is representative of four independent experiments.

consistent differences between whole-cell lysates prepared from VEGF-treated or control cells. It was not possible to obtain sufficient protein for MS-based identification from the DIGE gels themselves, nor was it possible to accurately match preparative gels, containing large amounts of protein, with the DIGE gels, so the protein spots determined to be different in the DIGE gels were not identified.

VEGF treatment reproducibly increased protein tyrosine phosphorylation as determined by immunoblots of one-dimensional gels, but these changes were not apparent on 2-D gels. An anti-pY antibody immunoprecipitated more proteins from VEGF-treated cells than from control cells, and the immunoreactivity of the IPed proteins towards anti-pY antibodies could be reduced by alkaline phosphatase treatment, indicating that the IPed proteins were likely to be tyrosine phosphorylated. Proteomic analysis of anti-pY IPs by 2-D electrophoresis and silver staining did not reveal major proteins in the expected positions when compared to the same IPs separated by SDS-PAGE and probed with an anti-pY antibody. However, a little-known protein, SLP2, was identified as a major component of anti-pY IPs, despite the lack of a major band at that molecular weight when the IPs were analysed by blotting with anti-pY antibodies.

VEGF treatment of endothelial cells is known to alter the phosphorylation status of a number of proteins in the short term, and alter the expression of proteins in both the short and longer term. Analysis of whole cell lysates revealed an acidic shift in Hsp27, demonstrating that 2-D separation allows the separation of post-translationally modified variants of a protein, and the identification of protein phosphorylation. Probable reasons for the lack of detection of proteins expected to be different between VEGF-treated and control samples is the low abundance of the VEGF-regulated proteins in the cell, and lack of adequate reproducibility in spot matching between gels and subsequent quantification of spot intensity, causing changes in more abundant proteins to go unnoticed.

Certain proteins, including cytoskeletal proteins such as actin and tropomyosin, metabolic enzymes such as enolase and triose phosphate isomerase, and chaperones such as Hsp60 and Hsp70, are highly abundant in cells and were easily identified by proteomic analysis of whole cell lysates

(data not shown). Many enzymes involved in signalling – those proteins likely to be affected by short-term VEGF treatment – are much lower abundance. This problem of differences in protein copy number within the cell, known as the dynamic range of protein expression, is a major challenge for proteomics-based techniques (reviewed by Corthals *et al.* 2000). Protein amplification systems, such as PCR for nucleic acids, are not available.

Others have also had difficulty with the dynamic range of protein expression. Analysis of the yeast proteome using high-resolution 2-D electrophoresis and MS identification failed to detect low abundance proteins, with the authors calculating that when using a 40 μg protein load, no proteins expressed lower than 50,000 copies per cell were detected (Gygi *et al.* 2000). Increasing the sample protein load to 500 μg allowed detection of proteins expressed at 1,000 copies per cell, but despite the use of narrow pH range IEF strips (1 pH unit) to try to maintain adequate spot resolution, resulted in many overlapping spots – that is, proteins migrating to the same position on the gel. When very large protein loads (50 mg, far beyond the capacity of 2-D electrophoresis) were separated by 1-D electrophoresis followed by multiple chromatographic steps, identification of low abundance proteins was improved. The authors suggested pre-fractionation techniques were necessary to obtain sufficient quantities of low-abundance proteins from large amounts of starting material. These simplified mixtures could then be analysed by 2-D electrophoresis.

Hsp27 is highly abundant in endothelial cells, and a large proportion of the protein is phosphorylated after VEGF treatment, allowing this effect to be observed in whole cell lysate analyses. To examine less abundant proteins, it was attempted to increase protein loading on analytical gels. While this was successful to a certain extent, experiments showed that increasing protein loading beyond around 200 μg reduces spot resolution on a 2-D gel, with vertical and especially horizontal streaking of abundant proteins becoming a particular problem, often leading to distortions in the 2-D pattern. Streaking occurs as highly abundant proteins become insoluble as they are concentrated in the same position on a gel. Matching spots between gels with poor spot patterns, and overlapping spots, became a problem at higher sample loads. A similar matching problem

occurred when trying to match analytical gels, with low protein loads and good spot resolution – used to identify differences, and preparative gels with high protein loads – to give enough protein for peptide mass fingerprinting.

The gel-gel spot matching problem was reduced using DIGE, where a control and VEGF-treated sample were run in the same gel. The sensitivity of DIGE appeared similar to silver staining when comparing DIGE gels later stained with silver. Using a fluorescent imager and automated spot detection enhanced the detection of low abundance proteins. The linear dynamic range of silver staining – the range over which observed stain intensity is proportional to the amount of protein present in a resolved spot – is reported to be around 200-fold (Lopez *et al.* 2000), whereas the dynamic range of the DIGE method is limited only by the characteristics of the fluorescent scanner used, in this study quoted by the manufacturer as 100,000-fold although lower than this in practice. The improved staining proportionality inherent in fluorescence-based methods allowed smaller differences in protein expression to be determined when compared to manual visual examination of separate silver-stained gels. However, between-gel spot matching is still required to compare replicate samples, and the spots still needed to be silver stained and matched to the scanned fluorescent image to allow picking of the spots for MS-based identification.

Even when using the DIGE method to analyse whole-cell lysates, the number of proteins identified as different between control and VEGF-treated samples was lower than expected when compared to published literature, and the average total number of spots detected per sample was around 700.

While it is unsurprising that changes in low abundance signalling molecules were not observed, higher abundance proteins also appeared to show little change. Using whole cell lysates, 2-D electrophoresis and silver staining to analyse the effect of 24 h VEGF stimulation on HUVEC, Pawlowska *et al.* (2005) reported a number of changes in high abundance proteins such as heat shock proteins and structural proteins, and also members of the protein synthetic systems. Increased expression of both Hsp27 and SLP2 were also reported. None of these changes in protein expression were confirmed by western blotting. The difference between Pawlowska's data and

that presented here may be related to cell culture conditions used – not adequately detailed in Pawlowska's paper. Cells used for proteomic analysis in this chapter were treated at confluency, minimising the degree of cell proliferation that would occur on VEGF stimulation. Internal feedback signalling within confluent cells may have prevented upregulation of proteins involved in protein synthetic pathways, for example.

Analysis of more dynamic cell systems than confluent HUVEC cultures, such as endothelial cells migrating in response to a VEGF gradient, may have been more appropriate, although a number of the VEGF-induced changes would have been in lower abundance signalling proteins. Bohman *et al.* (2005) studied immortalised endothelial cells undergoing VEGF-induced tubulogenesis within a collagen I matrix. Cells were retrieved from the gel using collagenase, with inhibitors of protein synthesis, proteolysis, and protein phosphatases to fix the cell state, and whole cell extracts were analysed by 2-D electrophoresis and fluorescent staining. Over 120 proteins were observed to change during tubulogenesis, a number of which were involved in cytoskeletal regulation and metabolism, which the authors attributed to the elongation of the endothelial cells as they form tubes. Hsp27 protein expression was reported to be downregulated after 16 h exposure to VEGF during tubulogenesis, and this was confirmed by western blotting. Comparing the Hsp27 results with those of Pawlowska *et al.* (2005) indicates that the expression of Hsp27, and probably many other proteins, in response to VEGF treatment is dependent on the cell culture system used.

Some proteins have been reported to undergo a large percentage increase in phosphorylation after VEGF stimulation – ERK phosphorylation has been reported to increase 5-fold (Gliki *et al.* 2001) – suggesting that a spot corresponding to the phosphorylated form of this protein should be observed on a 2-D gel and increase by a similar amount. The highest observed percentage increase in any protein spot using the DIGE method was less than 50%, suggesting that known changes (e.g. in phosphorylation of some proteins) were not being observed. This is probably due to low protein abundance, where even the DIGE method was insufficiently sensitive to detect these

proteins in a separated whole cell lysate. Only a small proportion of a cellular protein is usually phosphorylated after growth factor stimulation, with the result that the phosphorylated form is too low in abundance to observe, whereas reproducibility of the experiment is insufficient to detect the small percentage decrease in the unphosphorylated form of the protein. Again, the apparently large proportion of Hsp27 that is converted to the phosphorylated form was unusual and aided detection of this change.

Development of a cost-effective, reproducible, quantitative, MS-compatible staining technique with substantially improved sensitivity would certainly aid 2-D gel-based analyses of cell signalling. However, even if such a stain was available, it is likely that the spot pattern given by whole-cell lysates would be extremely complex, with many spots overlapping, requiring specific proteome fractions to be examined to simplify the 2-D spot pattern.

Variants of the pre-fractionation approach employed in this chapter, using anti-pY immunoprecipitation to isolate likely proteins of interest, have been used before to successfully analyse tyrosine phosphorylation occurring on epidermal growth factor (EGF) stimulation of HeLa cells (Pandey *et al.* 2000a; Steen *et al.* 2002) and to profile pY-containing proteins in cancer cells (Rush *et al.* 2005).

Tyrosine-phosphorylated proteins were immunoprecipitated, but when analysed on a 2-D gel and detected by silver staining, no differences were apparent between IPs from VEGF-treated and control cells. The absence of some proteins, such as the VEGF receptors, can be attributed to the known problems in analysing membrane proteins on 2-D gels – lysis buffers compatible with isoelectric focusing are often insufficiently harsh to solublise hydrophobic proteins. Common ionic detergents used in cell lysis buffers such as SDS and deoxycholate are incompatible with IEF and lead to heavy streaking of the spot pattern – only weaker non-ionic or zwitterionic detergents can be used, which are not as efficient as solublising transmembrane and other hydrophobic proteins (Rabilloud *et al.* 1997).

However, a number of proteins usually resident in the cytosol and known to be tyrosine phos-

phorylated in response to VEGF, such as mitogen-activated protein kinases, were not observed in 2-D-separated pY IPs, and despite clear differences in the degree of protein tyrosine phosphorylation observed in 1-D anti-pY blots of anti-pY IPs after 5 and 20 mins VEGF treatment, no obvious difference was observed in the intensity of spots in these same samples when analysed by 2-D electrophoresis.

Insufficient starting quantities of protein could have been a problem, as tyrosine phosphorylation is relatively rare compared to phosphorylation of serine and threonine. Olsen *et al.* (2006) reported that pY accounted for less than 2% of phosphorylated residues in EGF-stimulated HeLa cells. Six 15 cm dishes of cells (around 6 x 10^7 cells) were used for each 2-D-separated pY IP. This is comparable to other proteomic studies analysing pY immunoprecipitates by silver staining: Pandey *et al.* (2000a) used 5 x 10^9 suspension cells/sample, but Steen *et al.* (2002) used 1 x 10^8 adherent cells/sample, similar to my work.

Judging by silver stained gels, the vast majority of protein present in anti-pY IPs was the immunoprecipitating antibody. The number of cells used for immunoprecipitation could have been increased to get more protein onto the gel, but the presence of larger quantities of immunoprecipitating antibody in the IP would have led to major problems with streaking – this was observed when larger quantities of antibodies were used in a trial experiment (data not shown). The dominance of the immunoprecipitating antibody in the protein composition of the IP could be reduced by improved titering of the antibody – using just enough antibody required to IP the maximum amount pY proteins from the VEGF-treated cells.

Both Pandey *et al.* (2000a) and Steen *et al.* (2002) used a beads-conjugated pY antibody for immunoprecipitation, preventing contamination of the immunoprecipitate with antibody, with Steen additionally using the pY mimic phenyl phosphate to elute the IPed proteins from the antibody, which helped to ensure the pY dependence of the antigen-antibody interaction. Both studies used two different anti-pY antibodies to improve precipitation of pY-containing proteins, separated the resultant IPs using 1-D electrophoresis and silver stained the gels to detect proteins. In my hands,

in trial experiments an agarose-conjugated anti-pY antibody recovered less protein when compared to an unconjugated antibody when eluting directly with 2-D lysis buffer (data not shown), possibly due to incomplete elution of proteins from the IPing antibody, and so the unconjugated antibody approach was adopted. Other lysis buffers were avoided to prevent introduction of variability and protein losses from the precipitation/resuspension procedure that would be required to transfer the proteins to 2-D compatible buffers.

As the major problem was lack of pY-containing proteins being detected by silver staining, and not excess proteins causing overlapping spots, it may have been advantageous to use more cells, a conjugated antibody, eluted by heating in SDS-PAGE sample buffer, and separating IPs using 1-D gels. This approach may also have circumvented other known problems of 2-D gels such as insolubility of hydrophobic proteins and poor separation of large proteins, such that tyrosine phosphorylation of the VEGF receptors may have been observed. The ability to distinguish between multiple forms of the same protein, e.g. mono- and di-phosphorylated forms, would have been lost.

Using silver staining to detect pY IPed proteins may reduce the apparent effect of VEGF on the amount of protein present in 2-D-separated pY IPs when compared to control IPs. The spot pattern on distinct 2-D gels tended to develop at slightly different rates, probably due to differences in the contact individual gels had with the various staining solutions, and so required different amounts of time in developing solution to achieve an acceptable spot pattern. It is possible that control gels, having less immunoprecipitated protein present on them, were developed for longer than gels containing VEGF-treated samples, thus giving the false impression that similar amounts of protein were present in pY IPs from control and VEGF-treated cells. This would not be an issue using 1-D analysis of pY IPs, where separate samples are run on the same gel.

Using DIGE technology rather than silver staining to analyse pY immunoprecipitates on may improve detection of minor treatment-induced differences in tyrosine phosphorylation. However the DIGE normalisation method, which corrects for differences in the fluorescence intensity of

the two (or more) dyes used, assumes the majority of protein spots in each sample are of equal abundance, and corrects the fluorescence intensity of each dye to make this so. With drastically different protein samples, such as might be expected in VEGF-treated and control pY IPs, this would be invalid and would distort the results.

Gel and staining issues can be circumvented entirely by separating proteins using chromatographic techniques such as high performance liquid chromatography (HPLC), allowing large protein loads and dilute samples to be analysed with on-line protein identification. Coupling 2-D chromatography (charge-based separation via strong cation exchange, followed by hydrophobicity-based separation of these fractions via reversed phase chromatography) with an electrospray ionisation tandem mass spectrometer (ESI-MS/MS), in the LC-MS/MS configuration, allows proteins eluted off the column to be automatically identified (Link *et al.* 1999). This procedure has been used to identify almost 1500 proteins in yeast in a complex mixture (Washburn *et al.* 2001), but does not provide any quantitative information regarding protein expression.

With the advancement of mass spectrometry, development of isotope-based techniques now allow labelling of different samples, with either a heavy or a light variant, before mixing and analysis of the samples in the same LC-MS/MS run – a similar strategy to DIGE labelling for gel-based analyses (reviewed by Ong and Mann 2005). Quantification is based on the proportionality of a particular peptide-derived MS peak to the amount of peptide present in the analysed mixture. Three major strategies that have been employed are termed isotope-coded affinity tag (ICAT, Gygi *et al.* 1999a), stable isotope labelling by amino acids in cell culture (SILAC, Ong *et al.* 2002), and isobaric tag for relative and absolute quantification (ITRAQ, Ross *et al.* 2004).

The original ICAT reagents included a biotin group, either a heavy or light linker (8 Da difference in molecular weight due to deuterium/hydrogen differences), and a iodine-containing thiol-reactive group to bind cysteine residues. Two protein mixtures for comparison are labelled with either heavy or light ICAT reagent, the samples are then pooled and digested to peptides. Labelled peptides are isolated via the biotin group using an avidin column, and then separated and identified

by LC-MS/MS. The biotin-avidin capture method has been changed in other variants of the ICAT technique. Due to the small difference in mass, differently labelled peptides co-elute from the chromatography stage, and the ratio of that peptide (and therefore protein) in the original samples is determined by the size of the peptide peak produced during the first MS stage. The identity of the protein is determined by producing a peptide sequence tag using the MS/MS stage.

The SILAC strategy uses media deficient in a particular essential (i.e. media-derived) amino acid for cell growth. The media is supplemented with isotopically distinct versions of the absent amino acid, such that cells grown in the medium will incorporate the included isotope variant of the supplemented amino acid. Variation of amino acids in this way was reported not to influence tested cell behaviours such as proliferation. Protein samples were produced and separated by 1-D electrophoresis. Bands of interest were digested to peptides, and quantified by tandem MS. Quantification occurs at the first MS stage, as for ICAT. LC-MS/MS could be used rather than 1-D gels, band excision and MS/MS. The SILAC method avoids the need for the labelling and purification techniques used in ICAT, is not limited to cysteine-containing peptides (Ong *et al.* 2002 used deuterated leucine, although other amino acids could be used, perhaps in combinations, or a single amino acid but multiple isotopic variants), but is only suitable for cultured cells.

ITRAQ reagents consist of an amine-reactive group (NHS ester, same as used in DIGE), a balance group and a reporter group. The reporter group of distinct ITRAQ reagents varies in mass, but the balance group also varies in mass such that the overall mass of all ITRAQ reagents is identical. Labelling and separation is similar to ICAT – peptides are labelled on lysine or N-terminal amine groups with a particular ITRAQ reagent, and are separated and initially analysed by LC-MS. Unlike ICAT and SILAC, labelled peptides corresponding to different experimental groups produce seemingly identical ions in the first MS stage. Ions are then sent for fragmentation and analysis in the second MS stage. On fragmentation, ITRAQ-labelled peptides yield the original unmodified peptide, which is used for identification of the protein, the reporter group, and the balance group. The reporter groups from the distinct peptides, which have split from their balance group, now

have different masses to each other, are resolved in the MS/MS spectrum and can be used for quantification. At the time of writing, at least four distinct ITRAQ reagents were available.

ICAT, SILAC and ITRAQ can all be coupled to an LC-MS/MS separation and quantification approach and can be automated, allowing large scale quantification of many proteins in a sample. The SILAC method additionally avoids bias introduced by differences in labelling efficiency between samples. Lower abundance proteins are more likely to be observed using MS-based quantification rather than 2-D gels. Despite these advantages, all MS-based quantification methods suffer from certain drawbacks. Expensive equipment and expertise is necessary for successful analysis of complex protein mixtures. A major issue is that any unlabelled peptides, or peptides that are too hydrophobic or don't ionise well will be invisible to MS-based quantitative methods. Leucine-based SILAC and cysteine-based ICAT are expected to label and therefore detect around 50% and 20% of tryptic peptides respectively (Ong *et al.* 2002). Any post-translational modifications occurring in the region of a protein covered by an undetectable peptide will not be observed. In contrast, the position of a spot on a 2-D gel is based on the entire sequence of the protein, and so a modification anywhere in the protein will be resolved if the molecular weight or pI are sufficiently altered. Resolution on a 2-D gel often gives a pure protein, allowing less advanced (therefore cheaper and more available) mass spectrometers to be used for protein identification.

In addition to MS-based examinations of the proteome, antibody arrays are an emerging technique for examining changes in protein expression and modification. Antibody arrays (reviewed by Spisak *et al.* 2007), consisting of immobilised antibodies directed against a large number of proteins, are effectively a simultaneous immunoblot for a number of proteins of interest. This method may be useful for profiling the effect of a particular event such as cytokine/receptor interaction on a number of known signalling pathways and cellular systems, and has been used to examine protein phosphorylation (Gembitsky *et al.* 2004). However, the number of antibodies included in such an array is relatively small at around 200, and due to this limitation it is less that entirely novel findings will result as the antibodies present on the chip will be determined by the expected

results. The recognition of non-target proteins by such a large number of antibodies is also an unresolved problem with this emerging technology.

As discussed above, one of the major problems in proteomics is the ability to analyse low abundance proteins. Due to their repetitive structure and the availability of amplification techniques such as PCR, nucleic acids are far more amenable to analysis than proteins, and microarrays have been well used to examine changes in gene expression. Analysis of VEGF-induced changes in the endothelial expression of approx 18,000 genes were analysed in this laboratory using microarray technology (Liu *et al.* 2003). However, it is well established that changes in gene expression correlate poorly with changes in protein expression, probably due to differences in protein turnover, and variation in the importance of post-transcriptional control of protein expression (Gygi *et al.* 1999b, reviewed by Greenbaum *et al.* 2003). Proteins are the key effectors of the cell, and it is their expression that is important. Therefore any microarray hit must be followed up with western blotting to examine the effect on protein levels. Similarly, the absence of a microarray hit does not mean that the expression of that protein was not affected by the experimental condition. Importantly, microarrays will give no information on post-translational modifications occurring to proteins, such as protein phosphorylation, which can have a major impact on protein and cell function.

Proteomics directly examines protein levels, is able to detect activity-altering effects such as post-translational modifications and, via immunoprecipitation, protein-protein interactions, and can be used to specifically study defined cellular compartments such as the proteins present in a specific organelle.

The sheer number of expressed proteins, and their multiple post-translationally modified variants, is a major challenge for all proteomic strategies. For signalling studies, protein phosphorylation is an important post-translational modification, leading to changes in the activity or interactions of the affected protein, with subsequent effects on cellular behaviour. Characterisation of how protein phosphorylation changes in response to a stimulus such as VEGF administration would probably

give new insights into the signalling pathways involved. Purification of phospho-proteins would retain proteins of interest while simplifying the subset of proteins to be analysed.

As discussed above, while antibody-based approaches have been successful for purification of pY-containing proteins, the majority of protein phosphorylations occur on serine and, to a lesser degree, threonine. Other strategies for purification of pS and pT-containing proteins include metal affinity columns and chemical modification of phosphate groups.

Oda *et al.* (2001) chemically replaced phosphate groups in peptides with a thiol-containing group, which was then coupled to biotin. Avidin-based affinity chromatography was then used to purify biotinylated peptides, which were identified by MS/MS. Zhou *et al.* (2001) chemically modified each phosphate group to include a thiol group, which was then used for phospho (thio) peptide purification based on binding to an iodoacetyl-containing resin – a similar reaction to thiol modification after IEF by reaction with iodoacetamide. The thiol group was then chemically removed, regenerating the phosphate group. The protein mixture had previously been been alkylated with iodoacetamide to prevent cysteine-based purification. Both of these methods require multi-step chemical reactions which may not go to completion and may produce undesirable side reactions. The Oda biotin method produced less clear MS spectra than was obtained from non-biotinylated peptides and could not purify pY-containing peptides, whereas the Zhou reversible method recovered only 20% of the available phosphopeptides. Clearly it is important that phospho-peptide recovery is quantitative when comparing two samples.

Immobilised metal affinity chromatography (IMAC) has been used for some time to purify phosphopeptides from a protein digest, based on the binding of the negatively-charged phosphate group to positively-charged metal ions such as Fe^{3+} in the column (Andersson and Porath 1986). However, other non-phosphorylated negatively-charged peptides (such as those containing Asp or Glu) also bind to the column. Indeed all peptides contain a negatively-charged carboxyl group at their C-terminus. Ficarro *et al.* (2002) improved the IMAC strategy by reacting tryptic peptides with methanol to produce methyl esters, thus removing the charge on carboxyl groups. This approach

was reported to produce a large increase in the specificity of the IMAC method.

The specificity of the IMAC approach was enhanced by using titanium dioxide rather than the original Fe^{3+} as the affinity medium (Larsen *et al.* 2005). In a comprehensive study, Olsen *et al.* (2006) combined SILAC, phosphopeptide enrichment via TiO_2 columns, multi-dimensional chromatography and on-line tandem MS to determine the temporal phosphorylation of 6600 phosphorylation sites on more than 2000 proteins in response to EGF stimulation of HeLa cells, illustrating the power of this multi-faceted approach.

In summary, in addition to improved identification and quantification of differences in lower abundance proteins, and selective purification of important protein subsets such as phosphoproteins, the analysis of dynamic cell systems such as endothelial cells migrating in response to a VEGF gradient can be expected to yield significant insights in the signalling pathways activated by VEGF stimulation of endothelial cells.

Chapter 4

Results: VEGF regulation of Hsp27 phosphorylation

Analysis of VEGF signalling in HUVECs by 2-D electrophoresis led to the identification of a shift in Hsp27 from a more basic to a more acidic form, consistent with phosphorylation, after 10 mins treatment (figure 3.2). The fact that this shift was the major observable change noticed during short-term VEGF treatments aimed at investigating early signalling events indicated that Hsp27 was likely to be a major target of early responses to VEGF, and prompted investigation into its role in VEGF signalling and biological functions. This chapter describes studies intended to delineate the mechanisms involved in VEGF regulation of Hsp27 phosphorylation, chapter 5 describes studies into the role of Hsp27 in endothelial cell responses to VEGF.

4.1 Initial characterisation of VEGF-stimulated Hsp27 phosphorylation

4.1.1 VEGF stimulates phosphorylation of Hsp27 at serine residues 15, 78 and 82

Hsp27 had previously been reported to be phosphorylated at S15, S78 and S82 via the p38 MAPK pathway (discussed in section 1.5.3). Initial experiments were performed to characterise VEGF-

stimulated Hsp27 phosphorylation in the cell system used in this study, and to identify which sites are phosphorylated.

Using antibodies directed specifically to the various phosphorylation sites of Hsp27 it was determined that, in confluent serum-deprived HUVEC cultures, VEGF induces phosphorylation of Hsp27 at S15, S78 and S82 (figure 4.1). Treatment of cells with 25 ng/ml VEGF for different times, and for 10 mins at different concentrations, indicated that maximal Hsp27 phosphorylation was obtained 10–20 mins after VEGF addition, and with 5–100 ng/ml VEGF (figures 4.1 and 4.2). Unless stated, a VEGF concentration of 25 ng/ml was used for the remainder of the study, previously used in this and other laboratories to produce biological effects in endothelial cells, including HUVECs (for example, Gliki *et al.* 2001; Jia *et al.* 2004). This concentration of VEGF stimulated strong phosphorylation of the activation loop residues of protein kinase D (discussed in section 4.4) and p38 MAPK (figure 4.2).

SU5614, an inhibitor of VEGFR2 tyrosine kinase activity, reduced the VEGF-stimulated phosphorylation of Hsp27 at S15 and S82, and of PKD at S738/742 and S910, whereas H_2O_2-stimulated phosphorylation of Hsp27 was unaffected (figure 4.3), indicating that VEGF-stimulated phosphorylation of Hsp27 and PKD is likely to occur via VEGFR2.

4.1.2 2-D pattern of Hsp27 phospho-forms

2-D-separated lysates from HUVECs treated with VEGF for 10 mins showed a marked increase in the abundance of an acidic form of Hsp27, presumably a phosphorylated form (figure 3.2). Three approaches were used to determine what this acidic form of Hsp27 actually was – direct analysis of immunoprecipitated Hsp27 by tandem mass spectrometry, removal of phosphate from immunoprecipitated Hsp27 with alkaline phosphatase, and 2-D analysis of Hsp27 using phospho-specific antibodies.

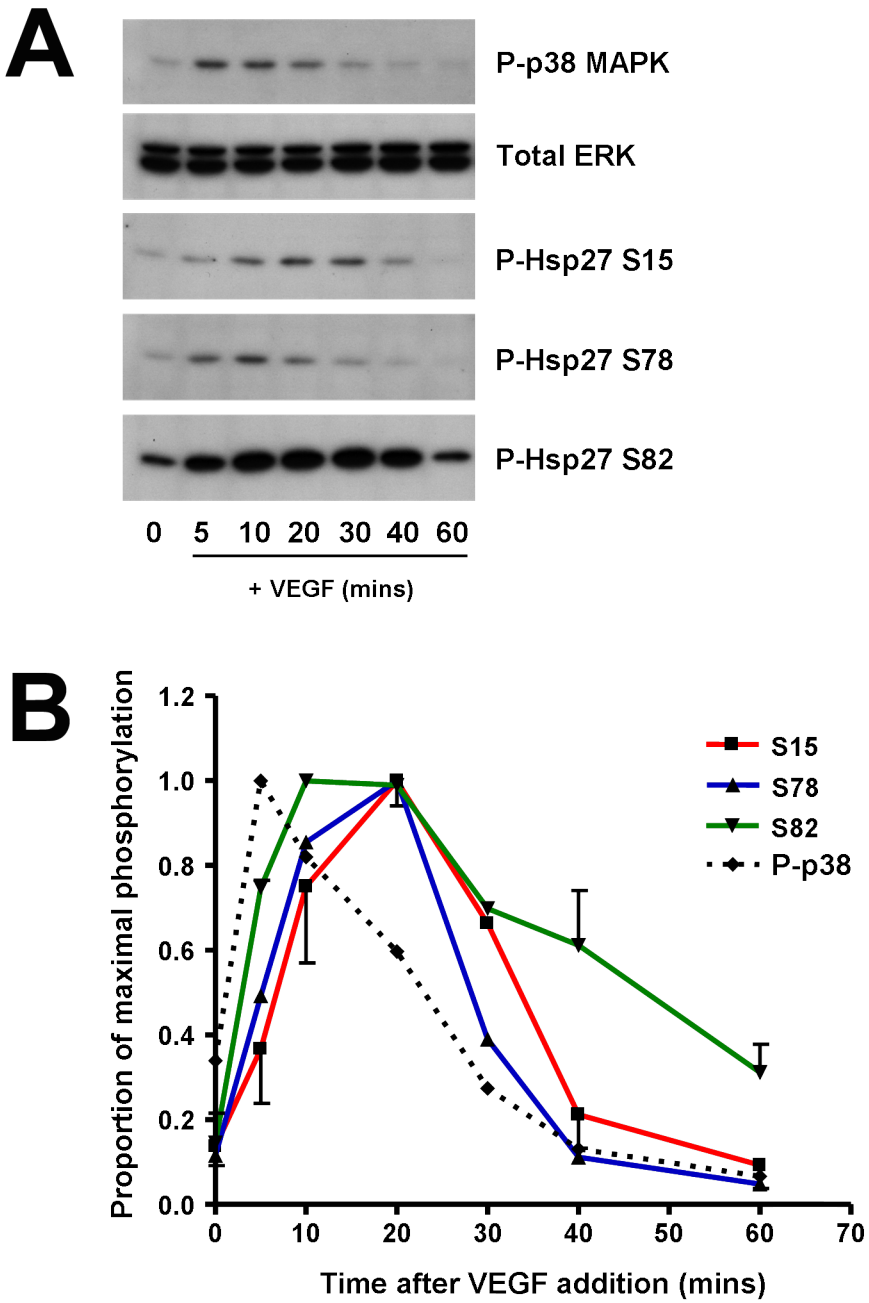

Figure 4.1: Time course of VEGF-induced Hsp27 phosphorylation
A. Confluent, serum-deprived HUVECs were treated with 25 ng/ml VEGF for the indicated times before lysis. Samples were then immunoblotted and probed with phospho-specific antibodies to the S15, S78 and S82 phosphorylations of Hsp27, phospho-p38 MAPK and phospho-ERK.
B. Quantification of band intensities from time course blots from (A). P-S15 and P-S82 data are means of three independent experiments, and error bars (SEM) are shown. P-S78 and P-p38 data are means of two independent experiments, error bars are not shown.

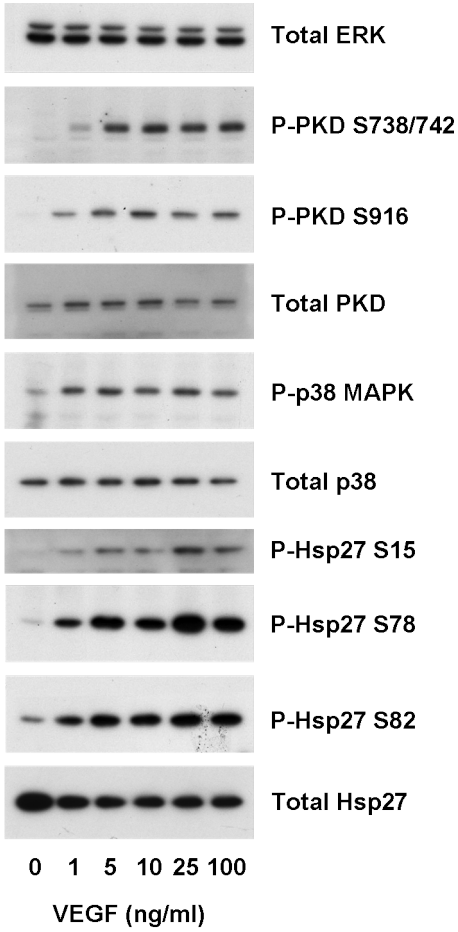

Figure 4.2: Effect of varying VEGF dose on phosphorylation of Hsp27, PKD and p38 MAPK
Serum-deprived, confluent HUVECs were treated for 15 mins with the indicated concentration of VEGF. Cells were then lysed, and samples were immunoblotted with the indicated antibodies. Results are representative of three independent experiments for P-S82, and two experiments for P-S15, P-S78, P-p38, and PKD P-S738/742 and P-S916.

4.1.2.1 Analysis of Hsp27 immunoprecipitates with tandem mass spectrometry

Hsp27 could be specifically immunoprecipitated from HUVEC lysates (figure 4.4), allowing further analysis of purified Hsp27 by subsequent procedures.

Hsp27 was immunoprecipitated from VEGF-treated HUVECs and separated on 2-D gels and both the acidic and basic spots (migrating similarly to spots A and B in figure 3.2A) were analysed by tandem mass spectrometry, a technique capable of identifying post-translational modifications. The tryptic peptides obtained, and the majority phosphorylation status, are indicated in figure 4.5A and B. Example tandem MS spectra for the peptide including the S82 residue are shown in figure 4.5C.

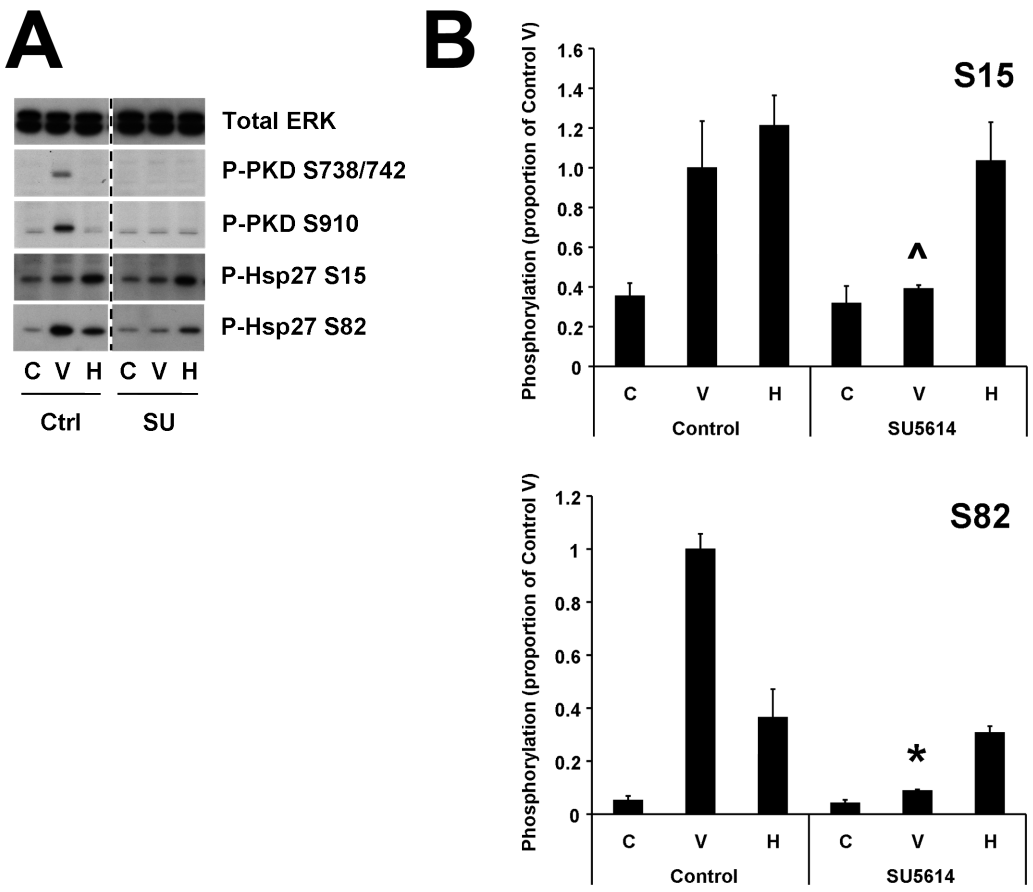

Figure 4.3: VEGF-stimulated phosphorylation of Hsp27 and PKD is inhibited by the VEGFR2 kinase inhibitor SU5614

A. Confluent, serum-deprived HUVECS were pre-incubated with either 5 μM SU5614 (SU) or solvent alone (0.1% DMSO, Ctrl) for 30 mins followed by 15 mins treatment with 25 ng/ml VEGF (V), 100 μM H_2O_2 (H), or no addition (C). Cells were then lysed, blotted, and probed with the indciated antibodies. The dotted line indicates that the Ctrl and SU samples, which were produced in the same experiment, were on separate membranes but blotted, probed and developed at the same time.

B. Quantification of the effect of SU5614 on phosphorylation of Hsp27 at S15 and S82. Values are given as a proportion of the phosphorylation in the Control V sample, and are means $\pm$ SEM from three independent experiments. Results were assessed by two-way ANOVA with differences located by Bonferroni's test for multiple comparisons. ^ significantly reduced compared to Control/VEGF ($p<0.05$). * significantly reduced compared to Control/VEGF ($p<0.001$).

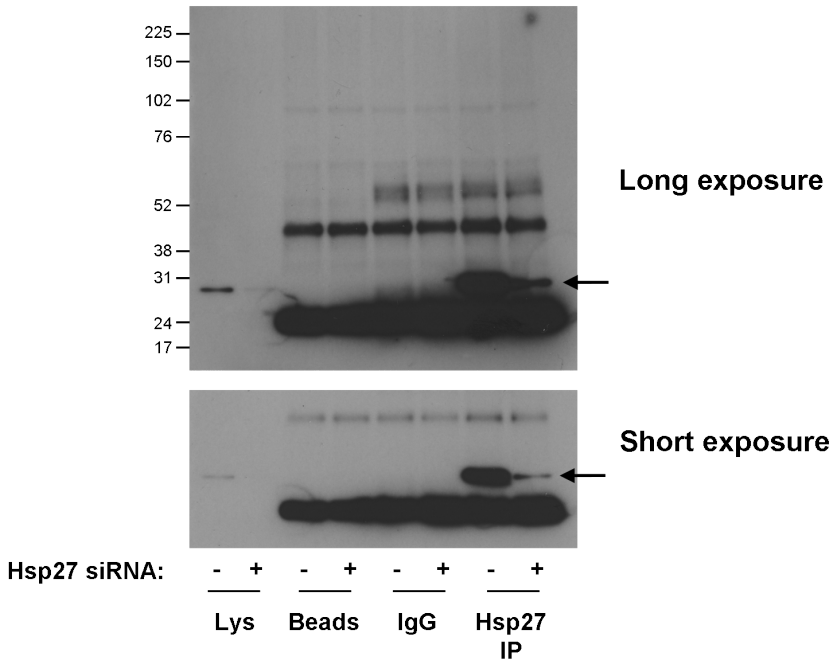

Figure 4.4: Hsp27 can be immunoprecipitated from HUVECs
HUVECs were treated for 48 h with anti-Hsp27 siRNA (+) or a control siRNA (-), and Hsp27 was immunoprecipitated. IPs were analysed by immunoblotting using a total Hsp27 antibody. Lys, lysate; Beads, Protein A/G beads only (no immunoprecipitating antibody); IgG, control rabbit IgG. Lysate loaded was a small proportion of the input lysate used in the immunoprecipitations. Arrows indicate expected Hsp27 band. Data is from a single experiment.

Multiple instances of the same S82-containing tryptic peptide were identified from both spot A and spot B. In spot A, the S82 residue was phosphorylated in 5 out of 7 instances, whereas in spot B the S82 residue was phosphorylated in 1 out of 17 instances. Multiple instances of an S15-containing tryptic peptide were also identified from spots A and B. In spot A, the S15 residue was phosphorylated in 0 out of 6 instances, and in spot B the S15 residue was phosphorylated in 0 out of 6 instances. The presence of phosphate at S78 could not be determined as tryptic peptides covering this residue were not identified. No other phosphorylated peptides, or other post-translational modifications, were identified from either spot. MS analysis of Hsp27 therefore indicated that the acidic spot (A) was phosphorylated on S82 but not S15, whereas the basic spot was unphosphorylated on both S82 and S15.

A

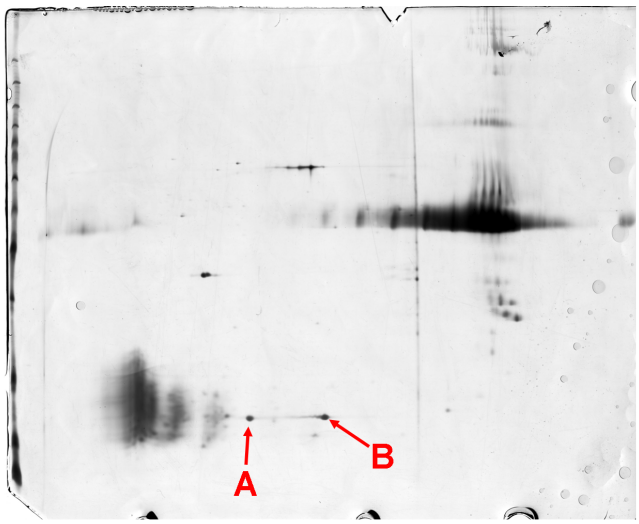

B

Spot A: Hsp27 phosphorylated at S82

MTER (RVPFSLLR) (GPSWDPFR) (DWYPHSR) (LFDQAFGLPR) LPEEWSQ
WLGGSSWPGYVRPLPPAAIESPAVAAPAYSRALSR (QLS*SGVSEIR) HTAD
RWR (VSLDVNHFAPDELTVK) (TKDGVVEITGK) HEERQDEHGYISRCFTR
(KYTLPPGVDPTQVSSSLSPEGTLTVEAPMPK) (LATQSNEITIPVTFESR)
(AQLGGPEAAK) SDETAAK

Spot B: Hsp27 unphosphorylated

MTER (RVPFSLLR) (GPSWDPFR) (DWYPHSR) (LFDQAFGLPR) (LPEEWSQ
WLGGSSWPGYVRPLPPAAIESPAVAAPAYSR) ALSR (QLS*SGVSEIR) HTAD
RWR (VSLDVNHFAPDELTVK) (TK (DGVVEITGK) HEER) QDEHGYISRCFTR
(K (YTLPPGVDPTQVSSSLSPEGTLTVEAPMPK) (LATQSNEITIPVTFESR)
(AQLGGPEAAK) SDETAAK

Figure 4.5: Hsp27 peptides identified via tandem mass spectrometry indicate the acidic form contains a phosphorylation at S82 (continued overleaf)

A. HUVECs were treated with VEGF for 15 mins, after which Hsp27 was immunoprecipitated. The IP was separated by 2-D electrophoresis and gels were silver stained. Two spots (A and B) were observed displaying the expected pattern for phosphorylated Hsp27 as previously observed in 2-D western blots and other immunoprecipitates, and corresponded to spots A and B from figure 3.2.

B. Spots A and B from part A were excised from the gel, digested with trypsin and analysed by tandem mass spectrometry. The identified peptides are enclosed in brackets and underlined, and are shown in the context of their position in the human Hsp27 protein reference sequence (Refseq accession NP_001531.1). S15, S78 and S82 are highlighted in red, and S82 is additionally indicated with an asterisk (*). The peptide containing S82 was phosphorylated in spot A and unphosphorylated in spot B.

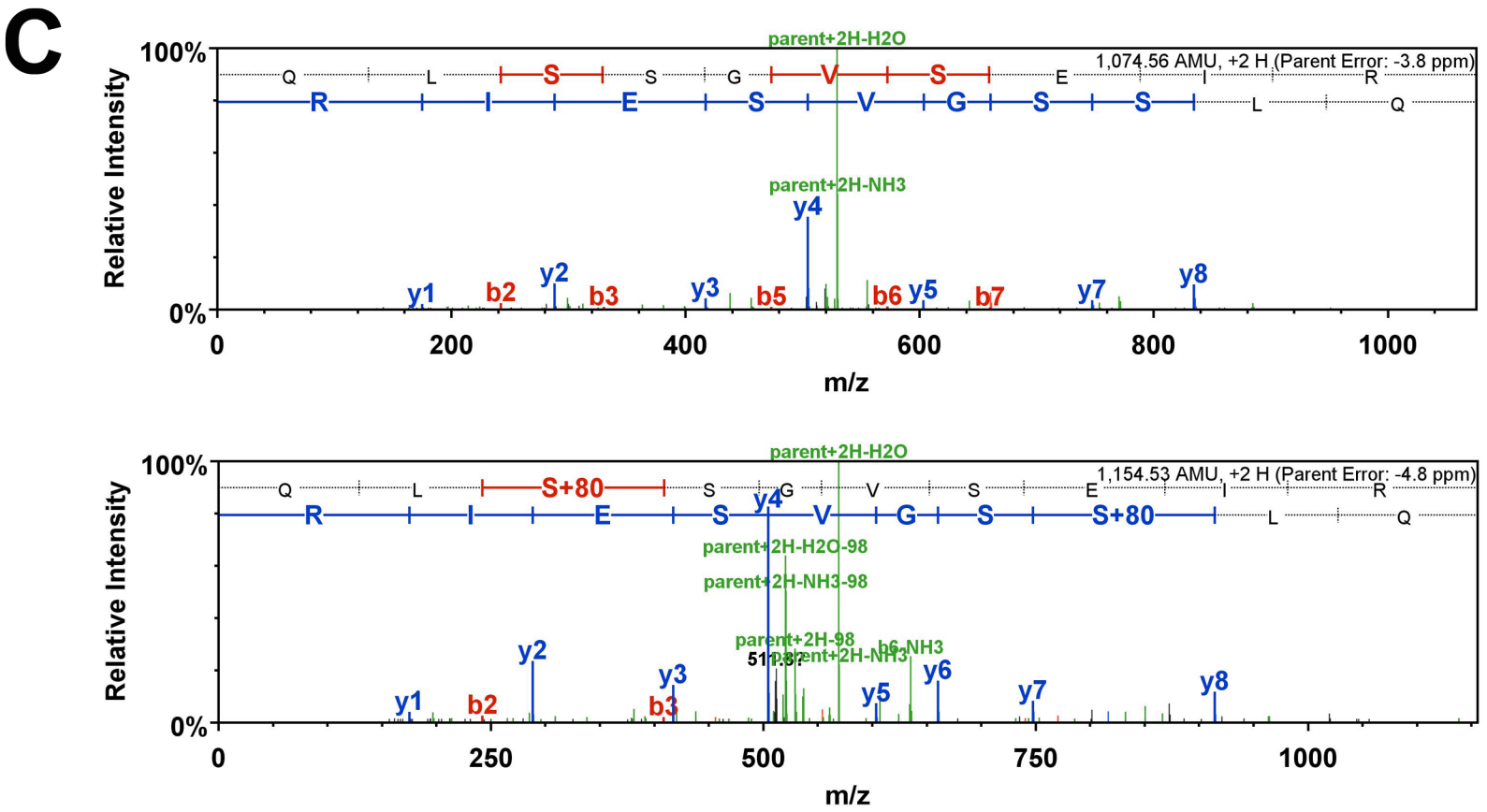

Figure 4.5: Hsp27 peptides identified via tandem mass spectrometry indicate the acidic form contains a phosphorylation at S82 (continued)

C. Tandem MS data output showing b- and y-ion series for the peptide QL$\underline{S}$SGVSEIR, identified in spot A (upper figure) and spot B (lower figure). To produce the b- and y-ion series, fragmentation occurs at the peptide bond with the charge being retained on N-terminal fragment for b-ions, and on the C-terminal fragment for y-ions. The mass difference corresponding to S82 is shown as b2–b3 or y7–y8. In spot A, S82 was identified as unphosphorylated by both b- and y-ion series, whereas in spot B S82 was identified as phosphorylated (+80 Da) by both the b- and y-ion series.

4.1.2.2 2-D analysis of Hsp27 immunoprecipitates with alkaline phosphatase treatment

While useful for determining specific phosphorylation sites, the tandem MS approach was unable to determine the presence of phosphate throughout the entire Hsp27 protein as the S78 phosphorylation site was not covered by identified tryptic peptides. Additionally, phosphate-containing peptides are often difficult to detect via MS-based methods, and the phosphate groups may be unintentionally lost during peptide fragmentation resulting in detection of an unphosphorylated peptide. To address these issues, alkaline phosphatase (AP) was used to remove phosphate groups from Ser, Thr and Tyr residues of proteins in Hsp27 immunoprecipitates. Phosphorylation results in an increase in the acidity of a protein, and treatment of a protein with AP should therefore reduce the acidity (increase the pI) of a protein that is already phosphorylated, without affecting the pI of an unphosphorylated protein. To discern whether a shift had actually occurred, samples treated with and without AP were run on separate 2-D gels and also in the same gel (figure 4.6).

In Hsp27 IPs from VEGF-treated cells, AP treatment eliminated Hsp27 phosphorylation at S78 and S82 as assessed by western blotting with a phospho-specific antibody (figure 4.6A). When analysed by 2-D electrophoresis, immunoprecipitated Hsp27 was present as two major spots. After AP treatment, IPed Hsp27 was present as a single spot, presumably representing unphosphorylated Hsp27, which had the same pI as the more basic spot from non-AP-treated Hsp27 IPs as indicated by the larger size of the basic spot but not the acidic spot in the blot of the mixed samples compared to the blot of non-AP-treated Hsp27 (figure 4.6B). Thus AP treatment did not affect the pI of the basic spot, indicating that this form is likely to be unphosphorylated, but increased the pI of the acidic spot to the same as that of the basic spot, indicating that the acidic form is phosphorylated.

4.1.2.3 2-D analysis of whole cell lysates using anti-Hsp27 phospho-specific antibodies

Western blotting data indicated that Hsp27 is phosphorylated at three different sites in response to VEGF treatment (figures 4.1, 4.2 and 4.3). To determine the relative abundance of the different phosphorylations produced, extracts of cells exposed to VEGF for 15 mins were analysed by 2-D

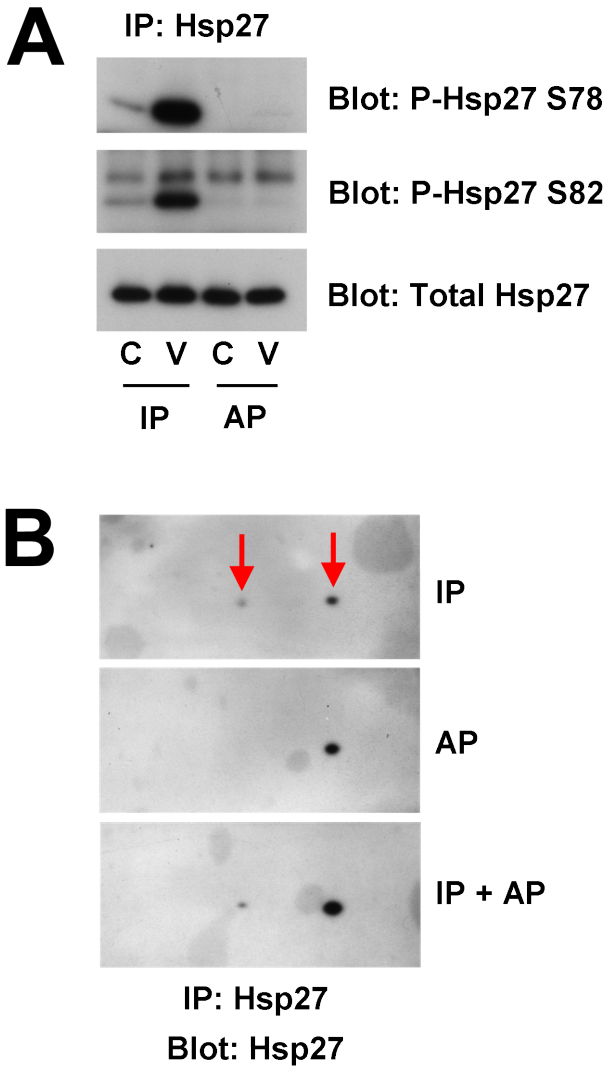

Figure 4.6: Effect of alkaline phosphatase treatment on 2-D spot pattern of an Hsp27 immunoprecipitate

Hsp27 was immunoprecipitated from confluent HUVECs treated for 15 mins with 25 ng/ml VEGF (V) or no addition (C) . The IPs were resuspended and divided into three aliquots. One aliquot (AP) was mixed with alkaline phosphatase to remove phosphate groups before quenching with concentrated SDS-PAGE buffer, whereas another remained on ice after immunoprecipitation before mixing with SDS-PAGE buffer (IP). The samples were then analysed as detailed below:

A. IPs were separated by 1-D electrophoresis, blotted and probed with the indicated antibodies. Representative of four independent experiments.

B. IPs from VEGF-treated cells were precipitated and resuspended in 2-D buffer, proteins were separated by 2-D electrophoresis, blotted and probed with the indicated antibodies. IP, Immunoprecipitate only; AP, alkaline phosphatase (AP)-treated immunoprecipitate only; IP + AP, both AP-treated and untreated immunoprecipitates were mixed and run on the same 2-D gel. The position of the two major Hsp27 species present are indicated. Data is representative of two independent experiments.

electrophoresis and probed with phospho-specific antibodies to Hsp27 (figure 4.7). Blots with total Hsp27 antibodies reproduced the pattern observed by staining 2-D gels (compare figure 3.2A with figure 4.7), but an additional acidic, low abundance spot, marked X, was observed after VEGF treatment.

None of the phospho-specific antibodies reacted with the basic spot B, consistent with it being unphosphorylated Hsp27. The major form of Hsp27 produced after 15 mins VEGF treatment, labelled A, co-migrated with the major phospho-S82-reactive spot, whereas the minor form of Hsp27 produced after VEGF treatment, labelled X, co-migrated with the major phospho-S78-reactive spot.

Due to the lack of S15 data, it was not possible using the results in figure 4.7 to determine whether the Hsp27 present in spot A was phosphorylated at S15. To address this question, HUVECs were pre-treated with the p38 MAPK inhibitor SB203580, which was observed in other experiments to dramatically reduce VEGF-induced phosphorylation at S15 and S78 but not S82 (described in section 4.2 and thereafter). SB203580 treatment did not alter the pI of the acidic form of Hsp27 present in lysates of VEGF-treated cells, or noticeably adjust the ratio between spots A and B (figure 4.8A), despite a strong reduction in S78 phosphorylation. These data suggest that the major component of spot A is Hsp27 mono-phosphorylated at S82.

Taken together, the results presented in this section from tandem MS, alkaline phosphatase treatment and phospho-specific antibodies indicate that that Hsp27 is predominantly unphosphorylated in unstimulated cells. The major quantitative change in Hsp27 after 15 mins treatment with VEGF is phosphorylation at S82 to produce mono-phosphorylated Hsp27. Even after VEGF stimulation for 15 mins, around half of Hsp27 present in HUVECs apparently remains unphosphorylated.

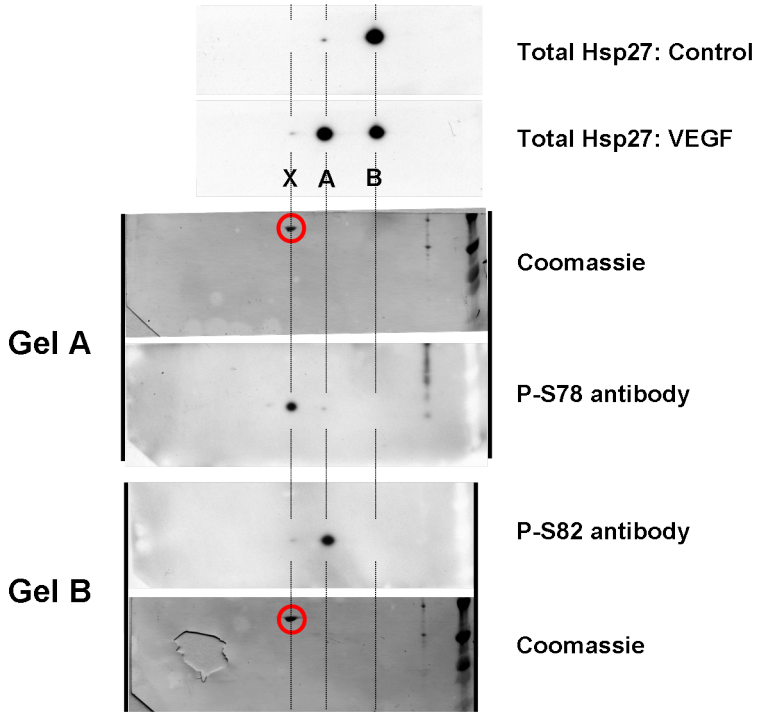

Figure 4.7: 2-D pattern of Hsp27 from VEGF-treated versus control-treated cells
Serum-deprived HUVECs were treated with 25 ng/ml VEGF or no addition (control) for 15 mins before lysis, 2-D separation using a linear pH 4–7 gradient, and immunoblotting with the indicated antibodies. An anti-phospho S15 antibody was also used but failed to produce a clean signal at the correct molecular weight. All blots are from the same VEGF-treated cell extract apart from the upper blot which is labelled control. After chemiluminescent detection, the membranes used for the S78 and S82 blots were coomassie stained and scanned. The images of the stained membranes were aligned with the corresponding blot (solid black lines along the edge of the blots and membranes), and then the strongly coomassie staining spot on the membranes (circled red) was used to align the membranes from the S78 and S82 membranes, and therefore blots, with each other. Dotted lines have been added to aid comparison between spot positions. Spots visible on the total Hsp27/VEGF-treated blot are labelled A, B, and X: A and B correspond to spots A and B observed on 2-D gels in figure 3.2, spot X was not identified from 2-D gels and is a different, more acidic form. Results are representative of two independent experiments.

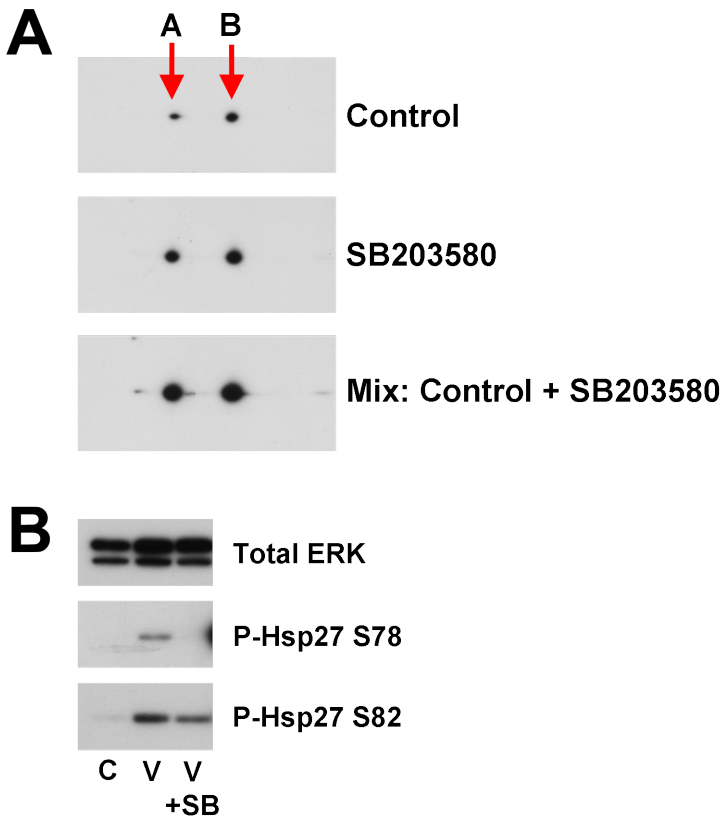

Figure 4.8: Effect of SB203580 on Hsp27 2-D spot pattern
Serum-deprived HUVECs were incubated for 30 mins with 5 μM SB203580 or solvent alone (0.1% v/v DMSO, Control), then treated with or without 25 ng/ml VEGF for 15 mins and lysed.
A. Lysates from VEGF-treated cells were separated by 2-D electrophoresis and blotted with a total Hsp27 antibody. Membranes were coomassie stained and used to align the blots as in figure 4.7. Mix indicates that the Control and SB203580 samples were mixed and run on the same 2-D gel.
B. The same lysates analysed in part (A) were immunoblotted and probed with the indicated antibodies. V+SB, SB203580 pre-treated and then VEGF-treated; V, VEGF-treated, no inhibitor; C, no inhibitor or VEGF.
Data is representative of two independent experiments.

4.2 A p38 MAPK-independent pathway contributes to VEGF-stimulated phosphorylation of Hsp27 at S82

Hsp27 has previously been reported to be phosphorylated at S15, S78 and S82 via the p38 MAPK pathway in response to various stimuli. The involvement of this pathway in VEGF-stimulated Hsp27 phosphorylation was examined using two approaches: pharmacological inhibition of p38 MAPK, and siRNA-mediated knockdown of p38α and MAPKAPK2.

4.2.1 p38 MAPK inhibition

Initially, the role of the p38 MAPK pathway in VEGF-stimulated Hsp27 phosphorylation was examined using the p38 inhibitors SB203580 and SB202190. SB203580 at 1 μM blocked phosphorylation of Hsp27 at S15 and S78, and completely prevented phosphorylation of MAPKAPK2, the downstream target of p38 MAPK reported to be responsible for directly phosphorylating Hsp27 (figure 4.9A). However S82 phosphorylation was less affected by SB203580, and doses of SB203580 up to 25 μM caused little additional inhibition (figure 4.9A). Similar experiments with a second, structurally-related pyridinyl imidazole-based inhibitor, SB202190, produced similar results. VEGF-induced phosphorylation of S82 was only partly inhibited by SB202190, whereas phosphorylation of S15 and S78 was blocked (figure 4.9B).

To determine whether the resistance of Hsp27 S82 phosphorylation to p38 MAPK inhibition was common to stimuli other than VEGF, phosphorylation induced by VEGF was compared to that induced by another p38 MAPK activator, tumour necrosis factor-α (TNFα). While VEGF-stimulated phosphorylation of S82 was only partially reduced by 5 μM SB203580 or SB202190, S82 phosphorylation induced by 100 U/ml TNFα was fully inhibited (figure 4.10A).

VEGF was then compared with a variety of stimuli previously demonstrated to induce Hsp27 phosphorylation: hydrogen peroxide (H_2O_2, 100 μM), TNFα (100 U/ml), interleukin-1β (IL-1β, 10 ng/ml), and the phorbol ester phorbol myristate acetate (PMA, 10 nM). All agents stimulated

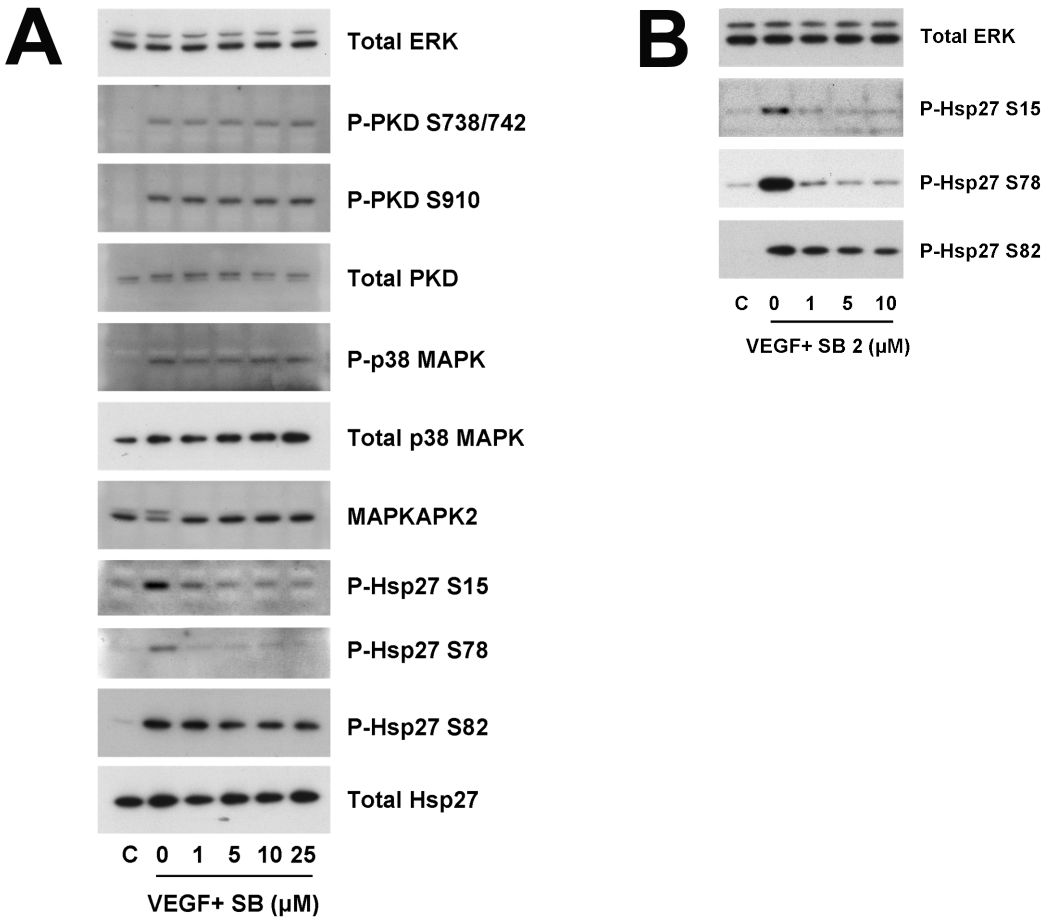

Figure 4.9: SB203580 does not completely inhibit VEGF-stimulated Hsp27 S82 phosphorylation

A and B. SB203580 (SB, A) and SB202190 (SB2, B) dose responses. Confluent, serum-deprived HUVECS were pre-incubated with the indicated concentrations of inhibitor or solvent alone (0.1% DMSO, C) for 30 mins followed by 15 mins treatment with 25 ng/ml VEGF or no addition (C). Cells were then lysed and immunoblotted using the indicated antibodies. The upper band of the MAPKAPK2 blot corresponds to the phosphorylated (active) form of MAPKAPK2, as reported on the manufacturer's antibody data sheet. SB203580 data representative of two independent experiments, SB202190 data from a single experiment.

phosphorylation of Hsp27 at S82, and that stimulated by H_2O_2, TNFα, and IL-1β was blocked by SB203580, but S82 phosphorylation induced by VEGF or PMA was resistant to p38 MAPK inhibition (figure 4.10B). In a separate experiment, 10 μM anisomycin (a protein synthesis inhibitor) also induced Hsp27 S82 phosphorylation, which was abrogated by SB203580 (figure 4.10C). The abilities of H_2O_2 and TNFα to induce Hsp27 phosphorylation at S15, S78 and S82, are shown in figures 4.13 and 4.16 respectively. The effects of 5 μM SB203580 on VEGF- or H_2O_2-stimulated phosphorylation of Hsp27 at all three residues are quantified in figure 4.13.

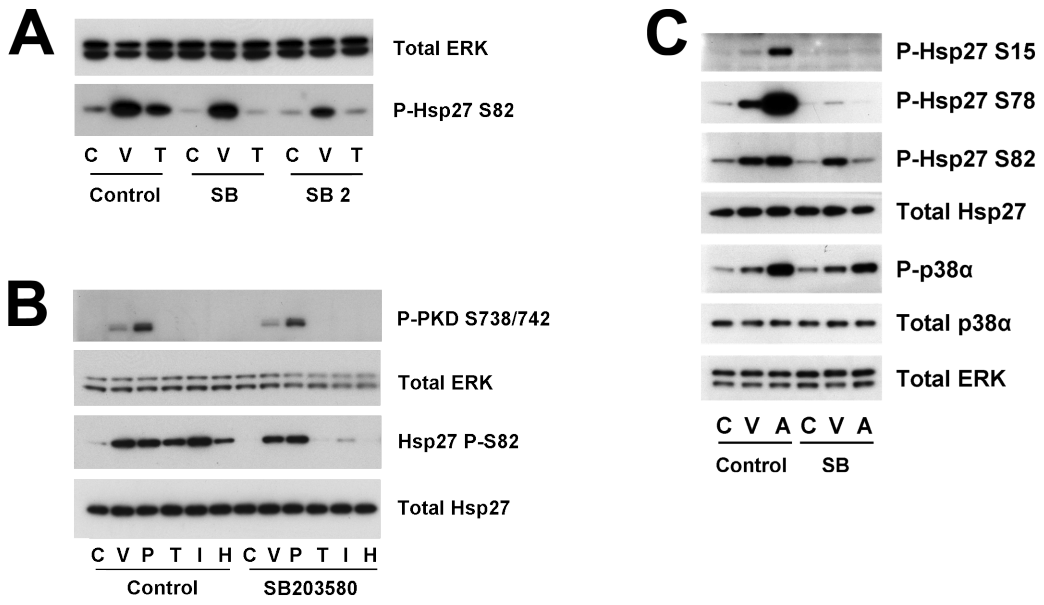

Figure 4.10: SB203580 differentially affects Hsp27 phosphorylation induced by VEGF and either TNFα, H_2O_2, IL-1β or anisomycin

A. Comparison of the effect of SB203580 and SB202190 on Hsp27 S82 phosphorylation stimulated by VEGF and TNFα. Confluent, serum-deprived HUVECS were pre-incubated with either 5 μM SB203580 (SB), 5 μM SB202190 (SB2) or solvent alone (0.1% DMSO, Control) for 30 mins followed by 15 mins treatment with 25 ng/ml VEGF, 100 U/ml TNFα, or no addition (C). Cells were then lysed, blotted, and probed with the indciated antibodies. Data is from a single experiment.

B. Comparison of the effect of p38 MAPK inhibition on Hsp27 S82 phosphorylation induced by various stimuli. Confluent, serum-deprived HUVECs were pre-incubated for 30 mins with either 5 μM SB203580 or solvent alone (0.1% DMSO, Control) followed by 15 mins treatment with either 25 ng/ml VEGF (V); 10 nM PMA (P); 100 U/ml TNFα (T); 10 ng/ml IL-1β (I); 100 μM H_2O_2 (H); or no addition (C). Cells were then lysed, blotted, and probed with the indicated antibodies. Data is from a single experiment.

C. Comparison of the effect of p38 MAPK inhibition on Hsp27 phosphorylation stimulated by VEGF and anisomycin. Confluent, serum-deprived HUVECs were pre-incubated for 30 mins with either 5 μM SB203580 (SB) or solvent alone (0.1% DMSO, Control) followed by 15 mins treatment with either 25 ng/ml VEGF (V); 10 μM anisomycin (A) or no addition (C). Cells were then lysed, blotted, and probed with the indicated antibodies. Data is representative of two independent experiments.

4.2.2 Knockdown of p38α and MAPKAPK2

Taken together, results from experiments using p38 MAPK inhibitors indicated that a p38 MAPK-independent pathway is involved in Hsp27 S82 phosphorylation stimulated by VEGF and PMA, whereas p38 MAPK appears to mediate VEGF-stimulated Hsp27 phosphorylation at S15 and S78, and all Hsp27 phosphorylations stimulated by TNFα, H_2O_2 and IL-1β. However, it was possible that a non-p38 target may be responsible for SB203580-dependent reductions in Hsp27 phosphorylation. Although regarded as a highly specific inhibitor of p38 MAPK (Davies *et al.* 2000), SB203580 is known to have p38-independent effects including activation of Raf (Eyers *et al.* 1999). In this study SB203580 consistently increased ERK phosphorylation (probably via Raf activation), and frequently led to increased phosphorylation of p38 MAPK itself (data not shown). Additionally, p38 MAPK has a number of isoforms and MAPKAPK2 is homologous to MAPKAPK3.

To determine whether the p38α/MAPKAPK2 pathway was the SB203580 target responsible for VEGF-induced phosphorylation of Hsp27 at S15 and S78, p38α and MAPKAPK2 protein expression was reduced in HUVECs with siRNAs. Representative blots demonstrating effective knockdown of p38 MAPK and MAPKAPK2 and the effect of these knockdowns on VEGF-induced Hsp27 phosphorylation are shown in figure 4.11A, with quantified data presented in figure 4.11B. Knockdown of p38α substantially reduced VEGF-stimulated phosphorylation of S15 and S78 (by 51% and 77% respectively), but only slightly affected VEGF-stimulated S82 phosphorylation (18% reduction). In contrast, TNFα-stimulated phosphorylation of all three residues was strongly decreased by p38α knockdown, with reductions of 56% at S15, 75% at S78, and 40% at S82. Knockdown of MAPKAPK2 showed a similar pattern, with VEGF-stimulated phosphorylation of S15 and S78 reduced by 76% and 85% respectively and S82 phosphorylation little affected, whereas TNFα-stimulated phosphorylation of all three residues was markedly reduced (by 77% at S15, 90% at S78, and 60% at S82). Thus the p38α–MAPKAPK2 pathway appears largely responsible for VEGF-induced phosphorylation of Hsp27 at S15 and S78, and plays a smaller role in

phosphorylation of S82, whereas it is the major pathway stimulated by TNFα for phosphorylation of Hsp27 at all three residues.

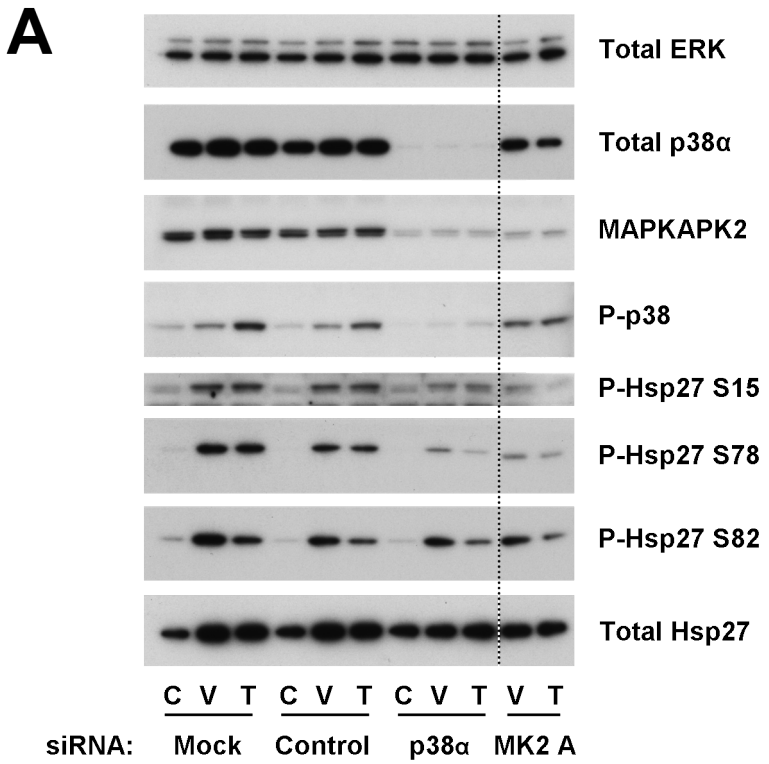

Figure 4.11: siRNAs directed against p38α or MAPKAPK2 do not reduce VEGF-induced phosphorylation of Hsp27 at S82 (continued overleaf)
A. HUVECs were transfected with 200 nM siRNA targeting p38α, MAPKAPK2 (MK2, siRNA A), a non-targeting siRNA (Control), or transfection reagent alone (Mock). After 48 h, serum-deprived cells were treated for 15 mins with 25 ng/ml VEGF (V) or 100 U/ml TNFα (T) or no addition (C) and lysed. Cell extracts were immunoblotted and probed with the indicated antibodies. Results are representative of five independent experiments. Quantification of the effect of the siRNAs on Hsp27 is shown in part B overleaf, and quantification of the effect of the siRNAs on p38α and MAPKAPK2 protein expression is given in figure 4.12B. The dotted line indicates that lanes were digitally removed from the blot, but all lanes shown were from the same blot, and all individual blots were performed in parallel on the same samples.

In addition to the effects on their intended target proteins, the siRNA targeting p38α reduced MAPKAPK2 protein expression by 83%, and two different siRNAs targeting MAPKAPK2 reduced p38α protein expression by 45% and 41% (figure 4.12), whereas neither the p38α siRNA nor the MAPKAPK2 siRNAs reduced total ERK expression.

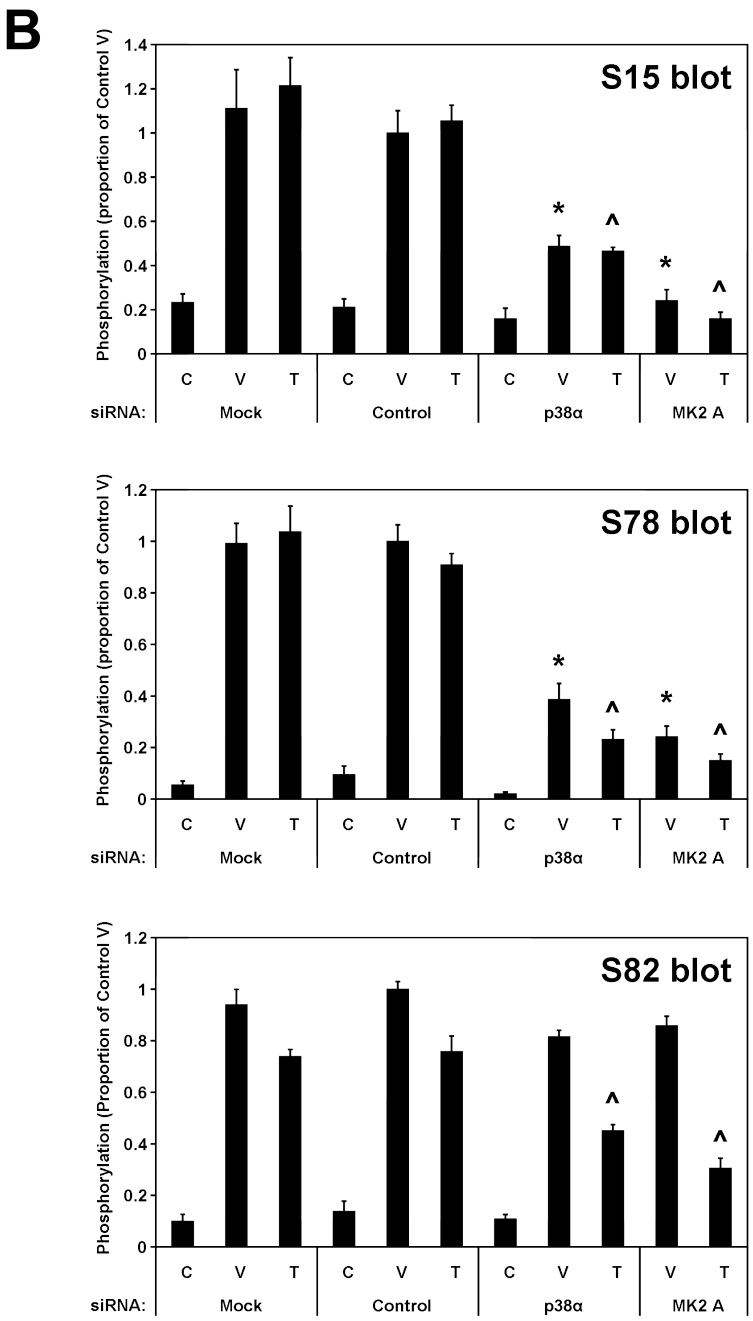

Figure 4.11: siRNAs directed against p38α MAPK or MAPKAPK2 do not markedly reduce VEGF-induced phosphorylation of Hsp27 at S82 (continued)
B. Quantification of results from part A (five independent experiments). Results were analysed by two-way ANOVA using Bonferroni's test for multiple pair-wise comparisons. * significantly different to Control/VEGF ($p<0.001$). ˆ significantly different to Control/TNFα ($p<0.001$). Mean knockdown of target protein achieved by siRNAs, compared to control siRNA: p38α 97%; MAPKAPK2 92%. Neither the MAPKAPK2 siRNA nor the p38α siRNA significantly affected Hsp27 protein levels.

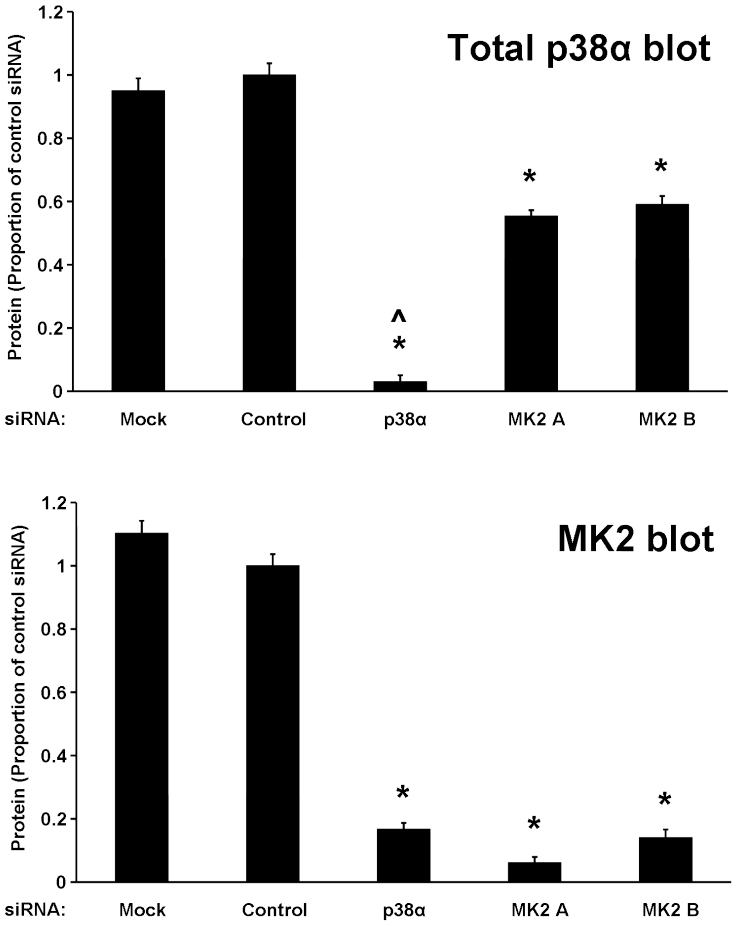

Figure 4.12: p38α siRNA reduces MAPKAPK2 protein levels, and MAPKAPK2 siRNA reduces p38α protein levels

Quantification of effects of siRNAs on p38 and MK2 protein levels, using results from figure 4.11A (five independent experiments). Data from an additional siRNA against MAPKAPK2, MK2 B, which was used in the same experiments and analysed on the same blots as those in figure 4.11, is included. MK2 B data was not included in data in figure 4.11B due to superior knockdown achieved by the MK2 A siRNA, and showed the same trend as that seen with MK2 A siRNA but to a lesser degree. Results were analysed by one-way ANOVA using Bonferroni's test for multiple pair-wise comparisons. * significantly reduced compared to control siRNA ($p<0.001$). ^ significantly reduced compared to both MK2 siRNAs ($p<0.001$).

4.3 Protein kinase C mediates VEGF-stimulated Hsp27 phosphorylation at S82

Experiments detailed in section 4.2 indicated that a p38 MAPK/MAPKAPK2-independent pathway was involved in VEGF-stimulated phosphorylation at S82, and prompted investigation into the intracellular enzymes involved in this pathway. Previous data from this and other laboratories has shown that protein kinase C (PKC) isoforms play a major role in VEGF signalling (see section 1.4.4), and work in this study showed that S82 phosphorylation induced by the PKC activator PMA was resistant to p38 MAPK inhibition (figure 4.10B), indicating that PKC may be an important mediator of Hsp27 S82 phosphorylation.

The involvement of protein kinase C in the SB203580-resistant phosphorylation of Hsp27 S82 was initially examined using pharmacological inhibitors. GF109203X (bisindolylmaleimide I) is a broad-spectrum PKC inhibitor, inhibiting classical and novel PKC isoforms but with reduced effectiveness against the atypical PKCs, whereas Gö6976 is commonly used as a selective inhibitor of the conventional/classical PKC isoforms α, β1, β2, and γ (Martiny-Baron *et al.* 1993). The effect of these PKC inhibitors alone and in combination with SB203580 on the VEGF- and H_2O_2-stimulated phosphorylation of Hsp27 was examined, and compared with the effect of SB203580 alone (figure 4.13).

As expected, SB203580 alone completely blocked H_2O_2-stimulated phosphorylation of Hsp27 at S15, S78 and S82, and strongly inhibited VEGF-induced phosphorylation at S15 and S78, but only partially reduced S82 phosphorylation (40% reduction). Both GF109203X and Gö6976 inhibited VEGF-stimulated phosphorylation at S82 without causing a statistically significant inhibition of of S15 and S78 phosphorylation, with GF109203X causing the greater reduction in S82 phosphorylation (76% reduction versus 62% reduction for Gö6976). When added in combination, SB203580 and GF109203X together reduced S82 phosphorylation to below control levels (96% reduction), whereas a comparatively large proportion of VEGF-induced S82 phosphorylation was

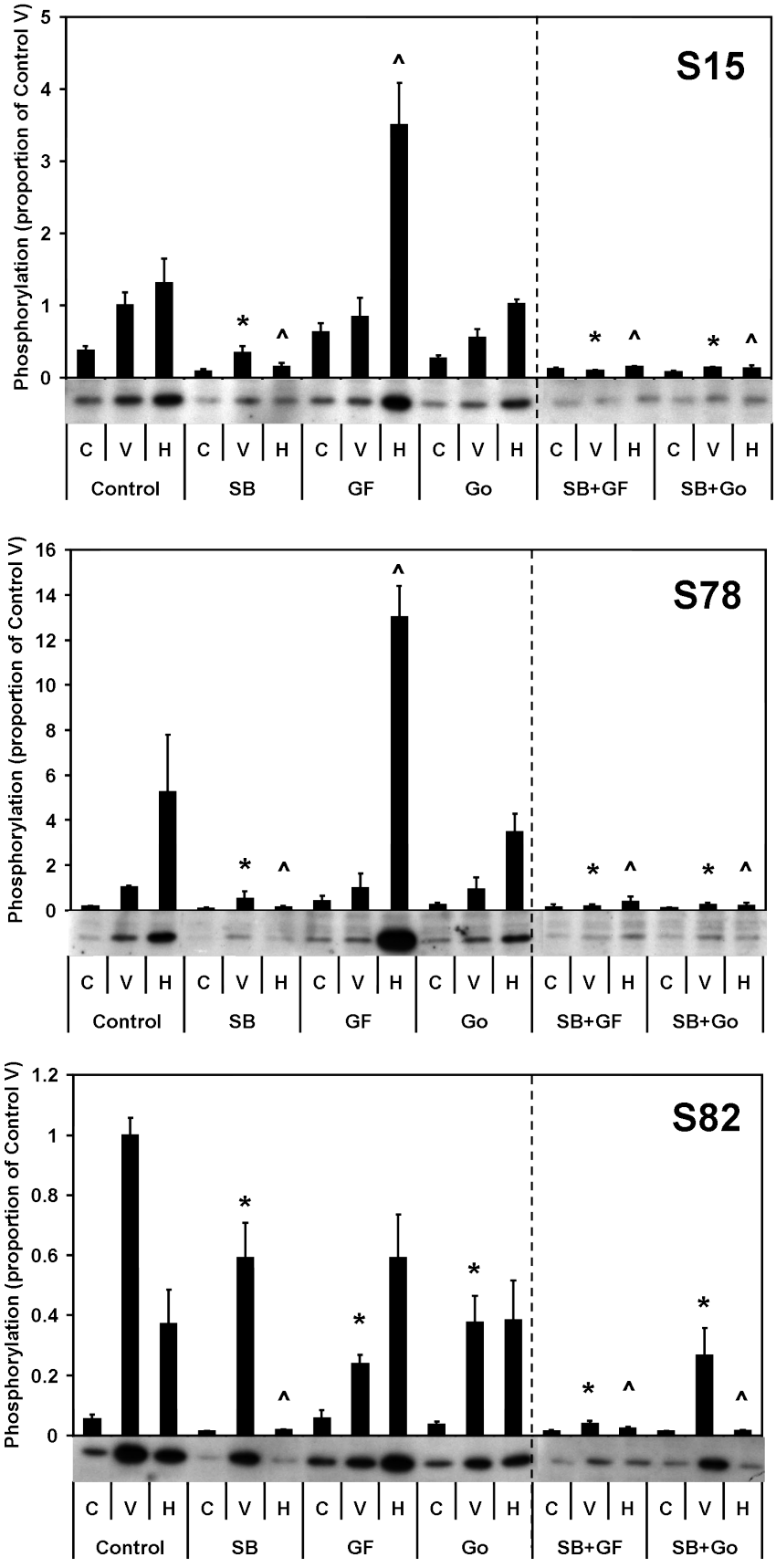

Figure 4.13: PKC is involved in phosphorylation of Hsp27 (caption overleaf)

Figure 4.13: PKC is involved in phosphorylation of Hsp27 (continued)
HUVECs were pre-incubated with either 5 μM SB203580 (SB), 3 μM GF109203X (GF), 1 μM Gö6976 (Go), solvent alone (Control), or the indicated combinations of inhibitors, followed by treatment for 15 mins with 25 ng/ml VEGF (V), H_2O_2 (100 μM, H) or no addition (C). Lysates were immunoblotted and probed with phospho-specific antibodies against Hsp27 as indicated. Results are given as the mean ($\pm$ SEM) proportion of the phosphorylation induced by Control V, and were analysed by two-way ANOVA with Bonferroni's test for multiple pair-wise comparisons. Representative blots are incorporated into each figure, dotted lines indicate that the samples for combinations of inhibitors were run on a separate gel run at the same time as that containing the other samples, due to insufficient lanes on the gel. * significantly different to Control/VEGF ($p<0.05$); ^ significantly different to Control/H_2O_2 ($p<0.05$). Total Hsp27 levels were similar in all samples. Cell treatments for these experiments was performed in conjunction with Dr. Ian Evans, Department of Medicine, UCL. Dr. Evans also carried out the P-S78 blots contributing to this figure.

not prevented by a Gö6976/SB203580 combination (27% S82 phosphorylation remaining).

Neither PKC inhibitor significantly inhibited phosphorylation in response to H_2O_2 at any residue, though surprisingly GF109203X increased phosphorylation at S15 and S78 more than 2-fold above the level induced by H_2O_2 alone without significantly affecting S82 phosphorylation. Control levels of phosphorylation were also increased by GF109203X at the same residues. The SB203580/GF109203X combination caused no more inhibition of H_2O_2-induced phosphorylation at all three residues than SB203580 alone.

The influence of different concentrations of GF109203X and Gö6976 on VEGF-stimulated Hsp27 phosphorylation was also examined. The effect of 1 μM and 6 μM GF109203X, and 0.2 μM and 3 μM Gö6976 on VEGF-induced Hsp27 phosphorylation at S78 and S82 was similar to that observed with 3 μM GF109203X and 1 μM Gö6976, the standard doses used in this study (figure 4.14). Greater inhibition of Hsp27 phosphorylation was observed at much higher inhibitor concentrations (15 μM GF109203X and 10 μM Gö6976), although p38 MAPK phosphorylation was little affected even at these concentrations.

In contrast to the effect of PKC inhibition on Hsp27 S82 phosphorylation, inhibition of the PI-3-K and ERK signalling cascades had little effect on phosphorylation of Hsp27, and when used in combination with SB203580 did not appear to reduce Hsp27 S82 phosphorylation further than observed with SB203580 alone (figure 4.15).

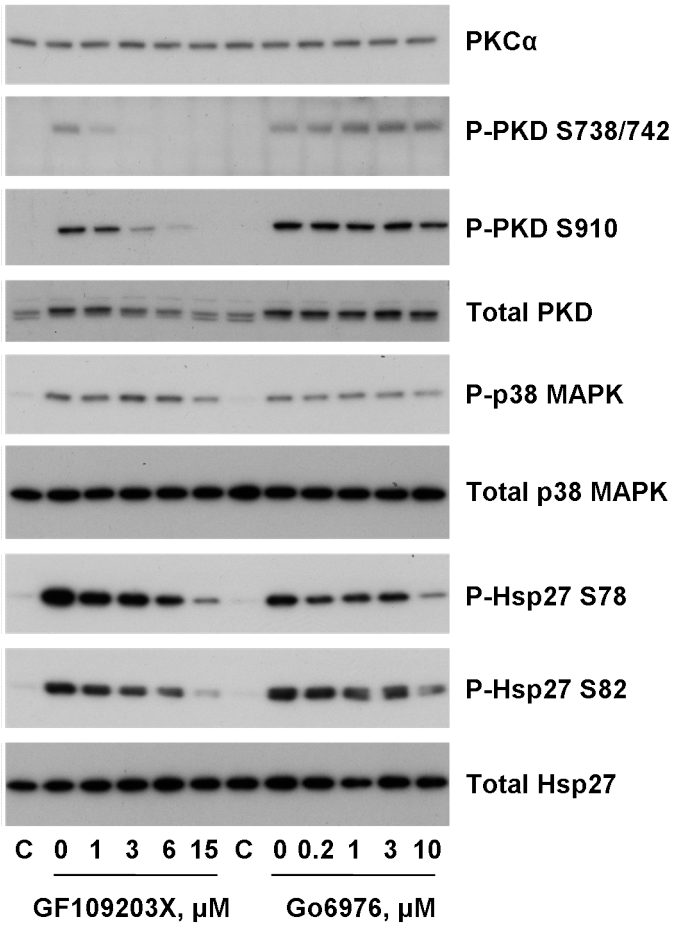

Figure 4.14: Effect of different PKC inhibitor concentrations on VEGF-induced phosphorylation of Hsp27 and PKD
Confluent HUVECs were pre-incubated for 30 mins with the indicated concentration of inhibitor (GF109203X or Gö6976), followed by 15 mins treatment with 25 ng/ml VEGF. Cells were then lysed, blotted and probed with the indicated antibodies. C, no VEGF or inhibitor (solvent alone: 0.5% v/v DMSO.)

4.3.1 Effect of PKC reduction on VEGF-induced Hsp27 phosphorylation

Together, results using kinase inhibitors indicated that PKC plays a major role in VEGF-stimulated phosphorylation of Hsp27 at S82, whereas H_2O_2 and TNFα stimulate Hsp27 phosphorylation via p38 MAPK. The involvement of PKC in VEGF-stimulated Hsp27 phosphorylation was also addressed using two methods to reduce PKC isoforms in cells: long term phorbol ester treatment, and PKC siRNAs.

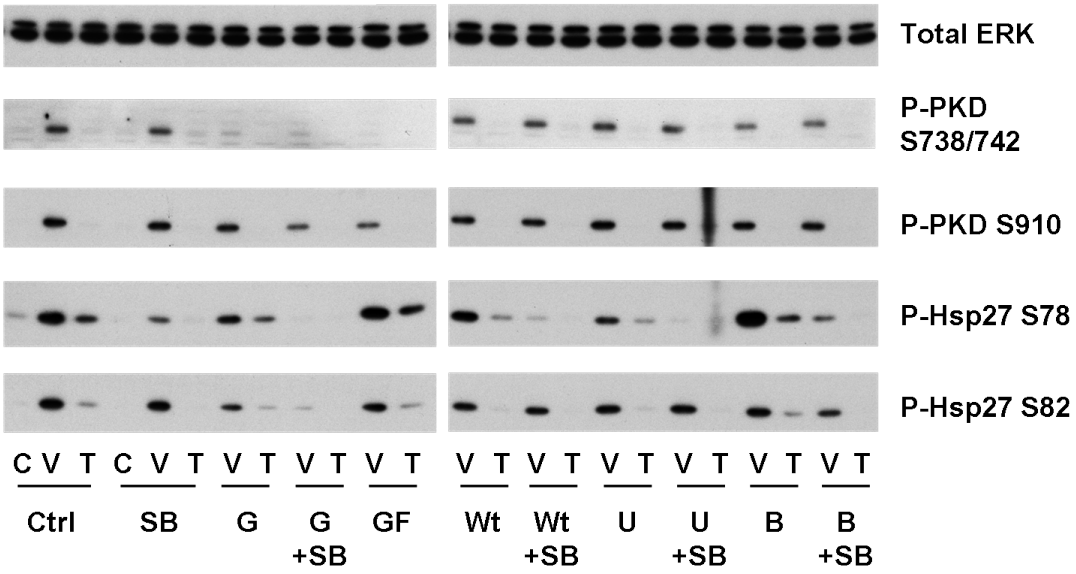

Figure 4.15: Inhibition of MEK or ERK has little effect on VEGF-stimulated Hsp27 S82 phosphorylation
HUVECs were pre-incubated with either 5 μM SB203580 (SB), 3 μM Gö6983 (G), 3 μM GF109203X (GF), 100 nM wortmannin (Wt), 10 μM U0126 (U), 10 μg/ml BAPTA-AM (B), or solvent alone (Control), or the indicated combinations of inhibitors, followed by treatment for 15 mins with 25 ng/ml VEGF (V), TNFα (100 U/ml, T) or no addition (C). Lysates were immunoblotted and probed with the indicated antibodies. Results are from a single experiment, but lack of effect of wortmannin, U0126 and BAPTA-AM (not in combination with SB203580) on Hsp27 S82 phosphorylation was also observed on at least two other occasions.

4.3.1.1 Phorbol ester-mediated PKC downregulation

Long-term treatment with phorbol esters, pharmacological analogues of the PKC activator diacylglycerol, has been used for many years as a way of downregulating the protein levels of conventional and novel subfamilies of PKC. Levels of atypical PKCs (which are not activated by diacylglycerol) and protein kinase D (Rennecke *et al.* 1996), are unaffected by this treatment.

Treatment of HUVECs with phorbol-12-myristate-13-acetate (PMA) for 28 h resulted in the loss of all detectable PKCα and PKCδ from the cells, and markedly reduced PKCϵ levels (figure 4.16A). VEGF-stimulated phosphorylation of Hsp27 at both S15 and S82 was strongly reduced by long-term PMA treatment (94% reduction in S15 phosphorylation, 84% reduction in S82 phosphorylation). TNFα-induced phosphorylation of S15 was also reduced by PMA, although by a smaller degree than that induced by VEGF (60% reduction), and TNFα-stimulated

phosphorylation of S82 was not affected by PMA. Thus, long-term treatments with PMA prevent phosphorylation of Hsp27 S82 induced by VEGF but not TNFα, again suggesting the importance of PKC in VEGF-stimulated phosphorylation at this residue. Possible reasons for the the effect of long-term PMA treatments on VEGF-stimulated S15 phosphorylation as discussed later.

Short-term PMA treatments (15 mins), aimed at activating rather than down-regulating PKC, induced phosphorylation of Hsp27 at S82 but not S15, indicating the importance of PKC in VEGF-induced phosphorylation of S82 but not S15 (figure 4.20B, third lane from left). PMA-stimulated S82 phosphorylation could not be blocked by SB203580, further suggesting the presence of a PKC-dependent, p38 MAPK independent pathway for phosphorylation of Hsp27 at S82.

4.3.1.2 Isoform-specific PKC knockdown

To examine the importance of individual PKC isoforms on VEGF-induced Hsp27 phosphorylation, three major PKC isoforms previously shown by this laboratory to translocate in HUVECs after VEGF stimulation, PKCs α, δ, and ϵ (Gliki *et al.* 2001), were separately knocked down in HUVECs using siRNA. Representative blots of the effect of PKC knockdowns on VEGF-stimulated Hsp27 phosphorylation are shown in figure 4.17, with the quantified effect on Hsp27 phosphorylation presented in figure 4.18.

The PKC siRNAs affected Hsp27 expression, with PKCα siRNA increasing Hsp27 expression by 43% and the other PKC siRNAs having smaller effects (14% increase in Hsp27 by the PKCδ siRNA, 6% decrease by the PKCϵ siRNA). It was also observed that knockdown of any of the three PKC isoforms examined also caused changes in the expression of the other two isoforms (figure 4.19), further complicating interpretation of results with these siRNAs.

Consistent effects on Hsp27 phosphorylation were observed. When correcting the results with anti-Hsp27 phospho-specific antibodies to total Hsp27 protein expression (figure 4.18A), PKCα and δ siRNAs reduced phosphorylation at S15 (48% and 49% reductions respectively) and S78 (50% and 49% reductions) by similar amounts, whereas PKCϵ knockdown had no significant ef-

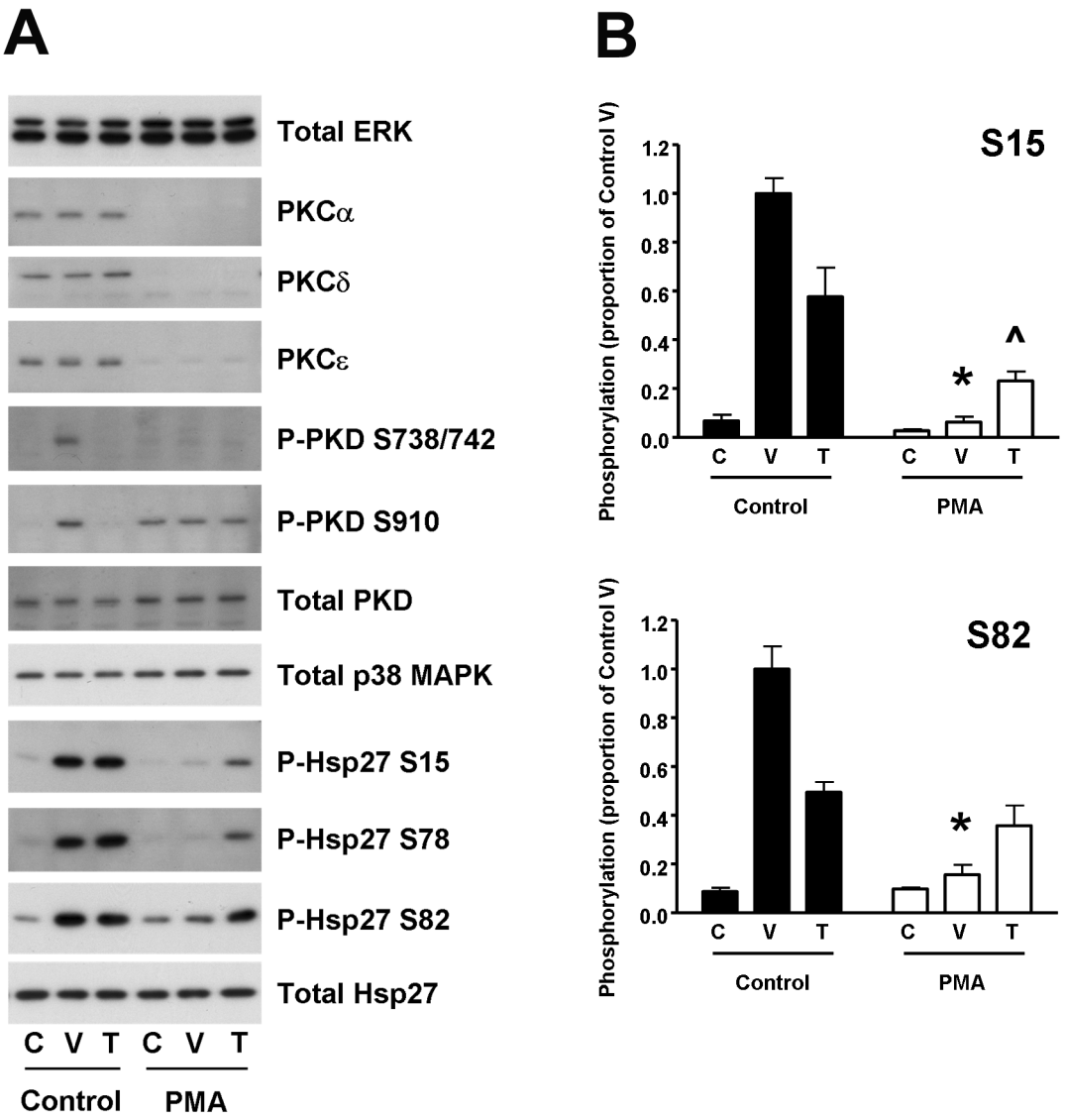

Figure 4.16: Phorbol ester-mediated PKC downregulation blocks VEGF-induced phosphorylation of Hsp27 at S82

A. Representative blots showing the effect of long-term treatment with phorbol ester on Hsp27 phosphorylation induced by VEGF and TNFα. Confluent HUVECs were treated for 28 h with either vehicle (0.1% DMSO, control) or 200 ng/ml (324 nM) phorbol-12-myristate-13-acetate (PMA), and subsequently treated for 15 mins with either no addition (C), 25 ng/ml VEGF (V) or 100 U/ml TNFα (T). Samples were then lysed and immunoblotted with antibodies as indicated. S78 data from a single experiment.

B. Quantification of results for Hsp27 S15 and S82 phosphorylation in control and PMA-treated cells (n=4), analysed by two-way ANOVA with Bonferroni's test for multiple comparisons. * Significantly different to control VEGF ($p<0.001$). ^ Significantly different to control TNFα ($p<0.01$).

fect on these phosphorylation sites. At S82, siRNAs against PKCα PKCδ and PKCϵ reduced phosphorylation by 32%, 25%, and 41% respectively. Without correcting signals obtained with phospho-specific antibodies to total Hsp27 expression (figure 4.18B), PKCα and δ siRNAs reduced phosphorylation at S15 (26% and 42% reductions respectively) and S78 (29% and 41% reductions) by similar amounts, whereas PKCϵ knockdown had no significant effect. At S82, siRNAs against PKCδ and PKCϵ reduced phosphorylation by 14% and 41% respectively, whereas an siRNA against PKCα had no significant effect. Both methods of analysing the results indicate a greater role for PKCϵ in VEGF-stimulated phosphorylation of S82 than phosphorylation of S15 or S78. A double knockdown of both PKCδ and PKCϵ did not apparently increase the reduction in VEGF-dependent PKD or Hsp27 phosphorylation when compared to the best-performing single knockdown (results not shown). Overall, knockdown of PKCα or PKCδ reduces VEGF-stimulated Hsp27 phosphorylation at S15 and S78, whereas the PKCϵ siRNA has a greater effect against S82.

4.4 Involvement of protein kinase D in VEGF-induced Hsp27 phosphorylation

4.4.1 PKD/PKCμ is phosphorylated in response to VEGF

While this work was in progress, it was shown that purified protein kinase D (PKD, also known as PKC$_\mu$) is able to phosphorylate an Hsp27-GST fusion protein at S82 but not S15 in an in vitro kinase assay (Doppler *et al.* 2005). Activation of protein kinase D is reported to involve transphosphorylation of the activation loop (S738/742) by an upstream kinase, thought to be PKC, and subsequent autophosphorylation at S910. Although S910 autophosphorylation may not be strictly required for activation, it is reported to correlate well with catalytic activity (section 1.6.3).

The potential role of PKD in VEGF-stimulated Hsp27 phosphorylation was examined. VEGF is able to induce phosphorylation of PKD at the activation loop and at the C-terminal site S910, with

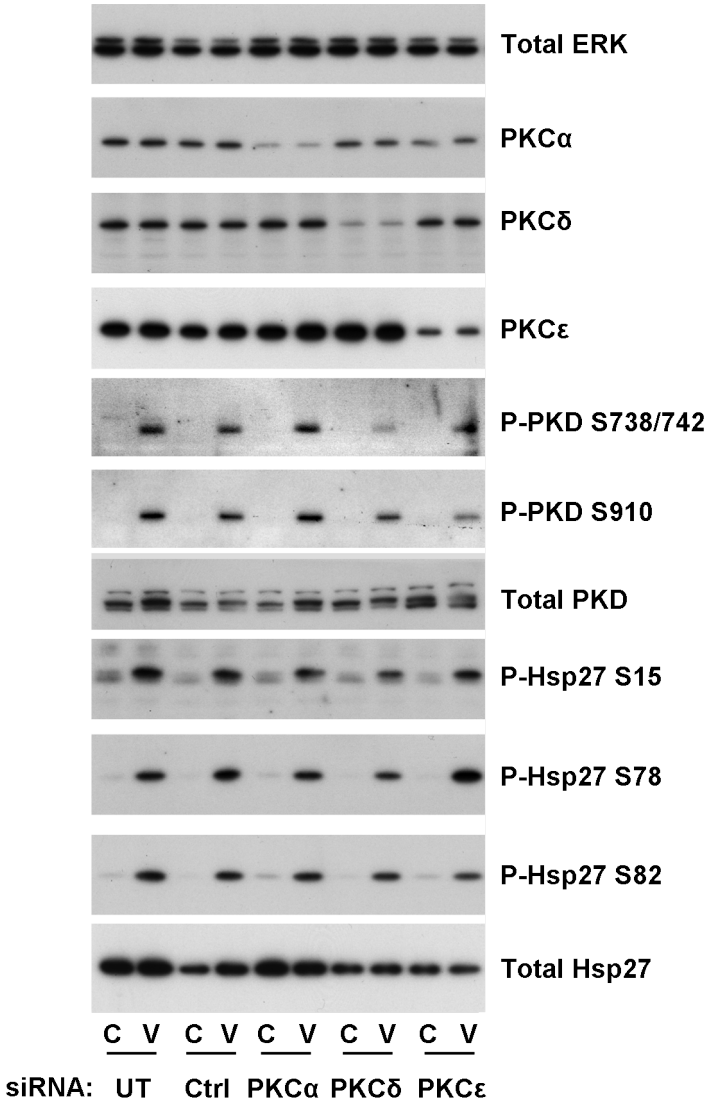

Figure 4.17: Effect of PKC knockdown on VEGF-stimulated phosphorylation of Hsp27 and PKD

HUVECs were incubated with 200 nM of the indicated siRNA (labelled on bottom of blot) for 48 h to knock down target proteins. Cells were then treated for 15 mins with 25 ng/ml VEGF (V) or no addition (C) and lysed. Lysates were immunoblotted and probed with the indicated antibodies. The effect of the siRNAs on Hsp27 phosphorylation is quantified in figure 4.18. UT, untransfected; Ctrl, control siRNA.

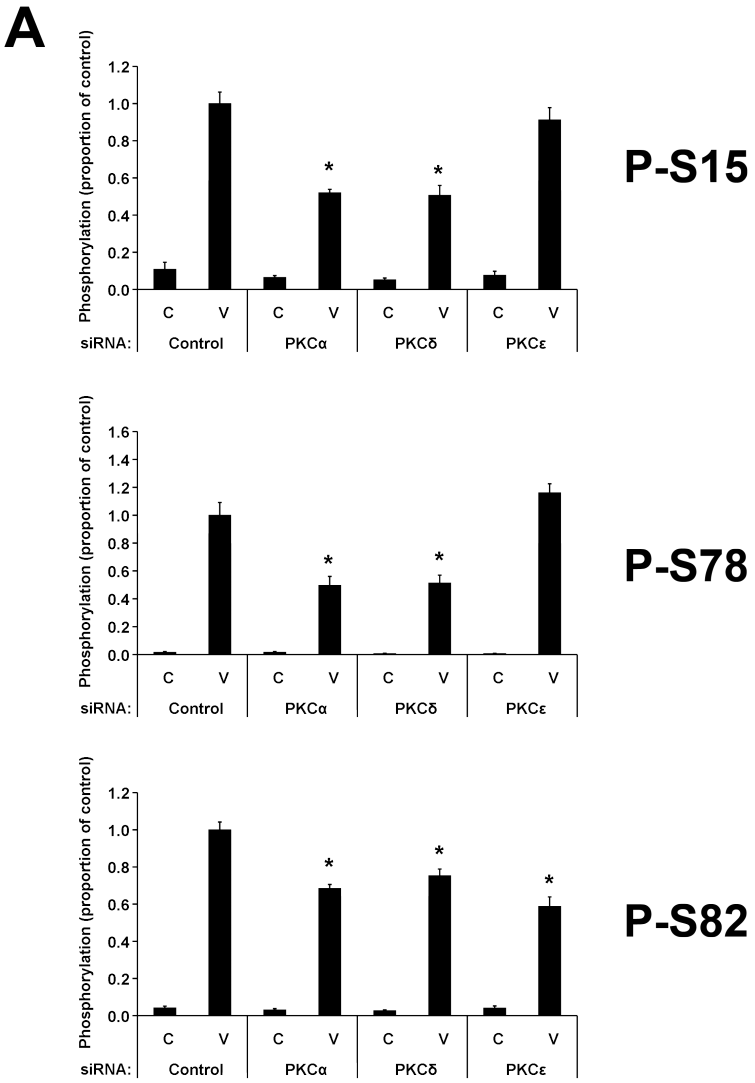

Figure 4.18: Effect of PKC knockdown on Hsp27 phosphorylation (continued overleaf) Quantification of the effects of PKC siRNAs on VEGF-stimulated Hsp27 phosphorylation, with results derived as described in figure 4.17. Blots were probed with phospho-specific antibodies targeting the indicated Hsp27 residue. Values are means $\pm$ SEM, and the number of independent experiments represented is: S15, 7; S78, 5; S82, 8. Statistical analysis via one-way ANOVA with Bonferroni's test for multiple pair-wise comparisons. Mean knockdown achieved by the siRNAs: PKCα 82%, PKCδ 90%, PKCϵ 76%
A. Phospho-Hsp27 data expressed as a ratio of the mean total Hsp27 signal for that siRNA to correct for the apparent increase in Hsp27 expression caused by the PKCα siRNA. * $p<0.001$ compared to control siRNA.

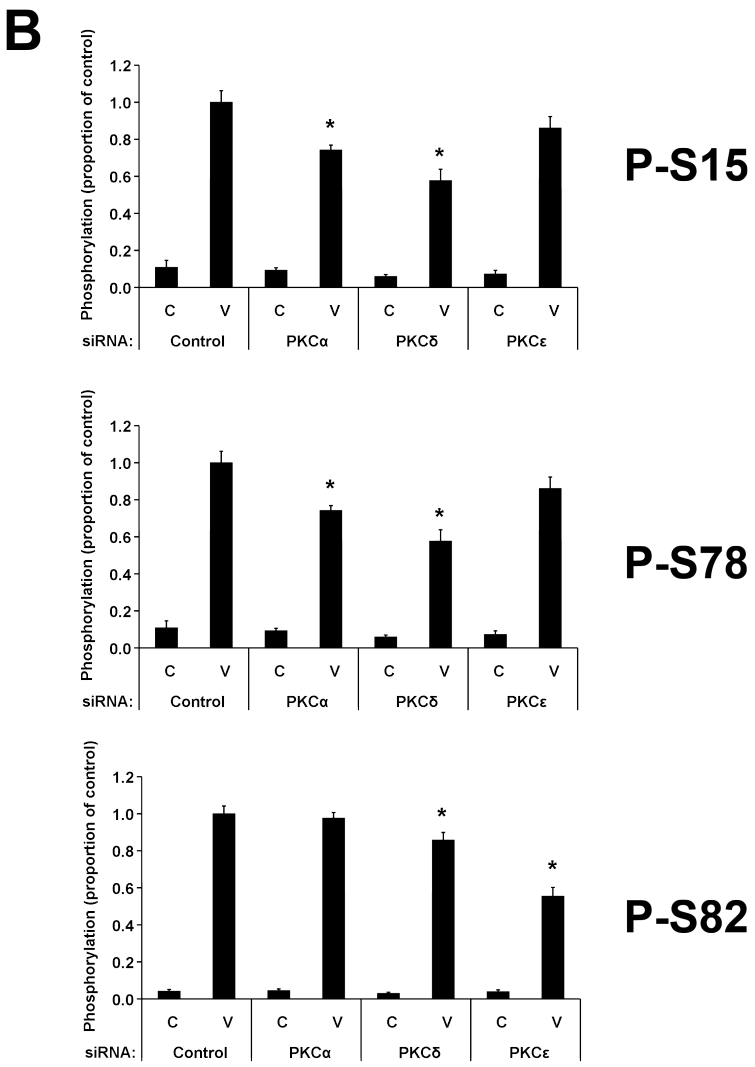

Figure 4.18: Effect of PKC knockdown on Hsp27 phosphorylation (continued)
B. Data presented in (A) not corrected to total Hsp27 levels. * $p<0.001$ compared to control siRNA, apart from P-S78 control siRNA vs PKCα siRNA and P-S82 control siRNA vs PKCδ siRNA, both $p<0.01$.

maximal phosphorylation of both sites occurring with 25 ng/ml VEGF after 10–20 mins (figure 4.2 and data not shown). VEGF-stimulated phosphorylation of PKD at S738/742 apparently occurred via VEGFR2 as it was blocked by the VEGFR2 tyrosine kinase inhibitor SU5614 (figure 4.3).

4.4.2 VEGF-stimulated PKD phosphorylation occurs via protein kinase C and not via p38 MAPK

VEGF-induced PKD phosphorylation was examined using the broad-spectrum PKC inhibitor GF109203X and the inhibitor of conventional/classical PKCs, Gö6976. 3 μM GF109203X

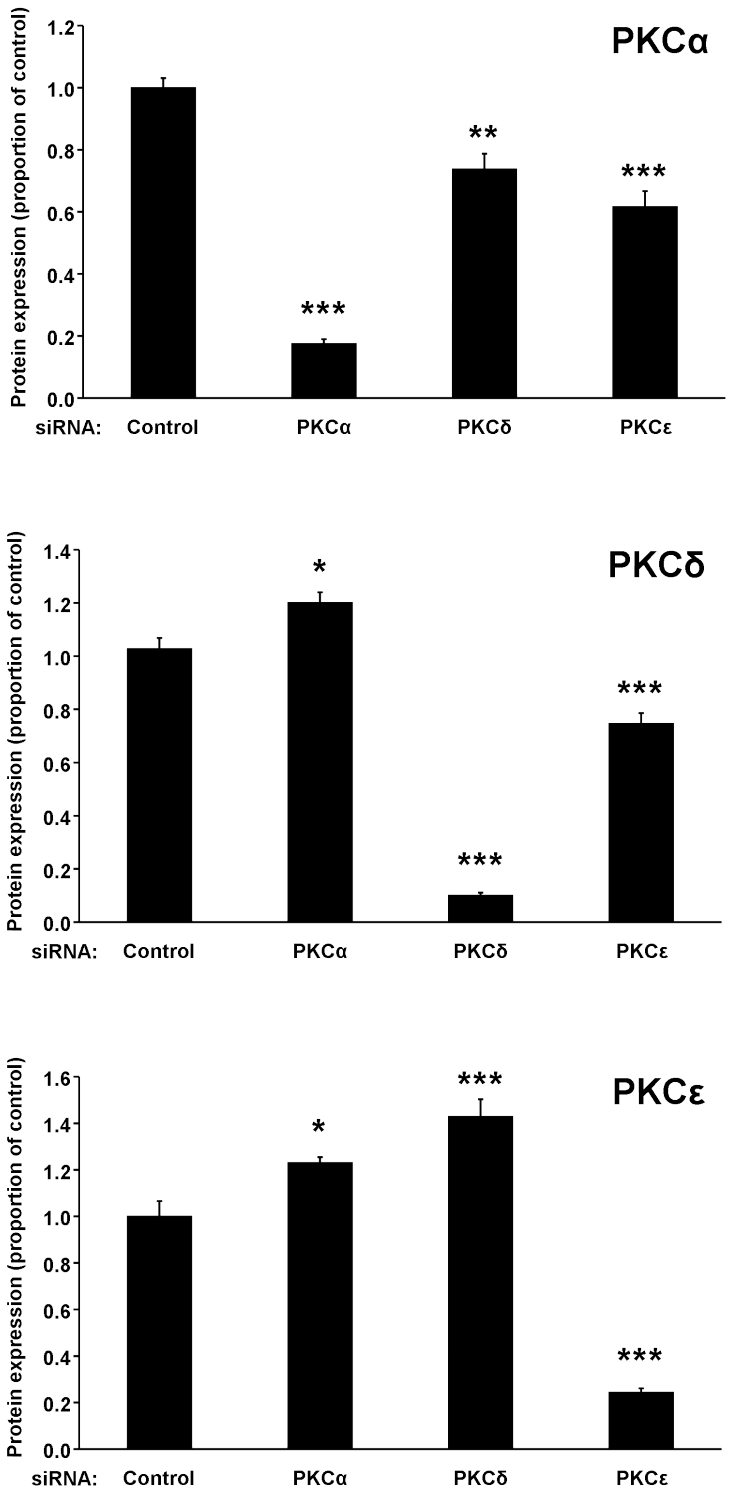

Figure 4.19: Effect of PKC knockdown on PKC protein expression
Quantification of the effects of PKC siRNAs on PKC expression, with results derived as described in figure 4.17. Blots were with antibodies reported not to cross-react with other PKC isoforms (indicated). Values are means ± SEM from five independent experiments. Statistical analysis via one-way ANOVA with Bonferroni's test for multiple pair-wise comparisons. * $p<0.05$ compared to control siRNA, ** $p<0.01$ compared to control siRNA, *** $p<0.001$ compared to control siRNA.

fully inhibited VEGF-induced phosphorylation of S738/742 and partially reduced phosphorylation at S910, whereas 1 μM Gö6976 and 5 μM SB203580 had no effect on either residue (figure 4.20A). Higher concentrations of GF109203X increased the degree of inhibition observed at S910, whereas concentrations of Gö6976 up to 10μM had little effect on VEGF-induced phosphorylation at either residue (figure 4.14). Concentrations of SB203580 up to 25μM had no effect on VEGF-stimulated phosphorylation at either S738/742 or S910 (figure 4.9A), and use of SB203580 in combination with either GF109203X or Gö6976 did not result in greater inhibition at either S738/742 or S910 than observed with the PKC inhibitor alone (figure 4.20A).

The involvement of the p38 MAPK pathway in PKD phosphorylation was further examined using the p38-activating stimuli H_2O_2, TNFα and IL-1β. These three stimuli all failed to induce S738/742 phosphorylation of PKD at concentrations sufficient to induce phosphorylation of Hsp27 at S82 (figure 4.10B). At higher concentrations, H_2O_2 did stimulate PKD phosphorylation, and this phosphorylation was not blocked by SB203580 (figure 4.20B). Interestingly, these higher H_2O_2 concentrations led to further increased p38 phosphorylation, but were associated with reductions in Hsp27 phosphorylation at both S15 and S82. Together, these data suggest that p38 MAPK activation is insufficient for PKD phosphorylation, and that high H_2O_2 concentrations activate an additional non-p38-mediated signalling pathway leading to PKD phosphorylation.

Overall, data from kinase inhibitors suggests that VEGF induces PKD phosphorylation via a non-classical PKC or PKCs, and that the p38 MAPK pathway is not involved. Additionally, studies with p38-activating stimuli indicate that PKD phosphorylation is not a consequence of Hsp27 phosphorylation.

4.4.3 Involvement of PKC isoforms in Hsp27 and PKD phosphorylation

To determine which PKC isoforms are responsible for the observed effects of the PKC inhibitors on VEGF-stimulated PKD phosphorylation, the amounts of PKCα, PKCδ, and PKCϵ present in HUVECs were separately reduced with siRNA. Knockdown of PKCδ and PKCϵ reduced S738/742

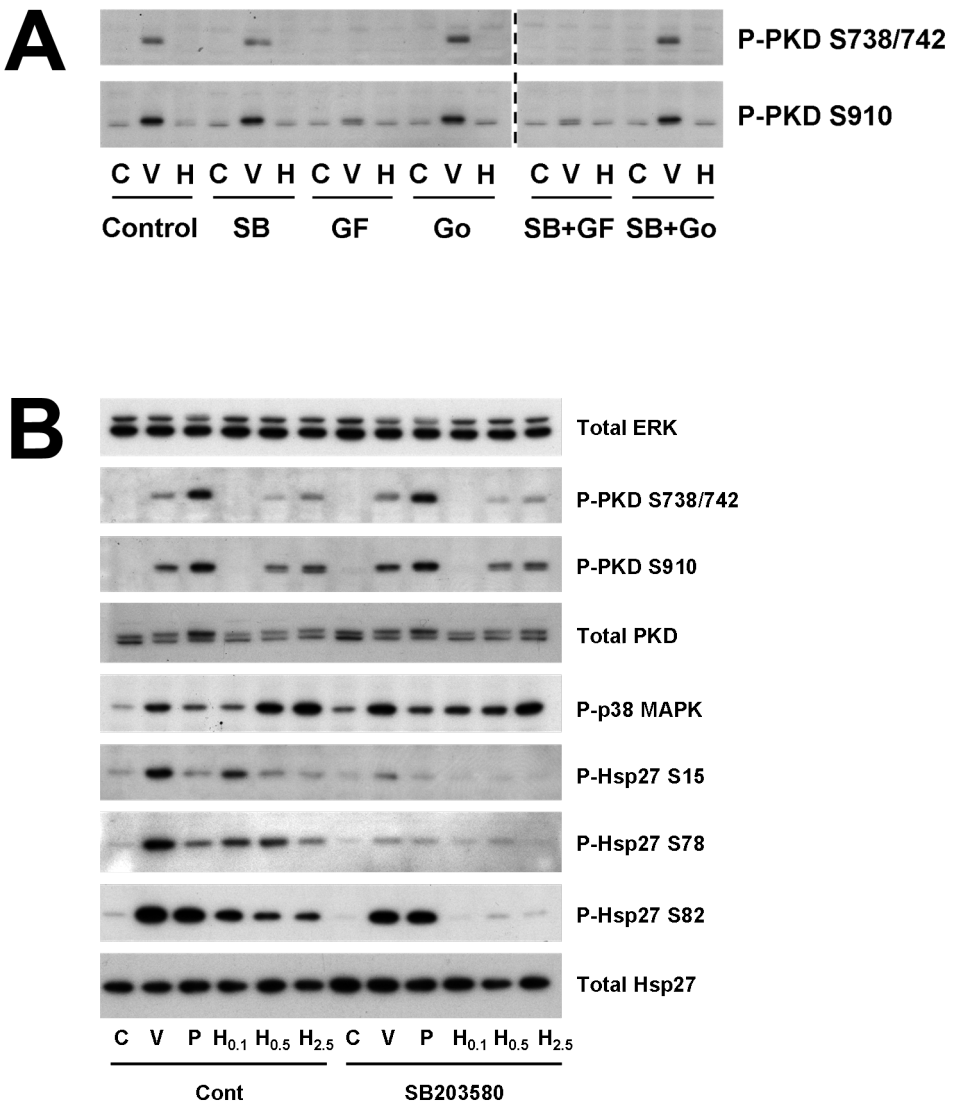

Figure 4.20: VEGF stimulates phosphorylation of protein kinase D by a PKC-dependent mechanism

A. VEGF-dependent phosphorylation of PKD is blocked by GF109203X but not Gö6976. HUVECs were pre-treated for 30 mins with either solvent alone (0.2% DMSO, Control), 5 μM SB203580 (SB), 3 μM GF109203X (GF), 1 μM Gö6976 (Go) or the indicated combinations of inhibitors, before 15 mins treatment with either no addition (C), 25 ng/ml VEGF (V) or 100 μM H_2O_2 (H). Immunoblots of lysates were probed for phospho-PKD (S738/742) and phospho-PKD (S910). Results are representative of three independent experiments.

B. H_2O_2 activates PKD at high concentrations. HUVECs were pre-treated for 30 mins with either solvent alone (0.1% DMSO, Cont) or 5 μM SB203580 followed by 15 mins treatment with either no addition (C), 25 ng/ml VEGF (V), 50 nM PMA (P), or the indicated concentration of H_2O_2 (H_x, where the subscript is the concentration of hydrogen peroxide used in mM). Immunoblots of lysates were probed with the antibodies indicated. Results are representative of two independent experiments.

phosphorylation by 57% and 25% respectively, whereas PKCα knockdown had no effect (figure 4.21, see figure 4.17 for representative blots). In contrast, none of the PKC siRNAs tested significantly reduced VEGF-stimulated phosphorylation at S910, although the mean reduction by the PKCϵ siRNA was 37%. A second, distinct siRNA targeted against PKCδ reduced VEGF-stimulated PKD phosphorylation at S738/742 to a similar degree to the original PKCδ siRNA (figure 4.22).

4.4.4 Importance of PKD in VEGF-induced Hsp27 phosphorylation

As VEGF stimulates PKD activation loop phosphorylation via PKC, and PKC is involved in the VEGF-induced SB203580-resistant phosphorylation of Hsp27 at S82, PKD is a potential mediator of VEGF-stimulated phosphorylation of S82. The importance of PKD in VEGF-stimulated phosphorylation was assessed using siRNA-mediated knockdown. Both PKD1 and PKD2 protein were detected in HUVECs by western blotting, and so both isoforms were examined. As the PKD2 siRNA reduced Hsp27 expression by a mean of 25%, densitometry results obtained with phospho-specific Hsp27 antibodies were expressed as a ratio of the total Hsp27 protein levels obtained using that particular siRNA.

PKD2 knockdown reduced VEGF-stimulated S82 phosphorylation occurring in the absence and presence of SB203580 by 34% and 70% respectively when compared to the inhibitor-matched control siRNA (figure 4.23). While tending to be lower than that seen with the control siRNA, PKD1 knockdown did not significantly affect VEGF-induced S82 phosphorylation. Neither PKD siRNA affected VEGF-stimulated phosphorylation of Hsp27 at S15 or S78 in the absence of SB203580, and phosphorylation at these residues in the presence of SB203580 was too low to quantify. Expression of p38 MAPK and MAPKAPK2 was not affected by either PKD siRNA.

Use of the PKD siRNAs also helped to clarify the specificity of the PKD antibodies used in this study. The total PKD antibody, expected to be specific for PKD1 (personal communication with Cell Signalling Technology), recognised two bands of approximately 115 kDa, the upper of which

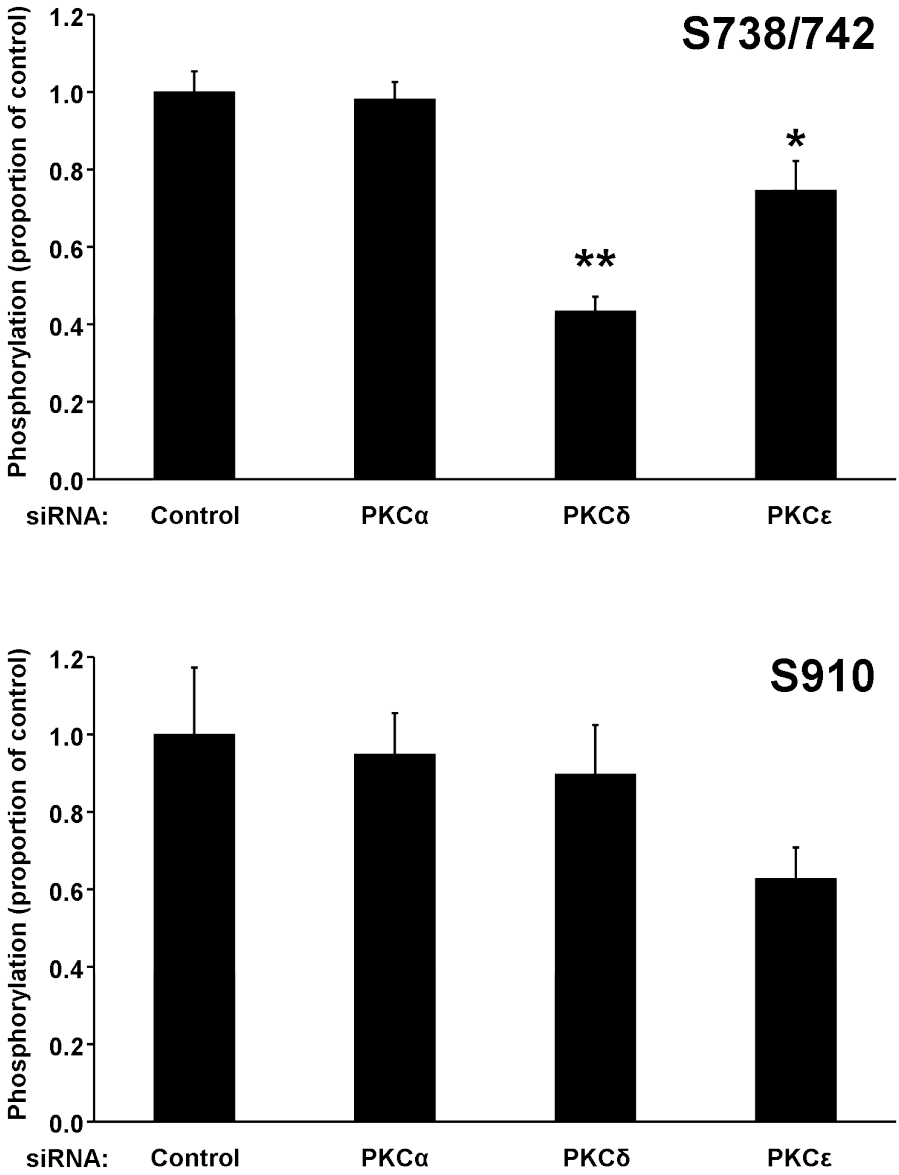

Figure 4.21: Effect of PKC siRNAs on VEGF-induced PKD phosphorylation
Quantification of the effects of PKC siRNAs on VEGF-stimulated PKD phosphorylation, with results derived as described in figure 4.17. HUVECs were incubated for 48 h with 200 nM of a non-targeting control siRNA (Control), or siRNAs targeting the indicated PKC isoform, and then treated for 15 mins with 25 ng/ml VEGF. Lysates were blotted and probed with phospho-specific antibodies to PKD phosphorylated at S738/742, or S910. The PKD residue represented is given in the upper right corner of each graph. Data is presented as mean signal obtained from the blot $\pm$ SEM, and the numbers of independent experiments represented are: S738/742, 8; S910, 4. Statistical analysis was via one-way ANOVA with Bonferroni's test for multiple pair-wise comparisons. * $p<0.05$ compared to control siRNA, ** $p<0.001$ compared to control siRNA. Mean knockdown of target protein achieved by the siRNAs: PKCα 82%, PKCδ 87%, PKCϵ 77%.

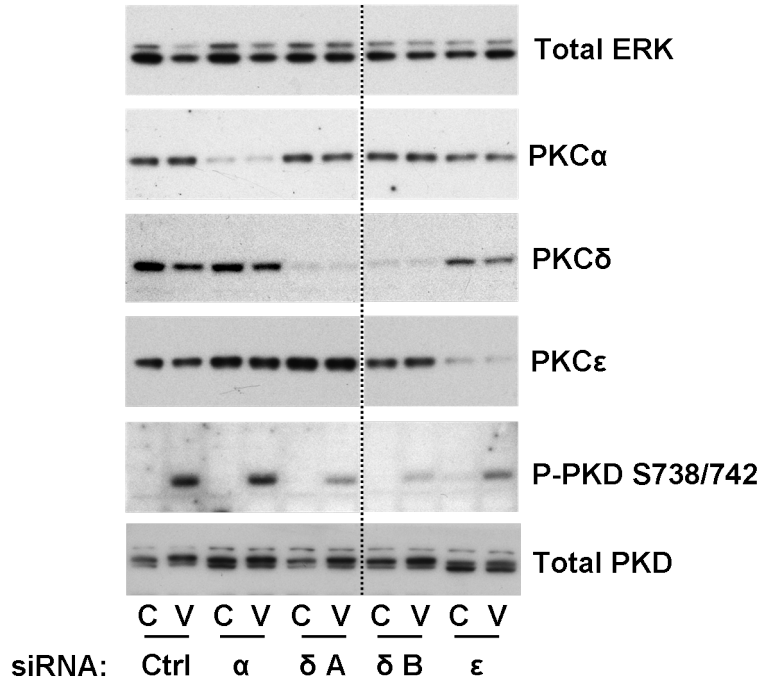

Figure 4.22: Two different PKCδ siRNAs reduce VEGF-stimulated phosphorylation of PKD
HUVECs were incubated with 200 nM siRNA for 48 h to reduce specific PKC isoforms, and then treated for 15 mins with 25 ng/ml VEGF (V) or no addition (C). Lysates were blotted and probed with the indicated antibodies. Ctrl, negative control siRNA; α, ϵ, siRNAs targeting these PKC isoforms; δ A, δ B, two different siRNAs targeting PKCδ (δ A is the siRNA used in all other PKCδ knockdown experiments in this thesis). Results are from a single experiment. The dotted line indicates that lanes were digitally removed from the blots, but all lanes shown are from the same blot.

was reduced by the PKD1 siRNA and the lower of which was reduced by the PKD2 siRNA. As the sequence-predicted molecular weights of unmodified PKD1 and PKD2 are 102 kDa and 97 kDa respectively, it was deduced that the total PKD antibody cross-reacts with PKD1 and PKD2, with the upper recognised band being PKD1 and the lower being PKD2. The signal derived from blots probed with the PKD2 antibody gave a single band at approximately 115 kDa, which was reduced by the PKD2 siRNA but not by the PKD1 siRNA, indicating that this antibody is likely to be specific for PKD2.

VEGF-induced phosphorylation of PKD detected by the P-PKD S738/742 antibody was reduced 64% by the PKD1 siRNA and 81% by the PKD2 siRNA, indicating that this antibody recognises both PKD1 and PKD2. In contrast, VEGF-induced phosphorylation of PKD detected by the P-PKD S910 antibody was reduced 85% by the PKD1 siRNA, but was unaffected by the

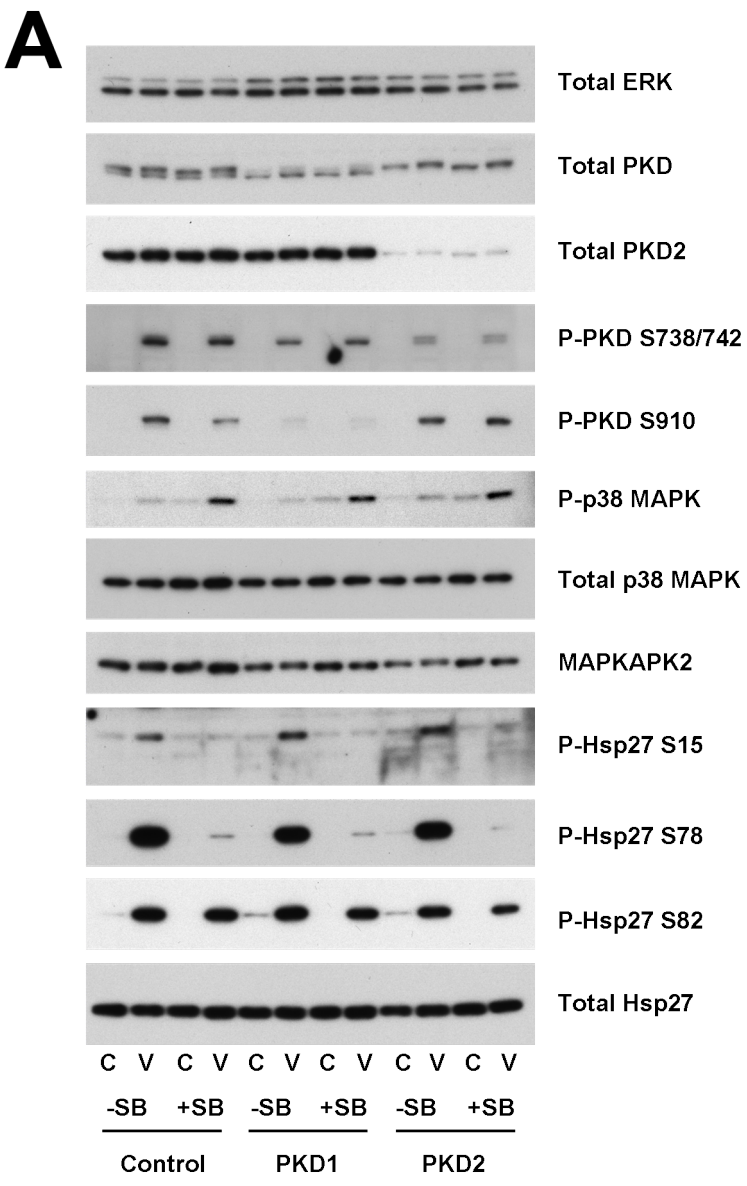

Figure 4.23: Effect of PKD knockdown on VEGF-induced Hsp27 and PKD phosphorylation (continued overleaf)

A. HUVECs were incubated for 48 h with 200 nM of a non-targeting siRNA (Control) or siRNAs targeting PKD1 or PKD2 as indicated. Cells were then pre-treated for 30 mins with 5 μM SB203580 (+SB) or solvent alone (0.1% v/v DMSO, -SB), then further treated for 15 mins with 25 ng/ml VEGF (V) or no addition (C). Cells were lysed, blotted and probed with the indicated antibodies.

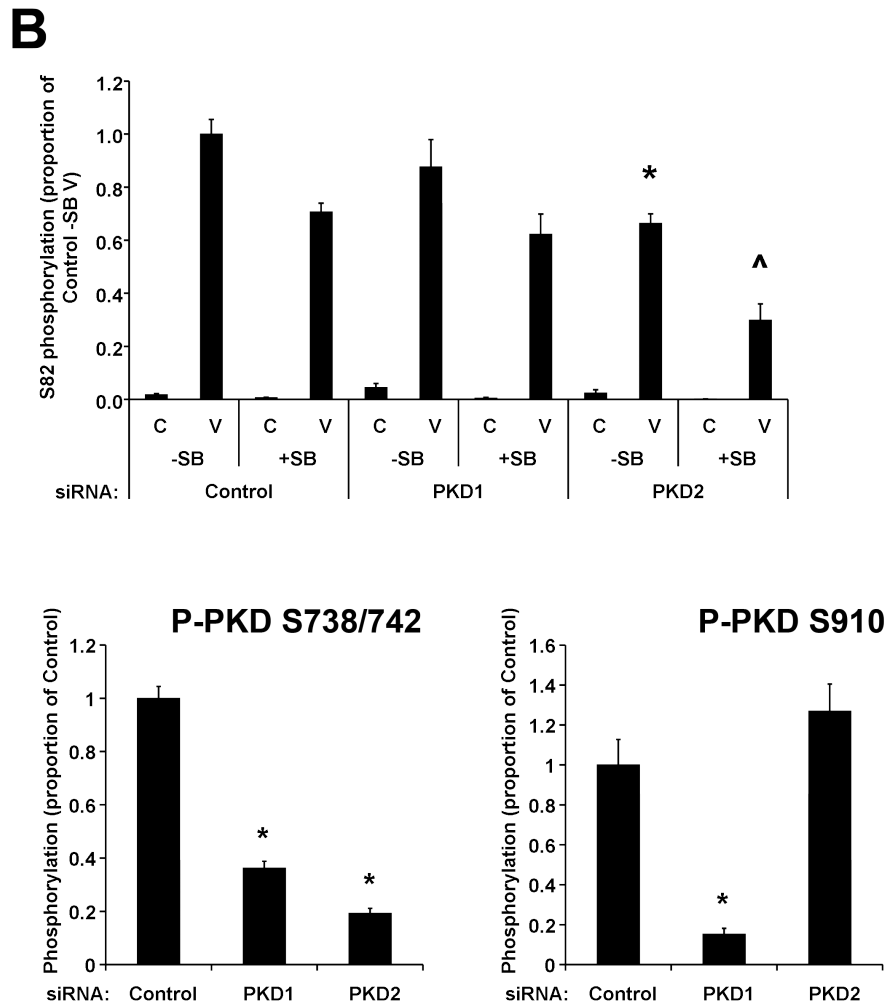

Figure 4.23: Effect of PKD knockdown on VEGF-induced Hsp27 and PKD phosphorylation (continued)

B. Upper: Quantification of the effect of PKD siRNAs on Hsp27 S82 phosphorylation. Results are means ± SEM from three independent experiments. In the three experiments analysed, the PKD2 siRNA reduced Hsp27 expression by a mean of 23%. To correct for this change in Hsp27 expression, the densitometry-quantified S82 phosphorylation result was divided by the corresponding result for total Hsp27, and the S82 phosphorylation/total Hsp27 ratio was used for graphing and statistical analysis. Statistical analysis via two-way ANOVA with Bonferroni's test for multiple pair-wise comparisons. * $p<0.01$ compared to control siRNA -SB, ^ $p<0.001$ compared to control siRNA +SB. Mean PKD2 knockdown was 90% compared to control siRNA, PKD1 knockdown was not be assessed due to the lack of a PKD1-specific antibody and the proximity of the PKD1- and PKD2-reactive bands in the total PKD blot, but the upper (PKD1) band detected in the total PKD blot was visually confirmed as substantially reduced in each experiment.

Lower: Quantification of the effect of PKD siRNAs on PKD phosphorylation. Results are derived from the same samples used for the Hsp27 S82 data, using only data from cells treated with VEGF in the absence of SB203580. Statistical analysis via one-way ANOVA with Bonferroni's test for multiple pair-wise comparisons. * P-S738/742: $p<0.001$ for control siRNA vs PKD1 or PKD2 siRNAs. * P-S910: $p<0.01$ for control siRNA vs PKD1 siRNA.

PKD2 siRNA (27% increase, non-significant), indicating that this antibody recognises PKD1 but not PKD2. These results are unsurprising given the high conservation of residues surrounding the activation loop phosphorylation sites, but low conservation of residues around the C-terminal phosphorylation site (figure 1.14).

4.4.5 Effect of siRNAs used in this study on non-target proteins

While siRNAs are designed to specifically reduce expression of a target gene, other genes may also be affected, complicating results. Recent studies reported that siRNAs targeting PKD2 and PKCϵ reduce expression of VEGFR2 (discussed below). To examine the possibility that the siRNAs used in this study may be affecting expression of other key proteins related to Hsp27 phosphorylation, the effect of these siRNAs on a variety of targets was examined. The siRNAs targeting PKD1, PKD2 and PKCϵ all reduced VEGFR2 expression (figure 4.24). Other siRNAs may have also slightly affected expression of some other proteins examined, although the consistency of these effects was not examined further.

4.4.6 Protein kinase D2 is able to directly phosphorylate Hsp27 at S82 only

Results from PKD siRNAs indicated that PKD2 is involved in VEGF-stimulated phosphorylation of Hsp27 S82 but not S15 or S78. Although data using phospho-specific antibodies to PKD showed that VEGF stimulated PKD phosphorylation, the effect of VEGF on PKD kinase activity was not examined using these experiments. To study the ability of VEGF to activate PKD2, and determine whether PKD2 is able to directly phosphorylate Hsp27 at S82, PKD2 was immunoprecipitated from VEGF-treated cells and mixed with recombinant Hsp27-GST fusion protein in vitro in an immune complex kinase assay.

PKD2 immunoprecipitated from HUVECs treated for 15 mins with VEGF phosphorylated recombinant Hsp27 at S82 in vitro in a time-dependent manner (figure 4.25). PKD2 immunoprecipitated from cells not treated with VEGF also phosphorylated Hsp27 at S82 but the rate of phosphory-

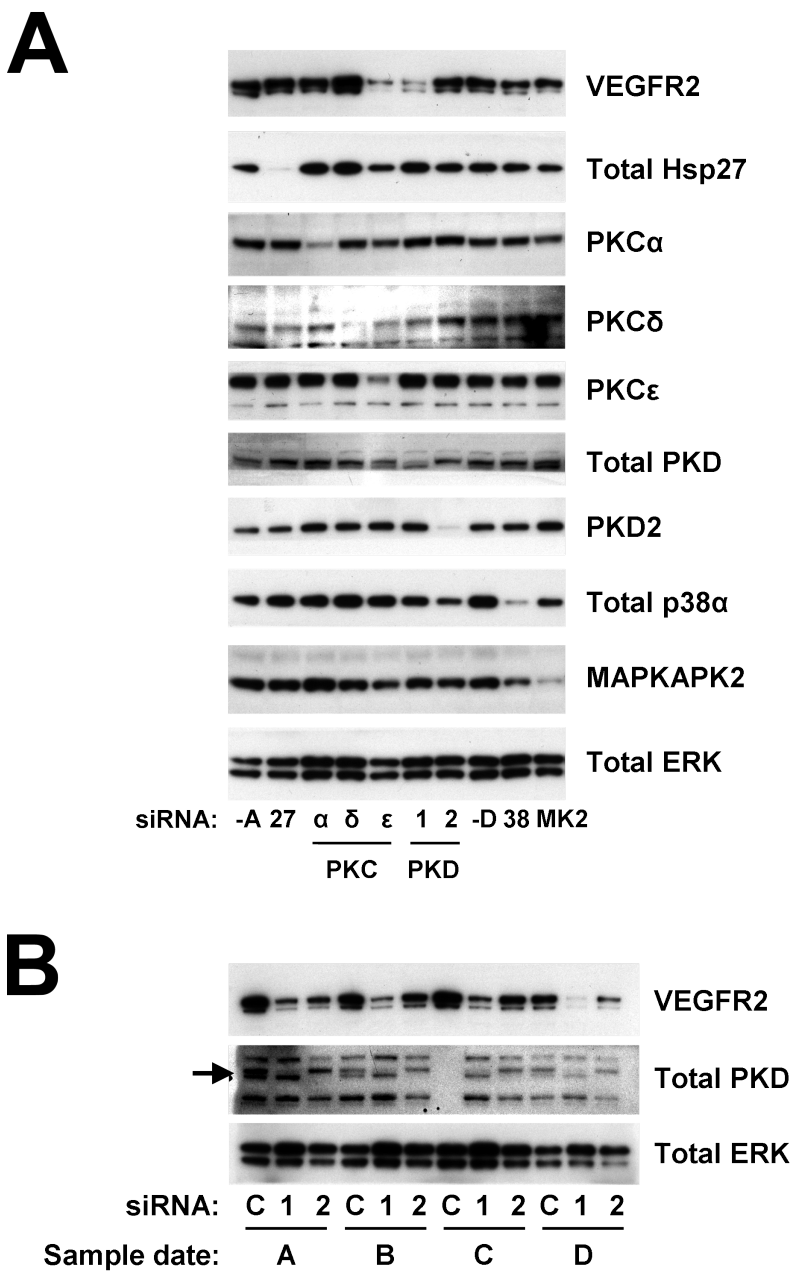

Figure 4.24: Effects of siRNAs on expression of selected proteins
A. HUVECs were treated for 48 h with 200 nM of the indicated siRNA, and were then lysed, blotted and probed with the indicated antibodies. siRNA abbreviations are: -A, Ambion non-targeting siRNA (control for all siRNAs used in this experiment except p38α and MAPKAPK2); 27, Hsp27 siRNA; -D, Dharmacon non-targeting siRNA (control for p38α and MAPKAPK2 siRNAs); 38, p38α siRNA. Data is from a single experiment, PKCϵ effect on VEGFR2 is representative of two independent experiments.
B. HUVECs were treated for 48 h with 200 nM siRNA targeting PKD1 (1), PKD2 (2), or a non-targeting control siRNA (C), and were then lysed, blotted and probed with the indicated antibodies. The total PKD doublet is indicated with an arrow. Samples from four independent experiments (A–D) are shown on the same blot for comparison. Insufficient lysate was available to run the total PKD blot for the date C, control siRNA sample – this lane is empty. This sample was blotted for total ERK and VEGFR2, as indicated.

lation was lower. Immunoprecipitated PKD2 did not phosphorylate Hsp27 at either S15 or S78. These data indicate PKD2 is able to phosphorylate Hsp27 at S82 in vitro, and that the Hsp27-phosphorylating activity of PKD2 is increased after VEGF stimulation. Similar experiments were not performed for PKD1 due to the lack of a PKD1-specific antibody.

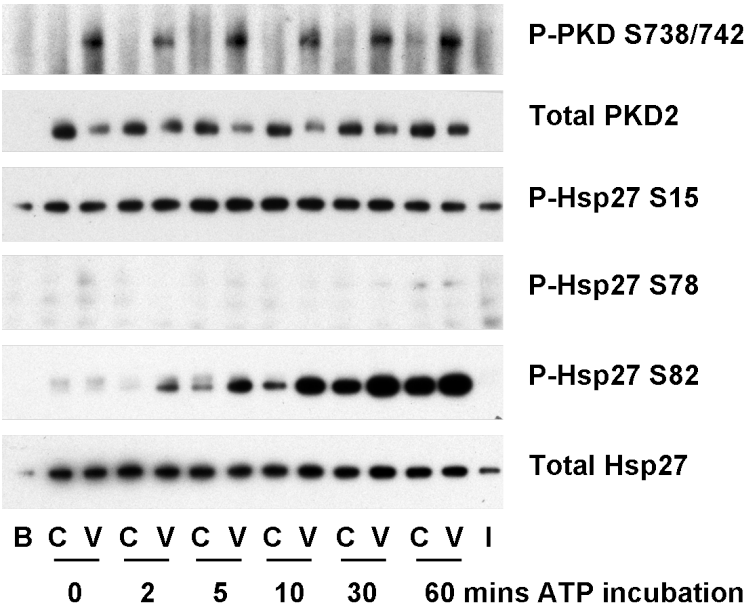

Figure 4.25: Protein kinase D2 can phosphorylate Hsp27 in a VEGF-dependent manner Confluent HUVECs were treated for 15 mins with either 25 ng/ml VEGF (V) or no addition (C). Cells were lysed and PKD2 was immunoprecipitated and incubated with Hsp27-GST and ATP in an immune complex kinase reaction. At the indicated times, an aliquot of the reaction mixture was removed and the reaction was quenched. Aliquots were subjected to immunoblotting with the indicated antibodies. B, beads only control (no immunoprecipitating antibody); I, control non-targeting IgG antibody. The band detected by the P-S15 antibody does not increase with ATP incubation time, and therefore does not apparently represent Hsp27 S15 phosphorylation by immunoprecipitated PKD. Results are representative of two independent experiments.

4.5 PKC mediates VEGF-stimulated Hsp27 S82 phosphorylation in Human Coronary Artery Endothelial Cells

The role of PKC in VEGF-stimulated Hsp27 phosphorylation was also examined in Human Coronary Artery Endothelial Cells (HCAEC). In initial studies, VEGF stimulated phosphorylation of Hsp27 and PKD in a concentration-dependent manner (figure 4.26A). Treatment of HCAEC with 25 ng/ml VEGF for 15 mins induced phosphorylation of Hsp27 at S15, S78 and S82; PKD at

S738/742 and S910; ERK1/2; and p38 MAPK, and these phosphorylations were inhibited by the VEGFR2 kinase inhibitor SU5614 (figure 4.26B). The VEGFR1 ligand PlGF1 did not increase phosphorylation of any molecule examined.

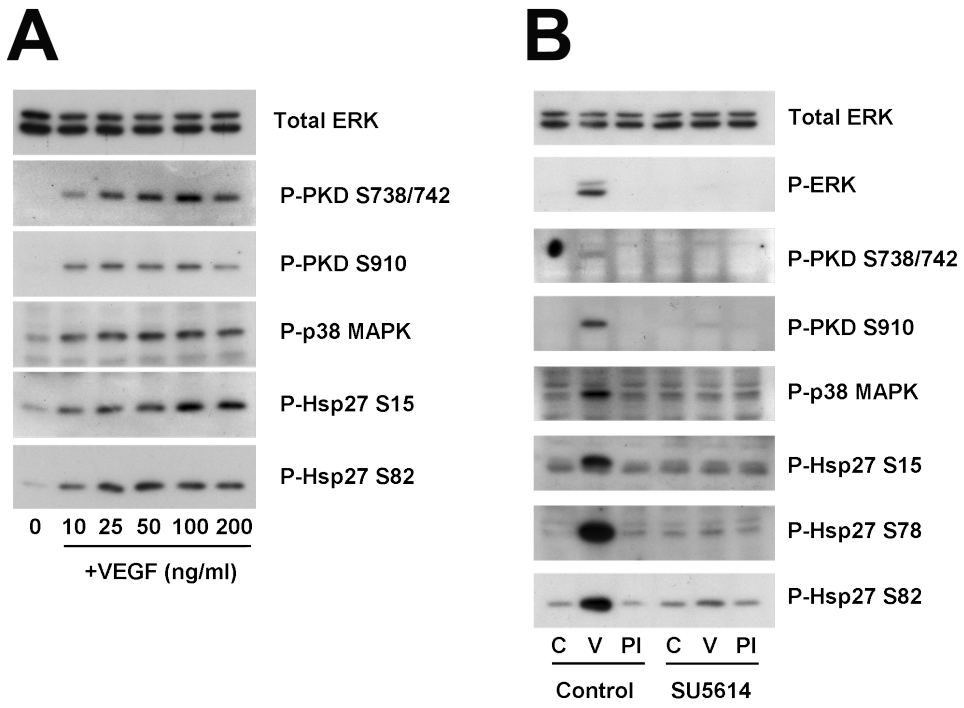

Figure 4.26: Initial characterisation of VEGF-induced phosphorylation of Hsp27 and PKD in human coronary artery endothelial cells
A. Effect of different VEGF concentrations on phosphorylation of Hsp27 and PKD. Serum-deprived, confluent HCAEC were incubated with the indicated concentrations of VEGF for 15 mins, before subsequent lysis and immunoblotting with the indicated antibodies. Results are from a single experiment.
B. Effect of the VEGF receptor tyrosine kinase inhibitor SU5614 on phosphorylation of Hsp27 and PKD. Serum-deprived, confluent HCAEC were incubated for 30 mins in the presence of 5 μM SU5614 or solvent alone (0.1% DMSO, control). Cells were then treated for 15 mins with no addition (C), 25 ng/ml VEGF (V) or 25 ng/ml PlGF1 (Pl) before lysis and blotting with the indicated antibodies. Results are from a single experiment.

The effects of inhibition of p38 MAPK and PKC on VEGF-induced phosphorylation of Hsp27 and p38 MAPK in HCAEC are shown in figure 4.27. GF109203X strongly reduced PKD phosphorylation at S738/742 and partially inhibited PKD phosphorylation at S910, whereas Gö6976 and SB203580 had no apparent effect on PKD phosphorylation.

SB203580 abrogated TNFα-stimulated phosphorylation of Hsp27 at S15, S78 and S82 and VEGF-induced phosphorylation at S15 and S78, but had little effect on VEGF-stimulated S82 phos-

phorylation. An SB203580/GF109203X combination dramatically reduced VEGF-stimulated Hsp27 S82 phosphorylation, and an SB203580/Gö6976 combination also strongly reduced VEGF-stimulated S82 phosphorylation, but to a lesser extent than the SB203580/GF109203X combination.

In summary, in HCAEC similar to the results from HUVECs, VEGF-induced Hsp27 S15 and S78 phosphorylation is blocked by p38 MAPK inhibition, whereas S82 phosphorylation is resistant to p38 MAPK inhibition, and a PKC-mediated pathway is likely to be responsible for p38 MAPK-independent S82 phosphorylation.

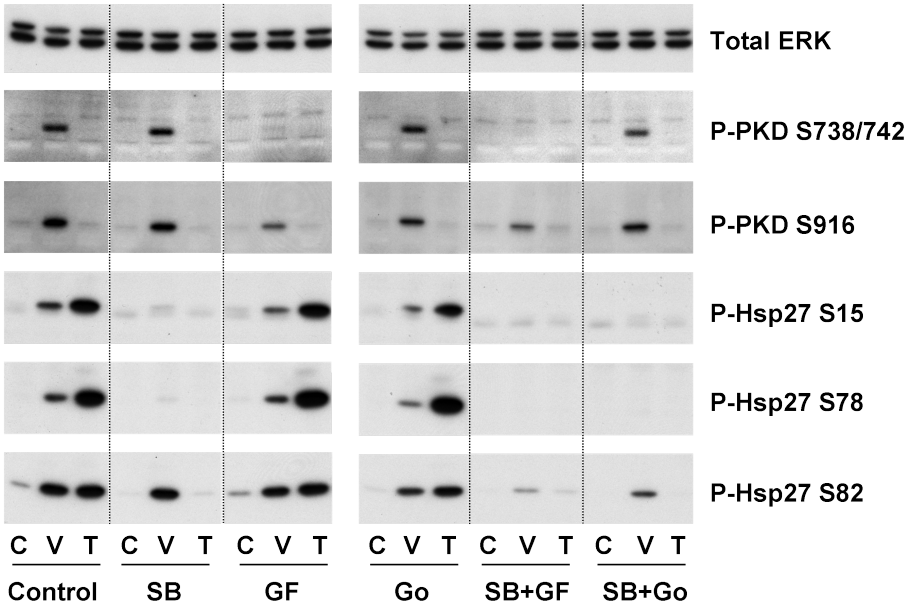

Figure 4.27: Effect of p38 and PKC inhibition on VEGF-stimulated Hsp27 phosphorylation in HCAEC
HCAECs were pre-incubated with solvent alone (0.1% v/v DMSO, Control), 5 μM SB203580 (SB), 3 μM GF109203X (GF), 1 μM Gö6976 (Go), or the indicated combinations of inhibitors. Cells were then treated for a further 15 mins treatment with 25 ng/ml VEGF (V), 100 U/ml TNFα (T), or no addition (C) and lysed. Lysates were analysed by western blotting with the indicated antibodies. Results are representative of two independent experiments. The dotted line indicated that lanes were digitally removed from the blot, but the remaining lanes were from the same membrane. The gap between lanes indicate that samples were from different membranes (due to a lack of available lanes), but were from the same experiment.

4.6 Discussion

As reported in chapter 3, alteration in the 2-D spot pattern of Hsp27 was a major observable change induced in the HUVEC proteome by 10 mins VEGF treatment, consistent with VEGF stimulating phosphorylation of Hsp27. Hsp27 is a highly abundant protein in HUVECs, and changes in a number of other early signalling proteins known to be phosphorylated in response to VEGF treatment (e.g. ERK, PI-3-K) were not detected on silver stained gels (section 3.2).

At the outset of this thesis, VEGF-stimulated phosphorylation of Hsp27 in endothelial cells had been reported to occur via a p38 MAPK/MAPKAPK2-mediated pathway (Rousseau *et al.* 1997), similar to the Hsp27-phosphorylating pathway activated by 'stress' stimuli such as H_2O_2, TNFα, IL-1, osmotic stress, anisomycin and others. In this chapter it has been shown that VEGF-stimulated Hsp27 S82 phosphorylation occurs via a PKC- and PKD-dependent pathway and is relatively independent of p38 MAPK, differing from the findings of Rousseau *et al.* (1997). In contrast, a p38 MAPK-dependent pathway is responsible for VEGF-stimulated phosphorylation of Hsp27 at S15 and S78, and for TNFα- and H_2O_2-stimulated phosphorylation at S15, S78 and S82. VEGF also stimulates a PKC-dependent, p38 MAPK-independent pathway to phosphorylate Hsp27 at S82 in HCAEC, indicating that this pathway is not restricted to HUVECs.

4.6.1 The major Hsp27 form produced after VEGF stimulation is phospho-S82 Hsp27

Blots with phospho-specific antibodies indicated that 15 mins VEGF treatment of HUVECs causes Hsp27 phosphorylation at S15, S78 and S82. Western blots of 2-D gels showed that Hsp27 occurs as two major 2-D-resolvable forms in VEGF-stimulated endothelial cells. Alkaline phosphatase treatment indicated that the basic form is likely to be unphosphorylated whereas the acidic form is phosphorylated. Analysis of Hsp27 by blotting with phospho-specific antibodies or by tandem mass spectrometry indicated that the acidic form is phosphorylated at S82, but not at S15 or S78.

Furthermore, 2-D western blot analysis of SB203580-treated HUVECs indicated that the relative amount of Hsp27 present in the acidic (phosphorylated) form was not altered by p38 MAPK inhibition, which prevents S15 and S78 phosphorylation but not S82 phosphorylation (discussed below), suggesting that the majority of the VEGF-increased acidic form of Hsp27 is phosphorylated at S82 only. Detection of unphosphorylated S82-containing peptides from the acidic Hsp27 form may have been generated by spontaneous dephosphorylation of an originally phosphorylated peptide, known to occur during MS procedures, or may have been due to the presence of Hsp27 phosphorylated at another residue.

Overall, it appears that the major new form of Hsp27 produced after 15 mins VEGF stimulation is mono-phosphorylated at S82, with around half of Hsp27 apparently remaining unphosphorylated. While this pattern may be characteristic of the treatment times employed in these experiments, time course studies showed that VEGF-stimulated Hsp27 phosphorylation at S15 and S78 did not alter substantially between 10–20 mins VEGF treatment and was reduced outside these times, suggesting that 15 mins VEGF treatment should induce approximately maximal phosphorylation at all three Hsp27 residues. Other studies have shown that anisomycin, heat shock and lipopolysaccharide cause much larger changes in Hsp27 phosphorylation, with almost all Hsp27 converted into phosphorylated forms (Saklatvala *et al.* 1991; Landry *et al.* 1992; Kotlyarov *et al.* 1999). VEGF may activate p38 MAPK/MAPKAPK2 to a lesser extent when compared to these stimuli. In agreement with this work, data from this thesis showed that p38 MAPK is more highly phosphorylated after anisomycin treatment than after VEGF treatment, which is reflected in greater anisomycin-stimulated phosphosphorylation of Hsp27 at S15 and S78 than was induced by VEGF.

Interestingly, the major spot detected by the P-S78 antibody was more acidic than the major spot detected by the P-S82 antibody, suggesting that P-S78-containing Hsp27 is multiply phosphorylated whereas P-S82-containing Hsp27 contains fewer phosphate groups (probably one, at S82). The absence of Hsp27 mono-phosphorylated at S78 may be due to a requirement for Hsp27 to be phosphorylated at S82 before S78 phosphorylation can occur, possibly due to opening up of

dimerised Hsp27 to allow enzyme access to other residues. Alternatively, the particular phosphorylation pattern observed may be characteristic of the VEGF treatment time used for the 2-D studies (15 mins), with shorter or longer treatment times altering the degree of phosphorylation on S15, S78 and S82.

4.6.2 VEGF stimulates a p38/MAPKAPK2-independent pathway to phosphorylation Hsp27 at S82

A number of groups have reported inhibition of Hsp27 phosphorylation in response to stress stimuli, such as TNFα and H_2O_2, by inhibition of the p38 MAPK/MAPKAPK2 pathway (discussed in section 1.5.3), and in this chapter the p38 MAPK inhibitor SB203580 abrogated Hsp27 phosphorylation at S15, S78 and S82 induced by these stimuli. While SB203580 prevented VEGF-stimulated phosphorylation of S15 and S78 in HUVECs, it was surprising that it showed relatively little effect on S82 phosphorylation. This is in contrast to the findings of Rousseau *et al.* (1997), also working in HUVECs, who reported that SB203580 largely prevented VEGF-stimulated incorporation of phosphate into Hsp27.

In this study SB202190, structurally related to SB203580, displayed a similar pattern of activity to SB203580. Additionally, siRNA-mediated knockdown of either p38α or MAPKAPK2 inhibited VEGF-stimulated phosphorylation of S15 and S78, and TNFα-stimulated phosphorylation at all three phosphorylation sites, but had no effect on VEGF-stimulated S82 phosphorylation.

In vitro, MAPKAPK2 phosphorylates S82 at a far higher rate than S78 or S15 based on the incorporation of radioactive phosphate into Hsp27 in an immune complex kinase assay (Stokoe *et al.* 1992b), and it is possible that the dose of SB203580 used in this study (5 μM) is too low to inhibit p38 sufficiently to prevent S82 phosphorylation. However, the phosphorylation of S82 by H_2O_2, TNFα and IL-1β (which stimulate Hsp27 S82 phosphorylation to a similar degree to VEGF) is almost completely blocked by SB203580. Indeed phosphorylation of Hsp27 by the protein synthesis anisomycin (10 μM), which induces phosphorylation of p38 MAPK and Hsp27 S78 to a much

greater extent than VEGF, and therefore is likely a stronger activator of p38 MAPK, is completely inhibited by 5 μM SB203580. SB203580 doses up to 25 μM and longer pre-incubation times with this inhibitor could not further reduce VEGF-stimulated S82 phosphorylation, suggesting its lack of effect is not due to insufficient dose. Furthermore, 1 μM SB203580 was sufficient to fully prevent the VEGF-induced phosphorylation of the downstream effector of p38 MAPK, MAPKAPK2 (the upper band in figure 4.9A), suggesting that the dose of SB203580 employed in these experiments (5 μM) is likely to be sufficient to prevent p38-mediated activation of MAPKAPK2. These data also suggest that MAPKAPK2 is unlikely to be involved in the p38-independent phosphorylation of S82. Overall, doses of SB203580 sufficient to inhibit MAPKAPK2 phosphorylation and Hsp27 phosphorylation by TNFα, H_2O_2 and IL-1β only partially reduce VEGF-stimulated Hsp27 S82 phosphorylation, indicating that VEGF activates a p38/MAPKAPK2-independent pathway which causes phosphorylation of Hsp27 at S82.

A number of isoforms of p38 MAPK and MAPKAPK2 exist (discussed in section 1.6.1). SB203580 is an inhibitor of the α and β isoforms of p38, but γ and δ forms of this protein also exist and a lack of effect with this inhibitor does not preclude the involvement of these additional forms. Indeed, p38δ mRNA is present in HUVECs, and overexpressed p38δ was activated by VEGF (Yashima *et al.* 2001). However, the same authors showed that p38δ appeared to be activated more strongly by TNFα than by VEGF, as determined by an immune complex kinase assay of the transcription factor ATF2. As TNFα-induced Hsp27 phosphorylation can be completely blocked by SB203580, this suggests that p38δ may not be important in Hsp27 phosphorylation in HUVECs. Indeed, p38α appeared to be the major p38 MAPK isoform activated by VEGF stimulation of HUVECs as siRNA-mediated p38α knockdown abrogated p38 MAPK activation loop phosphorylation as detected by an antibody which cross-reacts with all p38 MAPK isoforms. MAPKAPK3 may be involved in Hsp27 phosphorylation, but MAPKAPK2 and MAPKAPK3 are reported to be very similar, and the activity of both MAPKAPK2 and MAPKAPK3 can be prevented by SB203580 in response to a variety of stress stimuli (Clifton *et al.* 1996).

TNFα-stimulated phosphorylation of Hsp27 occurred via p38α and MAPKAPK2, as siRNAs against these proteins reduced TNFα-stimulated Hsp27 phosphorylation, and this is in agreement with the isoforms previously reported to be involved in Hsp27 phosphorylation (Adams *et al.* 2000; Ronkina *et al.* 2007). Indeed, phosphate incorporation into Hsp27 induced by UV, anisomycin and H_2O_2 was completely absent in p38α-null cardiomyocytes (Adams *et al.* 2000), indicating that p38α is essential for Hsp27 phosphorylation induced by these stimuli and other enzymes are unable to compensate. In contrast, the phorbol ester PMA stimulated Hsp27 phosphorylation in p38α-null cardiomyocytes, clearly indicating that a p38α-independent pathway, which can be activated by PMA but not by 'stress' stimuli exists, at least in cardiomyocytes.

Expression of p38α and MAPKAPK2 appeared to be interdependent. p38 MAPK knockdown significantly reduced MAPKAPK2 expression, and two different MAPKAPK2 siRNAs strongly reduced p38α expression, suggesting this is unlikely to be due to an off-target effect of the MAPKAPK2 siRNA. The co-regulation of p38 MAPK and MAPKAPK2 protein expression has been previously reported (Sudo *et al.* 2005; Kotlyarov *et al.* 2002, discussed in section 1.6.1.1).

4.6.3 PKC and PKD are involved in VEGF-stimulated, p38 independent phosphorylation of Hsp27 at S82

4.6.3.1 PKC inhibitors

Despite the known ability of phorbol esters and other PKC activators to induce Hsp27 phosphorylation, the involvement of PKC in Hsp27 phosphorylation appears to have been largely ignored after two findings: phorbol ester-induced PKC downregulation was shown to be ineffective in preventing Hsp27 phosphorylation induced by various stimuli including TNFα and, in HUVECs, interleukin-1 (Saklatvala *et al.* 1991), and MAPKAPK2 was shown to phosphorylate Hsp27 at a greater rate than PKC in vitro (Gaestel *et al.* 1991; Stokoe *et al.* 1992b).

The ability of PMA to stimulate Hsp27 phosphorylation in p38α-null cardiomyocytes (Adams

et al. 2000) suggested that PKC may mediate a p38-independent Hsp27-phosphorylating pathway. In agreement with this interpretation, in this chapter PMA stimulated Hsp27 S82 phosphorylation which was not prevented by SB203580. Interestingly, PMA only slightly increased phosphorylation of Hsp27 at S15 and S78 and had little effect on p38 MAPK activation loop phosphorylation, suggesting that the PMA-activated pathway stimulated Hsp27 phosphorylation at S82 specifically.

In this chapter, an inhibitor screen identified the broad specificity PKC inhibitor GF109203X as able to reduce VEGF-induced phosphorylation of Hsp27 at S82. When cells were pre-incubated with a combination of SB203580 and GF109203X, VEGF-induced S82 phosphorylation was almost completely blocked, indicating the additional pathway to phosphorylate Hsp27 involves PKC. The PKC involved in VEGF-stimulated S82 phosphorylation is unlikely to be an atypical isoform, as long-term PMA treatment (which does not downregulate the non-phorbol ester binding atypical isoforms) prevented phosphorylation of S82 induced by VEGF, but did not affect the ability of TNFα to cause phosphorylation of this residue. An SB203580/GF109203X combination was more effective than SB203580 in combination with the inhibitor of conventional PKC isoforms, Gö6976. Higher doses of both compound caused a greater degree of inhibition of VEGF-stimulated S82 phosphorylation, although whether this was due to more complete inhibition of target PKC isoforms or inhibition of other enzymes was not clear. However the standard concentrations used in this chapter (3 μM GF109203X, 1 μM Gö6976) were comparable to those used in published literature and identical to those previously used to treat HUVECs in this laboratory (Gliki *et al.* 2001).

At the standard doses used, GF109203X and Gö6976 did not affect p38 MAPK activation loop phosphorylation, nor did they reduce Hsp27 phosphorylation stimulated by TNFα or H_2O_2, indicating that they do not affect the p38/MAPKAPK2 pathway. However, long-term PMA treatment did reduce VEGF-stimulated phosphorylation at S15. This inhibition of VEGF-stimulated S15 phosphorylation after long-term PMA treatment may not be occurring via reductions in PKC activity, as PKC inhibition by GF109203X did not reduce S15 phosphorylation, and short-term PMA

treatments did not cause an increase in S15 phosphorylation. In addition to PKCs, other proteins also contain C1 domains and so are able to bind to and be influenced by phorbol esters (Colon-Gonzalez and Kazanietz 2006), leading to non-PKC effects of PMA administration.

A C1 domain-containing proteins may regulate the activity or expression of components of the p38 pathway. However, VEGF-stimulated S15 phosphorylation is more affected that TNFα-stimulated phosphorylation, suggesting a component upstream of p38 regulated by VEGF but not TNFα may be important. SiRNA-mediated downregulation of PKCϵ has recently been reported to reduce VEGFR2 expression and so VEGF-stimulated signalling (Rask-Madsen and King 2008, discussed below), and PMA-stimulated downregulation of PKCϵ and so VEGFR2 (or other VEGF signalling components) may contribute to the prevention of VEGF-stimulated Hsp27 phosphorylation by previous long-term PMA treatments.

Despite the involvement of PKC in VEGF-stimulated Hsp27 S82 phosphorylation, a p38 MAPK-dependent pathway also apparently contributes to phosphorylation of this residue. 10 μM GF109203X, the maximum dose used without a noticeable effect on VEGF-stimulated p38 activation loop phosphorylation, inhibited Hsp27 S82 phosphorylation to a lesser extent than an SB203580/GF109203X combination. Additionally, SB203580 and SB202190 consistently reduced VEGF-stimulated phosphorylation at S82, although the extent of this reduction was variable between experiments but always much lower than that the reduction observed with TNFα or H_2O_2-induced phosphorylation and was apparently little increased at higher inhibitor concentrations. The involvement of p38 MAPK in VEGF-stimulated Hsp27 S82 phosphorylation is unsurprising given that VEGF activates both PKCs and p38 MAPK, and the ability of p38 MAPK to phosphorylate S82.

4.6.3.2 PKC siRNAs

SiRNA-mediated downregulation of PKCα, δ or ϵ affected VEGF-stimulated Hsp27 phosphorylation. The results from these experiments are difficult to interpret, due to the effect of siRNAs

on other proteins including VEGFR2 and other PKC isoforms – knockdown of any of the PKCs significantly affected the expression of other PKC isoforms.

After almost all the experiments described in this chapter had been performed, Rask-Madsen and King (2008) reported that knockdown of PKCϵ by two different siRNAs (both different in sequence to the PKCϵ siRNA used in this thesis) reduced VEGFR2 expression and VEGF-stimulated phosphorylation of VEGFR2, ERK and Akt, and VEGF-stimulated DNA synthesis in BAECs. My subsequent experiments indicated that the PKCϵ siRNA used in this study also strongly reduced VEGFR2 expression, complicating the interpretation of the effects of the PKCϵ siRNA on VEGF-stimulated responses.

Rask-Madsen and King (2008) also reported that separate knockdown of PKCs α, δ and ϵ did not affect the expression of the other two PKC isoforms, and it is possible that the effects of PKC knockdown on the expression of other PKCs observed in this thesis were specific to the particular siRNAs used (e.g. via direct effects on non-target enzymes).

The influence of the PKCα siRNA in particular varied depending on whether or not the phospho-Hsp27 signal was corrected to total Hsp27 protein levels, which were apparently increased by the PKCα siRNA, although total protein normalisation before blotting was not performed (loading control total ERK appeared similar across all siRNAs). Hsp27 performs multiple cellular roles including a chaperone function, and is likely to be present in large quantities in the cytoplasm in case of need. The majority of Hsp27 in the cell may not have any signalling function, and so correction to total Hsp27 levels may be misleading, with the absolute quantity of phosphorylated Hsp27 being important for downstream signalling and/or cellular activity rather than the proportion of cellular Hsp27 phosphorylated.

The results with the PKCδ siRNA are somewhat surprising given that PKCδ is apparently responsible for PKD activation (discussed below) – a reduction in PKCδ protein levels sufficient to reduce PKD activation after VEGF treatment apparently had only a minor effect on VEGF-stimulated Hsp27 S82 phosphorylation, but a greater effect on VEGF-stimulated phosphorylation

of Hsp27 at S15 and S78. S15 and S78 do not conform to the believed PKD consensus phosphorylation site motif (Doppler *et al.* 2005), and were not detectably phosphorylated by immunoprecipitated PKD2 in an in vitro kinase assay. It is likely that the involvement of PKCα and/or PKCδ in phosphorylation of these sites is independent of PKD, either via direct phosphorylation of Hsp27 or by regulation of another Hsp27-phosphorylating kinase or an Hsp27 phosphatase. The effect of siRNA-mediated PKC isoform knockdown on p38 MAPK phosphorylation was not examined in detail, but various doses of the PKC inhibitors GF109203X up to 15 μM and Gö6976 up to 5 μM apparently had little effect on p38 MAPK phosphorylation. However, inhibition of VEGF-stimulated p38 MAPK activation loop phosphorylation by GF109203X has been reported previously (Yashima *et al.* 2001). PKCs may be involved in p38 MAPK-independent regulation of MAPKAPK2 activity, or may directly phosphorylate Hsp27. Direct phosphorylation of Hsp25 at S15 and S86 by PKCδ in an in vitro kinase assay has previously been reported (Lee *et al.* 2005).

The lack of effect of PKCδ knockdown on VEGF-stimulated Hsp27 S82 phosphorylation may be related to the knockdown rather than knockout characteristics of siRNA-mediated protein reduction. For an effect to be observed, knockdown must reduce the quantity of an enzyme sufficiently for its activity to become rate limiting for the pathway. For enzymes controlled post-transcriptionally, e.g. by phosphorylation, this may be difficult to achieve as a large pool of enzyme may be present in the cell with activation of only a proportion of the total cellular pool required to transmit a maximal signal to downstream targets. A partial reduction in PKCδ protein levels may have only a minor effect on the VEGF-induced increase in PKCδ enzyme activity, as this enzyme is subject to post-transcriptional control mechanisms (e.g. activation by diacylglycerol) rather than pure transcriptional control.

Thus although PKCδ was reported to mediate VEGF-stimulated ERK phosphorylation (Gliki *et al.* 2001), in my studies PKCδ knockdown did not noticeably affect VEGF-stimulated ERK phosphorylation, perhaps due to spare capacity in the system and insufficient knockdown, or compensation by other enzymes.

Other potential reasons for the lack of effect of PKCδ knockdown on VEGF-stimulated S82 phosphorylation include compensation by the p38 MAPK/MAPKAPK2 pathway and compensation of by other PKC enzymes. In addition to the analysed effects of PKCα, PKCδ and PKCϵ, western blotting indicated that PKCζ is expressed in the HUVECs used in this study. Previous work on HUVECs using the same cell source and culture conditions in this study also detected PKCζ but did not detect translocation of this isoform in response to VEGF treatment (Gliki *et al.* 2001). PKCs α, β, δ, ϵ, η, θ, and ζ have been detected in HUVECs by western blotting (Yamamura *et al.* 1996).

ERK and Akt are important kinases in endothelial cells, and their effects were examined in initial inhibitor screens. Akt has been reported to phosphorylate Hsp27 in vitro (Rane *et al.* 2003), with VEGF-stimulated Akt activation occurring via activation of PI-3-K (Gerber *et al.* 1998b). The PI-3-K inhibitors wortmannin (100 nM) and LY294002 (50 μM), which prevent VEGF-stimulated Akt activation, had no effect on VEGF-stimulated Hsp27 S82 phosphorylation, when used either alone or in combination with SB203580. The MEK1/2 inhibitor U0126 (10 μM), which completely prevents VEGF-stimulated phosphorylation of ERK1/2, was also ineffective alone or in combination with SB203580. Thus VEGF-stimulated Hsp27 phosphorylation is apparently independent of ERK and Akt.

4.6.3.3 PKD

While the work in this thesis was under way, a purified recombinant preparation of PKD (the exact PKD form used was unclear) was shown to phosphorylate Hsp27 at S82 but not S15 in an in vitro kinase assay (Doppler *et al.* 2005). Activation of PKD has been reported to involve transphosphorylation of its activation loop serine residues (S738 and S742 in human PKD1) by upstream novel PKC isoforms (Waldron *et al.* 2001), leading to autophosphorylation at a C-terminal phosphorylation site (S910 in human PKD1) (Matthews *et al.* 1999).

The PKD family contains three enzymes, PKD1, PKD2 and PKD3. siRNA-mediated knockdown

of PKD2 reduced VEGF-stimulated Hsp27 S82 phosphorylation, indicating the involvement of PKD. In the presence of SB203580, PKD2 knockdown further reduced VEGF-stimulated S82 phosphorylation, indicating that PKD2-mediated phosphorylation of S82 occurs via a p38 MAPK-independent pathway.

PKD1 knockdown did not cause a statistically significant reduction in VEGF-stimulated Hsp27 S82 phosphorylation in my hands, but a co-worker in the laboratory (Dr. Ian Evans) did observe a reduction albeit to a lesser extent than for PKD2 knockdown (data not shown, reported in Evans *et al.* 2008), and data presented in this chapter shows a trend for a reduction in S82 phosphorylation. Possible reasons for this discrepancy between investigators are variations in the degree of PKD1 knockdown obtained (which was not measured due to the blotting antibody detecting a doublet) and variation in the amount of PKD1 versus PKD2 expression in the specific cells used, through differing cell batches or culture conditions such as degree of confluence or 'completeness' of serum withdrawal before treatment. Expression of PKD1 and PKD2 is apparently similar based on blotting with the total PKD antibody, but the recognition of the two isoforms by the antibody may vary.

The greater effect observed with PKD2 knockdown rather than PKD1 knockdown could be caused by a number of factors – better knockdown of PKD2 than PKD1, better ability of PKD2 to compensate for PKD1 loss than vice versa (or better ability of another enzyme e.g. PKD3 to compensate for PKD1 loss than PKD2 loss), or a functional distinction between PKDs giving a greater quantitative role for PKD2 in S82 phosphorylation, e.g. more PKD2 than PKD1 is activated in response to VEGF, or PKD2 but not PKD1 may associate with a scaffolding molecule which promotes PKD2/Hsp27 interactions.

Recently two papers by the same group reported that PKD2 knockdown by two different siRNAs reduced VEGFR2 expression in HUVECs, whereas PKD1 knockdown had no effect (Hao *et al.* 2009a,b). The siRNA sequences used in these studies were not reported, but were from a different manufacturer and so may be distinct to that used in this thesis. While my experiments indicated

that PKD2 knockdown did indeed reduce VEGFR2 expression, the PKD1 siRNA caused a far greater reduction in VEGFR2 expression. As others observed no effect of PKD1 knockdown (Hao *et al.* 2009a,b), it is possible that the effect is specific to the siRNA sequence used in this study.

The effects of PKD siRNAs on VEGFR2 expression may contribute to the effects of these siRNAs on VEGF-stimulated Hsp27 S82 phosphorylation, making it difficult to determine the contribution of PKD to VEGF-stimulated cellular signalling. However, the PKD1 siRNA had little effect on VEGF-stimulated Hsp27 phosphorylation despite a marked reduction in VEGFR2 expression. While this lack of effect is somewhat surprising, explanations are possible. Perhaps activation of only a small percentage of VEGF receptors is sufficient for maximal VEGF-stimulated Hsp27 phosphorylation, or becomes sufficient through some compensatory signalling or amplification mechanism when VEGFR2 expression is low.

The PKD family also contains PKD3, reported to be ubiquitously expressed, of a similar size to the other PKDs, activated by phorbol esters and predicted to be recognised by the S738/742 antibody (PKD3 does not have a serine residue corresponding to S910 in PKD1). Overexpression of PKD3 rescued phorbol ester-stimulated Hsp27 S82 phosphorylation in PKD-null cells (Liu *et al.* 2007, discussed below). Although I did not examine PKD3 in this thesis, a co-worker (Dr. Ian Evans) detected PKD3 in HUVECs via western blotting (reported in Evans *et al.* 2008), and another group has also reported that PKD3 is expressed in HUVECs (Hao *et al.* 2009a). Further investigation into the role of this isoform in endothelial cells, and the possibility that it also phosphorylates Hsp27, is warranted.

In the presence of both PKD2 siRNA and SB203580, 30% of VEGF-stimulated S82 phosphorylation was not prevented, substantially more than that not prevented by an SB203580/GF109203X combination. This may be due to incomplete knockdown of PKD2, compensation of PKD2 function by another PKD isoform such as PKD1, or the existence of a PKC-mediated but PKD independent pathway such as direct phosphorylation of Hsp27 by a PKC isoform. Incomplete inhibition of p38 MAPK is possible but less likely given the effectiveness of SB203580 against S15 and S78,

and S82 phosphorylation induced by other stimuli.

Originally characterised as an inhibitor of novel PKC isoforms, Gö6976 has been reported to inhibit mouse PKD/PKD1 kinase activity (Gschwendt *et al.* 1996; Rybin *et al.* 2009), and has been used as a human PKD1 inhibitor in endothelial cells (Hao *et al.* 2009a). However it is not clear whether Gö6976 inhibits other PKD isoforms in addition to PKD1 such as PKD2 and PKD3. An SB203580/Gö6976 combination was less effective in inhibiting VEGF-stimulated Hsp27 S82 phosphorylation than an SB203580/GF109203X combination, possibly due to incomplete PKD inhibition by Gö6976 (e.g. due to insufficient concentration or lack of PKD2/PKD3 inhibition by Gö6976) but more complete inhibition of upstream PKCs by GF109203X. However, 1 μM Gö6976 strongly inhibited reported PKD-dependent events in ECs, including production of some inflammatory cytokines and phosphorylation of various proteins including Hsp27 (at S82), and histone deacetylases (HDACs) 5 and 7, indicating that 1 μM Gö6976 is likely to be sufficient to inhibit PKD in ECs (Hao *et al.* 2009a; Ha *et al.* 2008a,b). A PKC-dependent but PKD-independent pathway for VEGF-stimulated Hsp27 S82 phosphorylation, such as direct phosphorylation of Hsp27 by non-classical PKCs, may also exist and contribute to the differences in inhibition by the SB203580/GF109203X and SB203580/Gö6976 combinations.

In this thesis, PKD1 S910 phosphorylation was unaffected by Gö6976 but reduced by GF109203X, suggesting on the surface that Gö6976 may be present in insufficient dose to inhibit PKD1. However, Rybin *et al.* (2009) have recently re-examined the relationships between PKD phosphorylation and activity, and their results (discussed below) indicate that considerably higher doses of Gö6976 are required to inhibit phosphorylation of S910 than are required to inhibit phosphorylation of exogenous substrates. Therefore, lack of inhibition of PKD S910 phosphorylation does not indicate that Gö6976 is an ineffectual PKD inhibitor. It is likely that PKD1 was inhibited by the Gö6976 dose used in this study, which was the same dose used by Hao *et al.* (2009a) to inhibit PKD1.

While this thesis was in progress, the importance of PKD in Hsp27 S82 phosphorylation was re-

ported by two other groups (Liu *et al.* 2007; Yuan and Rozengurt 2007). Phosphorylation of Hsp27 at S15 or S78 was not examined in either study. Liu *et al.* (2007) generated PKD knockouts of the B-lymphocyte cell line DT40, which normally expresses PKDs 1 and 3 but not PKD2. Knockout of both PKD isoforms completely prevented phorbol ester-stimulated Hsp27 S82 phosphorylation, suggesting that PKC-mediated Hsp27 S82 phosphorylation may occur entirely via PKD isoforms. Liu *et al.* (2007) also reported functional redundancy between PKD isoforms – knockout of either PKD1 or PKD3 did not fully inhibit Hsp27 S82 phosphorylation, and expression of tagged PKD3 in PKD1/PKD3 double knockout cells rescued phorbol ester-stimulated S82 phosphorylation. Clearly, the situation in human endothelial cells, which express PKD2 and may express different PKC isoforms to DT40 cells, may be different. Additionally, phorbol ester-stimulated Hsp27 S82 phosphorylation appeared lower in PKD1-null cells than in wild-type lymphocytes, although quantification was not reported, suggesting that functional redundancy between PKD isoforms may not be complete.

Yuan and Rozengurt (2007) described Neurotensin-stimulated phosphorylation of Hsp27 S82 via a PKC and PKD1/2-dependent pathway in the PANC-1 adenocarcinoma cell line, similar to the work presented in this chapter. Their paper showed that while Neurotensin-stimulated S82 phosphorylation occurred via PKC/PKD, anisomycin-stimulated S82 phosphorylation occurred solely via p38 MAPK, agreeing with the results presented here showing that different stimuli use different pathways to stimulate Hsp27 S82 phosphorylation. Similar to this study, Yuan and Rozengurt (2007) also showed that siRNA-mediated PKD1 or PKD2 knockdown reduced Hsp27 S82 phosphorylation, with a greater reduction in S82 phosphorylation observed when the p38 MAPK inhibitor SB202190 was also used. Yuan and Rozengurt (2007) observed a still greater reduction in Neurotensin-stimulated Hsp27 S82 phosphorylation when both PKD1 and PKD2 siRNAs were used in combination, in the presence of SB202190.

The role of PKD in VEGF-stimulated S82 phosphorylation appears to involve direct phosphorylation: PKD2 immunoprecipitated from VEGF-treated cells directly phosphorylated recombinant

Hsp27 at S82 but not S78 or S15 in vitro. It is not precluded that the PKD2 antibody immunoprecipitated another direct Hsp27 kinase such as MAPKAPK2. However, also given that Hsp27 S82 is a consensus phosphorylation site for PKD (Doppler *et al.* 2005), and that PKD2 knockdown reduces VEGF-stimulated Hsp27 phosphorylation, it is likely that direct phosphorylation does occur. A co-worker, Dr. Ian Evans, also showed that purified recombinant PKD1 directly phosphorylated Hsp27 in vitro at S82 (shown in Evans *et al.* 2008). Direct phosphorylation of Hsp27 S82 but not S15 by PKD was initially reported by Doppler *et al.* (2005). Selective phosphorylation of Hsp27 at S82 only via activation of PKD rather than p38 MAPK provides a mechanism of producing Hsp27 phosphorylated at S82 only. As discussed above, results from blotting of 2-D gels indicated that S82-mono-phosphorylated Hsp27 is the major form of Hsp27 obtained after VEGF treatment, and the p38 MAPK pathway does not appear to be responsible for most S82-phosphorylated Hsp27. Thus PKC/PKD-mediated phosphorylation of Hsp27 may be a major in vivo mechanism responsible for Hsp27 phosphorylation.

Interestingly, PKD activation does not necessarily seem to lead to Hsp27 phosphorylation. 100 μM H_2O_2 did not detectably increase phosphorylation of PKD at the activation loop or of PKD1 at S910, but stimulated Hsp27 phosphorylation. Higher doses of H_2O_2 (500 μM, 2.5 mM) stimulated PKD activation loop phosphorylation to a similar degree to VEGF, and p38 MAPK phosphorylation to a much greater degree, but Hsp27 phosphorylation was less than that observed at lower H_2O_2 doses. Furthermore, the Hsp27 phosphorylation caused by H_2O_2 doses able to detectably stimulate PKD phosphorylation was almost completely inhibited by SB203580. Thus H_2O_2-stimulated PKD phosphorylation (and presumably PKD activity) has little effect on Hsp27 phosphorylation.

In contrast to these results, Waldron and Rozengurt (2000) showed that 100 μM–10 mM H_2O_2 caused increased phosphate incorporation into PKD in 3T3 fibroblasts – higher H_2O_2 doses caused greater phosphate incorporation within a particular time. In HeLa, a 10 min treatment with 10 μM H_2O_2 stimulates PKD activation loop phosphorylation (Storz *et al.* 2004). In BAEC, 30 mins

treatment with 100 μM H_2O_2 or 5–60 mins with 500 μM H_2O_2 induced phosphorylation of PKD at the activation loop (Zhang *et al.* 2005b), whereas TNFα had no effect.

The reason for the inability of lower concentrations of H_2O_2 to induce PKD activation in this chapter is unclear. The variability of H_2O_2-stimulated Hsp27 phosphorylation was generally higher than observed with other treatments (the main reason for using TNFα rather than H_2O_2 in later experiments), despite trying multiple batches of H_2O_2 and always freshly preparing the working solution by dilution from the manufacturer-supplied concentrated stock solution immediately before use. It is possible that the time and dose of H_2O_2 used in this study were too low to activate PKD – activation loop phosphorylation was observed at higher H_2O_2 doses. Alternatively, expression of catalase, which breaks down H_2O_2, may be higher in the HUVECs used in this study than in BAEC or other cell types.

4.6.4 VEGF stimulates PKD activation loop phosphorylation via PKCδ

Knockdown of either PKCδ or PKCϵ, two novel PKC isoforms, reduced VEGF-stimulated phosphorylation of the PKD activation loop (S738/742 in PKD1). This data agrees with data from inhibitor studies – GF109203X, but not the inhibitor of classical PKC isoforms Gö6976, completely blocked VEGF-induced phosphorylation of PKD at S738/742, and long-term phorbol ester treatment prevented the VEGF-stimulated increase in phosphorylation at these residues. The effects of PMA on VEGF-stimulated PKD phosphorylation could be due to either direct effects of the phorbol ester on PKD, or phorbol ester receptor (e.g. PKC)-mediated effects, but are not due to downregulation of PKD as total PKD levels are unaffected by PMA treatment. As discussed earlier, these results do not necessarily indicate the involvement of PKCϵ in VEGF-stimulated PKD phosphorylation as PKCϵ knockdown reduces VEGFR2 expression.

The lack of effect of PKCα siRNAs on VEGF-stimulated PKD activation loop phosphorylation in this study is in contrast to previous work in bovine aortic endothelial cells which showed that overexpression of a dominant negative PKCα construct blocked VEGF-induced PKD phosphory-

lation, whereas a dominant negative PKCδ construct had no effect (Wong and Jin 2005). The same authors also showed that 100 nM Gö6976 completely blocked VEGF-induced PKD activation loop phosphorylation. In this study, does of Gö6976 up to 5 μM had no effect on PKD phosphorylation either at the activation loop or at the C-terminal site (S910 in PKD1). The variations between data presented in this thesis and Wong and Jin (2005) may be due to differential PKC isoform expression between endothelial cell types obtained from different species and vascular beds. However in this thesis, GF109203X but not Gö6976 blocked VEGF-induced PKD activation loop phosphorylation in human coronary artery endothelial cells. Wong and Jin (2005) also reported that PKCα (and PKD) siRNAs reduced VEGF-stimulated ERK phosphorylation in HUVECs, whereas previous work with HUVECs in this laboratory, using the same culture medium as used in this thesis, showed that the classical PKC inhibitor Gö6976 had no effect on VEGF-induced ERK phosphorylation (Gliki *et al.* 2001). For unknown reasons, the work of Wong and Jin (2005) shows a greater role for PKCα than has been observed in data from this laboratory.

The involvement of novel PKC isoforms, rather than classical PKCs such as PKCα, in PKD activation loop phosphorylation has been widely reported in a number of other cell types (Rozengurt *et al.* 2005). Using dominant negative approaches, PKCδ (and not PKCϵ or PKCζ) has been reported to be the PKC isoform responsible for PKD activation loop phosphorylation in thrombin- or angiotensin II-stimulated vSMCs (Tan *et al.* 2003, 2004).

4.6.5 Complications in interpretation of PKD activation data

While activation loop phosphorylation is reported to be an initial step in PKD activation, phosphorylation of a C-terminal site (S910 in PKD1) has been reported to be due to autophosphorylation of PKD and to correlate well with PKD kinase activity (Matthews *et al.* 1999), and has been widely used as a surrogate marker for PKD activity. Surprisingly, given its effect on activation loop phosphorylation, PKCδ knockdown was ineffective in preventing S910 phosphorylation, which was non-significantly reduced by the PKCϵ siRNA. Differences in PKD isoform specificity between

the PKD phospho-specific antibodies, and recent studies re-examining the involvement of PKD phosphorylation in its activity, may help explain this apparent discrepancy.

4.6.5.1 Isoform specificity of PKD antibodies

The PKD antibodies used in this thesis, while raised against PKD1 peptides, are not all specific for this isoform. PKD2 has a very similar molecular weight to PKD1 and although the immunising antigens used to raise these antibodies are proprietary, the P-PKD S738/742 antibody is expected to cross-react with PKD2 and PKD3 (Dr. Robert Somogyi, Cell Signalling Technology, personal communication), which is unsurprising given the high degree of amino acid sequence homology around these residues (figure 1.14). This cross-reactivity appeared to occur in practice, with both PKD1 and PKD2 siRNAs able to reduce the VEGF-increased signal detected by blotting with this antibody. The reason only a single band is detected when blotting VEGF-treated HUVECs with this antibody, rather than the doublet produced due to cross-reactivity of the total PKD antibody with PKD1 and PKD2, may be because on activation both PKD1 and PKD2 undergo a mobility shift to a similar apparent electrophoretic mobility.

In contrast, the residues at the extreme C-terminus of PKD1 are not well conserved between PKD1 and PKD2, and an equivalent serine residue does not appear to be present in PKD3 at all (figure 1.14), suggesting that this antibody may be PKD1 specific. Although again the immunising peptide was not reported, the manufacturer expected this antibody to be PKD1 specific based on comparison of PKD isoform amino acid sequences (Dr. Robert Somogyi, Cell Signalling Technology, personal communication). Indeed, the signal obtained from VEGF-treated cells with the S910 antibody was affected by siRNA directed against PKD1 but not PKD2, suggesting that this antibody may well be specific for PKD1.

4.6.5.2 Function of PKD phosphorylation sites

The distinction between S738/742 as PKC-phosphorylated sites and S910 as an autophosphorylation site reflecting PKD activity may be too simplistic. Rybin *et al.* (2009) have recently examined the influence of mouse PKD phosphorylation on its ability to phosphorylate known substrates. Agreeing with work presented here, the authors showed that 5 μM Gö6976 did not inhibit PMA-stimulated PKD1 S916 phosphorylation in cardiomyocytes, but additionally showed that this concentration of Gö6976 prevented phosphorylation of the cAMP response element binding protein (CREB) at S133, a phosphorylation the same group had previously reported was performed by PKD (Ozgen *et al.* 2008).

Rybin *et al.* (2009) used in vitro kinase assays to show that PKD1 S916 phosphorylation had a lower [ATP] requirement than phosphorylation of substrate proteins such as CREB, and suggested that S916 phosphorylation may occur via an intramolecular mechanism rather than the intermolecular mechanism used for PKD-mediated phosphorylation of substrate proteins, although the relative importance of this mechanism in vivo was not addressed. Thus, lack of inhibition of PKD S910 phosphorylation does not indicate that Gö6976 is an ineffectual PKD inhibitor, although which isoforms are inhibited and how fully is not clear. Low PKD2/PKD3 inhibition by Gö6976 may partially explain the difference between the effect of SB203580/GF109203X and SB203580/Gö6976 combinations on VEGF-stimulated Hsp27 S82 phosphorylation.

The same paper showed that an S744A/S748A PKD1 mutant autophosphorylates on S916 but overall the entire enzyme incorporates relatively little phosphate, does not undergo a mobility shift and is unable to phosphorylate the exogenous substrates CREB and cardiac troponin I (cTnI), clearly dissociating S916 phosphorylation from PKD kinase activity towards its substrate proteins. Basal autophosphorylation may explain why in some experiments S910 phosphorylation was detected in the absence of cytokine stimulation and/or the presence of PKC inhibitors in a band of slightly higher mobility than observed in VEGF-stimulated PKD (figure 4.20A, for example).

Uncoupling of S738/742 and S910 phosphorylation may partially explain why in work presented in this chapter, PKCδ knockdown reduces PKD activation loop phosphorylation but does not affect PKD S910 phosphorylation. Alternatively PKCδ and PKCϵ may phosphorylate different PKD isoforms, with PKCϵ-mediated phosphorylation making the major contribution to PKD1 phosphorylation (detected by the S910 antibody) and PKCδ mainly phosphorylating PKD2. A variety of other schemes could also explain the observed effects of PKC siRNAs on PKD phosphorylation, such as PKCδ phosphorylating all PKD isoform activation loops, and PKCϵ contributing to transphosphorylation of other sites including PKD1 S910.

Rybin *et al.* (2009) also reported that overexpression of S916A PKD1 substantially increased phorbol ester-stimulated phosphorylation of PKD substrates (including Hsp27 S82) and so is catalytically active, but did not become phosphorylated at S748 after phorbol ester stimulation, indicating that S916 phosphorylation is required for S748 phosphorylation, and S916 phosphorylation may occur via autophosphorylation. Phosphorylation of the other activation loop serine, S744, was unaffected in the S916A mutant, and was reported to correlate well with PKD1 kinase activity (in the absence of inhibitors such as Gö6976), although this residue may also be autophosphorylated. Thus the phosphorylation of S738 and S742 may diverge – the P-PKD S738/742 antibody used in this thesis has been reported to primarily recognise S738 phosphorylation in PKD1, and diverges from the signal produced by a new S742-specific antibody (Rybin *et al.* 2009).

The major method used by Rybin *et al.* (2009) was overexpression of a PKD enzyme in intact cells, followed by its immunoprecipitation and kinase activity analysis by in vitro kinase assays. Clearly, the loss of normal cell structure and regulatory proteins may affect the results obtained. Although a particular phosphorylation is possible in vitro, the prevalence of that pathway in vivo may be less clear. However these data indicate potential reasons for uncoupling of phosphorylations at S738, S742, S910, and uncoupling of these phosphorylations from PKD1 kinase activity.

Overall, it appears that the signal detected by the S738/S742 antibody correlates well with *total* PKD activity (including both PKD1 and PKD2 activity) in the absence of PKC inhibitors, and the

signal detected by the S910 antibody may reflect *PKD1* activity in the absence of PKC and PKD inhibitors. When PKCs are inhibited or downregulated (e.g. by siRNAs), other mechanisms may come into play, such as PKD activation loop autophosphorylation, which may reduce the observed effect of these treatments.

4.6.6 Summary

VEGF activates PKC-, PKD- and p38 MAPK-dependent pathways to stimulate phosphorylation of Hsp27 at S82. The apparently major PKD-dependent pathway occurs partly by VEGF-stimulated PKCδ activation leading to activation of PKD2, which then can directly phosphorylate Hsp27 at S82 but not at other residues. Identification of the VEGF/PKCδ/PKD2/Hsp27 S82 pathway does not preclude the possibility that other PKD isoforms may also phosphorylate Hsp27 at S82, or that another PKC-mediated pathway may also be involved in Hsp27 phosphorylation. A summary of the signalling pathways involved in Hsp27 phosphorylation is shown in figure 4.28.

Activation of the PKC/PKD pathway by VEGF generates S82 mono-phosphorylated Hsp27, the major Hsp27 form produced after VEGF stimulation. S82 mono-phosphorylated Hsp27 may perform a different cellular role to S15/S78/S82 triply-phosphorylated Hsp27, for example by interacting with different proteins, causing p38 MAPK-mediated signalling to activate certain Hsp27-dependent cellular processes whereas PKD-mediated signalling may activate a different subset of Hsp27-dependent process. Work examining the functional role of Hsp27 and its phosphorylation site variants in endothelial cells is detailed in chapter 5.

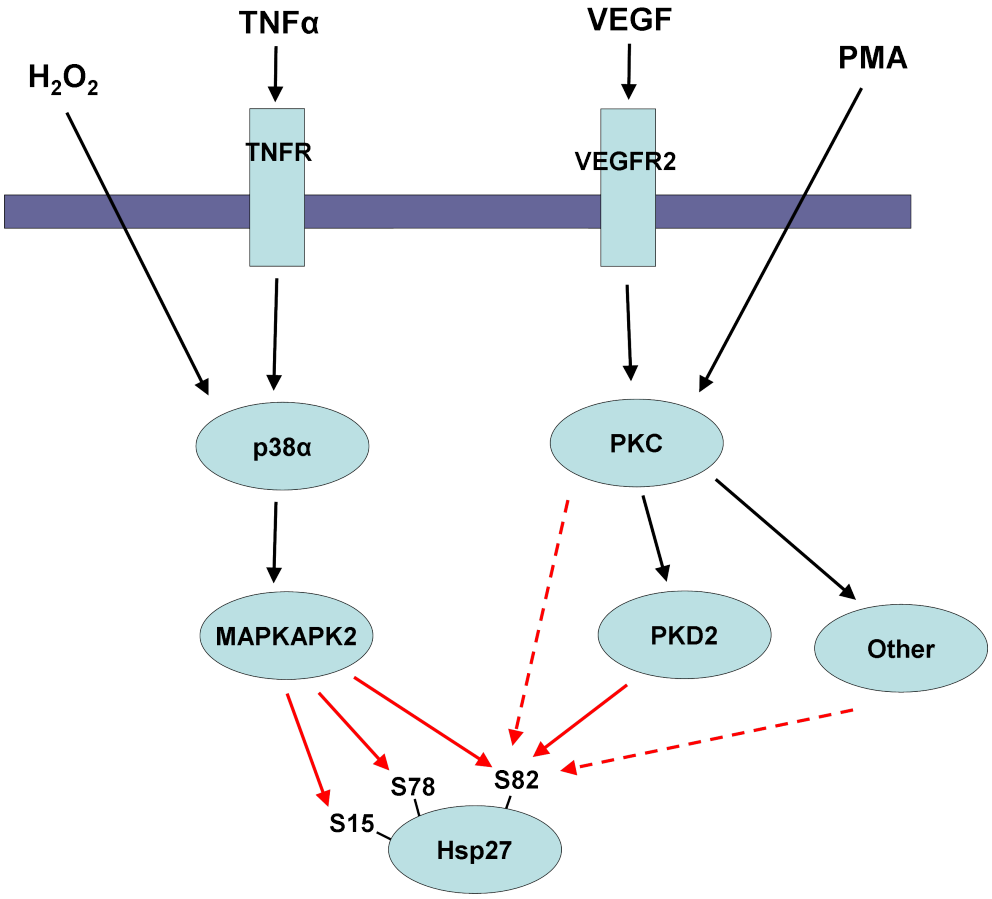

Figure 4.28: Proposed model for Hsp27 phosphorylation
Schematic diagram of the signalling pathways involved in Hsp27 phosphorylation stimulated by VEGF, PMA, TNFα and H_2O_2. Black arrows indicate signal transmission, red arrows indicate direct phosphorylation of Hsp27. Dashed red arrows indicate potential direct phosphorylation pathways not demonstrated in this thesis.
TNFα and H_2O_2 cause phosphorylation of Hsp27 at S15, S78 and S82 by activation of a pathway involving p38α and MAPKAPK2. Published work indicates that various cellular stresses including anisomycin, osmotic shock, UV irradiation and heat shock promote Hsp27 phosphorylation in other cell types via the p38 MAPK-mediated pathway.
VEGF also stimulates phosphorylation of Hsp27 via p38α/MAPKAPK2, but phosphorylates Hsp27 by a pathway involving PKC. PKCδ activates PKD2, which directly phosphorylates Hsp27 at S82. VEGF also causes PKC-dependent phosphorylation of PKD1, and this and other enzymes may be involved in VEGF-stimulated PKC-dependent Hsp27 phosphorylation. PKC may also directly phosphorylate Hsp27 at S82. PMA activates PKC but not p38α, resulting in phosphorylation of Hsp27 at S82 only.

Chapter 5

Results: The role of Hsp27 in VEGF-regulated functions in endothelial cells

Chapter 4 detailed evidence for the involvement of a p38-independent pathway mediated by PKC and PKD in VEGF-stimulated phosphorylation of Hsp27 at S82. In this chapter, the cellular role of Hsp27 was examined, concentrating on the PKC–Hsp27 pathway and the importance of S82 phosphorylation in VEGF-stimulated functions in ECs.

5.1 Overexpression of mutant and wild-type Hsp27 with adenovirus

To assess the importance of S82 phosphorylation in Hsp27 function, a number of adenoviruses were generated. In addition to a virus causing overexpression of wild-type Hsp27, three viruses expressing Hsp27 forms with mutations in phosphorylation sites were produced. Phosphorylatable serine residues were mutated to either aspartate (negatively charged, to mimic phosphorylation) or alanine (to prevent phosphorylation). The three separate mutant-expressing viruses produced Hsp27 forms containing the mutations S82A (prevents S82 phosphorylation); S82D (mimics S82 phosphorylation); or S15A S78A (prevents S15 and S78 phosphorylation). The Hsp27-expressing viruses were designed so that, if desired, endogenous Hsp27 could be reduced using Hsp27 siRNA, and replaced with the selected virus-encoded Hsp27 form. The Hsp27 forms

produced are schematically illustrated in figure 2.2. Viruses causing expression of β-galactosidase (referred to as the LacZ virus, same virus backbone as the Hsp27 viruses), and green fluorescent protein (GFP, different virus backbone to the other viruses) were also generated to use as controls for side effects of virus infection and protein overexpression.

On infection of HUVECs, all Hsp27-expressing viruses caused a multiplicity of infection (MOI)-dependent increase in Hsp27 expression in either the presence or absence of Hsp27 or control siRNA (figure 5.1A and data not shown). Immunoblots using phospho-specific antibodies directed against Hsp27 showed VEGF-treated cells infected with all Hsp27-expressing viruses had a higher than normal level of phosphorylation at S15, S78 and S82 unless a residue had been mutated to aspartic acid or alanine, where the detected level of phosphorylation of that residue was similar to that observed in LacZ-infected cells (figure 5.1B).

5.2 Cellular distribution of Hsp27

Firstly, I investigated whether VEGF might affect the overall cellular distribution of Hsp27 in endothelial cells. The influence of VEGF treatment on Hsp27 cellular location was examined by immunofluorescent staining. Treatment of HUVECs with VEGF for 5–60 mins did not produce a noticable shift in the location of Hsp27 staining, which remained predominantly cytoplasmic throughout (figure 5.2). The amount of Hsp27 present in the nucleus was much lower than in the cytoplasm. Additionally, Hsp27 was apparently excluded from certain cytoplasmic bodies of unknown identity.

5.3 VEGF-induced changes in Hsp27 quaternary structure

Hsp27 can self-associate into large oligomers, the size of which correlates with phosphorylation status (discussed in section 1.5.4). Some properties of Hsp27, such inhibition of actin polymerisation, may be restricted to particular oligomeric forms of the protein, and as such oligomerisation

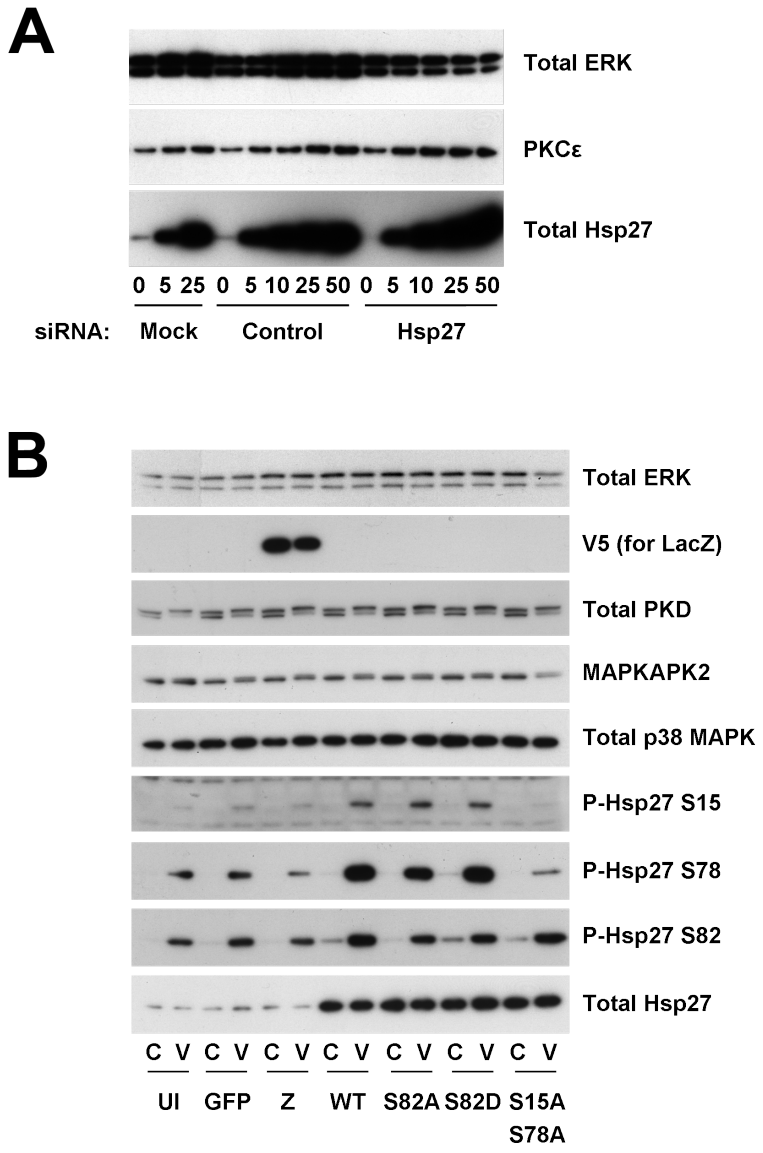

Figure 5.1: Overexpression of Hsp27 using adenoviruses
A. HUVECs were incubated with transfection reagent alone (Mock) or the indicated siRNA for 24 h, after which cells were incubated with adenovirus encoding wild-type Hsp27 at the indicated multiplicity of infection (MOI) for a further 48 h. Cells were then lysed and samples were immunoblotted and probed with the indicated antibodies. Data are from a single experiment.
B. HUVECs were incubated with adenovirus at an MOI of 20 (in the absence of siRNA) for 48 h, before cells were starved overnight and treated with (V) or without (C) 25 ng/ml VEGF. After 15 mins, cells were lysed and samples were immunoblotted and probed with the indicated antibodies. Representative of three independent experiments. Virus abbreviations are: UI, uninfected (no virus added); GFP, green fluorescent protein-expressing virus; Z, LacZ virus; WT, wild-type Hsp27 virus; S82A, S82D, S15A S78A, Hsp27 virus with this mutation (numbered serine residue is mutated to the indicated amino acid). V5 antibody detects the V5 epitope tag present on the modified β-galactosidase variant produced by the lacZ virus.

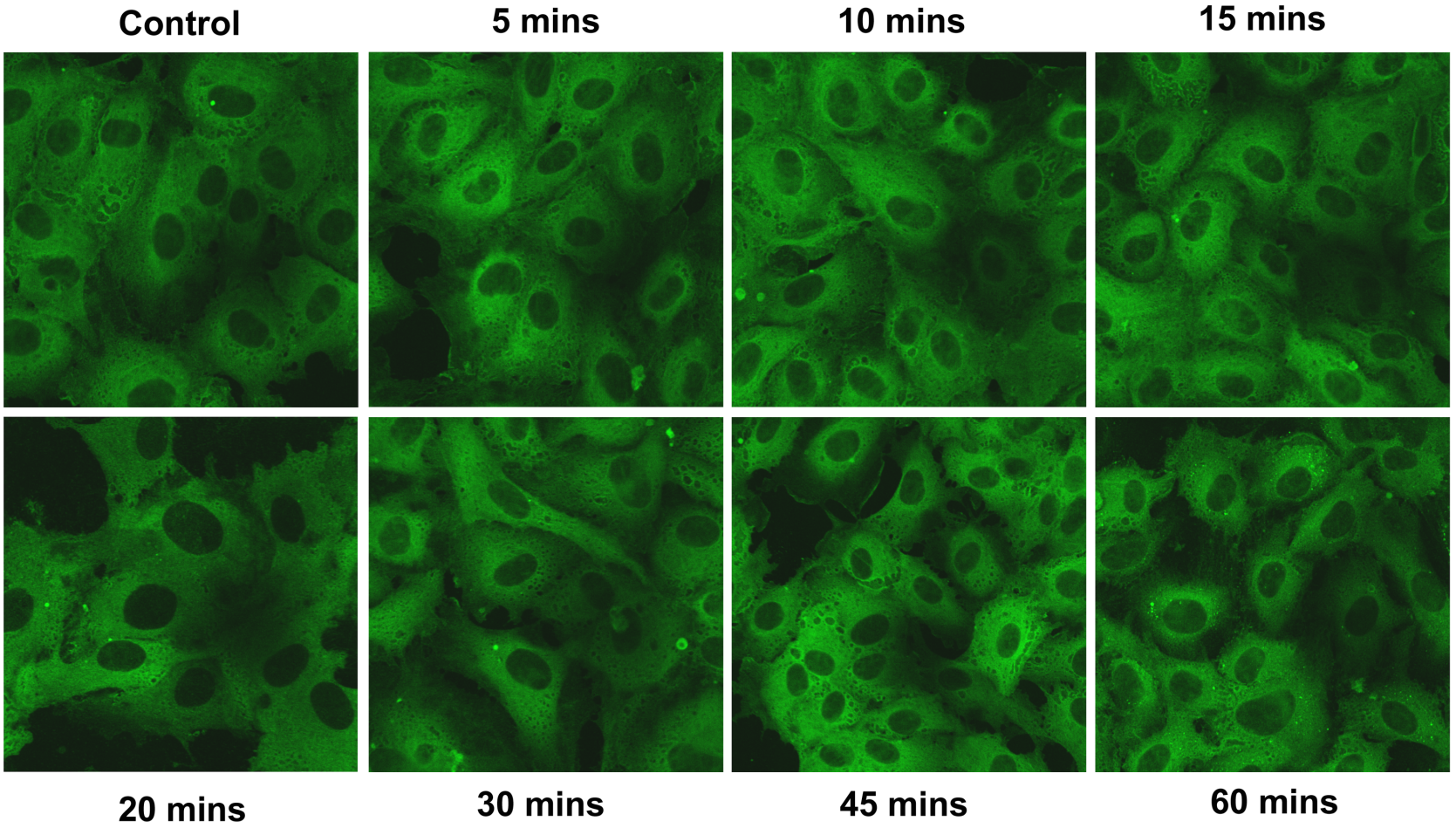

Figure 5.2: Hsp27 cellular distribution HUVECs grown on gelatin-coated coverslips were treated for the indicated time with 25 ng/ml VEGF or left untreated (control), after which cells were fixed and immunostained with polyclonal anti-Hsp27 antibody (FITC secondary antibody, green channel), with images acquired using a confocal microscope. No staining was observed in a control sample using secondary antibody only (no primary antibody, not shown). Data are from a single experiment, but a similar staining pattern and lack of VEGF effect was observed in two additional experiments using 10–15 mins treatment with VEGF.

status may be an important regulator of Hsp27 cellular function (section 1.5.4).

Glutaraldehyde-mediated protein cross-linking was used to examine VEGF-stimulated alterations in Hsp27 quaternary structure. Glutaraldeyde cross-linked Hsp27 gave a distinctive laddering pattern when analysed by SDS-PAGE, with more Hsp27 present in the higher molecular weight species at increased glutaraldehyde concentration (figure 5.3). In the presence of glutaraldehyde, the proportion of Hsp27 present in high molecular weight forms was reduced after 15 mins VEGF treatment when compared to control cells (figure 5.3), suggesting that VEGF leads to a reduction in the size of Hsp27 oligomers.

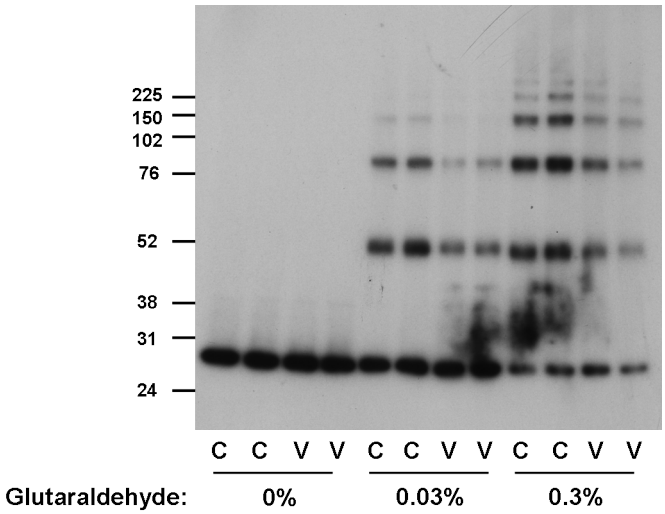

Figure 5.3: VEGF reduces the size of glutaraldehyde cross-linked Hsp27 oligomers
Serum-deprived HUVECs were treated with 25 ng/ml VEGF (V) or no addition (C) for 15 mins before cells were lysed and the extract was aliquoted. Separate aliquots of the same extract were treated for 30 mins using the indicated concentration of glutaraldehyde. After quenching, samples were separated and blotted, and Hsp27 was detected using a polyclonal anti-Hsp27 antibody. Position of molecular weight markers (in kDa) is given up the side of the blot. The experiment was performed in duplicate with respect to treatment and glutaraldehyde concentration (adjacent lanes on the blot). Results are representative of two independent experiments.

To determine the involvement of phosphorylation in the VEGF-stimulated reduction in Hsp27 oligomeric size, HUVECs were pre-treated with a combination of SB203580 and GF109203X, shown in chapter 4 to prevent VEGF-stimulated Hsp27 phosphorylation at S15, S78 and S82. This inhibitor combination prevented the VEGF-induced reduction in Hsp27 oligomeric size (figure 5.4).

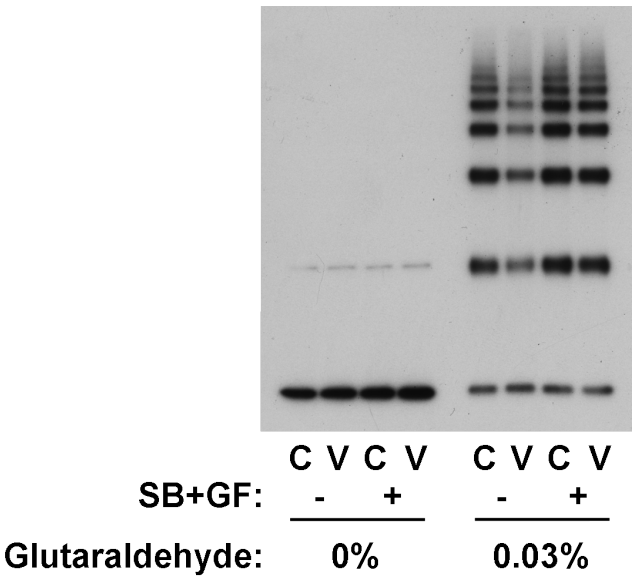

Figure 5.4: Pre-treatment of HUVECs with a combination of SB203580 and GF109203X prevents the VEGF-stimulated reduction in the size of glutaraldehyde cross-linked Hsp27 oligomers
Serum-deprived HUVECs were incubated in EBM containing 5 μM SB203580 and 3 μM GF109203X (SB+GF +) or solvent alone (0.2% v/v DMSO, SB+GF -) for 30 mins, and then treated with 25 ng/ml VEGF (V) or no addition (C) for 15 mins before cells were lysed and the extract aliquoted. Separate aliquots of the same extract were treated for 30 mins using the indicated concentration of glutaraldehyde. After quenching, samples were separated and blotted, and Hsp27 was detected using a polyclonal anti-Hsp27 antibody. Results are representative of two independent experiments.

To examine whether phosphorylation at S82 is an important determinant of Hsp27 oligomeric size, wild-type and mutant forms of Hsp27 were overexpressed in HUVECs using adenoviruses. Virus-produced Hsp27 showed a laddered pattern after glutaraldehyde cross-linking and SDS-PAGE and co-migrated with Hsp27 from uninfected cells (figure 5.5, long exposure), indicating that virus-produced Hsp27 forms similar oligomeric species to that seen with endogenous Hsp27. High molecular weight Hsp27 species were less prominent in extracts from cells overexpressing the S82D mutant than those overexpressing wild-type Hsp27, or the S82A or S15A+S78A mutants (figure 5.5).

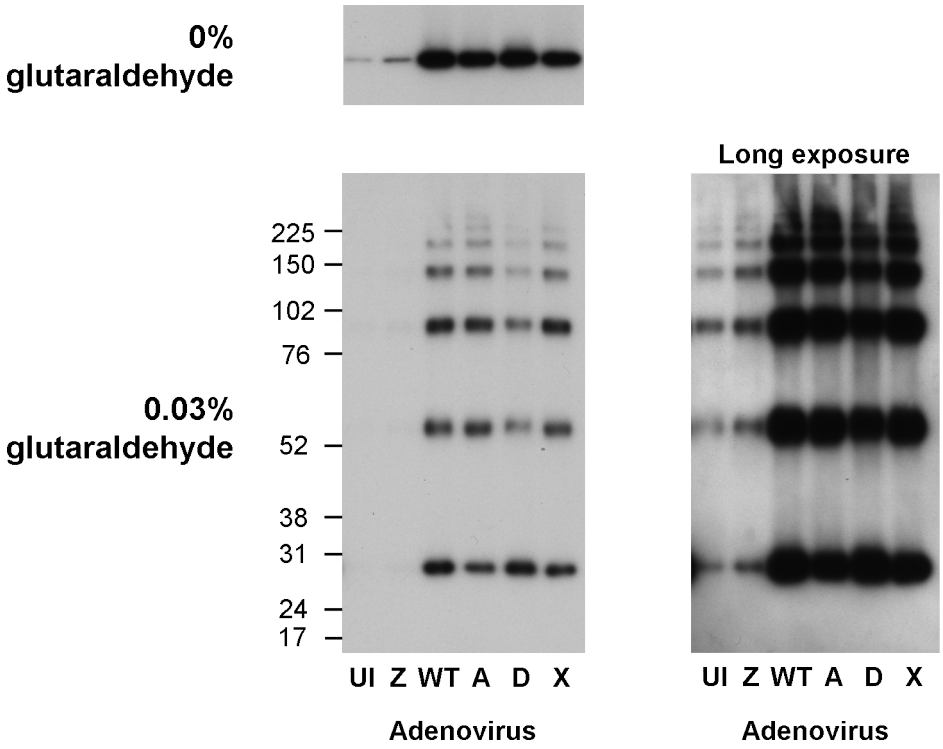

Figure 5.5: Hsp27 with an S82D mutation forms smaller cross-linked oligomers than unmutated Hsp27

HUVECs were treated for 24 h with siRNA against Hsp27 to reduce the level of endogenous Hsp27 protein present, before infection with adenovirus leading to overexpression of a normal or mutant form of Hsp27, or β-galactosidase. After 48 h, cells were lysed and the extract was aliquoted. Separate aliquots of the same extract were treated for 30 mins using the indicated concentration of glutaraldehyde. After quenching, samples were separated and blotted, and Hsp27 was detected using a polyclonal anti-Hsp27 antibody. Position of molecular weight markers (in kDa) is given up the side of the blot. Adenovirus abbreviations are: UI, uninfected (no virus added); Z, LacZ virus; WT, wild-type Hsp27 virus; A, Hsp27 virus with S82A mutation; S82D, Hsp27 virus with S82D mutation; X, Hsp27 virus with S15A S78A mutation. The rightmost blot is a longer exposure of the 0.03% gluaraldehyde blot on the left. Results are representative of three independent experiments.

5.4 Role of Hsp27 in VEGF-stimulated cell migration

5.4.1 Hsp27 knockdown reduces VEGF-stimulated HUVEC migration

The involvement of Hsp27 in cell migration was examined by depleting Hsp27 in HUVECs with siRNA and assessing the ability of these cells to migrate towards VEGF in a transwell assay. VEGF caused a $\sim$11-fold increase in HUVEC migration, which was reduced 38% by Hsp27 knockdown (figure 5.6B). The Hsp27 knockdown caused a large reduction in the amount of both total and VEGF-induced phospho-Hsp27 in these cells (figure 5.6A).

5.4.2 VEGF-stimulated HUVEC migration is dependent on PKC but not p38 MAPK

Results from chapter 4 showed that Hsp27 phosphorylation can occur via at least two distinct pathways – involving either p38 MAPK or PKC/PKD. Previous work has indicated a key role for p38 MAPK and p38 MAPK-mediated Hsp27 phosphorylation in VEGF-stimulated cell migration. It was therefore important to investigate the role of p38 MAPK and PKC/PKD in VEGF-stimulated HUVEC migration.

The p38 MAPK inhibitor SB203580 had little effect on VEGF-stimulated HUVEC migration at doses up to 25 μM (figure 5.7), 25 times that required for complete inhibtion of MAPKAPK2 phosphorylation (figure 4.10A). Knockdown of either p38α or MAPKAPK2 did not reduce VEGF-stimulated migration (figure 5.8). Similar degrees of knockdown inhibited TNFα-induced Hsp27 phosphorylation (figure 4.11B).

The broad-spectrum PKC inhibitor GF109203X markedly reduced VEGF-stimulated HUVEC migration (79% reduction), while SB203580 used in the same experiments had no effect (figure 5.9A).

To check the consistency of the results of p38 and PKC inhibition, the effects of a second p38

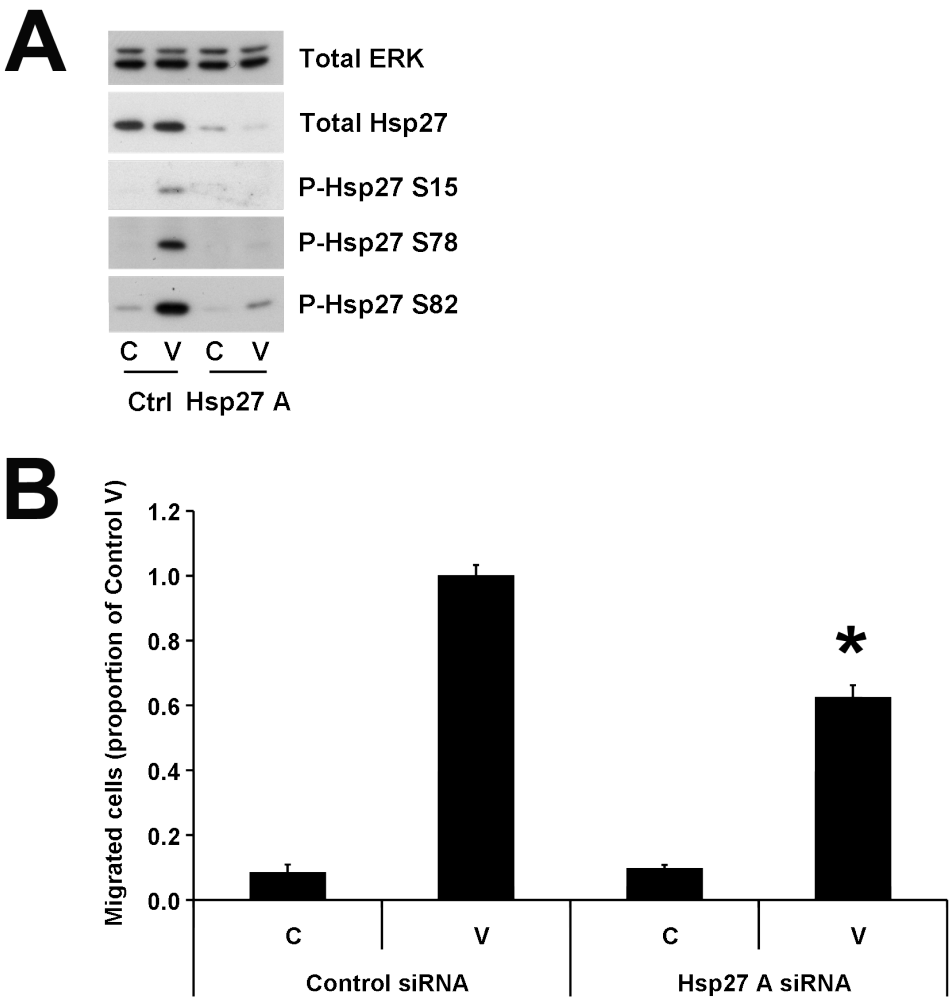

Figure 5.6: Hsp27 knockdown reduces HUVEC migration in response to VEGF
A. Representative blot showing Hsp27 knockdown achieved by the Hsp27 siRNA. 48 h after transfection with either Hsp27 siRNA A (Hsp27) or a non-targeting control siRNA (Control), cells were treated for 15 mins with 25 ng/ml VEGF (V) or no addition (C), before lysis and immunoblotting with the indicated antibodies.
B. Quantification of the effects of siRNA-mediated Hsp27 knockdown on VEGF-stimulated cell migration. 48 h after transfection with the either a non-targeting siRNA (Control) or an siRNA targeting Hsp27, HUVECs were trypsinised and added to the upper chamber of a transwell migration assay chamber. 25 ng/ml VEGF (V) or no addition (C) was added to the lower chamber and the cells were allowed to migrate at 37°C. After 4 h, the inserts were fixed, stained and the number of migrated cells was assessed by counting. Results are mean ± SEM from nine independent experiments, analysed by two-way ANOVA with Bonferronis test for multiple pair-wise comparisons. * $p<0.001$ compared to Control/VEGF-treated. Mean Hsp27 knockdown achieved by the siRNA was 91%.

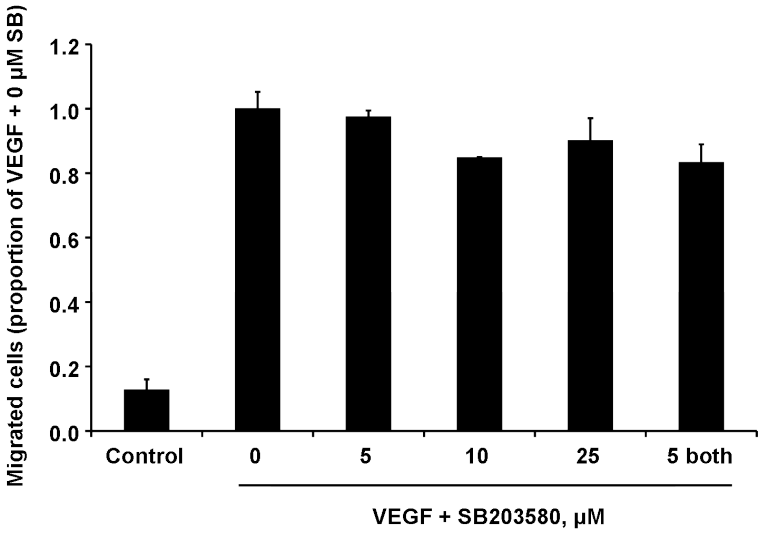

Figure 5.7: SB203580 does not inhibit migration towards VEGF
HUVECs were pre-incubated in suspension with either solvent alone (0.5% v/v DMSO, Ctrl) or the indicated concentration of SB203580. Migration was assessed in a transwell assay towards 25 ng/ml VEGF for 4 h, before cells were fixed, stained and counted. In one treatment group (5 both), 5 μM SB203580 was also added to the lower chamber to negate any possible diffusion of inhibitor away from the cells. Data are from three independent experiments. One-way ANOVA indicated no significant effect of any tested dose of SB203580.

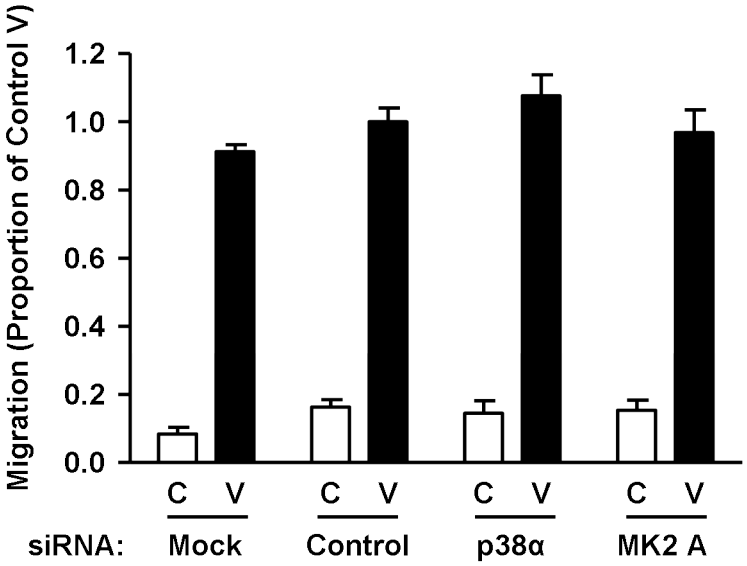

Figure 5.8: Knockdown of p38α or MAPKAPK2 does not reduce VEGF-stimulated migration
HUVECs were pre-treated for 48 h with siRNAs targeting p38α, MAPKAPK2 (siRNA A, MK2 A), a non-targeting control siRNA (Ctrl) or transfection reagent alone (Mock). Cells were trypsinised and migration was assessed in a transwell assay using 25 ng/ml VEGF (V) or no addition (C) as the chemoattractant. Results are means $\pm$ SEM of three independent experiments. Mean knockdown of target protein achieved by siRNAs, compared to control siRNA: p38α, 93%; MAPKAPK2, 88%. Analysis of VEGF-stimulated migration by one-way ANOVA indicated no significant effect achieved by any siRNA compared to the control siRNA.

MAPK inhibitor, SB202190, and a second broad-spectrum PKC inhibitor, Gö6983, were assessed in the same experiment. The broad-spectrum PKC inhibitor Gö6983 reduced VEGF-stimulated migration to a similar extent to GF109203X, whereas neither of the p38 MAPK inhibitors SB202190 and SB203580 reduced migration (figure 5.9B).

The PKD/classcial PKC inhibitor Gö6976 reduced VEGF-stimulated migration by 60%, similar to the reduction observed with GF109203X when used in the same assays (figure 5.10).

To determine which PKC isoforms are involved in VEGF-stimulated migration, PKCα, PKCδ, and PKCϵ were knocked down in cells with siRNA. PKCα knockdown reduced migration by 44%, whereas reduction of PKCδ increased migration by 55%, and PKCϵ knockdown had no significant effect (figure 5.11).

The involvement of protein kinase D in VEGF-stimulated migration was also examined using siRNA. PKD1 knockdown reduced VEGF-stimulated HUVEC migration by 42%, whereas PKD2 knockdown reduced migration by 47% (figure 5.12).

5.4.3 Effect of overexpression of Hsp27 mutants on migration

Both siRNA-mediated Hsp27 knockdown and inhibition of enzymes involved in Hsp27 phosphorylation reduced VEGF-stimulated HUVEC migration. To address the role of Hsp27 phosphorylation in VEGF-stimulated migration, HUVECs were infected with adenoviruses to overexpress either wild-type Hsp27 or an Hsp27 form with a selected phosphorylation site mutation.

The viruses were designed with the intention of reducing endogenous Hsp27 with siRNA and replacing the lost Hsp27 by adenovirus-mediated expression of the mutant Hsp27 form. While it was possible to knock down endogenous Hsp27 and overexpress adenovirus-synthesised Hsp27, initial experiments indicated that infection with any of the produced adenoviruses, including a LacZ control virus, caused a marked reduction in the migration of siRNA-treated HUVECs, and this reduction was dependent on virus MOI (Figure 5.13A illustrates the effect of the LacZ control

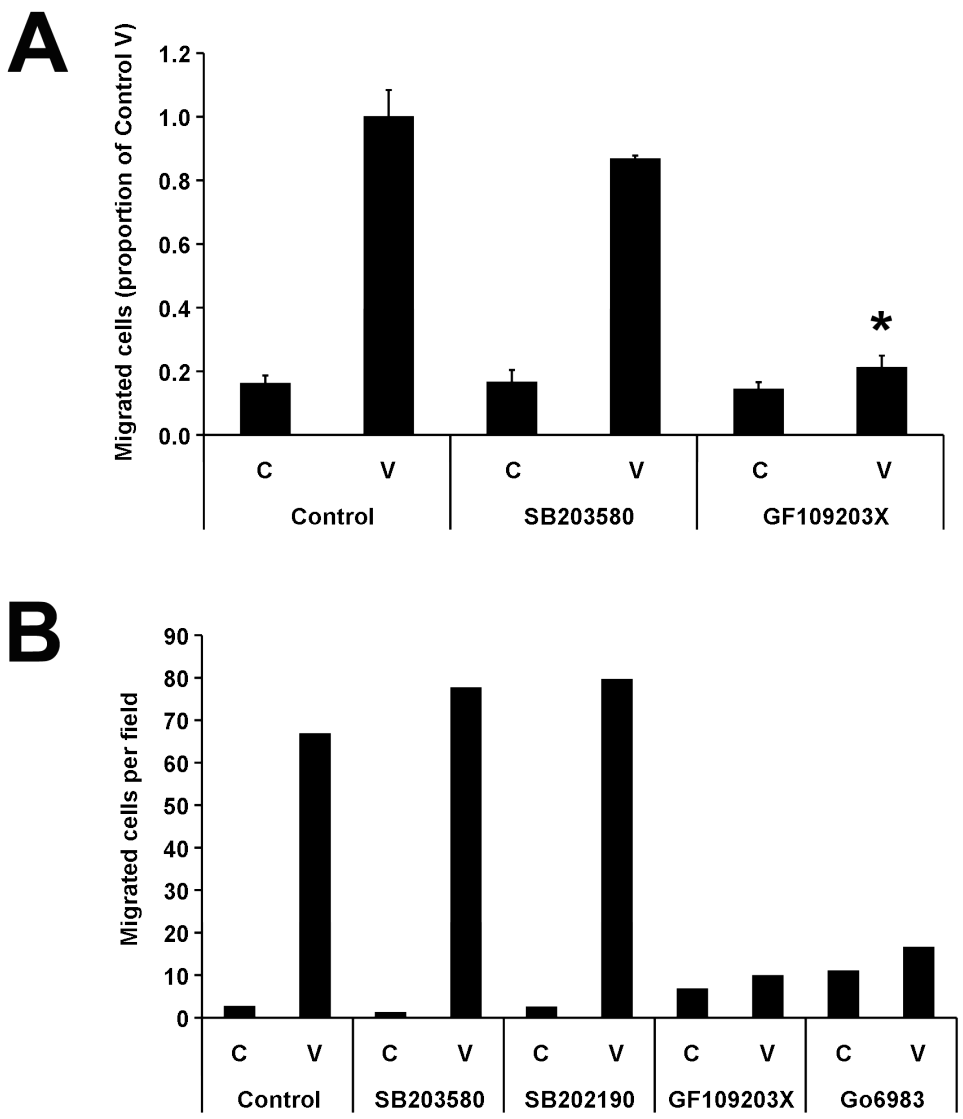

Figure 5.9: Inhibition of PKC but not p38 blocks VEGF-induced migration
A. HUVECs were trypsinised, resuspended and incubated in suspension in the presence of 5 μM SB203580, 3 μM GF109203X, or solvent alone (0.1% v/v DMSO, Control). Migration was assessed in a transwell assay using 25 ng/ml VEGF (V) or no addition (C) as the chemoattractant. After 4 h, cells were fixed, stained and counted. The number of migrated cells is expressed as a proportion of that observed in the Control/VEGF group, and are means $\pm$ SEM from three independent experiments. Differences were assessed by two-way ANOVA with Bonferronis test for multiple pair-wise comparisons. * significantly different to Control V ($p<0.001$).
B. HUVECs were trypsinised, resuspended and incubated in suspension in the presence of 5 μM SB203580, 5 μM SB202190, 3 μM GF109203X, 3 μM Gö6983 or solvent alone (0.1% v/v DMSO, Control). Migration was assessed in a transwell assay using 25 ng/ml VEGF (V) or no addition (C) as the chemoattractant. After 4 h, cells were fixed, stained and counted. Results are mean number of migrated cells observed from duplicate inserts. Data is from a single experment.

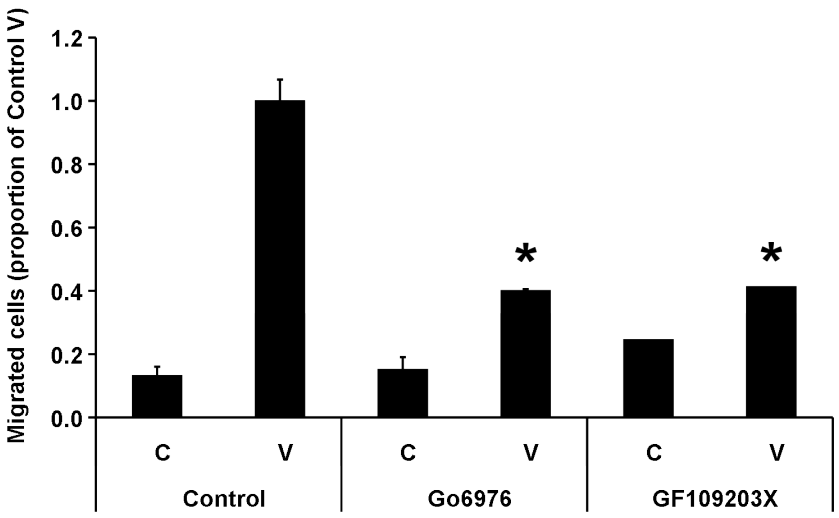

Figure 5.10: The inhibitor of conventional PKCs, Gö6976, reduces VEGF-stimulated HUVEC migration to the same extent as the broad-spectrum PKC inhibitor GF109203X
HUVECs were trypsinised, resuspended and incubated in suspension in the presence 3 μM GF109203X, 1 μM Gö6976, or solvent alone (0.1% v/v DMSO, Control). Migration was assessed in a transwell assay using 25 ng/ml VEGF (V) or no addition (C) as the chemoattractant. After 4 h, cells were fixed, stained and counted. The number of migrated cells is expressed as a proportion of that observed in the Control/VEGF group. Data are means $\pm$ SEM from three independent experiments for Control and Gö6976 (error bars shown). Only two of these experiments included GF109203X, and so error bars are not shown for this compound. Differences were assessed by two-way ANOVA with Bonferronis test for multiple pair-wise comparisons. * significantly different to Control V ($p<0.001$).

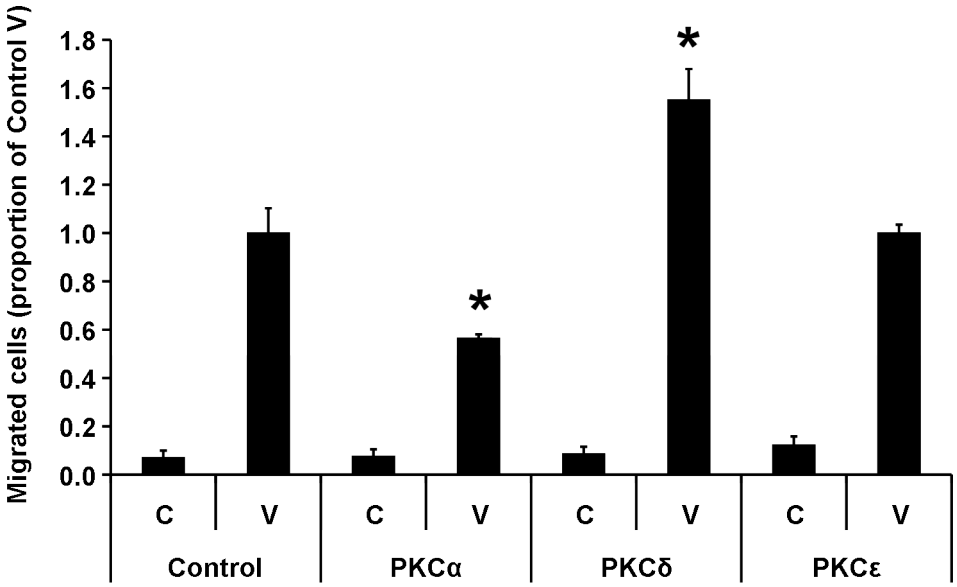

Figure 5.11: Knockdown of PKCα and PKCδ has opposing effects on VEGF-stimulated HUVEC migration
HUVECs were pre-treated for 48 h with siRNAs targeting the indicated PKC isoform, or a non-targeting control siRNA (Control). Cells were trypsinised and migration was assessed in a transwell assay using 25 ng/ml VEGF (V) or no addition (C) as the chemoattractant. Results are means $\pm$ SEM of three independent experiments. Mean knockdown of target protein achieved by siRNAs, compared to control siRNA: PKCα, 82%; PKCδ, 90%, PKCϵ, 76%. Differences were assessed by two-way ANOVA with Bonferroni's test for multiple pair-wise comparisons. * significantly different to Control siRNA V ($p<0.01$).

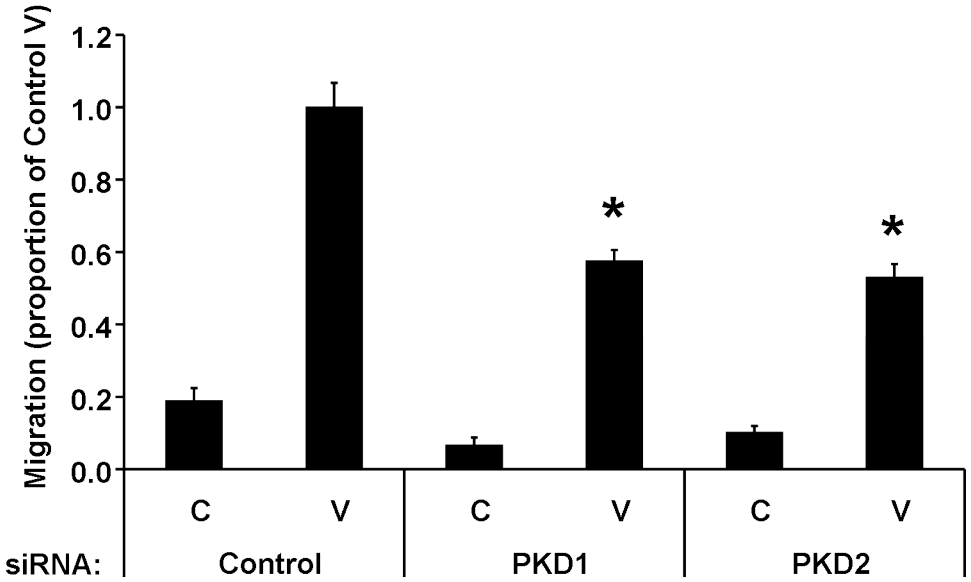

Figure 5.12: Effect of PKD knockdown on VEGF-induced cell migration
HUVECs were pre-treated for 48 h with siRNAs targeting the indicated PKD isoform, or with a non-targeting control siRNA (Control). Cells were trypsinised and migration was assessed in a transwell assay using 25 ng/ml VEGF (V) or no addition (C) as the chemoattractant. Results are means ± SEM of three independent experiments. The PKD2 siRNA reduced PKD2 expression by a mean of 86%, PKD1 knockdown was not quantitatively assessed due to the lack of a PKD1-specific antibody, but the upper band of a total PKD blot was strongly reduced in lysates prepared in parallel to each experiment. Differences were assessed by two-way ANOVA with Bonferroni's test for multiple pair-wise comparisons. * significantly lower than Control siRNA, VEGF treated group ($p<0.001$). There was no significant effect by the siRNAs on non-VEGF-stimulated migration.

virus on siRNA-transfected cells). In contrast, there did not appear to be an MOI-dependent effect of virus infection on the migration of HUVECs not treated with siRNA (figure 5.13B). In the light of these results, it was decided to concentrate on the effect of Hsp27-expressing viruses on HUVECs without prior siRNA transfection.

Wild-type Hsp27 or various mutant forms of Hsp27 (S82A; S82D; S15A+S78A) were overexpressed in HUVECs using adenovirus, and migration was assessed.

Overexpression of wild-type Hsp27 showed a trend towards increased migration in both the presence and absence of VEGF chemoattractant when compared to that observed with LacZ virus-infected cells, but this was not significant (figure 5.14A). Overexpression of either S82A, S82D or S15A S78A Hsp27 showed a trend towards reduction in both unstimulated and VEGF-stimulated migration, but these effects did not reach significance.

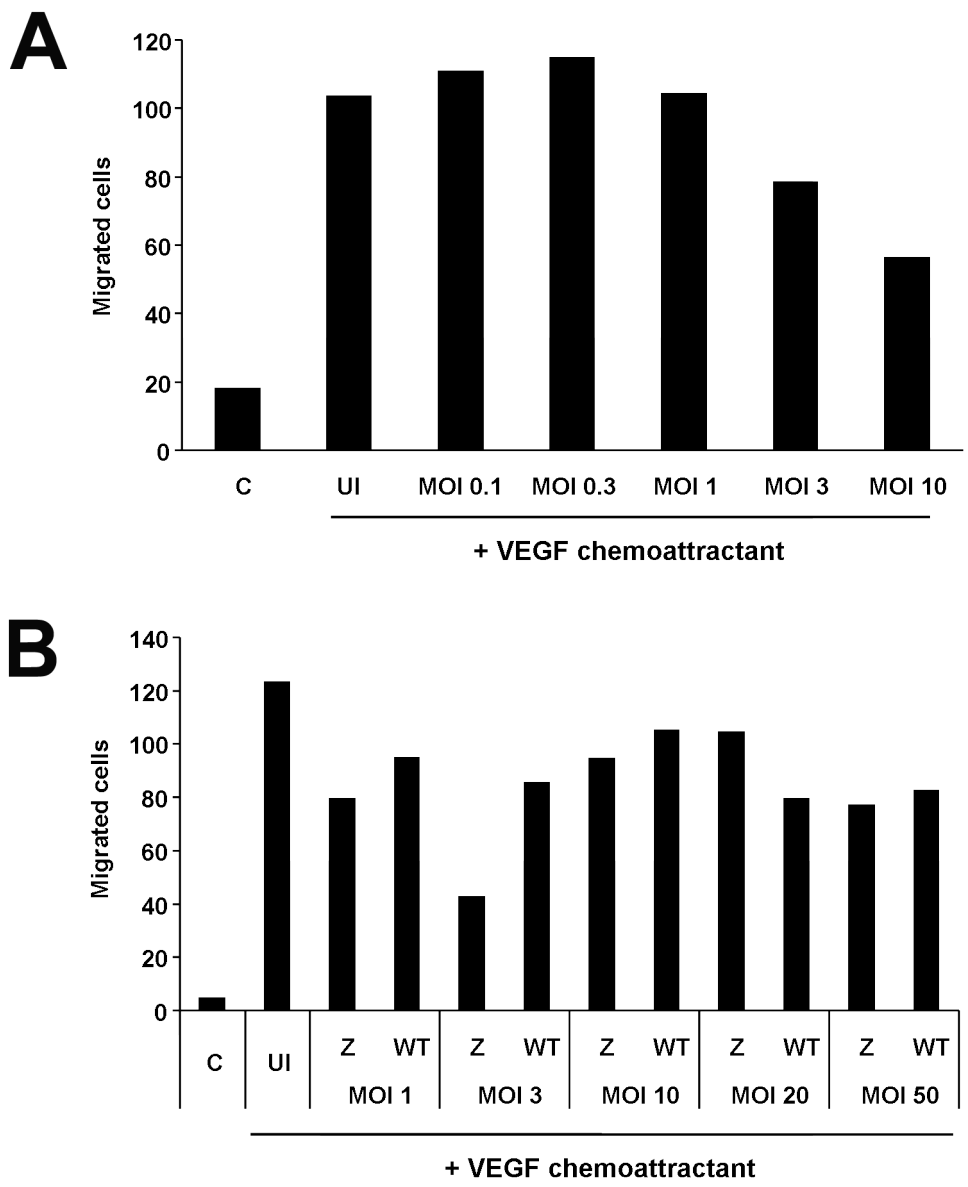

Figure 5.13: Comparison of the presence or absence of siRNA on the migration of HUVECs infected with adenovirus

A. HUVECs were transfected with a negative control siRNA for 24 h before the addition of LacZ adenovirus at the indicated MOI for a further 48 h. Cells were then trypsinised and migration was assessed in a transwell assay towards 25 ng/ml VEGF for 4 h, after which the cells were fixed, stained and counted. C, uninfected cells without VEGF chemoattractant; UI, uninfected cells with VEGF chemoattractant. Results are from a single experiment, but very little migration was observed in three additional experiments using Hsp27 siRNA and the various Hsp27 viruses at MOI 20.

B. HUVECs were infected with either LacZ (Z) or Hsp27 wild type-expressing (27) adenovirus at the indicated MOI. After 48 h, cells were trypsinised and migration was assessed in a transwell assay towards 25 ng/ml VEGF for 4 h, after which the cells were fixed, stained and counted. C, uninfected cells without VEGF chemoattractant; UI, uninfected cells with VEGF chemoattractant. Results are from a single experiment.

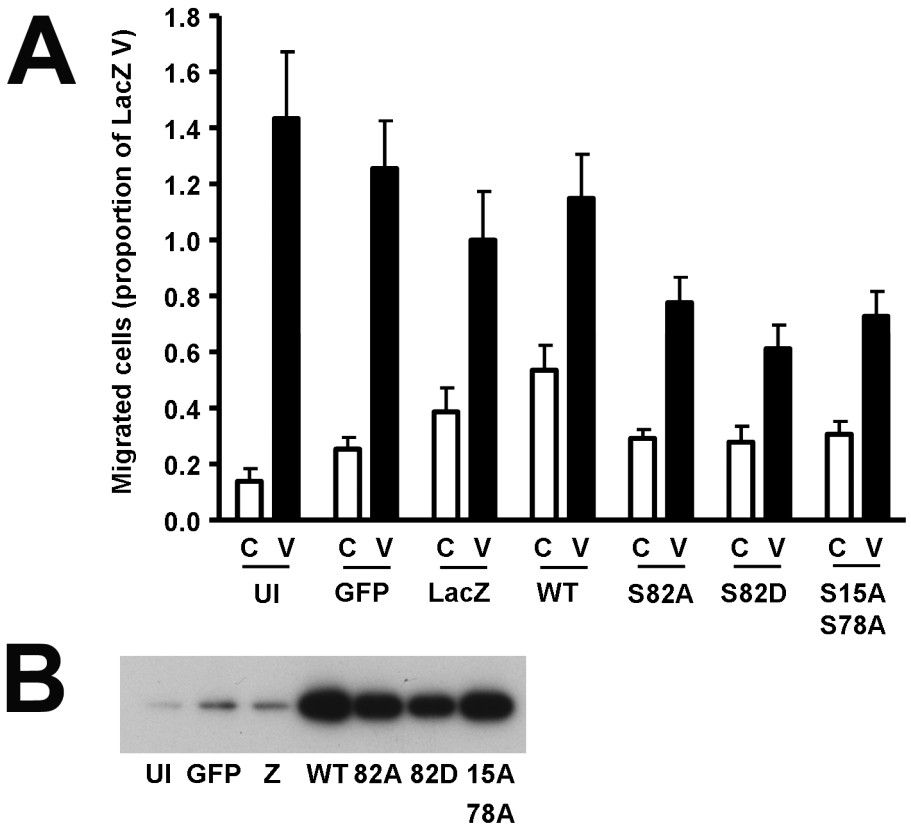

Figure 5.14: Effect of adenovirus-mediated overexpression of Hsp27 forms on migration
A. HUVECs were infected with the indicated adenovirus for 48 h at MOI of 20. Cells were then trypsinised and migration was assessed in a transwell assay towards 25 ng/ml VEGF (V) or no addition (C) for 4 h, after which the cells were fixed, stained and counted. Results are expressed as a proportion of the migration observed in the LacZ infected cells towards VEGF, and are mean $\pm$ SEM from six independent experiments. UI, uninfected; WT, wild type Hsp27 adenovirus; S..., Hsp27 adenovirus with the indicated mutation. Results were analysed by two-way ANOVA, with Bonferroni's test for multiple pairwise comparisons. No viruses significantly affected basal or VEGF-stimulated migration compared to LacZ virus.
B. Representative blot indicating the degree of overexpression caused by the viruses. Lysates prepared from cells infected in parallel with those used for the migration assays were immunoblotted and probed with an antibody to total Hsp27. Labels are as for part (A), but LacZ virus is represented by 'Z'.

5.5 Involvement of Hsp27 in apoptosis

The importance of Hsp27 in apoptosis induced by serum starvation was examined using annexin V staining to bind the membrane phospholipid phosphatidylinositol, usually present in the inner leaflet of the plasma membrane but translocated to the outer membrane during apoptosis, so becoming accessible to annexin V-based stains.

When included in the starvation medium, VEGF reduced the proportion of annexin V-positive cells by 38% in cells treated with a control siRNA and 23% in cells treated with an Hsp27 siRNA (figure 5.15a). Hsp27 knockdown increased the proportion of annexin V-stained cells by 36% in the absence of VEGF, and by 68% in the presence of VEGF.

Adenovirus-mediated expression of Hsp27 mutant forms was not used as an approach to examine the role of Hsp27 phosphorylation in apoptosis as initial experiments indicated that all viruses used (including the LacZ control virus) caused a strong resistance to apoptosis induced by serum starvation when compared to untransfected cells (figure 5.16). Work in this laboratory by other investigators found similar effects using other adenoviruses produced in the same way as the ones used in this study. In other experiments where virus-infected cells had been incubated overnight in 1% serum-containing medium, such as those involving VEGF treatment and lysis, it was consistently noted that virus-infected cells appeared more confluent, with less floating cells, than uninfected control cells (data not shown), possibly a manifestation of the same apoptosis-inhibiting effect.

5.6 Involvement of Hsp27 in VEGF-mediated tubulogenesis

The role of Hsp27 in tubulogenesis, the formation of tube-like structures composed of endothelial cells, was assessed in a cell culture system using siRNA-mediated knockdown of Hsp27. In cells treated with a control siRNA, VEGF increased tubulogenesis more than 2-fold above control levels (figure 5.17). Hsp27 knockdown reduced tubulogenesis in the absence of VEGF by 77%, and by

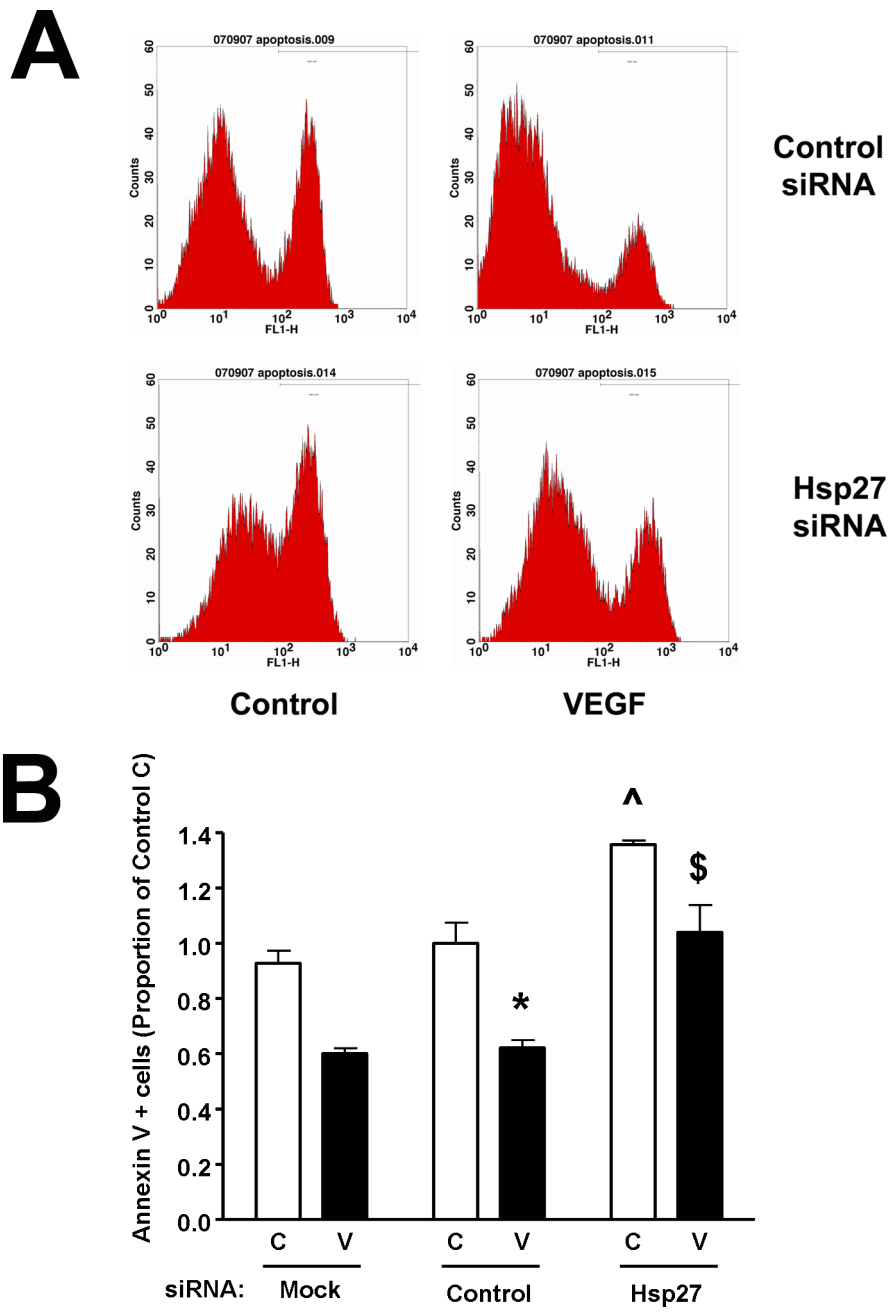

Figure 5.15: Hsp27 knockdown increases endothelial cell apoptosis in response to serum starvation (continued overleaf)

HUVECs were incubated with 200 nM siRNA targeting Hsp27, a non-targeting control siRNA, or transfection reagent alone (Mock) for 2 days. The medium was then changed and cells were incubated overnight in M199 basal medium in the presence (V) or absence (C) of 25 ng/ml VEGF to induce apoptosis. Live and dead cells were then harvested by trypsinisation and stained with fluorescein-conjugated annexin V. The proportion of stained and unstained cells was determined by flow cytometry.

A. Representative raw histograms illustrating the proportion of cells that are unstained and stained with annexin V. The x-axis represents annexin V staining intensity (detected on the FL-1 channel), the y-axis represents number of cells with that staining intensity. In each graph, the unstained cells are the leftmost population, the annexin V-stained cells are the rightmost population.

Figure 5.15: Hsp27 knockdown increases endothelial cell apoptosis in response to serum starvation (continued)

B. Quantitative data from apoptosis assays. Results are presented as the percentage of annexin V-positive cells, as a proportion of that observed in the control siRNA/no VEGF sample, and are given as mean ± SEM from four independent experiments. Data were analysed by two-way ANOVA with Bonferroni's test for multiple pair-wise comparisons. From the two-way ANOVA, the main effect of both siRNA (Mock, Control or Hsp27) and treatment (C or V) were significant ($p<0.001$) but the interaction term was not. * significantly lower than Control C ($p<0.01$), VEGF also increased survival in the presence of Hsp27 siRNA ($p<0.05$). ^ significantly higher than Control C ($p<0.01$). $ significantly higher than Control V ($p<0.001$). Mean Hsp27 knockdown achieved by the siRNA was 93%.

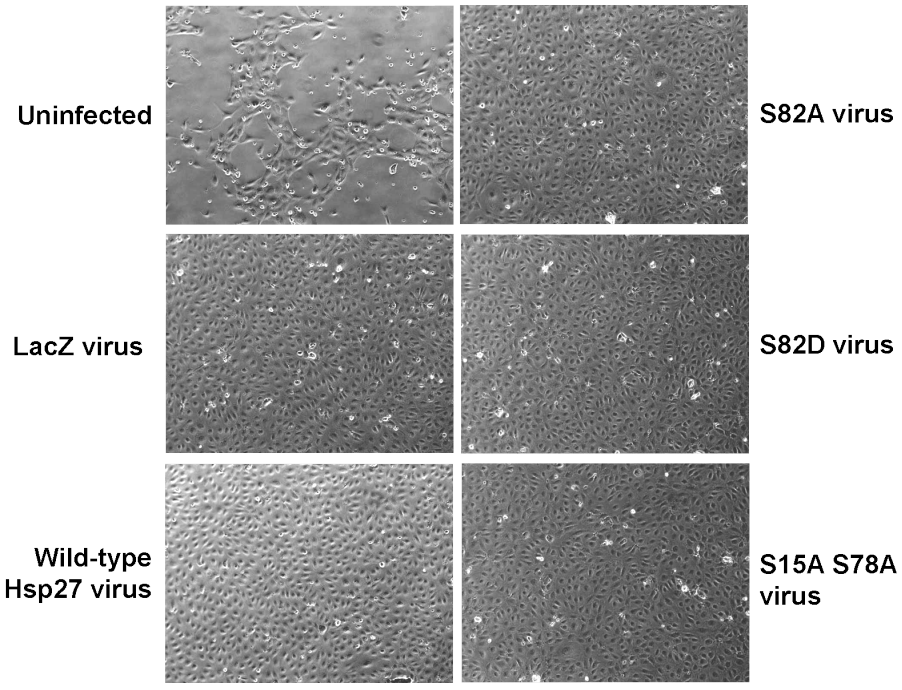

Figure 5.16: Adenovirus infection dramatically reduces endothelial cell apoptosis in response to serum starvation

HUVECs were infected with the indicated adenovirus at MOI 20 and then cultured for 2 days. Cells were then incubated in M199 basal medium overnight to induce apoptosis. Pictures of the cells were taken with an inverted light microscope using a x10 objective.

45% in VEGF treated cells.

As shown in chapter 4, Hsp27 phosphorylation can occur via the p38 MAPK or PKC pathways. The importance of these two pathways for tubulogenesis was studied using pharmacological inhibitors. The broad-spectrum PKC inhibitor GF109203X reduced VEGF-stimulated tubulogenesis to the levels observed in unstimulated cells, whereas the p38 MAPK inhibitor SB203580 had no significant effect (figure 5.18). In agreement with the SB203580 data, knockdown of neither p38α nor MAPKAPK2 significantly reduced tubulogenesis in either VEGF-treated or control cells (figure 5.19).

Due to the lack of a significant effect of the Hsp27-expressing viruses on migration, and the marked anti-apoptotic effect observed on virus infection, the adenoviruses were not used to examine tubulogenesis.

5.7 Discussion

Data reported in chapter 4 indicated that a p38 MAPK-independent, PKC/PKD-mediated pathway contributes to VEGF-stimulated phosphorylation of Hsp27 at S82, whereas the p38 MAPK/MAPKAPK2 pathway alone largely mediated VEGF-stimulated phosphorylation of Hsp27 at S15 or S78, and TNFα- and H_2O_2-stimulated Hsp27 phosphorylation at S15, S78 and S82. In this chapter, the role of Hsp27 in VEGF-stimulated cell activities was examined, with the aim of determining the biological relevance of PKC/PKD-mediated S82 phosphorylation for Hsp27 function.

Knockdown of Hsp27 via siRNA suppressed VEGF-stimulated HUVEC migration and tubulogenesis, and increased endothelial apoptosis in response to serum starvation, indicating that Hsp27 is involved in these VEGF-stimulated EC functions. An S82D Hsp27 mutant formed smaller oligomers than wild type Hsp27, similarly suggesting that S82 phosphorylation mediates the VEGF-stimulated reduction in Hsp27 oligomer size. However, overexpression of wild type or

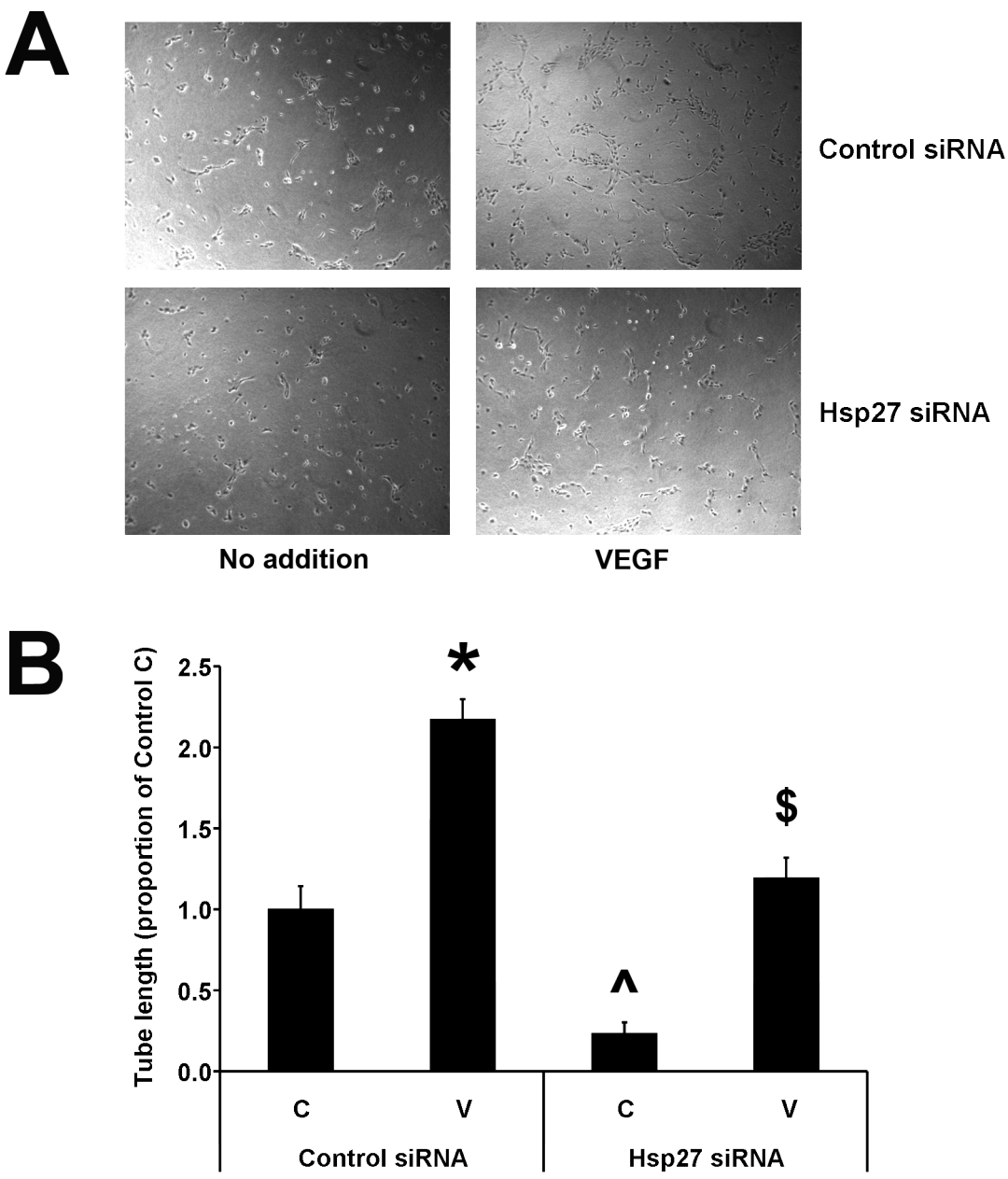

Figure 5.17: Effect of siRNA-mediated Hsp27 knockdown on VEGF-induced tubulogenesis

HUVECs were incubated for 48 h in the presence of an siRNA against Hsp27 or a non-targeting, control siRNA. Cells were then trypsinised and plated on to a collagen gel. VEGF (V, to a final concentration of 25 ng/ml) or no addition (C) was added to the cell suspension, and cells were incubated overnight at 37°C. The following day, pictures were taken of each well using an inverted light microscope and the length of the tubules present in each image was quantified.

A. Representative images of tubulogenesis on collagen in the presence of the siRNAs.

B. Quantification of the effect of Hsp27 siRNA on VEGF-induced tubulogenesis. Data is expressed as total tube length as a proportion of the Control siRNA/no VEGF group. Results are means ± SEM from three independent experiments. Differences between siRNAs were analysed by two-way ANOVA with Bonferroni's test for multiple pair-wise comparisons. In the two-way ANOVA, the main effects of siRNA and VEGF treatment were both significant, whereas the interaction term was not. * $p<0.001$ versus Control/C; ^ $p<0.05$ versus Control/C; \$ $p<0.01$ versus Control/V. Mean knockdown of target protein achieved by the Hsp27 siRNA was 93%.

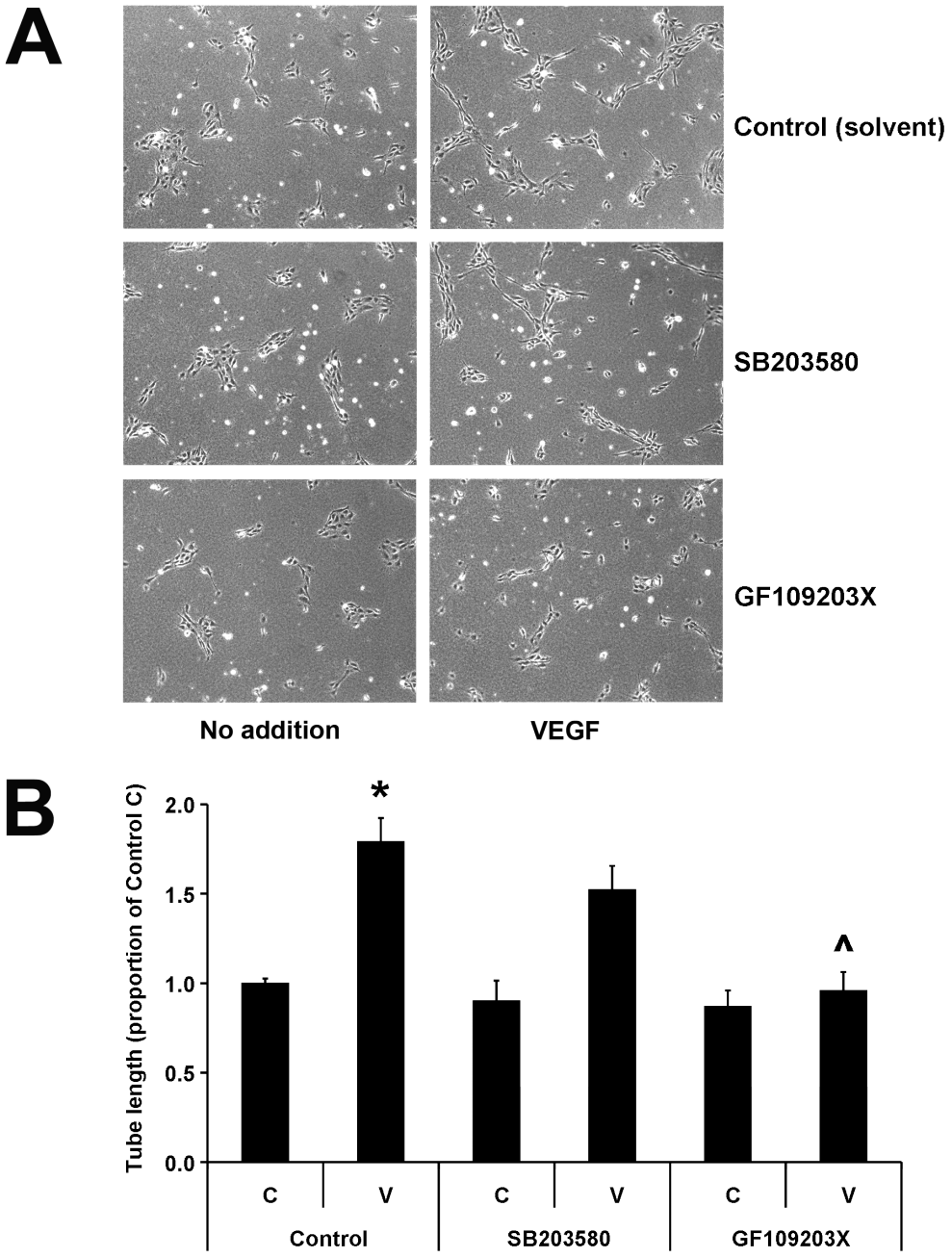

Figure 5.18: Inhibition of PKC but not p38 MAPK reduces VEGF-induced tubulogenesis

HUVECs were trypsinised and incubated in suspension for 30 mins in the presence of the indicated inhibitor, either 5 μM SB203580 (SB), 3 μM GF109203X (GF) or solvent only (0.1% DMSO, Control), before plating on to a collagen gel. VEGF (V, to a final concentration of 25 ng/ml) or no addition (C) was then added to the cell suspension, and cells were incubated overnight at 37°C. The following day, pictures were taken of each well and the length of the tubules present in each picture was quantified.

A. Representative images of tubulogenesis on collagen in the presence of the inhibitors.

B. Quantification of the effect of Hsp27 siRNA on VEGF-induced tubulogenesis. Data is expressed as total tube length as a proportion of the Control siRNA/no VEGF group. Results are means $\pm$ SEM from three independent experiments. Differences were analysed by two-way ANOVA with Bonferroni's test for multiple pair-wise comparisons. * significantly higher than Control/C ($p<0.01$). ^ significantly lower than Control/V ($p<0.01$).

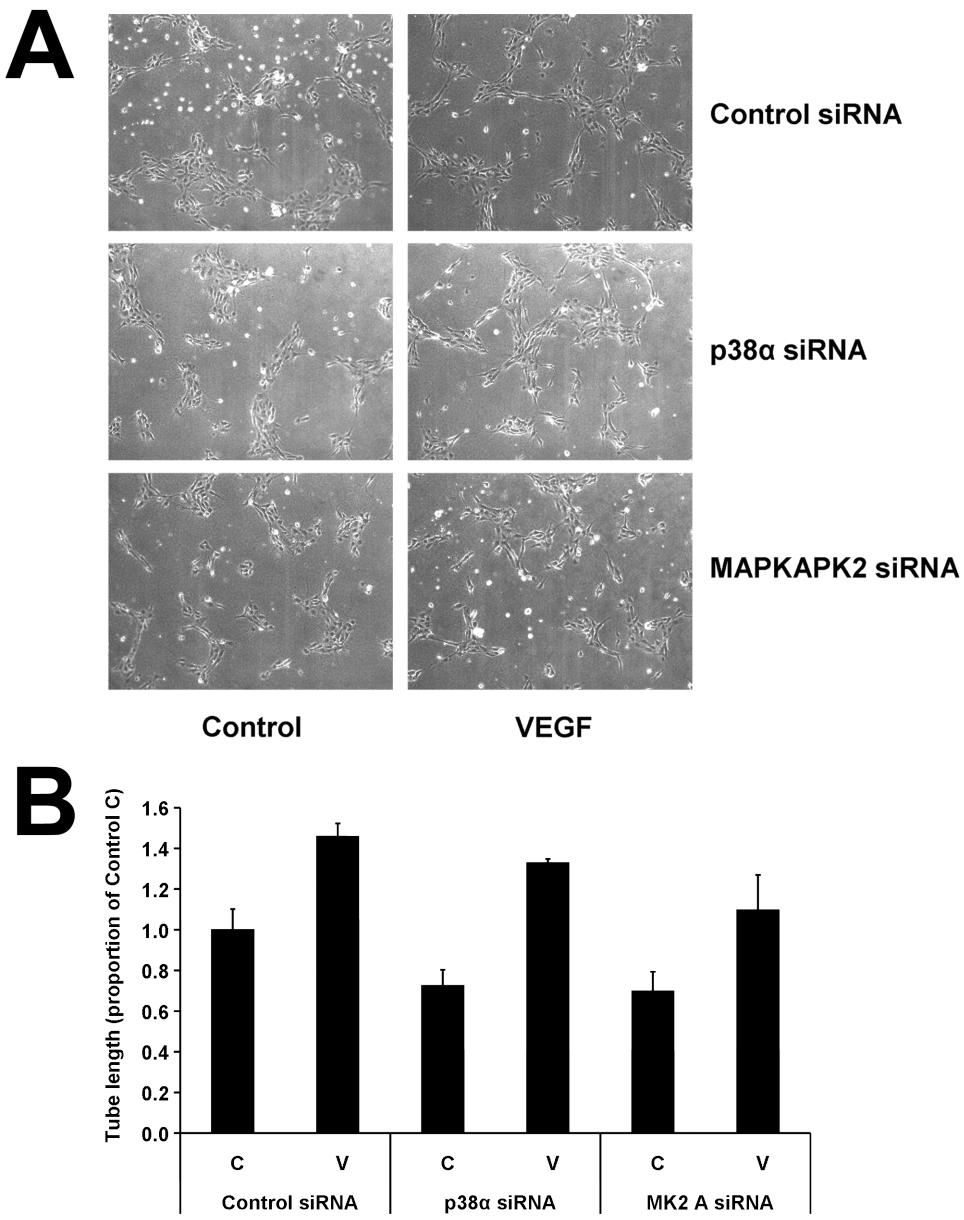

Figure 5.19: Effect of knockdown of p38α and MAPKAPK2 on VEGF-induced tubulogenesis

HUVECs were incubated for 48 h in the presence the indicated siRNA. Cells were then trypsinised and plated on to a collagen gel. VEGF (V, to a final concentration of 25 ng/ml) or no addition (C) was added to the cell suspension, and cells incubated were overnight at 37°C. The following day, pictures were taken of each well using an inverted light microscope and the length of the tubules present in each image was quantified.

A. Representative images of tubulogenesis on collagen in the presence of the siRNAs.

B. Quantification of the effect of p38α and MAPKAPK2 siRNAs on VEGF-induced tubulogenesis. Data is expressed as total tube length as a proportion of the Control siRNA/no VEGF group. Results are means $\pm$ SEM from three independent experiments, and were analysed by two-way ANOVA with Bonferroni's test for pair-wise comparisons. No significant differences were observed between siRNAs either with or without VEGF treatment. Mean knockdown of target protein achieved by siRNAs, compared to control siRNA: p38 88%, MK2 87%

mutant Hsp27 did not significantly alter VEGF-stimulated HUVEC migration when compared to a control virus. Inhibition of p38 MAPK or siRNA-mediated knockdown of p38α or MAPKAPK2 did not affect VEGF-stimulated migration or tubulogenesis, whereas inhibition or knockdown of PKC or PKD isoforms did alter VEGF-stimulated migration and tubulogenesis. Overall, it appears that PKC/PKD are more important mediators of VEGF-stimulated EC migration and tubulogenesis than p38/MAPKAPK2, although at least part of the involvement of PKC/PKD may be independent of Hsp27.

5.7.1 Cellular localisation of Hsp27

Hsp27 was observed to be distributed throughout the cytosol, although was apparently excluded from some cytoplasmic organelles. A greater portion of Hsp27 appeared to be present around the nucleus compared to the cell periphery, although this may be an artifact of a relatively thick optical section, as the cell is thinner at the edge than around the nucleus. No dramatic change in cellular localisation was observed after VEGF treatment. Time restrictions meant that examination of the influence of Hsp27 phosphorylation status using the Hsp27 phosphorylation site mutants was not performed.

Hsp27 has been reported to associate with actin filaments in ECs after heat shock (Loktionova *et al.* 1996), and to be present in the nucleus or cytoplasmic granules after heat shock (Arrigo and Welch 1987; Kato *et al.* 1993) in non-endothelial cells. While subtle changes in Hsp27 localisation may have occurred after VEGF treatment, large-scale changes were not observed. Hsp27 did not noticeably form filamentous structures, indicating that most Hsp27 is not associated with actin filaments either before or after VEGF treatment. It is possible that the use of confluent cells in these immunostaining experiments reduced any Hsp27 redistribution that may occur on VEGF stimulation of single cells, such as that leading to cell migration.

5.7.2 Role of phosphorylation in Hsp27 oligomerisation

Phosphorylation has previously been reported to influence the oligomeric size of Hsp27 (discussed in section 1.5.4.3). Data presented in this chapter shows that VEGF stimulation causes a reduction in the oligomeric size of Hsp27, and this can be prevented by pre-incubation of the cells with a combination of SB203580 and GF109203X, shown in the previous chapter to prevent VEGF-stimulated Hsp27 phosphorylation at S15, S78 and S82. Overexpressed S82D Hsp27 formed smaller oligomers than wild-type Hsp27, suggesting that S82 phosphorylation alone may be sufficient for VEGF-stimulated deoligomerisation of Hsp27. The reduction in oligomeric size observed in the S82D mutant was not due to the requirement of the S82 serine residue for maintenance of oligomeric structure as an S82A mutant formed large oligomers similar to wild-type Hsp27.

Hsp27 oligomers were observed in cells overexpressing S82D Hsp27. While some of the detected oligomer may be endogenous Hsp27, the degree of overexpression produced suggests that S82D Hsp27 itself also oligomerises. This finding is consistent with previous data on human Hsp27 showing that overexpressed wild type Hsp27 exists almost entirely as large species whereas an S78D S82D double mutant was present predominantly as smaller species but with some larger species also present (Rogalla *et al.* 1999).

In gel filtration studies, Hsp27 has consistently been reported to exist as two distinct populations of differing oligomeric size. Phosphorylation or phosphorylation-mimicking mutations result in an increase in the proportion of Hsp27 present as the smaller species. The two distinct populations observed in gel filtration studies are not clearly differentiated by the glutaraldehyde cross-linking method employed in this thesis, although the pattern observed with unmutated Hsp27 was broadly similar to that noted by Lambert *et al.* (1999). The proportion of Hsp27 present in large or small species, or whether Hsp27 exists as two discrete populations with regard to oligomeric size in ECs is not clear.

Human or hamster Hsp27 phosphorylated in vitro by MAPKAPK2, or containing

phosphorylation-mimicking mutations at all MAPKAPK2-phosphorylated serine residues (i.e. S15D S86D hamster Hsp27/S15D S78D S82D human Hsp27), has been reported to consist almost entirely of smaller species (Lambert *et al.* 1999; Rogalla *et al.* 1999). In the same studies, Hsp27 with phosphorylation-mimicking mutations at S78 and S82 (S86 in hamster Hsp27) forms a greater proportion of smaller species than Hsp27 with a phosphorylation-mimicking mutation at S15, suggesting that phosphorylation of S82 is more important than S15 for Hsp27 deoligomerisation.

Results from the previous chapter indicate that the majority of Hsp27 is unphosphorylated at S15 and S78, both before and after VEGF stimulation of HUVECs. The lack of formation of triply-phosphorylated Hsp27 is probably responsible for the partial reduction in Hsp27 oligomeric size observed after VEGF stimulation. Examination of the effect of SB203580 alone would have helped to exclude a significant role of S15 and S78 phosphorylation in the VEGF-induced reduction in Hsp27 oligomeric size.

The possibility that overexpression of S82A Hsp27 prevented VEGF-induced reductions in Hsp27 oligomeric size was not examined. VEGF stimulation modestly increased S82 phosphorylation of overexpressed wild-type Hsp27, whereas the total amount of Hsp27 present was strongly increased. Thus after VEGF stimulation, a lower proportion of Hsp27 is phosphorylated in Hsp27-overexpressing cells than in uninfected cells, which is likely to lead to greater difficulties in detecting VEGF-stimulated reductions in Hsp27 oligomerisation due to a higher background of unphosphorylated oligomeric Hsp27.

Overall the data obtained in this thesis support a role for phosphorylation status in modulation of Hsp27 oligomeric size, and indicate that the S82 phosphorylation occurring in VEGF-stimulated ECs is sufficient to reduce the size of VEGF-stimulated oligomers. The role of deoligomerisation in the function of Hsp27 in VEGF-stimulated cell functions is unclear, although effects on actin migration and chaperone functions are possible. For example, larger Hsp27 species are more effective molecular chaperones than smaller species (discussed in section 1.5.5.1.2).

5.7.3 Examination of VEGF-stimulated EC migration

5.7.3.1 Role of Hsp27

Although knockdown studies indicated a role for Hsp27 in VEGF-stimulated HUVEC migration, the role of Hsp27 phosphorylation is unclear. Overexpression of Hsp27 did not detectably increase migration in the absence or presence of VEGF, and overexpression of Hsp27 phosphorylation site mutants also had no significant effect on VEGF-stimulated migration, although a noticeable trend towards inhibition was seen with all mutants examined.

With the caveat that these effects did not reach statistical significance, the inhibitory effects of mutant Hsp27 adenoviruses suggest that prevention of phosphorylation, either at S82 or at both S15 and S78, inhibits VEGF-stimulated migration. However, they suggest that constitutively enhanced S82 phosphorylation, in so far as this is the effect of the S82D phospho-mimetic mutant, also inhibits the migratory response to VEGF. Since VEGF causes transient changes in Hsp27 phosphorylation, the effects of adenoviral Hsp27 site mutants suggests that constitutive blockade of enhancement of phosphorylation, or Hsp27 phosphorylation state cycling, may disrupt the role of Hsp27 in endothelial migration and other cell functions. The dynamic regulation of Hsp27 phosphorylation status is likely to be important in mediating VEGF-regulated cell movement.

Phosphorylation of Hsp27 has been proposed to release Hsp27 from capped actin filaments, allowing further actin polymerisation and lammelipodium extension, processes associated with migration (Rousseau *et al.* 2000a), and the inhibitory effect of the non-phosphorylatable Hsp27 mutants on migration is consistent with such a mechanism. The inhibitory effect of the S82D mutant may be due to an inability to stabilise newly formed actin filaments by capping them – transient capping may be important during migration. Alternatively, S82D Hsp27 may prevent directional migration by allowing excess actin polymerisation at the rear of the cell. Another possibility is that lack of large oligomeric chaperone-capable Hsp27 is sensed by the cell by some mechanism, which causes an emergency shut-down of non-essential cellular processes such as migration.

Stable overexpression of wild type Hsp27 was previously shown to enhance serum-stimulated HUVEC migration in a wound healing assay, whereas overexpression of an unphosphorylatable Hsp27 mutant inhibited migration (Piotrowicz *et al.* 1998). In a similar assay, oestrogen-stimulated BAEC migration is reduced by overexpression of a non-phosphorylatable Hsp27 mutant (Razandi *et al.* 2000), although a control for overexpression is apparently absent in the second study. In transwell assays similar to that used in this thesis, overexpression of unphosphorylatable Hsp27 inhibited PDGF-stimulated migration of vSMCs, although overexpression of wild-type Hsp27 had no effect (Hedges *et al.* 1999). Together these findings support the conclusion that Hsp27 phosphorylation plays an important role in migration of endothelial and other cell types.

Strong expression of endogenous Hsp27 in the HUVECs used in this thesis may have prevented any larger effects of overexpressed Hsp27 on migration, with sufficient endogenous wild-type Hsp27 present to fulfil the role of Hsp27 in migration. Transduction of HUVECs with control (lacZ or GFP) adenoviruses was consistently observed to increase Hsp27 expression though the effect was modest, suggesting that increased Hsp27 expression is a general consequence of adenoviral transduction in HUVECs. Attempts to increase the contribution of virus-encoded Hsp27 to VEGF-stimulated EC migration in this thesis were frustrated by a virus-induced reduction in cellular migration in siRNA treated cells. Attempts to rescue the Hsp27 siRNA-mediated reduction in VEGF-stimulated migration by overexpression of wild-type Hsp27 were also thwarted for the same reason. The basis of migration inhibition by an siRNA/virus combination is unclear, but may involve activation of cellular protective responses by siRNA transfection, which alters the effect of virus transduction on cellular behaviour.

Even in the absence of siRNA, the adenoviral vector may have significantly altered the migratory response of HUVECs, possibly altering the response to VEGF. Ramalingam *et al.* (2000) reported that transduction of HUVECs with adenovirus lacking the E1 region but containing the E4 region (such as the E1/E3-deleted vector used in this thesis) affected stromal-derived factor 1-stimulated migration. Migration induced by other stimuli was not examined. However, adenovirus vectors

produced by the same system as used in this thesis have been used by others to implicate various proteins in VEGF-stimulated HUVEC migration (Ha *et al.* 2008b).

5.7.3.2 Role of p38 MAPK

Inhibition of the p38/MAPKAPK2 pathway by p38 MAPK inhibition using pharmacological agents, or by knockdown of p38α or MAPKAPK2 using siRNAs, had no effect on VEGF-stimulated EC migration. However under the same conditions SB203580 or knockdown of p38α or MAPKAPK2 inhibited TNFα-stimulated Hsp27 phosphorylation (data presented in previous chapter), indicating the inhibitor and siRNAs were functional.

p38 MAPK has been suggested to be an important component of migratory signalling pathways in response to VEGF (Rousseau *et al.* 2000a), and other stimuli. In transwell assays, VEGF-stimulated HUVEC migration was inhibited by pre-treatment of cells with SB203580 (Rousseau *et al.* 1997; McMullen *et al.* 2004), or overexpression of kinase inactive p38 MAPK (McMullen *et al.* 2004). Overexpression of constitutively active MEK6, the upstream activator of p38 MAPK, increased HUVEC migration in the absence of other stimuli, and this could be prevented by co-expression of kinase-inactive p38 MAPK (McMullen *et al.* 2005).

Some of the differences between the results obtained in this thesis and that obtained by other groups may be due to methodological differences, including wound healing-type assays rather than transwell-type assays, and differences in specific cell type examined. However, Rousseau *et al.* (1997) and McMullen *et al.* (2004) used similar techniques to those employed in this thesis. The reason for the difference in results is unclear, particularly as Rousseau *et al.* (1997) and McMullen *et al.* (2004) also found that SB203580 strongly inhibited VEGF-stimulated incorporation of phosphate into Hsp27. Culture conditions, the source of endothelial cells and other factors discussed in the previous chapter may contribute to these differences, though they do not appear to adequately account for the discordance between my findings and previously published work.

In vivo, p38α (or its splice variants) are not essential for normal embryonic development (Adams

et al. 2000), and so cannot be essential for the VEGF-stimulated EC migration which occurs during vascular development. SB203580 has been reported to inhibit p38 MAPK isoforms p38α, β and β2 (Kumar *et al.* 1997; Goedert *et al.* 1997), and it is possible that a role of p38α in EC migration is compensated by p38β or β2 during development. p38β-null mice (lacking expression of p38β and β2, which are alternatively spliced forms of the same gene) are apparently normal (Beardmore *et al.* 2005), although p38α may compensate. Generation of p38α/β double null mice has not been reported. However, MAPKAPK2 activity was completely blocked in cells derived from p38α-null mice (Adams *et al.* 2000), indicating that p38 MAPK/MAPKAPK2-mediated phosphorylation of Hsp27 is unlikely to be important in developmental EC migration in vivo. Overall these data indicate that p38 MAPK may not be essential for vascular development or VEGF-stimulated migration, agreeing with the results presented in this thesis.

5.7.3.3 Role of PKD

GF109203X (or Gö6983) and Gö6976 caused similar reductions in VEGF-stimulated migration, suggesting that an enzyme inhibited by the more selective Gö6976 (i.e. a PKD or classical PKC isoform) may be primarily responsible. SiRNA-mediated knockdown of either PKD1 or PKD2 inhibited VEGF-stimulated migration by over 40%. As PKD2 knockdown reduced VEGF-stimulated Hsp27 S82 phosphorylation by less than 40% and PKD1 knockdown had no significant effect on Hsp27 phosphorylation, the effect of the PKD1 siRNA (and possibly both PKD siRNAs) on migration is unlikely to be mediated solely via inhibition of VEGF-stimulated Hsp27 S82 phosphorylation, and may be independent of effects on Hsp27.

Other groups have also reported the involvement of PKD1 and 2 in EC migration. siRNA-mediated knockdown of PKD1 (Qin *et al.* 2006, transwell assay) or overexpression of an S738A/S742A PKD1 double mutant (Qin *et al.* 2006, transwell) or kinase-dead PKD1 (Ha *et al.* 2008b, wound healing) inhibits VEGF-stimulated HUVEC migration in the indicated assays. Knockdown of PKD2 has also been reported to inhibit serum-stimulated HUVEC migration in a transwell assay

(Hao *et al.* 2009b).

As mentioned above, it is unlikely that the major influence of PKD1 on migration is via effects on Hsp27 phosphorylation. PKD1 has been shown to mediate VEGF-stimulated phosphorylation of histone deacetylases (HDACs) 5 and 7 in ECs. In wounding assays, overexpression of an S259A/S498A HDAC5 double mutant inhibited VEGF-stimulated HUVEC migration (Ha *et al.* 2008b), whereas overexpression of an S178A/S344A/S479A HDAC7 triple mutant inhibited VEGF-stimulated migration of bovine and human aortic ECs (Wang *et al.* 2008; Ha *et al.* 2008a). Thus inhibition of VEGF-stimulated HDAC phosphorylation may be at least partially responsible for the reduction in VEGF-stimulated HUVEC migration caused by PKD1 knockdown.

To my knowledge, the involvement of PKD2 in VEGF-stimulated migration has not been reported elsewhere, and the mechanism by which PKD2 knockdown reduced HUVEC migration in this thesis is unknown. As PKD2 knockdown alone (in the absence of SB203580) reduced VEGF-stimulated Hsp27 S82 phosphorylation, it is plausible that effects on Hsp27 phosphorylation are relevant to the effects of PKD2 knockdown on migration. PKD2 knockdown has also been reported to reduce the expression of growth factor receptors including VEGFR2 and FGFR1 (Hao *et al.* 2009b), and this may contribute to the reduction in VEGF-stimulated migration by the PKD2 siRNA. Reduction of VEGFR2 expression is unlikely to be the major reason for the reduction in migration given that the PKD1 siRNA reduced migration considerably more than the PKD2 siRNA but caused no additional inhibition of migration.

5.7.3.4 Role of PKC

In this thesis, the effect of PKC knockdown on VEGF-stimulated migration was isoform-specific. PKCα knockdown reduced migration, whereas PKCδ knockdown enhanced VEGF-stimulated migration and PKCϵ knockdown had little effect. The effects of Gö6976 and GF109203X probably result from inhibition of PKD1, PKD2 and PKCα, knockdown of which reduced VEGF-stimulated migration, although effects on other PKCs and non-PKC enzymes may contribute.

Previous results of isoform-specific PKC manipulation are consistent with those obtained in this thesis. Exactly how PKCα and PKCδ affect EC migration has not been examined, but PKC isoforms have been implicated in regulation of a number of cytoskeletal mediators (Larsson 2006).

Antisense-mediated reduction of PKCα expression reduced HUVEC migration in the presence of serum in a wound healing assay (Wang *et al.* 2002), and overexpression of PKCα in rat capillary ECs increases basal and hepatocyte growth factor-stimulated migration in a transwell assay (Harrington *et al.* 1997). Together, these data indicate that PKCα plays a pro-migratory role and that PKCα activity may be limiting in EC migration, although the involvement of PKCα in VEGF-stimulated EC migration was not directly addressed.

In a wound healing assay, overexpression of PKCδ in ECV immortalised ECs inhibits migration in the presence of VEGF, but not in the presence of serum (Shizukuda *et al.* 1999), suggesting that PKCδ inhibits VEGF-stimulated migration specifically. The authors hypothesised that a VEGF-stimulated, NO-mediated decrease in PKCδ activity, first observed after 8 h of VEGF stimulation, may contribute to VEGF stimulated migration (i.e. PKCδ activity is anti-angiogenic), and overexpression of PKCδ prevents this decrease and subsequent migration. In the transwell assays used in this thesis VEGF-stimulated migration occurs for only 4 h, although it is possible that PKCδ deactivation kinetics vary between transwell and wounding assays, possibly due to a greater need for cell detachment or breaking of cell-cell contacts or lack of a VEGF gradient in wound healing assays.

At first glance, the effects of the PKD siRNAs (which reduce migration) and the PKCδ siRNA (which inhibits PKD activation loop phosphorylation and so PKD activity, but increases migration) appear contradictory. However, the reduction in active PKD (after VEGF stimulation) obtained by PKCδ and PKD siRNAs may differ. As shown in the previous chapter, PKCδ knockdown reduced PKD activation loop phosphorylation by 57%, whereas PKD activation loop phosphorylation was reduced 64% by the PKD1 siRNA and 81% by the PKD2 siRNA. The actual reduction in VEGF-generated active PKD1 caused by the PKD1 siRNA may be greater than 64% as the signal detected

by the PKD P-S910 antibody, apparently PKD1 specific, was reduced by 85% in PKD1 siRNA-treated cells. If, for example, an 80% reduction in activation of either PKD1 or PKD2 is required for migration to be affected, then PKCδ knockdown would be insufficient to inhibit pro-migratory signals downstream of PKD (which would be affected by direct PKD knockdown), but may inhibit other anti-migratory processes which are not mediated by PKD. In short, the effects of the PKC siRNAs on migration may not occur via effects on PKD activity.

If the VEGF/VEGFR2 interaction is critical for VEGF-stimulated migration, the lack of effect of the PKCϵ siRNA on migration suggests that the reduction in VEGFR2 expression observed in cells treated with the PKCϵ siRNA is insufficient to retard VEGF-stimulated cell migration, and so may not impact upon functionally relevant VEGF-stimulated cell signalling. The decrease in VEGFR2 expression caused by the PKCϵ siRNA make it likely that the effects obtained with the PKCϵ siRNA detailed in the previous chapter (e.g. on PKD activation loop phosphorylation and Hsp27 S82 phosphorylation) may therefore indicate genuine effects of PKCϵ in VEGF-stimulated signalling rather than an indirect effect via VEGFR2 expression.

5.7.3.5 Proposed model for VEGF-stimulated HUVEC migration

Overall, the results obtained in this chapter indicate that Hsp27, PKCα, PKD1 and PKD2 are required for VEGF-stimulated HUVEC migration, whereas PKCδ appears to act primarily as an inhibitor of migration. It is unknown whether the effects of these enzymes are specific to VEGF-stimulated migration, or apply more generally to migration induced by other stimuli such as serum. While PKD2 may act partially via effects on Hsp27 phosphorylation, the effects of PKCα and PKD1 are likely to be largely independent of Hsp27. p38 MAPK does not appear to have a major role in VEGF-stimulated HUVEC migration. These relationships are summarised in figure 5.20.

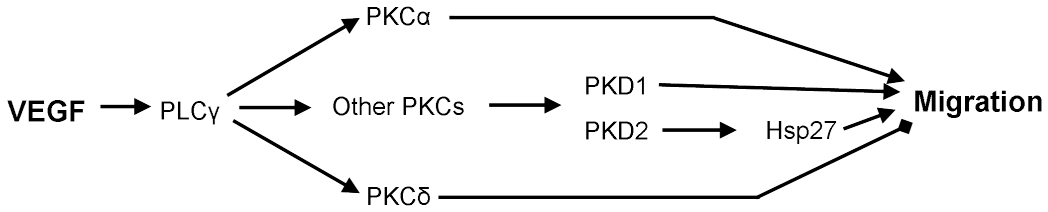

Figure 5.20: Proposed model for VEGF-stimulated migration via PKD/Hsp27
Schematic diagram of the PKC/PKD signalling pathways involved in VEGF-stimulated migration. Clearly a large number of proteins regulate a complex cellular event such as migration, only the enzymes experimentally examined in this thesis are illustrated. PKCα and PKCδ activate and inhibit VEGF-stimulated migration respectively (inhibition of migration by PKCδ is indicated with a diamond-tipped line). PKCδ and other PKCs may also affect migration via PKDs. PLCγ, though not directly examined in this thesis, is well established as a mediator of PKC activation. p38 MAPK/MAPKAPK2 does not appear to be important for VEGF-stimulated EC migration.

5.7.4 Role of Hsp27 in apoptosis

Virus-mediated overexpression of Hsp27 has previously been reported to reduce HUVEC apoptosis in a hypoxia–reoxygenation cell culture model (Kabakov *et al.* 2003). In this thesis, Hsp27 knockdown increased EC apoptosis induced by serum starvation. Hsp27 knockdown apparently increased EC apoptosis equally in the presence or absence of VEGF – that is, VEGF reduced apoptosis similarly in cells with and without Hsp27 knockdown. These data suggest that either Hsp27 knockdown was insufficiently complete to noticeably affect the VEGF-stimulated component of survival of serum starvation, or Hsp27-mediated survival pathways are not substantially affected by VEGF.

Hsp27 may have a role in VEGF-stimulated protection against apoptosis induced by methods other than serum starvation, e.g. using Fas ligand. Knockdown of Hsp27 sufficiently to impact upon a signalling role may be difficult to achieve given the abundance of Hsp27 in ECs, as it is possible that only a small fraction of this multi-functional protein is involved in signalling.

In this thesis, adenovirus transduction of HUVECs largely prevented apoptosis due to serum starvation, precluding the use of Hsp27-overexpressing viruses to examine the role of Hsp27 phosphorylation sites in protection against serum starvation-induced apoptosis. Transduction of HUVECs

with E1- E4+ adenovirus has previously been reported to prolong EC viability in the absence of serum, and this effect appeared dependent on sequences encoded by the E4 region as E1- E4- adenoviruses did not cause an increase in the survival of transduced ECs (Ramalingam *et al.* 1999).

While differences in the proportion of annexin V-stained cells between treatments have been attributed to effects of the treatments on apoptosis, effects on cell proliferation may also play a role. VEGF is a mitogen, and as the incubation time in the assay is similar to the doubling time of HUVECs (24–30 h, batch specific, as quoted by the supplier), VEGF-stimulated cell division could produce additional cells. These extra cells may die rapidly via apoptosis due to insufficient growth factor stimulus or some other factor, contributing to the number of apoptotic cells and giving the impression that VEGF has a lower survival effect than it does in reality. Alternatively, these extra cells may take some time to enter apoptosis, contributing to the number of live cells at the time the assay is terminated and giving the impression that VEGF promotes cell survival more strongly than in reality. Hsp27 knockdown may also have an effect on proliferation, causing similar effects. Separation of proliferation and apoptosis effects could have been performed by incubation of cells in the presence of modified nucleotides to inhibit cell proliferation during serum starvation, although arresting DNA synthesis may have led to alterations in cellular apoptosis rates. Alternatively a more rapid method for inducing apoptosis could have been used to avoid proliferation effects. However this assay has previously been used in a form similar to that used in this thesis to examine VEGF-stimulated HUVEC survival (Jia *et al.* 2004).

Overall, it appears that both VEGF and Hsp27 protect against serum starvation-induced HUVEC apoptosis, but Hsp27 does not appear to be essential (at least in large quantities) for VEGF-stimulated protective pathways.

5.7.5 Role of Hsp27 in tubulogenesis

Hsp27 knockdown reduced VEGF-stimulated tubulogenesis on 2-D collagen gels, and it is likely that reductions in migration and apoptosis contribute to this effect. Similar to the results obtained

for migration, blockade of the p38 MAPK pathway by SB203580 or knockdown of either p38α or MAPKAPK2 had no effect on VEGF-stimulated tubulogenesis, whereas PKC inhibition via GF109203X prevented VEGF-stimulated tubulogenesis.

The ability of Hsp27 knockdown or PKC inhibition to reduce VEGF-stimulated tubulogenesis is unsurprising given the effects of these approaches on migration and apoptosis. Interestingly, Hsp27 knockdown reduced basal tube formation (in the absence of VEGF), whereas GF109203X did not. Qualitatively, it appeared that Hsp27 siRNA-treated cells were more prone to die during the procedure resulting in fewer cells available for tubulogenesis, suggesting that apoptosis plays a significant part in this assay, at least in the effects of the Hsp27 siRNA.

Similar to the results obtained for VEGF-stimulated migration, reduction of p38 MAPK signalling did not significantly affect VEGF-stimulated tubulogenesis. SB203580 has been reported to slightly reduce tube formation in 3-D collagen gels by bovine skeletal muscle endothelial cells stimulated by a VEGF/hepatocyte growth factor combination (Yang *et al.* 2001). However as discussed above, p38α does not play an essential role in embryonic development and angiogenesis (Adams *et al.* 2000).

Tube formation in this assay was poor in that tubes were not particularly 'tube-like', although the assay was reproducible. Using a similar procedure, Dr. Dan Liu has shown more convincing tube formation in 2-D collagen assays (reported in Liu *et al.* 2008). Tube appearance is further improved on matrigel (Ha *et al.* 2008b), although the effect of VEGF may be further clouded by the addition of other factors and additional serum.

5.7.6 Summary

Hsp27 is involved in EC survival, and VEGF-stimulated migration and tubulogenesis. VEGF stimulates phosphorylation of Hsp27 predominantly at S82, which reduces Hsp27 oligomeric size and may affect its functional properties. Overexpression of wild-type Hsp27 or a number of Hsp27 phosphorylation site mutants did not significantly affect VEGF-stimulated migration, though ex-

pression of all phosphorylation site mutants showed a trend for reduced migration. PKC and PKD are involved in VEGF-stimulated migration, but at least part of the role of these enzymes on migration appears to be independent of Hsp27. The stress-activated p38 MAPK/MAPKAPK2 pathway does not appear to be important for VEGF-stimulated EC migration or tubulogenesis.

Chapter 6

Results: SLP2 in endothelial cells

6.1 Introduction

Stomatin-like protein 2 (SLP2) became of interest in this thesis when it was identified in a proteomics screen as a major component of phospho-tyrosine immunoprecipitates derived from HUVECs (see section 3.4.2).

Human SLP2 was originally identified from erythrocyte membranes as a ≈40 kDa peripheral membrane protein with amino acid sequence homology to previously identified stomatin and SLP1 due to the presence of a consensus sequence RX_2 (L/I/V) (S/A/N) X_6 (L/I/V) DX_2TX_2WG (L/I/V) (K/R/H) (L/I/V) X (K/R) (L/I/V) E (L/I/V) (K/R), where X is any amino acid (Wang and Morrow 2000). Since then another human stomatin homologue, SLP3, has been discovered, and SLP2 has been proposed to belong to a larger family including stomatin, the stomatin-like proteins and others, collectively termed slipins (Green and Young 2008). Stomatin itself is a 31 kDa transmembrane protein, lack of which is associated with erythrocyte abnormalities and the condition overhydrated hereditary stomatocytosis, a form of anaemia (Stewart 1997). However, stomatin-null mice have normal red blood cells, suggesting lack of stomatin is not the cause of this condition (Zhu *et al.* 1999). Stomatin and SLP3 have been reported to be involved in regulation of ion channels. MEC2, a homologue of stomatin, is involved in ion channel-mediated mechanosensation

(Huang *et al.* 1995), and SLP3 is essential for touch sensation in mice (Wetzel *et al.* 2007).

An alignment of the protein sequences of human stomatin, SLP1, SLP2 and SLP3 is shown in figure 6.1A. It is clear that there are substantial differences between stomatin and the stomatin-like protein sequences. SLP2 does not contain the N-terminal hydrophobic domain believed to be a membrane-spanning domain in stomatin, SLP1 and SLP3, and is not a transmembrane protein (Wang and Morrow 2000). Additionally, greater amino acid identity occurs between SLP2 homologues present in organisms as diverse as flies, nematodes and plants than between human stomatin and stomatin-like proteins (compare figures 6.1A and B). While BLAST did not detect homologous sequences in the yeast *S. cerevisae* or the bacterium *E. coli*, a later more comprehensive analysis indicates that SLP2 homologues are present in some bacteria and archaea (Green and Young 2008). The conservation of SLP2 itself throughout evolution, and its divergence from other members of the stomatin/SLP family suggests that SLP2 may have a distinct role from those of stomatin, SLP1 and SLP3.

At the time of my identification of SLP2 in endothelial cells, very little was known about SLP2 – literature searches for phrases such as 'stomatin-like protein 2', 'SLP2', or the gene name 'STOML2' in PubMed retrieved very few papers referring specifically to SLP2 – these papers identified the presence of SLP2 but did not examine its functional role.

At that time, SLP2 protein had been identified in a variety of human tissues, including heart, brain, placenta, lung, liver, skeletal muscle, kidney and pancreas – all tissues examined, indicating a wide tissue distribution (Wang and Morrow 2000). SLP2 had also been identified via proteomic analysis of caveolae/lipid raft-enriched HUVEC fractions (Sprenger *et al.* 2004). Tyrosine phosphorylation of SLP2 at Y124 had been observed via tandem mass spectrometry in the lymphoma cell line SU-DHL-1, although this phosphorylation was not observed in another lymphoma cell line, Karpas 299, in the same study (Rush *et al.* 2005).

Thus although SLP2 had been cloned and identified in human endothelial cells, and a tyrosine phosphorylation site identified, the functional and/or signalling roles of SLP2 were completely

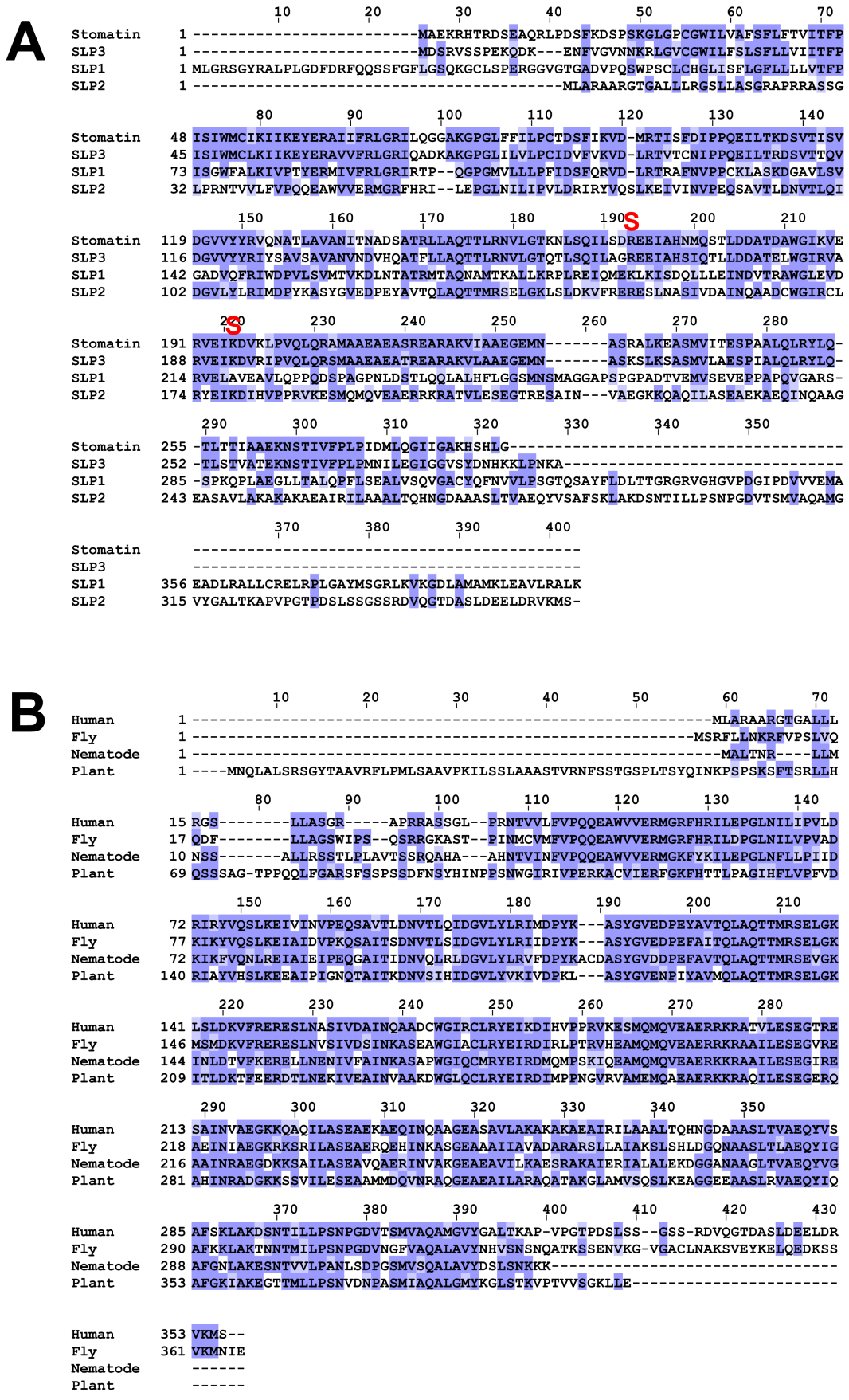

Figure 6.1: Alignment of human SLP2 protein sequence to stomatin family proteins (legend overleaf)

Figure 6.1: Alignment of human SLP2 protein sequence to stomatin family proteins (continued)
A. Reference protein sequences for human stomatin, SLP1, SLP2, and SLP3 were retrieved from the RefSeq database and aligned with ClustalX2. Residues are coloured according to Blossum62 score, with darker colours indicating better conservation. The first and last residues of the stomatin family consensus sequence RX_2 (L/I/V) (S/A/N) X_6 (L/I/V) DX_2TX_2WG (L/I/V) (K/R/H) (L/I/V) X (K/R) (L/I/V) E (L/I/V) (K/R) are indicated with an 'S'. The RefSeq database accession numbers for the protein sequences (all human) used for alignment were: Stomatin, NP_004090.4; SLP1, NP_004800.2; SLP2, NP_038470.1; SLP3, NP_660329.1.
B. Homologues of the human SLP2 protein sequence from (A) were located using BLASTp. The top RefSeq hits from common experimental organisms, the fly *Drosophila melanogaster* (RefSeq accession NP_611853.2, the nematode worm *Caenorhabditis elegans* (NP_492517.2), and the plant *Arabidopsis thaliana* (NP_200221.1), were aligned to the human SLP2 sequence using ClustalX2 as in (A). No BLASTp matches were found for *S. cerevisae* or *E. coli*.

unknown at the time SLP2 was identified during work for this thesis. In this chapter work examining SLP2 tyrosine phosphorylation, and SLP2 function in endothelial cells more generally, is presented. This data will then be discussed in the context of SLP2 data published during the course of this thesis.

6.2 SLP2 expression pattern and subcellular localisation of SLP2

As a starting point and to understand whether or not SLP2 is a widely expressed protein, the expression level of SLP2 in endothelial cells, smooth muscle cells, and a variety of cell lines was determined by immunoblotting. SLP2 was expressed in all cell types examined, at apparently similar levels, especially when compared to ERK and PKCα and some coomassie-stained protein bands, which were used for comparison purposes and displayed clear variations in expression levels between cell types (figure 6.2).

In initial studies on the sub-cellular localisation of SLP2, immunofluorescent staining of HUVECs showed a non-uniform distribution throughout the cytosol, in a pattern believed to be mitochondrial (data not shown). In subsequent experiments SLP2 staining substantially co-localised with that of Mitotracker Red, a dye that specifically accumulates in mitochondria (figure 6.3), indicating that SLP2 is a mitochondrial protein. SLP2 appeared to be present in all mitochondria, in

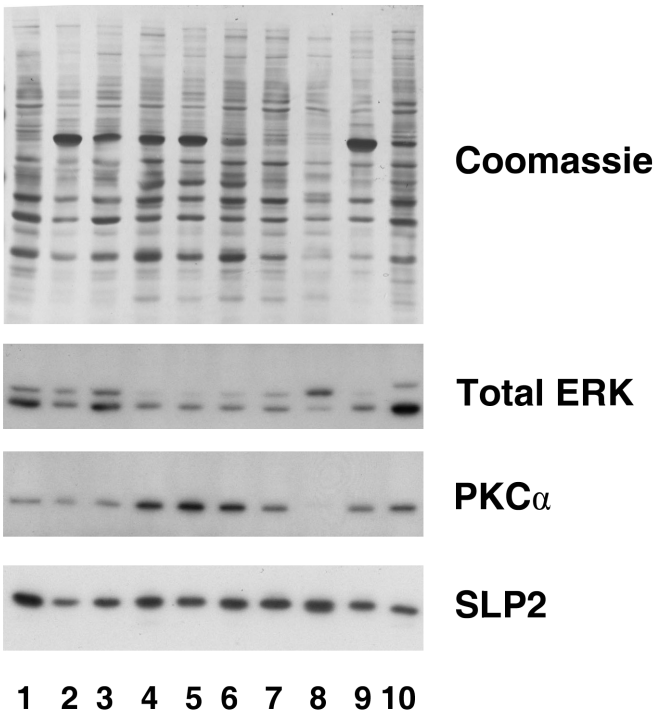

Figure 6.2: SLP2 protein expression in endothelial cells, smooth muscle cells, and a variety of cell lines
Lysates made from cultures of a variety of cell types were immunoblotted and probed with antibodies against the indicated target proteins. Equal loading was attempted by matching total protein loaded (assessed by a Bradford-type assay). After blotting, the membrane was stained with Coomassie R250 to show total protein loading. Lysates were numbered as follows: 1 HUVEC; 2 HCAEC; 3 Human coronary artery smooth muscle; 4 ACHN (kidney); 5 A549 (lung) (phosphate lysis buffer); 6 A549 (RIPA lysis buffer); 7 DU145 (prostate); 8 MCF7 (breast epithelium); 9 SKOV3 (ovary); 10 Porcine aortic endothelial cells. Lysates were protein assayed and supplied by Caroline Pellet-Many, Department of Medicine

that there did not appear to be patches of Mitotracker red-stained structures not stained for SLP2. Conversely, SLP2 did not occur in regions of the cell that did not accumulate Mitotracker Red.

6.3 SLP2 is present in anti-phosphotyrosine immunoprecipitates

SLP2 was identified by peptide mass fingerprinting as present in anti-pY immunoprecipitates prepared from both unstimulated and VEGF-stimulated HUVECs (figures 3.8 and 6.4). Total protein staining (e.g. silver staining) of 2-D-separated pY IPs always contained a spot migrating at the expected position for SLP2. A ≈40 kDa band present in anti-pY immunoprecipitates strongly reacted with an anti-SLP2 antibody (figure 6.4A), and together these data indicate that SLP2 is

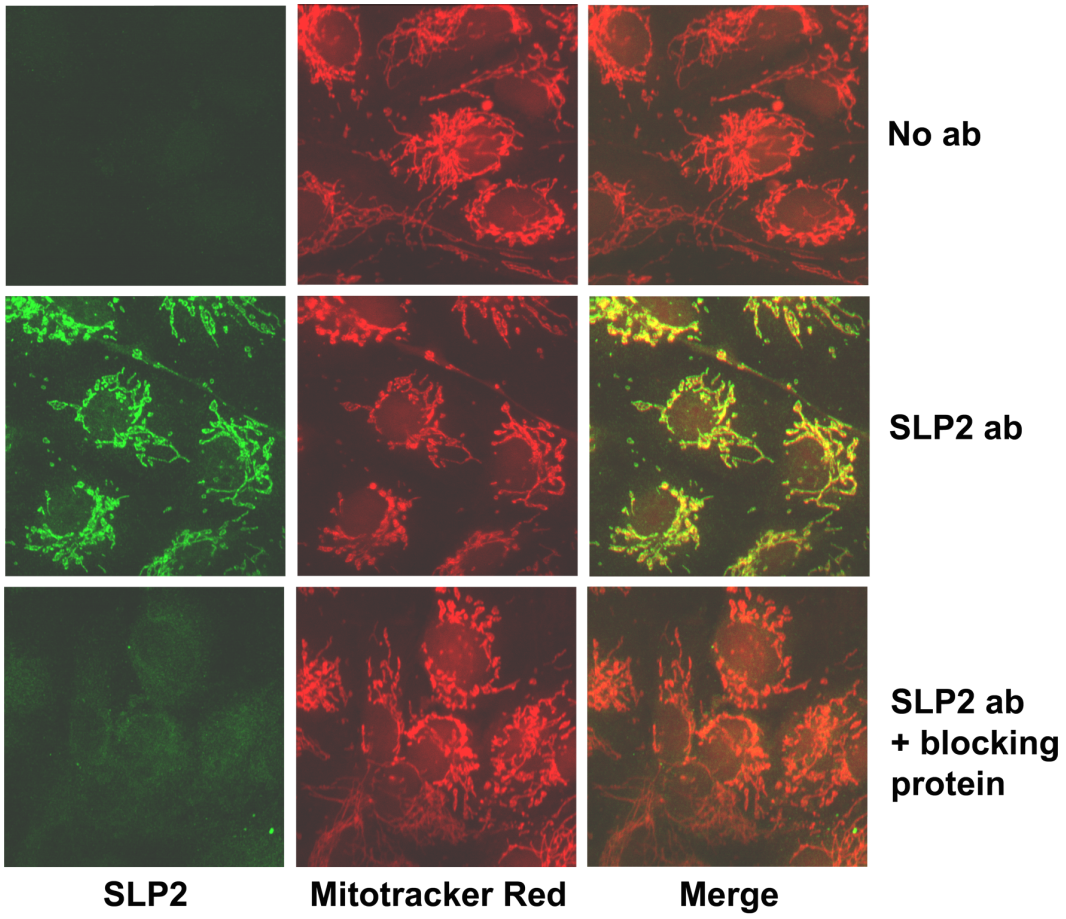

Figure 6.3: SLP2 is a mitochondrial protein
HUVECs grown on gelatin-coated coverslips were incubated in 400 nM Mitotracker Red in EGM for 30 mins to stain mitochondria (shown in red). Medium was then removed, and cells were washed, fixed, permeablised, blocked and incubated with an anti-SLP2 primary antibody followed by an Alexa fluor 488-conjugated secondary antibody (shown in green). In some samples, the SLP2 antibody was pre-blocked for 1 h at room temperature by addition of excess SLP2 recombinant protein before the antibody/blocking protein mixture was added to the cells. Images were acquired sequentially using a confocal microscope. Cells in the top row of images (No ab) shows cells without anti-SLP2 primary antibody but including the secondary reagent; the middle row (SLP2 ab) included both primary and secondary antibodies; and the bottom row (SLP2 ab + blocking protein) are images of cells incubated with pre-blocked primary and normal secondary antibodies. No adjustments have been made to the images after acquisition, and the same confocal settings were used to acquire all images. Blocking protein data is from one experiment, but co-localisation of SLP2 and Mitotracker Red was observed in three independent experiments.

indeed present in pY immunoprecipitates of HUVEC.

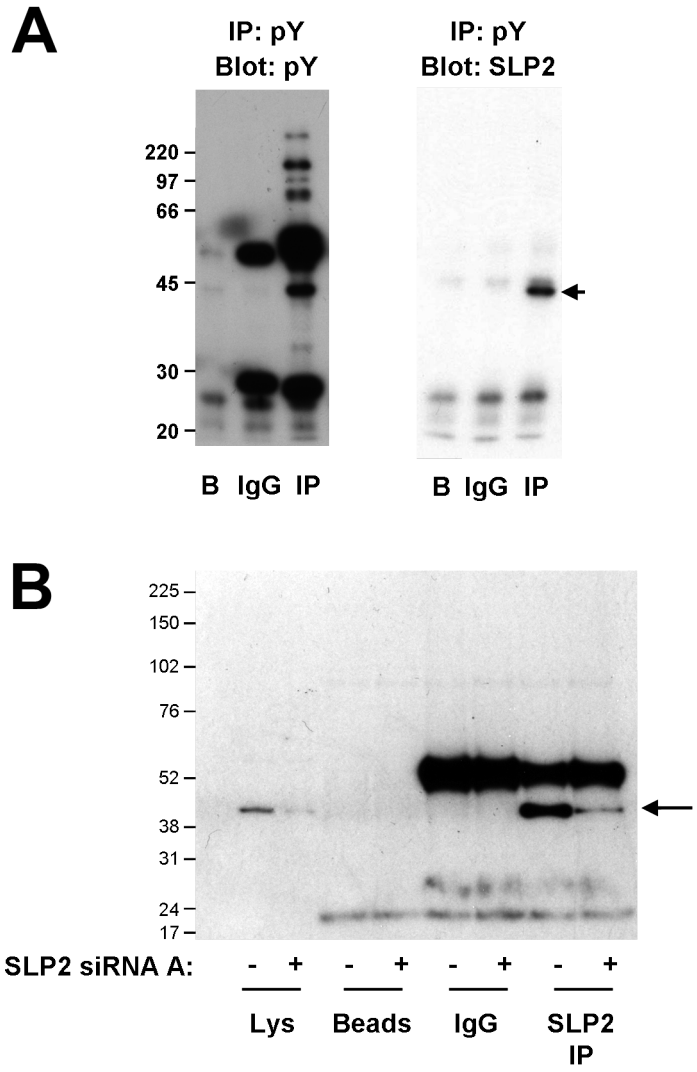

Figure 6.4: SLP2 is present in anti-phosphotyrosine immunoprecipitates
A. Phosphotyrosine-containing proteins were immunoprecipitated from HUVECs using an anti-pY monoclonal antibody. IPs were then immunoblotted and probed with antibodies directed against either pY (left) or SLP2 (right). Samples varied in the antibody used during the immunoprecipitation, and are: B, no primary antibody (protein A/G agarose beads alone); IgG, negative control antibody; IP, anti-pY antibody. Markers correspond to both blots. The arrowed band migrates in the expected position for SLP2. Markers correspond to both blots. Representative of three independent experiments.
B. HUVECs were treated for 48 h with SLP2 siRNA A (+) or a control siRNA (-), and SLP2 was immunoprecipitated. IPs were analysed by immunoblotting with SLP2 antibody. Lys, lysate; Beads, Protein A/G beads only (no immunoprecipitating antibody); IgG, control rabbit IgG. Lysate loaded was a small proportion of the input lysate used in the immunoprecipitations. Arrow indicates expected SLP2 band. Data is from a single experiment.

SLP2 could also be immunoprecipitated (figure 6.4B). Despite a number of attempts, it was not possible to convincingly detect an SLP2-sized band strongly reactive to anti-pY antibody in SLP2

immunoprecipitates (data not shown). To determine whether the anti-pY antibody immunoprecipitates SLP2 in a pY-dependent manner, pY-containing proteins were immunoprecipitated from lysates spiked with the pY analogue phenyl phosphate. The immunoprecipitation of pY-containing proteins was reduced in lysates spiked with phenyl phosphate, indicating that spiking inhibits binding of the anti-pY antibody to pY-containing proteins during immunoprecipitation (figure 6.5). Phenyl phosphate is acidic, but spiking did not apparently denature antibodies or the SLP2 antigen as immunoprecipitation of SLP2 by an anti-SLP2 antibody was not affected by spiking (figure 6.5). Phenyl phosphate spiking strongly reduced the immunoprecipitation of SLP2 by anti-pY antibody, suggesting that SLP2 is immunoprecipitated by anti-pY antibody in a pY-dependent manner.

6.3.1 SLP2 amino acid sequence analysis and examination of the effect of protein kinase A effectors on SLP2 2-D spot pattern

The human SLP2 reference protein sequence contains eight tyrosine residues, seven of which are conserved between human, mouse and zebrafish – these are Y75, Y106, Y117, Y124, Y175, Y282 and Y316 (human sequence numbering, figure 6.6). The other tyrosine residue, human Y113, is conserved between human and mouse SLP2.

It was believed that phosphorylation of one or more of these tyrosine residues may be responsible for the presence of SLP2 in anti-pY immunoprecipitates. To determine candidate enzymes that may be responsible for tyrosine phosphorylation of SLP2, the protein sequence of SLP2 was analysed using the Scansite 2.0 programme. At medium stringency settings a large number of hits were produced, but none of the phosphorylation sites predicted were tyrosine residues.

At high stringency Scansite produced only a single hit, predicting a protein kinase A (PKA) phosphorylation site at T203. T203 is conserved between human, mouse and zebrafish SLP2 (figure 6.6) although not present in the BLAST-identified SLP2 homologues listed in figure 6.1B. These sequence analysis studies prompted examination of the effect of inhibitors and activators targeting the PKA pathway.

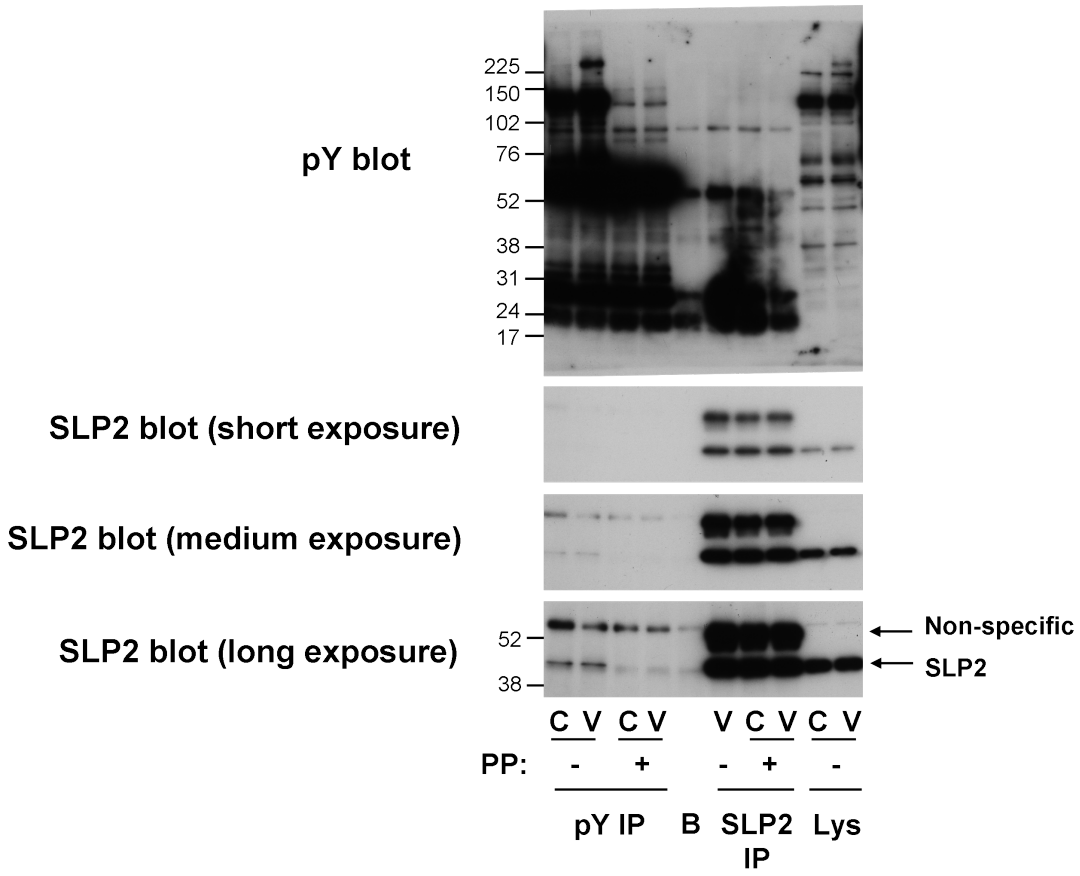

Figure 6.5: Anti-pY antibodies do not immunoprecipitate SLP2 in the presence of phenyl phosphate

HUVECs were preincubated with 1 mM sodium orthovanadate for 30 mins, before cells were treated with (V) or without (C) 25 ng/ml VEGF for 15 mins and lysed for immunoprecipitation. Pre-cleared lysates were mixed with an anti-pY antibody (pY IP) or SLP2 antibody (SLP2 IP) in the absence (-) or presence (+) of phenyl phosphate (PP, 25 mM final concentration) and immunoprecipitation was performed. Some of the pre-cleared lysates were heated in SDS-PAGE sample buffer without immunoprecipitation. Lysates (Lys) and IPs were then immunoblotted and probed with either anti-pY or anti-SLP2 antibody. Various exposures of the same SLP2 blot are shown. Positions of molecular weight markers (kDa) are indicated. The arrowed SLP2 band migrates in the expected position for SLP2. The arrowed non-specific band migrates in the expected position of IgG heavy chain. B, beads only control IP (no primary antibody used). Representative of two independent experiments. In a number of additional experiments excluding the anti-SLP2 IP, phenyl phosphate also reduced the IP of SLP2 by anti-pY.

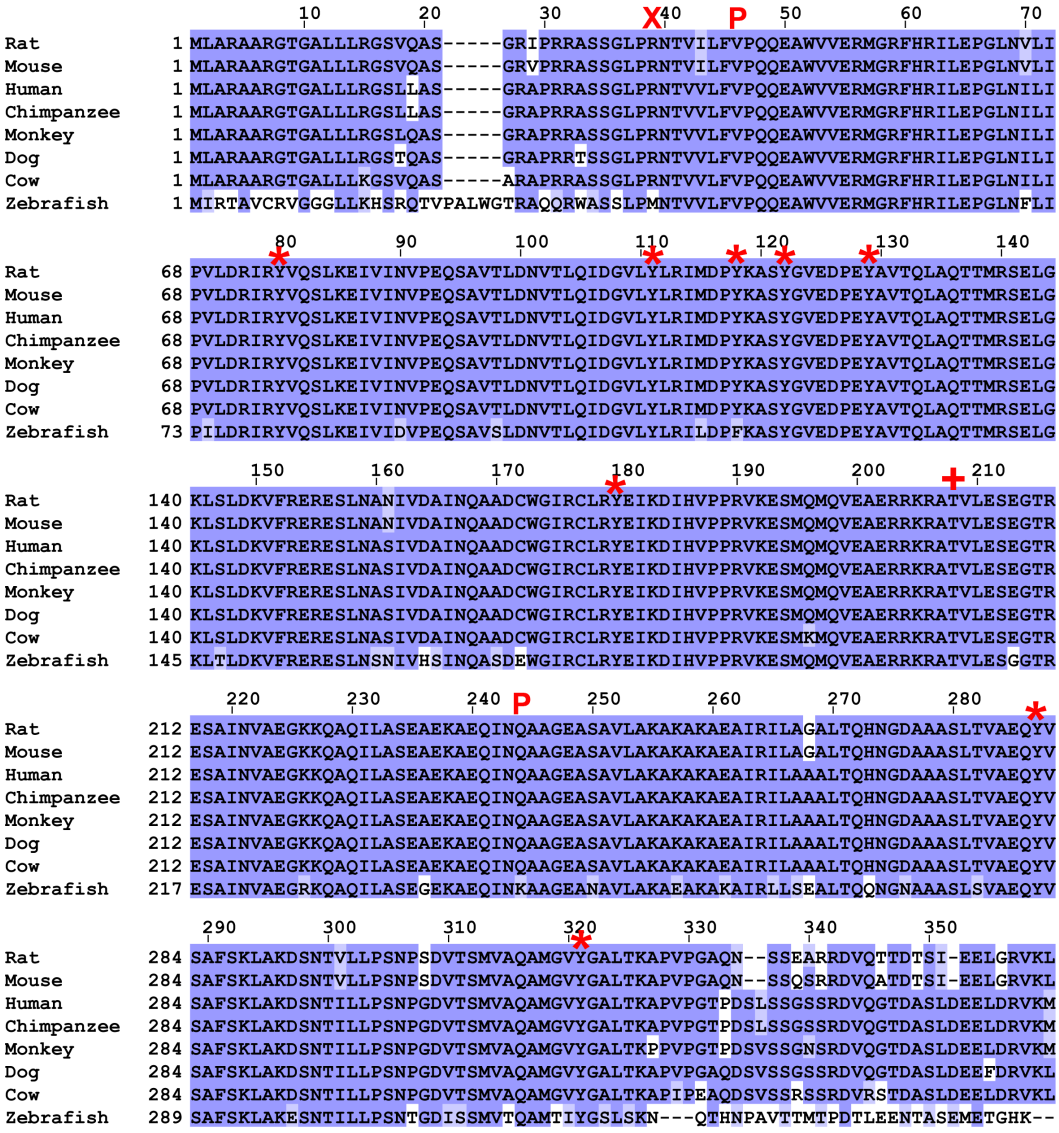

Figure 6.6: Alignment of human SLP2 protein sequence to homologues in other species
Protein sequences for SLP2 from human and other indicated species were retrieved from the RefSeq database, and aligned using ClustalX2. Residues are coloured according to Blossum62 score, with darker colours indicating better conservation. The eight tyrosine residues present in the human SLP2 sequence are highlighted with an asterisk (*). Analysis of the human SLP2 sequence by the Conserved Domain Database indicated that the PHB domain in human SLP2 runs from V41–Q239, the first and last residues are indicated with a red P. The initial 34 residues of the human sequence (last residue R34, indicated with a red X) were never identified by mass spectrometry despite peptide mass fingerprints being obtained from six independent protein samples.
The RefSeq database accession numbers for the protein sequences used for alignment were: human, NP_038470.1; chimpanzee, XP_520553.2; Rhesus monkey, XP_001091007.1; dog, XP_531986.2; cow, NP_001033157.1; rat, NP_001026816.1; mouse, NP_075720.1; zebrafish, NP_957325.1. The chimpanzee, monkey and dog sequences were listed as predicted proteins, and the zebrafish sequence as a hypothetical protein, but all sequences used were assigned RefSeq status. Both dog and chimpanzee have a number of predicted isoforms, with various extensions, insertions and deletions. The isoform most closely matching the human sequence was used for alignment in each case.

A number of pharmacological effectors of the cAMP/PKA pathway were tested for their effect on the SLP2 2-D spot pattern, which was used as an indicator of SLP2 phosphorylation status. No changes consistent with PKA-mediated phosphorylation were observed (figure 6.7). Although blots were not aligned exactly, three spots were visible in every blot, with the central spot being the largest, and comparison of spot patterns was based on the assumption that these three spots are the same molecular species in each blot. Given this, those changes that were observed seemed to be in the opposite direction to that expected if PKA phosphorylated SLP2 – the combinations of Forskolin + IBMX and dibutyryl cAMP + IBMX, expected to activate PKA, appeared to reduce the leftmost (acidic) spot compared to the large central spot (figure 6.7B). Additionally, a peptide including SLP2 T203 was identified from anti-pY immunoprecipitates by mass spectrometry, and was not phosphorylated (figure 6.10). Thus it appears that SLP2 is not basally phosphorylated on T203, and activators of PKA do not cause a noticeable increase in the acidity of SLP2, suggesting that PKA activation does not lead to SLP2 phosphorylation.

Many mitochondrial proteins are synthesised in the cytosol and then imported into mitochondria, often via an N-terminal targeting sequence which is cleaved after import (Neupert and Herrmann 2007). Further computational analysis of the SLP2 protein sequence predicted the presence of a mitochondrial targeting sequence at the N-terminus of SLP2. TargetP 1.1 predicted the last residue of the targeting sequence to be R34, and MitoProt II v1.101 predicted the last residue to be A28. In agreement with these predictions, the first 34 amino acids of SLP2 were not observed in the SLP2 peptide mass fingerprint in five tryptic digests from independent protein samples, regardless of whether SLP2 was obtained from SLP2 immunoprecipitates or pY immunoprecipitates, whereas the peptide covering residues N35–R51 was routinely observed (see figure 6.10 on page 349 for a list of identified peptides). Additionally, the observed isoelectric point of SLP2 on 2-D gels was $\approx$ 5.5 (compare with the location of the capZ and prohibitin 1 spots in figure 6.10, with Scansite-predicted pIs of 5.7 and 5.6 respectively, and β-actin, 41 kDa with a predicted pI of 5.5). The Scansite pI calculator predicted the pI of full-length SLP2 as 6.9, whereas the predicted pI of SLP2 lacking the first 34 residues is 5.3 (the calculated pI of the first 34 residues is 12.8).

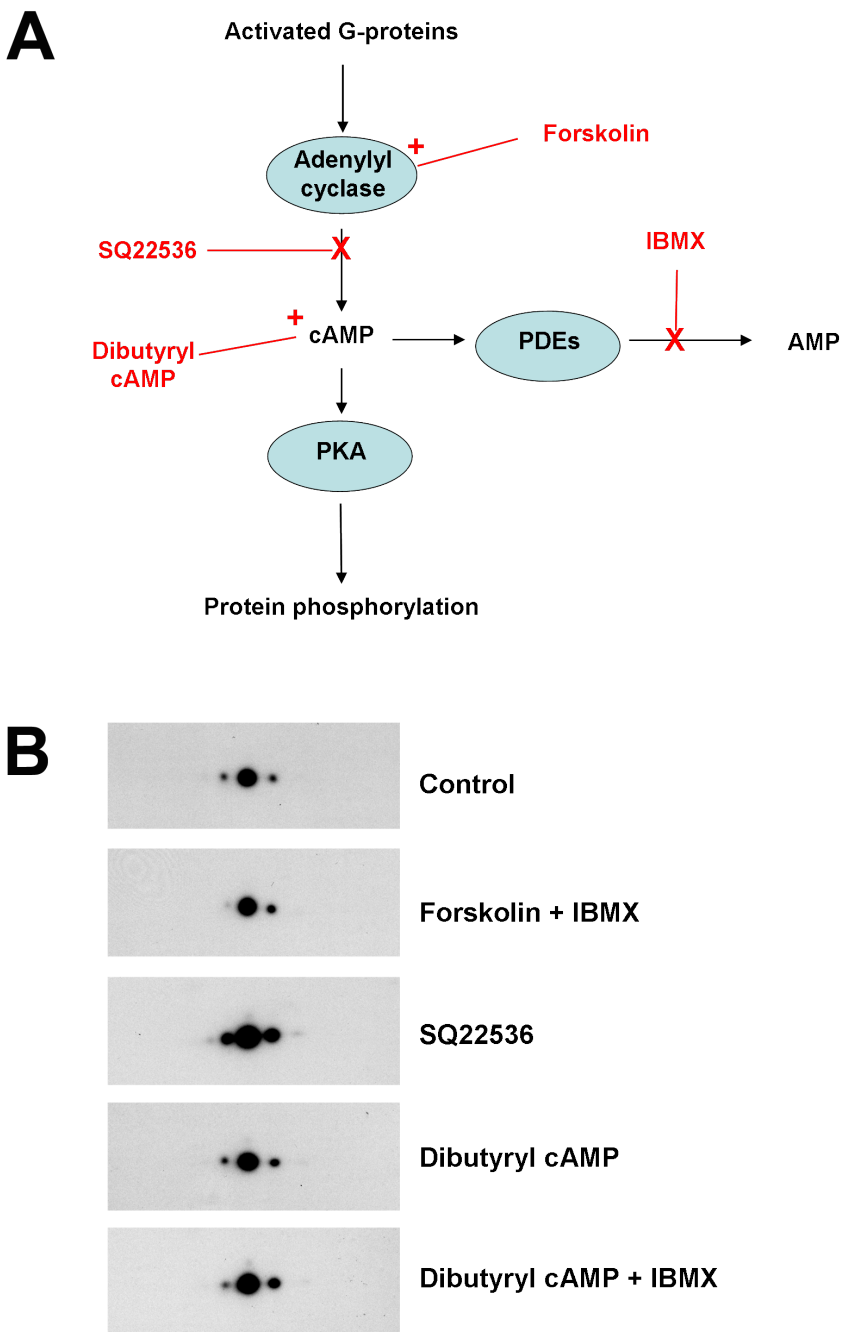

Figure 6.7: Influence of cAMP and protein kinase A manipulation on the SLP2 spot pattern

A. Schematic diagram of the cAMP/PKA pathway, illustrating the sites of action of the PKA effectors used in (B). Upstream stimuli lead to G-protein activation, which subsequently activates adenylyl cyclase so producing cAMP. cAMP activates PKA, which is then able to phosphorylate downstream proteins. cAMP is removed by phosphodiesterases (PDEs), which convert it to AMP. Adenylyl cyclase is activated by forskolin and inhibited by SQ22536. Dibutyryl cAMP is a cAMP mimic which activates PKA but is resistant to degradation by PDEs. 3-isobutyl-1-methylxanthine (IBMX) is a PDE inhibitor. PKA activity was expected to be increased by forskolin, dibutyryl cAMP, and IBMX, and reduced by SQ22536.

B. HUVECs were treated for 30 mins with either solvent alone (0.2% v/v DMSO, Control); 10 μM forskolin; 200 μM dibutyryl cAMP; 200 μM IBMX; 100 μM SQ22536; or the indicated combination of treatments. Cells were then lysed, and extracts were separated by 2-D electrophoresis, blotted, and probed with anti-SLP2 antibody. The acidic region is on the left. Data is from a single experiment.

Together these data suggest that SLP2 contains an N-terminal mitochondrial targeting peptide which is absent from the mature protein, which is presumably due to its cleavage after SLP2 entry into mitochondria (figure 6.3).

6.3.2 Effect of cytokines and kinase inhibitors on SLP2 2-D spot pattern and presence in phospho-tyrosine immunoprecipitates

As it was not possible to identify a consensus sequence for a specific tyrosine kinase using sequence analysis programmes, inhibitors targeting a variety of kinases were assayed for their effects on the SLP2 2-D spot pattern and on the amount of SLP2 recoverable from phosphotyrosine immunoprecipitates. Inhibitors targeting src family kinases (PP2), PKC (GF109203X), p38 MAPK (SB203580), and PI-3-K (Wortmannin), and a 30 mins treatment with serum, all failed to discernibly influence the SLP2 2-D spot pattern (figure 6.8). PP2, GF109203X, SB203580, wortmannin, and inhibitors of tyrosine kinases (herbimycin), tyrosine phosphatases (orthovanadate), MEK (U0126), and VEGFR2 (SU5614) failed to alter the amount of SLP2 detected in anti-pY immunoprecipitates (figure 6.9A). VEGF treatments of between 10 mins and 21 h duration also had no effect on the amount of SLP2 in anti-pY immunoprecipitates (figure 6.9B).

6.3.3 SLP2 may not be directly phosphorylated

Although SLP2 was always observed in anti-pY immunoprecipitates, as mentioned above, it was not possible to detect a band migrating in the position expected for SLP2 by probing SLP2 immunoprecipitates with the anti-pY antibody in immunoblots despite several attempts (section 6.3). It is possible that SLP2 is not directly tyrosine phosphorylated, but is closely associated with a pY-containing protein, and thus immunoprecipitated by the anti-pY antibody indirectly. That is, the anti-pY antibody binds to pY-containing protein X, which in turn binds to SLP2.

To examine whether SLP2 is directly tyrosine phosphorylated, SLP2 purified from anti-pY immunoprecipitates by 2-D electrophoresis was analysed by tandem mass spectrometry, a technique

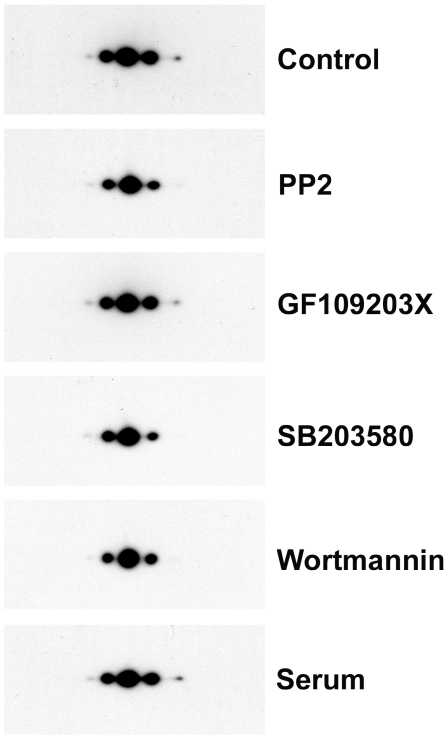

Figure 6.8: SLP2 spot pattern is unaffected by several kinase inhibitors
Confluent HUVECs were incubated for 30 mins in medium containing either 10% v/v serum; 3 μM PP2; 3 μM GF109203X; 5 μM SB203580; 100 nM wortmannin; or solvent alone (0.1% v/v DMSO, Control). Following lysis, 2-D separation (IEF pH 4–7, acidic on left) and transfer to membranes, blots were probed with anti-SLP2 antibodies to show the SLP2 spot pattern.

capable of determining the presence of post-translational modifications including phosphorylation. Commercial analysis performed by Alphalyse, which included phospho-peptide purification after trypsin digestion, did not identify any phospho-peptides present in SLP2. In-house analysis of SLP2 purified from an independent anti-pY immunoprecipitate run on a 2-D gel also failed to identify any phospho-peptides in SLP2, whereas it was possible to identify an Hsp27 peptide phosphorylated at S82 (see section 4.1.2.1) which was analysed at the same time. A peptide covering SLP2 residues 115–135 and so containing Y124, the SLP2 tyrosine phosphorylation site reported by Rush *et al.* (2005), was identified in both analyses and was not tyrosine phosphorylated. The peptides identified in the in-house analysis are shown in figure 6.10.

Although no phospho-peptides were identified using the tandem mass spectrometry approach described above, only three out of the eight human SLP2 tyrosine residues were covered by the mass spectrometry-identified peptides, leaving open the possibility that a phosphorylated tyrosine

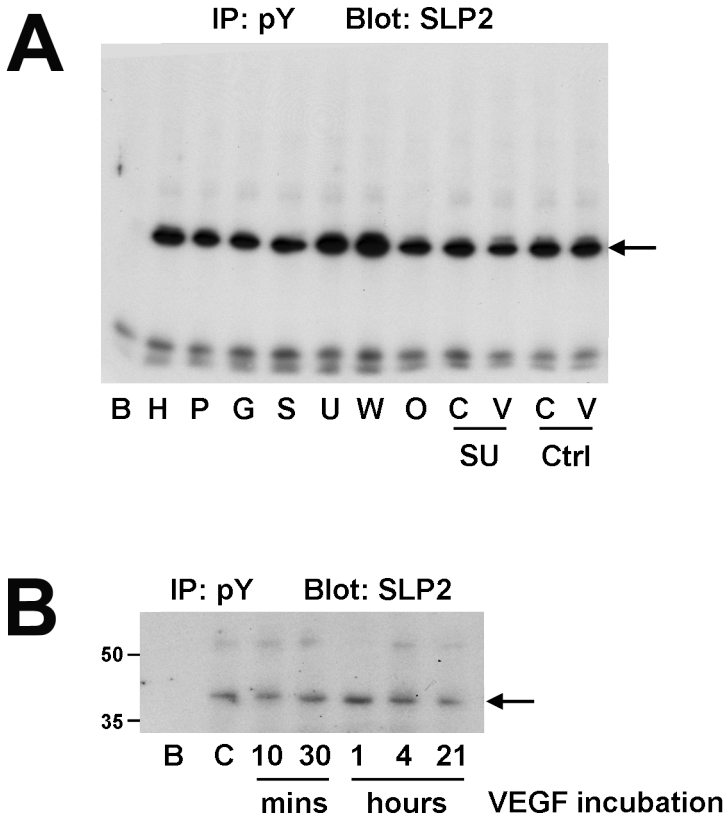

Figure 6.9: The quantity of SLP2 present in pY immunoprecipitates was not altered by a panel of treatments and inhibitors

A. HUVECs were incubated for 30 mins with either 1 μM herbimycin (H); 3 μM PP2 (P); 3 μM GF109203X (G); 5 μM SB203580 (S); 10 μM U0126 (U); 100 nM wortmannin (W); 1 mM orthovanadate (O); 5 μM SU5614 (SU); or solvent alone (Ctrl). Cells incubated with solvent alone or SU5614 were subsequently treated with 25 ng/ml VEGF (V) or no addition (C) for 15 mins, cells incubated with other inhibitors were not further treated. Cells were then lysed and phosphotyrosine-containing proteins were immunoprecipitated with an anti-pY antibody. Equal volumes of immunoprecipitates were then immunoblotted and probed with anti-SLP2 antibody. The arrowed band migrates at $\approx$ 40 kDa, the expected molecular weight of SLP2. B, beads only control (no immunoprecipitating antibody). Results are representative of two independent experiments. Apparent differences in the quantity of SLP2 present between immunoprecipitates were not consistent between experiments.

B. Effect of VEGF treatment on recovery of SLP2 by pY immunoprecipitation. HUVECs were left untreated (C) or incubated for the indicated time with 25 ng/ml VEGF, after which phosphotyrosine-containing proteins were immunoprecipitated with an anti-pY antibody. Equal volumes of immunoprecipitates were then immunoblotted and probed with anti-SLP2 antibody. The arrowed band migrates at the expected position for SLP2. B, beads only control (no immunoprecipitating antibody). Positions of molecular weight markers (kDa) are indicated. Results are from a single experiment.

MLARAARGTG ALLLRGSLLA SGRAPRRASS GLPR(NTVVLF VPQQEAWVVE
R)MGRFHR(ILE PGLNILIPVL DR)IRYVQSLK EIVINVPEQS AVTLDNVTLQ
IDGVLYLRIM DPYK(ASYGVE DPEY*AVTQLA QTTMR)SELGK LSLDKVFRER
ESLNASIVDA INQAADCWGI RCLRYEIKDI HVPPR(VKESM QMQVEAER)RK
R(AT*VLESEGT R)ESAINVAEG KK(QAQILASE AEK)(AEQINQA AGEASAVLAK)
AKAKAEAIRI LAAALTQHNG DAAASLTVAE QYVSAFSKLA K(DSNTILLPS
NPGDVTSMVA QAMGVYGALT K)(APVPGTPDS LSSGSSR)(DVQ GTDASLDEEL
DR)VKMS

Figure 6.10: Analysis of SLP2 from phospho-tyrosine immunoprecipitates by tandem mass spectrometry
Phosphotyrosine-containing proteins were immunoprecipitated from HUVECs using the anti-pY antibody, and were then separated by 2-D electrophoresis. The gel was silver stained and the spot corresponding to SLP2 was excised, digested with trypsin and analysed by tandem mass spectrometry. The identified peptides are enclosed in brackets and underlined, and are shown in the context of their position in the human SLP2 protein sequence. The tyrosine residues present in the SLP2 sequence are highlighted in red. The reported tyrosine phosphorylation site Y124 and the predicted PKA phosphorylation site T203, which were both contained in identified peptides, are indicated with an asterisk. No phosphorylation or any other modifications were detected in any of the identified peptides. This analysis was performed at the same time as the Hsp27 MS/MS analysis presented in figure 4.5, where a phosphorylated peptide was identified, indicating the ability of the procedure to identify phosphorylated peptides when present in a sample.

residue may occur in one of the unidentified sections of the SLP2 sequence. To address this issue, alkaline phosphatase (AP) treatment of anti-pY immunoprecipitates was used. As described in section 4.1.2.2, phosphorylation results in an increase in the acidity of a protein. Dephosphorylation with AP, which removes phosphate groups from Ser, Thr and Tyr residues, should therefore reduce the acidity of a protein that is already phosphorylated (such as SLP2 from pY IPs), causing a protein to appear more to the right (basic end) on a 2-D gel. To discern whether a shift had actually occurred, samples treated with and without AP were run on separate 2-D gels and also in the same gel (figure 6.11).

Alkaline phosphatase treatment largely eliminated tyrosine phosphorylation as detected by immunoblotting with an anti-pY antibody (figure 6.11A). However, AP treatment did not cause the potentially-phosphorylated SLP2 present in anti-pY IPs to shift to a more basic position, and the major SLP2 species present in both the IP and AP samples had the same isoelectric point before

and after AP treatment as shown by the increase in the size of the major SLP2 spot when the IP and AP-treated samples were run in the same gel (figure 6.11B).

Taken together with the tandem mass spectrometry data, the alkaline phosphatase experiments suggest that the SLP2 present in anti-pY immunoprecipitates is not directly phosphorylated.

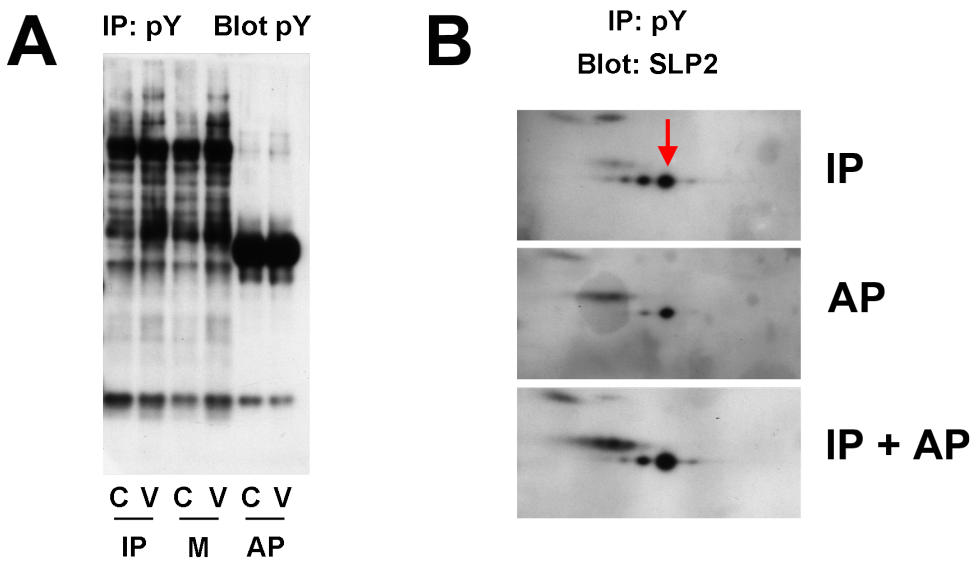

Figure 6.11: Effect of alkaline phosphatase treatment on 2-D spot pattern of an SLP2 immunoprecipitate
SLP2 was immunoprecipitated from confluent HUVECs treated for 15 mins with (V) or without (C) 25 ng/ml VEGF. The IPs were resuspended and divided into three aliquots. One aliquot (AP) was mixed with alkaline phosphatase to remove phosphate groups before quenching with concentrated SDS-PAGE buffer, another mimicked the conditions of alkaline phosphatase treatment (i.e. addition of alkaline phosphatase buffers and heating) but did not include the alkaline phosphatase protein (M), and the third remained on ice after immunoprecipitation before mixing with SDS-PAGE buffer (IP). The samples were then analysed as detailed below:
A. IPs were blotted and probed with anti-pY antibody.
B. IPs from VEGF-treated cells were precipitated and resuspended in 2-D buffer, proteins were separated by 2-D electrophoresis, blotted and probed with an anti-SLP2 antibody. IP, Immunoprecipitate only; AP, alkaline phosphatase (AP)-treated immunoprecipitate only; IP + AP, both AP-treated and untreated immunoprecipitates were mixed and run on the same 2-D gel. The position of the major SLP2 species present is indicated.
Results are representative of two independent experiments.

6.4 Analysis of SLP2 immunoprecipitates

If SLP2 itself is not directly tyrosine phosphorylated, SLP2 may be present in anti-pY immunoprecipitates because it is associated with a tyrosine phosphorylated protein. In an attempt to identify

SLP2-associated proteins, SLP2 immunoprecipitates derived from HUVECs were analysed by 2-D gel electrophoresis. A large number of proteins were present in the SLP2 immunoprecipitate that were not present in a beads-only control using the same lysate (figure 6.12, circled).

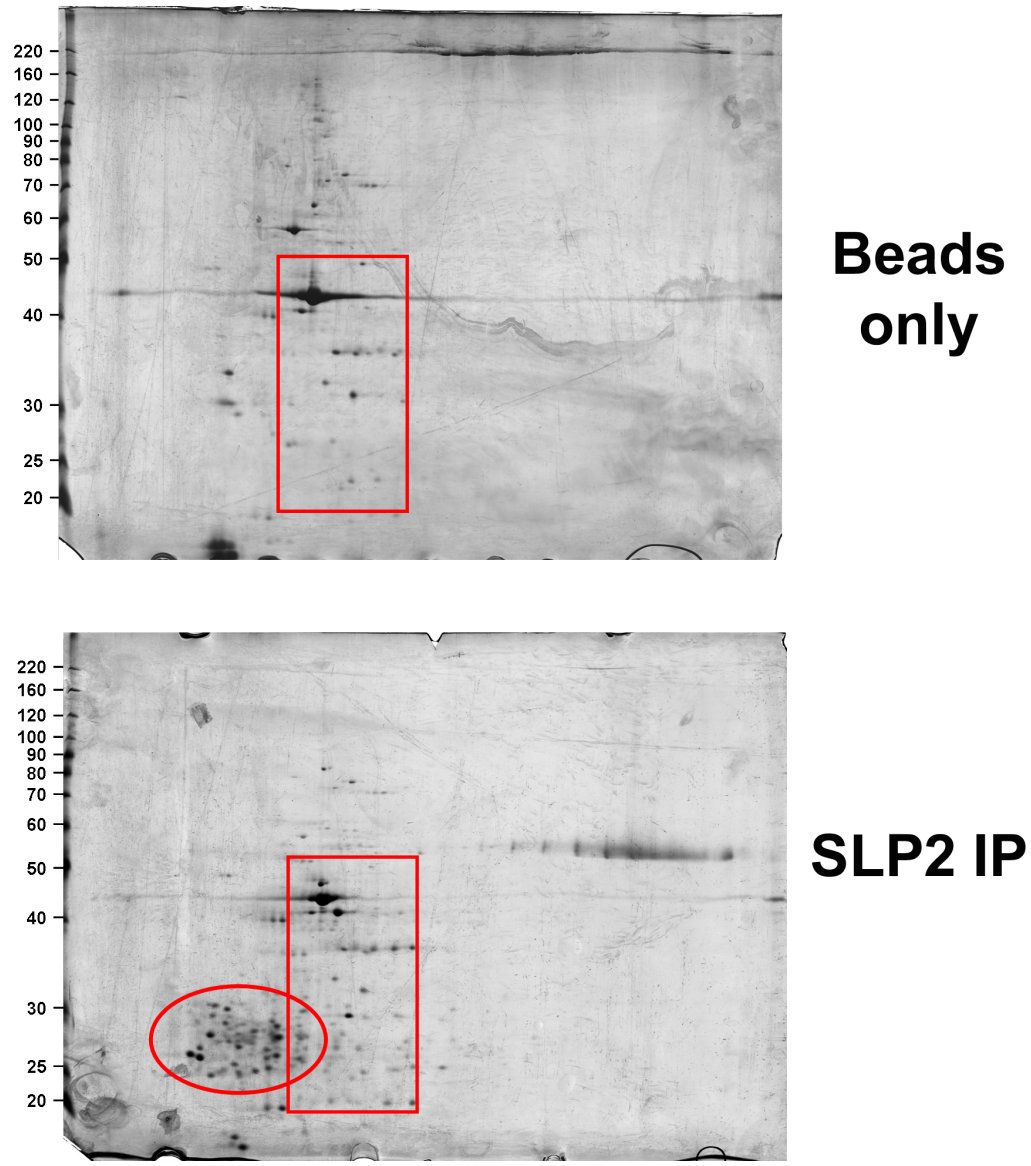

Figure 6.12: 2-D analysis of SLP2 immunoprecipitates
HUVECs were lysed in immunoprecipitation buffer, and SLP2 was immunoprecipitated with an anti-SLP2 antibody (SLP2 IP). A parallel, control immunoprecipitation was performed in which no immunoprecipitating antibody was used (i.e. protein A/G-agarose beads alone were used). Immunoprecipitates were separated by 2-D electrophoresis and gels were silver stained. The positions of molecular weight markers (kDa) are indicated. A large number of spots in the circled region are present in the SLP2 IP but not the beads-only control. The rectangle refers to figure 6.13. Data is from a single experiment.

One of the proteins present in all SLP2 immunoprecipitates analysed but not the beads only control was identified by MALDI-TOF MS as prohibitin 1 (Phb1, figure 6.13, a representative peptide

mass fingerprint is given in figure 6.14). Stomatin-like proteins and prohibitins are related proteins containing a stomatin/prohibitin/flotillin/HflK (SPFH) domain, also termed the prohibitin (Phb) domain (Browman *et al.* 2007, discussed later). Comparison of the SLP2, Phb1 and Phb2 amino acid sequences indicates that Phb1 and not Phb2 was the prohibitin isoform identified in SLP2 immunoprecipitates, as the MS-identified peptides listed in figure 6.14 are present in Phb1 but not Phb2. Sequence comparison of SLP2 with Phb1 also showed little amino acid identity between SLP2 and Phb1, making it unlikely that Phb1 is present in SLP2 due to direct immunoprecipitation (direct recognition by the SLP2 antibody).

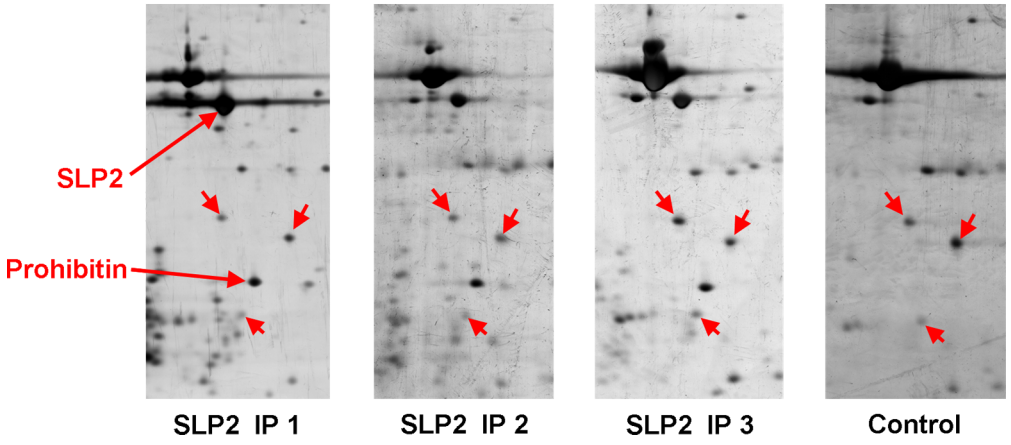

Figure 6.13: Prohibitin 1 is present in SLP2 immunoprecipitates
Comparison of the 2-D pattern of three independent SLP2 immunoprecipitates and one beads-only control, produced as in figure 6.12. The same region of each 2-D gel, corresponding to the area enclosed by the red rectangle in figure 6.12, is shown. Spots identified by peptide mass fingerprinting as SLP2 and Phb1 were identified in all three SLP2 immunoprecipitates, but these spots were not present in the control IP. What are believed to be the same three spots are indicated in all gels to aid visual comparison – the upper right of these spots was identified as the actin capping protein capZ in all three SLP2 IPs (sequence-predicted molecular weight 30 kDa and pI 5.6). The positions of SLP2, Phb1 and β-actin are indicated in the leftmost gel. Molecular weights of SLP2, Phb1 and β-actin (calculated from protein sequence) are 39 kDa, 30 kDa and 41 kDa respectively, and the predicted isoelectric points of Phb1 and β-actin are 5.6 and 5.5. The details of the MALDI-TOF identifications of Phb1 (number of matched peptides, sequence coverage) are: IP1 9, 36%; IP2 5, 21%; IP3 9, 35%. A representative spectrum is shown in figure 6.14.

SLP2 IPs immunoblotted with an anti-Phb1 antibody did not contain a strongly-recognised band migrating at the expected molecular weight for Phb1, despite the fact that Phb1 had been unambiguously identified by peptide mass fingerprinting in another aliquot of the same IP sample (data not shown). The anti-Phb1 antibody did, however, recognise a band of the appropriate molecular

A

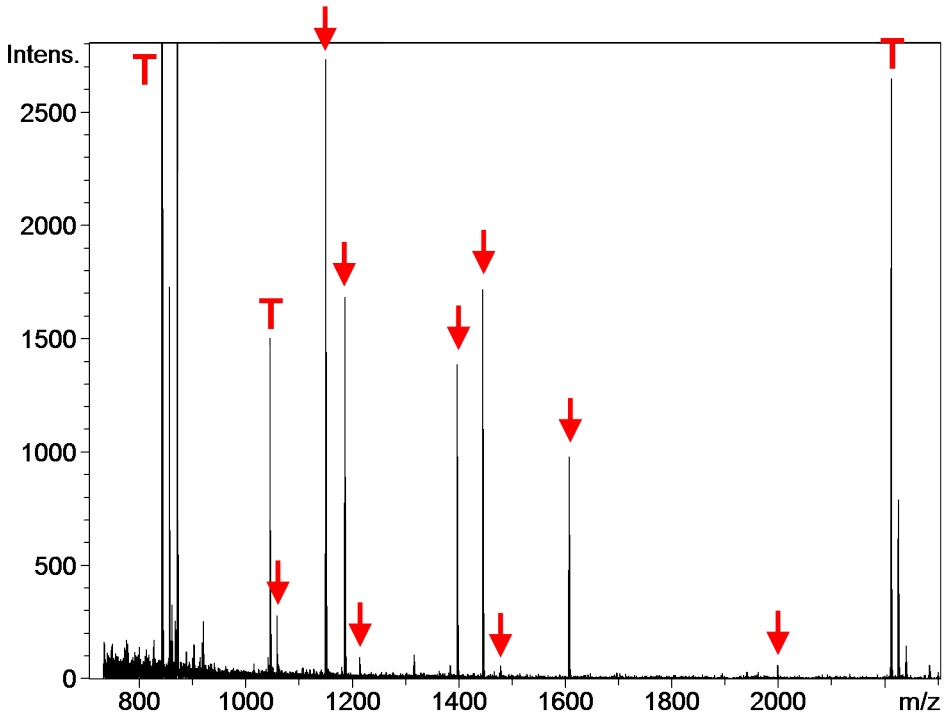

B

MAAKVFESIG KFGLALAVAG GVVNSALYNV DAGHRAVIFD RFRGVQDIVV
GEGTHFLIPW VQKPIIFDCR SRPRNVPVIT GSK(DLQNVNI TLR)(ILFRPVA
SQLPR)(IFTSI GEDYDER)(VLP SITTEILK)SV VAR(FDAGELI TQR)ELVSRQV
SDDLTERAAT FGLILDDVSL THLTFGKEFT EAVEAK(QVAQ QEAER)ARFVV
EKAEQQKKAA IISAEGDSK(A AELIANSLAT AGDGLIELR)(K LEAAEDIAYQ
LSR)SRNITYL PAGQSVLLQL PQ

Figure 6.14: Prohibitin 1 peptide mass fingerprint
A. Peptide mass fingerprint obtained for prohibitin 1 from SLP2 IP 1 in figure 6.13. The y-axis represents signal intensity, the x-axis represents mass-to-charge ratio (m/z) which, for the ions produced by MALDI-TOF, is equivalent to mass. Peaks identified as derived from Phb1 are indicated with arrows. The trypsin autolysis peptides at m/z 842.51, 1045.56 and 2211.10 are indicated with a 'T'. The graph has been scaled to show the less intense Phb1 peaks, and so some highly abundant trypsin peaks at m/z 800–900 are off the scale.
B. Amino acid sequence of human Phb1, showing the peptides identified using the mass spectrum from (A). The nine peptides covered 36% of the Phb1 amino acid sequence.

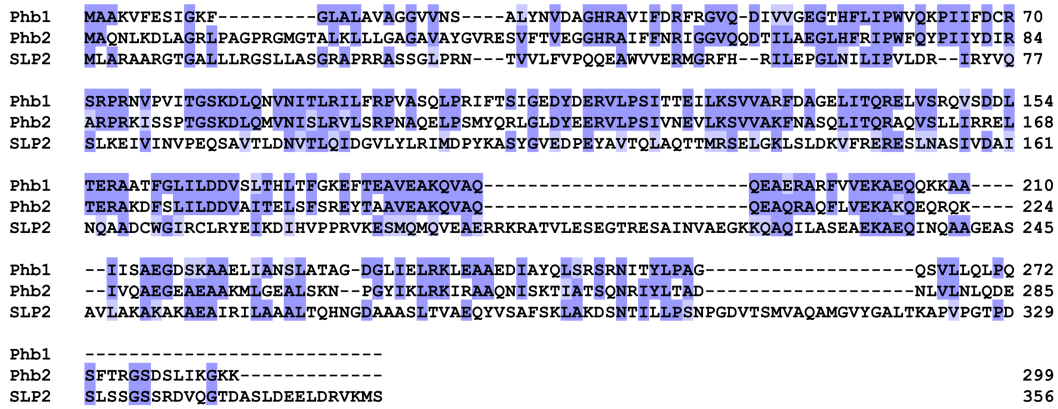

Figure 6.15: Alignment of human SLP2 and prohibitin protein sequences
Reference protein sequences for human SLP2, prohibitin 1 and prohibitin 2 were retrieved from the RefSeq database and aligned with ClustalX2. Residues are coloured according to Blossum62 score, with darker colours indicating better conservation. The RefSeq database accession numbers for the protein sequences (all human) used for alignment were: SLP2, NP_038470.1; Phb1, NP_002625.1; Phb2, NP_001138303.1. Phb2 has two transcript variants, but the proteins produced by these transcript variants are identical.

weight in HUVEC lysates analysed on the same membrane. Immunoprecipitation trials using the anti-Phb1 antibody were unsuccessful – immunoblots of these IPs with the same anti-prohibitin antibody used for immunoprecipitation did not recognise a band at the expected position for Phb1 (data not shown).

6.5 Examination of potential functions of SLP2

As the role of SLP2 in endothelial cells was completely unknown, two different siRNAs targeting SLP2 (SLP2 A and B) were used to address the effects of SLP2 knockdown on various endothelial cell functions. Given the mitochondrial location of SLP2 (figure 6.3), the role of SLP2 in the development of mitochondrial membrane potential and apoptosis was of particular interest.

6.5.1 Mitochondrial-related functions

The membrane potential of mitochondria is important in oxidative phosphorylation, and accumulation of the fluorescent dye TMRM can be used as a relative measure of mitochondrial membrane potential (section 2.9.1.1). Confocal microscopy confirmed that TMRM was accumulated, appar-

ently in a mitochondrial pattern, by HUVECs incubated for 2 h with 25 nM TMRM, the conditions used for TMRM experiments (figure 6.16A, compare with the Mitotracker Red pattern in figure 6.3). No consistent differences were observed in the TMRM staining pattern in cells treated with SLP2 siRNA compared to those treated with control siRNA.

To obtain quantitative data on the amount of TMRM accumulated by HUVECs, TMRM-treated cells were analysed by flow cytometry. SLP2 knockdown did not significantly affect accumulation of TMRM, despite 84–89% knockdown of SLP2 (figure 6.17).

6.5.2 Apoptosis

The importance of SLP2 in apoptosis was assessed using annexin V staining of serum-deprived HUVECs coupled with flow cytometry. The SLP2 A siRNA increased apoptosis by 24% compared to the control siRNA, whereas cells treated with the SLP2 B siRNA showed a non-significant 10% increase in apoptosis (figure 6.18). Both siRNAs reduced SLP2 protein levels by similar degrees (SLP2 A siRNA 91%, SLP2 B siRNA 93%) as assessed by western blotting of parallel samples.

6.5.3 Cell migration

The involvement of SLP2 in migration was also examined using SLP2 knockdown. Neither SLP2 A siRNA nor SLP2 B siRNA significantly affected HUVEC migration in response to VEGF.

6.6 Discussion

SLP2 came to attention during this thesis when it was identified as a major component of HUVEC-derived pY immunoprecipitates. As virtually nothing was known about SLP2, attempts were made to determine the reason for the presence of SLP2 in pY IPs, and the role of SLP2 in ECs more generally.

Results presented in this chapter indicate that while SLP2 is certainly present in pY IPs, SLP2

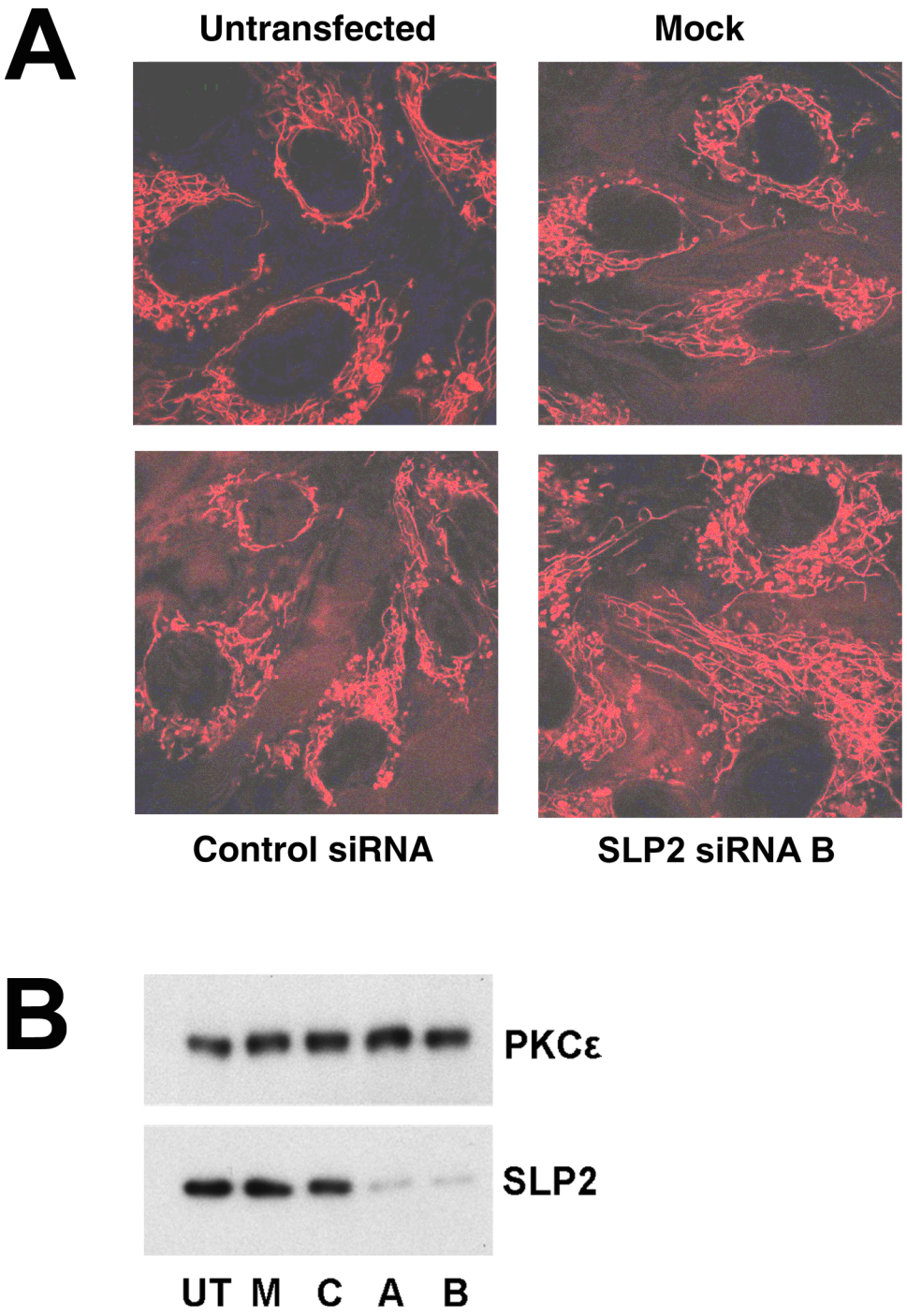

Figure 6.16: TMRM specifically accumulates in mitochondria
A. Confluent HUVECs grown on coverslips were incubated for 72 h with SLP2 siRNA B, a negative control siRNA (control), transfection reagent alone (mock) or were left untransfected. Cells were then incubated with the fluorescent dye TMRM (25 nM for 2 h), before live cell imaging with an inverted confocal microscope. The staining pattern is similar to that seen for Mitotracker Red in previous experiments. No differences were evident between SLP2 siRNA treated groups and controls, or any other groups, when viewing a number of separate fields. Data is from a single experiment.
B. Western blot indicating the SLP2 achieved by the siRNAs in this experiment.

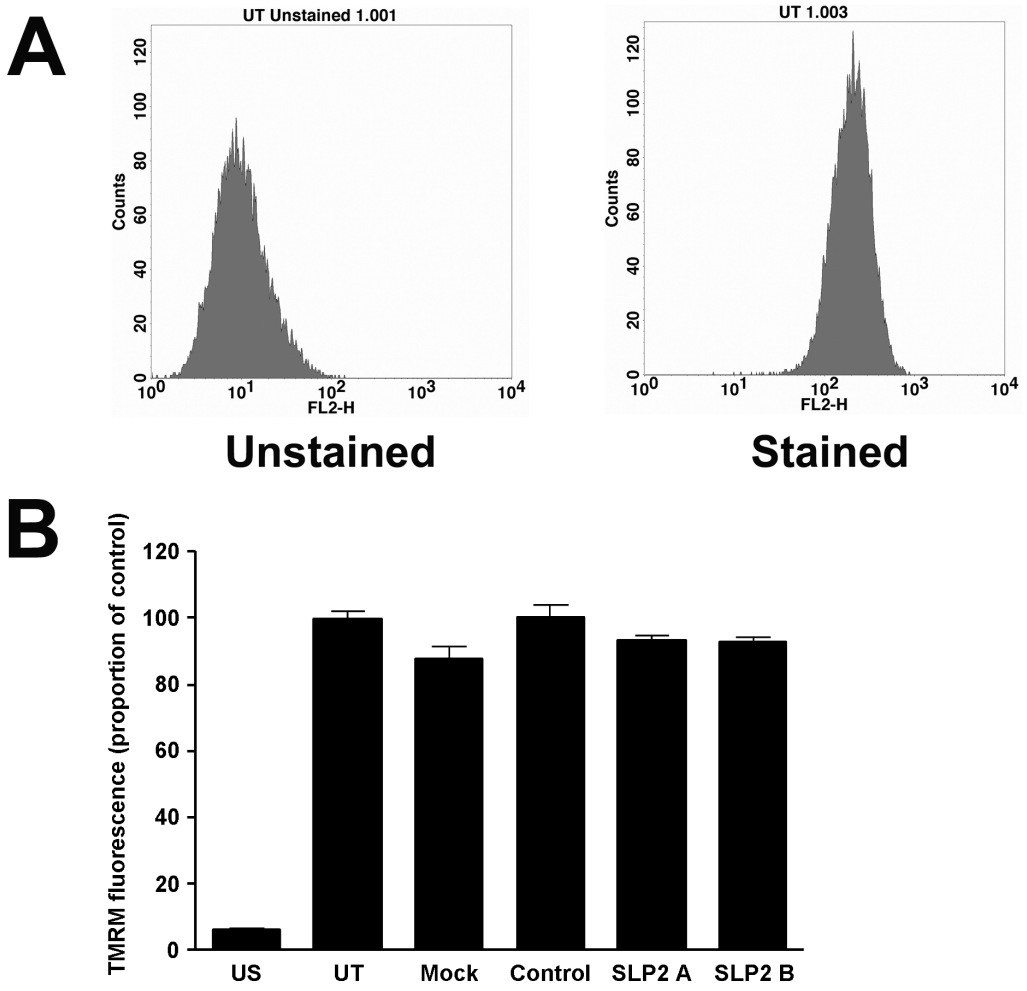

Figure 6.17: SLP2 knockdown does not affect accumulation of the mitochondrial potential-dependent dye TMRM

HUVECs were treated with siRNA for 72 h, followed by incubation with 25 nM TMRM for 2 h to label mitochondria. Cells were then resuspended in PBS and assessed for TMRM fluorescence using a flow cytometer.

A. Representative histogram from the CellQuest flow cytometry program, illustrating the effect of TMRM staining on the fluorescence recorded on the FL2 channel of the flow cytometer. Untransfected cells had been either incubated with TMRM (right panel) or not incubated with TMRM (left panel) as indicated.

B. Mean TMRM fluorescence of HUVECs treated with the indicated siRNA, as determined by flow cytometry. UT, untransfected cells; Mock, transfection reagent alone; Control, negative control siRNA; SLP2 A and B, two different siRNAs targeting SLP2; US, unstained untransfected cells (no TMRM added). Results are means $\pm$ SEM of four independent experiments. One-way ANOVA indicated no significant differences (except with unstained cells). Mean knockdown of target protein achieved by siRNAs, compared to control siRNA: SLP2 A 84%, SLP2 B 89%

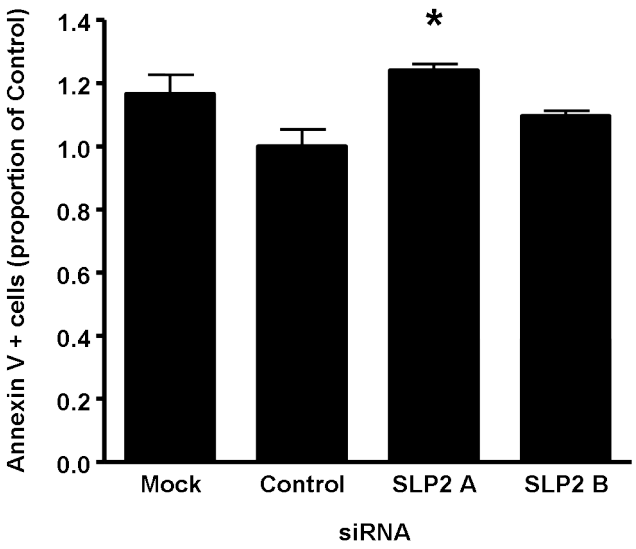

Figure 6.18: Effect of SLP2 knockdown on endothelial cell apoptosis
HUVECs were incubated with 200 nM of two different siRNAs targeting SLP2 (SLP2 A and SLP2 B), a non-targeting control siRNA, or transfection reagent alone (Mock) for 2 days. The medium was then changed and cells were incubated overnight in M199 basal medium to induce apoptosis. Live and dead cells were then harvested by trypsinisation and stained with FITC-conjugated annexin V. The proportion of stained (apoptotic) and unstained (healthy) cells was determined by flow cytometry, with 15,000 cells counted per sample. Results are presented as the proportion of annexin V-positive cells, compared to that observed in the control siRNA sample, and are given as mean $\pm$ SEM from four independent experiments. Data were analysed by one-way ANOVA with Bonferroni's test for multiple pair-wise comparisons. * SLP2 A siRNA significantly increased the proportion of annexin V-stained cells compared to the control siRNA ($p<0.05$). Mean knockdown of target protein achieved by siRNAs, compared to control siRNA: SLP2 A 91%, SLP2 B 93%

itself may not be directly tyrosine phosphorylated. I also found no evidence that a previously reported tyrosine phosphorylation site, Y124, was phosphorylated in HUVECs. However, the amount of SLP2 present in pY IPs was reduced by excess pY analogue, suggesting that SLP2 is present in pY IPs in a pY-dependent manner, possibly via association with a pY-containing protein. SLP2 appeared to associate with Phb1, but whether this contributed to its presence in pY IPs is unknown. SLP2 is a mitochondrial protein in HUVECs, and SLP2 maturation may involve cleavage of an N-terminal mitochondrial localisation peptide. Functionally, an $\approx$85% reduction in SLP2 protein levels did not noticeably affect mitochondrial morphology, nor did it significantly affect the mitochondrial membrane potential or VEGF-stimulated migration of HUVECs. SLP2 knockdown may have slightly increased apopotosis due to serum starvation, although the robustness of this effect is questionable as a second SLP2 siRNA had little effect.

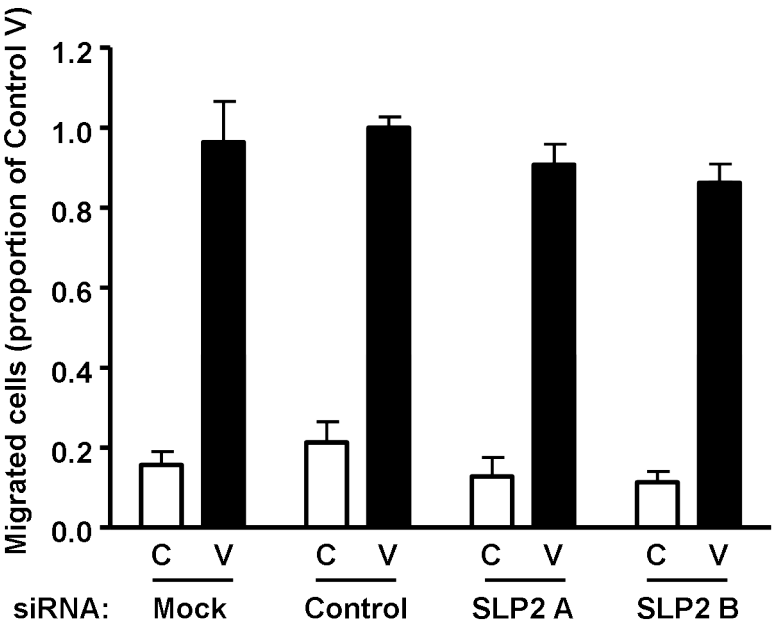

Figure 6.19: SLP2 knockdown does not affect HUVEC migration
HUVECs were pre-treated for 48 h with two different siRNAs targeting SLP2 (SLP2 A and B), a non-targeting control siRNA (Control) or transfection reagent alone (Mock). Cells were trypsinised and migration was assessed in a transwell assay using 25 ng/ml VEGF (V) or no addition (C) as the chemoattractant. Results are presented as the proportion of migration stimulated by VEGF (Control V), expressed as means ± SEM of five independent experiments. Two-way ANOVA indicated that while the effect of VEGF treatment was significant, the effect of siRNA was not. Mean knockdown of target protein achieved by siRNAs, compared to control siRNA: SLP2 A 90%, SLP2 B 93%.

Overall, the role of SLP2 in ECs is unclear from these experiments.

6.6.1 SLP2 is a mitochondrial protein in endothelial cells

SLP2 was originally identified as a peripheral membrane protein in erythrocytes (Wang and Morrow 2000). In this chapter, it was shown that SLP2 co-localises with the mitochondrial marker dye Mitotracker Red, indicating SLP2 is a mitochondrial protein in HUVECs. SLP2 has since been shown to co-localise with mitochondrial markers in HeLa cells, co-fractionate with mitochondrial marker proteins and has been detected in extracts of purified mitochondria (Da Cruz *et al.* 2003; Hajek *et al.* 2007; Da Cruz *et al.* 2008; Wang *et al.* 2009), strongly suggesting that SLP2 is indeed a mitochondrial protein. Incubation of isolated mitochondria with various detergent/protease mixtures, with subsequent analysis of the susceptibility of SLP2 to proteolysis, suggested that SLP2 was associated with the inner mitochondrial membrane, facing the intermembrane space (Hajek

et al. 2007; Da Cruz *et al.* 2008). SLP2 may have a distinct role in red blood cells, as these cells do not contain mitochondria (Sprague *et al.* 2007).

Amino acid sequence analysis suggested the presence of a mitochondrial targeting peptide, composed of approximately 34 amino acids at the N-terminus of SLP2. This region was never detected in a number of mass spectrometric analysis of SLP2, suggesting it could be absent in the mature protein. Absence of this region would adjust the SLP2 isoelectric point to a similar value to that observed by 2-D electrophoresis. The pI of SLP2 observed in this study (5.5) was similar to that observed previously when SLP2 was identified in HUVECs (5.3, Sprenger *et al.* 2004) and to that predicted for SLP2 lacking the N-terminal 34 amino acids (5.7), but dissimilar to that predicted for full-length SLP2 (6.9). While the absence of the 34 N-terminal amino acids from mass spectra may be due to a technical limitation, such as the inability of hydrophobic peptides generated from the SLP2 N-terminus to solublise or ionise properly, John *et al.* (2006) used a number of different proteolytic enzymes to generate different peptides from purified, human cell-derived SLP2, obtaining peptides covering the entire SLP2 sequence apart from the first 34 amino acids.

These first 34 amino acids are highly likely to contain a functional mitochondrial targeting sequence, at least part of which is then removed on import by proteolysis. Full-length in vitro synthesised SLP2 is imported into isolated mitochondria, leading to formation of a smaller SLP2 form suggesting proteolytic processing, and this import and size reduction is prevented by dissipation of the mitochondrial membrane potential (Hajek *et al.* 2007). The import signal is resident in the 50 N-terminal amino acids of SLP2 – tagged SLP2 lacking the 50 N-terminal amino acids was cytoplasmic when expressed in HeLa, whereas a fusion protein composed of the N-terminal 50 amino acids of SLP2 and GFP was mitochondrial as determined by fluorescent microscopy (Da Cruz *et al.* 2008).

6.6.2 Presence of SLP2 in pY immunoprecipitates

SLP2 was reproducibly observed in pY immunoprecipitates and, judging by silver staining of complete pY immunoprecipitates, appeared to be a major component of these immunoprecipitates. However, the anti-pY antibody did not strongly recognise an SLP2-sized band in SLP2 IPs. No post-translational modifications were identified in the peptides identified by MS/MS, and enzymatic dephosphorylation of pY IPs did not alter the isoelectric point of SLP2. Together, these data suggest that pY-containing SLP2 is not a major component of SLP2 IPs.

Analysis of the SLP2 protein sequence did not identify a strong tyrosine kinase consensus sequence. However, tyrosine phosphorylation sites are difficult to predict, and lack of a predicted site does not preclude the existence of a tyrosine phosphorylation site. Analysis of the EGF receptor using amino acid sequence analysis tools including that used in this chapter failed to predict five phosphorylation sites which were subsequently shown by MS/MS to be tyrosine phosphorylated (Steen *et al.* 2002).

If SLP2 is not directly phosphorylated on tyrosine residues, it may be present in pY immunoprecipitates due to direct recognition of a non-pY-containing region of SLP2 by the anti-pY antibody, i.e. an off-target effect. This appears unlikely, given that excess phenyl phosphate, a pY analogue, prevents immunoprecipitation of SLP2 by the anti-pY antibody. However, if phenyl phosphate is more strongly recognised by the anti-pY antibody than a non-pY-containing region of SLP2, it is conceivable that immunoprecipitation of SLP2 could be an off-target effect of the antibody which would still be prevented by excess phenyl phosphate. This possibility cannot be discounted.

SLP2 could be present in pY immunoprecipitates but not be tyrosine phosphorylated itself if it associates with a pY-containing protein. Given that SLP2 is a major component of pY immunoprecipitates, it might be expected that a large amount of pY-containing protein might need to be directly immunoprecipitated to enable such a large quantity of SLP2 to be co-precipitated. However, SLP2 has been reported to exist in large complexes, both as a homooligomer ((Reifschneider

et al. 2006), reported complex size 1800 kDa by variant native gel electrophoresis) and in complex with Mfn2 (Hajek *et al.* 2007) and prohibitins 1 and 2 (Da Cruz *et al.* 2008, approximate size of SLP2 complex 250 kDa by gel filtration). Data not shown in this thesis using glutaraldehyde cross-linking (as used for Hsp27 in the previous chapter) suggested that SLP2 may exist in a high molecular weight complex. As such, a strong association of a large complex containing a number of individual SLP2 protein molecules with a single pY-containing protein would explain the observed results - presence of a large amount of SLP2 in pY immunoprecipitates, but little pY-containing protein in SLP2 immunoprecipitates. Alternatively, the tyrosine phosphorylated protein associating with SLP2 could be SLP2 itself – that is, a very small proportion of SLP2 is tyrosine phosphorylated, with a large amount of unphosphorylated SLP2 complexing with it. This small proportion of pY-containing SLP2 could easily be missed when analysing SLP2 as a whole.

6.6.3 Association of SLP2 with mitochondrial proteins and influence on mitochondrial function

A large number of proteins were present in SLP2 immunoprecipitates but not in beads-only controls, indicating that these non-SLP2 proteins associate with the SLP2 antibody in some way, either directly (i.e. due to non-target recognition by the antibody) or indirectly via SLP2 (true association with SLP2) or via another protein. Prohibitin 1 was reproducibly identified in SLP2 immunoprecipitates via MALDI-TOF MS, but the anti-Phb1 antibody (the same antibody used by Da Cruz *et al.* 2008) did not convincingly recognise an appropriate band in SLP2 immunoprecipitates despite recognising prohibitin 1 in lysates. This may be because the Phb1 associated with SLP2 and so present in SLP2 immunoprecipitates is modified in some way so that it is not recognised by the monoclonal anti-Phb1 antibody.

Prohibitins (Phbs, reviewed by Artal-Sanz and Tavernarakis 2009) are predominantly mitochondrial proteins belonging to the SPFH (stomatin/prohibitin/flotillin/Hflk) family of proteins, which also includes SLP2. The role of the Phb domain (also called the SPFH domain) is unknown but

is present in a number of oligomeric lipid raft-associated proteins (that is, protein associate with membrane subdomains high in cholesterol), suggesting that it may be involved in lipid binding and/or oligomerisation (Browman *et al.* 2007). Two prohibitins have been identified in mammals, Phb1 and Phb2, which associate forming a heterodimer. Multiple heterodimers then associate to form a large complex at the inner mitochondrial membrane, and this complex is conserved between yeast and man. Multiple mitochondrial roles have been suggested for prohibitins including maintenance of normal cristae morphology, assistance of oxidative phosphorylation enzyme complex assembly/maintenance, roles in mitochondrial fission, and others (Artal-Sanz and Tavernarakis 2009).

Phb1 and 2 have previously been reported to associate with SLP2 in HeLa cells (Da Cruz *et al.* 2008). Immunoprecipitates of tagged SLP2 (using the tag for immunoprecipitation) contained both Phb1 and Phb2, and immunoprecipitated Phb1 contained tagged SLP2. Phb1 was also present in immunoprecipitates of endogenous SLP2 from mitochondrial lysates, indicating that association is not due to protein overexpression, although similar results have not been formally demonstrated for Phb2. Thus it appears from the work of Da Cruz *et al.* (2008) that SLP2 associates with Phb1 in mitochondria, and overexpression work suggests that Phb2 may also associate with SLP2.

Da Cruz *et al.* (2008) commented that only a very small fraction of endogenous Phb1 is present in SLP2 immunoprecipitates, suggesting that the inability to detect Phb1 in the immunoprecipitates of endogenous SLP2 produced in this thesis may be due to insufficient numbers of cells being used for immunoprecipitation. However silver-stained 2-D gels indicated that Phb1 appeared to be a major component of the SLP2 immunoprecipitates prepared in this thesis. Interestingly, Phb2 has been reported to be a tyrosine phosphorylated protein (at Y248), localising to the inner mitochondrial membrane of T-cells (Ross *et al.* 2008), and so SLP2 association with Phb2 could explain the presence of SLP2 in pY IPs.

In addition to prohibitins, SLP2 has been reported to associate with another inner mitochondrial membrane protein, mitofusin2 (Mfn2, Hajek *et al.* 2007), in formaldehyde-treated HeLa cells, with

formaldehyde cross-linking being used to preserve the interaction. Mfn2 is involved in adjustment of mitochondrial morphology via mitochondrial fusion and fission, which is thought to be involved in maintenance of the mitochondrial network and its adaptation to metabolic demand (van der Bliek 2009). Mfn2 itself, along with Opa1 and Mfn1, is required for mitochondrial fusion, whereas Drp1 is required for mitochondrial fission.

Despite the apparent association of SLP2 with Mfn2 and Phbs, both implicated in control of mitochondrial morphology, in this thesis siRNA-mediated reduction in endothelial cell SLP2 protein expression had no obvious effect on mitochondrial morphology. While reduction of SLP2 might be expected to enhance mitochondrial fragmentation by disrupting Mfn2-dependent fusion, others have also reported that SLP2 knockdown has no effect on normal mitochondrial morphology in HeLa cells (Hajek *et al.* 2007) and mouse embryonic fibroblasts (Tondera *et al.* 2009).

In addition to normal mitochondrial dynamics, it has recently been shown that mitochondria fuse in response to some cellular stresses (including cycloheximide, UV radiation and actinomycin D) in a process termed stress-induced mitochondrial hyperfusion (SIMH). SIMH requires Mfn1, Opa1 and SLP2, and short hairpin (sh)RNA-mediated knockdown of SLP2 causes proteolytic degradation of Opa1 and prevents UV-induced SIMH (Tondera *et al.* 2009). In the absence of SLP2, Opa1 is proteolytically cleaved, and overexpression of uncleavable Opa1 allowed SIMH to occur in SLP2-reduced cells, suggesting that SLP2 protects Opa1 from proteolytic cleavage.

SIMH may be a response to increase ATP production during stress – SIMH-inducing stimuli caused an increase in mitochondrial ATP production, which did not occur in cells unable to undergo SIMH due to absence of Opa1 or Mfn1, or in cells expressing SLP2 shRNA (Tondera *et al.* 2009). In unstimulated MEFs in the same study, mitochondrial membrane potential was not different between control and SLP2-reduced cells, although the details of how this was determined were not clear. In contrast, Hajek *et al.* (2007) reported that siRNA-mediated reduction of SLP2 protein expression by 95–98% in HeLa cells caused a 19% reduction in geometric mean TMRE fluorescence (interpreted as a reduction in mitochondrial membrane potential). In this thesis, an

siRNA-mediated ≈90% reduction in endothelial cell SLP2 protein expression did not significantly alter mean TMRM fluorescence using a similar method to Hajek *et al.* (2007). This may have been due to reduced SLP2 knockdown in the primary endothelial cells used in this chapter (Hajek *et al.* 2007 used a cell line, performing two rounds of siRNA treatment). However SLP2 knockdown by Tondera *et al.* (2009) appeared virtually complete, although quantitative data was not presented.

In summary, loss of SLP2 protein appears to lead to proteolysis of mitochondrial proteins including Phbs, Opa1, and components of the electron transport chain, suggesting that SLP2 is required for the stability of some of these proteins under normal and/or stress conditions, perhaps in some cases by stabilising a complex of these proteins.

6.6.4 Role of SLP2 in cell function

Release of cytochrome C from mitochondria is a cardinal event in apoptosis. In this thesis, it was unclear whether SLP2 reduction had increased EC apoptosis induced by serum starvation, as the size of the increase varied above and below the statistical significance threshold with two different siRNAs, despite similar reductions in SLP2 protein expression by the two siRNAs. However any effect present appeared low.

Tondera *et al.* (2009) reported that shRNA-mediated SLP2 knockdown increased the apoptosis of HeLa or MEFs in response to UV irradiation, and suggested that this was due to prevention of SIMH as cells deficient in Mfn1 were also sensitised to UV or actinomycin D-induced apoptosis. Serum starvation also caused SIMH and therefore SLP2 knockdown might be expected to sensitise cells to apoptosis due to loss of SIMH. It is possible that the degree of SLP2 knockdown obtained in this thesis was insufficient to observe this effect. However, a role for SIMH in protection of cells from serum starvation-induced apoptosis was not directly demonstrated, and may be less important in protection against this particular apoptotic trigger in endothelial cells, where other anti-apoptotic mechanisms may be more important.

SLP2 may have additional functions in other cell types. Red blood cells do not contain mitochon-

dria (Sprague *et al.* 2007), but contain SLP2 (Wang and Morrow 2000). Kirchhof *et al.* (2008) reported that a small proportion of SLP2 associates (possibly indirectly) with components of the T-cell receptor, a plasma membrane protein, and SLP2 knockdown reduced the duration of T-cell receptor signalling. A number of signalling proteins such as PLCγ, and other proteins including actin were also located in SLP2 IPs. A surprisingly large increase (not quantified) in the amount of SLP2 present in cell lysates was observed after T-cell stimulation, which may reflect increased mitochondrial density to fuel the needs of the activated T-cell. Overall, it is possible that SLP2 may have extra-mitochondrial functions, which may reflect its role as a scaffolding protein. In endothelial cells and a number of different cell types examined by others, SLP2 appears mitochondrial, suggesting SLP2 has a predominantly mitochondrial function in most cells.

SLP2 is overexpressed in a number of cancers (Zhang *et al.* 2006; Cao *et al.* 2007; Cui *et al.* 2007; Dowling *et al.* 2007), and increased SLP2 expression associates with increased clinical stage and reduced patient survival (Cao *et al.* 2007). Antisense SLP2 has been reported to reduce proliferation and attachment of the oesophageal cancer cell line KYSE450, and the weight of tumours formed by injected antisense SLP2-containing KYSE450 cells was dramatically reduced compared to control KYSE450 cells (Zhang *et al.* 2006). SLP2 overexpression may be a consequence of increased mitochondrial density as an adaptation to the metabolic demands of a rapidly-dividing cells, or may be due to a mitochondrial stress response such as the overexpression of SLP2 observed in SIMH. Low-power micrographs suggested that SLP2 is distributed throughout the cytoplasm of cancer cells, raising the possibility that the role of SLP2 in cancer is unrelated to its mitochondrial functions.

Chapter 7

General discussion

VEGF stimulates a number of biological effects, including angiogenesis in vivo and proliferation, migration and survival of cultured endothelial cells. The research undertaken for this thesis was initally directed towards identification of novel VEGF-activated signalling pathways in ECs which might be involved in mediating some of these functions.

7.1 Proteomics for analysis of intracellular signalling

Proteomic analysis of VEGF signalling, by gel separation of proteins followed by detection and MS-based identification, allowed the examination of post-translational modifications such as phosphorylation in addition to alterations in protein expression. Proteomic analysis of whole cell lysates identified Hsp27 as an abundant protein regulated by short-term VEGF treatments, but known VEGF-stimulated changes such as phosphorylation of VEGFR2, ERK and p38 MAPK which were observed via western blotting were not apparent in silver-stained 2-D gels. VEGF is known to increase protein tyrosine phosphorylation, but no differences were apparent during proteomics comparisons of pY immunoprecipitates from VEGF-treated and control cells. However, analysis did identify SLP2, a relatively unknown protein not previously reported to be tyrosine phosphorylated, as a major component of endothelial pY IPs. Further work on Hsp27 and SLP2 is discussed below.

A major problem for the proteomic approaches employed was the low abundance of many proteins involved in signalling. Some proteins (e.g. some metabolic enzymes, cytoskeletal proteins and chaperones) constitute a substantial proportion of total cellular protein, and so dominate when total protein detection, such as silver staining, is used. Even when examining pY immunoprecipitates, a high degree of constitutive tyrosine phosphorylation may have been a problem. Other intrinsic problems with the 2-D gel/total protein stain approach, such as difficulties in solubilising membrane proteins, difficulties in silver staining quantification, and problems in accurately matching spots between gels, may have contributed to the lack of identification of subtle changes. However, more spots were observed using total protein staining techniques than could be identified using mass spectrometry, and so improved staining sensitivity allowing detection of lower abundance proteins might by hampered by limited protein identification. Subcellular fractionation (to focus on a subset of the proteome) and scaling-up protein loading, coupled with a sensitive, accurate method to determine differences in protein expression would be required to markedly improve proteomic analysis of intracellular signalling.

7.2 Hsp27

Proteomic analysis identified Hsp27 phosphorylation as a major effect of VEGF stimulation of cultured ECs. At the outset of this work, Hsp27 had been identified as an actin capping protein and molecular chaperone, and had been implicated in a variety of roles including protection from apoptosis. Hsp27 expression increased in response to some cellular stresses in some cell types. Overexpression of Hsp27 protected cells from certain types of external stress, and had been implicated in survival of some cell types. Hsp27 had also been implicated in the migration of various cell types including cultured ECs (Piotrowicz *et al.* 1998). Phosphorylation of Hsp27 in response to cellular stresses and various cytokines, via a p38 MAPK/MAPKAPK2-dependent pathway had also been reported, with phosphorylation causing a reduction in Hsp27 oligomeric size and so possibly influencing its function (Lambert *et al.* 1999; Rogalla *et al.* 1999).

The results presented in chapters 4 and 5 indicated that VEGF rapidly stimulates phosphorylation of Hsp27 at S15, S78 and S82, with S82 the major phosphorylation site, and also causes a reduction in the oligomeric size of Hsp27. I determined that Hsp27 phosphorylation occurs via a PKC/PKD-dependent pathway, which acts in parallel to a p38α/MAPKAPK2-dependent pathway. Knockdown of Hsp27 suggested that Hsp27 is required for normal endothelial cell responses including VEGF-stimulated migration, protection from apoptosis and tubulogenesis.

7.2.1 Hsp27 phosphorylation

Stress-induced, p38 MAPK-mediated Hsp27 phosphorylation is well established. A major finding of this thesis was that VEGF-stimulated Hsp27 phosphorylation also occurs via a PKC/PKD-dependent pathway, which acts to phosphorylate Hsp27 at S82 but not S15 or S78. Stress stimuli examined (H_2O_2, TNFα, anisomycin) did not apparently activate PKD or cause PKC-dependent Hsp27 phosphorylation.

Whether activation of a PKC-dependent Hsp27-phosphorylating pathway, as opposed to the p38 MAPK-dependent pathway, has a functional relevance is unclear. Presumably, the PKC-dependent pathway acts to increase the abundance of S82 monophosphorylated Hsp27, the predominant form of Hsp27 occurring after VEGF stimulation. It is possible that PKC-dependent Hsp27 S82 phosphorylation is a non-consequential side effect of VEGF-stimulated activation of PKC, that is to say PKD or another PKC-dependent enzyme is able to non-functionally phosphorylate Hsp27, and the extra S82 monophosphorylated Hsp27 has no further effect in the cell, or any effect is tolerated. Perhaps an evolutionary solution to prevent PKC-dependent S82 phosphorylation, when PKC was activated for other purposes, was unnecessary. VEGF and other tyrosine kinases use PKC-mediated pathways for some processes where other stimuli use non-PKC-mediated pathways to achieve the same goal, such as activation of ERK, which can occur via PKC or via Ras.

However, S82 appears to be a key residue in terms of Hsp27 oligomerisation, and Hsp25 or Hsp27 mutants mimicking phosphorylation at S82 form smaller oligomers than those mimicking phos-

phorylation at S15 (Lambert *et al.* 1999; Rogalla *et al.* 1999). In this thesis, S82D mutation was sufficient to cause a reduction in Hsp27 oligomeric size.

Phosphorylation-induced deoligomerisation has been assumed to be an important mechanism of regulating the function of small Hsps such as Hsp27 (Haslbeck *et al.* 2005). In most studies, no distinction has been made between the effect of Hsp27 phosphorylation status, mutation of Hsp27 phosphorylation sites (to phospho-mimicking or phospho-null residues), and effects on Hsp27 oligomerisation status, and so it is not clear whether phosphorylation status or oligomeric size is the key property of Hsp27 regulating its function. One study that did make a distinction showed that unphosphorylated monomeric Hsp25 inhibited actin polymerisation whereas phosphorylated monomeric and unphosphorylated polymeric Hsp25 were ineffective (Benndorf *et al.* 1994), suggesting that phosphorylation status itself may be important in addition to oligomerisation state.

A number of studies have reported that overexpression of phospho-site mutants of Hsp27 or a homologue affects Hsp27 or cellular function differently compared to wild-type Hsp27, suggesting that some combination of phosphorylation and oligomerisation does modulate Hsp27 cellular function. Phospho-mimetic Hsp27 is less effective as a molecular chaperone in vitro than phospho-null Hsp27 (Rogalla *et al.* 1999; Theriault *et al.* 2004). Wild-type Hsp27 interacts with Akt whereas phospho-mimetic Hsp27 does not (Rane *et al.* 2003). Overexpression of unphosphorylatable Hsp27 inhibits VEGF-stimulated EC migration and PDGF-stimulated vSMC migration, whereas overexpression of wild-type Hsp27 either increased migration or had no effect (Piotrowicz *et al.* 1998; Hedges *et al.* 1999). Thus phosphorylation of Hsp27, possibly acting via effects on oligomeric structure, can modulate Hsp27 activities in vitro, interactions with binding partners and overall cellular function.

Given the reported importance of phosphorylation for at least some Hsp27 functions, it is possible that S82-monophosphorylated Hsp27 may have a distinct function to triply-phosphorylated Hsp27, and so a balance between p38- and PKC-dependent pathways for Hsp27 phosphorylation may be important in fine-tuning Hsp27-dependent responses. Examining migration in this thesis, mutation

of S82 to a phospho-mimicking or unphosphorylatable residue had no significant effect, although S82 monophosphorylated Hsp27 may be important in other functions. Alternatively, PKC/PKD-mediated phosphorylation and p38/MAPKAPK2-mediated phosphorylation may occur in different protein complexes or in different cellular locations.

p38 MAPK is strongly activated by stress stimuli, and prolonged activation is associated with induction of apoptosis. Perhaps S82-phosphorylated Hsp27 is required for VEGF-stimulated cell functions, but the degree of activation of the p38 MAPK cascade required to give adequate Hsp27 phosphorylation would be high enough to activate other unwanted signalling cascades (e.g. those leading to apoptosis). Further use of a PKC-mediated pathway would allow generation of sufficient phosphorylated Hsp27 without the need for high p38 activation.

Whatever the function, both PKC and PKD are involved in VEGF-stimulated Hsp27 S82 phosphorylation. Lack of a specific PKD inhibitor, and the incomplete removal of endothelial PKD using siRNA, prevented firm conclusions as to whether PKC stimulates Hsp27 phosphorylation solely via PKD. If Gö6976 inhibits all PKDs fully, then the effects of Gö6976 in combination with a p38 inhibitor would suggest that PKC may also stimulate Hsp27 phosphorylation via PKD-independent mechanisms. This issue is not clear from the data obtained.

PKC and PKD are required for endothelial migration, but it was not possible to determine the contribution of these enzymes to Hsp27-mediated effects on cell migration and other functions. While PKC/PKD knockdown or inhibition affected VEGF-stimulated cell migration, clearly these enzymes may be important signalling nodes and their manipulation may alter a number of downstream pathways in addition to affecting Hsp27. Knockdown of different PKC isoforms had different effects on migration, which were more dramatic than the effects of these knockdowns on Hsp27 phosphorylation, indicating that the major effects of PKC manipulation on migration are unlikely to be due to effects on Hsp27 phosphorylation. PKD may also target other migration-related proteins – in particular, PKD1 knockdown reduced migration to a greater degree than it reduced VEGF-stimulated Hsp27 S82 phosphorylation.

p38 MAPK was generally less important in VEGF-stimulated endothelial functions than has previously been suggested (Rousseau *et al.* 1997, 2000a). p38 inhibition or knockdown had surprisingly little effect on VEGF-stimulated migration and tubulogenesis, and p38 contributed only partially to VEGF-induced phosphorylation of Hsp27, a reportedly major downstream target postulated to be a key effector of p38 downstream signals. The idea that the p38 MAPK/MAPKAPK2 pathway regulates key migratory pathways may need to be revisited, as p38 MAPK activity is apparently not essential for VEGF-stimulated cell migration, as shown in this thesis, or for the plethora of cellular activities constituting normal mouse embryonic development (Adams *et al.* 2000). p38 MAPK may be essential for mediating some migratory (and other) signals in response to some stimuli, with either those signals or those stimuli redundant in development.

7.2.2 Hsp27 function

Hsp27 was shown to be required for VEGF-stimulated EC migration and protection from apoptosis. The nature of Hsp27 involvement in apoptosis was not examined in this thesis, but multiple effects on apoptotic signalling pathways have previously been reported (discussed in chapter 1).

The role Hsp27 plays in VEGF-stimulated EC migration is not clear. While Hsp27 knockdown reduces migration, in this thesis Hsp27 overexpression did not increase migration in the assay used, indicating that endogenous Hsp27 is sufficient for optimal migration. In other assays, where different cellular processes (e.g. adhesion) may be more important, additional Hsp27 may have led to enhanced migration.

Migration is driven by actin polymerisation, and Hsp27 has been reported to interact with actin as both a phosphorylation-dependent actin capping protein (capping in the unphosphorylated monomeric state) and as a stabiliser of intact actin filaments. While previous models have suggested that phosphorylation of Hsp27 causes removal of the Hsp27 cap from actin filaments to allow further actin extension, this seems unlikely to be the major Hsp27 migratory role impeded by Hsp27 knockdown – by this model less Hsp27, capping less actin filaments, might be expected

to increase migration by allowing enhanced actin polymerisation and laemellipodium extension. Actin capping at the trailing edge of a migrating cell may be important for directional movement, however. Loss of actin filament stabilisation, resulting in formation of actin filaments that are too transient to form appropriate structures, could compromise migration and this property may be more important in the effects of Hsp27 knockdown.

Hsp27 may also affect migration (and apoptosis and other cellular processes) indirectly by regulating other proteins (e.g. by direct interaction with these other proteins) which in turn affect downstream processes. For example, Hsp27 may have a specific role in the migration machinery, or it may have a general effect on cellular well-being, with consequential effects on many cellular processes.

Given apparent roles in cell migration, apoptosis and other functions, the redundancy of Hsp25 for mouse development and normal cellular behaviour (Huang *et al.* 2007), is surprising. Indeed, of those examined the only affected function in Hsp25-null cells was survival of thermal stress (Huang *et al.* 2007; migration was not examined by these authors). The relevance of thermal stress in mammals, which regulate their internal body temperature, is unclear although peripheral tissues may experience temperature fluctuations. Hsp27 may protect against other stresses which penetrate the body, such as radiation.

Hsp27 is one of a family of mammalian small Hsps. Any normal cellular roles of Hsp27 may be fulfilled by one or more of the other sHsps in Hsp25-null mice. If this occurs in practice, why is this compensation unable to cope with Hsp27 knockdown, leading to the functional effects observed in this thesis? Perhaps the conditions of cell culture assays (where the effect of the knockdown is assessed) stress the cells in ways not experienced inside an organism (perhaps siRNA transfection contributes to this stress), so a survival/damage limitation system not relevant to migration within an organism is relevant to migration in a culture assay. This interpretation suggests that Hsp27 may not, in fact, be important for cellular functions such as migration under ideal environmental conditions, and that the effect of Hsp27 on cellular function is a consequence of its chaperone

activity. Another possible interpretation is that production of Hsp27-compensating proteins occurs in vivo due to stimulation of a cell by an external signal, which does not occur in cell culture, and that Hsp27 is important for migration and other cellular functions. Given the reported interactions of Hsp27 apoptosis- and migration-related proteins, it seems likely that Hsp27 does have a genuine non-chaperone role in cellular function, although alternatively these interactions may be a result of promiscuous binding of a chaperone or scaffolding protein, or due to interaction of Hsp27 with a scaffolding protein.

7.3 SLP2

SLP2 was identified via proteomics as a component of pY immunoprecipitates. At the outset of this work, very little was known about SLP2 beyond its protein sequence and presence in a number of cell types. The results presented in chapter 6 indicated that SLP2 is a mitochondrial protein in ECs, and suggested that rather than SLP2 itself being tyrosine phosphorylated, it may be associated with a pY-containing protein. SLP2 knockdown did not significantly alter mitochondrial membrane potential, cell survival or VEGF-stimulated migration, and did not noticeably affect mitochondrial morphology.

Recent studies have begun to define the functional roles of SLP2. SLP2 is required for stress-induced mitochondrial hyperfusion, which may play a role in cellular resistance to certain toxins, and SLP2 knockdown increases cell susceptibility to UV-induced apoptosis (Tondera *et al.* 2009). Loss of SLP2 has also been reported to reduce mitochondrial membrane potential, required for ATP generation, although others were unable to reproduce this finding (Hajek *et al.* 2007; Tondera *et al.* 2009).

SLP2 associates with Mfn2 and prohibitins – indeed, association with prohibitin 1 was observed in this thesis – but the role of these associations is unclear. Mfn2 and prohibitins have roles in mitochondrial dynamics, but while Mfn2 is involved in normal mitochondrial dynamics SLP2 is not, and SLP2 but neither mitofusin 2 nor prohibitin is involved in SIMH (Tondera *et al.* 2009).

SLP2 has been shown to regulate the stability of some mitochondrial proteins including prohibitins and Opa1, and effects on the stability of these other mitochondrial proteins may contribute to the effects observed with SLP2 knockdown. For example, absence of SIMH in SLP2-reduced cells may reflect loss of Opa1 (Tondera *et al.* 2009). Phb domain proteins have previously been suggested to form membrane-associated protein scaffolds (Langhorst *et al.* 2005), and the Phb domain of podocin binds cholesterol (Huber *et al.* 2006). Binding of other proteins to SLP2 or other SLP2-associated proteins may stabilise them during certain cellular conditions, leading to protection from apoptosis.

The role of tyrosine phosphorylation in SLP2 function is enigmatic. As the majority of SLP2 does not appear to be tyrosine phosphorylated, SLP2 may be associated with a tyrosine-phosphorylated protein, which could be a small proportion of SLP2 itself or may be another protein. The Phb domain present in SLP2 is also present in other oligomerising proteins, and may itself be involved in oligomerisation. Potential hetero-oligomerisation between different Phb domain-containing proteins may possibly occur, and so other Phb domain-containing proteins are potential candidates for tyrosine-phosphorylated proteins associated with SLP2. At least one other Phb domain-containing protein, prohibitin 2, has been reported to be directly tyrosine phosphorylated. Tyrosine phosphorylation of either SLP2 or another protein in complex with SLP2 may regulate the stability of the entire complex, or may adjust its composition, with associated cellular effects.

7.4 Future work

Due to time and resource constraints, some of the areas of work in this thesis were not fully developed. Given more time, a number of additional studies would be likely to yield further insights into some of these areas.

7.4.1 Analysis of VEGF signalling

It was difficult to analyse signalling proteins using whole cell lysates – these proteins seemed too low in abundance to be detected within a whole cell lysate. Purification of a subset of interesting proteins, followed by their analysis using methods discussed in chapter 3 such as phosphoprotein/peptide enrichment, is likely to be more beneficial.

Determining the entire repertoire of phosphorylations and/or alterations in protein expression occurring after administration of a particular stimulus, might produce a list of proteins phosphorylated in response to the stimulus, but how these proteins are involved in stimulus-induced functions would not be clear. An alternative approach would be to perform an siRNA screen, assaying for a functional response or phosphorylation event that is of interest. This approach would identify the critical control proteins in a particular process, which could then be further investigated. Given the number of genes in human cells, this would be a major undertaking and would require a cost-effective high-throughput assay. The subset of siRNAs used could be limited to known signalling proteins, for example, or known actin binding proteins if migration was being studied, or some other subset of interest. Suitable high-throughput assays could include western blotting for a particular protein phosphorylation (if aiming to identify upstream enzymes), coulter counter proliferation assays, transwell migration assays, the MTT survival assay, and matrigel tubulogenesis. Some siRNAs may give insufficient knockdown and some effects may be missed, however any large effects due to knockdown of key rate-determining proteins would hopefully be observed.

Immunoprecipitation coupled with standard proteomics has been used to identify proteins interacting with the EGF receptor (Pandey *et al.* 2000a), and a similar IP/gel/mass spectrometry approach could be adopted for VEGFR2. Overexpression of tagged receptor could also be used. The stability of the receptor/associated proteins complex might be improved by administration of glutaraldehyde. Digestion of the entire complex with trypsin could provide peptides representing all members of the complex, although lysine-containing peptides would be lost if glutaraldehyde was used. Direct analysis of this peptide mixture by tandem mass spectrometry would avoid the

problems associated with gel analysis. With a sufficiently advanced mass spectrometer, quantification could be performed using stable isotope labelling by amino acids in cell culture (SILAC, discussed in section 3.5), or in later experiments using western blotting. The functional role of these interactions could later be examined with siRNA.

7.4.2 Hsp27

Despite the identification of a PKC-dependent pathway contributing to VEGF-stimulated Hsp27 S82 phosphorylation, the role of specific enzymes in VEGF-stimulated S82 phosphorylation is not clear.

To determine the role of p38-independent Hsp27 phosphorylation in VEGF-stimulated endothelial cell functions, and determine whether p38-independent pathways contribute to Hsp27 phosphorylation at S15 or S78, cells derived from p38-null mice could be used, such as those generated by Adams *et al.* (2000). Whether it would be possible to obtain sufficient endothelial cells from mice is a concern, possibly p38-null mouse embryonic fibroblasts overexpressing VEGFR2 could be used providing initial experiments indicated that VEGF stimulated a PKC-dependent S82-phosphorylating pathway. Alternatively, endothelial cells derived from the p38-deficient mice could be transformed by overexpression of the SV40 antigen and then cultured, similar to the method Adams *et al.* (2000) used to produce a cardiomyocyte line. Roles of signal transduction components implicated in Hsp27 signalling could also be tested using cells derived from mice lacking the enzyme of interest (e.g. PKD2-null mice). Alternatively, enzyme-null stable cell lines could be produced in a similar manner to that used by Matthews *et al.* (2006) to produce PKD1/PKD3 double null cells. In particular, it would be interesting to know whether PKD is entirely for responsible PKC-dependent Hsp27 phosphorylation, which could be accomplished by using PKD1/2/3-triply null cells.

In the cell culture studies performed during this thesis overexpression of wild-type or mutant Hsp27 had little effect on cellular functions, possibly due to high endogenous expression of Hsp27.

Attempts to reduce endogenous Hsp27 and re-express a desired Hsp27 from were successful but the virus/siRNA combination reduced cellular migration, preventing functional analysis of these cells. To circumvent these problems, and that of incomplete siRNA-mediated knockdown, overexpression of Hsp27 or mutants in cells completely devoid of Hsp27 (such as the mouse embryonic fibroblasts derived from Hsp25-null mice produced by Huang *et al.* 2007) could be performed, such that the overall levels of Hsp25 in wild-type/control virus and Hsp25-null/Hsp25 virus-infected cells were similar.

The most important question regarding VEGF-stimulated S82 phosphorylation is the role of this phosphorylation in an intact organism. Although Hsp25 expression is not required for normal mouse development, Huang *et al.* (2007) did not attempt to characterise the effect of Hsp25 absence on any models of disease. Hsp25/27 may be important in some pathological situations – Hsp27 overexpression is protective against ischaemia-reperfusion injury, suggesting that endogenous levels of Hsp27 may contribute to protection. Carrying out experiments on Langendorff perfused heart models similar to that performed by Hollander *et al.* (2004), using hearts derived from Hsp25-null mice, would allow examination of this question.

The effect of Hsp25 as a whole in disease models could be determined by crossing available Hsp25-null mice with a disease model mouse, for example the LDL receptor-null mouse for examining the potential role of Hsp25 in atherosclerosis. Clearly, mice homozygous for both the Hsp25 null mutation and the disease-inducing mutation would be required. For examination of the role of S82 phosphorylation, a mutant knock-in strategy could be employed to generate a mouse with the wild-type Hsp25 sequence replaced with an S86A Hsp25 sequence.

In terms of the role of Hsp27 in endothelial cells, angiogenic assays such as corneal neovascularisation or tumour growth assays would be of interest. Endothelial-specific Hsp25 knockouts (or endothelial-specific S86A Hsp25 knock-ins) would be useful in angiogenesis-related assays, to examine whether the endothelial Hsp25 is responsible for any effects. These could be produced by creating floxed Hsp25 mice, that is Hsp25 flanked by loxP sites, and then crossing these mice

with mice expressing the Cre recombinase under the control of an endothelial-specific promoter such as that for VE-cadherin or Tie2.

7.4.3 SLP2

Two major areas of the SLP2 studies warrant further investigation – the role of SLP2 in endothelial cells and the identity of the tyrosine-phosphorylated protein associated with SLP2 and whether this association affects the function of SLP2.

Clearly, SLP2-null mice would be useful in determining any non-redundant developmental role of SLP2. Creating floxed SLP2 mice would, with appropriate breeding, allow subsequent analysis of the role of SLP2 in individual cell types such as endothelial cells. A quicker, cell culture-based approach to examine SLP2 function might be to improve the siRNA-mediated knockdown of SLP2 and then perform functional assays (e.g. apoptosis, mitochondrial membrane potential). Using hardier cell lines which can survive multiple rounds of siRNA transfection (similar to the strategy of Hajek *et al.* 2007), or transducing cells with a lentivirus to continuously produce SLP2 shRNA, may produce greater knockdown and so make functional effects of SLP2 loss clearer.

SLP2 with all tyrosine residues mutated to phenylalanine, a tyrosine mimic lacking the phospho-acceptor hydroxyl group, would not be directly phosphorylated on tyrosine residues. Analysis of pY immunoprecipitates derived from SLP2-null or SLP2-reduced cells (e.g. those treated with SLP2 siRNA) expressing a tyrosine-null SLP2 mutant would allow the contribution of direct SLP2 tyrosine phosphorylation to the appearance of SLP2 in pY immunoprecipitates to be determined.

Searching for other SLP2 associating proteins, yeast two-hybrid screening may be useful. Over-expression of tagged SLP2 in cells, followed by immunoprecipitation and subsequent proteomic analysis of the retrieved complexes, may also allow improved specificity in identification of SLP2 interacting proteins, although these interactions would need to be sufficiently stable to survive the IP procedure. However, a tag may interfere with the interactions between SLP2 and other proteins, or with SLP2 oligomerisation.

Examination of the proteome of isolated mitochondria in SLP2-null or SLP2-reduced cells may allow identification of other proteins stabilised by SLP2 – large-scale loss of abundant proteins due to proteolysis may well be detected using total protein staining techniques providing quantification was sufficiently accurate (e.g. using difference gel electrophoresis or metabolic labelling). A candidate-based approach, blotting for known mitochondrial membrane proteins, may also identify SLP2-stabilised proteins. The identity of these proteins may give some insights into the function of SLP2.

References

Aase K, von Euler G, Li X, Ponten A, Thoren P, Cao R, Cao Y, Olofsson B, Gebre-Medhin S, Pekny M, Alitalo K, Betsholtz C, Eriksson U (2001) Vascular endothelial growth factor-B-deficient mice display an atrial conduction defect. *Circulation* 104(3):358–364

Abdel-Latif A, Bolli R, Tleyjeh IM, Montori VM, Perin EC, Hornung CA, Zuba-Surma EK, Al-Mallah M, Dawn B (2007) Adult bone marrow-derived cells for cardiac repair: a systematic review and meta-analysis. *Arch Intern Med* 167(10):989–997

Abeliovich A, Chen C, Goda Y, Silva AJ, Stevens CF, Tonegawa S (1993) Modified hippocampal long-term potentiation in PKC gamma-mutant mice. *Cell* 75(7):1253–1262

Abu-Ghazaleh R, Kabir J, Jia H, Lobo M, Zachary I (2001) Src mediates stimulation by vascular endothelial growth factor of the phosphorylation of focal adhesion kinase at tyrosine 861, and migration and anti-apoptosis in endothelial cells. *Biochem J* 360(Pt 1):255–264

Achen MG, Jeltsch M, Kukk E, Makinen T, Vitali A, Wilks AF, Alitalo K, Stacker SA (1998) Vascular endothelial growth factor D (VEGF-D) is a ligand for the tyrosine kinases VEGF receptor 2 (Flk1) and VEGF receptor 3 (Flt4). *Proc Natl Acad Sci U S A* 95(2):548–553

Adamis AP, Shima DT, Yeo KT, Yeo TK, Brown LF, Berse B, D'Amore PA, Folkman J (1993) Synthesis and secretion of vascular permeability factor/vascular endothelial growth factor by human retinal pigment epithelial cells. *Biochem Biophys Res Commun* 193(2):631–638

Adams RH, Alitalo K (2007) Molecular regulation of angiogenesis and lymphangiogenesis. *Nat Rev Mol Cell Biol* 8(6):464–478

Adams RH, Wilkinson GA, Weiss C, Diella F, Gale NW, Deutsch U, Risau W, Klein R (1999) Roles of ephrinB ligands and EphB receptors in cardiovascular development: demarcation of arterial/venous domains, vascular morphogenesis, and sprouting angiogenesis. *Genes Dev* 13(3):295–306

Adams RH, Porras A, Alonso G, Jones M, Vintersten K, Panelli S, Valladares A, Perez L, Klein R, Nebreda AR (2000) Essential role of p38alpha MAP kinase in placental but not embryonic cardiovascular development. *Mol Cell* 6(1):109–116

Adams RH, Diella F, Hennig S, Helmbacher F, Deutsch U, Klein R (2001) The cytoplasmic domain of the ligand ephrinB2 is required for vascular morphogenesis but not cranial neural crest migration. *Cell* 104(1):57–69

Aiello LP, Avery RL, Arrigg PG, Keyt BA, Jampel HD, Shah ST, Pasquale LR, Thieme H, Iwamoto MA, Park JE, (1994) Vascular endothelial growth factor in ocular fluid of patients with diabetic retinopathy and other retinal disorders. *N Engl J Med* 331(22):1480–1487

Aird WC (2007) Phenotypic heterogeneity of the endothelium: I. Structure, function, and mechanisms. *Circ Res* 100(2):158–173

Akhtar S, Benter IF (2007) Nonviral delivery of synthetic siRNAs in vivo. *J Clin Invest* 117(12):3623–3632

Alford KA, Glennie S, Turrell BR, Rawlinson L, Saklatvala J, Dean JL (2007) Heat shock protein 27 functions in inflammatory gene expression and transforming growth factor-beta-activated kinase-1 (TAK1)-mediated signaling. *J Biol Chem* 282(9):6232–6241

Allen M, Svensson L, Roach M, Hambor J, McNeish J, Gabel CA (2000) Deficiency of the stress kinase p38alpha results in embryonic lethality: characterization of the kinase dependence of stress responses of enzyme-deficient embryonic stem cells. *J Exp Med* 191(5):859–870

Alon T, Hemo I, Itin A, Pe'er J, Stone J, Keshet E (1995) Vascular endothelial growth factor acts as a survival factor for newly formed retinal vessels and has implications for retinopathy of prematurity. *Nat Med* 1(10):1024–1028

Altschul SF, Madden TL, Schaffer AA, Zhang J, Zhang Z, Miller W, Lipman DJ (1997) Gapped BLAST and PSI-BLAST: a new generation of protein database search programs. *Nucleic Acids Res* 25(17):3389–3402

Altschul SF, Wootton JC, Gertz EM, Agarwala R, Morgulis A, Schaffer AA, Yu YK (2005) Protein database searches using compositionally adjusted substitution matrices. *FEBS J* 272(20):5101–5109

Andersson L, Porath J (1986) Isolation of phosphoproteins by immobilized metal (Fe3+) affinity chromatography. *Anal Biochem* 154(1):250–254

Antonetti DA, Barber AJ, Hollinger LA, Wolpert EB, Gardner TW (1999) Vascular endothelial growth factor induces rapid phosphorylation of tight junction proteins occludin and zonula occluden 1. A potential mechanism for vascular permeability in diabetic retinopathy and tumors. *J Biol Chem* 274(33):23463–23467

Aramoto H, Breslin JW, Pappas PJ, Hobson RW, Duran WN (2004) Vascular endothelial growth factor stimulates differential signaling pathways in in vivo microcirculation. *Am J Physiol Heart Circ Physiol* 287(4):H1590–H1598

Arcaro A, Wymann MP (1993) Wortmannin is a potent phosphatidylinositol 3-kinase inhibitor: the role of phosphatidylinositol 3,4,5-trisphosphate in neutrophil responses. *Biochem J* 296 (Pt 2):297–301

Arnout J, Hoylaerts MF, Lijnen HR (2006) Haemostasis. *Handb Exp Pharmacol* (176 Pt 2):1–41

Arrigo AP, Welch WJ (1987) Characterization and purification of the small 28,000-dalton mammalian heat shock protein. *J Biol Chem* 262(32):15359–15369

Arrigo AP, Suhan JP, Welch WJ (1988) Dynamic changes in the structure and intracellular locale of the mammalian low-molecular-weight heat shock protein. *Mol Cell Biol* 8(12):5059–5071

Arrigo AP, Simon S, Gibert B, Kretz-Remy C, Nivon M, Czekalla A, Guillet D, Moulin M, Diaz-Latoud C, Vicart P (2007) Hsp27 (HspB1) and alphaB-crystallin (HspB5) as therapeutic targets. *FEBS Lett* 581(19):3665–3674

Artal-Sanz M, Tavernarakis N (2009) Prohibitin and mitochondrial biology. *Trends Endocrinol Metab* 20(8):394–401

Asahara T, Murohara T, Sullivan A, Silver M, van der Zee R, Li T, Witzenbichler B, Schatteman G, Isner JM (1997) Isolation of putative progenitor endothelial cells for angiogenesis. *Science* 275(5302):964–967

Asahara T, Takahashi T, Masuda H, Kalka C, Chen D, Iwaguro H, Inai Y, Silver M, Isner JM (1999) VEGF contributes to postnatal neovascularization by mobilizing bone marrow-derived endothelial progenitor cells. *EMBO J* 18(14):3964–3972

Ashikari-Hada S, Habuchi H, Kariya Y, Kimata K (2005) Heparin regulates vascular endothelial growth factor165-dependent mitogenic activity, tube formation, and its receptor phosphorylation of human endothelial cells. Comparison of the effects of heparin and modified heparins. *J Biol Chem* 280(36):31508–31515

Asirvatham AJ, Magner WJ, Tomasi TB (2009) miRNA regulation of cytokine genes. *Cytokine* 45(2):58–69

Autiero M, Waltenberger J, Communi D, Kranz A, Moons L, Lambrechts D, Kroll J, Plaisance S, De Mol M, Bono F, Kliche S, Fellbrich G, Ballmer-Hofer K, Maglione D, Mayr-Beyrle U, Dewerchin M, Dombrowski S, Stanimirovic D, Van HP, Dehio C, Hicklin DJ, Persico G, Herbert JM, Communi D, Shibuya M, Collen D, Conway EM, Carmeliet P (2003) Role of PlGF in the intra- and intermolecular cross talk between the VEGF receptors Flt1 and Flk1. *Nat Med* 9(7):936–943

Avkiran M, Rowland AJ, Cuello F, Haworth RS (2008) Protein kinase d in the cardiovascular system: emerging roles in health and disease. *Circ Res* 102(2):157–163

Azzouz M, Ralph GS, Storkebaum E, Walmsley LE, Mitrophanous KA, Kingsman SM, Carmeliet P, Mazarakis ND (2004) VEGF delivery with retrogradely transported lentivector prolongs survival in a mouse ALS model. *Nature* 429(6990):413–417

Bain J, McLauchlan H, Elliott M, Cohen P (2003) The specificities of protein kinase inhibitors: an update. *Biochem J* 371(Pt 1):199–204

Bain J, Plater L, Elliott M, Shpiro N, Hastie CJ, McLauchlan H, Klevernic I, Arthur JS, Alessi DR, Cohen P (2007) The selectivity of protein kinase inhibitors: a further update. *Biochem J* 408(3):297–315

Baldwin ME, Halford MM, Roufail S, Williams RA, Hibbs ML, Grail D, Kubo H, Stacker SA, Achen MG (2005) Vascular endothelial growth factor D is dispensable for development of the lymphatic system. *Mol Cell Biol* 25(6):2441–2449

Barchowsky A, Williams ME, Benz CC, Chepenik KP (1994) Oxidant-sensitive protein phosphorylation in endothelial cells. *Free Radic Biol Med* 16(6):771–777

Barleon B, Sozzani S, Zhou D, Weich HA, Mantovani A, Marme D (1996) Migration of human monocytes in response to vascular endothelial growth factor (VEGF) is mediated via the VEGF receptor flt-1. *Blood* 87(8):3336–3343

Bates DO, Harper SJ (2002) Regulation of vascular permeability by vascular endothelial growth factors. *Vascul Pharmacol* 39(4-5):225–237

Bates DO, Cui TG, Doughty JM, Winkler M, Sugiono M, Shields JD, Peat D, Gillatt D, Harper SJ (2002) VEGF165b, an inhibitory splice variant of vascular endothelial growth factor, is down-regulated in renal cell carcinoma. *Cancer Res* 62(14):4123–4131

Beardmore VA, Hinton HJ, Eftychi C, Apostolaki M, Armaka M, Darragh J, McIlrath J, Carr JM, Armit LJ, Clacher C, Malone L, Kollias G, Arthur JS (2005) Generation and characterization of p38beta (MAPK11) gene-targeted mice. *Mol Cell Biol* 25(23):10454–10464

Bellomo D, Headrick JP, Silins GU, Paterson CA, Thomas PS, Gartside M, Mould A, Cahill MM, Tonks ID, Grimmond SM, Townson S, Wells C, Little M, Cummings MC, Hayward NK, Kay GF (2000) Mice lacking the vascular endothelial growth factor-B gene (Vegfb) have smaller hearts, dysfunctional coronary vasculature, and impaired recovery from cardiac ischemia. *Circ Res* 86(2):E29–E35

Bellyei S, Szigeti A, Pozsgai E, Boronkai A, Gomori E, Hocsak E, Farkas R, Sumegi B, Gallyas J F (2007) Preventing apoptotic cell death by a novel small heat shock protein. *Eur J Cell Biol* 86(3):161–171

Ben-Levy R, Leighton IA, Doza YN, Attwood P, Morrice N, Marshall CJ, Cohen P (1995) Identification of novel phosphorylation sites required for activation of MAPKAP kinase-2. *EMBO J* 14(23):5920–5930

Ben-Levy R, Hooper S, Wilson R, Paterson HF, Marshall CJ (1998) Nuclear export of the stress-activated protein kinase p38 mediated by its substrate MAPKAP kinase-2. *Curr Biol* 8(19):1049–1057

Benndorf R, Hayess K, Ryazantsev S, Wieske M, Behlke J, Lutsch G (1994) Phosphorylation and supramolecular organization of murine small heat shock protein HSP25 abolish its actin polymerization-inhibiting activity. *J Biol Chem* 269(32):20780–20784

Benndorf R, Sun X, Gilmont RR, Biederman KJ, Molloy MP, Goodmurphy CW, Cheng H, Andrews PC, Welsh MJ (2001) HSP22, a new member of the small heat shock protein superfamily, interacts with mimic of phosphorylated HSP27 ((3D)HSP27). *J Biol Chem* 276(29):26753–26761

Berk AJ (2007) Adenoviridae: the viruses and their replication. In DM Knipe, PM Howley, editors, *Fields virology*, book chapter 63, 2355–2394. Lippincott, Williams and Wilkins, 5th edition

Beutler B, Milsark IW, Cerami AC (1985) Passive immunization against cachectin/tumor necrosis factor protects mice from lethal effect of endotoxin. *Science* 229(4716):869–871

Bevers EM, Comfurius P, Dekkers DW, Zwaal RF (1999) Lipid translocation across the plasma membrane of mammalian cells. *Biochim Biophys Acta* 1439(3):317–330

Bevilacqua MP, Pober JS, Wheeler ME, Cotran RS, Gimbrone MA (1985) Interleukin-1 activation of vascular endothelium. Effects on procoagulant activity and leukocyte adhesion. *Am J Pathol* 121(3):394–403

Bienfait HM, Baas F, Koelman JH, de Haan RJ, van Engelen BG, Gabreels-Festen AA, de Ongerboer V, Meggouh F, Weterman MA, De Jonghe P, Timmerman V, de Visser M (2007) Phenotype of Charcot-Marie-Tooth disease Type 2. *Neurology* 68(20):1658–1667

Bohman S, Matsumoto T, Suh K, Dimberg A, Jakobsson L, Yuspa S, Claesson-Welsh L (2005) Proteomic analysis of vascular endothelial growth factor-induced endothelial cell differentiation reveals a role for chloride intracellular channel 4 (CLIC4) in tubular morphogenesis. *J Biol Chem* 280(51):42397–42404

Bradley JR (2008) TNF-mediated inflammatory disease. *J Pathol* 214(2):149–160

Brancho D, Tanaka N, Jaeschke A, Ventura JJ, Kelkar N, Tanaka Y, Kyuuma M, Takeshita T, Flavell RA, Davis RJ (2003) Mechanism of p38 MAP kinase activation in vivo. *Genes Dev* 17(16):1969–1978

Braz JC, Gregory K, Pathak A, Zhao W, Sahin B, Klevitsky R, Kimball TF, Lorenz JN, Nairn AC, Liggett SB, Bodi I, Wang S, Schwartz A, Lakatta EG, Paoli-Roach AA, Robbins J, Hewett TE, Bibb JA, Westfall MV, Kranias EG, Molkentin JD (2004) PKC-alpha regulates cardiac contractility and propensity toward heart failure. *Nat Med* 10(3):248–254

Breier G, Albrecht U, Sterrer S, Risau W (1992) Expression of vascular endothelial growth factor during embryonic angiogenesis and endothelial cell differentiation. *Development* 114(2):521–532

Brightman MW, Reese TS (1969) Junctions between intimately apposed cell membranes in the vertebrate brain. *J Cell Biol* 40(3):648–677

Brock TA, Dvorak HF, Senger DR (1991) Tumor-secreted vascular permeability factor increases cytosolic Ca2+ and von Willebrand factor release in human endothelial cells. *Am J Pathol* 138(1):213–221

Brooks PC, Montgomery AM, Rosenfeld M, Reisfeld RA, Hu T, Klier G, Cheresh DA (1994) Integrin alpha v beta 3 antagonists promote tumor regression by inducing apoptosis of angiogenic blood vessels. *Cell* 79(7):1157–1164

Browman DT, Hoegg MB, Robbins SM (2007) The SPFH domain-containing proteins: more than lipid raft markers. *Trends Cell Biol* 17(8):394–402

Brown DM, Kaiser PK, Michels M, Soubrane G, Heier JS, Kim RY, Sy JP, Schneider S (2006) Ranibizumab versus verteporfin for neovascular age-related macular degeneration. *N Engl J Med* 355(14):1432–1444

Bruey JM, Ducasse C, Bonniaud P, Ravagnan L, Susin SA, Diaz-Latoud C, Gurbuxani S, Arrigo AP, Kroemer G, Solary E, Garrido C (2000a) Hsp27 negatively regulates cell death by interacting with cytochrome c. *Nat Cell Biol* 2(9):645–652

Bruey JM, Paul C, Fromentin A, Hilpert S, Arrigo AP, Solary E, Garrido C (2000b) Differential regulation of HSP27 oligomerization in tumor cells grown in vitro and in vivo. *Oncogene* 19(42):4855–4863

Brunet A, Bonni A, Zigmond MJ, Lin MZ, Juo P, Hu LS, Anderson MJ, Arden KC, Blenis J, Greenberg ME (1999) Akt promotes cell survival by phosphorylating and inhibiting a Forkhead transcription factor. *Cell* 96(6):857–868

Bryantsev AL, Kurchashova SY, Golyshev SA, Polyakov VY, Wunderink HF, Kanon B, Budagova KR, Kabakov AE, Kampinga HH (2007) Regulation of stress-induced intracellular sorting and chaperone function of Hsp27 (HspB1) in mammalian cells. *Biochem J* 407(3):407–417

Bukach OV, Glukhova AE, Seit-Nebi AS, Gusev NB (2009) Heterooligomeric complexes formed by human small heat shock proteins HspB1 (Hsp27) and HspB6 (Hsp20). *Biochim Biophys Acta* 1794(3):486–495

Butt E, Immler D, Meyer HE, Kotlyarov A, Laass K, Gaestel M (2001) Heat shock protein 27 is a substrate of cGMP-dependent protein kinase in intact human platelets: phosphorylation-induced actin polymerization caused by HSP27 mutants. *J Biol Chem* 276(10):7108–7113

Cai H (2005) Hydrogen peroxide regulation of endothelial function: origins, mechanisms, and consequences. *Cardiovasc Res* 68(1):26–36

Calderwood SK, Khaleque MA, Sawyer DB, Ciocca DR (2006) Heat shock proteins in cancer: chaperones of tumorigenesis. *Trends Biochem Sci* 31(3):164–172

Cao W, Zhang B, Liu Y, Li H, Zhang S, Fu L, Niu Y, Ning L, Cao X, Liu Z, Sun B (2007) High-level SLP-2 expression and HER-2/neu protein expression are associated with decreased breast cancer patient survival. *Am J Clin Pathol* 128(3):430–436

Cao Y, Linden P, Farnebo J, Cao R, Eriksson A, Kumar V, Qi JH, Claesson-Welsh L, Alitalo K (1998) Vascular endothelial growth factor C induces angiogenesis in vivo. *Proc Natl Acad Sci U S A* 95(24):14389–14394

Carmeliet P, Ferreira V, Breier G, Pollefeyt S, Kieckens L, Gertsenstein M, Fahrig M, Vandenhoeck A, Harpal K, Eberhardt C, Declercq C, Pawling J, Moons L, Collen D, Risau W, Nagy A (1996) Abnormal blood vessel development and lethality in embryos lacking a single VEGF allele. *Nature* 380(6573):435–439

Carmeliet P, Dor Y, Herbert JM, Fukumura D, Brusselmans K, Dewerchin M, Neeman M, Bono F, Abramovitch R, Maxwell P, Koch CJ, Ratcliffe P, Moons L, Jain RK, Collen D, Keshert E (1998) Role of HIF-1alpha in hypoxia-mediated apoptosis, cell proliferation and tumour angiogenesis. *Nature* 394(6692):485–490

Carmeliet P, Lampugnani MG, Moons L, Breviario F, Compernolle V, Bono F, Balconi G, Spagnuolo R, Oostuyse B, Dewerchin M, Zanetti A, Angellilo A, Mattot V, Nuyens D, Lutgens E, Clotman F, de Ruiter MC, Gittenberger-de GA, Poelmann R, Lupu F, Herbert JM, Collen D, Dejana E (1999a) Targeted deficiency or cytosolic truncation of the VE-cadherin gene in mice impairs VEGF-mediated endothelial survival and angiogenesis. *Cell* 98(2):147–157

Carmeliet P, Ng YS, Nuyens D, Theilmeier G, Brusselmans K, Cornelissen I, Ehler E, Kakkar VV, Stalmans I, Mattot V, Perriard JC, Dewerchin M, Flameng W, Nagy A, Lupu F, Moons L, Collen D, D'Amore PA, Shima DT (1999b) Impaired myocardial angiogenesis and ischemic cardiomyopathy in mice lacking the vascular endothelial growth factor isoforms VEGF164 and VEGF188. *Nat Med* 5(5):495–502

Carmeliet P, Moons L, Luttun A, Vincenti V, Compernolle V, De Mol M, Wu Y, Bono F, Devy L, Beck H, Scholz D, Acker T, DiPalma T, Dewerchin M, Noel A, Stalmans I, Barra A, Blacher S, Vandendriessche T, Ponten A, Eriksson U, Plate KH, Foidart JM, Schaper W, Charnock-Jones DS, Hicklin DJ, Herbert JM, Collen D, Persico MG (2001) Synergism between vascular endothelial growth factor and placental growth factor contributes to angiogenesis and plasma extravasation in pathological conditions. *Nat Med* 7(5):575–583

Carson SD, Hobbs JT, Tracy SM, Chapman NM (1999) Expression of the coxsackievirus and adenovirus receptor in cultured human umbilical vein endothelial cells: regulation in response to cell density. *J Virol* 73(8):7077–7079

Carswell EA, Old LJ, Kassel RL, Green S, Fiore N, Williamson B (1975) An endotoxin-induced serum factor that causes necrosis of tumors. *Proc Natl Acad Sci U S A* 72(9):3666–3670

Castrillo A, Pennington DJ, Otto F, Parker PJ, Owen MJ, Bosca L (2001) Protein kinase Cepsilon is required for macrophage activation and defense against bacterial infection. *J Exp Med* 194(9):1231–1242

Charette SJ, Lavoie JN, Lambert H, Landry J (2000) Inhibition of Daxx-mediated apoptosis by heat shock protein 27. *Mol Cell Biol* 20(20):7602–7612

Chaudhuri TK, Paul S (2006) Protein-misfolding diseases and chaperone-based therapeutic approaches. *FEBS J* 273(7):1331–1349

Chen H, Bagri A, Zupicich JA, Zou Y, Stoeckli E, Pleasure SJ, Lowenstein DH, Skarnes WC, Chedotal A, Tessier-Lavigne M (2000) Neuropilin-2 regulates the development of selective cranial and sensory nerves and hippocampal mossy fiber projections. *Neuron* 25(1):43–56

Chen SW, Park SW, Kim M, Brown KM, D'Agati VD, Lee HT (2009) Human heat shock protein 27 overexpressing mice are protected against hepatic ischemia and reperfusion injury. *Transplantation* 87(10):1478–1487

Chi JT, Chang HY, Haraldsen G, Jahnsen FL, Troyanskaya OG, Chang DS, Wang Z, Rockson SG, van de Rijn M, Botstein D, Brown PO (2003) Endothelial cell diversity revealed by global expression profiling. *Proc Natl Acad Sci U S A* 100(19):10623–10628

Chiti F, Dobson CM (2006) Protein misfolding, functional amyloid, and human disease. *Annu Rev Biochem* 75:333–366

Ciulla TA, Rosenfeld PJ (2009) Antivascular endothelial growth factor therapy for neovascular age-related macular degeneration. *Curr Opin Ophthalmol* 20(3):158–165

Claffey KP, Senger DR, Spiegelman BM (1995) Structural requirements for dimerization, glycosylation, secretion, and biological function of VPF/VEGF. *Biochim Biophys Acta* 1246(1):1–9

Clamp M, Cuff J, Searle SM, Barton GJ (2004) The Jalview Java alignment editor. *Bioinformatics* 20(3):426–427

Claros MG, Vincens P (1996) Computational method to predict mitochondrially imported proteins and their targeting sequences. *Eur J Biochem* 241(3):779–786

Clauss M, Weich H, Breier G, Knies U, Rockl W, Waltenberger J, Risau W (1996) The vascular endothelial growth factor receptor Flt-1 mediates biological activities. Implications for a functional role of placenta growth factor in monocyte activation and chemotaxis. *J Biol Chem* 271(30):17629–17634

Clayton JA, Chalothorn D, Faber JE (2008) Vascular endothelial growth factor-A specifies formation of native collaterals and regulates collateral growth in ischemia. *Circ Res* 103(9):1027–1036

Clifton AD, Young PR, Cohen P (1996) A comparison of the substrate specificity of MAPKAP kinase-2 and MAPKAP kinase-3 and their activation by cytokines and cellular stress. *FEBS Lett* 392(3):209–214

Cohen AW, Carbajal JM, Schaeffer J R C (1999) VEGF stimulates tyrosine phosphorylation of beta-catenin and small-pore endothelial barrier dysfunction. *Am J Physiol* 277(5 Pt 2):H2038–H2049

Colon-Gonzalez F, Kazanietz MG (2006) C1 domains exposed: from diacylglycerol binding to protein-protein interactions. *Biochim Biophys Acta* 1761(8):827–837

Concannon CG, Gorman AM, Samali A (2003) On the role of Hsp27 in regulating apoptosis. *Apoptosis* 8(1):61–70

Connolly DT, Heuvelman DM, Nelson R, Olander JV, Eppley BL, Delfino JJ, Siegel NR, Leimgruber RM, Feder J (1989) Tumor vascular permeability factor stimulates endothelial cell growth and angiogenesis. *J Clin Invest* 84(5):1470–1478

Corthals GL, Wasinger VC, Hochstrasser DF, Sanchez JC (2000) The dynamic range of protein expression: a challenge for proteomic research. *Electrophoresis* 21(6):1104–1115

Couturier M, Bahassi e, Van ML (1998) Bacterial death by DNA gyrase poisoning. *Trends Microbiol* 6(7):269–275

Cuenda A, Rouse J, Doza YN, Meier R, Cohen P, Gallagher TF, Young PR, Lee JC (1995) SB 203580 is a specific inhibitor of a MAP kinase homologue which is stimulated by cellular stresses and interleukin-1. *FEBS Lett* 364(2):229–233

Cui Z, Zhang L, Hua Z, Cao W, Feng W, Liu Z (2007) Stomatin-like protein 2 is overexpressed and related to cell growth in human endometrial adenocarcinoma. *Oncol Rep* 17(4):829–833

Cunningham SA, Tran TM, Arrate MP, Bjercke R, Brock TA (1999) KDR activation is crucial for VEGF165-mediated Ca2+ mobilization in human umbilical vein endothelial cells. *Am J Physiol* 276(1 Pt 1):C176–C181

Da Cruz S, Xenarios I, Langridge J, Vilbois F, Parone PA, Martinou JC (2003) Proteomic analysis of the mouse liver mitochondrial inner membrane. *J Biol Chem* 278(42):41566–41571

Da Cruz S, Parone PA, Gonzalo P, Bienvenut WV, Tondera D, Jourdain A, Quadroni M, Martinou JC (2008) SLP-2 interacts with prohibitins in the mitochondrial inner membrane and contributes to their stability. *Biochim Biophys Acta* 1783(5):904–911

Darbon JM, Issandou M, Tournier JF, Bayard F (1990) The respective 27 kDa and 28 kDa protein kinase C substrates in vascular endothelial and MCF-7 cells are most probably heat shock proteins. *Biochem Biophys Res Commun* 168(2):527–536

Datta SR, Dudek H, Tao X, Masters S, Fu H, Gotoh Y, Greenberg ME (1997) Akt phosphorylation of BAD couples survival signals to the cell-intrinsic death machinery. *Cell* 91(2):231–241

Davidson SM, Yellon D, Duchen MR (2007) Assessing mitochondrial potential, calcium, and redox state in isolated mammalian cells using confocal microscopy. *Methods Mol Biol* 372:421–430

Davies SP, Reddy H, Caivano M, Cohen P (2000) Specificity and mechanism of action of some commonly used protein kinase inhibitors. *Biochem J* 351(Pt 1):95–105

Dayanir V, Meyer RD, Lashkari K, Rahimi N (2001) Identification of tyrosine residues in vascular endothelial growth factor receptor-2/FLK-1 involved in activation of phosphatidylinositol 3-kinase and cell proliferation. *J Biol Chem* 276(21):17686–17692

de Martin R, Raidl M, Hofer E, Binder BR (1997) Adenovirus-mediated expression of green fluorescent protein. *Gene Ther* 4(5):493–495

De Vries C, Escobedo JA, Ueno H, Houck K, Ferrara N, Williams LT (1992) The fms-like tyrosine kinase, a receptor for vascular endothelial growth factor. *Science* 255(5047):989–991

Dejana E (2004) Endothelial cell-cell junctions: happy together. *Nat Rev Mol Cell Biol* 5(4):261–270

Deng CX, Wynshaw-Boris A, Shen MM, Daugherty C, Ornitz DM, Leder P (1994) Murine FGFR-1 is required for early postimplantation growth and axial organization. *Genes Dev* 8(24):3045–3057

Diaz-Latoud C, Buache E, Javouhey E, Arrigo AP (2005) Substitution of the unique cysteine residue of murine Hsp25 interferes with the protective activity of this stress protein through inhibition of dimer formation. *Antioxid Redox Signal* 7(3-4):436–445

Dimmeler S, Fleming I, Fisslthaler B, Hermann C, Busse R, Zeiher AM (1999) Activation of nitric oxide synthase in endothelial cells by Akt-dependent phosphorylation. *Nature* 399(6736):601–605

Dimmeler S, Dernbach E, Zeiher AM (2000) Phosphorylation of the endothelial nitric oxide synthase at ser-1177 is required for VEGF-induced endothelial cell migration. *FEBS Lett* 477(3):258–262

Dinarello CA (2009) Immunological and inflammatory functions of the interleukin-1 family. *Annu Rev Immunol* 27:519–550

Dixelius J, Makinen T, Wirzenius M, Karkkainen MJ, Wernstedt C, Alitalo K, Claesson-Welsh L (2003) Ligand-induced vascular endothelial growth factor receptor-3 (VEGFR-3) heterodimerization with VEGFR-2 in primary lymphatic endothelial cells regulates tyrosine phosphorylation sites. *J Biol Chem* 278(42):40973–40979

Donnini S, Machein MR, Plate KH, Weich HA (1999) Expression and localization of placenta growth factor and PlGF receptors in human meningiomas. *J Pathol* 189(1):66–71

Doppler H, Storz P, Li J, Comb MJ, Toker A (2005) A phosphorylation state-specific antibody recognizes Hsp27, a novel substrate of protein kinase D. *J Biol Chem* 280(15):15013–15019

Dougher M, Terman BI (1999) Autophosphorylation of KDR in the kinase domain is required for maximal VEGF-stimulated kinase activity and receptor internalization. *Oncogene* 18(8):1619–1627

Dougher-Vermazen M, Hulmes JD, Bohlen P, Terman BI (1994) Biological activity and phosphorylation sites of the bacterially expressed cytosolic domain of the KDR VEGF-receptor. *Biochem Biophys Res Commun* 205(1):728–738

Dowling P, Meleady P, Dowd A, Henry M, Glynn S, Clynes M (2007) Proteomic analysis of isolated membrane fractions from superinvasive cancer cells. *Biochim Biophys Acta* 1774(1):93–101

Doza YN, Cuenda A, Thomas GM, Cohen P, Nebreda AR (1995) Activation of the MAP kinase homologue RK requires the phosphorylation of Thr-180 and Tyr-182 and both residues are phosphorylated in chemically stressed KB cells. *FEBS Lett* 364(2):223–228

Dreher D, Vargas JR, Hochstrasser DF, Junod AF (1995) Effects of oxidative stress and Ca2+ agonists on molecular chaperones in human umbilical vein endothelial cells. *Electrophoresis* 16(7):1205–1214

Duchen MR, Surin A, Jacobson J (2003) Imaging mitochondrial function in intact cells. *Methods Enzymol* 361:353–389

Dumont DJ, Gradwohl G, Fong GH, Puri MC, Gertsenstein M, Auerbach A, Breitman ML (1994) Dominant-negative and targeted null mutations in the endothelial receptor tyrosine kinase, tek, reveal a critical role in vasculogenesis of the embryo. *Genes Dev* 8(16):1897–1909

Dumont DJ, Jussila L, Taipale J, Lymboussaki A, Mustonen T, Pajusola K, Breitman M, Alitalo K (1998) Cardiovascular failure in mouse embryos deficient in VEGF receptor-3. *Science* 282(5390):946–949

Dunn MJ (1999) Detection of total proteins on western blots of 2-D polyacrylamide gels. *Methods Mol Biol* 112:319–329

Duval M, Bedard-Goulet S, Delisle C, Gratton JP (2003) Vascular endothelial growth factor-dependent down-regulation of Flk-1/KDR involves Cbl-mediated ubiquitination. Consequences on nitric oxide production from endothelial cells. *J Biol Chem* 278(22):20091–20097

Ehrnsperger M, Graber S, Gaestel M, Buchner J (1997) Binding of non-native protein to Hsp25 during heat shock creates a reservoir of folding intermediates for reactivation. *EMBO J* 16(2):221–229

Ehrnsperger M, Lilie H, Gaestel M, Buchner J (1999) The dynamics of Hsp25 quaternary structure. Structure and function of different oligomeric species. *J Biol Chem* 274(21):14867–14874

Eichmann A, Yuan L, Moyon D, Lenoble F, Pardanaud L, Breant C (2005) Vascular development: from precursor cells to branched arterial and venous networks. *Int J Dev Biol* 49(2-3):259–267

Eliceiri BP, Paul R, Schwartzberg PL, Hood JD, Leng J, Cheresh DA (1999) Selective requirement for Src kinases during VEGF-induced angiogenesis and vascular permeability. *Mol Cell* 4(6):915–924

Emanuelsson O, Nielsen H, Brunak S, von Heijne G (2000) Predicting subcellular localization of proteins based on their N-terminal amino acid sequence. *J Mol Biol* 300(4):1005–1016

Engel K, Schultz H, Martin F, Kotlyarov A, Plath K, Hahn M, Heinemann U, Gaestel M (1995) Constitutive activation of mitogen-activated protein kinase-activated protein kinase 2 by mutation of phosphorylation sites and an A-helix motif. *J Biol Chem* 270(45):27213–27221

Engel K, Kotlyarov A, Gaestel M (1998) Leptomycin B-sensitive nuclear export of MAPKAP kinase 2 is regulated by phosphorylation. *EMBO J* 17(12):3363–3371

Enslen H, Raingeaud J, Davis RJ (1998) Selective activation of p38 mitogen-activated protein (MAP) kinase isoforms by the MAP kinase kinases MKK3 and MKK6. *J Biol Chem* 273(3):1741–1748

Epstein AC, Gleadle JM, McNeill LA, Hewitson KS, O'Rourke J, Mole DR, Mukherji M, Metzen E, Wilson MI, Dhanda A, Tian YM, Masson N, Hamilton DL, Jaakkola P, Barstead R, Hodgkin J, Maxwell PH, Pugh CW, Schofield CJ, Ratcliffe PJ (2001) C. elegans EGL-9 and mammalian homologs define a family of dioxygenases that regulate HIF by prolyl hydroxylation. *Cell* 107(1):43–54

Eremina V, Sood M, Haigh J, Nagy A, Lajoie G, Ferrara N, Gerber HP, Kikkawa Y, Miner JH, Quaggin SE (2003) Glomerular-specific alterations of VEGF-A expression lead to distinct congenital and acquired renal diseases. *J Clin Invest* 111(5):707–716

Esser S, Lampugnani MG, Corada M, Dejana E, Risau W (1998a) Vascular endothelial growth factor induces VE-cadherin tyrosine phosphorylation in endothelial cells. *J Cell Sci* 111 (Pt 13):1853–1865

Esser S, Wolburg K, Wolburg H, Breier G, Kurzchalia T, Risau W (1998b) Vascular endothelial growth factor induces endothelial fenestrations in vitro. *J Cell Biol* 140(4):947–959

Evans IM, Britton G, Zachary IC (2008) Vascular endothelial growth factor induces heat shock protein (HSP) 27 serine 82 phosphorylation and endothelial tubulogenesis via protein kinase D and independent of p38 kinase. *Cell Signal* 20(7):1375–1384

Evgrafov OV, Mersiyanova I, Irobi J, Van Den Bosch L, Dierick I, Leung CL, Schagina O, Verpoorten N, Van IK, Fedotov V, Dadali E, Auer-Grumbach M, Windpassinger C, Wagner K, Mitrovic Z, Hilton-Jones D, Talbot K, Martin JJ, Vasserman N, Tverskaya S, Polyakov A, Liem RK, Gettemans J, Robberecht W, De Jonghe P, Timmerman V (2004) Mutant small heat-shock protein 27 causes axonal Charcot-Marie-Tooth disease and distal hereditary motor neuropathy. *Nat Genet* 36(6):602–606

Ewan LC, Jopling HM, Jia H, Mittar S, Bagherzadeh A, Howell GJ, Walker JH, Zachary IC, Ponnambalam S (2006) Intrinsic tyrosine kinase activity is required for vascular endothelial growth factor receptor 2 ubiquitination, sorting and degradation in endothelial cells. *Traffic* 7(9):1270–1282

Eyers PA, van I d, Quinlan RA, Goedert M, Cohen P (1999) Use of a drug-resistant mutant of stress-activated protein kinase 2a/p38 to validate the in vivo specificity of SB 203580. *FEBS Lett* 451(2):191–196

Fabbri E, Brighenti L, Ottolenghi C (1991) Inhibition of adenylate cyclase of catfish and rat hepatocyte membranes by 9-(tetrahydro-2-furyl)adenine (SQ 22536). *J Enzyme Inhib* 5(2):87–98

Faucher C, Capdevielle J, Canal I, Ferrara P, Mazarguil H, McGuire WL, Darbon JM (1993) The 28-kDa protein whose phosphorylation is induced by protein kinase C activators in MCF-7 cells belongs to the family of low molecular mass heat shock proteins and is the estrogen-regulated 24-kDa protein. *J Biol Chem* 268(20):15168–15173

Feng D, Nagy JA, Hipp J, Dvorak HF, Dvorak AM (1996) Vesiculo-vacuolar organelles and the regulation of venule permeability to macromolecules by vascular permeability factor, histamine, and serotonin. *J Exp Med* 183(5):1981–1986

Feng D, Nagy JA, Dvorak HF, Dvorak AM (2002) Ultrastructural studies define soluble macromolecular, particulate, and cellular transendothelial cell pathways in venules, lymphatic vessels, and tumor-associated microvessels in man and animals. *Microsc Res Tech* 57(5):289–326

Ferns G, Shams S, Shafi S (2006) Heat shock protein 27: its potential role in vascular disease. *Int J Exp Pathol* 87(4):253–274

Ferrara N, Henzel WJ (1989) Pituitary follicular cells secrete a novel heparin-binding growth factor specific for vascular endothelial cells. *Biochem Biophys Res Commun* 161(2):851–858

Ferrara N, Winer J, Burton T, Rowland A, Siegel M, Phillips HS, Terrell T, Keller GA, Levinson AD (1993) Expression of vascular endothelial growth factor does not promote transformation but confers a growth advantage in vivo to Chinese hamster ovary cells. *J Clin Invest* 91(1):160–170

Ferrara N, Carver-Moore K, Chen H, Dowd M, Lu L, O'Shea KS, Powell-Braxton L, Hillan KJ, Moore MW (1996) Heterozygous embryonic lethality induced by targeted inactivation of the VEGF gene. *Nature* 380(6573):439–442

Ferrara N, Chen H, vis Smyth T, Gerber HP, Nguyen TN, Peers D, Chisholm V, Hillan KJ, Schwall RH (1998) Vascular endothelial growth factor is essential for corpus luteum angiogenesis. *Nat Med* 4(3):336–340

Ficarro SB, McCleland ML, Stukenberg PT, Burke DJ, Ross MM, Shabanowitz J, Hunt DF, White FM (2002) Phosphoproteome analysis by mass spectrometry and its application to Saccharomyces cerevisiae. *Nat Biotechnol* 20(3):301–305

Fischer C, Schneider M, Carmeliet P (2006) Principles and therapeutic implications of angiogenesis, vasculogenesis and arteriogenesis. *Handb Exp Pharmacol* (176 Pt 2):157–212

Fong GH, Rossant J, Gertsenstein M, Breitman ML (1995) Role of the Flt-1 receptor tyrosine kinase in regulating the assembly of vascular endothelium. *Nature* 376(6535):66–70

Fong GH, Zhang L, Bryce DM, Peng J (1999a) Increased hemangioblast commitment, not vascular disorganization, is the primary defect in flt-1 knock-out mice. *Development* 126(13):3015–3025

Fong TA, Shawver LK, Sun L, Tang C, App H, Powell TJ, Kim YH, Schreck R, Wang X, Risau W, Ullrich A, Hirth KP, McMahon G (1999b) SU5416 is a potent and selective inhibitor of the vascular endothelial growth factor receptor (Flk-1/KDR) that inhibits tyrosine kinase catalysis, tumor vascularization, and growth of multiple tumor types. *Cancer Res* 59(1):99–106

Foo SS, Turner CJ, Adams S, Compagni A, Aubyn D, Kogata N, Lindblom P, Shani M, Zicha D, Adams RH (2006) Ephrin-B2 controls cell motility and adhesion during blood-vessel-wall assembly. *Cell* 124(1):161–173

Freshney NW, Rawlinson L, Guesdon F, Jones E, Cowley S, Hsuan J, Saklatvala J (1994) Interleukin-1 activates a novel protein kinase cascade that results in the phosphorylation of Hsp27. *Cell* 78(6):1039–1049

Fuh G, Li B, Crowley C, Cunningham B, Wells JA (1998) Requirements for binding and signaling of the kinase domain receptor for vascular endothelial growth factor. *J Biol Chem* 273(18):11197–11204

Fukazawa H, Li PM, Yamamoto C, Murakami Y, Mizuno S, Uehara Y (1991) Specific inhibition of cytoplasmic protein tyrosine kinases by herbimycin A in vitro. *Biochem Pharmacol* 42(9):1661–1671

Gaestel M (2006) MAPKAP kinases - MKs - two's company, three's a crowd. *Nat Rev Mol Cell Biol* 7(2):120–130

Gaestel M, Schroder W, Benndorf R, Lippmann C, Buchner K, Hucho F, Erdmann VA, Bielka H (1991) Identification of the phosphorylation sites of the murine small heat shock protein hsp25. *J Biol Chem* 266(22):14721–14724

Gaestel M, Gotthardt R, Muller T (1993) Structure and organisation of a murine gene encoding small heat-shock protein Hsp25. *Gene* 128(2):279–283

Gamble JR, Drew J, Trezise L, Underwood A, Parsons M, Kasminkas L, Rudge J, Yancopoulos G, Vadas MA (2000) Angiopoietin-1 is an antipermeability and anti-inflammatory agent in vitro and targets cell junctions. *Circ Res* 87(7):603–607

Gampel A, Moss L, Jones MC, Brunton V, Norman JC, Mellor H (2006) VEGF regulates the mobilization of VEGFR2/KDR from an intracellular endothelial storage compartment. *Blood* 108(8):2624–2631

Garrido C, Ottavi P, Fromentin A, Hammann A, Arrigo AP, Chauffert B, Mehlen P (1997) HSP27 as a mediator of confluence-dependent resistance to cell death induced by anticancer drugs. *Cancer Res* 57(13):2661–2667

Garrido C, Fromentin A, Bonnotte B, Favre N, Moutet M, Arrigo AP, Mehlen P, Solary E (1998) Heat shock protein 27 enhances the tumorigenicity of immunogenic rat colon carcinoma cell clones. *Cancer Res* 58(23):5495–5499

Garrido C, Bruey JM, Fromentin A, Hammann A, Arrigo AP, Solary E (1999) HSP27 inhibits cytochrome c-dependent activation of procaspase-9. *FASEB J* 13(14):2061–2070

Gelinas DS, Bernatchez PN, Rollin S, Bazan NG, Sirois MG (2002) Immediate and delayed VEGF-mediated NO synthesis in endothelial cells: role of PI3K, PKC and PLC pathways. *Br J Pharmacol* 137(7):1021–1030

Gembitsky DS, Lawlor K, Jacovina A, Yaneva M, Tempst P (2004) A prototype antibody microarray platform to monitor changes in protein tyrosine phosphorylation. *Mol Cell Proteomics* 3(11):1102–1118

Gerber HP, Dixit V, Ferrara N (1998a) Vascular endothelial growth factor induces expression of the antiapoptotic proteins Bcl-2 and A1 in vascular endothelial cells. *J Biol Chem* 273(21):13313–13316

Gerber HP, McMurtrey A, Kowalski J, Yan M, Keyt BA, Dixit V, Ferrara N (1998b) Vascular endothelial growth factor regulates endothelial cell survival through the phosphatidylinositol 3'-kinase/Akt signal transduction pathway. Requirement for Flk-1/KDR activation. *J Biol Chem* 273(46):30336–30343

Gerety SS, Anderson DJ (2002) Cardiovascular ephrinB2 function is essential for embryonic angiogenesis. *Development* 129(6):1397–1410

Gerety SS, Wang HU, Chen ZF, Anderson DJ (1999) Symmetrical mutant phenotypes of the receptor EphB4 and its specific transmembrane ligand ephrin-B2 in cardiovascular development. *Mol Cell* 4(3):403–414

Gerhardt H, Golding M, Fruttiger M, Ruhrberg C, Lundkvist A, Abramsson A, Jeltsch M, Mitchell C, Alitalo K, Shima D, Betsholtz C (2003) VEGF guides angiogenic sprouting utilizing endothelial tip cell filopodia. *J Cell Biol* 161(6):1163–1177

Gernold M, Knauf U, Gaestel M, Stahl J, Kloetzel PM (1993) Development and tissue-specific distribution of mouse small heat shock protein hsp25. *Dev Genet* 14(2):103–111

Gewirtz AM (2007) On future's doorstep: RNA interference and the pharmacopeia of tomorrow. *J Clin Invest* 117(12):3612–3614

Gille H, Kowalski J, Li B, LeCouter J, Moffat B, Zioncheck TF, Pelletier N, Ferrara N (2001) Analysis of biological effects and signaling properties of Flt-1 (VEGFR-1) and KDR (VEGFR-2). A reassessment using novel receptor-specific vascular endothelial growth factor mutants. *J Biol Chem* 276(5):3222–3230

Gliki G, Abu-Ghazaleh R, Jezequel S, Wheeler-Jones C, Zachary I (2001) Vascular endothelial growth factor-induced prostacyclin production is mediated by a protein kinase C (PKC)-dependent activation of extracellular signal-regulated protein kinases 1 and 2 involving PKC-delta and by mobilization of intracellular Ca2+. *Biochem J* 353(Pt 3):503–512

Gluzman-Poltorak Z, Cohen T, Herzog Y, Neufeld G (2000) Neuropilin-2 is a receptor for the vascular endothelial growth factor (VEGF) forms VEGF-145 and VEGF-165 [corrected]. *J Biol Chem* 275(24):18040–18045

Goedert M, Cuenda A, Craxton M, Jakes R, Cohen P (1997) Activation of the novel stress-activated protein kinase SAPK4 by cytokines and cellular stresses is mediated by SKK3 (MKK6); comparison of its substrate specificity with that of other SAP kinases. *EMBO J* 16(12):3563–3571

Goligorsky MS, Abedi H, Noiri E, Takhtajan A, Lense S, Romanov V, Zachary I (1999) Nitric oxide modulation of focal adhesions in endothelial cells. *Am J Physiol* 276(6 Pt 1):C1271–C1281

Gordon JA (1991) Use of vanadate as protein-phosphotyrosine phosphatase inhibitor. *Methods Enzymol* 201:477–482

Gragoudas ES, Adamis AP, Cunningham J E T, Feinsod M, Guyer DR (2004) Pegaptanib for neovascular age-related macular degeneration. *N Engl J Med* 351(27):2805–2816

Graham FL, Smiley J, Russell WC, Nairn R (1977) Characteristics of a human cell line transformed by DNA from human adenovirus type 5. *J Gen Virol* 36(1):59–74

Gratton JP, Bernatchez P, Sessa WC (2004) Caveolae and caveolins in the cardiovascular system. *Circ Res* 94(11):1408–1417

Graupera M, Guillermet-Guibert J, Foukas LC, Phng LK, Cain RJ, Salpekar A, Pearce W, Meek S, Millan J, Cutillas PR, Smith AJ, Ridley AJ, Ruhrberg C, Gerhardt H, Vanhaesebroeck B (2008) Angiogenesis selectively requires the p110alpha isoform of PI3K to control endothelial cell migration. *Nature* 453(7195):662–666

Green DR (2005) Apoptotic pathways: ten minutes to dead. *Cell* 121(5):671–674

Green JB, Young JP (2008) Slipins: ancient origin, duplication and diversification of the stomatin protein family. *BMC Evol Biol* 8:44

Greenbaum D, Colangelo C, Williams K, Gerstein M (2003) Comparing protein abundance and mRNA expression levels on a genomic scale. *Genome Biol* 4(9):117

Gschwendt M, Dieterich S, Rennecke J, Kittstein W, Mueller HJ, Johannes FJ (1996) Inhibition of protein kinase C mu by various inhibitors. Differentiation from protein kinase c isoenzymes. *FEBS Lett* 392(2):77–80

Gu C, Rodriguez ER, Reimert DV, Shu T, Fritzsch B, Richards LJ, Kolodkin AL, Ginty DD (2003) Neuropilin-1 conveys semaphorin and VEGF signaling during neural and cardiovascular development. *Dev Cell* 5(1):45–57

Guay J, Lambert H, Gingras-Breton G, Lavoie JN, Huot J, Landry J (1997) Regulation of actin filament dynamics by p38 map kinase-mediated phosphorylation of heat shock protein 27. *J Cell Sci* 110 (Pt 3):357–368

Guo D, Jia Q, Song HY, Warren RS, Donner DB (1995) Vascular endothelial cell growth factor promotes tyrosine phosphorylation of mediators of signal transduction that contain SH2 domains. Association with endothelial cell proliferation. *J Biol Chem* 270(12):6729–6733

Gygi SP, Rist B, Gerber SA, Turecek F, Gelb MH, Aebersold R (1999a) Quantitative analysis of complex protein mixtures using isotope-coded affinity tags. *Nat Biotechnol* 17(10):994–999

Gygi SP, Rochon Y, Franza BR, Aebersold R (1999b) Correlation between protein and mRNA abundance in yeast. *Mol Cell Biol* 19(3):1720–1730

Gygi SP, Corthals GL, Zhang Y, Rochon Y, Aebersold R (2000) Evaluation of two-dimensional gel electrophoresis-based proteome analysis technology. *Proc Natl Acad Sci U S A* 97(17):9390–9395

Ha CH, Jhun BS, Kao HY, Jin ZG (2008a) VEGF stimulates HDAC7 phosphorylation and cytoplasmic accumulation modulating matrix metalloproteinase expression and angiogenesis. *Arterioscler Thromb Vasc Biol* 28(10):1782–1788

Ha CH, Wang W, Jhun BS, Wong C, Hausser A, Pfizenmaier K, McKinsey TA, Olson EN, Jin ZG (2008b) Protein kinase D-dependent phosphorylation and nuclear export of histone deacetylase 5 mediates vascular endothelial growth factor-induced gene expression and angiogenesis. *J Biol Chem* 283(21):14590–14599

Hajek P, Chomyn A, Attardi G (2007) Identification of a novel mitochondrial complex containing mitofusin 2 and stomatin-like protein 2. *J Biol Chem* 282(8):5670–5681

Hallmann R, Horn N, Selg M, Wendler O, Pausch F, Sorokin LM (2005) Expression and function of laminins in the embryonic and mature vasculature. *Physiol Rev* 85(3):979–1000

Hamdollah Zadeh MA, Glass CA, Magnussen A, Hancox JC, Bates DO (2008) VEGF-mediated elevated intracellular calcium and angiogenesis in human microvascular endothelial cells in vitro are inhibited by dominant negative TRPC6. *Microcirculation* 15(7):605–614

Han J, Lee JD, Bibbs L, Ulevitch RJ (1994) A MAP kinase targeted by endotoxin and hyperosmolarity in mammalian cells. *Science* 265(5173):808–811

Hanke JH, Gardner JP, Dow RL, Changelian PS, Brissette WH, Weringer EJ, Pollok BA, Connelly PA (1996) Discovery of a novel, potent, and Src family-selective tyrosine kinase inhibitor. Study of Lck- and FynT-dependent T cell activation. *J Biol Chem* 271(2):695–701

Hao Q, Wang L, Tang H (2009a) Vascular endothelial growth factor induces protein kinase D-dependent production of proinflammatory cytokines in endothelial cells. *Am J Physiol Cell Physiol* 296(4):C821–C827

Hao Q, Wang L, Zhao ZJ, Tang H (2009b) Identification of protein kinase d2 as a pivotal regulator of endothelial cell proliferation, migration, and angiogenesis. *J Biol Chem* 284(2):799–806

Harper SJ, Bates DO (2008) VEGF-A splicing: the key to anti-angiogenic therapeutics? *Nat Rev Cancer* 8(11):880–887

Harrington EO, Loffler J, Nelson PR, Kent KC, Simons M, Ware JA (1997) Enhancement of migration by protein kinase Calpha and inhibition of proliferation and cell cycle progression by protein kinase Cdelta in capillary endothelial cells. *J Biol Chem* 272(11):7390–7397

Haslbeck M, Ignatiou A, Saibil H, Helmich S, Frenzl E, Stromer T, Buchner J (2004) A domain in the N-terminal part of Hsp26 is essential for chaperone function and oligomerization. *J Mol Biol* 343(2):445–455

Haslbeck M, Franzmann T, Weinfurtner D, Buchner J (2005) Some like it hot: the structure and function of small heat-shock proteins. *Nat Struct Mol Biol* 12(10):842–846

Hastie LE, Patton WF, Hechtman HB, Shepro D (1997) H2O2-induced filamin redistribution in endothelial cells is modulated by the cyclic AMP-dependent protein kinase pathway. *J Cell Physiol* 172(3):373–381

Havasi A, Li Z, Wang Z, Martin JL, Botla V, Ruchalski K, Schwartz JH, Borkan SC (2008) Hsp27 inhibits Bax activation and apoptosis via a phosphatidylinositol 3-kinase-dependent mechanism. *J Biol Chem* 283(18):12305–12313

Hayashi A, Seki N, Hattori A, Kozuma S, Saito T (1999) PKCnu, a new member of the protein kinase C family, composes a fourth subfamily with PKCmu. *Biochim Biophys Acta* 1450(1):99–106

Hayden MS, Ghosh S (2008) Shared principles in NF-kappaB signaling. *Cell* 132(3):344–362

He H, Venema VJ, Gu X, Venema RC, Marrero MB, Caldwell RB (1999) Vascular endothelial growth factor signals endothelial cell production of nitric oxide and prostacyclin through flk-1/KDR activation of c-Src. *J Biol Chem* 274(35):25130–25135

Hedges JC, Dechert MA, Yamboliev IA, Martin JL, Hickey E, Weber LA, Gerthoffer WT (1999) A role for p38(MAPK)/HSP27 pathway in smooth muscle cell migration. *J Biol Chem* 274(34):24211–24219

Hellstrom M, Kalen M, Lindahl P, Abramsson A, Betsholtz C (1999) Role of PDGF-B and PDGFR-beta in recruitment of vascular smooth muscle cells and pericytes during embryonic blood vessel formation in the mouse. *Development* 126(14):3047–3055

Hellstrom M, Phng LK, Hofmann JJ, Wallgard E, Coultas L, Lindblom P, Alva J, Nilsson AK, Karlsson L, Gaiano N, Yoon K, Rossant J, Iruela-Arispe ML, Kalen M, Gerhardt H, Betsholtz C (2007) Dll4 signalling through Notch1 regulates formation of tip cells during angiogenesis. *Nature* 445(7129):776–780

Henikoff S, Henikoff JG (1992) Amino acid substitution matrices from protein blocks. *Proc Natl Acad Sci U S A* 89(22):10915–10919

Herzog Y, Guttmann-Raviv N, Neufeld G (2005) Segregation of arterial and venous markers in subpopulations of blood islands before vessel formation. *Dev Dyn* 232(4):1047–1055

Hickey E, Brandon SE, Potter R, Stein G, Stein J, Weber LA (1986) Sequence and organization of genes encoding the human 27 kDa heat shock protein. *Nucleic Acids Res* 14(10):4127–4145

Hiratsuka S, Minowa O, Kuno J, Noda T, Shibuya M (1998) Flt-1 lacking the tyrosine kinase domain is sufficient for normal development and angiogenesis in mice. *Proc Natl Acad Sci U S A* 95(16):9349–9354

Hiratsuka S, Maru Y, Okada A, Seiki M, Noda T, Shibuya M (2001) Involvement of Flt-1 tyrosine kinase (vascular endothelial growth factor receptor-1) in pathological angiogenesis. *Cancer Res* 61(3):1207–1213

Hiratsuka S, Nakao K, Nakamura K, Katsuki M, Maru Y, Shibuya M (2005) Membrane fixation of vascular endothelial growth factor receptor 1 ligand-binding domain is important for vasculogenesis and angiogenesis in mice. *Mol Cell Biol* 25(1):346–354

Hollander JM, Martin JL, Belke DD, Scott BT, Swanson E, Krishnamoorthy V, Dillmann WH (2004) Overexpression of wild-type heat shock protein 27 and a nonphosphorylatable heat shock protein 27 mutant protects against ischemia/reperfusion injury in a transgenic mouse model. *Circulation* 110(23):3544–3552

Holmes DI, Zachary I (2005) The vascular endothelial growth factor (VEGF) family: angiogenic factors in health and disease. *Genome Biol* 6(2):209

Holmqvist K, Cross MJ, Rolny C, Hagerkvist R, Rahimi N, Matsumoto T, Claesson-Welsh L, Welsh M (2004) The adaptor protein shb binds to tyrosine 1175 in vascular endothelial growth factor (VEGF) receptor-2 and regulates VEGF-dependent cellular migration. *J Biol Chem* 279(21):22267–22275

Houck KA, Ferrara N, Winer J, Cachianes G, Li B, Leung DW (1991) The vascular endothelial growth factor family: identification of a fourth molecular species and characterization of alternative splicing of RNA. *Mol Endocrinol* 5(12):1806–1814

Houck KA, Leung DW, Rowland AM, Winer J, Ferrara N (1992) Dual regulation of vascular endothelial growth factor bioavailability by genetic and proteolytic mechanisms. *J Biol Chem* 267(36):26031–26037

Houlden H, Laura M, Wavrant-De VF, Blake J, Wood N, Reilly MM (2008) Mutations in the HSP27 (HSPB1) gene cause dominant, recessive, and sporadic distal HMN/CMT type 2. *Neurology* 71(21):1660–1668

Huang L, Min JN, Masters S, Mivechi NF, Moskophidis D (2007) Insights into function and regulation of small heat shock protein 25 (HSPB1) in a mouse model with targeted gene disruption. *Genesis* 45(8):487–501

Huang M, Gu G, Ferguson EL, Chalfie M (1995) A stomatin-like protein necessary for mechanosensation in C. elegans. *Nature* 378(6554):292–295

Huber TB, Schermer B, Muller RU, Hohne M, Bartram M, Calixto A, Hagmann H, Reinhardt C, Koos F, Kunzelmann K, Shirokova E, Krautwurst D, Harteneck C, Simons M, Pavenstadt H, Kerjaschki D, Thiele C, Walz G, Chalfie M, Benzing T (2006) Podocin and MEC-2 bind cholesterol to regulate the activity of associated ion channels. *Proc Natl Acad Sci U S A* 103(46):17079–17086

Huot J, Houle F, Spitz DR, Landry J (1996) HSP27 phosphorylation-mediated resistance against actin fragmentation and cell death induced by oxidative stress. *Cancer Res* 56(2):273–279

Huot J, Houle F, Marceau F, Landry J (1997) Oxidative stress-induced actin reorganization mediated by the p38 mitogen-activated protein kinase/heat shock protein 27 pathway in vascular endothelial cells. *Circ Res* 80(3):383–392

Hurwitz H, Fehrenbacher L, Novotny W, Cartwright T, Hainsworth J, Heim W, Berlin J, Baron A, Griffing S, Holmgren E, Ferrara N, Fyfe G, Rogers B, Ross R, Kabbinavar F (2004) Bevacizumab plus irinotecan, fluorouracil, and leucovorin for metastatic colorectal cancer. *N Engl J Med* 350(23):2335–2342

Ichijo H, Nishida E, Irie K, ten DP, Saitoh M, Moriguchi T, Takagi M, Matsumoto K, Miyazono K, Gotoh Y (1997) Induction of apoptosis by ASK1, a mammalian MAPKKK that activates SAPK/JNK and p38 signaling pathways. *Science* 275(5296):90–94

Iglesias T, Waldron RT, Rozengurt E (1998) Identification of in vivo phosphorylation sites required for protein kinase D activation. *J Biol Chem* 273(42):27662–27667

Ihle JN (2000) The challenges of translating knockout phenotypes into gene function. *Cell* 102(2):131–134

Ikeda E, Achen MG, Breier G, Risau W (1995) Hypoxia-induced transcriptional activation and increased mRNA stability of vascular endothelial growth factor in C6 glioma cells. *J Biol Chem* 270(34):19761–19766

Ilan N, Mahooti S, Madri JA (1998) Distinct signal transduction pathways are utilized during the tube formation and survival phases of in vitro angiogenesis. *J Cell Sci* 111 (Pt 24):3621–3631

Ilic D, Furuta Y, Kanazawa S, Takeda N, Sobue K, Nakatsuji N, Nomura S, Fujimoto J, Okada M, Yamamoto T (1995) Reduced cell motility and enhanced focal adhesion contact formation in cells from FAK-deficient mice. *Nature* 377(6549):539–544

Issandou M, Rozengurt E (1989) Diacylglycerols, unlike phorbol esters, do not induce homologous desensitization or down-regulation of protein kinase C in Swiss 3T3 cells. *Biochem Biophys Res Commun* 163(1):201–208

Ito N, Wernstedt C, Engstrom U, Claesson-Welsh L (1998) Identification of vascular endothelial growth factor receptor-1 tyrosine phosphorylation sites and binding of SH2 domain-containing molecules. *J Biol Chem* 273(36):23410–23418

Jain RK, Duda DG, Clark JW, Loeffler JS (2006) Lessons from phase III clinical trials on anti-VEGF therapy for cancer. *Nat Clin Pract Oncol* 3(1):24–40

Jakob U, Gaestel M, Engel K, Buchner J (1993) Small heat shock proteins are molecular chaperones. *J Biol Chem* 268(3):1517–1520

Jeltsch M, Kaipainen A, Joukov V, Meng X, Lakso M, Rauvala H, Swartz M, Fukumura D, Jain RK, Alitalo K (1997) Hyperplasia of lymphatic vessels in VEGF-C transgenic mice. *Science* 276(5317):1423–1425

Jia H, Jezequel S, Lohr M, Shaikh S, Davis D, Soker S, Selwood D, Zachary I (2001a) Peptides encoded by exon 6 of VEGF inhibit endothelial cell biological responses and angiogenesis induced by VEGF. *Biochem Biophys Res Commun* 283(1):164–173

Jia H, Bagherzadeh A, Bicknell R, Duchen MR, Liu D, Zachary I (2004) Vascular endothelial growth factor (VEGF)-D and VEGF-A differentially regulate KDR-mediated signaling and biological function in vascular endothelial cells. *J Biol Chem* 279(34):36148–36157

Jia Y, Ransom RF, Shibanuma M, Liu C, Welsh MJ, Smoyer WE (2001b) Identification and characterization of hic-5/ARA55 as an hsp27 binding protein. *J Biol Chem* 276(43):39911–39918

Jo N, Mailhos C, Ju M, Cheung E, Bradley J, Nishijima K, Robinson GS, Adamis AP, Shima DT (2006) Inhibition of platelet-derived growth factor B signaling enhances the efficacy of anti-vascular endothelial growth factor therapy in multiple models of ocular neovascularization. *Am J Pathol* 168(6):2036–2053

Johannes FJ, Prestle J, Eis S, Oberhagemann P, Pfizenmaier K (1994) PKCu is a novel, atypical member of the protein kinase C family. *J Biol Chem* 269(8):6140–6148

Johannes FJ, Prestle J, Dieterich S, Oberhagemann P, Link G, Pfizenmaier K (1995) Characterization of activators and inhibitors of protein kinase C mu. *Eur J Biochem* 227(1-2):303–307

John JP, Anrather D, Pollak A, Lubec G (2006) Mass spectrometrical verification of stomatin-like protein 2 (SLP-2) primary structure. *Proteins* 64(2):543–551

Joukov V, Pajusola K, Kaipainen A, Chilov D, Lahtinen I, Kukk E, Saksela O, Kalkkinen N, Alitalo K (1996) A novel vascular endothelial growth factor, VEGF-C, is a ligand for the Flt4 (VEGFR-3) and KDR (VEGFR-2) receptor tyrosine kinases. *EMBO J* 15(2):290–298

Joukov V, Sorsa T, Kumar V, Jeltsch M, Claesson-Welsh L, Cao Y, Saksela O, Kalkkinen N, Alitalo K (1997) Proteolytic processing regulates receptor specificity and activity of VEGF-C. *EMBO J* 16(13):3898–3911

Kabakov AE, Budagova KR, Bryantsev AL, Latchman DS (2003) Heat shock protein 70 or heat shock protein 27 overexpressed in human endothelial cells during posthypoxic reoxygenation can protect from delayed apoptosis. *Cell Stress Chaperones* 8(4):335–347

Kabakov AE, Budagova KR, Malyutina YV, Latchman DS, Csermely P (2004) Pharmacological attenuation of apoptosis in reoxygenated endothelial cells. *Cell Mol Life Sci* 61(24):3076–3086

Kaelin WG, Ratcliffe PJ (2008) Oxygen sensing by metazoans: the central role of the HIF hydroxylase pathway. *Mol Cell* 30(4):393–402

Kaipainen A, Korhonen J, Mustonen T, van V H, Fang GH, Dumont D, Breitman M, Alitalo K (1995) Expression of the fms-like tyrosine kinase 4 gene becomes restricted to lymphatic endothelium during development. *Proc Natl Acad Sci U S A* 92(8):3566–3570

Kamata H, Honda S, Maeda S, Chang L, Hirata H, Karin M (2005) Reactive oxygen species promote TNFalpha-induced death and sustained JNK activation by inhibiting MAP kinase phosphatases. *Cell* 120(5):649–661

Kamba T, McDonald DM (2007) Mechanisms of adverse effects of anti-VEGF therapy for cancer. *Br J Cancer* 96(12):1788–1795

Karkkainen MJ, Haiko P, Sainio K, Partanen J, Taipale J, Petrova TV, Jeltsch M, Jackson DG, Talikka M, Rauvala H, Betsholtz C, Alitalo K (2004) Vascular endothelial growth factor C is required for sprouting of the first lymphatic vessels from embryonic veins. *Nat Immunol* 5(1):74–80

Kato K, Goto S, Hasegawa K, Shinohara H, Inaguma Y (1993) Responses to heat shock of alpha B crystallin and HSP28 in U373 MG human glioma cells. *Biochim Biophys Acta* 1175(3):257–262

Kato K, Hasegawa K, Goto S, Inaguma Y (1994) Dissociation as a result of phosphorylation of an aggregated form of the small stress protein, hsp27. *J Biol Chem* 269(15):11274–11278

Kawamura H, Li X, Harper SJ, Bates DO, Claesson-Welsh L (2008) Vascular endothelial growth factor (VEGF)-A165b is a weak in vitro agonist for VEGF receptor-2 due to lack of coreceptor binding and deficient regulation of kinase activity. *Cancer Res* 68(12):4683–4692

Kawasaki T, Kitsukawa T, Bekku Y, Matsuda Y, Sanbo M, Yagi T, Fujisawa H (1999) A requirement for neuropilin-1 in embryonic vessel formation. *Development* 126(21):4895–4902

Keck PJ, Hauser SD, Krivi G, Sanzo K, Warren T, Feder J, Connolly DT (1989) Vascular permeability factor, an endothelial cell mitogen related to PDGF. *Science* 246(4935):1309–1312

Kendall RL, Thomas KA (1993) Inhibition of vascular endothelial cell growth factor activity by an endogenously encoded soluble receptor. *Proc Natl Acad Sci U S A* 90(22):10705–10709

Kennedy SG, Kandel ES, Cross TK, Hay N (1999) Akt/Protein kinase B inhibits cell death by preventing the release of cytochrome c from mitochondria. *Mol Cell Biol* 19(8):5800–5810

Keyt BA, Berleau LT, Nguyen HV, Chen H, Heinsohn H, Vandlen R, Ferrara N (1996) The carboxyl-terminal domain (111-165) of vascular endothelial growth factor is critical for its mitogenic potency. *J Biol Chem* 271(13):7788–7795

Kiemer AK, Weber NC, Furst R, Bildner N, Kulhanek-Heinze S, Vollmar AM (2002) Inhibition of p38 MAPK activation via induction of MKP-1: atrial natriuretic peptide reduces TNF-alpha-induced actin polymerization and endothelial permeability. *Circ Res* 90(8):874–881

Kim KJ, Li B, Winer J, Armanini M, Gillett N, Phillips HS, Ferrara N (1993) Inhibition of vascular endothelial growth factor-induced angiogenesis suppresses tumour growth in vivo. *Nature* 362(6423):841–844

Kim KK, Kim R, Kim SH (1998) Crystal structure of a small heat-shock protein. *Nature* 394(6693):595–599

Kirchhof MG, Chau LA, Lemke CD, Vardhana S, Darlington PJ, Marquez ME, Taylor R, Rizkalla K, Blanca I, Dustin ML, Madrenas J (2008) Modulation of T cell activation by stomatin-like protein 2. *J Immunol* 181(3):1927–1936

Kitsukawa T, Shimizu M, Sanbo M, Hirata T, Taniguchi M, Bekku Y, Yagi T, Fujisawa H (1997) Neuropilin-semaphorin III/D-mediated chemorepulsive signals play a crucial role in peripheral nerve projection in mice. *Neuron* 19(5):995–1005

Knauf U, Jakob U, Engel K, Buchner J, Gaestel M (1994) Stress- and mitogen-induced phosphorylation of the small heat shock protein Hsp25 by MAPKAP kinase 2 is not essential for chaperone properties and cellular thermoresistance. *EMBO J* 13(1):54–60

Korff T, Dandekar G, Pfaff D, Fuller T, Goettsch W, Morawietz H, Schaffner F, Augustin HG (2006) Endothelial ephrinB2 is controlled by microenvironmental determinants and associates context-dependently with CD31. *Arterioscler Thromb Vasc Biol* 26(3):468–474

Kostenko S, Johannessen M, Moens U (2009) PKA-induced F-actin rearrangement requires phosphorylation of Hsp27 by the MAPKAP kinase MK5. *Cell Signal* 21(5):712–718

Kotch LE, Iyer NV, Laughner E, Semenza GL (1999) Defective vascularization of HIF-1alpha-null embryos is not associated with VEGF deficiency but with mesenchymal cell death. *Dev Biol* 209(2):254–267

Kotlyarov A, Neininger A, Schubert C, Eckert R, Birchmeier C, Volk HD, Gaestel M (1999) MAPKAP kinase 2 is essential for LPS-induced TNF-alpha biosynthesis. *Nat Cell Biol* 1(2):94–97

Kotlyarov A, Yannoni Y, Fritz S, Laass K, Telliez JB, Pitman D, Lin LL, Gaestel M (2002) Distinct cellular functions of MK2. *Mol Cell Biol* 22(13):4827–4835

Kou R, SenBanerjee S, Jain MK, Michel T (2005) Differential regulation of vascular endothelial growth factor receptors (VEGFR) revealed by RNA interference: interactions of VEGFR-1 and VEGFR-2 in endothelial cell signaling. *Biochemistry* 44(45):15064–15073

Kramer RH, Bensch KG, Davison PM, Karasek MA (1984) Basal lamina formation by cultured microvascular endothelial cells. *J Cell Biol* 99(2):692–698

Krilleke D, DeErkenez A, Schubert W, Giri I, Robinson GS, Ng YS, Shima DT (2007) Molecular mapping and functional characterization of the VEGF164 heparin-binding domain. *J Biol Chem* 282(38):28045–28056

Kroll J, Waltenberger J (1997) The vascular endothelial growth factor receptor KDR activates multiple signal transduction pathways in porcine aortic endothelial cells. *J Biol Chem* 272(51):32521–32527

Kroll J, Waltenberger J (1998) VEGF-A induces expression of eNOS and iNOS in endothelial cells via VEGF receptor-2 (KDR). *Biochem Biophys Res Commun* 252(3):743–746

Kruidering M, van de Water B, Zhan Y, Baelde JJ, Heer E, Mulder GJ, Stevens JL, Nagelkerke JF (1998) Cisplatin effects on F-actin and matrix proteins precede renal tubular cell detachment and apoptosis in vitro. *Cell Death Differ* 5(7):601–614

Ku DD, Zaleski JK, Liu S, Brock TA (1993) Vascular endothelial growth factor induces EDRF-dependent relaxation in coronary arteries. *Am J Physiol* 265(2 Pt 2):H586–H592

Kubota Y, Kleinman HK, Martin GR, Lawley TJ (1988) Role of laminin and basement membrane in the morphological differentiation of human endothelial cells into capillary-like structures. *J Cell Biol* 107(4):1589–1598

Kuijper S, Turner CJ, Adams RH (2007) Regulation of angiogenesis by Eph-ephrin interactions. *Trends Cardiovasc Med* 17(5):145–151

Kuldo JM, Westra J, Asgeirsdottir SA, Kok RJ, Oosterhuis K, Rots MG, Schouten JP, Limburg PC, Molema G (2005) Differential effects of NF-kappaB and p38 MAPK inhibitors and combinations thereof on TNF-alpha- and IL-1beta-induced proinflammatory status of endothelial cells in vitro. *Am J Physiol Cell Physiol* 289(5):C1229–C1239

Kumar S, McDonnell PC, Gum RJ, Hand AT, Lee JC, Young PR (1997) Novel homologues of CSBP/p38 MAP kinase: activation, substrate specificity and sensitivity to inhibition by pyridinyl imidazoles. *Biochem Biophys Res Commun* 235(3):533–538

Kumar S, Jiang MS, Adams JL, Lee JC (1999) Pyridinylimidazole compound SB 203580 inhibits the activity but not the activation of p38 mitogen-activated protein kinase. *Biochem Biophys Res Commun* 263(3):825–831

Labow M, Shuster D, Zetterstrom M, Nunes P, Terry R, Cullinan EB, Bartfai T, Solorzano C, Moldawer LL, Chizzonite R, McIntyre KW (1997) Absence of IL-1 signaling and reduced inflammatory response in IL-1 type I receptor-deficient mice. *J Immunol* 159(5):2452–2461

Lacorre DA, Baekkevold ES, Garrido I, Brandtzaeg P, Haraldsen G, Amalric F, Girard JP (2004) Plasticity of endothelial cells: rapid dedifferentiation of freshly isolated high endothelial venule endothelial cells outside the lymphoid tissue microenvironment. *Blood* 103(11):4164–4172

Laitinen M, Zachary I, Breier G, Pakkanen T, Hakkinen T, Luoma J, Abedi H, Risau W, Soma M, Laakso M, Martin JF, Yla-Herttuala S (1997) VEGF gene transfer reduces intimal thickening via increased production of nitric oxide in carotid arteries. *Hum Gene Ther* 8(15):1737–1744

Lamalice L, Houle F, Jourdan G, Huot J (2004) Phosphorylation of tyrosine 1214 on VEGFR2 is required for VEGF-induced activation of Cdc42 upstream of SAPK2/p38. *Oncogene* 23(2):434–445

Lambert H, Charette SJ, Bernier AF, Guimond A, Landry J (1999) HSP27 multimerization mediated by phosphorylation-sensitive intermolecular interactions at the amino terminus. *J Biol Chem* 274(14):9378–9385

Lamoreaux WJ, Fitzgerald ME, Reiner A, Hasty KA, Charles ST (1998) Vascular endothelial growth factor increases release of gelatinase A and decreases release of tissue inhibitor of metalloproteinases by microvascular endothelial cells in vitro. *Microvasc Res* 55(1):29–42

Lampugnani MG, Orsenigo F, Gagliani MC, Tacchetti C, Dejana E (2006) Vascular endothelial cadherin controls VEGFR-2 internalization and signaling from intracellular compartments. *J Cell Biol* 174(4):593–604

Landry J, Chretien P, Lambert H, Hickey E, Weber LA (1989) Heat shock resistance conferred by expression of the human HSP27 gene in rodent cells. *J Cell Biol* 109(1):7–15

Landry J, Lambert H, Zhou M, Lavoie JN, Hickey E, Weber LA, Anderson CW (1992) Human HSP27 is phosphorylated at serines 78 and 82 by heat shock and mitogen-activated kinases that recognize the same amino acid motif as S6 kinase II. *J Biol Chem* 267(2):794–803

Langhorst MF, Reuter A, Stuermer CA (2005) Scaffolding microdomains and beyond: the function of reggie/flotillin proteins. *Cell Mol Life Sci* 62(19-20):2228–2240

Lanneau D, Brunet M, Frisan E, Solary E, Fontenay M, Garrido C (2008) Heat shock proteins: essential proteins for apoptosis regulation. *J Cell Mol Med* 12(3):743–761

Larcher F, Murillas R, Bolontrade M, Conti CJ, Jorcano JL (1998) VEGF/VPF overexpression in skin of transgenic mice induces angiogenesis, vascular hyperpermeability and accelerated tumor development. *Oncogene* 17(3):303–311

Larkin MA, Blackshields G, Brown NP, Chenna R, McGettigan PA, McWilliam H, Valentin F, Wallace IM, Wilm A, Lopez R, Thompson JD, Gibson TJ, Higgins DG (2007) Clustal W and Clustal X version 2.0. *Bioinformatics* 23(21):2947–2948

Laroia G, Cuesta R, Brewer G, Schneider RJ (1999) Control of mRNA decay by heat shock-ubiquitin-proteasome pathway. *Science* 284(5413):499–502

Larsen MR, Thingholm TE, Jensen ON, Roepstorff P, Jorgensen TJ (2005) Highly selective enrichment of phosphorylated peptides from peptide mixtures using titanium dioxide microcolumns. *Mol Cell Proteomics* 4(7):873–886

Larsson C (2006) Protein kinase C and the regulation of the actin cytoskeleton. *Cell Signal* 18(3):276–284

Lasa M, Mahtani KR, Finch A, Brewer G, Saklatvala J, Clark AR (2000) Regulation of cyclooxygenase 2 mRNA stability by the mitogen-activated protein kinase p38 signaling cascade. *Mol Cell Biol* 20(12):4265–4274

Lavoie JN, Gingras-Breton G, Tanguay RM, Landry J (1993a) Induction of Chinese hamster HSP27 gene expression in mouse cells confers resistance to heat shock. HSP27 stabilization of the microfilament organization. *J Biol Chem* 268(5):3420–3429

Lavoie JN, Hickey E, Weber LA, Landry J (1993b) Modulation of actin microfilament dynamics and fluid phase pinocytosis by phosphorylation of heat shock protein 27. *J Biol Chem* 268(32):24210–24214

Lavoie JN, Lambert H, Hickey E, Weber LA, Landry J (1995) Modulation of cellular thermoresistance and actin filament stability accompanies phosphorylation-induced changes in the oligomeric structure of heat shock protein 27. *Mol Cell Biol* 15(1):505–516

Lawson ND, Weinstein BM (2002) In vivo imaging of embryonic vascular development using transgenic zebrafish. *Dev Biol* 248(2):307–318

Le Boeuf F, Houle F, Huot J (2004) Regulation of vascular endothelial growth factor receptor 2-mediated phosphorylation of focal adhesion kinase by heat shock protein 90 and Src kinase activities. *J Biol Chem* 279(37):39175–39185

Lee JC, Laydon JT, McDonnell PC, Gallagher TF, Kumar S, Green D, McNulty D, Blumenthal MJ, Heys JR, Landvatter SW, (1994) A protein kinase involved in the regulation of inflammatory cytokine biosynthesis. *Nature* 372(6508):739–746

Lee JW, Kwak HJ, Lee JJ, Kim YN, Lee JW, Park MJ, Jung SE, Hong SI, Lee JH, Lee JS (2008) HSP27 regulates cell adhesion and invasion via modulation of focal adhesion kinase and MMP-2 expression. *Eur J Cell Biol* 87(6):377–387

Lee S, Chen TT, Barber CL, Jordan MC, Murdock J, Desai S, Ferrara N, Nagy A, Roos KP, Iruela-Arispe ML (2007) Autocrine VEGF signaling is required for vascular homeostasis. *Cell* 130(4):691–703

Lee SH, Schloss DJ, Swain JL (2000) Maintenance of vascular integrity in the embryo requires signaling through the fibroblast growth factor receptor. *J Biol Chem* 275(43):33679–33687

Lee TY, Rosenthal A, Gotlieb AI (1996) Transition of aortic endothelial cells from resting to migrating cells is associated with three sequential patterns of microfilament organization. *J Vasc Res* 33(1):13–24

Lee YJ, Lee DH, Cho CK, Bae S, Jhon GJ, Lee SJ, Soh JW, Lee YS (2005) HSP25 inhibits protein kinase C delta-mediated cell death through direct interaction. *J Biol Chem* 280(18):18108–18119

Leitges M, Schmedt C, Guinamard R, Davoust J, Schaal S, Stabel S, Tarakhovsky A (1996) Immunodeficiency in protein kinase cbeta-deficient mice. *Science* 273(5276):788–791

Leitges M, Sanz L, Martin P, Duran A, Braun U, Garcia JF, Camacho F, az Meco MT, Rennert PD, Moscat J (2001) Targeted disruption of the zetaPKC gene results in the impairment of the NF-kappaB pathway. *Mol Cell* 8(4):771–780

Leslie JD, Ariza-McNaughton L, Bermange AL, McAdow R, Johnson SL, Lewis J (2007) Endothelial signalling by the Notch ligand Delta-like 4 restricts angiogenesis. *Development* 134(5):839–844

Leung DW, Cachianes G, Kuang WJ, Goeddel DV, Ferrara N (1989) Vascular endothelial growth factor is a secreted angiogenic mitogen. *Science* 246(4935):1306–1309

Ley K, Reutershan J (2006) Leucocyte-endothelial interactions in health and disease. *Handb Exp Pharmacol* (176 Pt 2):97–133

Li B, Ogasawara AK, Yang R, Wei W, He GW, Zioncheck TF, Bunting S, de Vos AM, Jin H (2002) KDR (VEGF receptor 2) is the major mediator for the hypotensive effect of VEGF. *Hypertension* 39(6):1095–1100

Li S, Piotrowicz RS, Levin EG, Shyy YJ, Chien S (1996) Fluid shear stress induces the phosphorylation of small heat shock proteins in vascular endothelial cells. *Am J Physiol* 271(3 Pt 1):C994–1000

Liberek K, Lewandowska A, Zietkiewicz S (2008) Chaperones in control of protein disaggregation. *EMBO J* 27(2):328–335

Liem DA, Honda HM, Zhang J, Woo D, Ping P (2007) Past and present course of cardioprotection against ischemia-reperfusion injury. *J Appl Physiol* 103(6):2129–2136

Lin MT, Yen ML, Lin CY, Kuo ML (2003) Inhibition of vascular endothelial growth factor-induced angiogenesis by resveratrol through interruption of Src-dependent vascular endothelial cadherin tyrosine phosphorylation. *Mol Pharmacol* 64(5):1029–1036

Lin Y, Weisdorf DJ, Solovey A, Hebbel RP (2000) Origins of circulating endothelial cells and endothelial outgrowth from blood. *J Clin Invest* 105(1):71–77

Link AJ, Eng J, Schieltz DM, Carmack E, Mize GJ, Morris DR, Garvik BM, Yates I J R (1999) Direct analysis of protein complexes using mass spectrometry. *Nat Biotechnol* 17(7):676–682

Liu D, Jia H, Holmes DI, Stannard A, Zachary I (2003) Vascular endothelial growth factor-regulated gene expression in endothelial cells: KDR-mediated induction of Egr3 and the related nuclear receptors Nur77, Nurr1, and Nor1. *Arterioscler Thromb Vasc Biol* 23(11):2002–2007

Liu D, Evans I, Britton G, Zachary I (2008) The zinc-finger transcription factor, early growth response 3, mediates VEGF-induced angiogenesis. *Oncogene* 27(21):2989–2998

Liu P, Scharenberg AM, Cantrell DA, Matthews SA (2007) Protein kinase D enzymes are dispensable for proliferation, survival and antigen receptor-regulated NFkappaB activity in vertebrate B-cells. *FEBS Lett* 581(7):1377–1382

Loktionova SA, Ilyinskaya OP, Gabai VL, Kabakov AE (1996) Distinct effects of heat shock and ATP depletion on distribution and isoform patterns of human Hsp27 in endothelial cells. *FEBS Lett* 392(2):100–104

Lopez MF, Berggren K, Chernokalskaya E, Lazarev A, Robinson M, Patton WF (2000) A comparison of silver stain and SYPRO Ruby Protein Gel Stain with respect to protein detection in two-dimensional gels and identification by peptide mass profiling. *Electrophoresis* 21(17):3673–3683

Machida K, Mayer BJ (2005) The SH2 domain: versatile signaling module and pharmaceutical target. *Biochim Biophys Acta* 1747(1):1–25

Mackay F, Loetscher H, Stueber D, Gehr G, Lesslauer W (1993) Tumor necrosis factor alpha (TNF-alpha)-induced cell adhesion to human endothelial cells is under dominant control of one TNF receptor type, TNF-R55. *J Exp Med* 177(5):1277–1286

Madge LA, Pober JS (2001) TNF signaling in vascular endothelial cells. *Exp Mol Pathol* 70(3):317–325

Maes C, Carmeliet P, Moermans K, Stockmans I, Smets N, Collen D, Bouillon R, Carmeliet G (2002) Impaired angiogenesis and endochondral bone formation in mice lacking the vascular endothelial growth factor isoforms VEGF164 and VEGF188. *Mech Dev* 111(1-2):61–73

Maes C, Stockmans I, Moermans K, Van LR, Smets N, Carmeliet P, Bouillon R, Carmeliet G (2004) Soluble VEGF isoforms are essential for establishing epiphyseal vascularization and regulating chondrocyte development and survival. *J Clin Invest* 113(2):188–199

Maglione D, Guerriero V, Viglietto G, li Bovi P, Persico MG (1991) Isolation of a human placenta cDNA coding for a protein related to the vascular permeability factor. *Proc Natl Acad Sci U S A* 88(20):9267–9271

Maharaj AS, D'Amore PA (2007) Roles for VEGF in the adult. *Microvasc Res* 74(2-3):100–113

Maisonpierre PC, Suri C, Jones PF, Bartunkova S, Wiegand SJ, Radziejewski C, Compton D, McClain J, Aldrich TH, Papadopoulos N, Daly TJ, Davis S, Sato TN, Yancopoulos GD (1997) Angiopoietin-2, a natural antagonist for Tie2 that disrupts in vivo angiogenesis. *Science* 277(5322):55–60

Maizels ET, Peters CA, Kline M, Cutler J R E, Shanmugam M, Hunzicker-Dunn M (1998) Heat-shock protein-25/27 phosphorylation by the delta isoform of protein kinase C. *Biochem J* 332 (Pt 3):703–712

Makinen T, Jussila L, Veikkola T, Karpanen T, Kettunen MI, Pulkkanen KJ, Kauppinen R, Jackson DG, Kubo H, Nishikawa S, Yla-Herttuala S, Alitalo K (2001) Inhibition of lymphangiogenesis with resulting lymphedema in transgenic mice expressing soluble VEGF receptor-3. *Nat Med* 7(2):199–205

Makinen T, Norrmen C, Petrova TV (2007) Molecular mechanisms of lymphatic vascular development. *Cell Mol Life Sci* 64(15):1915–1929

Marchler-Bauer A, Anderson JB, Derbyshire MK, Weese-Scott C, Gonzales NR, Gwadz M, Hao L, He S, Hurwitz DI, Jackson JD, Ke Z, Krylov D, Lanczycki CJ, Liebert CA, Liu C, Lu F, Lu S, Marchler GH, Mullokandov M, Song JS, Thanki N, Yamashita RA, Yin JJ, Zhang D, Bryant SH (2007) CDD: a conserved domain database for interactive domain family analysis. *Nucleic Acids Res* 35(Database issue):D237–D240

Marconcini L, Marchio S, Morbidelli L, Cartocci E, Albini A, Ziche M, Bussolino F, Oliviero S (1999) c-fos-induced growth factor/vascular endothelial growth factor D induces angiogenesis in vivo and in vitro. *Proc Natl Acad Sci U S A* 96(17):9671–9676

Marino MW, Dunn A, Grail D, Inglese M, Noguchi Y, Richards E, Jungbluth A, Wada H, Moore M, Williamson B, Basu S, Old LJ (1997) Characterization of tumor necrosis factor-deficient mice. *Proc Natl Acad Sci U S A* 94(15):8093–8098

Martin JL, Mestril R, Hilal-Dandan R, Brunton LL, Dillmann WH (1997) Small heat shock proteins and protection against ischemic injury in cardiac myocytes. *Circulation* 96(12):4343–4348

Martin JL, Hickey E, Weber LA, Dillmann WH, Mestril R (1999) Influence of phosphorylation and oligomerization on the protective role of the small heat shock protein 27 in rat adult cardiomyocytes. *Gene Expr* 7(4-6):349–355

Martiny-Baron G, Kazanietz MG, Mischak H, Blumberg PM, Kochs G, Hug H, Marme D, Schachtele C (1993) Selective inhibition of protein kinase C isozymes by the indolocarbazole Go 6976. *J Biol Chem* 268(13):9194–9197

Matoba T, Shimokawa H, Nakashima M, Hirakawa Y, Mukai Y, Hirano K, Kanaide H, Takeshita A (2000) Hydrogen peroxide is an endothelium-derived hyperpolarizing factor in mice. *J Clin Invest* 106(12):1521–1530

Matsumoto T, Bohman S, Dixelius J, Berge T, Dimberg A, Magnusson P, Wang L, Wikner C, Qi JH, Wernstedt C, Wu J, Bruheim S, Mugishima H, Mukhopadhyay D, Spurkland A, Claesson-Welsh L (2005) VEGF receptor-2 Y951 signaling and a role for the adapter molecule TSAd in tumor angiogenesis. *EMBO J* 24(13):2342–2353

Matthews SA, Pettit GR, Rozengurt E (1997) Bryostatin 1 induces biphasic activation of protein kinase D in intact cells. *J Biol Chem* 272(32):20245–20250

Matthews SA, Rozengurt E, Cantrell D (1999) Characterization of serine 916 as an in vivo autophosphorylation site for protein kinase D/Protein kinase Cmu. *J Biol Chem* 274(37):26543–26549

Matthews SA, Liu P, Spitaler M, Olson EN, McKinsey TA, Cantrell DA, Scharenberg AM (2006) Essential role for protein kinase D family kinases in the regulation of class II histone deacetylases in B lymphocytes. *Mol Cell Biol* 26(4):1569–1577

McCollum AK, Teneyck CJ, Sauer BM, Toft DO, Erlichman C (2006) Up-regulation of heat shock protein 27 induces resistance to 17-allylamino-demethoxygeldanamycin through a glutathione-mediated mechanism. *Cancer Res* 66(22):10967–10975

McLaughlin MM, Kumar S, McDonnell PC, Van HS, Lee JC, Livi GP, Young PR (1996) Identification of mitogen-activated protein (MAP) kinase-activated protein kinase-3, a novel substrate of CSBP p38 MAP kinase. *J Biol Chem* 271(14):8488–8492

McMillan DR, Xiao X, Shao L, Graves K, Benjamin IJ (1998) Targeted disruption of heat shock transcription factor 1 abolishes thermotolerance and protection against heat-inducible apoptosis. *J Biol Chem* 273(13):7523–7528

McMullen M, Keller R, Sussman M, Pumiglia K (2004) Vascular endothelial growth factor-mediated activation of p38 is dependent upon Src and RAFTK/Pyk2. *Oncogene* 23(6):1275–1282

McMullen ME, Bryant PW, Glembotski CC, Vincent PA, Pumiglia KM (2005) Activation of p38 has opposing effects on the proliferation and migration of endothelial cells. *J Biol Chem* 280(22):20995–21003

Mechtcheriakova D, Schabbauer G, Lucerna M, Clauss M, de Martin R, Binder BR, Hofer E (2001) Specificity, diversity, and convergence in VEGF and TNF-alpha signaling events leading to tissue factor up-regulation via EGR-1 in endothelial cells. *FASEB J* 15(1):230–242

Meeson AP, Argilla M, Ko K, Witte L, Lang RA (1999) VEGF deprivation-induced apoptosis is a component of programmed capillary regression. *Development* 126(7):1407–1415

Mehlen P, Kretz-Remy C, Preville X, Arrigo AP (1996a) Human hsp27, Drosophila hsp27 and human alphaB-crystallin expression-mediated increase in glutathione is essential for the protective activity of these proteins against TNFalpha-induced cell death. *EMBO J* 15(11):2695–2706

Mehlen P, Schulze-Osthoff K, Arrigo AP (1996b) Small stress proteins as novel regulators of apoptosis. Heat shock protein 27 blocks Fas/APO-1- and staurosporine-induced cell death. *J Biol Chem* 271(28):16510–16514

Mehlen P, Hickey E, Weber LA, Arrigo AP (1997a) Large unphosphorylated aggregates as the active form of hsp27 which controls intracellular reactive oxygen species and glutathione levels and generates a protection against TNFalpha in NIH-3T3-ras cells. *Biochem Biophys Res Commun* 241(1):187–192

Mehlen P, Mehlen A, Godet J, Arrigo AP (1997b) hsp27 as a switch between differentiation and apoptosis in murine embryonic stem cells. *J Biol Chem* 272(50):31657–31665

Mehta D, Malik AB (2006) Signaling mechanisms regulating endothelial permeability. *Physiol Rev* 86(1):279–367

Mellor H, Parker PJ (1998) The extended protein kinase C superfamily. *Biochem J* 332 (Pt 2):281–292

Michel JB (2003) Anoikis in the cardiovascular system: known and unknown extracellular mediators. *Arterioscler Thromb Vasc Biol* 23(12):2146–2154

Migdal M, Huppertz B, Tessler S, Comforti A, Shibuya M, Reich R, Baumann H, Neufeld G (1998) Neuropilin-1 is a placenta growth factor-2 receptor. *J Biol Chem* 273(35):22272–22278

Millauer B, Wizigmann-Voos S, Schnurch H, Martinez R, Moller NP, Risau W, Ullrich A (1993) High affinity VEGF binding and developmental expression suggest Flk-1 as a major regulator of vasculogenesis and angiogenesis. *Cell* 72(6):835–846

Miquerol L, Langille BL, Nagy A (2000) Embryonic development is disrupted by modest increases in vascular endothelial growth factor gene expression. *Development* 127(18):3941–3946

Miron T, Wilchek M, Geiger B (1988) Characterization of an inhibitor of actin polymerization in vinculin-rich fraction of turkey gizzard smooth muscle. *Eur J Biochem* 178(2):543–553

Miron T, Vancompernolle K, Vandekerckhove J, Wilchek M, Geiger B (1991) A 25-kD inhibitor of actin polymerization is a low molecular mass heat shock protein. *J Cell Biol* 114(2):255–261

Mitra SK, Hanson DA, Schlaepfer DD (2005) Focal adhesion kinase: in command and control of cell motility. *Nat Rev Mol Cell Biol* 6(1):56–68

Mittar S, Ulyatt C, Howell GJ, Bruns AF, Zachary I, Walker JH, Ponnambalam S (2009) VEGFR1 receptor tyrosine kinase localization to the Golgi apparatus is calcium-dependent. *Exp Cell Res* 315(5):877–889

Miyamoto A, Nakayama K, Imaki H, Hirose S, Jiang Y, Abe M, Tsukiyama T, Nagahama H, Ohno S, Hatakeyama S, Nakayama KI (2002) Increased proliferation of B cells and auto-immunity in mice lacking protein kinase Cdelta. *Nature* 416(6883):865–869

Modur V, Zimmerman GA, Prescott SM, McIntyre TM (1996) Endothelial cell inflammatory responses to tumor necrosis factor alpha. Ceramide-dependent and -independent mitogen-activated protein kinase cascades. *J Biol Chem* 271(22):13094–13102

Moncada S (2006) Adventures in vascular biology: a tale of two mediators. *Philos Trans R Soc Lond B Biol Sci* 361(1469):735–759

Morbidelli L, Birkenhaeger R, Roeckl W, Granger HJ, Kaerst U, Weich HA, Ziche M (1997) Distinct capillary density and progression promoted by vascular endothelial growth factor-A homodimers and heterodimers. *Angiogenesis* 1(1):117–130

Mounier N, Arrigo AP (2002) Actin cytoskeleton and small heat shock proteins: how do they interact? *Cell Stress Chaperones* 7(2):167–176

Mukherjee S, Tessema M, Wandinger-Ness A (2006) Vesicular trafficking of tyrosine kinase receptors and associated proteins in the regulation of signaling and vascular function. *Circ Res* 98(6):743–756

Muller WA, Gimbrone MA (1986) Plasmalemmal proteins of cultured vascular endothelial cells exhibit apical-basal polarity: analysis by surface-selective iodination. *J Cell Biol* 103(6 Pt 1):2389–2402

Muller YA, Li B, Christinger HW, Wells JA, Cunningham BC, de Vos AM (1997) Vascular endothelial growth factor: crystal structure and functional mapping of the kinase domain receptor binding site. *Proc Natl Acad Sci U S A* 94(14):7192–7197

Murohara T, Horowitz JR, Silver M, Tsurumi Y, Chen D, Sullivan A, Isner JM (1998) Vascular endothelial growth factor/vascular permeability factor enhances vascular permeability via nitric oxide and prostacyclin. *Circulation* 97(1):99–107

Nawroth PP, Handley DA, Esmon CT, Stern DM (1986) Interleukin 1 induces endothelial cell procoagulant while suppressing cell-surface anticoagulant activity. *Proc Natl Acad Sci U S A* 83(10):3460–3464

Neupert W, Herrmann JM (2007) Translocation of proteins into mitochondria. *Annu Rev Biochem* 76:723–749

New L, Jiang Y, Zhao M, Liu K, Zhu W, Flood LJ, Kato Y, Parry GC, Han J (1998) PRAK, a novel protein kinase regulated by the p38 MAP kinase. *EMBO J* 17(12):3372–3384

Newton AC (2001) Protein kinase C: structural and spatial regulation by phosphorylation, cofactors, and macromolecular interactions. *Chem Rev* 101(8):2353–2364

Newton AC (2003) Regulation of the ABC kinases by phosphorylation: protein kinase C as a paradigm. *Biochem J* 370(Pt 2):361–371

Ng EW, Shima DT, Calias P, Cunningham J E T, Guyer DR, Adamis AP (2006) Pegaptanib, a targeted anti-VEGF aptamer for ocular vascular disease. *Nat Rev Drug Discov* 5(2):123–132

Nguyen A, Chen P, Cai H (2004) Role of CaMKII in hydrogen peroxide activation of ERK1/2, p38 MAPK, HSP27 and actin reorganization in endothelial cells. *FEBS Lett* 572(1-3):307–313

Nicosia RF, Nicosia SV, Smith M (1994) Vascular endothelial growth factor, platelet-derived growth factor, and insulin-like growth factor-1 promote rat aortic angiogenesis in vitro. *Am J Pathol* 145(5):1023–1029

Nielsen H, Engelbrecht J, Brunak S, von HG (1997) Identification of prokaryotic and eukaryotic signal peptides and prediction of their cleavage sites. *Protein Eng* 10(1):1–6

Nishijima K, Ng YS, Zhong L, Bradley J, Schubert W, Jo N, Akita J, Samuelsson SJ, Robinson GS, Adamis AP, Shima DT (2007) Vascular endothelial growth factor-A is a survival factor for retinal neurons and a critical neuroprotectant during the adaptive response to ischemic injury. *Am J Pathol* 171(1):53–67

Nishitoh H, Saitoh M, Mochida Y, Takeda K, Nakano H, Rothe M, Miyazono K, Ichijo H (1998) ASK1 is essential for JNK/SAPK activation by TRAF2. *Mol Cell* 2(3):389–395

Nissen NN, Polverini PJ, Koch AE, Volin MV, Gamelli RL, DiPietro LA (1998) Vascular endothelial growth factor mediates angiogenic activity during the proliferative phase of wound healing. *Am J Pathol* 152(6):1445–1452

Norrby K (1996) Vascular endothelial growth factor and de novo mammalian angiogenesis. *Microvasc Res* 51(2):153–163

Obenauer JC, Cantley LC, Yaffe MB (2003) Scansite 2.0: Proteome-wide prediction of cell signaling interactions using short sequence motifs. *Nucleic Acids Res* 31(13):3635–3641

Oda Y, Nagasu T, Chait BT (2001) Enrichment analysis of phosphorylated proteins as a tool for probing the phosphoproteome. *Nat Biotechnol* 19(4):379–382

Ogawa S, Oku A, Sawano A, Yamaguchi S, Yazaki Y, Shibuya M (1998) A novel type of vascular endothelial growth factor, VEGF-E (NZ-7 VEGF), preferentially utilizes KDR/Flk-1 receptor and carries a potent mitotic activity without heparin-binding domain. *J Biol Chem* 273(47):31273–31282

Olofsson B, Korpelainen E, Pepper MS, Mandriota SJ, Aase K, Kumar V, Gunji Y, Jeltsch MM, Shibuya M, Alitalo K, Eriksson U (1998) Vascular endothelial growth factor B (VEGF-B) binds to VEGF receptor-1 and regulates plasminogen activator activity in endothelial cells. *Proc Natl Acad Sci U S A* 95(20):11709–11714

Olsen JV, Ong SE, Mann M (2004) Trypsin cleaves exclusively C-terminal to arginine and lysine residues. *Mol Cell Proteomics* 3(6):608–614

Olsen JV, Blagoev B, Gnad F, Macek B, Kumar C, Mortensen P, Mann M (2006) Global, in vivo, and site-specific phosphorylation dynamics in signaling networks. *Cell* 127(3):635–648

Olsson AK, Dimberg A, Kreuger J, Claesson-Welsh L (2006) VEGF receptor signalling - in control of vascular function. *Nat Rev Mol Cell Biol* 7(5):359–371

Ong SE, Mann M (2005) Mass spectrometry-based proteomics turns quantitative. *Nat Chem Biol* 1(5):252–262

Ong SE, Blagoev B, Kratchmarova I, Kristensen DB, Steen H, Pandey A, Mann M (2002) Stable isotope labeling by amino acids in cell culture, SILAC, as a simple and accurate approach to expression proteomics. *Mol Cell Proteomics* 1(5):376–386

Oosthuyse B, Moons L, Storkebaum E, Beck H, Nuyens D, Brusselmans K, Van DJ, Hellings P, Gorselink M, Heymans S, Theilmeier G, Dewerchin M, Laudenbach V, Vermylen P, Raat H, Acker T, Vleminckx V, Van Den Bosch L, Cashman N, Fujisawa H, Drost MR, Sciot R, Bruyninckx F, Hicklin DJ, Ince C, Gressens P, Lupu F, Plate KH, Robberecht W, Herbert JM, Collen D, Carmeliet P (2001) Deletion of the hypoxia-response element in the vascular endothelial growth factor promoter causes motor neuron degeneration. *Nat Genet* 28(2):131–138

Owens DM, Keyse SM (2007) Differential regulation of MAP kinase signalling by dual-specificity protein phosphatases. *Oncogene* 26(22):3203–3213

Ozgen N, Obreztchikova M, Guo J, Elouardighi H, Dorn GW, Wilson BA, Steinberg SF (2008) Protein kinase D links Gq-coupled receptors to cAMP response element-binding protein (CREB)-Ser133 phosphorylation in the heart. *J Biol Chem* 283(25):17009–17019

Pages G, Pouyssegur J (2005) Transcriptional regulation of the Vascular Endothelial Growth Factor gene–a concert of activating factors. *Cardiovasc Res* 65(3):564–573

Pan Q, Chathery Y, Wu Y, Rathore N, Tong RK, Peale F, Bagri A, Tessier-Lavigne M, Koch AW, Watts RJ (2007) Neuropilin-1 binds to VEGF121 and regulates endothelial cell migration and sprouting. *J Biol Chem* 282(33):24049–24056

Pandey A, Podtelejnikov AV, Blagoev B, Bustelo XR, Mann M, Lodish HF (2000a) Analysis of receptor signaling pathways by mass spectrometry: identification of vav-2 as a substrate of the epidermal and platelet-derived growth factor receptors. *Proc Natl Acad Sci U S A* 97(1):179–184

Pandey P, Farber R, Nakazawa A, Kumar S, Bharti A, Nalin C, Weichselbaum R, Kufe D, Kharbanda S (2000b) Hsp27 functions as a negative regulator of cytochrome c-dependent activation of procaspase-3. *Oncogene* 19(16):1975–1981

Parcellier A, Schmitt E, Gurbuxani S, Seigneurin-Berny D, Pance A, Chantome A, Plenchette S, Khochbin S, Solary E, Garrido C (2003) HSP27 is a ubiquitin-binding protein involved in I-kappaBalpha proteasomal degradation. *Mol Cell Biol* 23(16):5790–5802

Pareyson D (2007) Axonal Charcot-Marie-Tooth disease: the fog is only slowly lifting. *Neurology* 68(20):1649–1650

Park JE, Keller GA, Ferrara N (1993) The vascular endothelial growth factor (VEGF) isoforms: differential deposition into the subepithelial extracellular matrix and bioactivity of extracellular matrix-bound VEGF. *Mol Biol Cell* 4(12):1317–1326

Park JE, Chen HH, Winer J, Houck KA, Ferrara N (1994) Placenta growth factor. Potentiation of vascular endothelial growth factor bioactivity, in vitro and in vivo, and high affinity binding to Flt-1 but not to Flk-1/KDR. *J Biol Chem* 269(41):25646–25654

Park SW, Chen SW, Kim M, D'Agati VD, Lee HT (2009) Human heat shock protein 27 overexpressing mice are protected against acute kidney injury after hepatic ischemia and reperfusion. *Am J Physiol Renal Physiol*

Paul C, Manero F, Gonin S, Kretz-Remy C, Virot S, Arrigo AP (2002) Hsp27 as a negative regulator of cytochrome C release. *Mol Cell Biol* 22(3):816–834

Pawlowska Z, Baranska P, Jerczynska H, Koziolkiewicz W, Cierniewski CS (2005) Heat shock proteins and other components of cellular machinery for protein synthesis are up-regulated in vascular endothelial cell growth factor-activated human endothelial cells. *Proteomics* 5(5):1217–1227

Pellet-Many C, Frankel P, Jia H, Zachary I (2008) Neuropilins: structure, function and role in disease. *Biochem J* 411(2):211–226

Pepper MS, Ferrara N, Orci L, Montesano R (1991) Vascular endothelial growth factor (VEGF) induces plasminogen activators and plasminogen activator inhibitor-1 in microvascular endothelial cells. *Biochem Biophys Res Commun* 181(2):902–906

Pepper MS, Ferrara N, Orci L, Montesano R (1992) Potent synergism between vascular endothelial growth factor and basic fibroblast growth factor in the induction of angiogenesis in vitro. *Biochem Biophys Res Commun* 189(2):824–831

Peschon JJ, Torrance DS, Stocking KL, Glaccum MB, Otten C, Willis CR, Charrier K, Morrissey PJ, Ware CB, Mohler KM (1998) TNF receptor-deficient mice reveal divergent roles for p55 and p75 in several models of inflammation. *J Immunol* 160(2):943–952

Pfeffer K, Matsuyama T, Kundig TM, Wakeham A, Kishihara K, Shahinian A, Wiegmann K, Ohashi PS, Kronke M, Mak TW (1993) Mice deficient for the 55 kd tumor necrosis factor receptor are resistant to endotoxic shock, yet succumb to L. monocytogenes infection. *Cell* 73(3):457–467

Piotrowicz RS, Weber LA, Hickey E, Levin EG (1995) Accelerated growth and senescence of arterial endothelial cells expressing the small molecular weight heat-shock protein HSP27. *FASEB J* 9(11):1079–1084

Piotrowicz RS, Hickey E, Levin EG (1998) Heat shock protein 27 kDa expression and phosphorylation regulates endothelial cell migration. *FASEB J* 12(14):1481–1490

Pober JS, Min W (2006) Endothelial cell dysfunction, injury and death. *Handb Exp Pharmacol* 176 Pt 2:135–156

Pober JS, Sessa WC (2007) Evolving functions of endothelial cells in inflammation. *Nat Rev Immunol* 7(10):803–815

Pober JS, Lapierre LA, Stolpen AH, Brock TA, Springer TA, Fiers W, Bevilacqua MP, Mendrick DL, Gimbrone MA (1987) Activation of cultured human endothelial cells by recombinant lymphotoxin: comparison with tumor necrosis factor and interleukin 1 species. *J Immunol* 138(10):3319–3324

Pocock G, Richards CD (2006) *Human Physiology: The Basis of Medicine*. Oxford University Press, Oxford, 3rd edition

Portig I, Pankuweit S, Lottspeich F, Maisch B (1996) Identification of stress proteins in endothelial cells. *Electrophoresis* 17(4):803–808

Pruitt KD, Tatusova T, Maglott DR (2007) NCBI reference sequences (RefSeq): a curated non-redundant sequence database of genomes, transcripts and proteins. *Nucleic Acids Res* 35(Database issue):D61–D65

Qin L, Zeng H, Zhao D (2006) Requirement of protein kinase D tyrosine phosphorylation for VEGF-A165-induced angiogenesis through its interaction and regulation of phospholipase Cgamma phosphorylation. *J Biol Chem* 281(43):32550–32558

Quinn TP, Peters KG, De Vries C, Ferrara N, Williams LT (1993) Fetal liver kinase 1 is a receptor for vascular endothelial growth factor and is selectively expressed in vascular endothelium. *Proc Natl Acad Sci U S A* 90(16):7533–7537

Rabilloud T, Adessi C, Giraudel A, Lunardi J (1997) Improvement of the solubilization of proteins in two-dimensional electrophoresis with immobilized pH gradients. *Electrophoresis* 18(3-4):307–316

Raingeaud J, Gupta S, Rogers JS, Dickens M, Han J, Ulevitch RJ, Davis RJ (1995) Pro-inflammatory cytokines and environmental stress cause p38 mitogen-activated protein kinase activation by dual phosphorylation on tyrosine and threonine. *J Biol Chem* 270(13):7420–7426

Raingeaud J, Whitmarsh AJ, Barrett T, Derijard B, Davis RJ (1996) MKK3- and MKK6-regulated gene expression is mediated by the p38 mitogen-activated protein kinase signal transduction pathway. *Mol Cell Biol* 16(3):1247–1255

Ramagli LS (1999) Quantifying protein in 2-D PAGE solubilization buffers. *Methods Mol Biol* 112:99–103

Ramalingam R, Rafii S, Worgall S, Brough DE, Crystal RG (1999) E1(-)E4(+) adenoviral gene transfer vectors function as a "pro-life" signal to promote survival of primary human endothelial cells. *Blood* 93(9):2936–2944

Ramalingam R, Worgall S, Rafii S, Crystal RG (2000) Downregulation of CXCR4 gene expression in primary human endothelial cells following infection with E1(-)E4(+) adenovirus gene transfer vectors. *Mol Ther* 2(4):381–386

Raman M, Chen W, Cobb MH (2007) Differential regulation and properties of MAPKs. *Oncogene* 26(22):3100–3112

Rane MJ, Coxon PY, Powell DW, Webster R, Klein JB, Pierce W, Ping P, McLeish KR (2001) p38 Kinase-dependent MAPKAPK-2 activation functions as 3-phosphoinositide-dependent kinase-2 for Akt in human neutrophils. *J Biol Chem* 276(5):3517–3523

Rane MJ, Pan Y, Singh S, Powell DW, Wu R, Cummins T, Chen Q, McLeish KR, Klein JB (2003) Heat shock protein 27 controls apoptosis by regulating Akt activation. *J Biol Chem* 278(30):27828–27835

Rask-Madsen C, King GL (2008) Differential regulation of VEGF signaling by PKC-alpha and PKC-epsilon in endothelial cells. *Arterioscler Thromb Vasc Biol* 28(5):919–924

Ratcliffe KE, Tao Q, Yavuz B, Stoletov KV, Spring SC, Terman BI (2002) Sck is expressed in endothelial cells and participates in vascular endothelial growth factor-induced signaling. *Oncogene* 21(41):6307–6316

Razandi M, Pedram A, Levin ER (2000) Estrogen signals to the preservation of endothelial cell form and function. *J Biol Chem* 275(49):38540–38546

Razani B, Engelman JA, Wang XB, Schubert W, Zhang XL, Marks CB, Macaluso F, Russell RG, Li M, Pestell RG, Di Vizio D, Hou J H, Kneitz B, Lagaud G, Christ GJ, Edelmann W, Lisanti MP (2001) Caveolin-1 null mice are viable but show evidence of hyperproliferative and vascular abnormalities. *J Biol Chem* 276(41):38121–38138

Reifschneider NH, Goto S, Nakamoto H, Takahashi R, Sugawa M, Dencher NA, Krause F (2006) Defining the mitochondrial proteomes from five rat organs in a physiologically significant context using 2D blue-native/SDS-PAGE. *J Proteome Res* 5(5):1117–1132

Rennecke J, Johannes FJ, Richter KH, Kittstein W, Marks F, Gschwendt M (1996) Immunological demonstration of protein kinase C mu in murine tissues and various cell lines. Differential recognition of phosphorylated forms and lack of down-regulation upon 12-O-tetradecanoylphorphol-13-acetate treatment of cells. *Eur J Biochem* 242(2):428–432

Ribatti D (2005) The crucial role of vascular permeability factor/vascular endothelial growth factor in angiogenesis: a historical review. *Br J Haematol* 128(3):303–309

Riccioni T, Cirielli C, Wang X, Passaniti A, Capogrossi MC (1998) Adenovirus-mediated wild-type p53 overexpression inhibits endothelial cell differentiation in vitro and angiogenesis in vivo. *Gene Ther* 5(6):747–754

Risau W, Flamme I (1995) Vasculogenesis. *Annu Rev Cell Dev Biol* 11:73–91

Rissanen TT, Markkanen JE, Gruchala M, Heikura T, Puranen A, Kettunen MI, Kholova I, Kauppinen RA, Achen MG, Stacker SA, Alitalo K, Yla-Herttuala S (2003) VEGF-D is the strongest angiogenic and lymphangiogenic effector among VEGFs delivered into skeletal muscle via adenoviruses. *Circ Res* 92(10):1098–1106

Rissanen TT, Korpisalo P, Markkanen JE, Liimatainen T, Orden MR, Kholova I, de Goede A, Heikura T, Grohn OH, Yla-Herttuala S (2005) Blood flow remodels growing vasculature during vascular endothelial growth factor gene therapy and determines between capillary arterialization and sprouting angiogenesis. *Circulation* 112(25):3937–3946

Robaye B, Hepburn A, Lecocq R, Fiers W, Boeynaems JM, Dumont JE (1989) Tumor necrosis factor-alpha induces the phosphorylation of 28kDa stress proteins in endothelial cells: possible role in protection against cytotoxicity? *Biochem Biophys Res Commun* 163(1):301–308

Roberts WG, Palade GE (1995) Increased microvascular permeability and endothelial fenestration induced by vascular endothelial growth factor. *J Cell Sci* 108 (Pt 6):2369–2379

Robinson CJ, Stringer SE (2001) The splice variants of vascular endothelial growth factor (VEGF) and their receptors. *J Cell Sci* 114(Pt 5):853–865

Roca C, Adams RH (2007) Regulation of vascular morphogenesis by Notch signaling. *Genes Dev* 21(20):2511–2524

Rodriguez-Pena A, Rozengurt E (1984) Disappearance of Ca2+-sensitive, phospholipid-dependent protein kinase activity in phorbol ester-treated 3T3 cells. *Biochem Biophys Res Commun* 120(3):1053–1059

Rogalla T, Ehrnsperger M, Preville X, Kotlyarov A, Lutsch G, Ducasse C, Paul C, Wieske M, Arrigo AP, Buchner J, Gaestel M (1999) Regulation of Hsp27 oligomerization, chaperone function, and protective activity against oxidative stress/tumor necrosis factor alpha by phosphorylation. *J Biol Chem* 274(27):18947–18956

Romer LH, Birukov KG, Garcia JG (2006) Focal adhesions: paradigm for a signaling nexus. *Circ Res* 98(5):606–616

Ron D, Walter P (2007) Signal integration in the endoplasmic reticulum unfolded protein response. *Nat Rev Mol Cell Biol* 8(7):519–529

Ronkina N, Kotlyarov A, ttrich Breiholz O, Kracht M, Hitti E, Milarski K, Askew R, Marusic S, Lin LL, Gaestel M, Telliez JB (2007) The mitogen-activated protein kinase (MAPK)-activated protein kinases MK2 and MK3 cooperate in stimulation of tumor necrosis factor biosynthesis and stabilization of p38 MAPK. *Mol Cell Biol* 27(1):170–181

Rosenfeld PJ, Brown DM, Heier JS, Boyer DS, Kaiser PK, Chung CY, Kim RY (2006) Ranibizumab for neovascular age-related macular degeneration. *N Engl J Med* 355(14):1419–1431

Roskoski R (2008) VEGF receptor protein-tyrosine kinases: structure and regulation. *Biochem Biophys Res Commun* 375(3):287–291

Rosnoblet C, Vischer UM, Gerard RD, Irminger JC, Halban PA, Kruithof EK (1999) Storage of tissue-type plasminogen activator in Weibel-Palade bodies of human endothelial cells. *Arterioscler Thromb Vasc Biol* 19(7):1796–1803

Ross JA, Nagy ZS, Kirken RA (2008) The PHB1/2 phosphocomplex is required for mitochondrial homeostasis and survival of human T cells. *J Biol Chem* 283(8):4699–4713

Ross PL, Huang YN, Marchese JN, Williamson B, Parker K, Hattan S, Khainovski N, Pillai S, Dey S, Daniels S, Purkayastha S, Juhasz P, Martin S, Bartlet-Jones M, He F, Jacobson A, Pappin DJ (2004) Multiplexed protein quantitation in Saccharomyces cerevisiae using amine-reactive isobaric tagging reagents. *Mol Cell Proteomics* 3(12):1154–1169

Rothe J, Lesslauer W, Lotscher H, Lang Y, Koebel P, Kontgen F, Althage A, Zinkernagel R, Steinmetz M, Bluethmann H (1993) Mice lacking the tumour necrosis factor receptor 1 are resistant to TNF-mediated toxicity but highly susceptible to infection by Listeria monocytogenes. *Nature* 364(6440):798–802

Rouse J, Cohen P, Trigon S, Morange M, onso Llamazares A, Zamanillo D, Hunt T, Nebreda AR (1994) A novel kinase cascade triggered by stress and heat shock that stimulates MAPKAP kinase-2 and phosphorylation of the small heat shock proteins. *Cell* 78(6):1027–1037

Rousseau S, Houle F, Landry J, Huot J (1997) p38 MAP kinase activation by vascular endothelial growth factor mediates actin reorganization and cell migration in human endothelial cells. *Oncogene* 15(18):2169–2177

Rousseau S, Houle F, Huot J (2000a) Integrating the VEGF signals leading to actin-based motility in vascular endothelial cells. *Trends Cardiovasc Med* 10(8):321–327

Rousseau S, Houle F, Kotanides H, Witte L, Waltenberger J, Landry J, Huot J (2000b) Vascular endothelial growth factor (VEGF)-driven actin-based motility is mediated by VEGFR2 and requires concerted activation of stress-activated protein kinase 2 (SAPK2/p38) and geldanamycin-sensitive phosphorylation of focal adhesion kinase. *J Biol Chem* 275(14):10661–10672

Rousseau S, Dolado I, Beardmore V, Shpiro N, Marquez R, Nebreda AR, Arthur JS, Case LM, Tessier-Lavigne M, Gaestel M, Cuenda A, Cohen P (2006) CXCL12 and C5a trigger cell migration via a PAK1/2-p38alpha MAPK-MAPKAP-K2-HSP27 pathway. *Cell Signal* 18(11):1897–1905

Rozengurt E, Rey O, Waldron RT (2005) Protein kinase D signaling. *J Biol Chem* 280(14):13205–13208

Ruhrberg C, Gerhardt H, Golding M, Watson R, Ioannidou S, Fujisawa H, Betsholtz C, Shima DT (2002) Spatially restricted patterning cues provided by heparin-binding VEGF-A control blood vessel branching morphogenesis. *Genes Dev* 16(20):2684–2698

Rush J, Moritz A, Lee KA, Guo A, Goss VL, Spek EJ, Zhang H, Zha XM, Polakiewicz RD, Comb MJ (2005) Immunoaffinity profiling of tyrosine phosphorylation in cancer cells. *Nat Biotechnol* 23(1):94–101

Russell WC (2000) Update on adenovirus and its vectors. *J Gen Virol* 81(Pt 11):2573–2604

Rybin VO, Guo J, Steinberg SF (2009) Protein Kinase D1 Autophosphorylation via Distinct Mechanisms at Ser744/Ser748 and Ser916. *J Biol Chem* 284(4):2332–2343

Sabio G, Arthur JS, Kuma Y, Peggie M, Carr J, Murray-Tait V, Centeno F, Goedert M, Morrice NA, Cuenda A (2005) p38gamma regulates the localisation of SAP97 in the cytoskeleton by modulating its interaction with GKAP. *EMBO J* 24(6):1134–1145

Saitoh M, Nishitoh H, Fujii M, Takeda K, Tobiume K, Sawada Y, Kawabata M, Miyazono K, Ichijo H (1998) Mammalian thioredoxin is a direct inhibitor of apoptosis signal-regulating kinase (ASK) 1. *EMBO J* 17(9):2596–2606

Saklatvala J, Kaur P, Guesdon F (1991) Phosphorylation of the small heat-shock protein is regulated by interleukin 1, tumour necrosis factor, growth factors, bradykinin and ATP. *Biochem J* 277 (Pt 3):635–642

Sakurai Y, Ohgimoto K, Kataoka Y, Yoshida N, Shibuya M (2005) Essential role of Flk-1 (VEGF receptor 2) tyrosine residue 1173 in vasculogenesis in mice. *Proc Natl Acad Sci U S A* 102(4):1076–1081

Salomoni P, Khelifi AF (2006) Daxx: death or survival protein? *Trends Cell Biol* 16(2):97–104

Salven P, Lymboussaki A, Heikkila P, Jaaskela-Saari H, Enholm B, Aase K, von EG, Eriksson U, Alitalo K, Joensuu H (1998) Vascular endothelial growth factors VEGF-B and VEGF-C are expressed in human tumors. *Am J Pathol* 153(1):103–108

Sambrook J, Fritsch EF, Maniatis T (1989) *Molecular Cloning: A Laboratory Manual*. Cold Spring Harbor Laboratory Press, New York, 2nd edition

Santell L, Bartfeld NS, Levin EG (1992) Identification of a protein transiently phosphorylated by activators of endothelial cell function as the heat-shock protein HSP27. A possible role for protein kinase C. *Biochem J* 284 (Pt 3):705–710

Saraste A, Pulkki K (2000) Morphologic and biochemical hallmarks of apoptosis. *Cardiovasc Res* 45(3):528–537

Sato TN, Tozawa Y, Deutsch U, Wolburg-Buchholz K, Fujiwara Y, Gendron-Maguire M, Gridley T, Wolburg H, Risau W, Qin Y (1995) Distinct roles of the receptor tyrosine kinases Tie-1 and Tie-2 in blood vessel formation. *Nature* 376(6535):70–74

Schneider GB, Hamano H, Cooper LF (1998) In vivo evaluation of hsp27 as an inhibitor of actin polymerization: hsp27 limits actin stress fiber and focal adhesion formation after heat shock. *J Cell Physiol* 177(4):575–584

Seamon KB, Daly JW (1981) Forskolin: a unique diterpene activator of cyclic AMP-generating systems. *J Cyclic Nucleotide Res* 7(4):201–224

Senger DR, Galli SJ, Dvorak AM, Perruzzi CA, Harvey VS, Dvorak HF (1983) Tumor cells secrete a vascular permeability factor that promotes accumulation of ascites fluid. *Science* 219(4587):983–985

Senger DR, Connolly DT, Van de Water L, Feder J, Dvorak HF (1990) Purification and NH2-terminal amino acid sequence of guinea pig tumor-secreted vascular permeability factor. *Cancer Res* 50(6):1774–1778

Shalaby F, Rossant J, Yamaguchi TP, Gertsenstein M, Wu XF, Breitman ML, Schuh AC (1995) Failure of blood-island formation and vasculogenesis in Flk-1-deficient mice. *Nature* 376(6535):62–66

Shaw RJ, Cantley LC (2006) Ras, PI(3)K and mTOR signalling controls tumour cell growth. *Nature* 441(7092):424–430

Shi Y, Kotlyarov A, Laabeta K, Gruber AD, Butt E, Marcus K, Meyer HE, Friedrich A, Volk HD, Gaestel M (2003) Elimination of protein kinase MK5/PRAK activity by targeted homologous recombination. *Mol Cell Biol* 23(21):7732–7741

Shing Y, Folkman J, Sullivan R, Butterfield C, Murray J, Klagsbrun M (1984) Heparin affinity: purification of a tumor-derived capillary endothelial cell growth factor. *Science* 223(4642):1296–1299

Shizukuda Y, Tang S, Yokota R, Ware JA (1999) Vascular endothelial growth factor-induced endothelial cell migration and proliferation depend on a nitric oxide-mediated decrease in protein kinase Cdelta activity. *Circ Res* 85(3):247–256

Shweiki D, Itin A, Soffer D, Keshet E (1992) Vascular endothelial growth factor induced by hypoxia may mediate hypoxia-initiated angiogenesis. *Nature* 359(6398):843–845

Siekmann AF, Lawson ND (2007) Notch signalling limits angiogenic cell behaviour in developing zebrafish arteries. *Nature* 445(7129):781–784

Silva R, D'Amico G, Hodivala-Dilke KM, Reynolds LE (2008) Integrins: the keys to unlocking angiogenesis. *Arterioscler Thromb Vasc Biol* 28(10):1703–1713

Silvestre JS, Tamarat R, Ebrahimian TG, Le-Roux A, Clergue M, Emmanuel F, Duriez M, Schwartz B, Branellec D, Levy BI (2003) Vascular endothelial growth factor-B promotes in vivo angiogenesis. *Circ Res* 93(2):114–123

Sinsimer KS, Gratacos FM, Knapinska AM, Lu J, Krause CD, Wierzbowski AV, Maher LR, Scrudato S, Rivera YM, Gupta S, Turrin DK, De La Cruz MP, Pestka S, Brewer G (2008) Chaperone Hsp27, a novel subunit of AUF1 protein complexes, functions in AU-rich element-mediated mRNA decay. *Mol Cell Biol* 28(17):5223–5237

Slowik MR, De Luca LG, Fiers W, Pober JS (1993) Tumor necrosis factor activates human endothelial cells through the p55 tumor necrosis factor receptor but the p75 receptor contributes to activation at low tumor necrosis factor concentration. *Am J Pathol* 143(6):1724–1730

Soker S, Takashima S, Miao HQ, Neufeld G, Klagsbrun M (1998) Neuropilin-1 is expressed by endothelial and tumor cells as an isoform-specific receptor for vascular endothelial growth factor. *Cell* 92(6):735–745

Soloff RS, Katayama C, Lin MY, Feramisco JR, Hedrick SM (2004) Targeted deletion of protein kinase C lambda reveals a distribution of functions between the two atypical protein kinase C isoforms. *J Immunol* 173(5):3250–3260

Sondell M, Sundler F, Kanje M (2000) Vascular endothelial growth factor is a neurotrophic factor which stimulates axonal outgrowth through the flk-1 receptor. *Eur J Neurosci* 12(12):4243–4254

Sonveaux P, Martinive P, DeWever J, Batova Z, Daneau G, Pelat M, Ghisdal P, Gregoire V, Dessy C, Balligand JL, Feron O (2004) Caveolin-1 expression is critical for vascular endothelial growth factor-induced ischemic hindlimb collateralization and nitric oxide-mediated angiogenesis. *Circ Res* 95(2):154–161

Spisak S, Tulassay Z, Molnar B, Guttman A (2007) Protein microchips in biomedicine and biomarker discovery. *Electrophoresis* 28(23):4261–4273

Sprague RS, Stephenson AH, Ellsworth ML (2007) Red not dead: signaling in and from erythrocytes. *Trends Endocrinol Metab* 18(9):350–355

Sprenger RR, Speijer D, Back JW, De Koster CG, Pannekoek H, Horrevoets AJ (2004) Comparative proteomics of human endothelial cell caveolae and rafts using two-dimensional gel electrophoresis and mass spectrometry. *Electrophoresis* 25(1):156–172

Srinivasan R, Forman S, Quinlan RA, Ohanian J, Ohanian V (2008) Regulation of contractility by Hsp27 and Hic-5 in rat mesenteric small arteries. *Am J Physiol Heart Circ Physiol* 294(2):H961–H969

Stacker SA, Stenvers K, Caesar C, Vitali A, Domagala T, Nice E, Roufail S, Simpson RJ, Moritz R, Karpanen T, Alitalo K, Achen MG (1999) Biosynthesis of vascular endothelial growth factor-D involves proteolytic processing which generates non-covalent homodimers. *J Biol Chem* 274(45):32127–32136

Stalmans I, Ng YS, Rohan R, Fruttiger M, Bouche A, Yuce A, Fujisawa H, Hermans B, Shani M, Jansen S, Hicklin D, Anderson DJ, Gardiner T, Hammes HP, Moons L, Dewerchin M, Collen D, Carmeliet P, D'Amore PA (2002) Arteriolar and venular patterning in retinas of mice selectively expressing VEGF isoforms. *J Clin Invest* 109(3):327–336

Stan RV (2007) Endothelial stomatal and fenestral diaphragms in normal vessels and angiogenesis. *J Cell Mol Med* 11(4):621–643

Stan RV, Kubitza M, Palade GE (1999) PV-1 is a component of the fenestral and stomatal diaphragms in fenestrated endothelia. *Proc Natl Acad Sci U S A* 96(23):13203–13207

Steen H, Kuster B, Fernandez M, Pandey A, Mann M (2002) Tyrosine phosphorylation mapping of the epidermal growth factor receptor signaling pathway. *J Biol Chem* 277(2):1031–1039

Stewart DJ, Kutryk MJ, Fitchett D, Freeman M, Camack N, Su Y, Della SA, Bilodeau L, Burton JR, Proulx G, Radhakrishnan S (2009) VEGF gene therapy fails to improve perfusion of ischemic myocardium in patients with advanced coronary disease: results of the NORTHERN trial. *Mol Ther* 17(6):1109–1115

Stewart GW (1997) Stomatin. *Int J Biochem Cell Biol* 29(2):271–274

Stokoe D, Campbell DG, Nakielny S, Hidaka H, Leevers SJ, Marshall C, Cohen P (1992a) MAPKAP kinase-2; a novel protein kinase activated by mitogen-activated protein kinase. *EMBO J* 11(11):3985–3994

Stokoe D, Engel K, Campbell DG, Cohen P, Gaestel M (1992b) Identification of MAPKAP kinase 2 as a major enzyme responsible for the phosphorylation of the small mammalian heat shock proteins. *FEBS Lett* 313(3):307–313

Storz P, Doppler H, Toker A (2004) Protein kinase Cdelta selectively regulates protein kinase D-dependent activation of NF-kappaB in oxidative stress signaling. *Mol Cell Biol* 24(7):2614–2626

Stromer T, Fischer E, Richter K, Haslbeck M, Buchner J (2004) Analysis of the regulation of the molecular chaperone Hsp26 by temperature-induced dissociation: the N-terminal domain is important for oligomer assembly and the binding of unfolding proteins. *J Biol Chem* 279(12):11222–11228

Sturany S, Van LJ, Muller F, Wilda M, Hameister H, Hocker M, Brey A, Gern U, Vandenheede J, Gress T, Adler G, Seufferlein T (2001) Molecular cloning and characterization of the human protein kinase D2. A novel member of the protein kinase D family of serine threonine kinases. *J Biol Chem* 276(5):3310–3318

Sudo T, Kawai K, Matsuzaki H, Osada H (2005) p38 mitogen-activated protein kinase plays a key role in regulating MAPKAPK2 expression. *Biochem Biophys Res Commun* 337(2):415–421

Sugimoto H, Hamano Y, Charytan D, Cosgrove D, Kieran M, Sudhakar A, Kalluri R (2003) Neutralization of circulating vascular endothelial growth factor (VEGF) by anti-VEGF antibodies and soluble VEGF receptor 1 (sFlt-1) induces proteinuria. *J Biol Chem* 278(15):12605–12608

Sun L, Tran N, Tang F, App H, Hirth P, McMahon G, Tang C (1998) Synthesis and biological evaluations of 3-substituted indolin-2-ones: a novel class of tyrosine kinase inhibitors that exhibit selectivity toward particular receptor tyrosine kinases. *J Med Chem* 41(14):2588–2603

Sun Z, Arendt CW, Ellmeier W, Schaeffer EM, Sunshine MJ, Gandhi L, Annes J, Petrzilka D, Kupfer A, Schwartzberg PL, Littman DR (2000) PKC-theta is required for TCR-induced NF-kappaB activation in mature but not immature T lymphocytes. *Nature* 404(6776):402–407

Sundberg C, Kowanetz M, Brown LF, Detmar M, Dvorak HF (2002) Stable expression of angiopoietin-1 and other markers by cultured pericytes: phenotypic similarities to a subpopulation of cells in maturing vessels during later stages of angiogenesis in vivo. *Lab Invest* 82(4):387–401

Suri C, Jones PF, Patan S, Bartunkova S, Maisonpierre PC, Davis S, Sato TN, Yancopoulos GD (1996) Requisite role of angiopoietin-1, a ligand for the TIE2 receptor, during embryonic angiogenesis. *Cell* 87(7):1171–1180

Swarup G, Cohen S, Garbers DL (1982) Inhibition of membrane phosphotyrosyl-protein phosphatase activity by vanadate. *Biochem Biophys Res Commun* 107(3):1104–1109

Takahashi H, Hattori S, Iwamatsu A, Takizawa H, Shibuya M (2004) A novel snake venom vascular endothelial growth factor (VEGF) predominantly induces vascular permeability through preferential signaling via VEGF receptor-1. *J Biol Chem* 279(44):46304–46314

Takahashi T, Kalka C, Masuda H, Chen D, Silver M, Kearney M, Magner M, Isner JM, Asahara T (1999a) Ischemia- and cytokine-induced mobilization of bone marrow-derived endothelial progenitor cells for neovascularization. *Nat Med* 5(4):434–438

Takahashi T, Ueno H, Shibuya M (1999b) VEGF activates protein kinase C-dependent, but Ras-independent Raf-MEK-MAP kinase pathway for DNA synthesis in primary endothelial cells. *Oncogene* 18(13):2221–2230

Takahashi T, Yamaguchi S, Chida K, Shibuya M (2001) A single autophosphorylation site on KDR/Flk-1 is essential for VEGF-A-dependent activation of PLC-gamma and DNA synthesis in vascular endothelial cells. *EMBO J* 20(11):2768–2778

Takai Y, Kishimoto A, Iwasa Y, Kawahara Y, Mori T, Nishizuka Y (1979) Calcium-dependent activation of a multifunctional protein kinase by membrane phospholipids. *J Biol Chem* 254(10):3692–3695

Takashima S, Kitakaze M, Asakura M, Asanuma H, Sanada S, Tashiro F, Niwa H, Miyazaki JJ, Hirota S, Kitamura Y, Kitsukawa T, Fujisawa H, Klagsbrun M, Hori M (2002) Targeting of both mouse neuropilin-1 and neuropilin-2 genes severely impairs developmental yolk sac and embryonic angiogenesis. *Proc Natl Acad Sci U S A* 99(6):3657–3662

Tan M, Xu X, Ohba M, Ogawa W, Cui MZ (2003) Thrombin rapidly induces protein kinase D phosphorylation, and protein kinase C delta mediates the activation. *J Biol Chem* 278(5):2824–2828

Tan M, Xu X, Ohba M, Cui MZ (2004) Angiotensin II-induced protein kinase D activation is regulated by protein kinase Cdelta and mediated via the angiotensin II type 1 receptor in vascular smooth muscle cells. *Arterioscler Thromb Vasc Biol* 24(12):2271–2276

Taylor RP, Benjamin IJ (2005) Small heat shock proteins: a new classification scheme in mammals. *J Mol Cell Cardiol* 38(3):433–444

Tessler S, Rockwell P, Hicklin D, Cohen T, Levi BZ, Witte L, Lemischka IR, Neufeld G (1994) Heparin modulates the interaction of VEGF165 with soluble and cell associated flk-1 receptors. *J Biol Chem* 269(17):12456–12461

Thakker GD, Hajjar DP, Muller WA, Rosengart TK (1999) The role of phosphatidylinositol 3-kinase in vascular endothelial growth factor signaling. *J Biol Chem* 274(15):10002–10007

Theriault JR, Lambert H, Chavez-Zobel AT, Charest G, Lavigne P, Landry J (2004) Essential role of the NH2-terminal WD/EPF motif in the phosphorylation-activated protective function of mammalian Hsp27. *J Biol Chem* 279(22):23463–23471

Thurston G, Suri C, Smith K, McClain J, Sato TN, Yancopoulos GD, McDonald DM (1999) Leakage-resistant blood vessels in mice transgenically overexpressing angiopoietin-1. *Science* 286(5449):2511–2514

Thurston G, Rudge JS, Ioffe E, Zhou H, Ross L, Croll SD, Glazer N, Holash J, McDonald DM, Yancopoulos GD (2000) Angiopoietin-1 protects the adult vasculature against plasma leakage. *Nat Med* 6(4):460–463

Tischer E, Mitchell R, Hartman T, Silva M, Gospodarowicz D, Fiddes JC, Abraham JA (1991) The human gene for vascular endothelial growth factor. Multiple protein forms are encoded through alternative exon splicing. *J Biol Chem* 266(18):11947–11954

Tondera D, Grandemange S, Jourdain A, Karbowski M, Mattenberger Y, Herzig S, Da CS, Clerc P, Raschke I, Merkwirth C, Ehses S, Krause F, Chan DC, Alexander C, Bauer C, Youle R, Langer T, Martinou JC (2009) SLP-2 is required for stress-induced mitochondrial hyperfusion. *EMBO J* 28(11):1589–1600

Toullec D, Pianetti P, Coste H, Bellevergue P, Grand-Perret T, Ajakane M, Baudet V, Boissin P, Boursier E, Loriolle F, (1991) The bisindolylmaleimide GF 109203X is a potent and selective inhibitor of protein kinase C. *J Biol Chem* 266(24):15771–15781

Tran J, Rak J, Sheehan C, Saibil SD, LaCasse E, Korneluk RG, Kerbel RS (1999) Marked induction of the IAP family antiapoptotic proteins survivin and XIAP by VEGF in vascular endothelial cells. *Biochem Biophys Res Commun* 264(3):781–788

Trinklein ND, Murray JI, Hartman SJ, Botstein D, Myers RM (2004) The role of heat shock transcription factor 1 in the genome-wide regulation of the mammalian heat shock response. *Mol Biol Cell* 15(3):1254–1261

Uehara Y, Fukazawa H, Murakami Y, Mizuno S (1989) Irreversible inhibition of v-src tyrosine kinase activity by herbimycin A and its abrogation by sulfhydryl compounds. *Biochem Biophys Res Commun* 163(2):803–809

Ushio-Fukai M, Tang Y, Fukai T, Dikalov SI, Ma Y, Fujimoto M, Quinn MT, Pagano PJ, Johnson C, Alexander RW (2002) Novel role of gp91(phox)-containing NAD(P)H oxidase in vascular endothelial growth factor-induced signaling and angiogenesis. *Circ Res* 91(12):1160–1167

Valverde AM, Sinnett-Smith J, Van LJ, Rozengurt E (1994) Molecular cloning and characterization of protein kinase D: a target for diacylglycerol and phorbol esters with a distinctive catalytic domain. *Proc Natl Acad Sci U S A* 91(18):8572–8576

van der Bliek AM (2009) Fussy mitochondria fuse in response to stress. *EMBO J* 28(11):1533–1534

van der Zee R, Murohara T, Luo Z, Zollmann F, Passeri J, Lekutat C, Isner JM (1997) Vascular endothelial growth factor/vascular permeability factor augments nitric oxide release from quiescent rabbit and human vascular endothelium. *Circulation* 95(4):1030–1037

Van Lint JV, Sinnett-Smith J, Rozengurt E (1995) Expression and characterization of PKD, a phorbol ester and diacylglycerol-stimulated serine protein kinase. *J Biol Chem* 270(3):1455–1461

van Montfort RL, Basha E, Friedrich KL, Slingsby C, Vierling E (2001) Crystal structure and assembly of a eukaryotic small heat shock protein. *Nat Struct Biol* 8(12):1025–1030

Vander Heide RS (2002) Increased expression of HSP27 protects canine myocytes from simulated ischemia-reperfusion injury. *Am J Physiol Heart Circ Physiol* 282(3):H935–H941

Veikkola T, Jussila L, Makinen T, Karpanen T, Jeltsch M, Petrova TV, Kubo H, Thurston G, McDonald DM, Achen MG, Stacker SA, Alitalo K (2001) Signalling via vascular endothelial growth factor receptor-3 is sufficient for lymphangiogenesis in transgenic mice. *EMBO J* 20(6):1223–1231

Vertii A, Hakim C, Kotlyarov A, Gaestel M (2006) Analysis of properties of small heat shock protein Hsp25 in MAPK-activated protein kinase 2 (MK2)-deficient cells: MK2-dependent insolubilization of Hsp25 oligomers correlates with susceptibility to stress. *J Biol Chem* 281(37):26966–26975

Vestweber D (2008) VE-cadherin: the major endothelial adhesion molecule controlling cellular junctions and blood vessel formation. *Arterioscler Thromb Vasc Biol* 28(2):223–232

Vogeli KM, Jin SW, Martin GR, Stainier DY (2006) A common progenitor for haematopoietic and endothelial lineages in the zebrafish gastrula. *Nature* 443(7109):337–339

Voss OH, Batra S, Kolattukudy SJ, Gonzalez-Mejia ME, Smith JB, Doseff AI (2007) Binding of caspase-3 prodomain to heat shock protein 27 regulates monocyte apoptosis by inhibiting caspase-3 proteolytic activation. *J Biol Chem* 282(34):25088–25099

Wadgaonkar R, Pierce JW, Somnay K, Damico RL, Crow MT, Collins T, Garcia JG (2004) Regulation of c-Jun N-terminal kinase and p38 kinase pathways in endothelial cells. *Am J Respir Cell Mol Biol* 31(4):423–431

Wagner M, Hermanns I, Bittinger F, Kirkpatrick CJ (1999) Induction of stress proteins in human endothelial cells by heavy metal ions and heat shock. *Am J Physiol* 277(5 Pt 1):L1026–L1033

Waldron RT, Rozengurt E (2000) Oxidative stress induces protein kinase D activation in intact cells. Involvement of Src and dependence on protein kinase C. *J Biol Chem* 275(22):17114–17121

Waldron RT, Rozengurt E (2003) Protein kinase C phosphorylates protein kinase D activation loop Ser744 and Ser748 and releases autoinhibition by the pleckstrin homology domain. *J Biol Chem* 278(1):154–163

Waldron RT, Rey O, Iglesias T, Tugal T, Cantrell D, Rozengurt E (2001) Activation loop Ser744 and Ser748 in protein kinase D are transphosphorylated in vivo. *J Biol Chem* 276(35):32606–32615

Waltenberger J, Claesson-Welsh L, Siegbahn A, Shibuya M, Heldin CH (1994) Different signal transduction properties of KDR and Flt1, two receptors for vascular endothelial growth factor. *J Biol Chem* 269(43):26988–26995

Walter DH, Hink U, Asahara T, Van BE, Horowitz J, Tsurumi Y, Vandlen R, Heinsohn H, Keyt B, Ferrara N, Symes JF, Isner JM (1996) The in vivo bioactivity of vascular endothelial growth factor/vascular permeability factor is independent of N-linked glycosylation. *Lab Invest* 74(2):546–556

Wang A, Nomura M, Patan S, Ware JA (2002) Inhibition of protein kinase Calpha prevents endothelial cell migration and vascular tube formation in vitro and myocardial neovascularization in vivo. *Circ Res* 90(5):609–616

Wang HU, Chen ZF, Anderson DJ (1998) Molecular distinction and angiogenic interaction between embryonic arteries and veins revealed by ephrin-B2 and its receptor Eph-B4. *Cell* 93(5):741–753

Wang S, Li X, Parra M, Verdin E, Bassel-Duby R, Olson EN (2008) Control of endothelial cell proliferation and migration by VEGF signaling to histone deacetylase 7. *Proc Natl Acad Sci U S A* 105(22):7738–7743

Wang Y, Morrow JS (2000) Identification and characterization of human SLP-2, a novel homologue of stomatin (band 7.2b) present in erythrocytes and other tissues. *J Biol Chem* 275(11):8062–8071

Wang Y, Cao W, Yu Z, Liu Z (2009) Downregulation of a mitochondria associated protein SLP-2 inhibits tumor cell motility, proliferation and enhances cell sensitivity to chemotherapeutic reagents. *Cancer Biol Ther* 8(17)

Washburn MP, Wolters D, Yates I J R (2001) Large-scale analysis of the yeast proteome by multidimensional protein identification technology. *Nat Biotechnol* 19(3):242–247

Westerheide SD, Morimoto RI (2005) Heat shock response modulators as therapeutic tools for diseases of protein conformation. *J Biol Chem* 280(39):33097–33100

Wetzel C, Hu J, Riethmacher D, Benckendorff A, Harder L, Eilers A, Moshourab R, Kozlenkov A, Labuz D, Caspani O, Erdmann B, Machelska H, Heppenstall PA, Lewin GR (2007) A stomatin-domain protein essential for touch sensation in the mouse. *Nature* 445(7124):206–209

Wheeler-Jones C, Abu-Ghazaleh R, Cospedal R, Houliston RA, Martin J, Zachary I (1997) Vascular endothelial growth factor stimulates prostacyclin production and activation of cytosolic phospholipase A2 in endothelial cells via p42/p44 mitogen-activated protein kinase. *FEBS Lett* 420(1):28–32

Wieske M, Benndorf R, Behlke J, Dolling R, Grelle G, Bielka H, Lutsch G (2001) Defined sequence segments of the small heat shock proteins HSP25 and alphaB-crystallin inhibit actin polymerization. *Eur J Biochem* 268(7):2083–2090

Wiesmann C, Fuh G, Christinger HW, Eigenbrot C, Wells JA, de Vos AM (1997) Crystal structure at 1.7 A resolution of VEGF in complex with domain 2 of the Flt-1 receptor. *Cell* 91(5):695–704

Wilson K, Walker J (2005) *Principles and Techniques of Biochemistry and Molecular Biology*. Cambridge University Press, New York, 6th edition

Wilting J, Christ B, Bokeloh M, Weich HA (1993) In vivo effects of vascular endothelial growth factor on the chicken chorioallantoic membrane. *Cell Tissue Res* 274(1):163–172

Winzen R, Kracht M, Ritter B, Wilhelm A, Chen CY, Shyu AB, Muller M, Gaestel M, Resch K, Holtmann H (1999) The p38 MAP kinase pathway signals for cytokine-induced mRNA stabilization via MAP kinase-activated protein kinase 2 and an AU-rich region-targeted mechanism. *EMBO J* 18(18):4969–4980

Wise LM, Veikkola T, Mercer AA, Savory LJ, Fleming SB, Caesar C, Vitali A, Makinen T, Alitalo K, Stacker SA (1999) Vascular endothelial growth factor (VEGF)-like protein from orf virus NZ2 binds to VEGFR2 and neuropilin-1. *Proc Natl Acad Sci U S A* 96(6):3071–3076

Wong C, Jin ZG (2005) Protein kinase C-dependent protein kinase D activation modulates ERK signal pathway and endothelial cell proliferation by vascular endothelial growth factor. *J Biol Chem* 280(39):33262–33269

Wu HM, Yuan Y, Zawieja DC, Tinsley J, Granger HJ (1999) Role of phospholipase C, protein kinase C, and calcium in VEGF-induced venular hyperpermeability. *Am J Physiol* 276(2 Pt 2):H535–H542

Wu LW, Mayo LD, Dunbar JD, Kessler KM, Baerwald MR, Jaffe EA, Wang D, Warren RS, Donner DB (2000) Utilization of distinct signaling pathways by receptors for vascular endothelial cell growth factor and other mitogens in the induction of endothelial cell proliferation. *J Biol Chem* 275(7):5096–5103

Xu L, Chen S, Bergan RC (2006) MAPKAPK2 and HSP27 are downstream effectors of p38 MAP kinase-mediated matrix metalloproteinase type 2 activation and cell invasion in human prostate cancer. *Oncogene* 25(21):2987–2998

Yacyshyn OK, Lai PF, Forse K, Teichert-Kuliszewska K, Jurasz P, Stewart DJ (2009) Tyrosine phosphatase beta regulates angiopoietin-Tie2 signaling in human endothelial cells. *Angiogenesis* 12(1):25–33

Yamaguchi TP, Dumont DJ, Conlon RA, Breitman ML, Rossant J (1993) flk-1, an flt-related receptor tyrosine kinase is an early marker for endothelial cell precursors. *Development* 118(2):489–498

Yamaguchi TP, Harpal K, Henkemeyer M, Rossant J (1994) fgfr-1 is required for embryonic growth and mesodermal patterning during mouse gastrulation. *Genes Dev* 8(24):3032–3044

Yamamura S, Nelson PR, Kent KC (1996) Role of protein kinase C in attachment, spreading, and migration of human endothelial cells. *J Surg Res* 63(1):349–354

Yamaoka-Tojo M, Ushio-Fukai M, Hilenski L, Dikalov SI, Chen YE, Tojo T, Fukai T, Fujimoto M, Patrushev NA, Wang N, Kontos CD, Bloom GS, Alexander RW (2004) IQGAP1, a novel vascular endothelial growth factor receptor binding protein, is involved in reactive oxygen species–dependent endothelial migration and proliferation. *Circ Res* 95(3):276–283

Yamazaki D, Suetsugu S, Miki H, Kataoka Y, Nishikawa S, Fujiwara T, Yoshida N, Takenawa T (2003) WAVE2 is required for directed cell migration and cardiovascular development. *Nature* 424(6947):452–456

Yan JX, Wait R, Berkelman T, Harry RA, Westbrook JA, Wheeler CH, Dunn MJ (2000) A modified silver staining protocol for visualization of proteins compatible with matrix-assisted laser desorption/ionization and electrospray ionization-mass spectrometry. *Electrophoresis* 21(17):3666–3672

Yang K, Cepko CL (1996) Flk-1, a receptor for vascular endothelial growth factor (VEGF), is expressed by retinal progenitor cells. *J Neurosci* 16(19):6089–6099

Yang S, Xin X, Zlot C, Ingle G, Fuh G, Li B, Moffat B, de Vos AM, Gerritsen ME (2001) Vascular endothelial cell growth factor-driven endothelial tube formation is mediated by vascular endothelial cell growth factor receptor-2, a kinase insert domain-containing receptor. *Arterioscler Thromb Vasc Biol* 21(12):1934–1940

Yang S, Toy K, Ingle G, Zlot C, Williams PM, Fuh G, Li B, de Vos A, Gerritsen ME (2002) Vascular endothelial growth factor-induced genes in human umbilical vein endothelial cells: relative roles of KDR and Flt-1 receptors. *Arterioscler Thromb Vasc Biol* 22(11):1797–1803

Yashima R, Abe M, Tanaka K, Ueno H, Shitara K, Takenoshita S, Sato Y (2001) Heterogeneity of the signal transduction pathways for VEGF-induced MAPKs activation in human vascular endothelial cells. *J Cell Physiol* 188(2):201–210

Yla-Herttuala S, Rissanen TT, Vajanto I, Hartikainen J (2007) Vascular endothelial growth factors: biology and current status of clinical applications in cardiovascular medicine. *J Am Coll Cardiol* 49(10):1015–1026

Young PR, McLaughlin MM, Kumar S, Kassis S, Doyle ML, McNulty D, Gallagher TF, Fisher S, McDonnell PC, Carr SA, Huddleston MJ, Seibel G, Porter TG, Livi GP, Adams JL, Lee JC (1997) Pyridinyl imidazole inhibitors of p38 mitogen-activated protein kinase bind in the ATP site. *J Biol Chem* 272(18):12116–12121

Young S, Parker PJ, Ullrich A, Stabel S (1987) Down-regulation of protein kinase C is due to an increased rate of degradation. *Biochem J* 244(3):775–779

Yu Y, Sato JD (1999) MAP kinases, phosphatidylinositol 3-kinase, and p70 S6 kinase mediate the mitogenic response of human endothelial cells to vascular endothelial growth factor. *J Cell Physiol* 178(2):235–246

Yuan J, Rozengurt E (2007) PKD, PKD2, and p38 MAPK mediate Hsp27 serine-82 phosphorylation induced by neurotensin in pancreatic cancer PANC-1 cells. *J Cell Biochem* 103(2):648–662

Yuan L, Moyon D, Pardanaud L, Breant C, Karkkainen MJ, Alitalo K, Eichmann A (2002) Abnormal lymphatic vessel development in neuropilin 2 mutant mice. *Development* 129(20):4797–4806

Zachary I, Mathur A, Yla-Herttuala S, Martin J (2000) Vascular protection: A novel nonangiogenic cardiovascular role for vascular endothelial growth factor. *Arterioscler Thromb Vasc Biol* 20(6):1512–1520

Zanetti M, Katusic ZS, O'Brien T (2002) Adenoviral-mediated overexpression of catalase inhibits endothelial cell proliferation. *Am J Physiol Heart Circ Physiol* 283(6):H2620–H2626

Zantema A, Verlaan-De Vries M, Maasdam D, Bol S, van der Eb A (1992) Heat shock protein 27 and alpha B-crystallin can form a complex, which dissociates by heat shock. *J Biol Chem* 267(18):12936–12941

Zelzer E, McLean W, Ng YS, Fukai N, Reginato AM, Lovejoy S, D'Amore PA, Olsen BR (2002) Skeletal defects in VEGF(120/120) mice reveal multiple roles for VEGF in skeletogenesis. *Development* 129(8):1893–1904

Zhang L, Ding F, Cao W, Liu Z, Liu W, Yu Z, Wu Y, Li W, Li Y, Liu Z (2006) Stomatin-like protein 2 is overexpressed in cancer and involved in regulating cell growth and cell adhesion in human esophageal squamous cell carcinoma. *Clin Cancer Res* 12(5):1639–1646

Zhang R, Luo D, Miao R, Bai L, Ge Q, Sessa WC, Min W (2005a) Hsp90-Akt phosphorylates ASK1 and inhibits ASK1-mediated apoptosis. *Oncogene* 24(24):3954–3963

Zhang W, Zheng S, Storz P, Min W (2005b) Protein kinase D specifically mediates apoptosis signal-regulating kinase 1-JNK signaling induced by H2O2 but not tumor necrosis factor. *J Biol Chem* 280(19):19036–19044

Zheng C, Lin Z, Zhao ZJ, Yang Y, Niu H, Shen X (2006) MAPK-activated protein kinase-2 (MK2)-mediated formation and phosphorylation-regulated dissociation of the signal complex consisting of p38, MK2, Akt, and Hsp27. *J Biol Chem* 281(48):37215–37226

Zhou H, Watts JD, Aebersold R (2001) A systematic approach to the analysis of protein phosphorylation. *Nat Biotechnol* 19(4):375–378

Zhou M, Lambert H, Landry J (1993) Transient activation of a distinct serine protein kinase is responsible for 27-kDa heat shock protein phosphorylation in mitogen-stimulated and heat-shocked cells. *J Biol Chem* 268(1):35–43

Zhu Y, Paszty C, Turetsky T, Tsai S, Kuypers FA, Lee G, Cooper P, Gallagher PG, Stevens ME, Rubin E, Mohandas N, Mentzer WC (1999) Stomatocytosis is absent in "stomatin"-deficient murine red blood cells. *Blood* 93(7):2404–2410

Ziche M, Morbidelli L, Choudhuri R, Zhang HT, Donnini S, Granger HJ, Bicknell R (1997) Nitric oxide synthase lies downstream from vascular endothelial growth factor-induced but not basic fibroblast growth factor-induced angiogenesis. *J Clin Invest* 99(11):2625–2634

Zor T, Selinger Z (1996) Linearization of the Bradford protein assay increases its sensitivity: theoretical and experimental studies. *Anal Biochem* 236(2):302–308

Zugaza JL, Waldron RT, Sinnett-Smith J, Rozengurt E (1997) Bombesin, vasopressin, endothelin, bradykinin, and platelet-derived growth factor rapidly activate protein kinase D through a protein kinase C-dependent signal transduction pathway. *J Biol Chem* 272(38):23952–23960